A. A. Ilyshin, V. S. Lensky

Strength of Materials.

A. A. ILYUSHIN *and* V. S. LENSKY

Strength of Materials

TRANSLATED BY

J. K. LUSHER

TRANSLATION EDITED BY

S. C. REDSHAW

PERGAMON PRESS

OXFORD · LONDON · EDINBURGH · NEW YORK
TORONTO · SYDNEY · PARIS · BRAUNSCHWEIG

Pergamon Press Ltd., Headington Hill Hall, Oxford
4 & 5 Fitzroy Square, London W.1

Pergamon Press (Scotland) Ltd., 2 & 3 Teviot Place, Edinburgh 1

Pergamon Press Inc., 44–01 21st Street, Long Island City, New York 11101

Pergamon of Canada, Ltd., 6 Adelaide Street East, Toronto, Ontario

Pergamon Press (Aust.) Pty. Ltd., 20–22 Margaret Street, Sydney, N.S.W.

Pergamon Press S.A.R.L., 24 rue des Écoles, Paris 5e

Vieweg & Sohn GmbH, Burgplatz 1, Braunschweig

Copyright © 1967
Pergamon Press Ltd.

First English edition 1967

Library of Congress Catalog Card No. 66–12655

This is a translation of the book
Сопротивление Материалов *(Soprotivlenye Materialov)*
published by Gosizdfizmat, Moscow

2464/67

CONTENTS

PREFACE ix

INTRODUCTION 1

CHAPTER I. STRESSES AND STRAINS 9

1. Structural Characteristics of Materials 9
2. Internal Interaction of Particles in a Body 20
3. Investigation of the State of Stress at a Point 27
4. Principal Normal and Shearing Stresses 30
5. Octahedral Stresses 38
6. Deformation in the Neighbourhood of a Point 43
7. The Work done by Internal Forces 53
8. External Forces 58
9. Examples of Surface Forces 60
10. Body Forces 62
11. Examples of Mass Forces 64
12. Equilibrium Conditions and the General Method for finding Stresses, Strains, and Displacements in a Body 64
13. Problems for Solution on Chapter I 67

CHAPTER II. ELASTO-PLASTIC DEFORMATION OF RODS 69

1. The Mechanical Properties of Various Materials 69
2. The Effect of Various Factors on the Mechanical Properties of Materials 80
3. The Mechanism of Plastic Deformation 100
4. Rods of Variable Cross-section. The Method of Elastic Solutions 104
5. Frameworks 109
6. The Solution of Pin-jointed Frameworks 118
7. The Resistance of a Material to Shear 126
8. Torsion of a Circular Rod 130
9. Combined Stress State in a Beam 135
10. Stresses and Strains in a Beam 141
11. Eccentric Loading. Core Points 149

12. The Carrying Capacity of a Beam 153
13. The Deflection of a Beam 156
14. A Beam on an Elastic Foundation 160
15. Longitudinal–Transverse Bending. The Stability of a Beam in Compression 164
16. The Stability of a Rod beyond the Elastic Limit 169

CHAPTER III. ELASTICITY AND PLASTICITY IN A STATE OF COMPOUND STRESS 176

1. Three-dimensional Elasticity of Materials 176
2. General Properties of Elasto-plastic Strains in Solid Bodies 178
3. *P–p* Experiments 183
4. *P–M* Experiments and the Basic Principles of Plasticity 189
5. The Generalization of Hooke's Law and the Laws of Small Elasto-plastic Strains 196
6. The Conditions of Plasticity 202
7. Deformation of a Pipe under Internal and External Pressure (Lamé's Problem) 207
8. Plastic Deformation of a Hollow Sphere 216
9. Thin-walled Containers 218
10. Shearing Stress Distribution in a Beam 220

CHAPTER IV. PLASTIC FLOW 226

1. The Strength and Plasticity of a Heated Metal 226
2. Finite Strains and the Tensor of Rate of Deformation 230
3. The Relation between Stresses and Strains in the Theory of Plastic Flow 235
4. Surface Friction 237
5. The Compression of a Strip between Rigid Plates 242
6. Extrusion of Plates and Strips 246
7. Flow over Rigid Plane Surfaces 250
8. Examples 256

CHAPTER V. CREEP OF MATERIALS 261

1. Dependence of the Properties of Materials on Time 261
2. Mechanical Theories of Creep 273
3. Creep in a State of Compound Stress 278
4. A Tube under Pressure (Plane Strain) 284
5. The Method of Similarity in the Determination of Steady Creep 286

CHAPTER VI. DYNAMIC RESISTANCE OF MATERIALS 291

1. Dynamic Forces of Resistance 291
2. The Effect of Rate of Strain on the Yield Point 293
3. The Effect of Rate of Strain on the Ultimate Tensile Stress 295
4. Delayed Yield and Delayed Failure 296
5. Stress–Strain Curve for Dynamic Loading 298
6. The Theory of Impact 304
7. Longitudinal Waves in Rods 307
8. Transverse Waves 312
9. Reflection of Longitudinal Elastic Waves 312
10. Impact of a Rod on a Stationary Obstacle 315
11. The Measuring Rod Theory 321
12. Derivation of the Dynamic $\sigma \sim \varepsilon$ Diagram from the Distribution of Residual Strains 322
13. The Method of Impulses 325
14. Spalling and Resistance to Bursting 326
15. Hollow Charges 329
16. Penetration of one Body by Another 333
17. Impact on Structures 338

CHAPTER VII. VIBRATIONS OF ELASTIC BODIES AND FATIGUE OF MATERIALS 339

1. The Behaviour of Materials and Structures under Oscillating Loads 339
2. Longitudinal Standing Waves and Longitudinal Vibrations in Rods 341
3. Torsional Vibrations in Rods 348
4. Bending Oscillations in Rods 351
5. Fatigue 356
6. Factors influencing Fatigue Characteristics 361
7. The Development of Fatigue Failures 364

CHAPTER VIII. METHODS AND EQUIPMENT FOR MECHANICAL TESTING 367

1. Introduction 367
2. Preparation of the Specimen 367
3. Geometry of the Specimen 370
4. Static Testing Machines 372
5. Dynamic Testing Machines 383
6. The Measurement of Small Displacements 395
7. Force Measuring Devices 403

8. Mechanical, Optical and Optical–Mechanical Methods of Measuring Strains 408
9. Electrical Methods of Measuring Strains 417
10. The Photoelastic Method of Stress Analysis 424
11. Photographic Recording 431

INDEX 437

PREFACE

MODERN structures and equipment are often subjected to extremely complex conditions such as high or very low temperatures, large plastic strains, high rates of deformation, radio-active radiation, the deleterious effects of certain substances, large pressures, etc. It is apparent then that the science of the resistance of materials, being a branch of the mechanics of a solid deformable body, must take into account as much information as possible concerning the strength of materials and their behaviour under load, in order to be able to formulate the general principles of the relations between the physical and mechanical parameters which describe the behaviour of materials under load, and to develop a theory which represents accurately the real conditions to which a structure is subjected.

The development of the theory of the resistance of materials means, on the one hand, a perfection of the methods of analysis and a widening of the class of problems which previously belonged to the theory of applied elasticity. On the other hand, this development comprises a study of new phenomena and aims to widen the physical principles of this science and to give us a general approach to a wider field of problems belonging to different branches of technology. The latter is becoming more essential in the training of research specialists in the universities and technical institutes.

This book is based on lectures on the strength of materials given by the authors with the above aim in mind, during the course of a number of years in the mechanical–mathematical department of Moscow University. Although perhaps it is not exhaustive, the book does give, together with problems on the equilibrium and stability of simple structural elements under elastic and elastic-plastic deformation, information on plastic flow of materials under pressure, creep of materials, their dynamic resistance, vibrations and propagation of elastic and plastic waves and the effect of temperature, rate of deformation, radiation, etc., on the strength and plasticity of materials. It also gives a description of

experimental techniques used in investigating the mechanical properties of materials.

The mathematics is not advanced and contains nothing more involved than the normal differential equations. In some parts of the book methods of solution are given only in general form with a few illustrative examples. The qualified reader will, no doubt, be able to bridge the gaps which this approach may leave, and those studying the book will be able to apply the methods illustrated to various other problems.

The authors would welcome readers' advice and comments which would assist them in realizing their aims and hope that they will point out methods of improving the contents and presentation of the book.

The authors are indebted to their fellow workers in the chair of the elasticity department, to the undergraduate and post-graduate students in the mechanical–mathematical department of Moscow State University who made suggestions regarding the scope of the book and assisted in the preparation of the manuscript.

INTRODUCTION

THE strength of materials is the study of solid bodies under the action of external forces under working conditions, and of their resistance to deformation and failure. It sets out methods of analysis of structural elements and components of machinery with respect to their strength and deformability. It is, therefore, a branch of the mechanics of solid deformable bodies.

The resistance of materials includes a study of the following: (1) the materials of solid bodies (for example, steel, alloys, concrete) and their mechanical properties; (2) bodies of different shape and different usages such as rods, beams, plates, shells and others encountered in structures and machinery (for example in metal bridges, hydro-electric stations, the hulls of ships, aircraft, rockets, motors, instruments. etc.), bars, strips and plates during rolling, stamping and pressing operations, etc.; (3) the external forces acting on bodies and the mechanical effects on these bodies of, for example, the force of gravity, aero-hydrodynamic forces of gas and liquid pressure, forces of external friction and pressure, contact forces arising from the interaction of one body with other bodies, centrifugal and other forces of inertia, dynamic forces from motors and machines, etc.; (4) other external effects: temperature, chemically active media, radiation, etc.

The criteria on which the suitability and strength of any structural element can be assessed vary and depend entirely on its particular function.

In many cases they reduce to the requirement that the element retains its dimensions and shape under its working conditions for a long period of time, and that it does so to a high degree of accuracy. This refers to industrial and to civil structures, to production machinery (for example, to presses and rolling mills, to machine-tools, etc.), and to the hulls of ships and aircraft, etc.

On the other hand, under certain conditions, they reduce to the requirement that the body has to withstand, without failure, large plastic deformations in order easily to assume some other predeter-

mined shape. This applies to heated metal ingots which, by a process of rolling, pressing or forging, are formed into sheet metal, rails, shaped beams and many other products; in a number of cases it also applies to cold sheet metal from which curved panels are made on special mills for aircraft, motor cars and instruments.

In other cases the suitability of a component is assessed by its capacity to deform under working conditions without failure until such time that the load reaches a specified value, and then to fail at this load in a definite manner. This refers to certain measuring instruments, warning systems, etc., which contain a "weak element", the failure of which at a definite load prevents further action of the forces on the structure and thus protects it from serious damage.

The reasons why a component is unsound can be extremely different, but in the end they all amount either to the fact that it was incorrectly designed and stressed, or that the material was incorrectly chosen, or its properties insufficiently studied; or that the external forces, temperature and other conditions were inaccurately assessed. Failure, which often starts at just one point, then causes failure of the whole body.

The basic property of all solid bodies in practice is their elasticity—their capacity, up to certain limits, to deform reversibly under the action of external loads in such a way that after the removal of the external causes of the deformation, the deformation itself disappears. The concept of a deformable elastic body is the basis of the study of the resistance of materials.

The cause of catastrophes, failures of structures and machinery is often to be found in the occurrence of vibration. Since all bodies are to some extent elastic, they possess a number of natural frequencies of oscillation. This is the frequency of the oscillations which a body will perform if the external forces causing deformation are suddenly removed. If, for example, a rod with hinged ends is loaded by a force at the centre, and if then this force is suddenly removed, the rod will perform oscillations so that at every instant its curved axis forms a half-wave of a sine curve with nodal (stationary) points at the points of support (Fig. 1a). If now this rod is loaded by two equal but opposite forces applied at the quarter span points, and if these forces are then removed, the shape of the deflected axis of the rod will, with the resulting oscillations, be represented by a full sine wave with three nodal points: two at the supports and one at the centre (Fig. 1b). The frequency of the oscil-

lations in the second case will be four times larger than in the first case. An elastic body has an infinite number of such simple forms of oscillations and their corresponding frequencies. In the general case these different possible forms of oscillations are superimposed one on the other, and in some conditions, one shape and its corresponding frequency will be predominant, and under other conditions, another. It was due to the large oscillations which arose from wind action, that the Tacoma Bridge in the U.S.A.—one of the largest bridges in the world—failed in 1940. As soon as resonance conditions arise (when the frequency of the external forces coincides with one of the natural frequencies of oscillation) there is the possibility that the amplitude of the corresponding wave forms will sharply increase and that the structure will therefore fail. In technology however, it is not always possible or indeed necessary to avoid

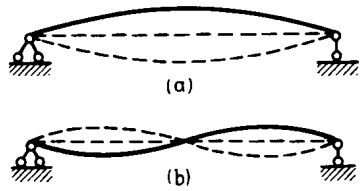

FIG. 1.

the state of resonance. There exist machines in the laboratory and in industry which are constructed in a special way and which work on the resonance principle. Examples would be certain machines for experiments in the field of vibration and fatigue.

A frequent cause of the failure of a structure is the instability of individual elements. This phenomenon is similar to the sudden buckling of a slender ruler held vertically on the table when a load greater than some critical value is applied to it. In the history of engineering many cases are known of serious accidents and tragedies when the cause of failure of bridges, buildings, ships and other structures was found to be loss of stability. We might, for instance, quote the failure of the large gasholder of 600,000 cubic metres capacity in Hamburg, which during a test filling on 7 December 1909 collapsed due to loss of stability in one of the elements of the support structure.

A cause of large deformations in a body can be the occurrence, in certain parts or throughout the whole body, of the state of

plasticity or yielding, when a small increase in the load causes large strains in the body. It should be realized that almost all solid materials display to a certain extent the properties of plasticity, and at high pressures even materials which we normally call brittle can yield without failure. For example, rock masses in the earth's crust flow under conditions of high hydrostatic pressure and undergo large plastic deformations.

The cause of large plastic deformations and the failure of components of machines working at high temperatures, for example the blades and guide vanes of gas turbines, the casing of jet engines, etc., is the creep of metals. This property is similar to the yielding of a wax rod when a load is hung from it: depending on the temperature such a rod will extend rapidly or slowly at constant load, and will finally break.

A very frequent cause of failure of the working parts of machines, for example, shafts in engines and other equipment, is the fatigue of the material, which can arise if a body is subjected to repetitive loading. The shafts of engines make millions of revolutions during the working life of the engine and each revolution is accompanied by the application of an alternating load. We make use of the property of fatigue when we wish to break a wire and bend it sharply backwards and forwards; the less we bend the wire each time, the greater the number of times we must repeat the operation before it breaks. A study of this phenomenon has shown that fatigue occurs in bodies only if the amplitude of the deformation at the points of greatest deformation exceeds some definite critical value. If during a process of oscillation the greatest deformation does not exceed the critical value, the component will function without a failure of the fatigue type for a practically indefinite period.

The materials of all bodies possess internal friction which in the vast majority of cases depends on the speed of the relative movement of particles of the body and increases with increase in this speed. The concept of internal friction covers all the many different types of internal dissipative forces. It is due to the existence of internal friction and also the ever present friction between the body and its surroundings that the vibrations which occur after the removal of a periodic disturbing force are quickly damped. The resistance of bodies to deformation always depends to a certain extent on the rate of deformation, which is related to the rate of application of the external loads. With very high rates of deformation, arising for

example, from shock loading, the resistance of metals to transition into the plastic state at normal temperature can increase by two or three times, and the resistance to deformation of polymers (for example, rubber) increases considerably even within the limits of elastic deformation.

When external forces are applied to a body all the features mentioned above can be present, and to a certain extent they determine the strength of the body. And if failure of the body does occur it never occurs throughout the whole body at once, but starts at one or several points and then spreads through the body at finite speed.

If we consider the enormous number of different types of bodies with which we have to deal in practice, the different materials and their properties, the types of interaction between bodies and the forces acting on them, the different temperature ranges and other conditions, it appears at first a hopeless task to attempt a general scientific approach to the solution of problems on the strength of solid bodies. An external effect on the boundary surface of a body of reasonably large dimensions penetrates inside the body and reaches its different elementary particles—molecules, ions, atoms—in different ways. If one considers that large solid bodies, for example metal bodies, with linear dimensions of from a millimetre to several tens of metres and more, which we are normally concerned with in engineering practice, contain 10^{20}–10^{40} atoms, it becomes clear that it would be hopeless to try to evaluate the effect on every single atom. However the atomic nature of bodies does give us an idea of why a solid body is able to deform (it is apparently because the distance between atoms changes, together with their relative positions and also the dimensions of the atoms themselves), how large all the many possible changes in shape and dimensions of the body can be (excluding the deformation of the atom itself, each atom, considered as a material point, has three degrees of freedom), and it also gives us an idea as to the nature of the change in the interaction between individual atoms (the occurrence of repulsive or attractive forces as atoms approach each other or move apart). The atomic nature of bodies illustrates that the study of the strength of solid bodies involves the study of the relative changes in position of small elements in the body, i.e. strains, and the resulting changes in the interaction between these elements, i.e. internal stresses.

But if we reject the idea of attempting to take the atom as the starting point for studying the strength and laws of resistance to

deformation and failure of different materials simply because no methods are known which will allow us to take into account the different interactions of all the many atoms in the body, then the question arises: what small part of the whole body should be taken as the basic element for studying the internal strains and stresses in the body, bearing in mind that at all such points the situation will be different?

Solid bodies, as is well known, can be divided into amorphous and crystalline. It is assumed that in amorphous bodies, typical examples of which are ordinary glass and bakelite, the atoms and molecules are distributed at random, with no orientation, and amorphous bodies are, therefore, isotropic, i.e. their mechanical, optical and electrical properties are identical in all directions. The characteristic linear dimension of an amorphous material is the mean inter-atomic distance. Crystalline bodies on the other hand, typical examples of which are metals, do have an ordered structure and their elementary particles (atoms, ions) are arranged in a definite order. For example, iron has a cubic lattice. A piece of iron, however, is not a crystal, but a polycrystalline body composed of grains which are crystals (crystallites), the dimensions of which are of the order of 0·1 mm or more, i.e. considerably greater than the inter-atomic distances. Each crystal is anisotropic, i.e. it has different properties in different directions and is therefore characterized not only by its dimensions and shape, but by its orientation in space defined with reference to its physical properties. But even an individual grain cannot be taken as the basic small element for studying the internal stresses and strains in large bodies, for more or less the same reasons as for the atom; here conditions are complicated by the fact that the shapes of the grains are irregular and varied, and the relative orientation of the grains is, in general, random.

In mechanics we take as the elementary volume for investigating internal stresses and strains in a body, a small volume which is such that in practice it contains very many atoms and even very many grains, but mathematically it is assumed to be infinitely small. It is assumed that displacements, stresses and strains are continuous differentiable functions of the coordinates of the internal points of the body and of time. It is assumed also, that the internal stresses which arise due to external effects depend at every point only on the strain which occurs at that point due to external effects, and

on temperature and time. Thus, in addition to the concept of an "absolutely solid body" there arises in mechanics a new concept of a "material continuum" or "continuous medium" and, in particular, of a "solid continous deformable body". This concept has proved to be extremely useful not only in a theoretical and analytical respect, in that it has enabled the powerful apparatus of mathematics to be applied to strength analysis, but it has also been of great value in experimental work, since it has shown that in an investigation of the strength of solid bodies only mechanical properties are important, i.e. the relation between stress, strains, time and temperature, and not the whole set of complex interactions which define fully the physical state of the real solid body. From this concept were devised special experimental methods of investigating the mechanical properties of materials. There was developed, more than a hundred years ago, the mechanics of solid bodies or continuums and such basic sciences dealing with the strength of solid bodies as the resistance of materials, structural mechanics, the theory of elasticity and the theory of plasticity.

The contents of this book can be divided into three main parts: (1) the basic concepts of displacements, internal stresses, strains and the work of internal forces, and also the process of loading a small element of a solid body; (2) the basic mechanical properties of solid bodies such as elasticity and ideal plasticity, ductility, creep and relaxation, viscosity and dynamic resistance, fatigue and failure; (3) basic kinematic and geometrical hypotheses which simplify the mathematical formulation of problems on stresses, strains, displacements and failures of solid bodies under various external forces, and also the basic equations and methods of solution of problems on the deformation and strength of bodies. The methods of the Strength of Materials differ from the more precise methods of the theory of elasticity and plasticity in that a number of simplifying assumptions are made of a kinematic and geometrical nature, but they remain, nevertheless, sufficiently accurate in the majority of cases.

CHAPTER I

STRESSES AND STRAINS

1. Structural Characteristics of Materials

The material most commonly used in engineering is metal. The study of metals and their internal structure is a special part of such branches of science as the physics of metals, which deals with the theoretical bases of their structure in relation to their different physical properties (electrical conductivity, thermal conductivity, etc.), and physical metallurgy and metallography, which are mainly concerned with technological processes of producing metals and their alloys.

Metals differ from many other materials in their crystalline structure, i.e. the geometrically regular and ordered arrangement of their atoms which makes up a crystal space lattice. The existence of this crystal structure is revealed by X-ray analysis. The various types of crystal bodies are characterized by the geometry of the arrangement of their elementary particles, the atoms, which defines one or other type of crystal lattice, and also by the structure of the atoms.

In the majority of metals the crystal lattices are of three types: body-centred cubic, face-centred cubic and hexagonal.

In an elementary cell of a body-centred cubic lattice the atoms are situated at the corners of a cube and at its centre (Fig. 2a). Such a lattice has one characteristic dimension called the lattice parameter—the length of the edge of the cube, a.

The atoms in a face-centred cubic lattice are located at the corners of a cube and at the centre of the faces (Fig. 2b). This type of lattice is defined by one parameter, the length of the side of the cube, a.

The elementary cell of the hexagonal lattice comprises a right six-sided prism with base of side a and height c, where a and a/c are the two parameters which characterize this type of lattice. The atoms in this elementary cell are positioned at every corner of

the prism, and in addition there are three atoms at the centres of the three opposite triangular prisms which are formed by the three diagonal planes which pass through the axis of the hexagonal prism (Fig. 2c).

The linear lattice parameters a are of the order of 2–5 Å (1 Å = 10^{-8} cm). For example for γ iron (see below) $a = 3{\cdot}56$ Å, for α iron the parameter $a = 2{\cdot}86$ Å, for copper $a = 3{\cdot}61$ Å, for aluminium $a = 4{\cdot}04$ Å. If we consider that atoms have a linear dimension (a diameter) of the same order, we can see that the atoms must occupy very nearly the whole of the volume of the elementary cell. Atoms in a lattice are sometimes depicted, therefore, as closely

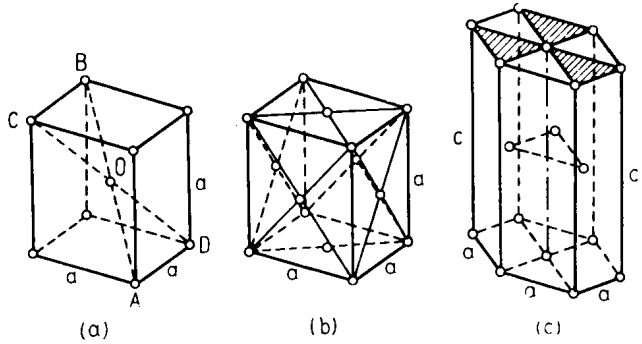

FIG. 2.

packed spheres. The degree to which the lattice as a whole is filled and the intensity of the inter-atomic forces can be characterized by a coordination number—the number of atoms at an equal distance from a datum: the greater the coordination number, the smaller is the space in the lattice not occupied by the atoms.

The number of atoms which belong to an elementary cell is called the basis of this cell.

The point is that in a body-centred lattice, for example (Fig. 2a), atoms A and D do not belong solely to the cell shown, since they are at the same time essential elements of neighbouring cells. In order to determine the number of atoms per unit cell, we give all the atoms identical small displacements, parallel, for example, to the diagonal AB (or in general, in a direction not lying in a boundary plane of the cell). Then all the atoms except A and O move beyond the boundaries of the cell. This shows that the basis of a body-

centred cubic structure is 2. The basis of a face-centred cubic lattice is 4.

The forces of interaction of the atoms in the lattice are of an involved nature, the basis of which is considered to be the existence of electrostatic forces between the atoms. Electrons circuit the nucleus of the atom in several orbits, the number of electrons being equal to the number of the element in Mendeleev's periodic table i.e. to the positive charge of the nucleus, so that the atom as a whole is electrically neutral. Chemical combinations take place due to the electrons in the outer orbit being shared. These shared electrons form a so-called electron gas. On account of these shared electrons, the atoms become positively charged ions, which are surrounded by an electron gas, which gives rise to forces between the atoms (ions) in a crystal lattice. The existence of this electron gas explains, in particular, the high electrical conductivity of metals.

In a crystal lattice it is possible to draw a number of planes which contain a certain number of atoms per unit area. From the point of view of the strength of the material, the planes passing through the greatest number of atoms are of most importance (for example, the plane *ABCD* in Fig. 2a). It is along these planes—called slip-planes or gliding planes—that shearing can most easily take place when a force is applied to the body. Tearing of the particles takes place along these lines during a brittle type of failure.

The geometrically regular arrangement of atoms in a crystal lattice gives rise to anisotropy of the monocrystal, i.e. a difference in its properties (electrical conductivity, thermal conductivity, optical properties and mechanical properties) in different directions. For example, for a monocrystal of copper the fracture load per unit area in tension varies in different directions from 12–35 kg/mm^2, i.e. by three times, and the extension at failure referred to the initial length, varies from 10–50 per cent, i.e. by five times. Anisotropy of a crystalline body is, therefore, an important property from the point of view of the mechanical characteristics of a material.

In real crystals there are always disturbances in the regularity of the structure: distortion of the lattices, curvature of the slip planes, the presence of vacancies—spaces unoccupied by atoms. The presence of these defects, such as vacancy in a monocrystal, can be detected with the aid of an electron microscope. Without going into the causes of such defects, we might note that they do explain

some mechanical effects. For example the presence of vacancies, "holes", facilitates plastic deformation which is associated with the sliding of one row (plane) of atoms over another.

The metals we are normally concerned with are polycrystalline bodies made from ingots which are formed by the hardening of the molten metal in cooling and which are then subjected to heat treatment. All such bodies have a granular structure, i.e. they are made up of a number of grains of irregular shape, each of which can, as a first approximation, be considered as a monocrystal, and the rela-

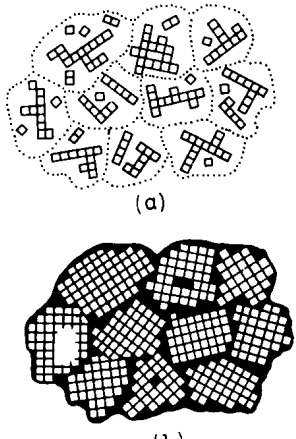

FIG. 3.

tive orientation of the crystals of neighbouring grains can be considered as random and dependent mainly on the direction of growth of the crystals from different centres of crystallization (Fig. 3)

In order to investigate the dimensions and disposition of the grains in a metal we make use of methods of macrostructural and microstructural analysis. The macrostructure of a metal can be determined by visual examination without magnification or with only slight magnification of the surface of the specimen, which should be previously cleaned, emery-papered, polished and etched with special reagents. Occasionally the macrostructure can be determined from the type of fracture of a specimen. In order to study the microstructure we normally proceed as follows. We cut out a specimen with a flat surface, which we carefully grind, polish and then etch

with special reagents. Under microscopic examination we can then see clearly the boundaries of each grain. The production of photographs of this polished surface is called photo-micrography. If this method is applied to a specimen previously subjected to plastic deformation it is possible to establish the directions of the slip planes, i.e. to determine the relative orientation of the crystal lattices in different grains. In recent years, isotopes have been used in the study of the structure of polished sections. For example, steel is a solid solution of carbon (less than 2 per cent) in iron, and during the formation of the grains, compounds of carbon accumulate at the boundaries of the grains. If the carbon is given radio-active properties it is possible to establish the positions of these accumulations. The picture of the distribution of grains obtained in this way is identical to that observed under the microscope after the surface of the specimen has been pickled.

Depending on the rate of cooling and the heat treatment, the grains of the same metal can have different dimensions—which has a bearing on the mechanical properties of the metal. In fine-grained steel, the representative mean dimension of one grain is 0·01–0·1 mm; in coarse-grained steel, it is up to 10 mm. Normally metals with a fine-grained structure are the strongest.

For every metal, for a given rate of solidifying and for a given heat-treatment, the dimensions of the grains are on an average the same. Thus, in addition to the parameters of the crystal lattice, each metal has a further characteristic dimension—the mean grain size d, which corresponds to a definite type of heat treatment.

The magnitude of the lattice parameter in some metals can also alter suddenly depending on the temperature. It has been found that during the cooling process of a hardened metal so-called allotropic transformations can take place which are associated with the re-arrangement of the lattice structure and with the re-grouping of atoms. Each type of lattice and each value of the lattice parameter correspond to a particular phase of the metal. For example, iron after solidifying at a temperature $T = 1535\,^{\circ}\mathrm{C}$ goes into the $\alpha(\delta)$-phase, characterized by a body-centred cubic lattice with parameter $a = 2{\cdot}93$ Å. After a certain time during the cooling process (time is represented by the abscissal in Fig. 4) at a temperature of 1390 °C, iron undergoes an allotropic transformation and changes to the γ-phase with a face-centred cubic structure having parameter $a = 3{\cdot}56$ Å. At a temperature of 910 °C this phase changes to the

$\alpha(\beta)$-phase with a body-centred cubic structure (and with $a = 2{\cdot}90$ Å). Finally, at 768 °C change to the α-phase with a body-centred cubic structure occurs ($a = 2{\cdot}86$ °Å). The horizontal plateaux in Fig. 4 correspond to the time required for the atoms to re-arrange themselves during the allotropic transformations which take place at constant temperature.

The different phases of a given metal have rather different physical properties. For example $\alpha(\beta)$-phase iron is non-magnetic whereas the α-phase does possess the well known magnetic properties of iron.

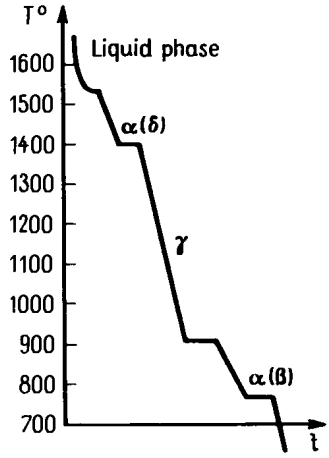

FIG. 4.

The regrouping of atoms during an allotropic transformation leads to a noticeable change in volume. For instance, in going from the α to the β-phase, tin changes its volume by 26 per cent. These changes in volume are associated with the occurrence of considerable internal stresses which frequently lead to the formation of cracks. For example, tin, if it is kept for a long time at a temperature of about -20 °C, starts to break up from spontaneous cracking. This phenomenon is known by the name of "tin pest".

The above-mentioned specific linear dimensions of the structure of a metal—the lattice parameter a, and the mean grain size d enable us to make the approximation of considering a metal as a continuous medium instead of a body made up of small discrete particles, and apply to it infinitesimal calculus. However, we

need to establish one further specific linear dimension — the orientation parameter of the grains.

As has already been pointed out, the grains in a metal, for a given heat-treatment, have approximately the same specific linear dimension d (on an average). But the orientation of the grains, generally speaking, is arbitrary and random, providing there are no special forms of treatment which could to some extent orientate the grains.

The orientation of a grain, considered as a first approximation as a monocrystal, can be characterized by the position in space of a

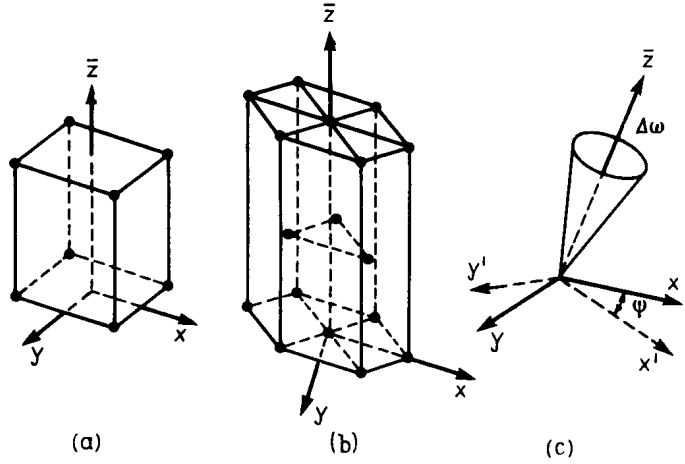

FIG. 5.

vector which is related in a definite way with some characteristic direction in the crystal lattice and with the rotation of the grain about this vector.

The three parameters (three direction cosines of the vector, related by an expression of the form $\alpha^2 + \beta^2 + \gamma^2 = 1$, and the angle of rotation) determine completely the orientation of the grain. For example, for a metal with a cubic crystal lattice (body-centred or face-centred) we can drawn the vector z along one of the central axes of the cube, and the axes of x and y, perpendicular to the direction of the vector z can be connected to the crystal lattice in the manner indicated in Fig. 5a. For a metal with a hexagonal structure the vector z would be collinear whit the central axis of the six-sided prism and the x and y-axes could be in the plane of the

lower base of the prism (Fig. 5b). We will take the described orientation of a grain as our datum and compare the orientation of other grains. The orientation of another grain can differ, first of all, by an angle of rotation, i.e. its x' and y' axes could be rotated about the direction of z through and angle ψ (Fig. 5c), and secondly, its orientation vector z' could be inclined relative to the vector z.

We shall attempt to determine how many identically orientated grains there are along any given line, i.e. how large is the distance between identically orientated grains.

Strictly speaking, in view of the completely arbitrary orientation which we have assumed to take place in the process of crystallization, we can say that in any finite volume of metal there are not, in general, two grains absolutely identically orientated. The probability of such an event, speaking in the language of the theory of probability, is zero, and the required mean distance between identically orientated grains is infinitely large. However, we must bear in mind the fact that every practical calculation is made, not with absolute accuracy, but with the admission of some error. For example, modern quantum mechanics, in investigating the atom, does not enable us to determine simultaneously and exactly both the position of a particle (an electron) and its velocity.

In normal engineering calculations in the strength of materials, an error of 3–5 per cent is admissible. There is no point, therefore, in the above problem of considering as identically orientated only those grains whose vectors z and z' are exactly parallel and whose axes x and x' are parallel ($\psi = 0$). We shall consider grains to be identically orientated if their deviation in ψ from the given angle ψ does not exceed some quantity $\Delta\psi$, and if the inclination of their orientation vector z' to the vector z is within the limits of a solid angle $\Delta\omega$ (Fig. 5c). The quantities $\Delta\psi$ and $\Delta\omega$, which we shall call the permitted deviations (or tolerances) in ψ and ω, are chosen according to the accuracy of all the subsequent calculations and of the physical laws which are to be applied.

We call the mean distance l between grains identically orientated in the above sense, the parameter of grain orientation. The exact solution to the problem of finding the orientation parameter is within the province of the theory of probability, which deals with the same kind of random processes as our present problem. But it is possible to solve this problem to a sufficient degree of accuracy by elementary methods.

We note, first of all, that the total range of variation of the quantity ψ is not 2π as it might appear at first. In the case of a cubic lattice, for example, two unit cells for which ψ differs by $\pi/2$ must be considered identically orientated in view of the symmetry of the arrangement of their atoms. Therefore, in general, the range of variation of ψ is $2\pi k_\psi$:

$$0 \leqq \psi \leqq 2\pi k_\psi.$$

For a cubic lattice $k_\psi = \frac{1}{4}$, for a hexagonal lattice $k_\psi = \frac{1}{3}$. In the same way, the range of variation of ω is $4\pi k_\omega$:

$$0 \leqq \omega \leqq 4\pi k_\omega.$$

For example, for a hexagonal lattice, a change in direction of the vector z by π gives coincidence. Therefore for such a lattice $k_\omega = \frac{1}{2}$.

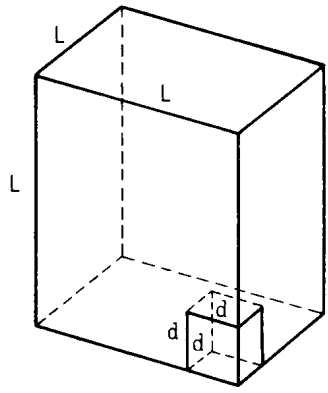

FIG. 6.

Let us consider a cube, the length of whose edge L, is considerably greater than the dimension l, which we require to find (Fig. 6). If we consider the grains as closely packed cubes with edge d (d is the mean diameter of a grain), then the number of grains in the large cube is $N = L^3/d^3$.

The orientation of the N different grains corresponds to the different values of ψ and ω over their whole range of variation. Amongst them there will be N_ω grains which differ in the orientation of their vector z from some chosen grain within the limits of $\Delta\omega$. With a normally large number of grains N, orientated at

random, the number N_ω comprises the same proportion of N as $\Delta\omega$ does of the total range of variation:

$$N_\omega = N\frac{\Delta\omega}{4\pi k_\omega}.$$

The orientations of these N_ω grains correspond to different values of ψ within the total range of variation. Consequently, by analogy with the above, there are $N_{\psi\omega}$ grains amongst them, which differ from some chosen grain by a deviation in ψ not greater than $\Delta\psi$ and therefore

$$N_{\psi\omega} = N_\omega\frac{\Delta\psi}{2\pi k_\psi}.$$

Substituting the value of N_ω, we get that:

$$N_{\psi\omega} = N\frac{\Delta\psi\,\Delta\omega}{8\pi^2 k_\psi k_\omega}.$$

All these $N_{\psi\omega}$ grains must be considered identically orientated, if $\Delta\psi$ and $\Delta\omega$ are the permitted deviations.

On the other hand, if l is the required mean distance between identically orientated grains, then

$$N_{\psi\omega} = \frac{L^3}{l^3} = \frac{L^3}{d^3}\frac{d^3}{l^3} = N\frac{d^3}{l^3}.$$

Comparing the two expressions for $N_{\psi\omega}$, we find that

$$\frac{d^3}{l^3} = \frac{\Delta\psi\,\Delta\omega}{8\pi^2 k_\psi k_\omega},$$

from which

$$l = 2d\sqrt[3]{\left(\frac{\pi^2 k_\psi k_\omega}{\Delta\psi\,\Delta\omega}\right)}.$$

This formula gives the orientation parameter l, if the permitted deviations $\Delta\psi$ and $\Delta\omega$ are given, and providing the coefficients k_ψ and k_ω for the type of lattice are known.

Usually there is no point in giving different permitted deviations for $\Delta\psi$ and for the angle of inclination of the vector z. Bearing in mind that the solid angle $\Delta\omega$ is a part of the area of the surface of a sphere of unit radius with centre at the origin of coordinates delineated by a cone (Fig. 5b), we can put $\Delta\omega = (\Delta\psi)^2$. Then the formula for the orientation parameter l becomes

$$l = \frac{2d}{\Delta\psi}\sqrt[3]{(\pi^2 k_\psi k_\omega)}.$$

It can be seen that the smaller the permitted deviation $\Delta\psi$, i.e. the greater the accuracy of the calculations, the greater is the orientation parameter l. Let us consider a permitted deviation of 2 per cent of 2π, which corresponds to determining the orientation to an accuracy of ± 7 degrees or a value of $\Delta\psi = 0{\cdot}2$. For a hexagonal lattice we have that $k_\psi = \frac{1}{3}$, $k_\omega = \frac{1}{2}$ and consequently,

$$l = \frac{2d}{0{\cdot}2}\sqrt[3]{\left(\frac{\pi^2}{6}\right)} \approx 12d.$$

For a cubic lattice $k_\psi = \frac{1}{4}$, $k_\omega = \frac{1}{4}$ and we find that

$$l = \frac{2d}{0{\cdot}2}\sqrt[3]{\left(\frac{\pi^2}{16}\right)} \approx 8{\cdot}5d.$$

In the first case one in 1700 grains approximately have the given orientation (with a permitted deviation $\Delta\psi = 0{\cdot}2$) and in the second case, one in 650 grains.

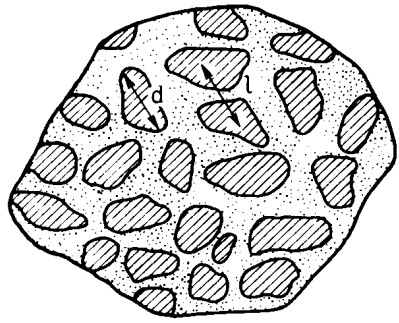

FIG. 7.

Some materials used in engineering practice and met with in nature are non-homogeneous. An example is concrete. It can consist of mortar with the dimensions of the grains of sand from 0·1 mm–1 mm; or it can be coarse aggregate concrete. Since the grains of sand are usually anisotropic the former type of concrete has an orientation parameter $l \approx 10\,d$—the mean distance between identically orientated sand particles (with a permitted deviation $\Delta\psi = 0{\cdot}2$). In coarse aggregate concrete the mass of cement and sand matrix contains larger particles (gravel, crushed rock) and the characteristic linear dimension of the particles (from 10–50 mm) is of the same order as the distance between their centres (Fig. 7).

Since these particles normally have a polycrystalline structure the orientation parameter in this case can be taken as $l \approx d$.

2. Internal Interaction of Particles in a Body

In order to investigate the internal interaction between different parts of a body the strength of materials and the theory of elasticity make use of the method of sections, which means that the body is imagined to be cut into two parts, one part being discarded and its action on the remaining part (i.e. the internal forces holding together particles on either side of the section) is replaced by forces distributed over the surface of the section. In this way the forces

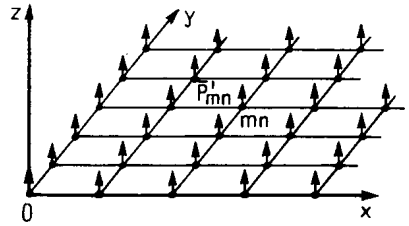

Fig. 8.

of internal interaction are treated as external forces and operated upon according to the normal rules of theoretical mechanics.

Let us consider first of all a single grain with specific linear dimension d, and for simplicity we shall assume that the material of the grain has a body centred cubic lattice with parameter a. In order to investigate the internal forces of interaction within the grain we imagine it to be cut by a plane parallel to the face of the crystal lattice and discard the upper part of the grain. We shall take the axes Ox and Oy in the plane of the section (or more accurately, in the plane of the upper layer of atoms of the remaining lower part of the grain) and directed along the edges of the cubic lattice (Fig. 8); we shall take the axis Oz perpendicular to Ox and Oy in the direction of the discarded part. Each atom in the plane (xy) can be given a double index mn, corresponding to the coordinates of the atom

$$x' = ma, \quad y' = na, \quad z' = 0$$

in the chosen system of coordinates. Alternatively the position of an atom mn can be given a by vector

$$\boldsymbol{r}_{mn} = x'\boldsymbol{i} + y'\boldsymbol{j} + z'\boldsymbol{k},$$

where $\boldsymbol{i}, \boldsymbol{j}, \boldsymbol{k}$ are unit vectors directed along the axes x, y, z.

Let us suppose that the atom is in a natural state, i.e. in such a state that in the absence of external forces and other external effects (for example, non-uniform heating) the lattice in the grain is completely regular and undistorted. In actual fact there will always be some distortion of the lattice. For example, close to the surface of the grain there is the effect of forces of the surface tension type, but these distortions will not, apparently, penetrate further into the grain than a few lattice parameters. In such a natural state, in view of the symmetry of the arrangement of the atoms, the forces $\boldsymbol{P}'_{mn}$ acting on the various atoms mn situated in the plane (xy) are the same in magnitude and act in a direction perpendicular to the plane of the section, i.e.

$$\boldsymbol{P}'_{mn} = \text{const.} \quad (m, n = 1, 2, 3, \ldots).$$

If there is some external effect (heating, external force, etc.), which penetrates into the grain, all the vectors $\boldsymbol{P}'_{mn}$ change in magnitude and direction and become the vectors $\boldsymbol{P}''_{mn}$. Each atom moves from its initial position and its displacement is characterized by a displacement vector $\boldsymbol{u}_{mn}$, with components u_{mn}, v_{mn}, w_{mn} along the axes x, y, z:

$$\boldsymbol{u}_{mn} = u_{mn}\boldsymbol{i} + v_{mn}\boldsymbol{j} + w_{mn}\boldsymbol{k},$$

so that the new coordinates of the atom mn become

$$x'' = x' + u_{mn}, \quad y'' = y' + v_{mn}, \quad z'' = z' + w_{mn}.$$

In future we shall be very much concerned with these distortions of the vectors $\boldsymbol{P}'_{mn}$ and the displacements associated with external effects.

The distortion of the coordinates of the atoms and of the vectors $\boldsymbol{P}'_{mn}$ is different for different atoms. We will consider these distortions regular if for a regular change in the suffixes of the atoms $(m \to m + 1 \to m + 2 \to \cdots \to m + M;\ n \to n + 1 \to n + 2 \to \cdots \to n + N)$ the distortions

$$\boldsymbol{P}_{mn} = \boldsymbol{P}''_{mn} - \boldsymbol{P}'_{mn},$$
$$\boldsymbol{u}_{mn} = \boldsymbol{r}''_{mn} - \boldsymbol{r}'_{mn}$$

vary monotonically for sufficiently large M and N (this must be the case over some interval). The distortions for two neighbouring atoms will differ only slightly , so that the quantities

$$\frac{\boldsymbol{P}_{m+1,\,n} - \boldsymbol{P}_{mn}}{|\boldsymbol{P}_{mn}|}, \quad \frac{\boldsymbol{P}_{m,\,n+1} - \boldsymbol{P}_{mn}}{|\boldsymbol{P}_{mn}|}, \quad \frac{\boldsymbol{u}_{m+1,\,n} - \boldsymbol{u}_{mn}}{|\boldsymbol{u}_{mn}|}$$

will be small compared to unity.

We can treat only conventionally the atoms as points, since with their electron envelope they occupy practically the whole of the crystal cell; for this reason the treatment of the inter-atomic forces as concentrated forces applied at the nodes of the crystal lattice

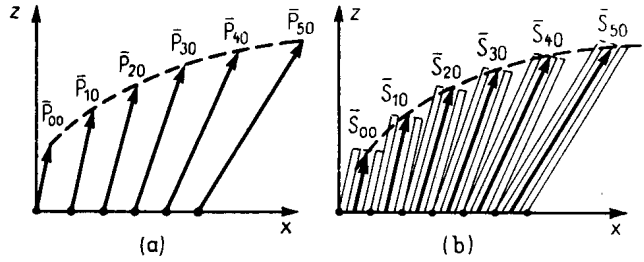

FIG. 9.

is a very relative one. Therefore, we can also consider the force of interaction as uniformly distributed over the whole face of the unit cell to which atom mn belongs. Therefore, as a characteristic of the force acting on the atom mn, having coordinates x, y, z (we are considering now only additional forces which arise from some external effect, i.e. the changes $\boldsymbol{P}_{mn} = \boldsymbol{P}''_{mn} - \boldsymbol{P}'_{mn}$), we can introduce the vector

$$\boldsymbol{S}_{(mn)} = \frac{\boldsymbol{P}_{mn}}{a^2},$$

which is called the stress vector at the point (x, y, z) in the plane (xy). In the same way we shall assume that the displacement vector $\boldsymbol{u}_{mn}$ refers to all points on the face of the cell, and that all points of every face of a unit cell of the crystal lattice undergo the same displacement.

In this way we have replaced the discrete distribution of forces of interaction by a step-continuous distribution. Figures 9a and b show the corresponding curves (distribution curves) along one of

the coordinate lines $y = \text{const}$. Similar curves can also be drawn from any coordinate line $x = \text{const}$.

This replacement of concentrated forces by stresses uniformly distributed over each elementary face is, of course, a convention. The exact way in which inter-atomic forces are distributed is not known. Taking as a basic assumption, therefore, the regularity of the above changes in the vectors our next step is to characterize the forces of internal interaction by a stress vector $\boldsymbol{S}$, which is continuous and differentiable with respect to the coordinates x, y, i.e. we shall replace the step curve of stress distribution (Fig. 9b) by a curve with a continuous distribution (Fig. 10).

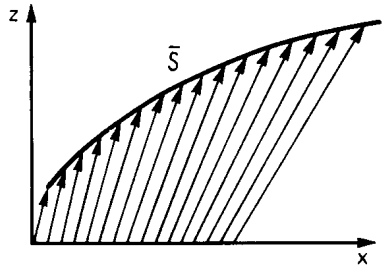

FIG. 10.

In the same way we shall consider the displacement vector $\boldsymbol{u}$ as a continuous and differentiable function of the coordinates x, y.

The change from a discrete to a continuous distribution means that, for the characteristics of strength and deformation under the action of external forces, only the mean values of the stresses and displacements over the area of the elementary cell are important. Mathematically this change corresponds to a replacement of finite difference ratios by differential relations:

$$\frac{\boldsymbol{P}_{m+1,\,n} - \boldsymbol{P}_{m,\,n}}{a^3} \to \frac{\boldsymbol{S}_{(m+1,\,n)} - \boldsymbol{S}_{(m,\,n)}}{a} \to \frac{\partial \boldsymbol{S}}{\partial x},$$

$$\frac{\boldsymbol{P}_{m,\,n+1} - \boldsymbol{P}_{m,\,n}}{a^3} \to \frac{\boldsymbol{S}_{(m,\,n+1)} - \boldsymbol{S}_{(m,\,n)}}{a} \to \frac{\partial \boldsymbol{S}}{\partial y},$$

$$\frac{\boldsymbol{u}_{m+1,\,n} - \boldsymbol{u}_{m,\,n}}{a} \to \frac{\boldsymbol{u}_{(m+1,\,n)} - \boldsymbol{u}_{(m,\,n)}}{a} \to \frac{\partial \boldsymbol{u}}{\partial x},$$

$$\frac{\boldsymbol{u}_{m,\,n+1} - \boldsymbol{u}_{m,\,n}}{a} \to \frac{\boldsymbol{u}_{(m,\,n+1)} - \boldsymbol{u}_{(m,\,n)}}{a} \to \frac{\partial \boldsymbol{u}}{\partial y}.$$

Instead of the area a^2 of the face of the elementary crystal cell we can now take any small element of area $dx\,dy$ on which there acts the force vector $\boldsymbol{S}\,dx\,dy$.

We shall now modify our notation for the stresses. We have been considering so far a section which we took as the plane (xy). Let us give the stress acting on the section the suffix z, i.e. let us define it as $\boldsymbol{S}_z$. This indicates that we are considering a stress on an element of a surface passing through the point (x, y, z) and perpendicular to the z-axis. If we had initially taken sections in planes parallel to the two other faces of the crystal cell, i.e. in the planes (xz) and

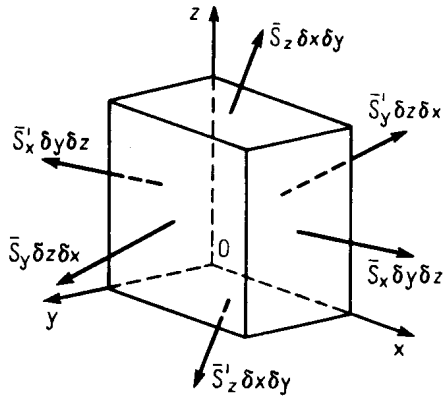

FIG. 11.

(yz), then the stresses acting on elements of area in these planes containing the point (x, y, z) would, in general, differ from $\boldsymbol{S}_z$. We shall denote these stresses as $\boldsymbol{S}_y$ and $\boldsymbol{S}_x$ respectively. The three stress vectors $\boldsymbol{S}_x$, $\boldsymbol{S}_y$, $\boldsymbol{S}_z$ acting on three mutually perpendicular surfaces containing the point under consideration are called a stress tensor. Thus, in contrast to a vector, which is defined by three scalar quantities (components), a stress tensor is defined by three vectors.

The stresses $\boldsymbol{S}_x$, $\boldsymbol{S}_y$, $\boldsymbol{S}_z$ are continuous in their corresponding planes with respect to the coordinates y, z; z, x; x, y respectively. It can easily be shown that each of them is also continuous with respect to the third coordinate. In order to do so, let us consider an elementary parallelepiped with edges δx, δy, δz parallel to the edges of a cube of the crystal lattice (Fig. 11). The resultant forces acting

on each face of the parallelepiped are expressed in the form of vectors applied at the centre of each face.

If body forces $\boldsymbol{F}(x, y, z)$ distributed throughout the whole volume of the body are applied (for example centrifugal forces, gravitational forces, etc.) then the condition of equilibrium of the elementary parallelepiped is of the form

$$(\boldsymbol{S} + \boldsymbol{S}'_x)\,\delta y\,\delta z + (\boldsymbol{S}_y + \boldsymbol{S}'_y)\,\delta z\,\delta x + (\boldsymbol{S}_z + \boldsymbol{S}'_z)\,\delta x\,\delta y + \boldsymbol{F}\delta x\,\delta y\,\delta z = 0$$

Decreasing infinitely the length of each side in turn, we get that as $\delta x \to 0$ $\boldsymbol{S}'_x \to -\boldsymbol{S}_x$; as $\delta_y \to 0$ $\boldsymbol{S}'_y \to -\boldsymbol{S}_y$; as $\delta_z \to 0$ $\boldsymbol{S}'_z \to -\boldsymbol{S}_z$. This proves the continuity of each of the vectors $\boldsymbol{S}_x$, $\boldsymbol{S}_y$, $\boldsymbol{S}_z$ with respect to all coordinates. The limiting equality of the type $\boldsymbol{S}'_x = -\boldsymbol{S}_x$ is obvious. It simply shows that the forces applied by one

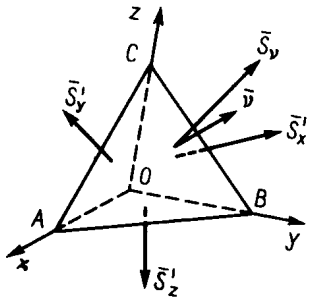

FIG. 12.

side of the body on the other are equal in magnitude and opposite in direction to the forces applied by this other side on the first.

Let us now imagine a cut to be made in the vicinity of the point O (which for convenience we shall take as the origin of coordinates) at an inclined angle to all the coordinate surfaces. In addition, we will make cuts along the coordinate planes, in this way forming the pyramid $OABC$ (Fig. 12). The orientation of the surface ABC is characterized by the unit vector

$$\boldsymbol{\nu} = \boldsymbol{i}l + \boldsymbol{j}m + \boldsymbol{k}n,$$

where

$$l = \cos(x, \nu), \quad m = \cos(y, \nu), \quad n = \cos(z, \nu).$$

If the area of the triangle ABC is f, then

$$\text{area of triangle } BOC = fl,$$
$$\text{area of triangle } AOC = fm,$$
$$\text{area of triangle } AOB = fn.$$

The equilibrium equation for the pyramid $OABC$ if body forces $\boldsymbol{F}$ act is of the form

$$S_\nu f + S_x' fl + S_y' fm + S_z' fn + Ff\frac{h}{3} = 0,$$

where S_ν denotes the stress on the surface ABC with normal $\boldsymbol{\nu}$, and h is the height of the perpendicular from the point O to the face ABC. Dividing by f and letting $h \to 0$, i.e. letting the inclined plane move to one passing through the point O characterized by normal $\boldsymbol{\nu}$, we get that

$$S_\nu = -S_x' l - S_y' m - S_z' n$$

or

$$S_\nu = S_x l + S_y m + S_z n. \tag{1.1}$$

(In Fig. 12 the pyramid is formed by discarding the parts situated in the directions of the negative semi-axes Ox, Oy, Oz. On the areas with external normals along the axes Ox, Oy, Oz, the stresses, as was pointed out above, are of opposite sign.)

Formula (1.1), which is one of the fundamental equations in the strength of materials, enables us to determine the stress on any surface containing a given point if the stresses on areas perpendicular to the coordinate axes are known. In other words, if S_x, S_y, S_z are known functions of the coordinates x, y, z, the stress tensor (S_x, S_y, S_z) defines completely the state of stress of a grain.

If the area f and the normal $\boldsymbol{\nu}$ refer to a smooth surface intersecting a grain, then movement along this surface will be accompanied by a continuous change in the direction of the normal $\boldsymbol{\nu}$ and a continuous change in the coordinates x, y, z. Since, as has already been proved, the vectors S_x, S_y, S_z vary continuously, so also will the vector S_ν. We must, however, remember that physically this continuity only applies within the limits of dimensions not exceeding the lattice parameter.

The above discussions are valid for a monocrystal and for an individual grain. In a body of considerable size with a large number of irregularly orientated grains the stress vectors S_x (x, y, z), S_y (x, y, z), S_z (x, y, z) are continuous only within the limits of each grain. On the boundaries of the grains these vectors are in general subjected to discontinuities, since the orientation of the crystal lattices of neighbouring grains is different.

However, if we take into account the grain orientation parameter l mentioned in § 1, we can represent the forces of internal interaction in a polycrystalline body by a continuous vector S_ν in the same way

as for a monocrystal. From this point of view a polycrystalline body is assumed to be made up of homogeneous complexes of grains, l being the specific dimension of each complex. This means that a small cube of polycrystalline material with side l comprises in effect an elementary homogeneous cubic lattice, and for a number of these lattices together all the arguments which referred to a monocrystal are valid. The essential difference is that inside one grain all the conclusions concerning continuity are valid for extremely small areas which are greater than the lattice parameter a, whereas in a polycrystalline body there exists continuity over very small areas the minimum dimension of which exceeds the orientation parameter l. Similar remarks would apply to non-homogeneous bodies such as concrete. Here the orientation parameter, as was mentioned above, is of the order of the dimensions of the aggregate.

3. Investigation of the State of Stress at a Point

Making use of the results of the previous section we shall consider a solid body as a material continuum, i.e. as a solid body with a continuous distribution of material.

If we imagine such a continuum to be cut by some plane R (Fig. 13) and if we discard one part A, then the effect of the discarded part on the remaining part B must be replaced by continuously distributed forces. On a small area ΔF in the plane of the section with normal $\boldsymbol{\nu}$ and containing some point N there will act a force $\Delta \boldsymbol{P}_\nu$ which is the resultant of the forces distributed over this small area. If we refer this force to the area ΔF (i.e. replace the actual distribution of internal forces by a uniform distribution), then in the limit, as the boundary of the area ΔF reduces to the point N, we get the quantity

$$\boldsymbol{S}_\nu = \lim_{\Delta F \to 0} \frac{\Delta \boldsymbol{P}_\nu}{\Delta F},$$

which is called the stress at the point (or the actual stress) acting on a small area with normal $\boldsymbol{\nu}$†. If we project this stress vector onto the normal $\boldsymbol{\nu}$, we obtain the vector of the normal stress σ_ν. The projection of the vector $\boldsymbol{S}_\nu$ on the plane of the area ΔF gives the

† In tending to the limit the direction of the vector $\boldsymbol{S}_\nu$ can differ slightly from the direction of the vector $\Delta \boldsymbol{P}_\nu$.

vector of the shearing stress τ_ν. The suffix "ν" in all cases indicates the orientation of the area on which the particular stress acts. From the law of action and reaction it follows that reversing the direction of ν (which corresponds to discarding not the part A, but the part B in Fig. 13) reverses the direction of the vector S_ν, so that $S_{-\nu} = -S_\nu$, from which it follows that $\sigma_\nu = -\sigma_{-\nu}$, $\tau_\nu = -\tau_\nu$.

Considering other elementary areas containing the point N, i.e., drawing other sections through this point, we can obtain an infinite number of values of S_ν which, in general, are different. This infinite number of values of S_ν characterizes the state of stress (or the stress state) at the point N. However, as has already been pointed out when we were considering formula (1.1), to describe

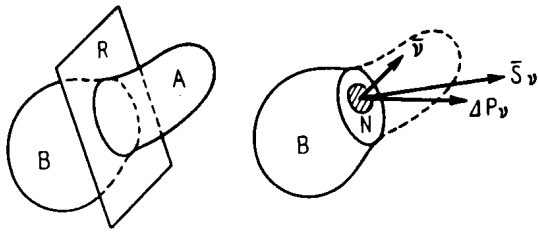

FIG. 13.

the stress state at a given point there is no need to know the values of the stress vectors on all the infinite number of areas containing this point; if we know the stress vectors S_x, S_y, S_z, on three orthogonal areas, which we can take as parts of the coordinate planes (yz), (zx), (xy), then the stress on any area containing this point can be found from formula (1.1). The vectors S_x, S_y, S_z, as a has already been pointed out, make up the stress tensor (S). Each of them can be resolved into components along the coordinate axes:

$$\left.\begin{aligned} S_x &= \sigma_{xx}\,i + \sigma_{xy}\,j + \sigma_{xz}\,k, \\ S_y &= \sigma_{yx}\,i + \sigma_{yy}\,j + \sigma_{yz}\,k, \\ S_z &= \sigma_{zx}\,i + \sigma_{zy}\,j + \sigma_{zz}\,k. \end{aligned}\right\} \qquad (1.1')$$

The nine scalar quantities $\sigma_{xx}, \sigma_{yy}, \ldots, \sigma_{xy}$ are called components of the stress tensor. The first letter in the suffix indicates the direction of the normal to the area on which the stress acts, and the second letter corresponds to the axis on which the stress vector is

projected.† For example, σ_{zy} represents the magnitude of the projection on the axis Oy of the stress vector acting on an area with normal parallel to the axis Oz. Thus the stress state at a point is defined completely by the nine quantities σ_{ij}, the components of the stress tensor, where the values of $i, j = 1, 2, 3$ correspond to the directions of the axes Ox, Oy, Oz.

If the values of the vectors $\boldsymbol{S}_x, \boldsymbol{S}_y, \boldsymbol{S}_z$ are known, i.e., if the values of the nine quantities σ_{ij} are known at all point in the body, in other words, if the vectors $\boldsymbol{S}_x, \boldsymbol{S}_y, \boldsymbol{S}_z$ are known functions of the coordinates x, y, z and of time t, then the stress state of the body is fully defined.

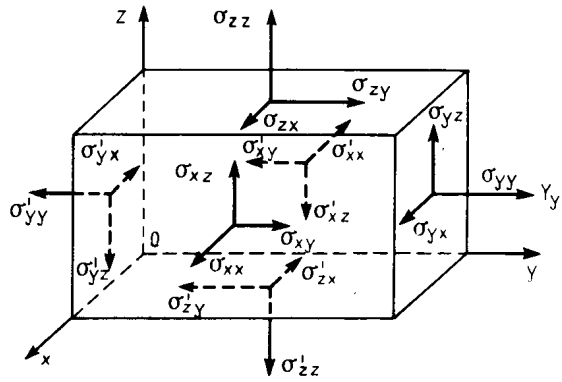

FIG. 14.

There are certain relations between the nine components of the stress tensor (S). In order to find them let us draw three pairs of planes, parallel to the coordinate planes, at distances apart of $\delta x, \delta y, \delta z$, so that the point under consideration lies within the parallelepiped so formed. If we imagine this parallelepiped removed from the body and replace the effect of the discarded part by resultant internal forces applied at the centre of each face and then resolve each resultant along the coordinate axes, we obtain the picture shown in Fig. 14, in which the forces acting on each face are given in the form of components of the stress tensor. For example, the force in the direction of the x-axis acting on the

† Sometimes, in order to emphasize the difference, we will write $\tau_{xy}, \tau_{xz}, \ldots, \tau_{yz}$ for shearing stresses instead of $\sigma_{xy}, \sigma_{xz}, \ldots, \sigma_{zy}$.

right-hand face of the parallelepiped is $\sigma_{yx}\,\delta x\,\delta z$. The values of these forces on the faces of the parallelepiped, together with the mass forces, give the stresses at every point within the parallelepiped.

Since the parallelepiped is in equilibrium, the sum of the moments of all forces about each of the coordinate axes must be zero. Taking mass forces $F(x, y, z)$ into account with components X, Y, Z, along the axes, the condition that the moment of all the forces about the axis Ox vanishes can be written in the form

$$(\sigma_{yy} - \sigma'_{yy})\frac{\delta z}{2}\delta x\,\delta z - \sigma_{yz}\,\delta y\delta x\,\delta z + \sigma_{zy}\,\delta z\,\delta x\,\delta y$$
$$- (\sigma_{zz} - \sigma'_{zz})\frac{\delta y}{2}\delta x\,\delta y + (\sigma_{xy} - \sigma'_{xy})\frac{\delta z}{2}\delta y\,\delta z$$
$$- (\sigma_{xz} - \sigma'_{xz})\frac{\delta y}{2}\delta y\,\delta z + Y\frac{\delta z}{2}\delta x\,\delta y\,\delta z - Z\frac{\delta y}{2}\delta x\delta y\delta z = 0.$$

Letting the dimensions of the edges of the parallelepiped tend to zero, i.e., letting $\delta x \to 0$, $\delta y \to 0$, $\delta z \to 0$, we arrive at the limiting equalities $\sigma_{yy} = \sigma'_{yy}, \sigma_{zz} = \sigma'_{zz}, \sigma_{xy} = \sigma'_{xy}, \sigma_{xz} = \sigma'_{xz}$. Dividing then by the product $\delta x\,\delta y\,\delta z$, we get that $\sigma_{yz} = \sigma_{zy}$. Equating to zero the sum of the moments of the forces about the axes Oy and Oz, we obtain the final set of three equalities $(i \neq j)$:

$$\sigma_{ij} = \sigma_{ji}.$$

These equalities express the law of complementary shearing stresses which states that the components of the shearing stresses at a point on two mutually perpendicular areas passing through this point are equal in magnitude and directed either both towards this line of section (the right-hand and upper face in Fig. 14), or away from it (the front and lower faces in Fig. 14). This law, apparently applies for any two perpendicular areas (and not only coordinate planes).

4. Principal Normal and Shearing Stresses

The state of stress at a point is a physical state which depends on the properties of the material and the external forces. We have already described it by the components of a stress tensor in a system of coordinates arbitrarily orientated in space. We shall attempt to find a system of coordinates in which the state of stress is described in a more simple and physically natural way. Three

such axes, which are called principal axes of stress, and which are analogous to the principal axes of a second order surface or the principal axes of inertia, exist at every point in the body. In order to determine the direction of these axes we work out the normal component σ_ν of the stress $\boldsymbol{S}_\nu$ acting on an arbitrary area with normal $\boldsymbol{\nu}$:

$$\sigma_\nu = \boldsymbol{S}_\nu \boldsymbol{\nu} \equiv (\boldsymbol{S}_x l + \boldsymbol{S}_y m + \boldsymbol{S}_z n)(\boldsymbol{i} l + \boldsymbol{j} m + \boldsymbol{k} n).$$

Taking into account the expressions (1.1′) for $\boldsymbol{S}_x$, $\boldsymbol{S}_y$, $\boldsymbol{S}_z$ in terms of the components σ_{ij} and the law of complementary shearing stresses, we get that

$$\sigma_\nu = \sigma_{xx} l^2 + \sigma_{yy} m^2 + \sigma_{zz} n^2 + 2\sigma_{yz} mn + 2\sigma_{zx} nl + 2\sigma_{xy} lm. \quad (1.2)$$

We will try to find the areas containing the given point, the normal stresses on which assume a stationary value. The orientation of an area can be described by the vector of its normal $\boldsymbol{\nu}$, i.e., by the direction cosines l, m, n, which are related by the expression

$$l^2 + m^2 + n^2 = 1.$$

We thus require to find the conditional maximum of the quantity σ_ν. To do so, as is well known, it is sufficient to find the unconditional maximum of the function

$$\Sigma = \sigma_\nu - \sigma'(l^2 + m^2 + n^2 - 1).$$

From the relations

$$\frac{\partial \Sigma}{\partial l} = 0, \quad \frac{\partial \Sigma}{\partial m} = 0, \quad \frac{\partial \Sigma}{\partial n} = 0,$$

we arrive at a set of linear homogeneous equations in the quantities l, m, n:

$$\left.\begin{aligned} (\sigma_{xx} - \sigma') l + \sigma_{xy} m + \sigma_{xz} n &= 0, \\ \sigma_{yx} l + (\sigma_{yy} - \sigma') m + \sigma_{yz} n &= 0, \\ \sigma_{zx} l + \sigma_{zy} m + (\sigma_{zz} - \sigma') n &= 0. \end{aligned}\right\} \quad (1.3)$$

Since the quantities l, m, n, in view of the equality $l^2 + m^2 + n^2 = 1$ cannot be zero simultaneously, the determinant of the coefficients of this set of equations must vanish:

$$\begin{vmatrix} \sigma_{xx} - \sigma' & \sigma_{xy} & \sigma_{xz} \\ \sigma_{yx} & \sigma_{yy} - \sigma' & \sigma_{yz} \\ \sigma_{zx} & \sigma_{zy} & \sigma_{zz} - \sigma' \end{vmatrix} = 0. \quad (1.4)$$

This determinant is symmetrical about the leading diagonal. The condition that it vanishes gives the well known secular equation in

the quantity σ', which has three real roots. These three values of σ' are called the principal normal stresses or simply the principal stresses $\sigma_1, \sigma_2, \sigma_3$.

The secular eqn. (1.4) can be re-written in the form

$$-\sigma'^3 + I_1\sigma'^2 - I_2\sigma' + I_3 = 0,$$

where

$$\left.\begin{aligned} I_1 &= \sigma_{xx} + \sigma_{yy} + \sigma_{zz}, \\ I_2 &= \sigma_{xx}\sigma_{yy} + \sigma_{yy}\sigma_{zz} + \sigma_{zz}\sigma_{xx} - \sigma_{yz}^2 - \sigma_{zx}^2 - \sigma_{xy}^2, \\ I_3 &= \begin{vmatrix} \sigma_{xx} & \sigma_{xy} & \sigma_{xz} \\ \sigma_{yx} & \sigma_{yy} & \sigma_{yz} \\ \sigma_{zx} & \sigma_{zy} & \sigma_{zz} \end{vmatrix}, \end{aligned}\right\} \tag{1.5}$$

and from the property of the roots of a cubic equation we have that:

$$\left.\begin{aligned} I_1 &= \sigma_1 + \sigma_2 + \sigma_3, \\ I_2 &= \sigma_1\sigma_2 + \sigma_2\sigma_3 + \sigma_3\sigma_1, \\ I_3 &= \sigma_1\sigma_2\sigma_3. \end{aligned}\right\} \tag{1.6}$$

The stress state at a point is a physical state which cannot depend on the choice of coordinate axes. Therefore the coefficients of the cubic equation which gives the principal stresses will also be independent of the choice of axes, i.e. the quantities I_1, I_2, I_3 are invariants of the stress tensor with respect to rotation of the co-ordinate axes. This can be seen from the relations (1.6) which give the quantities I_1, I_2, I_3 in terms of the values of the principal stresses.

Substituting in turn the values of $\sigma_1, \sigma_2, \sigma_3$ in the eqns. (1.3), and each time taking into account the equality $l^2 + m^2 + n^2 = 1$, we find three sets of values (l_1, m_1, n_1), (l_2, m_2, n_2) (l_3, m_3, n_3) which give the principal directions of stress at the point, i.e. three surfaces which are called principal surfaces.

It can be shown from eqns. (1.3) that the principal directions are orthogonal ($\boldsymbol{\nu}_1\boldsymbol{\nu}_2 = \boldsymbol{\nu}_2\boldsymbol{\nu}_3 = \boldsymbol{\nu}_3\boldsymbol{\nu}_1 = 0$). We can now find the stresses acting on the principal surfaces. Let us consider the expression $\boldsymbol{S}_\nu - \boldsymbol{\nu}\sigma'$, where σ' represents one of the principal stresses. Since, from the basic formula (1.1),

$$\left.\begin{aligned} X_\nu &= \sigma_{xx}l + \sigma_{yx}m + \sigma_{zx}n, \\ Y_\nu &= \sigma_{xy}l + \sigma_{yy}m + \sigma_{zy}n, \\ Z_\nu &= \sigma_{xz}l + \sigma_{yz}m + \sigma_{zz}n, \end{aligned}\right\} \tag{1.7}$$

then for the projection of the vector $S_\nu - \nu\sigma'$ on the x-axis we have that:

$$X_\nu - l\sigma' = (\sigma_{xx} - \sigma')\, l + \sigma_{yx} m + \sigma_{zx} n = 0$$

from the first of eqns. (1.3). Similarly

$$Y_\nu - m\sigma' = 0, \quad Z_\nu - n\sigma' = 0,$$

i.e. $S_\nu = \nu\sigma'$. This means that on each of the principal surfaces there is only a normal stress equal to the corresponding principal stress, and there are no shearing stresses.

Thus at every point of the body there always exist three orthogonal surfaces on which the normal stresses assume stationary values and on which there are no shearing stresses:

$$S_{\nu_1} = \sigma_1 \nu_1; \quad S_{\nu_2} = \sigma_2 \nu_2; \quad S_{\nu_3} = \sigma_3 \nu_3.$$

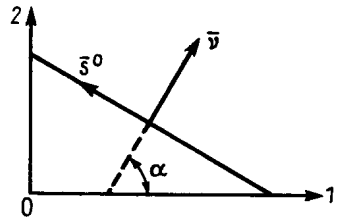

FIG. 15.

In general the orientation of the principal surfaces and the values of the principal stresses vary continuously from point to point.

If we enclose the point under consideration by an elementary parallelepiped with faces parallel to the principal surfaces at this point, then on the faces of this parallelepiped there will act only normal stresses equal to the principal stresses. Since the state of stress within the prallelepiped is defined only by the stresses on its faces (and mass forces), then this means that the state of stress at a point is fully defined by the principal stresses and by the orientation of the principal surfaces. This is a physically natural and important characteristic of the state of stress at a point.

We can now find the surfaces on which the shearing stresses assume stationary values. Let us consider a surface parallel to one of the principal axes, for example, the axis 3 with normal ν inclined to the principal axis 1 at an angle α (Fig. 15). The basic formula (1.1) can be re-written in the form

$$S_\nu = S_1 l + S_2 m + S_3 n$$

or, since

$$\boldsymbol{S}_1 = \sigma_1 \boldsymbol{\nu}_1 = \sigma_1 \boldsymbol{i}, \quad \boldsymbol{S}_2 = \sigma_2 \boldsymbol{\nu}_2 = \sigma_2 \boldsymbol{j}, \quad \boldsymbol{S}_3 = \sigma_3 \boldsymbol{\nu}_3 = \sigma_3 \boldsymbol{k},$$

then

$$\boldsymbol{S}_\nu = \sigma_1 l \boldsymbol{i} + \sigma_2 m \boldsymbol{j} + \sigma_3 n \boldsymbol{k}.$$

For the chosen surface $l = \cos\alpha$, $m = \sin\alpha$, $n = 0$, so that

$$\boldsymbol{S}_\nu = \sigma_1 \cos\alpha \boldsymbol{i} + \sigma_2 \sin\alpha \boldsymbol{j},$$

$$\boldsymbol{\nu} = \cos\alpha \boldsymbol{i} + \sin\alpha \boldsymbol{j},$$

$$\boldsymbol{s}^0 = -\sin\alpha \boldsymbol{i} + \cos\alpha \boldsymbol{j}.$$

For the normal and shearing stresses on this surface we have that (Fig. 15):

$$\left.\begin{aligned} \sigma = \boldsymbol{S}_\nu \boldsymbol{\nu} = \sigma_1 \cos^2\alpha + \sigma_2 \sin^2\alpha = \frac{\sigma_1 + \sigma_2}{2} + \frac{\sigma_1 - \sigma_2}{2} \cos 2\alpha, \\ \tau_\nu = \boldsymbol{S}_\nu \boldsymbol{s}^0 = (-\sigma_1 + \sigma_2) \sin\alpha \cos\alpha = -\frac{\sigma_1 - \sigma_2}{2} \sin 2\alpha. \end{aligned}\right\} \tag{1.8}$$

From the condition $\partial\tau_\nu / \partial\alpha = 0$ we get that $\sigma_1 - \sigma_2 = 0$, or $\cos 2\alpha = 0$ and $\sigma_1 \neq \sigma_2$.

In the first case the shearing stresses are zero on any surface parallel to the principal axis 3, i.e. all such surfaces are principal surfaces. This is one of the possible particular cases. In the second case we find that $\alpha = \pm\pi/4$, i.e. the maximum value of the shearing stress, which is $\pm(\sigma_1 - \sigma_2)/2$ occurs on surfaces inclined at an angle of 45° to the principal surfaces. Considering the other coordinate surfaces we can, by a similar procedure, arrive at the conclusion that there are three pairs of surfaces inclined at angles of 45° to the principal surfaces on which the shearing stresses assume stationary values equal respectively to

$$\left.\begin{aligned} \tau_{12} = \frac{\sigma_1 - \sigma_2}{2}, \\ \tau_{23} = \frac{\sigma_2 - \sigma_3}{2}, \\ \tau_{31} = \frac{\sigma_3 - \sigma_1}{2}. \end{aligned}\right\} \tag{1.9}$$

Relations of the type of formulae (1.8) suggest a simple method of finding the principal directions and principal stresses and of describing graphically the stress state at a point.

Let us suppose first of all that the axis Oz of the rectangular system of coordinates $Oxyz$ coincides with one of the principal axes (for example with the axis 3), and that the x-axis forms an angle α with the principal axis 1. The normal stress σ_{xx} and the shearing stress $\tau_{xy} = \sigma_{xy}$ on a plane AB perpendicular to the x-axis (Fig. 16) are given by formulae (1.8), and the normal and shearing stresses σ_{yy} and $\tau_{yx} = \sigma_{yx}$ on the plane AC perpendicular to the y-axis are given by the same formula by replacing α by $\alpha + \pi/2$, and by the law of complementary shearing stresses $\sigma_{yx} = \sigma_{xy}$:

$$\left.\begin{aligned} \sigma_{xx} &= \frac{\sigma_1 + \sigma_2}{2} + \frac{\sigma_1 - \sigma_2}{2}\cos 2\alpha, \\ \sigma_{yy} &= \frac{\sigma_1 + \sigma_2}{2} - \frac{\sigma_1 - \sigma_2}{2}\cos 2\alpha, \\ \tau_{xy} \equiv \sigma_{xy} &= \sigma_{yx} = -\frac{\sigma_1 - \sigma_2}{2}\sin 2\alpha. \end{aligned}\right\} \tag{1.10}$$

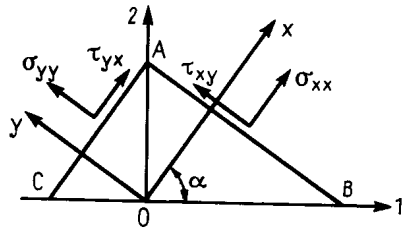

FIG. 16.

These expressions can be looked upon as a set of equations for determining the principal stresses σ_1 and σ_2 and the angle α, which gives the orientation of the principal axes for given stress components σ_{xx}, σ_{yy}, τ_{xy} in the arbitrarily orientated system of coordinates. For example, in order to determine the angle α we substract the first expression from the second and divide the third expression by this result. We then get that:

$$\tan 2\alpha = \frac{2\tau_{xy}}{\sigma_{yy} - \sigma_{xx}}. \tag{1.11}$$

The maximum shearing stress $\tau_{12} = (\sigma_1 - \sigma_2)/2$ can be found by substracting the first expression from the second, squaring and adding to the square of the third expression:

$$\tau_{12} = \frac{\sigma_1 - \sigma_2}{2} = \sqrt{\left[\tau_{xy}^2 + \left(\frac{\sigma_{xx} - \sigma_{yy}}{2}\right)^2\right]}. \tag{1.12}$$

If we also take into account the result of adding the first two expressions

$$\sigma_{xx} + \sigma_{yy} = \sigma_1 + \sigma_2,$$

we get for the principal stresses that:

$$\left.\begin{aligned} \sigma_1 &= \frac{\sigma_{xx} + \sigma_{yy}}{2} + \sqrt{\left[\tau_{xy}^2 + \left(\frac{\sigma_{xx} - \sigma_{yy}}{2}\right)^2\right]}, \\ \sigma_2 &= \frac{\sigma_{xx} + \sigma_{yy}}{2} - \sqrt{\left[\tau_{xy}^2 + \left(\frac{\sigma_{xx} - \sigma_{yy}}{2}\right)^2\right]}. \end{aligned}\right\} \tag{1.13}$$

These algebraic results can be represented graphically.

We set out along the axis of abscissae the values of the normal stresses, and along the axis of ordinates the values of shearing stresses. We shall assume that $\sigma_1 > \sigma_2$ (this is of no significance) and we mark off on the axis of abscissae the points A and B corresponding to these values (Fig. 17).

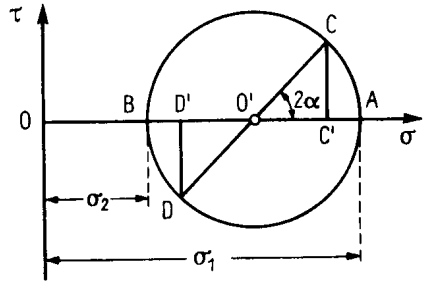

FIG. 17.

With the point O', the mid-point of AB (its abscissa OO' is $(\sigma_1 + \sigma_2)/2$), as centre, we describe a circle of radius $(\sigma_1 - \sigma_2)/2$. This circle will pass through the points A and B. We draw the diameter CD inclined at some angle 2α to the axis of abscissae, and from the points C and D we drop perpendiculars CC' and DD' onto the axis of abscissae. It is now easy to see that the lengths OC', OD' and $CC' = DD'$ represent to the scale of the drawing the stress components σ_{xx}, σ_{yy} and τ_{xy} respectively in the system of coordinates

for which the axis Ox is inclined to the principal axis 1 at an angle α (Fig. 16). For,

$$OC' = OO' + O'C' = OO' + O'C\cos 2\alpha$$

$$= \frac{\sigma_1 + \sigma_2}{2} + \frac{\sigma_1 - \sigma_2}{2}\cos 2\alpha,$$

$$OD' = OO' - O'D' = \frac{\sigma_1 + \sigma_2}{2} - \frac{\sigma_1 - \sigma_2}{2}\cos 2\alpha,$$

$$CC' = DD' = OC\sin 2\alpha = \frac{\sigma_1 - \sigma_2}{2}\sin 2\alpha.$$

It can be seen that the maximum values of CC' and DD' (i.e. the maximum values of shearing stresses) are equal to the radius of the circle $(\sigma_1 - \sigma_2)/2$ and occur when $2\alpha = \pi/2$, i.e. when $\alpha = \pi/4$.

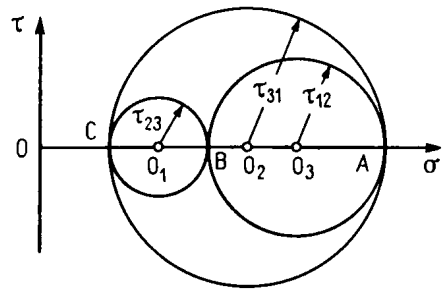

FIG. 18.

The figure constructed in Fig. 17 is called Mohr's diagram (or Mohr's circle). By making use of this figure it is easy to determine graphically the stresses on any surface, i.e. Mohr's circle describes the state of stress at a point.

In the above construction of Mohr's circle diagram we worked on the assumption that the principal stresses σ_1 and σ_2 are known. But it is easy to construct this diagram knowing the stress components σ_{xx}, σ_{yy}, τ_{xy} in any system of coordinates (when the z-axis coincides with the principal axis 3). For the abscissa of the centre of the circle O' is given by formulae (1.13) as $(\sigma_{xx} + \sigma_{yy})/2$. This means that the centre of the circle O' lies midway between the points C' and D' ($OC' = \sigma_{xx}$, $OD' = \sigma_{yy}$). Drawing a perpendicular from the point C' (or D') and marking off along it $CC' = \tau_{xy}$, we

find the point C on the circle. A circle then drawn with radius OC' will be Mohr's circle. The position of the points of its intersection with the axis of abscissae A and B give the values of the principal stresses σ_1 and σ_2, and the angle $CO'A$ gives the orientation of the principal directions relative to the x-axis.

We are now no longer restricted by the requirement that the z-axis must coincide with the principal axis 3. Let us mark the points A, B, C on the axis of abscissae corresponding to the principal stresses $\sigma_1, \sigma_2, \sigma_3$ (Fig. 18). If we now draw circles with diameters AB, BC and AC, their radii will be equal respectively to $\tau_{12}, \tau_{23}, \tau_{31}$, i.e. to the maximum shearing stresses, and if $\sigma_1 > \sigma_2 > \sigma_3$ (this can always be assumed since the order of numbering the principal axes is arbitrary), then τ_{31} is the greatest of the maximum shearing stresses.

5. Octahedral Stresses

The principal normal stresses are a natural physical characteristic of the state of stress at a point. However, the stress state can be described just as naturally in another way—a way which is more closely related to the physical state in the neighbourhood of the point considered. Let us suppose that the directions of the principal axes 1, 2, 3 are known. Let us mark off along each of the semi-axes equal intervals from the origin of coordinates (which is taken as coincident with the point under consideration), and then draw planes in each octant so that each plane passes through the three points lying on different axes. In this way we form an octahedron the faces of which are identically inclined to the principal axes (Fig. 19), so that the direction cosines of the normals to all the faces have the same numerical value:

$$l = \pm m = \pm n = \pm \frac{1}{\sqrt{3}}.$$

For example, for the face in the first octant $l = m = n = 1/\sqrt{3}$.

Let us evaluate the stresses acting on the faces of this octahedron. On the principal surfaces we have principal stresses $\sigma_1, \sigma_2, \sigma_3$: $\boldsymbol{S}_1 = \sigma_1 \boldsymbol{i}$, $\boldsymbol{S}_2 = \sigma_2 \boldsymbol{j}$, $\boldsymbol{S}_3 = \sigma_3 \boldsymbol{k}$ where $\boldsymbol{i}, \boldsymbol{j}, \boldsymbol{k}$ are the unit vectors of the principal axes. From formula (1.1) the stress on a face of the octahedron will be

$$\boldsymbol{S}_\nu = \boldsymbol{S}_1 l + \boldsymbol{S}_2 m + \boldsymbol{S}_3 n = \sigma_1 l \boldsymbol{i} + \sigma_2 m \boldsymbol{j} + \sigma_3 n \boldsymbol{k};$$

since $\boldsymbol{\nu} = l\boldsymbol{i} + m\boldsymbol{j} + n\boldsymbol{k}$, the normal stress σ_ν on the face of the octahedron will be

$$\sigma_\nu = \boldsymbol{S}_\nu = \sigma_1 l^2 + \sigma_2 m^2 + \sigma_3 n^2 = \tfrac{1}{3}(\sigma_1 + \sigma_2 + \sigma_3)$$
$$= \tfrac{1}{3} I_1 = \sigma.$$

The quantity $\sigma = \frac{1}{3}(\sigma_1 + \sigma_2 + \sigma_3)$ is called the mean normal stress (or hydrostatic stress). From the formula for σ_ν we see that the normal stresses on all faces of the octahedron are the same and equal to the mean normal stress.

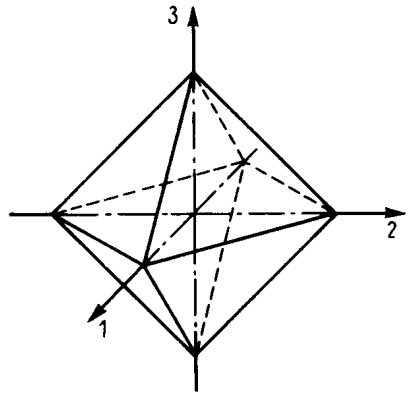

FIG. 19.

The shearing stress on a face of the octahedron can be evaluated from the formula

$$\tau_\nu^2 = \boldsymbol{S}_\nu^2 - \sigma_\nu^2.$$

Substituting here the values of $\boldsymbol{S}_\nu$ and $\sigma_\nu = \sigma$, we get that

$$\tau_\nu = 1/3 \sqrt{[(\sigma_1 - \sigma_2)^2 + (\sigma_2 - \sigma_3)^2 + (\sigma_3 - \sigma_1)^2]}$$
$$= 2/3 \sqrt{(\tau_{12}^2 + \tau_{23}^2 + z\tau_{31}^2)}. \qquad (1.14)$$

The quantity τ_ν is called the octahedral shearing stress. The magnitude of the vector τ_ν is given by (1.14), and its angle of inclination to the edge of the octahedron is φ_ν, which we shall call the angle of octahedral shearing stress. Thus the same normal stresses σ and the same shearing stresses τ_ν act on all faces of the octahedron. The former, which subject the octahedron to an all-round compression or tension, give rise to a change in volume, as a result of which the octahedron, since the pressure is uniform, does

not change its shape. The latter cause a change in shape, but do not contribute to the change in volume. This can be explained as follows. Let us suppose that the body is subjected to an external hydrostatic pressure p. This leads to a change in the principal stresses $\sigma_1, \sigma_2, \sigma_3$ and in the mean normal stress σ by the quantity p:

$$\sigma_1' = \sigma_1 - p, \quad \sigma_2' = \sigma_2 - p, \quad \sigma_3' = \sigma_3 - p, \quad \sigma' = \sigma - p.$$

This is not reflected in the magnitude of the octahedral shearing stress, since $\sigma_1' - \sigma_2' = \sigma_1 - \sigma_2$, $\sigma_2' - \sigma_3' = \sigma_2 - \sigma_3$, $\sigma_3' - \sigma_1' = \sigma_3 - \sigma_1$ and, therefore, $\tau_v' = \tau_v$.

This division of a stress into a part that gives rise only to a change in volume and a part that gives rise only to a change in shape is a very important and useful technique in studying the behaviour of materials under stress. It can be represented in general form by expressing the stress components in the form

$$\sigma_{ij} = \sigma_{ij}' + \sigma_{ij}'', \tag{1.15}$$

where $\sigma_{ij}' = \sigma_{ij} - \sigma\,\delta_{ij}$, $\sigma_{ij}'' = \sigma\,\delta_{ij}$. Here δ_{ij} is the so-called Kronecker delta: $\delta_{ij} = 1$ for $i = j$ and $\delta_{ij} = 0$ for $i \neq j$. The quantities σ_{ij}' form a so-called stress deviator and the quantities σ_{ij}'', a spherical stress tensor. It is apparent that the mean normal stress (i.e. the first invariant) of the stress deviator is zero,

$$I_1' = \sigma_{xx}' + \sigma_{yy}' + \sigma'_{zz} = \sigma_{xx} - \sigma + \sigma_{yy} - \sigma + \sigma_{zz} - \sigma = 0,$$

and that the spherical stress tensor does not define the shearing stresses. The octahedral shearing stress is related only to the second invariant of the stress deviator. For, by definition (see formulae (1.5) and (1.6)), we have that:

$$\begin{aligned} I_2' &= \sigma_{xx}'\sigma_{yy}' + \sigma_{yy}'\sigma_{zz}' + \sigma_{zz}'\sigma_{xx}' - \sigma_{yz}'^2 - \sigma_{zx}'^2 - \sigma_{xy}'^2 \\ &= (\sigma_1 - \sigma)(\sigma_2 - \sigma) + (\sigma_2 - \sigma)(\sigma_3 - \sigma) + (\sigma_3 - \sigma)(\sigma_1 - \sigma) \\ &= -\tfrac{1}{6}[(\sigma_1 - \sigma_2)^2 + (\sigma_2 - \sigma_3)^2 + (\sigma_3 - \sigma_1)^2]. \end{aligned}$$

Comparing this with formula (1.14) for τ_v, we see that

$$\tau_v = \sqrt{\left(-\frac{2}{3} I_2'\right)}. \tag{1.16}$$

We can now express τ_v in terms of the components of the stress tensor σ_{ij}. We first of all substitute the expression for I_2' in terms

of σ'_{ij} in formula (1.16), and then substitute for σ'_{ij} in terms of σ_{ij} and σ. As a result we get that:

$$\tau_\nu = 1/3\sqrt{[(\sigma_{xx} - \sigma_{yy})^2 + (\sigma_{yy} - \sigma_{zz})^2 + (\sigma_{zz} - \sigma_{xx})^2 + 6(\sigma_{yz}^2 + \sigma_{zx}^2 + \sigma_{xy}^2)]}. \tag{1.17}$$

Instead of the octahedral shearing stress we often make use of the quantity σ_i, which is called the intensity of stress:

$$\sigma_i = \frac{3}{\sqrt{2}}\tau_\nu. \tag{1.18}$$

It is convenient to introduce this quantity, proportional to τ_ν. For example, for a long cylindrical rod in simple tension the intensity of stress σ_i is equal to the tensile stress.

Let us now compare the magnitudes of the octahedral shearing stress and the greatest of the principal shearing stresses. From formula (1.14) for τ_ν we see that τ_ν is always less than the greatest of the shearing stresses. In order to evaluate the difference between them let us consider the expression

$$\frac{\tau_\nu^2}{\tau_{max}^2} = \frac{4}{9}\frac{\tau_{max}^2 + \tau_{av}^2 + \tau_{min}^2}{\tau_{max}^2}.$$

Since $\tau_{12} + \tau_{23} + \tau_{31} = 0$, $\tau_{av} = -\tau_{max} - \tau_{min}$ and τ_{max} and τ_{min} must necessarily be of opposite sign. Therefore

$$\frac{\tau_\nu^2}{\tau_{max}^2} = \frac{8}{9}\frac{\tau_{max}^2 + \tau_{max}\tau_{min} + \tau_{min}^2}{\tau_{max}^2}.$$

We define $\xi = \tau_{min}/\tau_{max}$, and, bearing in mind the above remark concerning the signs of τ_{max} and τ_{min}, $\xi \leqq 0$; then

$$\frac{\tau_\nu^2}{\tau_{max}^2} = \frac{8}{9}(\xi^2 + \xi + 1).$$

This quantity becomes a minimum when $\xi = -\frac{1}{2}$, increasing monotonically as ξ changes from $-\frac{1}{2}$ to 0 and from $-\frac{1}{2}$ to $-\infty$. But ξ cannot assume a value less than -1. The value of $\xi = -1$ corresponds to the equality $\tau_{max} = -\tau_{min}$ when τ_{av} is zero. This means that the quantity τ_ν^2/τ_{max}^2 varies within the limits

$$\frac{2}{3} \leqq \frac{\tau_\nu^2}{\tau_{max}^2} \leqq \frac{8}{9}$$

or

$$\frac{\sqrt{2}}{\sqrt{3}} \leqq \left|\frac{\tau_\nu}{\tau_{max}}\right| \leqq \frac{2\sqrt{2}}{3}.$$

The lower limit of variation of τ_ν/τ_{max} is 0·866 of the upper limit. Therefore, if we take the relation

$$\tau_\nu = 0{\cdot}933\,\frac{2\sqrt{2}}{3}\,|\tau_{max}|,$$

it cannot be in error by more than $\pm 6{\cdot}7$ per cent. This result will be used later in comparing various approaches to the question of establishing the criteria for the transition of materials into the plastic state.

The question now arises of comparing two states of stress. The problem can be formulated as follows: in a particular coordinate system *Oxyz* the stress components σ_{ij} are known at two points in the body; we require to compare these states of stress. We shall give two methods of approach.

(1). An approximate comparison. The values of the mean normal stress σ and the octahedral shearing stress τ_ν are calculated for the two states of stress, and a comparison is made on the basis of these two stresses. The existence of inequalities of the type $\sigma' > \sigma''$ and $\tau'_\nu > \tau''_\nu$ for steel, for example, shows that the first state of stress is nearer to failure than the second.

(2). An exact comparison. The principal stresses are calculated and compared; an alternative would be a comparison of the Mohr's circles.

Example. Compare the three states of stress (in kg/mm²)

$$\begin{cases} \sigma'_{xx} = 3, & \sigma'_{yy} = 9, & \sigma'_{zz} = 3, \\ \sigma'_{xy} = 4, & \sigma'_{yz} = 0, & \sigma'_{zx} = 0; \end{cases}$$

$$\begin{cases} \sigma''_{xx} = 10, & \sigma''_{yy} = 3, & \sigma''_{zz} = 2, \\ \sigma''_{xy} = 0, & \sigma''_{yz} = 0, & \sigma''_{zx} = 3; \end{cases}$$

$$\begin{cases} \sigma'''_{xx} = 3, & \sigma'''_{yy} = -7, & \sigma'''_{zz} = -5, \\ \sigma'''_{xy} = 0, & \sigma'''_{yz} = 0, & \sigma'''_{zx} = 0. \end{cases}$$

Using the approximate method we calculate the values of σ and τ_ν:

$$\sigma' = \tfrac{1}{3}(\sigma'_{xx} + \sigma'_{yy} + \sigma'_{zz}) = 5,$$

$$\sigma'' = \tfrac{1}{3}(\sigma''_{xx} + \sigma''_{yy} + \sigma''_{zz}) = 5,$$

$$\sigma''' = \tfrac{1}{3}(\sigma'''_{xx} + \sigma'''_{yy} + \sigma'''_{zz}) = -3;$$

$$\tau'_\nu = \tfrac{1}{3}\sqrt{(36 + 36 + 6 \times 16)} = \tfrac{2}{3}\sqrt{42} \approx 4{\cdot}32,$$

$$\tau''_\nu = \tfrac{1}{3}\sqrt{(49 + 1 + 64 + 6 \times 9)} = \tfrac{2}{3}\sqrt{42} \approx 4{\cdot}32,$$

$$\tau'''_\nu = \tfrac{1}{3}\sqrt{(100 + 4 + 64)} = \tfrac{2}{3}\sqrt{42} \approx 4{\cdot}32.$$

The first two states of stress are the same, but the third differs from both of these by an additional hydrostatic stress (pressure) of -8.

For an exact solution we compare the Mohr's circles. Since $\sigma'_{yz} = \sigma'_{zx} = 0$, the z-axis in the first state of stress is a principal axis. The radius of the Mohr's circle is therefore

$$\tau_{12} = \sqrt{\left[\sigma'^2_{xy} + \left(\frac{\sigma'_{xy} - \sigma'_{yy}}{2}\right)^2\right]} = 5,$$

and the abscissa of the centre of the circle is

$$\frac{\sigma'_{xx} + \sigma'_{yy}}{2} = 6.$$

The principal stresses are $\sigma_1 = 6 + 5 = 11$, $\sigma_2 = 6 - 5 = 1$, $\sigma_3 = \sigma'_{zz} = 3$.

In the second state of stress $\sigma''_{xy} = \sigma''_{yz} = 0$, i.e., the y-axis is a principal axis. The radius of the Mohr's circle is

$$\tau_{31} = \sqrt{\left[\sigma''^2_{zx} + \left(\frac{\sigma''_{zz} - \sigma''_{xx}}{2}\right)^2\right]} = 5,$$

and the abscissa of the centre is

$$\frac{\sigma''_{zz} + \sigma''_{xx}}{2} = 6.$$

The principal stresses are $\sigma_1 = 6 + 5 = 11$, $\sigma_2 = \sigma''_{yy} = 3$, $\sigma_3 = 6 - 5 = 1$. Therefore the first two states of stress are exactly the same.

In the third state of stress the x, y, and z-axes are principal axes so that $\sigma_1 = 3$, $\sigma_2 = -7$, $\sigma_3 = -5$ and the greatest shearing stress is

$$\tau_{\max} \quad \frac{\sigma_1 - \sigma_2}{2} \quad 5.$$

Therefore, in the third state of stress the greatest shearing stress is the same as in the first two cases, and the normal stress is less.

6. Deformation in the Neighbourhood of a Point

As was pointed out in § 2, our deductions as to the possibility of replacing a discrete distribution by the mean continuous distribution apply not only to stresses, but also to the displacements of physical particles of the body, which cause changes in the distances between the atoms in the crystals and changes in the forces of interaction between elementary particles, i.e. the stresses which were considered in the preceding sections. In studying the strains which arise in a body due to external forces, we shall, therefore, consider a polycrystalline body as a homogeneous continuous medium occupying a part of space.

Let us consider the deformation in the neighbourhood of some point (x, y, z) in the body. The deformation of a body is defined as a change in the shape and dimensions (volume) of the body. The deformation of the whole body is made up of the strains in elements of volume in the body which change their dimensions and shape, these changes, in general, being different for different elements of volume. In order to characterize the deformation in the neighbourhood of the point under consideration therefore, we must find quantities which enable us to determine the change in length of any line (fibre) of the material which passes through this point, and also

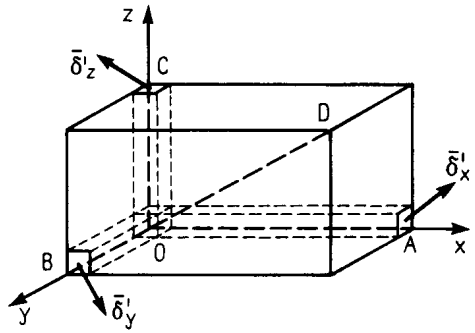

FIG. 20.

the change in the angle between any two lines radiating from this point.

Let us suppose that $\mathfrak{D}(x, y, z)$ is the displacement vector at a particular point O, which we can take as the origin of a rectangular rectilinear system of coordinates $Oxyz$. We define u, v, w as the components of this vector along the coordinate axes, and $\boldsymbol{i}, \boldsymbol{j}, \boldsymbol{k}$ as the unit vectors of the coordinate axes. We then have that:

$$\mathfrak{D} = u\boldsymbol{i} + v\boldsymbol{j} + w\boldsymbol{k}.$$

As an element of volume in the neighbourhood of the point O, we shall consider a small rectangular parallelepiped, with edges dx, dy dz (Fig. 20). We wish to find the strains which arise due to the fact that the displacements are different for different points, i.e. due to the fact that the vector $\mathfrak{D}$ is a function of the coordinates of the point. We need, therefore, to find the relative displacements, i.e.,

the difference between the displacement of the point O and the displacements of points lying in the neighbourhood of O.

If we draw prisms of small cross-sectional area along the edges OA, OB, OC of the elementary parallelepiped (i.e. fibres made up of physical particles) and define the displacements of the ends A, B, C of these fibres relative to the point O as $\boldsymbol{\delta}'_x$, $\boldsymbol{\delta}'_y$, $\boldsymbol{\delta}'_z$ (the suffixes x, y, z indicate the direction of the fibre before deformation), it will readily be seen that the magnitudes (and directions) of $\boldsymbol{\delta}'_x$, $\boldsymbol{\delta}'_y$, $\boldsymbol{\delta}'_z$ depend on the distances from O of A, B and C. It is convenient, therefore, to describe relative displacement by a vector referred to the distance from the point O:

$$\boldsymbol{\delta}_x = \frac{\boldsymbol{\delta}'_x}{dx}, \quad \boldsymbol{\delta}_y = \frac{\boldsymbol{\delta}'_y}{dy}, \quad \boldsymbol{\delta}_z = \frac{\boldsymbol{\delta}'_z}{dz}.$$

By definition, we have that:

$$\boldsymbol{\delta}'_x = \mathfrak{D}(x + dx, y, z) - \mathfrak{D}(x, y, z) = \frac{\partial \mathfrak{D}}{\partial x} dx + \cdots$$

The series of dots indicates that there are further small terms of higher order. Discarding these terms, we get that:

$$\delta_x = \frac{\partial \mathfrak{D}}{\partial x}, \quad \delta_y = \frac{\partial \mathfrak{D}}{\partial y}, \quad \delta_z = \frac{\partial \mathfrak{D}}{\partial z}$$

or

$$\left.\begin{aligned} \boldsymbol{\delta}_x &= \frac{\partial u}{\partial x}\boldsymbol{i} + \frac{\partial v}{\partial x}\boldsymbol{j} + \frac{\partial w}{\partial x}\boldsymbol{k}, \\ \boldsymbol{\delta}_y &= \frac{\partial u}{\partial y}\boldsymbol{i} + \frac{\partial v}{\partial y}\boldsymbol{j} + \frac{\partial w}{\partial y}\boldsymbol{k}, \\ \boldsymbol{\delta}_z &= \frac{\partial u}{\partial z}\boldsymbol{i} + \frac{\partial v}{\partial z}\boldsymbol{j} + \frac{\partial w}{\partial z}\boldsymbol{k}. \end{aligned}\right\} \tag{1.19}$$

Let us now consider the displacement of some physical linear element ds with direction cosines l, m, n. Let us suppose that this fibre is the diagonal OD of the elementary parallelepiped of Fig. 20, so that

$$l = \frac{dx}{ds}, \quad m = \frac{dy}{ds}, \quad n = \frac{dz}{ds}.$$

Defining the relative displacement of the point D as $\boldsymbol{\delta}_r$, we have that

$$\begin{aligned} \boldsymbol{\delta}_r ds &= \mathfrak{D}(x + dx, \ y + dy, \ z + dz) - \mathfrak{D}(x, y, z) \\ &= \frac{\partial \mathfrak{D}}{\partial x} dx + \frac{\partial \mathfrak{D}}{\partial y} dy + \frac{\partial \mathfrak{D}}{\partial z} dz + \cdots \end{aligned}$$

But $\partial\mathfrak{D}/\partial x$, $\partial\mathfrak{D}/\partial y$, $\partial\mathfrak{D}/\partial z$ are the relative displacements of the projections of the point D on the axes Ox, Oy, Oz which above were defined as $\boldsymbol{\delta}_x$, $\boldsymbol{\delta}_y$, $\boldsymbol{\delta}_z$. Therefore, ignoring small quantities of a higher order and dividing by ds, we get that:

$$\boldsymbol{\delta}_\nu = \boldsymbol{\delta}_x l + \boldsymbol{\delta}_y m + \boldsymbol{\delta}_z n. \tag{1.20}$$

Formula (1.20) is analogous to formula (1.1) for stresses: $\boldsymbol{S}_\nu = \boldsymbol{S}_x l + \boldsymbol{S}_y m + \boldsymbol{S}_z n$. We conclude therefore that the three vectors of relative displacements $\boldsymbol{\delta}_x$, $\boldsymbol{\delta}_y$, $\boldsymbol{\delta}_z$, or the nine scalar quantities $\partial u/\partial x$, $\partial u/\partial y$, ..., $\partial w/\partial z$ comprise a tensor, which we shall call the tensor of relative displacements ($\mathfrak{D}'$).

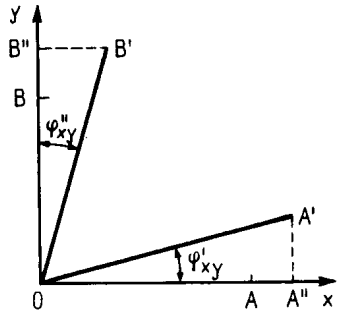

FIG. 21.

Let us consider two fibres OA and OB, which before deformation are directed along the axes Ox and Oy (Fig. 21). After deformation the projections of these fibres on the (xy) plane will be OA' and OB'. Taking the lengths of OA and OB as unity, we have that:

$$AA'' = \frac{\partial u}{\partial x}, \quad A'A'' = \frac{\partial v}{\partial x}, \quad BB'' = \frac{\partial v}{\partial y}, \quad B'B'' = \frac{\partial u}{\partial y}.$$

We shall assume that the deformation is small, so that $|\partial u_i/\partial x_j| \ll 1$. Then AA'' and BB'' represent (to the accuracy of terms of the second order of smallness) the relative extensions of the fibres OA and OB. Due to the fact that the angles of rotation are small, we have that

$$\varphi'_{xy} \equiv \angle AOA' \approx \tan\varphi'_{xy} \approx \frac{\partial v}{\partial x},$$

$$\varphi''_{xy} \equiv \angle BOB' \approx \tan\varphi''_{xy} \approx \frac{\partial u}{\partial y}.$$

The sum $\varphi'_{xy} + \varphi''_{xy}$ is a measure of the change in the angle (which, before deformation was a right-angle) between the fibres OA and OB as a result of the deformation. The changes in the angles between fibres which before deformation were perpendicular to each other are called shearing strains. Thus if we introduce the nine quantities

$$\varepsilon_{ij} = \frac{1}{2}\left(\frac{\partial u_i}{\partial x_j} + \frac{\partial u_j}{\partial x_i}\right) \quad (i,j = 1, 2, 3), \tag{1.21}$$

the three quantities ε_{ii} are the relative extensions of fibres directed (before deformation) along the coordinate axes, and the three quantities $\varepsilon_{ij} = \varepsilon_{ji}$ for $i \neq j$ are half the shear strains $\gamma_{ij} = 2\varepsilon_{ij}$ between these fibres. The quantities ε_{ij} form a strain tensor and are called strain components. The reason why half, and not whole, shear strains occur in the strain tensor, whereas in the stress tensor we have the full value for the shear stresses, can be explained as follows. The stresses σ_{xy} and σ_{yx} are equal and each acts on an area perpendicular to the axes Ox and Oy; at the same time, γ_{xy} is a change in angle due to a combined displacement of fibres directed along the axes Ox and Oy.

The region of the point O is subjected by the deformation to a rotation as a whole. The rotations about the axes Ox, Oy, Oz are, apparently, equal respectively to (see Fig. 21)

$$\omega_x = \frac{1}{2}\left(\frac{\partial w}{\partial y} - \frac{\partial v}{\partial z}\right), \quad \omega_y = \frac{1}{2}\left(\frac{\partial u}{\partial z} - \frac{\partial w}{\partial x}\right), \quad \omega_z = \frac{1}{2}\left(\frac{\partial v}{\partial x} - \frac{\partial u}{\partial y}\right), \tag{1.22}$$

so that the resultant vector of rotation is

$$\boldsymbol{\omega} = \operatorname{rot} \mathfrak{D}. \tag{1.23}$$

These quantities do not characterize the deformation in the neighbourhood of the point. The relative displacements of the ends of the fibres due purely to deformation are therefore expressed, not by formulae (1.19), but by the formulae

$$\left.\begin{aligned} \boldsymbol{\delta}_x &= \varepsilon_{xx}\boldsymbol{i} + \varepsilon_{xy}\boldsymbol{j} + \varepsilon_{xz}\boldsymbol{k}, \\ \boldsymbol{\delta}_y &= \varepsilon_{yx}\boldsymbol{i} + \varepsilon_{yy}\boldsymbol{j} + \varepsilon_{yz}\boldsymbol{k}, \\ \boldsymbol{\delta}_z &= \varepsilon_{zx}\boldsymbol{i} + \varepsilon_{zy}\boldsymbol{j} + \varepsilon_{zz}\boldsymbol{k}. \end{aligned}\right\} \tag{1.24}$$

These formulae are completely analogous to formulae (1.1′) for stresses. We can therefore, without repeating a process similar to that of §§ 4 and 5, establish results analogous to those for stresses.

We will show, in particular, that if we know the strain components (1.21) we can evaluate the relative extension of a fibre arbitrarily orientated relative to the axes Ox, Oy, Oz. Suppose the direction of some fibre is given by the unit vector $\boldsymbol{\nu} = l\boldsymbol{i} = m\boldsymbol{j} + n\boldsymbol{k}$ (Fig. 22). Since we are considering small strains and since, consequently, the angle of rotation of the fibre φ_ν is small, the relative extension of a fibre can be taken as the ratio of the projection of the displacement vector on the fibre, to the length of the fibre

$$\varepsilon_\nu = \frac{\boldsymbol{\delta}_\nu ds\boldsymbol{\nu}}{ds} = \boldsymbol{\delta}_\nu \boldsymbol{\nu}.$$

This formula is analogous to the expression for the normal stress on an area with normal $\boldsymbol{\nu}$: $\sigma_\nu = \boldsymbol{S}_\nu \boldsymbol{\nu}$. Taking into account formulae (1.20) and (1.24) we get that:

$$\varepsilon_\nu = \varepsilon_{xx}l^2 + \varepsilon_{yy}m^2 + \varepsilon_{zz}n^2 + 2\varepsilon_{yz}mn + 2\varepsilon_{zx}nl + 2\varepsilon_{xy}lm, \quad (1.25)$$

which is completely analogous to formula (1.2) for stresses.

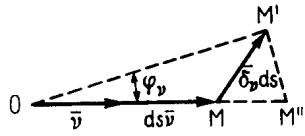

FIG. 22.

We might also wish to find the directions in which extensions of fibres assume maximum values. To do so we must find the stationary value of the function

$$F(l, m, n) \equiv \varepsilon_\nu - \varepsilon'(l^2 + m^2 + n^2 - 1).$$

Here, as was the case for stresses (see § 5), we arrive at a secular equation

$$-\varepsilon'^3 + J_1\varepsilon'^2 - J_2\varepsilon' + J_3 = 0, \quad (1.26)$$

where

$$J_1 \equiv \theta = \varepsilon_{xx} + \varepsilon_{yy} + \varepsilon_{zz},$$

$$J_2 = \varepsilon_{xx}\varepsilon_{yy} + \varepsilon_{yy}\varepsilon_{zz} + \varepsilon_{zz}\varepsilon_{xx} - \varepsilon_{yz}^2 - \varepsilon_{zx}^2 - \varepsilon_{zy}^2,$$

and J_3 is a determinant made up of the quantities ε_{ij}. The quantities J_1, J_2, J_3 are invariants of the strain tensor with respect to rotation of the coordinate axes.

Equation (1.26) has three real roots $\varepsilon_1, \varepsilon_2, \varepsilon_3$, which are the principal extensions. The directions of fibres which experience these principal extensions are called principal directions or principal axes of strain. The extensions of these fibres are the extremal extensions of all the many fibres radiating from the same point. The principal axes are orthogonal, and there is no shearing strain between the principal fibres.

Let us consider a unit cube with edges directed along the principal axes 1, 2, 3. Since there is no shearing strain between the principal axes, the cube, after deformation, becomes a rectangular parallelepiped with edges $1 + \varepsilon_1$, $1 + \varepsilon_2$, $1 + \varepsilon_3$. The relative change in volume, bearing in mind that $\varepsilon_1, \varepsilon_2, \varepsilon_3$ are small, will be

$$\theta = \frac{\Delta V}{V} = (1 + \varepsilon_1)(1 + \varepsilon_2)(1 + \varepsilon_3) - 1 = \varepsilon_1 + \varepsilon_2 + \varepsilon_3 = J_1.$$

The quantity θ is called simply the volumetric strain. We often make use of a quantity known as the average strain (or average elongation)

$$\varepsilon = \frac{1}{3}\theta = \frac{1}{3}(\varepsilon_1 + \varepsilon_2 + \varepsilon_3).$$

Since the mass of the cube does not alter during deformation, we have that

$$\varrho_0 1 = \varrho(1 + \theta),$$

where ϱ_0 and ϱ are the densities before and after deformation. Therefore,

$$\varrho = \frac{\varrho_0}{1 + \theta} \approx \varrho_0(1 - \theta).$$

It can be shown that in order to determine the angle of rotation of any fibre, or the change in the angle between any two fibres, it is sufficient to know the six strain components (1.21) (or, what amounts to the same thing, the principal extensions and the orientation of the principal axes of strain). For this purpose we shall confine ourselves to two mutually perpendicular fibres lying in one of the principal planes. This enables us at the same time to find the directions of the maximum shearing strains.

Let us consider two mutually perpendicular fibres OC and OD (Fig. 23) in the (xy) plane, the z-axis being taken as coincident with the principal axis of strain 3, so that

$$\varepsilon_{zz} = \varepsilon_3, \quad \varepsilon_{yz} = \varepsilon_{zx} = 0,$$

Let us take the length of the fibre OC as ds and the unit vector along OC as $\boldsymbol{\nu}$. If the relative displacements (independent of the rotation of the region as a whole) of the point C and of the points A and B (the projections of the point C on the axes Ox and Oy) are defined as $\boldsymbol{\delta}_\nu$, $\boldsymbol{\delta}_x$, $\boldsymbol{\delta}_y$, then

$$\boldsymbol{\delta}_\nu = \boldsymbol{\delta}_x l + \boldsymbol{\delta}_y m,$$
$$\boldsymbol{\delta}_x = \varepsilon_{xx}\boldsymbol{i} + \varepsilon_{xy}\boldsymbol{j},$$
$$\boldsymbol{\delta}_y = \varepsilon_{xy}\boldsymbol{i} + \varepsilon_{yy}\boldsymbol{j}.$$

Since $\boldsymbol{\nu} = l\boldsymbol{i} + m\boldsymbol{j} = \boldsymbol{i}\cos\alpha + \boldsymbol{j}\sin\alpha$, then

$$\boldsymbol{\delta}_\nu = \boldsymbol{\delta}_x \cos\alpha + \boldsymbol{\delta}_y \sin\alpha.$$

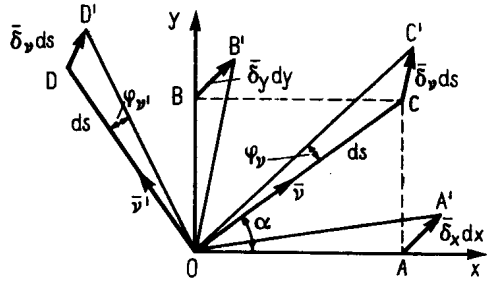

FIG. 23.

We obtain an analogous formula for the relative displacement of the end of the fibre OD by replacing α by $\alpha + \pi/2$, i.e.

$$\boldsymbol{\delta}_{\nu'} = -\boldsymbol{\delta}_x \sin\alpha + \boldsymbol{\delta}_y \cos\alpha,$$

where $\boldsymbol{\nu}' = -\boldsymbol{i}\sin\alpha + \boldsymbol{j}\cos\alpha$.

The tangent of the angle of rotation of the fibre OC is

$$\tan\varphi_\nu = \frac{\boldsymbol{\delta}_\nu ds \boldsymbol{\nu}'}{ds} = \boldsymbol{\delta}_\nu \boldsymbol{\nu}'.$$

Similarly $\tan\varphi_{\nu'} = \boldsymbol{\delta}_{\nu'}\boldsymbol{\nu}$. The shearing strain between fibres OC and OD is

$$2\varepsilon_{\nu\nu'} = \varphi_\nu + \varphi_{\nu'} \tan\varphi_\nu + \tan\varphi_{\nu'} = \boldsymbol{\delta}_\nu \boldsymbol{\nu}' + \boldsymbol{\delta}_{\nu'}\boldsymbol{\nu}$$
$$= -(\varepsilon_{xx} - \varepsilon_{yy})\sin 2\alpha + 2\varepsilon_{xy}\cos 2\alpha.$$

Taking into account also that the relative extensions of fibres OC and OD are

$$\varepsilon_\nu = \boldsymbol{\delta}_\nu \boldsymbol{\nu} = \boldsymbol{\nu}\boldsymbol{\delta}_x \cos\alpha + \boldsymbol{\nu}\boldsymbol{\delta}_y \sin\alpha,$$
$$\varepsilon_{\nu'} = \boldsymbol{\delta}_{\nu'}\boldsymbol{\nu}' = -\boldsymbol{\nu}'\boldsymbol{\delta}_x \sin\alpha + \boldsymbol{\nu}'\boldsymbol{\delta}_y \cos\alpha,$$

we get that:

$$\varepsilon_\nu = (i\varepsilon_{xx}\cos\alpha + j\varepsilon_{xy}\cos\alpha + i\varepsilon_{xy}\sin\alpha + j\varepsilon_{yy}\sin\alpha)(i\cos\alpha + j\sin\alpha)$$

$$= \frac{\varepsilon_{xx} + \varepsilon_{yy}}{2} + \frac{\varepsilon_{xx} - \varepsilon_{yy}}{2}\cos 2\alpha + \varepsilon_{xy}\sin 2\alpha.$$

As a result, we have that

$$\left.\begin{aligned} \varepsilon_\nu &= \frac{\varepsilon_{xx} + \varepsilon_{yy}}{2} + \frac{\varepsilon_{xx} - \varepsilon_{yy}}{2}\cos 2\alpha + \varepsilon_{xy}\sin 2\alpha, \\ \varepsilon_{\nu'} &= \frac{\varepsilon_{xx} + \varepsilon_{yy}}{2} - \frac{\varepsilon_{xx} - \varepsilon_{yy}}{2}\cos 2\alpha - \varepsilon_{xy}\sin 2\alpha, \\ \varepsilon_{\nu\nu'} &= -\frac{\varepsilon_{xx} - \varepsilon_{yy}}{2}\sin 2\alpha + \varepsilon_{xy}\cos 2\alpha. \end{aligned}\right\} \quad (1.27)$$

If the directions of ν and ν' are the principal axes of strain, so that $\varepsilon_{\nu\nu'} = 0$, $\varepsilon_\nu = \varepsilon_1$, $\varepsilon_{\nu'} = \varepsilon_2$, then by solving (1.27) for ε_{xx}, ε_{yy}, ε_{xy} we obtain formulae which are completely analogous to formulae (1.10) for stresses:

$$\left.\begin{aligned} \varepsilon_{xx} &= \frac{\varepsilon_1 + \varepsilon_2}{2} + \frac{\varepsilon_1 - \varepsilon_2}{2}\cos 2\alpha, \\ \varepsilon_{yy} &= \frac{\varepsilon_1 + \varepsilon_2}{2} - \frac{\varepsilon_1 - \varepsilon_2}{2}\cos 2\alpha, \\ \varepsilon_{xy} &= -\frac{\varepsilon_1 - \varepsilon_2}{2}\sin 2\alpha, \end{aligned}\right\} \quad (1.28)$$

and it can be seen that the greatest shearing strain in the principal plane (1, 2) is when $2\alpha = 90°$, i.e. it occurs between fibres forming angles of 45° to the principal axes of strain. In determining the directions of the principal axes, i.e. the angle α, we have, from the third formula of (1.27), that:

$$\tan 2\alpha = \frac{2\varepsilon_{xy}}{\varepsilon_{xx} - \varepsilon_{yy}}. \quad (1.29)$$

We see that in order to describe the deformed state in the vicinity of some point we can make use of a geometrical figure—a Mohr's circle diagram, with relative extensions as abscissae and half the shearing strains as ordinates.

From the last of formulae (1.28) we have for the principal shearing strains, that

$$\gamma_{12} = 2\varepsilon_{12} = \varepsilon_1 - \varepsilon_2,$$
$$\gamma_{23} = 2\varepsilon_{23} = \varepsilon_2 - \varepsilon_3,$$
$$\gamma_{31} = 2\varepsilon_{31} = \varepsilon_3 - \varepsilon_1,$$

where the expressions for γ_{23}, γ_{31} are derived by analogy with γ_{12}.

For the relative extension ε_ν and the rotation of the octahedral fibre η_ν, i.e. of a material element which before deformation is equally inclined to the three principal axes of strain, we get (by a similar procedure to that for the octahedral stresses) that:

$$\left.\begin{aligned} \varepsilon_\nu &= \varepsilon = \tfrac{1}{3}(\varepsilon_1 + \varepsilon_2 + \varepsilon_3), \\ \eta_\nu &= \tfrac{2}{3}\sqrt{(\varepsilon_{12}^2 + \varepsilon_{23}^2 + \varepsilon_{31}^2)}, \end{aligned}\right\} \tag{1.30}$$

so that the octahedral shearing strain γ_ν is

$$\begin{aligned} \gamma_\nu = 2\eta_\nu &= \tfrac{2}{3}\sqrt{(\gamma_{12}^2 + \gamma_{23}^2 + \gamma_{31}^2)} \\ &= \tfrac{2}{3}\sqrt{[(\varepsilon_1 - \varepsilon_2)^2 + (\varepsilon_2 - \varepsilon_3)^2 + (\varepsilon_3 - \varepsilon_1)^2]} \\ &= \tfrac{2}{3}\sqrt{[(\varepsilon_{xx} - \varepsilon_{yy})^2 + (\varepsilon_{yy} - \varepsilon_{zz})^2 + (\varepsilon_{zz} - \varepsilon_{xx})^2 + 6(\varepsilon_{yz}^2 + \varepsilon_{zx}^2 + \varepsilon_{xy}^2)]}. \end{aligned} \tag{1.31}$$

For convenience we introduce also the intensity of strain

$$\begin{aligned} \varepsilon_i &= \frac{\gamma_\nu}{\sqrt{2}} \\ &= \frac{\sqrt{2}}{3}\sqrt{[(\varepsilon_{xx} - \varepsilon_{yy})^2 + (\varepsilon_{yy} - \varepsilon_{zz})^2 + (\varepsilon_{zz} - \varepsilon_{xx})^2 + 6(\varepsilon_{yz}^2 + \varepsilon_{zx}^2 + \varepsilon_{xy}^2)]}. \end{aligned} \tag{1.32}$$

Finally, any strain can be divided into two parts: one, associated with a change of shape without change in volume—the deviator part; the other, associated only with a change in volume—the spherical part:

$$\left.\begin{aligned} &\varepsilon_{ij} = \varepsilon'_{ij} + \varepsilon''_{ij}, \\ \text{where} \quad &\varepsilon'_{ij} = \varepsilon_{ij} - \varepsilon\delta_{ij}, \quad \varepsilon''_{ij} = \varepsilon\delta_{ij}. \end{aligned}\right\} \tag{1.33}$$

In other words the strain tensor is in fact the sum of a spherical tensor and a strain deviator.

7. The Work done by Internal Forces

The internal mechanical state of a body is described by the stresses and strains at all points in it. The former depend on the internal forces of interaction between the particles, and the latter on the displacements of these particles. The additional forces of internal interaction between elementary particles of the material, which arise during the deformation, do work in the displacements of these particles. This work can be expressed in terms of stresses and strains which can be looked upon as generalized forces and generalized displacements respectively.

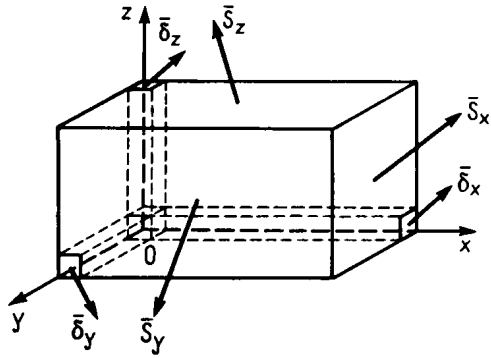

Fig. 24.

Let us consider a unit cube inside the body with edges parallel to the coordinate axes (Fig. 24). At a certain instant of time t the stresses on its faces will be $\boldsymbol{S}_x$, $\boldsymbol{S}_y$, $\boldsymbol{S}_z$ and the relative displacements of fibres lying along the axes will be $\boldsymbol{\delta}_x$, $\boldsymbol{\delta}_y$, $\boldsymbol{\delta}_z$. After a time dt these displacements will receive the following increments:

$$\Delta\boldsymbol{\delta}_x = \frac{\partial\boldsymbol{\delta}_x}{\partial t}dt, \quad \Delta\boldsymbol{\delta}_y = \frac{\partial\boldsymbol{\delta}_y}{\partial t}dt, \quad \Delta\boldsymbol{\delta}_z = \frac{\partial\boldsymbol{\delta}_z}{\partial t}dt.$$

The changes in the stress vectors can be neglected, since in the expressions for the work done in the increments in the displacements, the increments in the stresses would give terms of a higher order of smallness. Referring the vectors $\Delta\boldsymbol{\delta}_x, \Delta\boldsymbol{\delta}_y, \Delta\boldsymbol{\delta}_z$ to the centres of corresponding faces of the cube, we obtain for the increment of work, the expression

$$\Delta W = \boldsymbol{S}_x\Delta\boldsymbol{\delta}_x + \boldsymbol{S}_y\Delta\boldsymbol{\delta}_y + \boldsymbol{S}_z\Delta\boldsymbol{\delta}_z$$

(the sum of the scalar products of the force vectors with the displacement vectors of their points of application), or, since $\boldsymbol{S}_i = \sigma_{ix}\boldsymbol{i} + \sigma_{iy}\boldsymbol{j} + \sigma_{iz}\boldsymbol{k}$ and $\Delta\boldsymbol{\delta}_i = \Delta\varepsilon_{ix}\boldsymbol{i} + \Delta_{iy}\boldsymbol{j} + \Delta\varepsilon_{iz}\boldsymbol{k}$ and since $\Delta\varepsilon_{ij} = \Delta\varepsilon_{ji}$ and $\sigma_{ij} = \sigma_{ji}$, by multiplying out and collecting similar terms, we get that

$$\Delta W = \sigma_{xx}\Delta\varepsilon_{xx} + \sigma_{yy}\Delta\varepsilon_{yy} + \sigma_{zz}\Delta\varepsilon_{zz} + 2\sigma_{yz}\Delta\varepsilon_{yz} + 2\sigma_{zx}\Delta\varepsilon_{zx} + 2\sigma_{xy}\Delta\varepsilon_{xy} = \sum_{i,j=1}^{3}\sigma_{ij}\Delta\varepsilon_{ij} \tag{1.34}$$

We can explain this result by an example of plane deformation. Let us consider a square in the (xy) plane with side of unit length (Fig. 25). The shearing strain can be represented as that due to

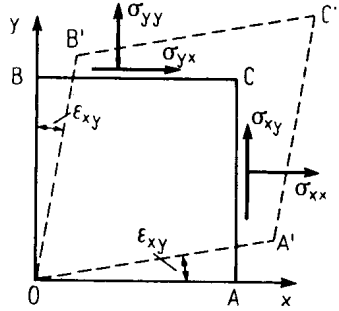

FIG. 25.

rotations of fibres OA and OB through equal angles ε_{xy}. If we consider unit thickness in the z-direction, the stresses will be numerically equal to the resultant forces applied to the sides. Let us consider the work done by each force. The force σ_{xx} does work in the displacements in the direction of the axis Ox; therefore the work associated with this stress component is $\sigma_{xx}\Delta\varepsilon_{xx}$. In the same way the stress component σ_{yy} is associated with a work $\sigma_{yy}\Delta\varepsilon_{yy}$. Due to the shearing strain of the side AC (in this case upwards) the force σ_{xy} does work, and due to the shear strain of the face BC (to the right) the force σ_{yx} does work, so that the work due to shear is $\sigma_{xy}\Delta\varepsilon_{xy} + \Delta\varepsilon_{yx}\sigma_{yx}$ or, since $\sigma_{yx} = \sigma_{xy}$, this work is $2\sigma_{xy}\Delta\varepsilon_{xy}$.

During a time t the work done on unit volume will be

$$W = \int_0^t (\boldsymbol{S}_x\Delta\boldsymbol{\delta}_x + \boldsymbol{S}_y\Delta\boldsymbol{\delta}_y + \boldsymbol{S}_z\Delta\boldsymbol{\delta}_z),$$

and the work done by the internal forces throughout the whole body during time t will be

$$V = \iiint W \, dx \, dy \, dz.$$

Since the stress and strain tensors can be represented in the form of spherical tensors and deviators it is expedient to divide the work into that done in changing the volume of the body, and that done in changing the shape of the body without change of volume. Substituting in formula (1.34) $\sigma_{ij} = \sigma'_{ij} + \sigma''_{ij}$ and $\varepsilon_{ij} = \varepsilon'_{ij} + \varepsilon''_{ij}$ we get that

$$\begin{aligned} \Delta W &= \sum_{i,j=1}^{3} (\sigma'_{ij} + \sigma''_{ij})(\Delta\varepsilon'_{ij} + \Delta\varepsilon''_{ij}) \\ &= \sum_{i,j=1}^{3} \sigma'_{ij} \Delta\varepsilon'_{ij} + \sum_{i,j=1}^{3} \sigma''_{ij} \Delta\varepsilon''_{ij} + \sum_{i,j=1}^{3} \sigma'_{ij} \Delta\varepsilon''_{ij} + \sum_{i,j=1}^{3} \sigma''_{ij} \Delta\varepsilon'_{ij} \\ &= \sum_{i,j=1}^{3} \sigma'_{ij} \Delta\varepsilon'_{ij} + 3\sigma \Delta\varepsilon + \Delta\varepsilon \sum_{i=1}^{3} \sigma'_{ii} + \sigma \sum_{i=1}^{3} \Delta\varepsilon'_{ii}. \end{aligned}$$

Since $$\sum_{i=1}^{3} \sigma'_{ii} = 0 \quad \text{and} \quad \sum_{i=1}^{3} \varepsilon'_{ii} = 0,$$

$$\Delta W = \Delta W_i + \Delta W_\theta,$$

where $$\Delta W_i = \sum_{i,j=1}^{3} \sigma'_{ij} \Delta\varepsilon'_{ij} \tag{1.35}$$

is the element in the work done in changing the shape of the body, and

$$\Delta W_\theta = 3\sigma \Delta\varepsilon = \sigma \Delta\theta \tag{1.36}$$

is the element in the work done in changing the volume.

Examples. **1.** *Simple Uniaxial Tension or Compression.* Let us suppose that the state of stress at every point in the body is given by the components

$$\sigma_{xx} = \sigma_1, \quad \sigma_{yy} = \sigma_{zz} = \sigma_{yz} = \sigma_{zx} = \sigma_{xy} = 0.$$

This state of stress occurs in cylindrical bodies (rods) subjected to uniform tension or compression (depending on the sign of σ_1) in the direction of the axis, which we have taken as the axis Ox. We note that the axis Ox is here a principal axis. Any direction perpendicular to the axis Ox is also a principal axis, since $\sigma_2 = \sigma_3 = 0$.

Let us find the increment in the work; from formula (1.34) we have that:

$$\Delta W = \sigma_{xx} \Delta\varepsilon_{xx}$$

(we note that ε_{yy} and ε_{zz} are not zero, but their increments do not appear in the expression for the work since $\sigma_{yy} = \sigma_{zz} = 0$). If we put $\varepsilon_{xx} = \varepsilon_1$, the work done by the internal forces per unit volume after a time t, during which the strain ε_{xx} increases from zero to ε_1, is

$$W = \int_0^{\varepsilon_1} \sigma_1 \, d\varepsilon_1 .$$

If the longitudinal stress σ_1 is a single-valued function of the strain ε_1, the work done per unit volume is given by the area under the $\sigma_1 \sim \varepsilon_1$ curve (Fig. 26).

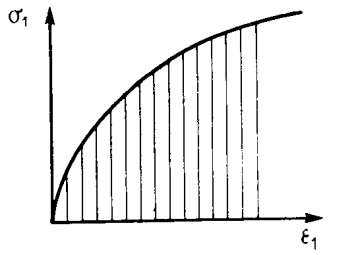

FIG. 26.

2. *Hydrostatic Uniform Tension (or Compression).* Let us suppose that the state of stress at every point in the body is given by the components

$$\sigma_{xx} = \sigma_{yy} = \sigma_{zz} = \sigma, \quad \sigma_{yz} = \sigma_{zx} = \sigma_{xy} = 0.$$

This state of stress occurs in bodies subjected to an all-round (hydrostatic) pressure $p = -\sigma$. The axes Ox, Oy, Oz are in this case principal axes (since $\sigma_{yz} = \sigma_{zx} = \sigma_{xy} = 0$). Moreover, any other axis will also be a principal axis. For in the equations for the principal directions

$$\begin{aligned}
(\sigma_{xx} - \sigma')\, l + \sigma_{xy} m + \sigma_{xz} n &= 0, \\
\sigma_{yx} l + (\sigma_{yy} - \sigma')\, m + \sigma_{yz} n &= 0, \\
\sigma_{zx} l + \sigma_{zy} m + (\sigma_{zz} - \sigma')\, n &= 0
\end{aligned}$$

the coefficients in the diagonal terms are zero, since σ' must be replaced by one of the principal stresses, i.e. always by σ, and a condition of the problem is that $\sigma_{xx} = \sigma_{yy} = \sigma_{zz} = \sigma$. The coefficients of the other terms must also be zero, i.e. the direction cosines of the principal directions l, m, n are indeterminate. The stress deviator is zero: $\sigma'_{ij} = 0$. Therefore

$$\Delta W_i = \sum_{i,j=1}^{3} \sigma'_{ij} \Delta \varepsilon'_{ij} = 0,$$

$$\Delta W = \Delta W_0 = \sigma \Delta \theta .$$

During a time t the work done by the internal forces per unit volume is

$$W = \int_0^{\theta} \sigma \, d\theta = \frac{1}{\varrho_\theta} \int_{\varrho_\theta}^{\varrho} p \, d\varrho,$$

where ϱ_0 and ϱ are the densities before deformation and at time t. In solid bodies, as well as in gases, the pressure depends on the density and temperature.

3. *Plane Shear Strain.* Suppose that the conditions at some point in the body are given by the strain components

$$\varepsilon_{xy} = \tfrac{1}{2}\gamma \neq 0, \quad \varepsilon_{xx} = \varepsilon_{yy} = \varepsilon_{zz} = \varepsilon_{yz} = \varepsilon_{zx} = 0.$$

This state of deformation is called pure shear. The increment in the work done per unit volume is

$$\Delta W = \Delta W_i + \Delta W_\theta,$$

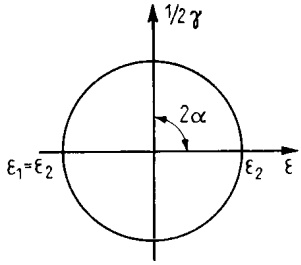

FIG. 27.

and in this particular case

$$\Delta W_i = 2\sigma_{xy} \Delta\varepsilon_{xy} = \tau \Delta\gamma, \quad \Delta W_\theta = 0,$$

since $\varepsilon_{xx} = \varepsilon_{yy} = \varepsilon_{zz} = 0$; τ is defined as the shearing stress σ_{xy}. If the relation $\tau \sim \gamma$ is known for pure shear, then the work done by the internal forces per unit volume during a time t is

$$W = \int_0^{\gamma} \tau \, d\gamma.$$

By definition of state of pure shear, one of the principal extensions (in our case ε_3) is zero. The other principal strains are equal in magnitude and opposite in sign. For, as follows from formulae (1.28), in this case the abscissa of the centre of the Mohr's circle (Fig. 27) is

$$\frac{\varepsilon_1 + \varepsilon_2}{2} = \frac{\varepsilon_{xx} + \varepsilon_{yy}}{2} = 0,$$

i.e. it is at the origin of coordinates and therefore $\varepsilon_1 = -\varepsilon_2$. The radius of the Mohr's circle is $(\varepsilon_1 - \varepsilon_2)/2 = \varepsilon_{xy} - \frac{1}{2}\gamma$ since, from (1.29), $2\alpha = \pi/2$. Therefore $-\varepsilon_1 = +\varepsilon_2 = \gamma$, and the shearing strain γ in the (xy) plane is a maximum.

8. External Forces

The state of stress and strain in a body arises due to external influences. It should be noted that these external influences need not necessarily be forces. They might take the form, for instance, of a non-uniform temperature increase in the body which leads to a non-uniform temperature strain which gives rise to so-called thermal stresses. They might also take the form of stresses which arise during the solidification process of the metal, during which, as a result of the interaction of the newly formed grains and the matrix, there occur so-called initial stresses.

The external forces acting on the body can be divided into two types:

(1) Surface forces acting on the boundary of the body from the surrounding medium, and (2) mass forces (or body forces), acting in general at all points within the body. Both types can be continuous or step-continuous functions of the coordinates of a point (and of time).

Examples of surface forces are the forces due to water and wind pressure and contact forces due to the interaction between the body considered and other bodies.

In introducing the concept of stresses we made use of the method of sections. The surface of a body, its boundary with the surrounding medium, can also be considered as a section and we can talk of external stresses applied to the body and arising due to the effect of the surface forces. If $\boldsymbol{\nu}$ is the external normal to the surface of a body at some point, we can write for the stress vector acting on an element of the area of the surface containing this point the expression

$$\boldsymbol{T}_\nu = T_x\boldsymbol{i} + T_y\boldsymbol{j} + T_z\boldsymbol{k},$$

where $\boldsymbol{T}_\nu$ has the dimensions of a stress $[\boldsymbol{T}_\nu] = \text{kg/cm}^2$ and is a function of the coordinates of the point on the surface of the body. From the equilibrium conditions we see that if we take a section in the body in a surface parallel and very close to the surface of the body, i.e. if we take a very thin layer of the body bounded by its surface and the surface of this section, then the vector of the internal stresses (acting on the layer from the side of the section) will be equal to the vector of the stress which is applied from outside:

$$\boldsymbol{S}_\nu = \boldsymbol{T}_\nu.$$

In terms of the projections on the axes, this relation can be written in the form

$$\left.\begin{aligned} \sigma_{xx}l + \sigma_{xy}m + \sigma_{xz}n &= T_x, \\ \sigma_{yx}l + \sigma_{yy}m + \sigma_{yz}n &= T_y, \\ \sigma_{zx}l + \sigma_{zy}m + \sigma_{zz}n &= T_z. \end{aligned}\right\} \tag{1.37}$$

These expressions, which are analogous to (1.7), establish the three relations on the surface of the body between the six components of the internal stresses, which are usually unknown functions, and the external surface forces applied to the body, which are given functions. We see then that the problem of finding the internal stresses even on the surface is statically indeterminate.

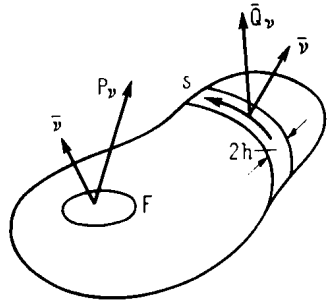

FIG. 28.

It sometimes happens that the surface forces are distributed over a narrow strip on the surface of the body, the width of which $2h$ is small compared with the characteristic dimension of the body (Fig. 28). The exact nature of the distribution of the external stresses over the width of the strip is then of little importance and only their integral over the length of the strip is important. The stress distributed over the strip can then be replaced by a force distributed over the centre line of the strip s:

$$\boldsymbol{Q}_\nu = \int_{-h}^{+h} \boldsymbol{T}_\nu \, dh = \boldsymbol{Q}_\nu(s);$$

where $[\boldsymbol{Q}_\nu] =$ kg/cm.

In cases when the external stress is applied only to a small area F of the surface of the body (for example in the case of a contact force applied to a small area), it is often important to know only

the resultant vector and not the exact nature of the distribution of the external stresses. The distributed stresses can then be replaced by a concentrated force

$$\boldsymbol{P}_{\nu} = \iint_{F} \boldsymbol{T}_{\nu}\, dF,$$

where $[\boldsymbol{P}_{\nu}]$ = kg. It should be remembered, however, that in actual fact a force always acts over an area of finite dimensions and the assumption of a concentrated force is a device which can only give correct values to the internal stresses at sufficient distance from the point or line of application of concentrated forces of the type $\boldsymbol{P}_{\nu}$.

9. Examples of Surface Forces

(a) A Dam. If we consider a section of a dam in a plane perpendicular to its axis, and if we take the x-axis in the surface of the water in the upstream direction, and the z-axis vertically downwards, then in the case of a dam with a vertical upstream face ($\boldsymbol{\nu} = \boldsymbol{i}$) (Fig. 29), we would have that:

$$\boldsymbol{T}_{\nu} = \boldsymbol{T}_{x} = T_{x}\boldsymbol{i} = -p\boldsymbol{i},$$

where $p = \varrho g z$, and ϱ is the density of water, g is the acceleration due to gravity, so that

$$T_{x} = -p = -\varrho g z,$$
$$T_{y} = T_{z} = 0.$$

(b) A Ship. Let us consider a section of a ship in a plane perpendicular to the axis of the ship at a place where the hull is almost

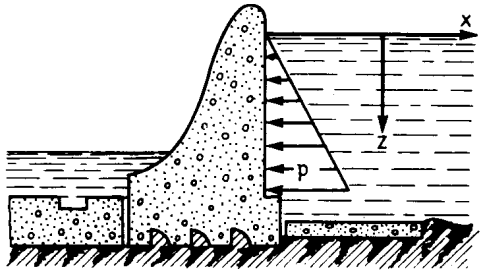

Fig. 29.

cylindrical. The pressure from the water increases linearly with the depth and is always normal to the surface of the ship (Fig. 30). If we take the directions of the axes as in the previous case, we will have that:

$$T_\nu = -p\boldsymbol{\nu} = -p(\boldsymbol{i}\cos\varphi + \boldsymbol{k}\sin\varphi),$$
$$T_x = -\varrho gz\cos\varphi, \quad T_y = 0, \quad T_z = -\varrho gz\sin\varphi.$$

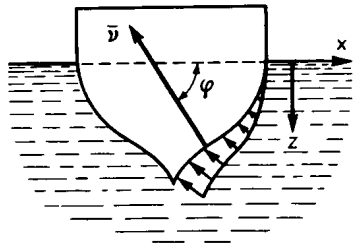

FIG. 30.

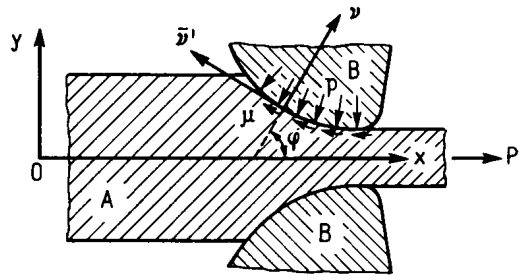

FIG. 31.

(c) Drawing a Strip of Metal through a Die. The metal strip A is drawn by the force P through the die B (Fig. 31). In this case, in order to investigate the stresses in the strip we represent the action of the die (that is a passive force in this case) on the surface of the strip by surface forces: a force due to pressure and a force due to dry friction. We will take the x-axis as in the direction in which the strip moves, and the y-axis will be taken as vertically upwards. The pressure acts at right angles to the surface and is a function of the coordinate x (since the equation of the boundary of the die cross-section $y = f(x)$ is known). The friction force acts along the tangent to the surface of the strip in a direction opposite to the movement, and is also a function of the coordinate x. If the pressure is p, then the friction force per unit area is μp, where μ is the coefficient of friction. If $\boldsymbol{\nu}$ and $\boldsymbol{\nu}'$ are the

unit vectors of the normal and tangent at some point M on the surface, then

$$\boldsymbol{T}_\nu = -p\boldsymbol{\nu} + \mu p\boldsymbol{\nu}';$$

since

$$\boldsymbol{\nu} = \boldsymbol{i}\cos\varphi + \boldsymbol{j}\sin\varphi,$$

$$\boldsymbol{\nu}' = -\boldsymbol{i}\sin\varphi + \boldsymbol{j}\cos\varphi,$$

then

$$T_x = -p(\cos\varphi + \mu\sin\varphi),$$

$$T_y = -p(\sin\varphi - \mu\cos\varphi).$$

10. Body Forces

Due to gravitational affects when a body under consideration is situated in the field of gravity, and due to inertia and electromagnetic forces, etc., there can arise external forces which act on every part of the volume of the body. A force of this type referred to unit mass of the body is called a mass force; and when referred to unit volume of the body it is called a body force.

If the resultant vector of forces of this type acting on an element of volume Δv having a mass $\Delta m = \varrho\,\Delta v$ (ϱ is the density) is $\Delta\boldsymbol{R}$, then $\boldsymbol{R} = \lim_{\Delta v \to 0} \Delta\boldsymbol{R}/\Delta m$ is the vector of the mass force at the point to which the volume Δv reduces, and

$$\varrho\boldsymbol{R} = \lim_{\Delta v \to 0} \frac{\Delta\boldsymbol{R}}{\Delta v} = \varrho R_x\boldsymbol{i} + \varrho R_y\boldsymbol{j} + \varrho R_z\boldsymbol{k} \tag{1.38}$$

is the vector of the body force at the point to which the volume reduces, their dimensions being

$$[\boldsymbol{R}] = \text{cm/sec}^2, \quad [\varrho R] = \text{kg/cm}^3.$$

Mass or body forces are sometimes distributed, not throughout the volume of the body, but only over a part of it in the form of a layer of thickness $2h$, which is small compared with the dimensions of the body. Their exact distribution over the thickness of the layer is then often of no importance; in this case if $\boldsymbol{\nu}$ is the normal to some central surface of the layer we have that the force $\boldsymbol{Q}_\nu = \int_{-h}^{+h} \boldsymbol{R}\,dv$, or $\varrho\boldsymbol{Q}_\nu = \int_{-h}^{+h} \varrho\boldsymbol{R}\,dv$, where $\boldsymbol{Q}_\nu$ is a function of the coordinates of a point on the central surface of the layer, the dimensions of $\boldsymbol{Q}_\nu$ and $\varrho\boldsymbol{Q}_\nu$ being $[\boldsymbol{Q}_\nu] = \text{cm}^2/\text{sec}^2$, $[\varrho\boldsymbol{Q}_\nu] = \text{kg/cm}^2$, i.e. in the latter case the dimension of a stress.

This case is met with, for example, in the theory of plates, when we are not concerned with the distribution of the force over the thickness of the plate, but with the force which is applied per unit area of the plate in plan.

Sometimes mass forces act only on a part of the body which can be in the form of a cord with cross-section F the dimensions of which are small compared with the dimensions of the body (Fig. 32), and the exact distribution of forces over the cross-section of the cord is of no interest to us. We then consider the forces

$$\boldsymbol{Q}_S = \int\int_F \boldsymbol{R}\, dF \quad \text{or} \quad \varrho \boldsymbol{Q}_S = \int\int_F \varrho \boldsymbol{R}\, dF,$$

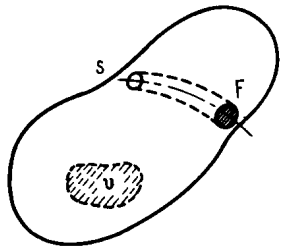

FIG. 32.

which are functions of a point on the axial line S of the tube. Their dimensions are

$$[\boldsymbol{Q}_S] = \text{cm}^3/\text{sec}^2, \quad [\varrho \boldsymbol{Q}_S] = \text{kg/cm}.$$

Such a force distributed along a line is considered, for example, in examining a beam under the action of its own weight, when we require to know only the weight applied per unit length of the beam and not the exact distribution of the weight over the cross-section of the beam.

Finally, it might happen that the mass forces act only on a small volume v within the body (Fig. 32) and that the dimensions of this volume are small compared with the dimensions of the body, when only the integral effect of these forces is important. We then consider a concentrated force

$$\boldsymbol{Q}_v = \iiint_v \boldsymbol{R}\, dV \quad \text{or} \quad \boldsymbol{P} = \varrho \boldsymbol{Q}_v,$$

and their dimensions are respectively

$$[\boldsymbol{Q}_v] = \text{cm}^4/\text{sec}^2, \quad [\boldsymbol{P}] = \text{kg}.$$

Whether or not we are able replace the exact distribution of forces by their integral effects depends on the particular conditions of each specific problem.

11. Examples of Mass Forces

(a) The force of gravity. If we take the z-axis as vertically downwards then $\boldsymbol{R} = g\boldsymbol{k}$, so that

$$R_x = R_y = 0, \quad R_z = g, \quad \varrho R_z = \varrho g = \gamma,$$

where γ is the specific weight.

(b) Centrifugal forces in a rotating disc. Let us suppose that a disc of thickness $2h$ is rotated about its axis z at a constant angular velocity ω. The centripetal acceleration in a radial direction is $j_r = -r\omega^2$, and the acceleration in a circumferential direction is zero, $j_\varphi = 0$. If $\boldsymbol{r}_0$ and $\boldsymbol{s}_0$ are the unit vectors in radial and circumferential directions, then $\boldsymbol{R} = -j_r\boldsymbol{r}_0$, i.e.

$$R_r = r\omega^2, \quad R_q = R_z = 0; \quad \varrho R_r = \varrho r\omega^2.$$

The mean mass force through the thickness of the disc is

$$\boldsymbol{Q}_r = \int_{-h}^{+h} \boldsymbol{R}\, dz = 2hr\omega^2\boldsymbol{r}_0,$$

where $h = h(r, q)$ and $\boldsymbol{Q}_r = \boldsymbol{Q}_r(r, \varphi)$.

(c) The self weight of a horizontal beam. If the y-axis is in an upward vertical direction, then

$$\boldsymbol{R} = -g\boldsymbol{j}, \quad R_x = R_z = 0, \quad R_y = -g.$$

The mean mass force over the area of cross-section is $\boldsymbol{Q}_S = -Fg\boldsymbol{j}$, and the mean body force is $\varrho\boldsymbol{Q}_S = -\varrho gF\boldsymbol{j}$, so that

$$q = \varrho Q_{Sy} = \varrho gF.$$

12. Equilibrium Conditions and the General Method for Finding Stresses, Strains, and Displacements in a Body

Let us suppose that the body is under the action of a given set of surface and body forces (Fig. 33):

$$\boldsymbol{T}_v = T_x\boldsymbol{i} + T_y\boldsymbol{j} + T_z\boldsymbol{k},$$
$$\varrho\boldsymbol{R} = \varrho R_x\boldsymbol{i} + \varrho R_y\boldsymbol{j} + \varrho R_z\boldsymbol{k}.$$

For the body to be in equilibrium the resultant vector and the resultant moment of all external forces (including the reactions of restraints if they exist) must vanish:

$$\left.\begin{aligned} \iint_F \boldsymbol{T}_\nu \, dF + \iiint_V \varrho \boldsymbol{R} \, dv = 0, \\ \iint_F \boldsymbol{T}_\nu \times \boldsymbol{r} \, dF + \iiint_V \varrho \boldsymbol{R} \times \boldsymbol{r} \, dv = 0, \end{aligned}\right\} \tag{1.39}$$

where F is the surface area and V is the volume of the whole body. If the conditions were not satisfied the body would not only have an internal movement of particles associated with strains, but it

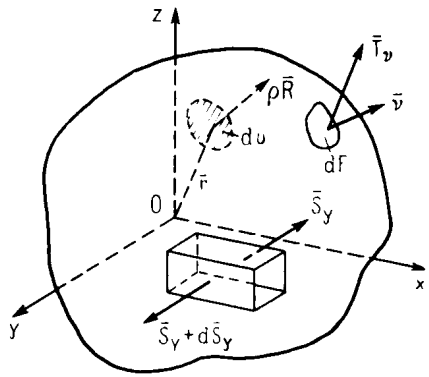

FIG. 33.

would also accelerate in space. We will consider, therefore, that these conditions are satisfied identically, or that limitations are imposed on the reactions of the restraints, if they exist.

A necessary and sufficient condition for the equilibrium of a body is that every internal part of the body, including elements on its surface, is in equilibrium. Consequently, for any volume V within the body bounded by some surface F, the relations (1.39) must be satisfied in which $\boldsymbol{T}_\nu$ must be replaced by $\boldsymbol{S}_\nu$—the stress vector on an element of area of the surface F. On the bounding surface of the body the relation between the internal forces (stresses) and the external surface forces, which was dealt with in § 8, is of the form

$$\boldsymbol{S}_\nu \equiv \boldsymbol{S}_x l + \boldsymbol{S}_y m + \boldsymbol{S}_z n = \boldsymbol{T}_\nu. \tag{1.40}$$

Let us consider an elementary parallelepiped within the body with edges dx, dy, dz (see Fig. 33). The forces acting on unit area of the faces normal to the axis Oy are shown in the figure; their resultant is $(\partial \boldsymbol{S}_y/\partial y)\, dy\, dx\, dz$. Taking similar expressions for the resultant forces acting on the other faces, and taking into account the effect of mass forces, we obtain the equilibrium condition in the form

$$\frac{\partial \boldsymbol{S}_x}{\partial x} + \frac{\partial \boldsymbol{S}_y}{\partial y} + \frac{\partial \boldsymbol{S}_z}{\partial z} + \varrho \boldsymbol{R} = 0. \tag{1.41}$$

It can be shown that the condition (1.39) can be derived from (1.40) and (1.41).

It is known from theoretical mechanics that the equilibrium conditions for a body (or for any volume within the body) can be written in the form of a Lagrange variational equation:

$$\Delta V \equiv \iiint_v \Delta W \, dv \equiv \iiint_v (\boldsymbol{S}_x \Delta \boldsymbol{\delta}_x + \boldsymbol{S}_y \Delta \boldsymbol{\delta}_y + \boldsymbol{S}_z \Delta \boldsymbol{\delta}_z)\, dv = \Delta' A, \tag{1.42}$$

where $\Delta' A$ is the elementary work done by the external forces and $\Delta \boldsymbol{\delta}_x, \Delta \boldsymbol{\delta}_y, \Delta \boldsymbol{\delta}_z$ refer to the displacements $\Delta \mathfrak{D}$ which must be compatible with the restraints (internal or external) made to the body. Such displacements are called kinematically admissible.

If, as is usually the case, the external forces acting on the body—mass and surface forces—are given, and it is required to find the stresses in the body, i.e. the three vector functions $\boldsymbol{S}_x$, $\boldsymbol{S}_y$, $\boldsymbol{S}_z$, then we have one differential eqn. (1.41) with the boundary condition (1.40) or their equivalent variational eqn. (1.42). Thus the equations of statics give only one equation for the relation between the three functions $\boldsymbol{S}_x$, $\boldsymbol{S}_y$, $\boldsymbol{S}_z$, i.e. the problem of finding the internal stresses in a body is statically indeterminate. This is understandable, since so far we have considered entirely independently internal stresses and internal strains. In actual fact the internal forces of interaction (stresses) between the particles of real bodies depend on the change in position of these particles relative to one another, for example, on the change in distance between the atoms, i.e. there are relations between the stresses and strains which impose additional conditions on the stresses, since the displacements in a medium (continuum) must be continuous functions of the coordinates.

13. Problems for Solution on Chapter I

1. A boiler of diameter 2 m and length 5 m is subjected to an internal pressure of 12 atm. Find the principal tensile stresses in the cylindrical part of the walls of the boiler, the greatest shearing stresses and the octahedral stresses, if the thickness of the wall of the boiler is 1 cm. The radial compressive stresses in the wall can be neglected.

2. At every point in a body

$$\sigma_{xx} = 0, \quad \sigma_{yy} = 300 \text{ kg/cm}^2, \quad \sigma_{zz} = 100 \text{ kg/cm}^2,$$
$$\sigma_{yz} = 100\sqrt{3} \text{ kg/cm}^2, \quad \sigma_{zx} = \sigma_{xy} = 0.$$

Find the orientation of the principal axes of stress, the magnitudes of the principal stresses, of the octahedral stresses and the maximum shearing stresses.

3. Compare the following two states of plane stress (by the exact and approximate methods):

(1) $\sigma_{xx} = 5, \quad \sigma_{yy} = -1, \quad \sigma_{xy} = -3\sqrt{3}, \quad \sigma_{yz} = \sigma_{zx} = \sigma_{zz} = 0;$

(2) $\sigma_{xx} = 2, \quad \sigma_{yy} = 2, \quad \sigma_{xy} = 6, \quad \sigma_{yz} = \sigma_{zx} = \sigma_{zz} = 0.$

4. A cylindrical rod of cross-sectional area 2 cm^2 is subjected to a tensile force along its axis of 1·2 ton. Find the maximum shearing stresses and the orientation of the surfaces on which they act. Find the octahedral stresses.

5. At a point in a body

$$\sigma_{xx} = 500 \text{ kg/cm}^2, \quad \sigma_{yy} = 0, \quad \sigma_{zz} = -300 \text{ kg/cm}^2,$$
$$\sigma_{yz} = -750 \text{ kg/cm}^2, \quad \sigma_{zx} = 800 \text{ kg/cm}^2, \quad \sigma_{xy} = 500 \text{ kg/cm}^2.$$

Find the normal, shearing and resultant stresses on an area, the direction cosines of the normal to which are

$$l = \frac{1}{2}, \quad m = \frac{1}{2}, \quad n = \frac{1}{\sqrt{2}}.$$

6. The principal stresses are

$$\sigma_1 = 500 \text{ kg/cm}^2, \quad \sigma_2 = -500 \text{ kg/cm}^2, \quad \sigma_3 = 750 \text{ kg/cm}^2.$$

Find the normal, shearing and resultant stresses on an octahedral plane. Compare the magnitude of the octahedral shearing stress with the maximum shearing stress. Construct the Mohr's circle diagram.

7. Compare the two states of stress (by the exact and approximate methods):

(1) $\sigma_{xx} = 11, \quad \sigma_{yy} = 1, \quad \sigma_{zz} = 3, \quad \sigma_{yz} = \sigma_{zx} = \sigma_{xy} = 0;$

(2) $\sigma_{xx} = 9, \quad \sigma_{yy} = 3, \quad \sigma_{zz} = 3, \quad \sigma_{yz} = \sigma_{xy} = 0, \quad \sigma_{zx} = 4.$

8. At a point in a body

$$\varepsilon_{xx} = 0{\cdot}001, \quad \varepsilon_{yy} = -0{\cdot}0005, \quad \varepsilon_{zz} = 0{\cdot}0005,$$
$$2\varepsilon_{yz} = 0{\cdot}001, \quad 2\varepsilon_{zx} = -0{\cdot}0008, \quad 2\varepsilon_{xy} = 0{\cdot}003.$$

Find the principal extensions and the principal strain directions. Check that the principal axes are mutually perpendicular.

9. Show that the strains

$$\varepsilon_{xx} = 0{\cdot}0005, \qquad \varepsilon_{yy} = -0{\cdot}000375, \quad \varepsilon_{zz} = -0{\cdot}000125,$$

$$2\varepsilon_{yz} = 0{\cdot}00025\sqrt{3}, \quad 2\varepsilon_{zx} = 0{\cdot}0005\sqrt{3}, \quad 2\varepsilon_{xy} = -0{\cdot}0015$$

correspond to a state of plane deformation, of pure shear.

10. Derive formulae (1.30) for extensions and rotations of an octahedral fibre (its direction cosines being $l = m = n = 1/\sqrt{3}$).

11. Write down the condition (1.41) in the form of equations containing the components σ_{ij} of the stress tensor and the components X, Y, Z of the mass forces along the coordinate axes.

CHAPTER II

ELASTO-PLASTIC DEFORMATION OF RODS

1. The Mechanical Properties of Various Materials

The internal forces, stresses, which we considered in the preceding section are related to the change in the relative positions of elementary particles (atoms, ions) which takes place due to external influences (external forces—body and surface forces, and temperature). The stresses, therefore, have a functional relation with the strains which occur due to the action of external forces on the body. This relation can be conveniently expressed in the form of a relation between the stress and strain tensors:

$$(\sigma_{ij}) = \Phi(\varepsilon_{ij}).$$

To determine this relation and to find the stresses and strains which occur for a given external loading is a fundamental problem in the mechanics of a continuous media.

The relation between the stresses and strains in a body can be found in principle by a study of the atomic structure of the material and the laws of interaction between elementary particles. There are, however, serious difficulties in this method, not only for a polycrystalline body having a complex structure, but even for a monocrystal. These difficulties have not as yet been fully overcome and different suppositions exist for numerous questions on the mechanism of deformation which to some extent explain different aspects of the process of deformation and the occurrence of internal forces of interaction, but so far no reliable quantitative relations have been found by this method.

In mechanics, therefore, the relation between stresses and strains is found as a statistically mean characteristic by experiments on bodies of relatively large dimensions. These experiments, however, are accompanied by serious difficulties which must be overcome.

One of these is that the measuring equipment in existence until very recently did not enable us to measure mechanical quantities (stresses, strains) inside a body. It was only possible to measure the relative displacements of particle situated on the surface of the body under investigation (the specimen). As regards stresses, since we have no means of measuring them directly, we must be content with making an estimate of their magnitude on the basis of the total force acting on the body (when this is possible), or by measuring certain physical properties of the material (which forms the basis of, for example, the optical method of measuring stresses, which will be dealt with later), or finally, from the relative movement of particles, i.e. by the strains, if the relation between stresses and strains has already been found by one of the previous methods.

In order to overcome these difficulties in investigating the properties of materials, the experiments are so arranged, the specimens so shaped and the loads applied in such a way that we can be reasonably certain that the state of stress and strain at all points in the part of the body under investigation is uniform. In this way, by measuring the strains on the surface of the body, we can obtain an estimate of the strains within the body, and by measuring the resultant external forces we can estimate the stresses in the body. In so doing it is assumed that the body is homogeneous, continuous, and before deformation isotropic (quasi-isotropic). This is the case, for example, for a thin wire in tension, when the stresses can be considered to be equal at all cross-sections and at all points on the cross-section, so that in order to find their magnitude we need only divide the tensile force by the cross-sectional area. There are cases when, for example, in a thin-walled cylinder with a torque applied at its ends, the shearing stresses at every cross-section and at all points of each cross-section are equal and can therefore be evaluated from the magnitude of the torque, which can easily be measured.

Experiments on the behaviour of cylindrical specimens in tension and compression can be used to illustrate important characteristic properties of a material. For various groups of materials typical standard dimensions and shapes of specimens have been established in an effort to standardize certain experiments. For plastic metals (iron, steel, copper, aluminium, nickel, etc.), a long specimen of circular section is used. The central part of the cylindrical specimen is called the working portion or gage length (Fig. 34), and allmeasure-

ments, (longitudinal extensions, changes in diameter) are taken within this portion; its length l should be 5–10 times greater than the diameter d. This allows us to assume a state of uniform stress and strain at least near the centre of the gage length. The ends of the specimen, which are connected to the jaws of the testing machine, are thickened and sometimes threaded. The state of stress and strain in the thickened ends is not uniform and this non-uniformity extends a little way into the gage length of the specimen.

The tensile or compressive force transmitted by the jaws of the testing machine to the specimen is measured by a manometer (in machines with hydraulic loading), by the position of the weights on a lever balance (in machines of the lever type) or by some

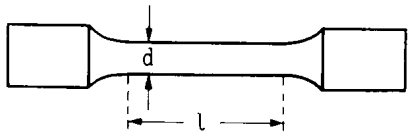

FIG. 34.

other means. In some cases a load is applied simply by hanging weights on the specimen. In compression tests short prismatic specimens are used ($l \approx d - 2d$) and arrangements are made to eliminate friction on the ends (the use of oil, conical shapes with the angle of inclination equal to the angle of friction, etc.).

Assuming a uniform state of stress in the gage length of the specimen, and having measured the tensile (or compressive) force P, the magnitude of the normal stress on areas perpendicular to the axis of the specimen (which we shall take as the x-axis) can be found by dividing the force P by the area of the cross-section F_0 in the undeformed state:

$$\sigma_{xx} \equiv \sigma_1 = \frac{P}{F_0},$$

and

$$\sigma_{yy} = \sigma_{zz} = \sigma_{yz} = \sigma_{zx} = \sigma_{xy} = 0,$$

so that the axis of the specimen is a principal axis of stress. As regards the other principal axes, any direction perpendicular to the axis of the specimen is a principal axis of stress.

This assumption of uniform stress is equivalent to the so-called assumption of plane sections, which is often used in the strength of

materials and which states that cross-sections which are plane before deformation remain plane after deformation, i.e. that the longitudinal displacements of all physical particles of material at a given cross-section are the same:

$$\varepsilon_{xx} = \frac{\partial u}{\partial x} = \varepsilon_1 = \text{const.}, \quad \frac{\partial u}{\partial y} = \frac{\partial u}{\partial z} = 0.$$

Similarly, for the transverse strains it is assumed that:

$$\varepsilon_{yy} = \varepsilon_{zz} = \frac{\partial v}{\partial y} = \frac{\partial w}{\partial z} = \varepsilon_2 = \varepsilon_3 = \text{const.},$$

$$\frac{\partial v}{\partial x} = \frac{\partial v}{\partial z} = \frac{\partial w}{\partial x} = \frac{\partial w}{\partial y} = 0.$$

The assumption that plane sections remain plane has been confirmed by numerous experiments. This means that at all points on a cross-section and at all sections the strains are equal, and from the assumption that $(\sigma_{ij}) = \Phi(\varepsilon_{ij})$ it follows that the stresses also are equal at all points on the cross-section and at all sections on which the assumption of plane sections applies.

The stress obtained by dividing the tensile (or compressive) force by the initial area of the cross-section is called the nominal stress,† in contrast to the actual or true stress, which is obtained by dividing the force by the cross-sectional area after deformation. For small strains this distinction is of no significance.

For the present, in order to investigate the nominal normal stress on the cross-section and the relative longitudinal strain $\partial u/\partial x$ we shall define them as σ and ε:

$$\sigma \equiv \sigma_1 \equiv \sigma_{xx} = \frac{P}{F_0},$$

$$\varepsilon \equiv \varepsilon_1 \equiv \frac{\partial u}{\partial x} = \frac{\Delta l}{l_0},$$

where l_0 is the length of the working part (or that part of it over which the extensions are measured) before deformation, Δl is the change in this length under load, i.e. the total extension.

A typical diagram of the relation between the stress σ and the strain ε is shown in Fig. 35. The diagram shows several characteristic points which correspond to characteristic values of the stresses (and strains).

† The terms "standard stress" and "conventional stress" are also used.

1. The limit of proportionality σ_p (the point A on the diagram) is the greatest stress for which there still exists a linear relation between stresses and strains. Most materials give diagrams with a linear part such as this.

2. The elastic limit σ_e (the point B) is the greatest stress for which, although the relation between stresses and strains is no longer linear, on removing the load, no plastic (residual) strain remains in the specimen. The elastic energy stored in the body during deformation within the elastic limit is totally recovered during the unloading process.

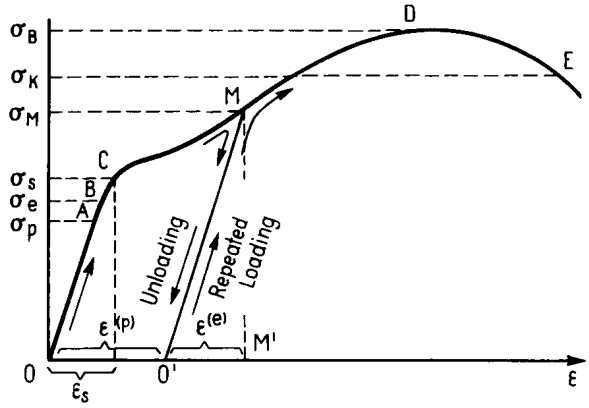

FIG. 35.

Usually the points A and B are very close together and they are often looked upon as one and the same point.

3. The yield point σ_s (the point C) is the stress at which non-reversible strains are first noticed: if the specimen is loaded beyond the stress σ_s and the load then removed, residual strains, too large to neglect, remain in the specimen. The strains which occur in the specimen for stresses which exceed the yield point are called plastic strains or, more precisely, elasto-plastic strains. For some materials (for example mild steel) the point C is the start of a definite kink in the diagram which corresponds to a continued extension of the specimen without increase in the tensile force. In this case the material has a well defined yield point which we shall call σ_T. If there is no such kink an estimate of the load at which residual strains first

occur depends on the accuracy of the measurements or the nature of the problem. We therefore introduce the concept of a proof stress which is the stress at which there first occurs a residual strain of a certain magnitude. The magnitude of this residual strain in percentages is indicated by a second suffix. For example $\sigma_{s(0\cdot2)}$ means that for a stress not exceeding $\sigma_{s(0\cdot2)}$ the residual strain will not exceed 0·2 per cent.

With materials which have a kink in their $\sigma \sim \varepsilon$ curve accurate experiments show a temporary increase in stress before yield occurs. In this case we call this maximum stress the upper yield point, and the value of σ_T corresponding to the bottom of the kink, the lower yield point.

4. The maximum or ultimate stress σ_B is the stress at which the strain ceases to be uniform; a neck appears in the specimen (a local decrease in cross-sectional area) the area of which can be very much

FIG. 36.

less than the area of the working part of the specimen before deformation (Fig. 36). Failure occurs at this neck at a stress σ_K (see Fig. 35). The deformation process, from the moment necking occurs to the moment of failure, takes place with a decreasing tensile force. But if the actual stress were measured, referred to the smallest cross-sectional area at the neck $\sigma_{actual} = P/F$, it would be found that the stress does in fact increase up to the moment of failure. The process of necking is not as simple as the extension of the specimen before the formation of the neck: uniformity of strain is destroyed both from section to section, and over every cross-section in the neck. Many theoretical and experimental investigations of this problem have been carried out.

From the diagram of the relation between nominal stress and strain, and from measurements made during the test of the change in diameter of the specimen, we can obtain the relation between the actual stress and strain.

Typical properties of materials which are illustrated by the stress–strain diagram (Fig. 35) are as follows. First of all we note the

property of elasticity for small strains not exceeding the elastic limit, which is expressed mathematically by Hooke's law:

$$\sigma = E\varepsilon \quad \text{for} \quad \varepsilon < \varepsilon_S = \frac{\sigma_S}{E}, \tag{2.1}$$

where E is the linear modulus of elasticity or Young's modulus. The dimensions of the modulus of elasticity are those of a stress. The linear modulus of elasticity characterizes the resistance of a material to elastic compressive or tensile strain: the greater the value of E, the less is the relative extension for the same tensile stress. For steel $E = 2 \times 10^6$ kg/cm^2, for copper $E = 0{\cdot}9 \times 10^6$ kg/cm^2, for aluminium $E = 0{\cdot}75 \times 10^6$ kg/cm^2.

If during the experiment we measure the change in magnitude of the cross-section, we will find that in tension the size of the cross-section decreases and that in compression it increases, and providing the stress does not exceed the yield point, the ratio of the transverse strain to the axial strain remains constant:

$$\varepsilon_2 = \varepsilon_3 = -\nu\varepsilon_1 \quad \text{for} \quad \varepsilon_1 \leqq \varepsilon_S\,. \tag{2.2}$$

The constant ν, known as Poisson's ratio, is the second constant which characterizes the elastic properties of an isotropic material. The quantities E and ν are called the elastic constants of the material. For many materials ν is approximately 0·3. In general, for all materials

$$0 \leqq \nu \leqq 0{\cdot}5.$$

The value of $\nu = 0$ corresponds to a material the cross-sectional area of which does not alter with tension or compression. Cork has these properties (approximately). The value of $\nu = 0{\cdot}5$ corresponds to an incompressible material the volume of which does not change during deformation. Rubber has a value of ν of approximately 0·5.

Beyond the yield point ν ceases to be a constant and its magnitude depends on the strain.

For tension beyond the yield point, for elasto-plastic strains, the material continues to resist deformation. The quantity $d\sigma/d\varepsilon$, which is the slope of the tangent to the $\sigma \sim \varepsilon$ curve (to the scale of the diagram), is called the strain hardening modulus. For a great many metals

$$\frac{d\sigma}{d\varepsilon} \ll E \quad \text{for} \quad \varepsilon > 2\varepsilon_S.$$

This inequality, which shows a considerable weakening in the resistance of material to deformation beyond the yield point, characterizes a second typical property of the majority of materials.

If we extend the specimen to some point M on the $\sigma \sim \varepsilon$ curve (see Fig. 35) and then start gradually to unload the specimen, the relation between stress and strain will be represented by the straight line MO' which is parallel to the elastic portion OA obtained during the first loading. After removal of all the load a residual strain is observed in the specimen, corresponding to the interval OO'. If then the specimen is loaded once more the relation between stress and strain will, up to the stress at which the unloading was commenced, be represented by the line $O'M$ and after further increase in load the relation will follow the previous curve MD, which it would have followed had the specimen not been unloaded. Thus, with a repeated loading the material is elastic up to the stress σ_{SM}, which is called the local yield point and exceeds the initial yield point σ_S. This increase in the yield point with a repeated loading is called strain hardening.

The property of elastic unloading and elastic repeated loading is the third typical property of a material.

Any deformation beyond the yield point consists of two parts: an elastic part $\varepsilon^{(e)}$, which disappears after removal of the load, and a plastic (residual) part $\varepsilon^{(p)}$, which remains in the body after unloading:

$$\varepsilon = \varepsilon^{(e)} + \varepsilon^{(p)},$$

where

$$\varepsilon^{(e)} = \sigma/E,$$

so that

$$\varepsilon = \sigma/E + \varepsilon^{(p)}, \tag{2.3}$$

and

$$\varepsilon^{(p)} = 0 \quad \text{for} \quad \varepsilon < \varepsilon_S .$$

A characteristic property of the process of elasto-plastic deformation is the absence of a unique relation between stresses and strains. Whereas below the elastic limit the value of the stress given by formula (2.1) defines uniquely the magnitude of the strain, beyond the elastic limit it is important to know the way in which the stress reached this value. If a stress σ' is reached with a monotonic increase in strain (which is called an active strain), then the strain ε' corresponding to σ' is given directly by the $\sigma \sim \varepsilon$ curve

(Fig. 37); if this stress is reached after unloading (a passive strain) from a higher stress σ'', then the strain ε'' corresponding to σ' is determined by taking into account the law of elastic unloading; if it is reached by unloading from a stress σ''' it will correspond to a third value of strain ε'''. This distinguishes elasto-plastic deformation from non-linear elastic deformation, for which the $\sigma \sim \varepsilon$ relation is non-linear but reversible, so that during unloading it follows the same curve. For example, for a rubber cord in tension the $\sigma \sim \varepsilon$ relation gives an S-shaped curve (Fig. 38), and the same curve is followed approximately during unloading.

The irreversibility of elasto-plastic deformation gives rise to an irreversible dissipation of the energy expended in deforming

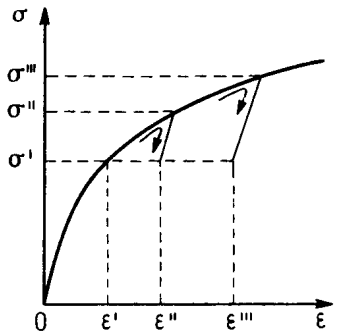

FIG. 37.

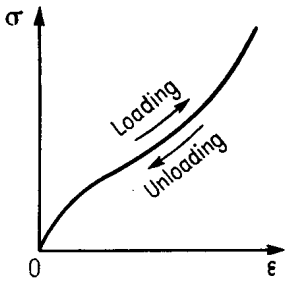

FIG. 38.

the specimen. The total work done during deformation, the mechanical strain energy, as we know (see § 7, Chapter I), is given by the area $OAMM'$ (see Fig. 35) under the $\sigma \sim \varepsilon$ curve. The area $O'MM'$ represents the reversible (elastic) part of the strain energy and the area $OAMO'$, the irreversible part.

The relation between stress and strain $\sigma = \Phi(\varepsilon)$ is sometimes conveniently written in the form

$$\sigma = E\varepsilon[1 - \omega(\varepsilon)], \tag{2.4}$$

where

$$\omega(\varepsilon) = 0 \quad \text{for} \quad \varepsilon \leqq \varepsilon_S,$$
$$0 \leqq \omega(\varepsilon) < 1 \quad \text{for} \quad \varepsilon > \varepsilon_S.$$

The function $\omega(\varepsilon)$ can be found if the stress-strain curve is drawn. For, from (2.4) we have that,

$$\omega(\varepsilon) = \frac{E\varepsilon - \Phi(\varepsilon)}{E\varepsilon},$$

i.e. if the elastic part is prolonged and if then a perpendicular AB is dropped onto the ε-axis from the point A on this line corresponding to the strain ε (Fig. 39a), then $\omega(\varepsilon)$ is equal to the ratio of $AC : AB$. A typical graph of the variation of the function $\omega(\varepsilon)$ is shown in Fig. 39b. For small elasto-plastic strains the function $\omega(\varepsilon)$ can be looked upon as a small parameter.

The curved parts of the $\sigma \sim \varepsilon$ curve can be very different for different materials, and therefore the function $\omega(\varepsilon)$ will also be different. Since the curvature of this part of the curve is often not very great, in order to simplify and standardize the computations, we sometimes replace the curved part by a straight line, so that the

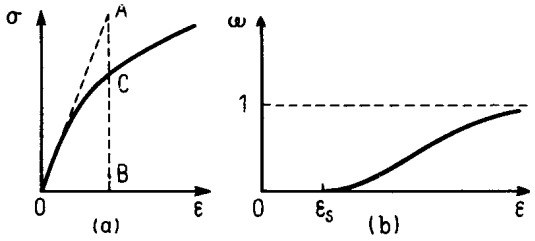

FIG. 39.

whole diagram is represented by an open polygon as shown in Fig. 40. In this case we talk of a simplified linear diagram.

The slope of the part of the diagram beyond the yield point is called the strain hardening modulus E'. In this case

$$\omega = 0 \quad \text{for} \quad \varepsilon \leqq \varepsilon_S,$$

$$\omega = \lambda\left(1 - \frac{\varepsilon_S}{|\varepsilon|}\right) \quad \text{for} \quad \varepsilon \geqq \varepsilon_S,$$

where

$$\lambda = \frac{E - E'}{E}. \tag{2.5}$$

Often $E' \ll E$ so that λ is approximately unity.

If after unloading from some stress beyond the yield point a load of opposite sign is applied to the specimen, plastic strains appear at a stress of $\sigma_{SM'}$, which is not only less than the local yield point σ_{SM}, but less than the initial yield point σ_S. This lowering of the yield point for loadings of opposite sign is known as Bauschinger's

effect. In the case of linear strain hardening this effect is represented in the form of an open polygon $OAMM'N$ (Fig. 40).

If we increase the load of opposite sign as far as the point N on the $\sigma \sim \varepsilon$ curve and then remove the load and apply a load in the previous sense, transition to an elastic-plastic state occurs at a point N' at a stress less than σ_S (the initial yield point for compression is assumed to be equal to the yield point for tension). If we once more repeat the whole cycle a point in the $(\sigma\varepsilon)$ plane will decribe the closed polygon $MM'NN'$. The area inside this polygon is proportional to the energy dissipated during one cycle.

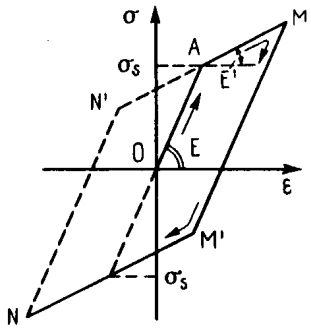

FIG. 40.

The properties described above are typical of many materials. There are, however, materials which have different properties. A number of materials do not have a straight elastic portion on their stress–strain curves (cast steel, cast iron and other cast metals). But for a decreasing load the $\sigma \sim \varepsilon$ relation is a straight line parallel to the tangent to the $\sigma \sim \varepsilon$ curve at the origin of coordinates. This straight line determines the elasticity modulus. After a comparatively small initial deformation these materials do have an elastic portion.

Some materials (cast iron, concrete, rock) are very strong in compression but are comparatively weak in tension. The stress–strain curve for such materials is not symmetrical, so that $\sigma_B^{(+)} < \sigma_B^{(-)}$ (Fig. 41), and failure under tension occurs after very small plastic strains.

Certain brittle steels have a considerable elastic region but fail in tension very close to the elastic limit, so that there are almost no residual strains after failure. In order to reveal the plastic

properties of these steels we proceed in the following way. The specimen is placed in a massive metal ring which is compressed together with the specimen (Fig. 42). In this way the ring exerts a lateral pressure which enables brittle steels to display a noticeable range of plastic strain. In order to find the part of the force which is taken by the ring a separate experiment is performed, the ring being compressed without the specimen and with the opening filled. The difference in the forces determines the difference between the properties of the specimen and the properties of the ring. Rocks situated deep in the earth are under conditions similar to the specimen

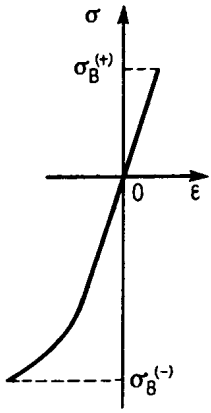

FIG. 41.

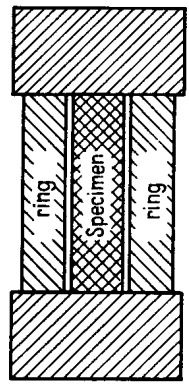

FIG. 42.

in the ring, under conditions of high all-round pressure. This explains the large plastic deformations in layers of rock, in spite of their brittleness under normal tensile and compressive tests on specimens.

2. The Effect of Various Factors on the Mechanical Properties of Materials

The typical properties we have described so far do not cover all the properties of the materials to which they refer. In every material there are deviations from these typical properties which are associated with the effect of temperature, time, rate of deformation and the surrounding media, etc. Some of these effects will be dealt with in detail later but at present we shall only describe them briefly.

(a) *The Strain of Rate Effect*

The rate of deformation $\dot{\varepsilon}$ is defined as the change in strain with time

$$\dot{\varepsilon} = \frac{d\varepsilon}{dt} = \frac{1}{l_0}\frac{d\Delta l}{dt} = \frac{v}{l_0},$$

where v is the rate of stretching of a specimen of length l_0 (i.e. the rate of movement of one end of the working portion relative to the other). In normal statical tensile or compressive testing machines rates of deformation can be attained from 1×10^{-4}/sec to 1×10^{-1}/sec. In order to attain high speeds of deformation special

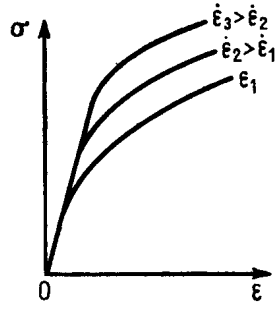

FIG. 43.

dynamical testing machines have been constructed. In a pneumatic dynamic testing machine in the materials laboratory of Moscow University a speed of deformation of the order of 1×10^4/sec and more can be obtained.

Metals display a relation between their mechanical characteristics and the rate of deformation, so that if we find the $\sigma \sim \varepsilon$ curves for different fixed strain rates these curves will be different for different strain rates (Fig. 43). Their elastic parts will be found to coincide approximately, but their curved parts are higher, the higher the rate of deformation. The increase in the ultimate strength of electrolytic copper, for example, can be approximately expressed by the formula

$$\sigma_B = \sigma_0(1 + 0{\cdot}012 \ln 10^4\dot{\varepsilon}),$$

where $\sigma_0 = 300$ kg/cm^2 is the ultimate stress at a strain rate of 1×10^{-4}/sec. It can be seen that the ultimate stress depends

only slightly on the rate of deformation, and for a noticeable increase it is necessary to increase the rate of deformation several times. For example at a rate of deformation $\dot{\varepsilon} = 1 \times 10^{-2}$/sec we have that $\sigma_B = 1{\cdot}05\,\sigma_0$, i.e. an increase of only 5 per cent, and for $\dot{\varepsilon} = 1 \times 10^{3}$/sec, i.e. for an increase in the rate of deformation of 10^7 times, we have that $\sigma_B \approx 1{\cdot}19\,\sigma_0$, i.e. an increase of 19 per cent. The yield point increases more noticeably. In mild steels the yield point under impact loads is two to three times higher than its static value.

(b) *Relaxation*

If a specimen has extended a certain amount and is then held in a fixed position, then after a certain time the force holding the specimen at this given extension (and therefore the stress) will decrease and tend asymptotically to some particular value (Fig. 44). This decrease in stresses under constand strains is called relaxation. It is only slightly noticeable in metals at room temperature and only becomes noticeable at high temperatures. With certain mate-

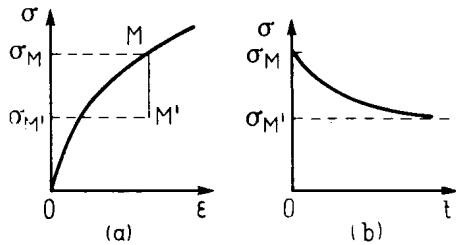

FIG. 44.

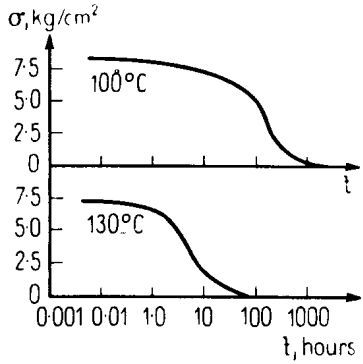

FIG. 45.

rials (for example lead, high polymers) this effect is noticeable even at room temperatures. With certain types of rubber, if they are kept at a high temperature and if intensive rearrangement of the molecular structure occurs, the stress can decrease to zero. Figure 45 shows this process in vulcanized rubber at a relative extension of 50 per cent.

(c) *Creep and Recovery*

If at some stage in the extension of a specimen the tensile force (tensile stress) is fixed, deformation of the specimen will continue quickly at first and then more slowly, and the rate of deformation then becomes approximately constant (Fig. 46). In some cases this

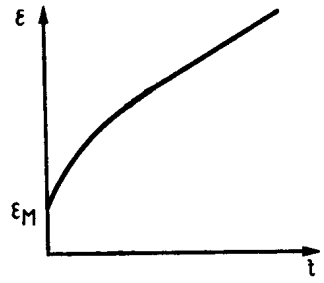

FIG. 46.

continuous increase in strain, which is known as creep, tends asymptotically to some limiting value; in other materials the decrease in the rate of deformation after a certain time gives way to an increased rate and failure occurs. At room temperature the phenomenon of creep is only slightly noticeable and becomes noticeable only at high temperatures. However it should often be taken into account at normal temperatures, especially in structures which are intended for prolonged use. For example the occurrence of creep in massive concrete structures is of particular importance.

Qualitatively creep can be described by Maxwell's equation:

$$E\frac{d\varepsilon^{(p)}}{dt} = \frac{\sigma}{T},$$

where T is the so-called time of relaxation. Since plastic deformation can be represented as the difference between the total strain and the elastic strain

$$\varepsilon^{(p)} = \varepsilon - \varepsilon^{(e)} = \varepsilon - \frac{\sigma}{E},$$

Maxwell's equation can be rewritten in the form

$$\frac{d\sigma}{dt} = E\frac{d\varepsilon}{dt} - \frac{\sigma}{T}.$$

If we put σ = const. in this equation it will describe creep at a constant rate $\dot{\varepsilon} = \sigma/ET$. If we put ε = const. then we define a relaxation process according to the law $\sigma = \sigma_0 e^{(t-t_0)/T}$.

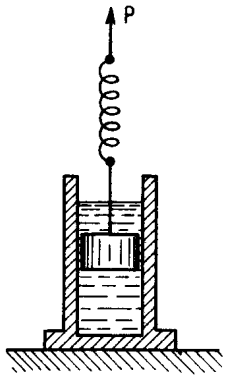

FIG. 47.

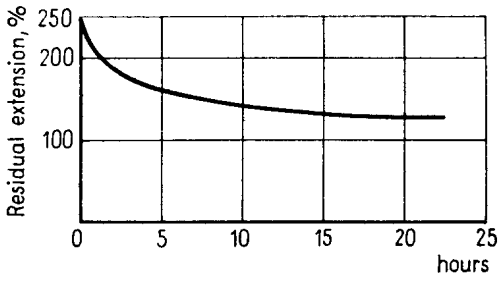

FIG. 48.

Maxwell's equation is not in accordance with the quantitative relations observed in real bodies and it only enables us to have a better understanding of the qualitative side of the processes which take place. There is an interesting mechanical model which corresponds to Maxwell's equation and which enables us to see the interaction of the properties of elasticity and viscosity in bodies. This model is made of a spring joined to a "dash-pot" in the

form of a piston moving in a viscous liquid, the speed of which is proportional to the applied force (Fig. 47).

A phenomenon which is associated with creep is recovery. If a body is deformed beyond the elastic limit and if then the external forces are removed, the resulting deformation will decrease. For example the length of a specimen of non-vulcanized rubber extended by 390 per cent and held for a long time at this extension will decrease after removal of the forces, at first very rapidly and then more slowly (Fig. 48).

(d) *Hysteresis*

If a specimen is extended to a point M on the $\sigma \sim \varepsilon$ curve and then unloaded and reloaded, it will be found that the point on the $\sigma \sim \varepsilon$ curve corresponding to this process will not move exactly

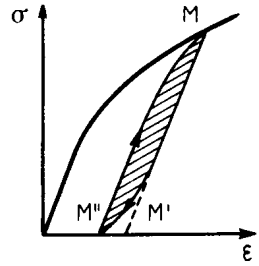

FIG. 49.

along the line MM' parallel to the elastic portion, but will describe some closed curve called a hysteresis loop (Fig. 49). The right-hand loop of this curve, which corresponds to the unloading, is tangential to the line MM' at the point M, and the left-hand loop has a tangent at the point M'' parallel to the line MM'. This phenomenon is observed also with elastic strains. The area under the hysteresis loop is proportional to the part of mechanical energy which is expended in the form of heat during the closed cycle of unloading and loading. The dissipation of energy in this way is one of the reaons for the damping of free elastic vibrations.

We will now deal in a little more detail with the effects of heat treatment, temperature and radiation.

(e) *The Effect of Heat Treatment*

The characteristics of a metal of a given chemical composition depend very much on the heat treatment to which it has been subjected. The purpose of heat treatment is to achieve by controlled heating and cooling a change in the micro-structure, and in this way a change in the physical–mechanical properties of a metal. The various allotropic and structural changes in a metal which accompany a change in temperature do not take place instantaneously, but require a certain definite time. For example, in the diagram of

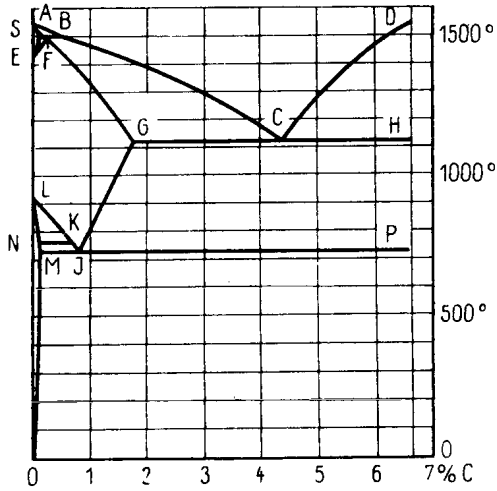

FIG. 50.

allotropic changes for iron (Fig. 4, Chapter I) we see that there are horizontal portions. The full cycle, therefore, of these changes will be completed only if the change in temperature takes place sufficiently slowly.

The structural and physical properties of a metal can be represented by a so-called constitution diagram. As an example let us consider the equilibrium diagram for the iron–carbon system which refers to steels and cast irons (Fig. 50). Along the axis of abscissae we set out the percentage composition of carbon, and along the axis of ordinates the temperature (centigrades); the different states of the alloy are bounded by lines in this plane.

The temperature at the start of the solidification depends on the carbon content; for a fixed carbon content the solidification does not finish at this temperature: a considerable decrease in temperature is necessary for the mixture of solid and liquid phases to solidify completely. This distinguishes alloys from pure metals. The line *ABCD* in Fig. 50, which is called the liquidus, gives the temperature at the start of solidification for different carbon contents. Above this line the system is completely in a liquid state. The line *ESFGCH* (the solidus) defines the completion of solidification: below this the system is entirely in a solid state. Within the area *BFGCB* there exists a mixture of a liquid phase and a solid phase in the form of austenite (a solid solution of carbon in γ-iron). The area *DCH* represents a mixture of the liquid phase with cementite (the compound Fe_3C). In the small area *ASE* there occurs a solid solution of carbon in δ-iron. In the area *EFGJKL* we have austenite. In the area *HCGJP*, a eutectic—an alloy composed of solid grains of austenite and cementite. A eutectoid reaction occurs along the line *MJP*—the austenite divides up into ferrite (a solid solution of carbon in α-iron) and cementite. In the narrow region *LMO* there is ferrite. In the area *LMJ*, ferrite and austenite. This diagram is explained as follows. If a liquid solution of iron and carbon with a given carbon content is slowly cooled, its state will be given by the region containing a point, the abscissa of which gives the carbon content and the ordinate of which the temperature at the instant considered. The size of the grains and of other crystalline formations depends on the régime of temperature changes.

Alloys with a carbon content less than 2 per cent are known as steels. Alloys with a greater carbon content are known as cast irons.

In order to remove initial internal stresses caused by distortions of the crystal structure due to deformation in the cold state (during mechanical working) a process known as annealing is carried out, which aims at obtaining an equilibrium structure corresponding to the appropriate position on the constitution diagram and at improving the mechanical workability of the steel. The process consists of heating the metal to a temperature above the line *LKJG* (but below *EFG*), keeping it at this temperature for a considerable time, and then slowly cooling. Providing the temperature is not too far above the line *LKJG*, cooling slowly gives a strong fine-grained structure.

Annealing causes a lowering of the yield point (and the elastic limit), and decreases the tensile strength but improves its cutting and pressing properties. In addition, the process results in an increase in ductility: failure occurs only after considerable extension. It is therefore possible to subject an annealed metal to severe changes in shape without failure.

Quenching leads to a structure not in equilibrium and untypical of the alloy at room temperature as shown on the constitution diagram. The quenching process consists of heating the metal to some temperature beyond the critical temperature and then cooling at such a high rate that there is insufficient time for all the changes in phase to take place, so that a structure results which is characteristic of the state of the metal at a higher temperature. For example, if a steel is heated to a point above the line *LKJG* (Fig. 50), kept at that temperature for some time, and then rapidly cooled, there takes place in the homogeneous austenite a change of the γ-iron into α-iron without separation of the carbide Fe_3C in solution. The crystal lattice is therefore distorted and stressed. This solution is known as martensite. We see then, that a quenched steel has initial stresses. The distribution of these stresses is not uniform, since different parts of the product cool at different rates and consequently experience different structural changes.

Quenching makes a steel stronger (it raises the elastic limit and the ultimate tensile stress) but it also makes it less ductile (more brittle). For example a medium carbon steel (C = 0·45; Mn = 0·77; Si = 0·21; S = 0·02; P = 0·013)† annealed at 800°C (with sand cooling) has $\sigma_S = 5000$ kg/cm^2, $\sigma_B = 5900$ kg/cm^2 and a percentage elongation at failure $\delta = 20$ per cent at room temperature. After quenching in water from 800°C and tempering (see below) at 540° the same steel has $\sigma_S = 8700$ kg/cm^2, $\sigma_B = 9500$ kg/cm^2 and $\delta = 12$ per cent.

Tempering is used to improve the properties obtained after quenching. It consists of heating the metal and maintaining it for some time at an elevated temperature below the critical temperature. The rate of heating and the time the metal is kept at this temperature controls the process of partial breakdown of the solid solution and the formation of a fine-grained structure. As a result the strength of the metal is improved and its ductility slightly increased.

† The numbers indicate the percentage content of the various elements.

Normalizing consists of keeping the metal at a temperature beyond the critical and then cooling in still air. Due to the slow (compared with quenching) rate of cooling the changes are able partially to take place, but a structure results which is untypical of the metal at that temperature as shown on its constitution diagram.

For the above medium carbon steel, after normalizing from 870°C (after one hour at this temperature) the results were $\sigma_S = 4400$ kg/cm^2, $\sigma_B = 7900$ kg/cm^2, $\delta = 12$ per cent, i.e. compared with the annealed steel the yield point was lowered and the ultimate tensile stress was considerably increased.

The effect of various heat treatments on the mechanical properties of various types of steels are illustrated in Table 1.

The important influence of heat treatment on the properties of metals makes it necessary, both in structural design and in the laboratory investigation of materials, to take into account these

TABLE 1. THE EFFECT OF HEAT TREATMENT ON MECHANICAL PROPERTIES

Material	Treatment	Mechanical properties		
		σ_S [kg/cm^2]	σ_B [kg/cm^2]	δ [%]
Steel 15	Anneal, 1 hr, 900°C	2410	4300	36
	Normalize, 1 hr, 900°C	2400	4540	35
Steel 40X	Anneal, 1 hr, 900°C	3450	6600	19
	Normalize, 1 hr, 900°C	4350	7650	21
	Quench from 820°C in water and temper at 450°C (3 hr)	10490	12700	10
Steel 30XGSA	Anneal, 1 hr 950°C	4120	7210	21·5
	Normalize, 1 hr, 950°C	4850	8390	20·5
	Anneal from 780°C with rate of cooling 5°/hr	3230	6300	26·2
	Quench from 950°C in oil and temper at 500°C (3 hr)	9630	11130	13
Steel 25X 2MFA	Anneal at 900°C	3910	6390	25
	Normalize, 920°C	8420	11270	16
	Quench from 920°C in oil and temper at 650°C (2 hr)	9190	9790	16·6

influences and to specify the treatment most suitable for the given conditions.

(f) *The Effect of Temperature*

Temperature influences the yield point, the ultimate stress, ductility, and also the elastic properties of the material—the modulus of elasticity and Poisson's ratio. The general tendency of the effect of temperature on the properties of a material is that an increase in temperature causes the yield point at first to increase slightly and then to decrease; the tensile strength decreases more rapidly, so that the strain hardening becomes less.

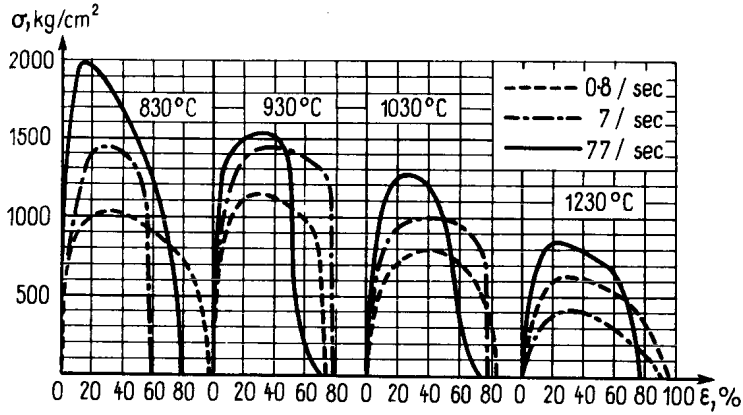

FIG. 51.

At a sufficiently high temperature the ultimate stress becomes practically equal to the yield point. This creates very favourable conditions for hot working. An exception, however, is aluminothermic chromium, the ultimate tensile stress of which increases from 470 to 1000 kg/cm² for an increase in temperature from 20° to 1100°C. The effect of high temperatures on the mechanical properties of some steels is shown in Table 2.†

The effect of temperature and rate of deformation is illustrated in Fig. 51, which has been compiled from the results of tensile tests carried out by Inoue (Japan) on tempered low carbon steel (C = 0·12; Mn = 0·55; Si = 0·33; P = 0·01; S = 0·23), which at

† See, for example, A. A. Shmykov, *Spravochnik Termista*, Mashgiz, 1956.

room temperature has $\sigma_B = 6240\ \text{kg/cm}^2$ and $\delta = 28{\cdot}4$ per cent. A noticeable feature of this diagram is the decrease in the size of each curve corresponding to a given rate of deformation, with

TABLE 2. THE EFFECT OF TEMPERATURE ON MECHANICAL PROPERTIES

Type of steel	Heat treatment	Temperature of test [°C]	σ_S [kg/cm²]	σ_B [kg/cm²]	δ [%]
25X2MFA	Anneal at 900°C	20	3910	6390	25
		500	3280	5200	25
		550	3620	4680	24
	Quench from 920°C in oil and temper at 650°C	20	9190	9790	19·6
		550	6640	6900	15·3
30XMA	Anneal at 860°C	20	3660	6820	22·3
		400	3070	5680	26
	Normalize at 850°C	20	4750	7630	20·3
		400	5350	7650	18
		500	3860	5520	21·5
	Quench from 880°C in oil and temper at 650°C	20	7870	8950	22·6
		400	5870	7480	22·8
		500	4970	5570	23·3
Heat-resistant 1X13(Z1)		100	5200	6800	14
		500	3000	4200	18
		700	700	1000	63
		800	100	400	69
Heat-resistant X(9C2 CX8)		20	8400	9000	19
		400	4900	8300	17
		600	4000	5400	14
		800	400	700	24
Stainless 2X13	Normalize at 1200°C	20	5200	7200	21
		400	4050	5300	16·5
		550	2850	3500	36·5
Stainless X10C2M	Quench from 1100°C in oil, temper at 800°C	20	6800	9600	19
		100	5800	8600	13·5
		400	4900	7800	13
		600	3750	4400	30
		700	2050	2250	41
X18H25C2	Quench from 1200°C in water and then soak at 800°C (for 8 hr)	20	5500	8550	17·2
		400	4250	7250	14·5
		600	4030	5800	13·3
		800	2500	2650	8·5

increase in temperature. At a fixed temperature the curve corresponding to the highest rate of deformation is the highest. Less obvious, but nevertheless noticeable, is the decrease in the modulus of elasticity (the inclination of the initial part of the curve to the ε-axis) with increase in temperature. From the results of these experiments the author has established the expression

$$\sigma = C\varepsilon^n \dot{\varepsilon}^m e^{A/kT},$$

where C, m, n, A, k are constants and T is the absolute temperature.

Figure 52 represents graphically the relation between temperature and the tensile strength (the continuous line) and the elongation

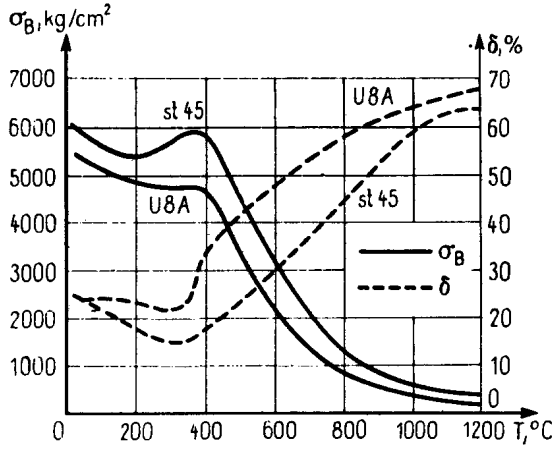

FIG. 52.

at failure (the dotted line) for steel 45 and tool steel U8A. It can be seen that for both steels these relations in general have the same form.

A number of authors have suggested that the relation between the mechanical properties and temperature can be expressed by the formula

$$\frac{K_2}{K_1} = e^{-\alpha(t_2 - t_1)},$$

where K_1 and K_2 are the values of some mechanical property at temperatures t_1 and t_2, and α is some constant. This relation presupposes that in every case the mechanical properties vary mono-

tonically. Although this is so for a number of materials and the above formula in these cases can be used, it can be seen from Fig. 52 that this formula cannot be applied universally.

Lowering the temperature below 0°C leads, for a great number of steels, to a rise in the yield point and ultimate tensile stress accompanied by a decrease in ductility. Some steels, however, behave differently in this respect, and in non-ferrous metals, as a rule, a noticeable increase in ductility is observed after a considerable decrease in temperature. The effect of low temperature on the mechanical properties of some materials can be seen from Table 3.

Young's modulus increases slightly with decrease in temperature. For example, the elasticity modulus of stainless steels increases by approximately 10 per cent after a decrease in temperature to -200°C.

A change in temperature leads in a number of cases to a change in the basic features of the stress–strain curve. Some low carbon steels which have a smooth stress–strain curve at room temperature, that is, the stress increases monotonically with increase in extension, give a well defined yield point at low temperatures.

The effect of temperature on the mechanical properties of metals is sometimes very similar to the effect of rate of deformation, and it is considered that their effects are in an opposite sense: a decrease in temperature has the same effect as an increase in the rate of deformation and vice versa. A number of attempts have been made to relate these effects quantitatively. For example, for steels it is thought that a decrease in temperature by 61°C is equivalent to an increase in rate of deformation by 1000 times.

In actual fact however, although qualitatively this may be the case, a number of exceptions could be quoted and this relation should not be looked upon as a general rule.

It might also be added that at high temperatures the corrosive action of the surrounding medium (for example, gases in internal combustion engines and in rocket motors) is intensified, and this leads to a weakening of the internal bonding forces in the metal and the occurrence of cracks. A rapid flow of gas over a metal product especially at a high temperature, when the likelihood of sublimation is increased, can cause erosion of the surface and weaken the structure.

Ceramics, concrete and natural stone are only slightly sensitive to changes in temperature except at high temperatures when chemical changes might take place.

TABLE 3. THE EFFECT OF LOW TEMPERATURES ON MECHANICAL PROPERTIES[a]

Material	σ_S [kg/cm^2]			σ_B [kg/cm^2]			δ [%]		
	+17°C	−196°C	−253°C	+17°C	−196°C	−253°C	+17°C	−196°C	−253°C
Steel 1010 (annealed)	2300	7200	–	3700	7300	8400	35	4	0
Steel 1020 (annealed)	2900	8000	–	4900	8700	10600	29	12	0
Steel 1050 (annealed)	4100	9800	–	6900	11400	13900	22	16	0
Steel 12XN2 (annealed)	–	–	–	5100	8600	11900	25	20	0
Steel EY2 (annealed)	–	–	–	7700	17000	13200	60	42	20
Aluminium	–	–	–	1200	2100	3500	29	42	45
Copper	–	–	–	2400	3800	4600	29	41	48
Molybdenum	–	–	–	4900	5400	5400	3	0	0
Brass	–	–	–	4200	5900	6400	38	42	41
Duralumin	–	–	–	4100	5200	6800	15	16	16
Silumin	–	–	–	1300	1300	2300	1·2	0·8	1·4

[a] See, for example, G. V. Uzhik, *Strength and Plasticity of Materials at Low Temperature*, Academy of Sciences publication, U.S.S.R. 1957.

Materials of organic origin (rubber, plastics) at low temperatures usually become so brittle that they are no longer useful as structural materials. Their use at high temperatures is also limited due to their rapid softening. In addition, if they are maintained at even slightly elevated temperatures deep oxidizing processes occur which severely weaken the material (a well-known example is the perishing of rubber).

(g) *The Effect of Radio-active Radiation*

The components of atomic reactors, atomic motors and the equipment used in them are subjected to intense radio-active radiation and especially to neutron bombardment. Over the last ten years many observations and experimental investigations have been made on the effect of this radiation on the mechanical properties of materials. It has been discovered that the effect is so important that in no circumstances should it be ignored in the design or construction.

The way in which a metal is affected by neutron bombardment can be described as follows. As it passes through the crystal lattice the neutron collides with the atoms; in so doing its velocity is decreased and its path becomes more and more irregular. The atoms displaced by the neutron and now moving at high velocity collide in their turn with other atoms and dislodge them from their positions in the lattice, sometimes occupying the vacated places, and sometimes leaving them unoccupied. A large number of the atoms in the path of the neutron are dislodged and forced into the interatomic space of the lattice. It has been estimated that an intense neutron bombardment displaces 5 per cent of the atoms. The formation of a large number of vacancies and interstitials is in itself sufficient to alter considerably the elastic-plastic properties of the material. In addition the atomic lattice in the narrow "tunnel" around the path of the neutron quickly takes on an intense oscillatory motion, corresponding to a high temperature (of the order of 10,000°C) followed by a rapid damping (which takes place over approximately 10^{-10} sec). This has a local effect similar to quenching. The damage of the crystal lattice leads to a non-uniform change in volume within the body and to the occurence of initial stresses.

The amount by which the mechanical properties are affected depends on the dose of radiation, which is measured by the number

of neutrons entering the body per 1 cm^2 of surface. If n is the number of neutrons per unit volume of the neutron beam and v their velocity, then in t sec nvt neutrons enter the body through 1 cm^2 of surface. The unit of dosage of radiation is defined as nvt.

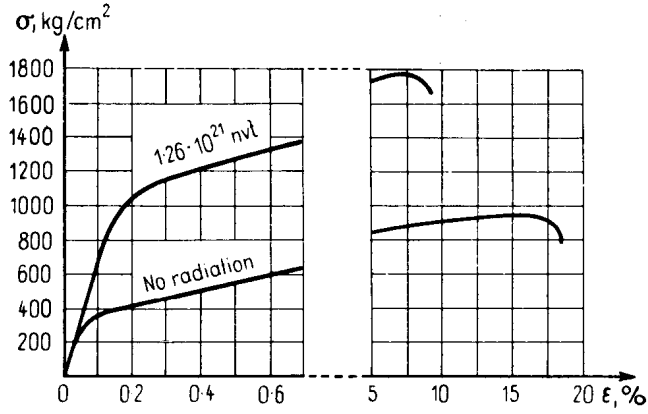

FIG. 53.

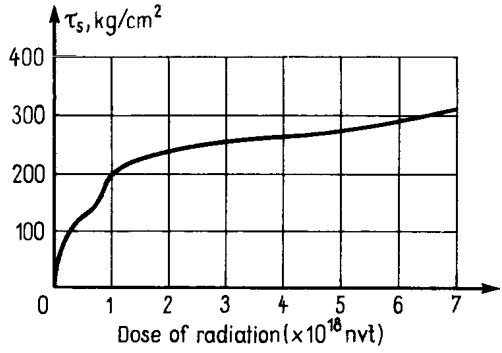

FIG. 54.

Figure 53 shows the stress–strain curves for specimens of an aluminium alloy 2SO. The lower curve refers to a specimen which has not been subjected to radiation, and the upper to a specimen which has received a dose of $1{\cdot}26 \times 10^{21}$ neutrons/cm^2. For the former specimen, $\sigma_{S(0{\cdot}2)} = 480$ kg/cm^2, $\sigma_B = 950$ kg/cm^2, $\delta = 38$ per cent; for the latter $\sigma_{S(0{\cdot}2)} = 1200$ kg/cm^2, $\sigma_B = 1830$ kg/cm^2,

$\delta = 21$ per cent. Note the considerable increase in the ultimate tensile stress and the yield point and the decrease in ductility. This is typical of the change in the mechanical properties of most of the metals investigated. Figure 54 shows the curve of the variation in the yield point in shear for a monocrystal of copper with change in dose.

The effect on the elasticity modulus of materials is less noticeable. Theoretical reasoning suggests that for copper, for example, the modulus of elasticity should increase by 5–7 per cent due to 1 per cent interstitials in the crystal lattice. An increase in the elasticity

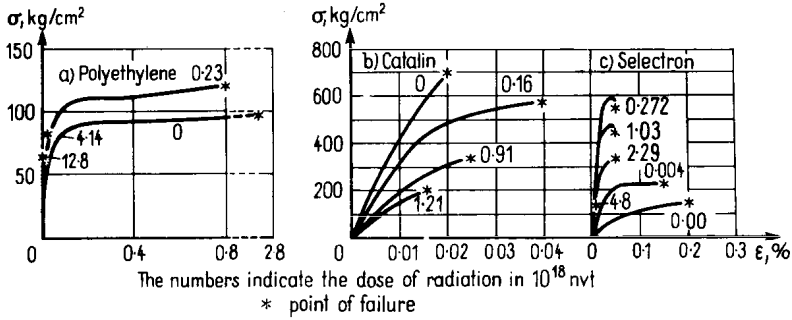

FIG. 55.

modulus of 10 per cent has been obtained in a heavy particles cyclotron. Approximately the same increase has been obtained after neutron bombardment in a reactor. For small doses of radiation (up to 10^{12}–10^{13} *nvt*) the following theoretical formula for the elasticity modulus E_r of a material after radiation agrees with experiment:

$$\frac{1}{E_r} = \frac{1}{E} + \frac{A}{(1 + BN)^2},$$

where E is the elasticity modulus for the material before radiation, A and B are contants and N is the dose of radiation in *nvt*.

As a rule the changes in the mechanical properties of metals brought about by neutron bombardment are permanent changes at room temperature. In one series of experiments part of the specimens were tested over six months after radiation and no real deviations from the properties observed immediately after radiation

were noticed. But the changes in properties brought about by radiation can be fully or partially removed by annealing. Since in atomic plants many elements are working under conditions of high temperature, they are subjected simultaneously to two opposite effects: the effect of radio-active radiation, which changes their mechanical properties, and a high temperature anneal. Since, as we have seen from the above examples, the effects of radiation are very important, it is essential to take into account the two simultaneous and opposite effects.

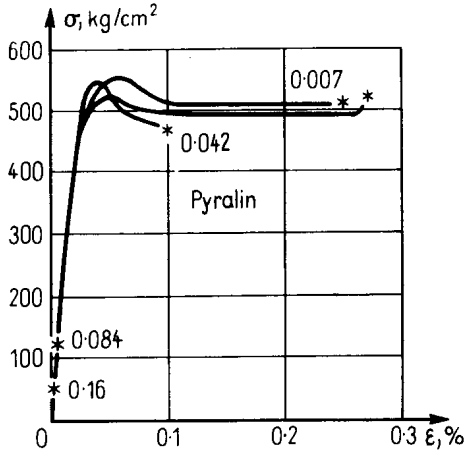

Fig. 56.

Plastics, which are widely used in nuclear engineering as structural materials, are mostly more sensitive to radiation than metals. It is noticed, as a rule, that the material becomes extremely brittle, less ductile and fails after only a small extension. For some plastics the yield point remains practically constant, whereas for others it rapidly decreases, or alternatively, it sometimes rapidly increases. Typical examples of these three types are shown in Fig. 55, the results for which were obtained by the Oak Ridge National Laboratory (U.S.A.). The curves in Fig. 55a refer to polyethylene, those in Fig. 55b to catalin, and those in 55c to selectron. Extensions per unit length are measured along the axes of abscissae and stresses along the axes of ordinates. The numbers on the curves indicate the dose of radiation in 10^{18} *nvt*, and the asterisks indicate the points of failure.

TABLE 4. CHANGE IN MECHANICAL PROPERTIES AFTER RADIATION

Material	Mechanical and heat treatment	Dose of radiation (*nvt*)	Yield point [kg/cm²]		UTS [kg/cm²]		Percentage elongation [%]	
			Before radiation	After radiation	Before radiation	After radiation	Before radiation	After radiation
Al. alloy 2SO	anneal	$1{\cdot}26 \times 10^{21}$	480	1200	950	1830	38	21
Al. alloy 2SH14	cold work	$1{\cdot}26 \times 10^{21}$	1160	1680	1210	1830	6	5·5
Al. alloy 52SO	anneal	$1{\cdot}26 \times 10^{21}$	1030	1600	2040	2620	34	30·5
Al. alloy 61SO	cold work	$1{\cdot}26 \times 10^{21}$	675	1800	1270	2600	28·8	22·4
Al. alloy A54S	reduction by 50%	$1{\cdot}26 \times 10^{21}$	3350	3560	3820	4050	8·8	12·5
Stainless steel 316	anneal	9×10^{20}	—	—	5550	10900	—	—
Stainless steel 410	case harden	9×10^{19}	3080	4270	4900	5250	—	—
Stainless steel 440C	temper	9×10^{19}	13000	14300	13900	16800	—	—
Monel metal	—	9×10^{19}	—	—	5950	6700	33	10

A further characteristic can be seen from Fig. 55b: a small dose of radiation has caused an increase in the ductility of catalin. Figure 56 shows the stress–strain curves (with the same definitions as in Fig. 55) for pyralin. The outstanding feature here is that the shape of the curve changes only slightly, whereas the point of failure is considerably displaced towards the origin of coordinates, even for small doses of radiation.

Table 4 gives some of the known data on the effect of neutron bombardment on the yield point, the ultimate tensile strength and the percentage elongation.

It should be noted that the existing data on the effect of radiation has been obtained in different laboratories under different temperature and radiation conditions, and for this reason it is very difficult to correlate the results.

The effect of various factors on the elasto-plastic properties of materials which have been briefly dealt with in this section, in particular, those which depend on time (creep, rate of deformation), will be considered in more detail in the subsequent chapters. Here, as also in the following section, a material which at some fixed temperature assumes a given physical state, determined by the conditions of manufacture and of heat treatment, will be considered to have the property of ideal plasticity, which does not depend on time. It will therefore be assumed that the behaviour of the material under load is determined by the properties described in § 1 of this chapter.

3. The Mechanism of Plastic Deformation

A number of suggestions have been made concerning the mechanism of plastic deformation which allow us to a certain extent to give a qualitative explanation of phenomena observed in experiments with specimens of considerable dimensions.

With elastic deformation the elementary particles (atoms, ions, molecules) return to their mean position after the removal of the load. But with plastic deformation the shape and volume of the body are not restored after unloading and the particles therefore experience irreversible relative displacements and do not re-occupy their previous mean positions after plastic deformation.

If we observe the surface of a specimen under tension we are able even with the naked eye to see that plastic deformation causes thin dark and light strips on the surface of the specimen, called

Lüders lines, inclined approximately at 45° to the axis of the specimen. This indicates that there is intensive shearing of the material on a plane intersecting the specimen in this direction. There can be either one or several of these shearing planes, and the greater the plastic deformation the greater their number, so that as a result they fill the whole volume of the working portion of the specimen. The result is as if the specimen were made up of plates inclined at 45° to its axis which slide over each other during the plastic deformation (Fig. 57). In monocrystal specimens these layers are called blocks and the shear planes are identified with the slip planes which

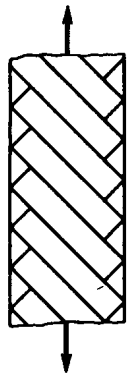

FIG. 57.

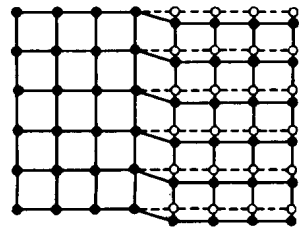

FIG. 58.

were mentioned in § 1 of Chapter I. This mechanism of plastic deformation is called a slip mechanism. The growth in resistance to plastic deformation is connected with the rotation of these blocks to a position in which the resistance to shear increases. This slipping of one layer of atoms over another in the crystal lattice takes place both in elastic and in plastic deformation (Fig. 58). But a simultaneous slip of one layer of atoms relative to another by one lattice parameter (the parameter a), which is necessary for an irreversible plastic deformation, would require in an ideal lattice a tensile force much greater than that which is in actual fact required to give plastic deformation of the specimen. The shearing strain between the layers would be of the order of unity and consequently the stress would be of the order of the elasticity modulus, which is not so in actual fact (the yield point is several times less than the elasticity modulus). Shear of the whole layer does not therefore take

place. Slip is the result of a complex process which takes place in the crystal lattice of each grain and in the intercrystalline material.

One of the slip mechanisms in crystal materials is associated with dislocation in the crystal lattice. Dislocation is a particular sort of disruption of the regular lattice, when, for example, it contains an extra half-plane of atoms AB (Fig. 59), so that above the plane CD there is in each horizontal row one atom more than in the rows below this plane. Figure 59 shows only one section of the lattice. A similar state exists in other planes so that dislocation is not confined to the point A but takes place along a line perpendicular to the plane of the paper (linear dislocation). The lattice

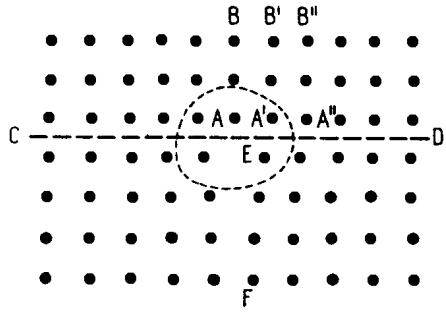

FIG. 59.

around the point A is of course considerably distorted. Let us assume now that there are forces acting on the crystal which are trying to move the upper part to the right relative to the lower part. The plane AB, together with the other planes is moved slightly to the right. At some value of the forces it occupies a position closer to the plane EF than the plane $A'B'$; the plane $A'B'$ loses its previous connection with the plane EF, its place is occupied by the plane AB, and the dislocation moves from the point A to the point A'. But in this position the interaction between the planes $A'B'$ and $A''B''$ is the same as that between the planes AB and $A'B'$. Consequently the dislocation will not remain in the position A' but will move to a position A'' and so on, until it arrives at the face of the crystal or grain. The speed at which the dislocation moves can often be very high. As a result the part of the crystal above the plane CD is displaced to the right by one lattice parameter relative

to the lower part. Although this result is the same as if the upper part had moved relative to the lower part by one lattice parameter, the forces necessary to bring about these processes are completely different. In the dislocational mechanism the force required is defined as a quantity which is sufficient for a distortion of the lattice such that only one plane AB is displaced by one lattice parameter and not all planes at once.

In order to explain the many effects of plastic deformation let us consider a more involved model of dislocation. If, for example, a crystal lattice contains impurity atoms and linear dislocation takes

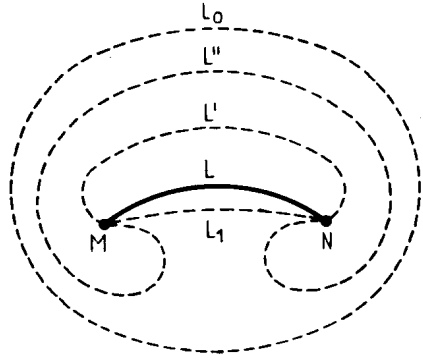

FIG. 60.

place through these points in the lattice, calculation of the interatomic forces shows that the dislocation is, so to speak, anchored (or pinned down) to these points. During the process of plastic deformation the linear dislocation which remains fixed at the points M and N becomes curved (Fig. 60 is a view from above relative to Fig. 59). The regions of dislocation with the greater curvature are displaced more rapidly than those with small curvature. The dislocation therefore occupies successively the positions MLN, $ML'N$, $ML''N$. At some instant the lower loops meet. The dislocation then divides into two parts: into a linear dislocation $ML_1'N$, which is completely similar to the initial dislocation MLN and into a dislocation loop L_0 which spreads in all directions. With increase in stress the dislocation ML_1N can repeat the whole cycle of the dislocation MLN. This mechanism is called the Frank–Ried "dislocation source". There are also linear dislocations which are anchored at several points and for which, at sufficiently high stresses, some of the connections are

broken. Since the movement of a pinned-down dislocation is more difficult than a free linear dislocation the strengthening effect of certain alloying admixtures which are present in the form of substitutional solutions becomes apparent.

The dislocation theory of plastic deformation enables us to give a qualitative explanation to such effects as the influence of temperature, rate of deformation and time. For example, at a high temperature the vibrations in the lattice in general assist movement of the dislocation.

Plastic deformation is sometimes explained by the processes of diffusion of molecules. Every molecule in a solid body performs thermal oscillations about a position of stable equilibrium and is situated in a so-called "energy source" formed by the neighbouring molecules. Sometimes the temperature fluctuations give the molecule sufficient energy to overcome the potential barrier (activation energy), and then the molecule moves to some neighbouring position: the molecules change places and a slow random movement of molecules takes place. As there is no order in this process no deformation of the body takes place. If a stress acts (for example a tensile stress) the height of the energy barriers falls especially in the direction of maximum shearing stress (in favourably orientated grains) and at a definite stress the molecules are able to diffuse preferentially in this direction. Vacancies in the lattice and interstitial atoms also diffuse. This diffusion leads to an irreversible deformation.

4. Rods of Variable Cross-section. The Method of Elastic Solutions

The properties of materials outlined in the previous paragraphs which are revealed by tensile or compressive tests on a cylindrical specimen give an adequate description of the behaviour of a cylindrical rod under tensile (or compressive) loading. If therefore in some structure made up of rods of constant cross-section the tensile or compressive forces in each rod are known, then the quantities necessary for estimating the strength and deformation (stresses, strains, load at failure) can be found directly from the stress–strain curve for a specimen of the material of the structure, it being assumed that they do not depend on the shape of the cross-section.

The behaviour of a rod of variable cross-section in tension or

compression is slightly more complicated. This problem illustrates the so-called method of elastic solutions, which is the general method of solving problems for small plastic deformations.

By a rod of variable cross-section we shall mean an oblong body the lateral surface of which is formed by moving along the x-axis the centre of gravity of an area bounded by a plane contour (lying in the yz plane), with a simultaneous change in shape of this contour (Fig. 6); the area of the cross-section is a known function $F(x)$. If mass forces $R_x(x)$ act on this rod in the direction of the axis Ox then it is essential to know the magnitude of the body force per unit length of the rod

$$Q(x) = F(x)\varrho R_x(x).$$

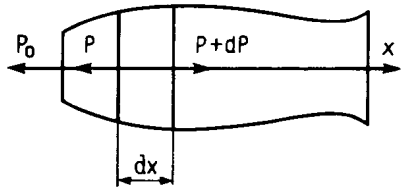

FIG. 61.

Considering the condition of equilibrium of an element of the rod of length dx (see Fig. 61), taking into account the mass forces, we arrive at the differential equation in the force P on the section x: For uniformly distributed stress σ (see below) we obtain the equation

$$\frac{dP}{dx} = -Q(x).$$

$$\frac{d(\sigma F)}{dx} = -Q(x).$$

In the case of a rod of constant cross-section we have that:

$$\frac{d\sigma}{dx} = -\frac{Q(x)}{F}.$$

If the forces acting on the rod are such that the material is nowhere stressed beyond the yield point, then $\sigma = E\varepsilon = E\,du/dx$ and the previous equation for a rod of constant cross-section reduces to a second order differential equation in the axial displacement $u(x)$:

$$\frac{d^2u}{dx^2} = -\frac{Q(x)}{EF}. \tag{2.6}$$

The quantity EF is called the stiffness of the rod in tension or compression.

Let us suppose also that on the left-hand end of the rod $x = 0$ there acts external forces which reduce to a force P_0 acting in the direction of the axis Ox. The determination of the stresses, as has already been pointed out, is a statically indeterminate problem, and in order to solve it by the methods of the strength of materials it is necessary to make certain assumptions concerning the nature of the strains. We make use again of the assumption that plane sections remain plane, and assume also that the displacements at all points on the cross-section are the same, so that

$$u = u(x), \quad \varepsilon \equiv \frac{du}{dx} = \varepsilon(x).$$

The stress will then be:

$$\sigma = \frac{P}{F} = E\varepsilon[1 - \omega(\varepsilon)],$$

where P is the tensile force at the section x. The magnitude of this force can be found if we imagine the rod cut at a distance x from the left-hand end, discard the right-hand part of the rod and then write down the equilibrium condition for the remaining left-hand part:

$$P(x) \equiv F\sigma = -\int_0^x Q(x)\,dx + P_0. \tag{2.7}$$

If all points of the rod deform elastically the strains are given by Hooke's law:

$$\varepsilon = \frac{\sigma}{E} = \frac{P_0}{EF} - \frac{1}{EF}\int_0^x Q(x)\,dx.$$

If at some section the stress exceeds the yield point, then if we know the relation $\sigma = \Phi(\varepsilon)$ or $\varepsilon = du/dx = \Phi^{-1}(\sigma)$ we can find by integration

$$u - u_0 = \int_0^x \Phi^{-1}(\sigma)\,dx, \tag{2.8}$$

where u_0 is the displacement of the left-hand end.

(2.7) can be rewritten, by making use of the relation between stresses and strains (2.4), in the form

$$E\frac{du}{dx}\left[1 - \omega\left(\frac{du}{dx}\right)\right] = \frac{P_0}{F} - \frac{1}{F}\int_0^x Q(x)\,dx, \tag{2.7'}$$

If we take over the term containing ω to the right-hand side and integrate with respect to x, we get that:

$$u - u_0 = \frac{P_0}{E}\int_0^x \frac{dx}{F} - \frac{1}{E}\int_0^x \left(\frac{1}{F}\int_0^x Q(x)\,dx\right) dx + \int_0^x \omega \frac{du}{dx}\,dx.$$

The second term can be transformed by Dirichlet's formula:

$$\int_0^x \frac{dx}{F}\int_0^x Q(x)\,dx = \int_0^x [\psi(x) - \psi(\eta)]\,Q(\eta)\,d\eta,$$

where we have introduced the definition

$$\psi(x) = \int_0^x \frac{dx}{F}.$$

Then

$$u - u_0 = \frac{P_0}{E}\psi(x) - \frac{1}{E}\int_0^x [\psi(x) - \psi(\eta)]\,Q(\eta)\,d\eta + \int_0^x \omega \frac{du}{dx}\,dx. \tag{2.9}$$

For the rod considered the following problems could arise:

(a) It is required to find the displacements for given mass forces and given values of P_0 and P_1 on the ends of the rod. The external loads must comprise a system which is statically equivalent to zero in order that the body should be in equilibrium. Therefore,

$$P_1 = P_0 - \int_0^l Q(x)\,dx \tag{2.10}$$

(this relation can be obtained directly from formula (2.7) for $P(x)$ when $x = l$, where l is the length of the rod). Making use of the assumption of plane sections, we can find the stress from formula (2.7) and the displacement from formula (2.9).

For given loads the stresses can be found from the equations of statics with the one limitation imposed on the strains by the assumption that plane sections remain plane; the problem in this case is statically determinate.

(b) The external conditions are given but the stresses cannot be found from the equations of statics by making use only of the assumption that plane sections remain plane, and it is necessary to take

into account other relations between the strains implied by the problem. The problem in this case is statically indeterminate. These conditions arise, for example, if for given mass forces limitations are imposed on the displacements of the ends of the rod by the external conditions. Let us suppose that the ends of the rod are fixed in flexible supports, the reactions of which depend on the displacements (for example elastic supports). Then an additional condition imposed on the strain is in the form of a relation between the relative displacement of the ends and the reactions of the supports:

$$u_1 - u_0 = f(P_0, P_1). \tag{2.11}$$

If both supports are rigid and do not move, then $f = 0$. If the left support is rigid and the right elastic, then $u_0 = 0$, $u_1 = -kP_1$ where k is the coefficient of elasticity of the support.

In statically indeterminate problems, therefore, we are always concerned with equations of three types:

(1) The equations of statics;

(2) The relations between strains and perhaps external forces;

(3) The physical law of the relation between stresses and strains.

These equations give a complete system which enables us to find the unknown reactions of the supports, the stresses and strains.

In the case of a rod of variable cross-section these equations reduce to a system of three equations obtained from (2.10), (2.9), (2.11), (2.7):

$$\left.\begin{aligned} P_1 &= P_0 - \int_0^l Q(x)\,dx, \\ f(P_0, P_1) &= \frac{P_0}{E}\psi(l) - \frac{1}{E}\int_0^l [\psi(l) - \psi(\eta)]\,Q(\eta)\,d\eta + \int_0^l \omega\varepsilon\,dx, \\ \varepsilon(x) &= \frac{P_0}{EF} - \frac{1}{EF}\int_0^x Q(x)\,dx + \omega(\varepsilon)\,\varepsilon(x), \end{aligned}\right\} \tag{2.12}$$

in which the unknowns are P_0, P_1 and $\varepsilon(x)$. The stress can then be found from the relation $\sigma = \Phi(\varepsilon)$. For elastic strains $\omega = 0$ and this system can be solved very simply; the first two equations form an independent set in the unknowns P_0 and P_1, and when they have been solved we find $\varepsilon(x)$ from the third equation.

With plastic strains the problem becomes more involved. As an approximate solution to this set of equations we shall apply the method of elastic solutions, i.e. the method of successive approximations considering ω as a small parameter.

As a first approximation we put $\omega = 0$ in (2.12), i.e. we find P_0', P_1' and ε' corresponding to a rod which is absolutely elastic.† Then from the first two equations we find P_0' and P_1', and from the third we find:

$$\varepsilon'(x) = \frac{P_0'}{EF} - \frac{1}{EF}\int_0^x Q(x)\,dx.$$

If $|\varepsilon'| < \varepsilon_S$ for any x, this means that no plastic strains occur in the rod. But let us consider the case when this is not so. From the conditions $|\varepsilon'|(x) \geqq \varepsilon_S$ we find a range Ω' of values of x where, as a first approximation, there will be plastic strains. In this range we find from the $\sigma \sim \varepsilon$ curve $\omega'(x) = \omega(\varepsilon')$ and substitute in the second equation of (2.12), the integral containing $\omega'\varepsilon'\,dx$ being taken over the range Ω'; now, solving the first and second equations for the forces, we find P_0'' and P_1'', and from the third we get that:

$$\varepsilon''(x) = \frac{P_0''}{EF} - \frac{1}{EF}\int_0^x Q(x)\,dx + \omega'(x)\,\varepsilon'(x)$$

and, therefore, $\omega'' = \omega(\varepsilon'')$ can be found as a function of x. This gives the values of the required quantities as a second approximation.

Putting $|\varepsilon''(x)| \geqq \varepsilon_S$ we find the range of plasticity Ω'' as a second approximation. If ε'' and ω'' are substituted in the second equation of (2.12), and if we then solve it with the first equation, we find P_0''', P_1''' as a third approximation and then ε''', ω''' and so on. This converging process in the limit gives an exact solution to the problem. It is rapidly convergent, so that the second or third approximation usually gives sufficient accuracy.

5. Frameworks

Many engineering structures (bridges, cranes, ships' hulls, aircraft structures, radio masts, etc.), are made up in some way or another of a number of rods joined together by bolts, rivets or

† The first approximation is therefore called the elastic solution or the elastic approximation.

welds. The number of rods which go to make up the structure can be very large.

Depending on the degree of stiffness of the rods themselves and their connections, framework structures can be divided for purposes of design into two categories: stiff-jointed and pin-jointed. In an ideal pin-jointed framework (or truss) the relative rotation of the rods meeting at a joint is not restrained by the joint. In a stiff-jointed framework (or frame) however the connection of the rods are assumed to be rigid, so that rotation of one rod relative to the others at that joint is impossible. In practice neither of these assumptions is absolutely valid, but we can always decide for any particular case

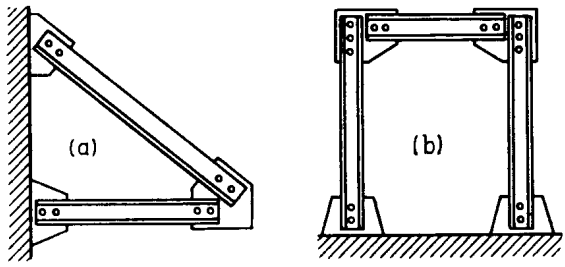

FIG. 62.

whether the behaviour of the system corresponds more closely to hinged or fixed joints and design accordingly.

The most simple approach is as follows. Providing that if we replace the actual joints by hinges the system does not become a mechanism which can, without deformation of its components, move about stationary points, it is permissible to treat the system as pin-jointed (Fig. 62a). If, however, the system does become a mechanism (Fig. 62b) it must be considered as stiff-jointed.

A framework system is characterized by:

(a) the number of rods N_c in the system,
(b) the number of nodal points N_y,
(c) the number of supports N_0 and the properties of these supports,
(d) the external forces applied to the system,
(e) the elasto-plastic properties of the material of the rods which make up the system.

Let us consider first of all those frameworks which can be considered as pin-jointed, that is, those for which we can consider the connections and supports as hinged.

Hinged joints can be classified according to the number of degrees of freedom which they have. Hinged supports can be of three different types.

(1) Hinged supports with two degrees of freedom. These can be represented as an absolutely rigid support rod OA which is pinned

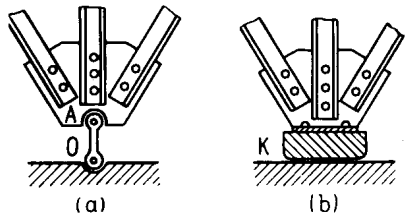

FIG. 63.

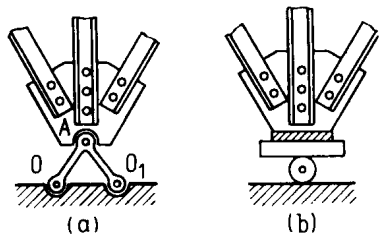

FIG. 64.

to a fixed hinge O and a movable hinge (the support joint) A, at which several rods meet and which is able to move slightly in a plane perpendicular to the support rod (Fig. 63a).

In practice these conditions are realized if the support joint is fixed to a bearing plate K which can slide freely in the plane of the support (Fig. 63b): this can be brought about by resting the bearing plate on two layers of mutually perpendicular rollers.

(2) Hinged supports with one degree of freedom. These can be represented as two absolutely rigid support rods hinged to the surface of the support at the points O and O_1 (Fig. 64a) and to the support joint A. This allows movement of the joint A in a direction perpendicular to the plane OAO_1. In practice this type of support

is made up either of a cylindrical roller (Fig. 64b) or of a slide which is able to move only in one direction.

(3) Hinged supports which have no degree of freedom. These can be represented by three supports rods O_1A, O_2A, O_3A converging at the support joint (Fig. 65a). In practice a support of this type is made of a spherical ended rod with a step-bearing (Fig. 65b).

The above hinged supports can be part of a simple support system or part of a compound support system.

A simple support joint is one which is connected to some fixed surface (a plane for example). Each type of support imposes a certain number of conditions on the movement of the support

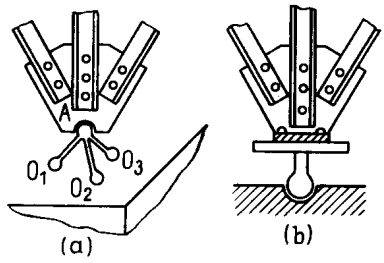

FIG. 65.

joint. In order to derive the equations for these conditions we shall assume that the plane of the fixed support (or element of the supporting surface) is positioned so that its normal $\boldsymbol{\nu}$ coincides with the direction in which movement is restrained. (This is done purely for convenience: in actual fact the position of the plane of the support is immaterial.) In the case of a support of the first type, represented by a support rod OA (Fig. 63a), the normal $\boldsymbol{\nu}$ coincides with the direction of this rod, i.e. with the direction of the normal to the plane on which the support lies. We choose two perpendicular directions in this support plane, which are characterized by the unit vectors $\boldsymbol{\nu}'$ and $\boldsymbol{\nu}''$, so that

$$\boldsymbol{\nu}\boldsymbol{\nu}' = \boldsymbol{\nu}'\boldsymbol{\nu}'' = \boldsymbol{\nu}''\boldsymbol{\nu} = 0.$$

In a support of the first type displacements are possible only in the directions $\boldsymbol{\nu}'$ and $\boldsymbol{\nu}''$. In the case of a support of the second type we take as the direction $\boldsymbol{\nu}'$ the second direction in which movement is restrained, so that movement is possible in the direction $\boldsymbol{\nu}''$.

In a support of the third type movement is not possible in any of the directions $\boldsymbol{\nu}$, $\boldsymbol{\nu}'$ or $\boldsymbol{\nu}''$. If there are several supports, each will be characterized by its own three vectors $\boldsymbol{\nu}_n$, $\boldsymbol{\nu}'_n$, $\boldsymbol{\nu}''_n$. If we choose some fixed rectangular system of coordinates having unit vectors $\boldsymbol{i}, \boldsymbol{j}, \boldsymbol{k}$ along the directions of the axes, we can compile a table of direction cosines of the unit vectors $\boldsymbol{\nu}_n$, $\boldsymbol{\nu}'_n$, $\boldsymbol{\nu}''_n$.

	ν_n	ν'_n	ν''_n
i	l_n	l'_n	l''_n
j	m_n	m'_n	m''_n
k	n_n	n'_n	n''_n

The values of $l_n, l'_n, \ldots, n''_n$ are known, as they are determined by the directions of $\boldsymbol{\nu}_n$, $\boldsymbol{\nu}'_n$, $\boldsymbol{\nu}''_n$ at each support.

Considering the nth support joint, we can write down the following expression for the displacement vector of this joint

$$\boldsymbol{\delta}_n = 0\boldsymbol{\nu}_n + \delta'_n\boldsymbol{\nu}'_n + \delta''_n\boldsymbol{\nu}''_n.$$

But

$$\boldsymbol{\delta}_n = u_n\boldsymbol{i} + v_n\boldsymbol{j} + w_n\boldsymbol{k}.$$

Therefore

$$\left.\begin{aligned} u_n &= \boldsymbol{\delta}_n\boldsymbol{i} = \delta'_n l'_n + \delta''_n l''_n, \\ v_n &= \boldsymbol{\delta}_n\boldsymbol{j} = \delta'_n m'_n + \delta''_n m''_n, \\ w_n &= \boldsymbol{\delta}_n\boldsymbol{k} = \delta'_n n'_n + \delta''_n n''_n. \end{aligned}\right\} \tag{2.13}$$

The expressions (2.13) can be looked upon as the parametric equations of compatibility.

In the case of a support of the first type $\delta'_n \neq 0$ and $\delta''_n \neq 0$ and they are arbitrary, so that the three components u_n, v_n, w_n of the displacement can be expressed in terms of the two independent quantities δ'_n and δ''_n. Eliminating these two independent quantities we obtain one equation of compatibility. A support of the first type therefore, corresponds to one equation of compatibility.

In the case of a support of the second type $\delta'_n = 0$ and δ''_n is arbitrary. In this case eqn. (2.13) give two equations of compatibility, which in parametric form can be written as

$$u_n = \delta''_n l''_n, \quad v_n = \delta''_n m''_n, \quad w_n = \delta''_n n''_n.$$

Eliminating the arbitrary quantity, we obtain two equations of compatibility.

In the case of a support of the third type (a fixed support) $\delta_n' = \delta_n'' = 0$ and (2.13) gives three equations of compatibility:

$$u_n = v_n = w_n = 0.$$

A compound support is one in which part of the support joints are attached to one absolutely rigid body, which is taken as fixed, and part are situated on another absolutely rigid body, which can move relative to the former body on account of the deformation of the system of rods joining them. As an example we might take the engine supports shown in Fig. 66. The engine A which we can take as an absolutely rigid, movable body is attached through a

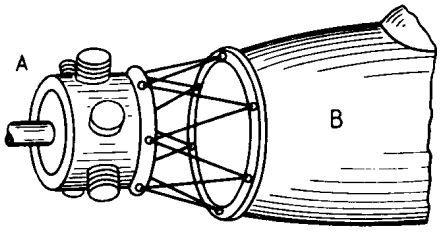

FIG. 66.

system of rods to the fuselage B of the aircraft, which can be taken as an absolutely rigid fixed body.

In order to calculate the stresses and strains in each rod it is necessary to find the displacements of all the support joints attached to the movable body. In order to demonstrate the method of solving compound supports, let us suppose that all the support joints are of the third type (fixed) and situated in one support plane on the movable, absolutely rigid body, so that $\boldsymbol{\nu}$, $\boldsymbol{\nu}'$, $\boldsymbol{\nu}''$ are fixed to this plane. The absolutely rigid support body has six degrees of freedom given by the components of the vector of the translational displacement $\boldsymbol{d}$ of some point O and the components of the rotation vector $\boldsymbol{\omega}$:

$$\boldsymbol{d} = d\boldsymbol{\nu} + d'\boldsymbol{\nu}' + d''\boldsymbol{\nu}'',$$

$$\boldsymbol{\omega} = p\boldsymbol{\nu} + q\boldsymbol{\nu}' + r\boldsymbol{\nu}''.$$

Here d, d', d'', p, q, r are independent quantities.

Let us consider the displacement of the nth joint (Fig. 67) situated at the point O_n with radius vector ϱ_n relative to O:

$$\varrho_n = \varrho_n \nu + \varrho_n' \nu' + \varrho_n'' \nu''.$$

It is made up of a translational movement and a rotational movement, so that for the displacement vector δ_n we have:

$$\delta_n = d + \varrho_n \times \omega.$$

But if we choose some fixed rectangular system of coordinates with unit vectors i, j, k, then

$$\delta_n = u_n i + v_n j + w_n k.$$

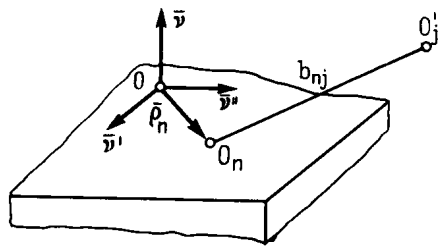

FIG. 67.

Consequently

$$u_n = \delta_n i = di + (\varrho_n \times \omega) i = di + (i \times \varrho_n) \omega.$$

If l, l', l'' are the cosines of the angles between the directions ν, ν', ν'' and the direction i, then, since

$$i \times \varrho_n = -\varrho_{nz} j + \varrho_{ny} k,$$

we have that

$$u_n = dl + d'l' + d''l'' + (-\varrho_{nz} j + \varrho_{ny} k) \cdot \omega.$$

Also,

$$\varrho_{nx} = \varrho_n i = \varrho_n l + \varrho_n' l' + \varrho_n'' l'',$$
$$\varrho_{ny} = \varrho_n j = \varrho_n m + \varrho_n' m' + \varrho_n'' m'',$$
$$\varrho_{nz} = \varrho_n k = \varrho_n n + \varrho_n' n' + \varrho_n'' n''$$

and

$$\omega i = pl + ql' + rl'',$$
$$\omega j = pm + qm' + rm'',$$
$$\omega k = pn + qn' + rn''.$$

Therefore

$$\left.\begin{aligned} u_n &= dl + d'l' + d''l'' + p(\varrho_{ny}n - \varrho_{nz}m) + q(\varrho_{ny}n' - \varrho_{nz}m') \\ &\quad + r(\varrho_{ny}n'' - \varrho_{nz}m''), \\ v_n &= dm + d'm' + d''m'' + p(\varrho_{nz}l - \varrho_{nx}n) + q(\varrho_{nz}l' - \varrho_{nx}n') \\ &\quad + r(\varrho_{nz}l'' - \varrho_{nx}n''), \\ w_n &= dn + d'n' + d''n'' + p(\varrho_{nx}m - \varrho_{ny}l) + q(\varrho_{nx}m' - \varrho_{ny}l') \\ &\quad + r(\varrho_{nx}m'' - \varrho_{ny}l''). \end{aligned}\right\} \tag{2.14}$$

Thus the displacement of any support point can be expressed in terms of the six independent quantities d, d', d'', p, q, r which define the movement of the absolutely rigid body. There might be less than six of these quantities if confinements are imposed on the absolutely rigid body.

If the displacements of the nth and ith joints, which connect a rod of length b_{ni}, are known,

$$\boldsymbol{\delta}_n = u_n\boldsymbol{i} + v_n\boldsymbol{j} + w_n\boldsymbol{k},$$
$$\boldsymbol{\delta}_i = u_i\boldsymbol{i} + v_i\boldsymbol{j} + w_i\boldsymbol{k},$$

then the relative extension of this rod is

$$\varepsilon_{ni} = \frac{1}{b_{ni}}(\boldsymbol{\delta}_i - \boldsymbol{\delta}_n)\,\boldsymbol{\nu}_{ni},$$

where $\boldsymbol{\nu}_{ni}$ is a unit vector in the direction of the rod b_{ni}, or

$$\varepsilon_{ni} = \frac{1}{b_{ni}}[(u_i - u_n)\,l_{ni} + (v_i - v_n)\,m_{ni} + (w_i - w_n)\,n_{ni}]. \tag{2.15}$$

Let us now consider the nth internal (not support) joint of a pin-jointed framework made up of k_n rods. There might be applied to this joint, apart from the forces transmitted by the rods, an external force $\boldsymbol{P}_n$. This might be, for example, part of the weight of the rods. The problem is, for a given force $\boldsymbol{P}_n$ and conditions at the supports, to find the tensile of compressive forces S_{ni} in each rod, and then to find the stresses and strains. The number of unknown forces S_{ni} is equal to the number of rods N_c. Since each internal joint has three degrees of freedom the number of degrees of freedom of the framework is

$$N_{cc} = 3N_y + N_{co}, \tag{2.16}$$

where N_y is the number of internal joints and N_{co} is the number of degrees of freedom of all the supports.†

Since the number of independent equations of statics which can be derived for a mechanical system is equal to the number of degrees of freedom, the possibility of determining the forces in all the rods of the framework solely from the equations of statics depends on the difference between the number of unknown forces, which is equal to the number of rods, and the number of independent equations of statics, which is equal to the number of degrees of freedom. This difference L is called the number of "redundancies":

$$L = N_c - N_{cc}. \tag{2.17}$$

If $L = 0$ the number of unknown forces is equal to the number of equations of statics, and the framework is statically determinate. If $L > 0$ the number of unknown forces in the rods is greater than the number of equations of statics and the framework is statically indeterminate. If $L < 0$ the framework is able to move without deformation of the rods, i.e. it is a mechanism.

It should be noted that the condition that $L \geqq 0$ is necessary, but not sufficient, for the framework not to be a mechanism. For, it is possible to join to a statically indeterminate system containing L_1 redundancies, a mechanism made up of k_1 rods and having k_2 degrees of freedom, so that $k_1 - k_2 = L_1$. Then in general $L = 0$, but the system would contain a mechanism. In many specific cases, therefore, it is necessary not only to calculate the number of "redundacies" L, but, in addition, to carry out a kinematic analysis of the system considering the rods as absolutely rigid.

Examples. **1.** In a plane pin-jointed framework (Fig. 68) $N_c = 15$, $N_y = 7$, $N_{co} = 1$ (the left-hand support is fixed, the right-hand has one degree of freedom). In the case of a plane framework each internal joint has two degrees of freedom. Therefore

$$N_{cc} = 2N_y + N_{co} = 2 \times 7 + 1 - 15,$$

and from formula (2.17)

$$L = N_c - N_{cc} = 15 - 15 = 0.$$

The framework is a statically determinate truss.

† The number of degrees of freedom of all the supports N_{co} can be given in the form $N_{co} = 2N_0^{(1)} + N_0^{(2)}$, where $N_0^{(1)}$ is the number of supports of the first type (with two degrees of freedom) and $N_0^{(2)}$ is the number of supports of the second type (with one degree of freedom).

2. In a plane framework (Fig. 69) $N_c = 15$, $N_y = 7$, $N_{co} = 1$

$$N_{cc} = 2N_y + N_{co} = 15, \quad L = N_c - N_{cc} = 0.$$

This system, however, is not statically determinate; it is a mechanism. It ceases to be a mechanism if the support B is fixed. It would then become a statically indeterminate framework ($N_c = 15$, $N_{co} = 0$, $N_y = 7$, $L = 15 - 14 = 1$).

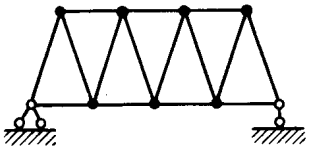

FIG. 68.

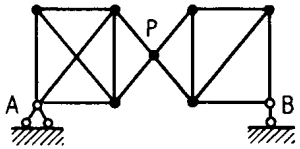

FIG. 69.

6. THE SOLUTION OF PIN-JOINTED FRAMEWORKS

(a) *Statically Determinate Frameworks*

In order to obtain the reactions of the supports we write the equilibrium equation for the framework as a whole:

$$\left.\begin{aligned} \sum_n \boldsymbol{P}_n + \sum_k \boldsymbol{R}_{vk} = 0, \\ \sum_n \boldsymbol{r}_n \times \boldsymbol{P}_n + \sum_k \boldsymbol{r}_k \times \boldsymbol{R}_{vk} = 0, \end{aligned}\right\} \tag{2.18}$$

where $\boldsymbol{P}_n$ are the external forces applied at the joints, $\boldsymbol{r}_n$ the radius vector of the nth internal joint, $\boldsymbol{R}_{vk}$ the reaction of the kth support, $\boldsymbol{r}_k$ the radius vector of this support. In order to find the reactions at the supports from these six equations the latter must be arranged to impose on the truss six equations of compatibility. Since a support of the first sort imposes one equation of compatibility, a support of the second sort, two, and of the third sort three equations of compatibility, the condition that the truss is statically determinate, $L = 0$, must be supplemented by the further condition that the number of unknown quantities—the reactions of the supports—is six. If the truss has six supports of the first type ($N_{co} = 12$), then the determination of the six reactions from (2.18) is a matter of resolving the given set of external forces $\boldsymbol{P}_n$ into six directions.

Having found the reactions of the supports we can find the forces in the rods, starting with an external or support joint at which not more than three rods converge, and making use of the equilibrium equations for the joint, considered as a material point. (In the case

of a plane framework we start with a joint at which two rods converge.) We then move to the next joint, and so on. If we define $\boldsymbol{\nu}_{ni}$ as the unit vector in a direction from the joint n to the joint i along a rod of length b_{ni} between theset wo joints, then for every nth joint we have an equilibrium equation

$$\sum_i S_{ni}\boldsymbol{\nu}_{ni} + \boldsymbol{P}_n + \boldsymbol{R}_{\nu k} = 0, \tag{2.19}$$

where S_{ni} is the force in the rod, $\boldsymbol{\nu}_{ni} = l_{ni}\boldsymbol{i} + m_{ni}\boldsymbol{j} + n_{ni}\boldsymbol{k}$ and $\boldsymbol{R}_{\nu k} = 0$ if $k \neq n$ (i.e. if the joint considered is not a support joint). If we start the calculation as shown above (i.e. from a joint where $i \leqq 3$), then eqn. (2.19), which is equivalent to three scalar equations, will contain not more than three unknowns.

If we define the projections of the vector $\boldsymbol{P}_m + \boldsymbol{R}_{\nu k}$ ($\boldsymbol{R}_{\nu k} = 0$ for $k \neq m$) on the axes as X_m, Y_m, Z_m, analysis of the framework shows that the force in the rod b_{ni} can be written in the form

$$S_{ni} = \sum_m (X_m k_{mx}^{(ni)} + Y_m k_{my}^{(ni)} + Z_m k_{mz}^{(ni)}),$$

where $k_{mx}^{(ni)}$, $k_{my}^{(ni)}$, $k_{mz}^{(ni)}$ are so-called influence coefficients. For example, $k_{mx}^{(ni)}$ is the force which is set up in the rod ni under the action of a unit force in the direction of the x-axis applied at the mth joint.

From the forces we can then find the stresses in the rods

$$\sigma_{ni} = \frac{S_{ni}}{F_{ni}},$$

where F_{ni} is the cross-sectional area of the rod ni, and then, making use of the $\sigma = \Phi_1(\varepsilon)$ curve, we can find the strains

$$\varepsilon_{ni} = \Phi_1^{-1}\left(\frac{S_{ni}}{F_{ni}}\right).$$

Substituting these values in formulae (2.15), we obtain the equations

$$(u_i - u_n)\, l_{ni} + (v_i - v_n)\, m_{ni} + (w_i - w_n)\, n_{ni} = \varepsilon_{ni} b_{ni},$$

which, together with equations of compatibility of the type (2.13) or (2.14), give a complete set of equations for finding the displacements of all the joints. If, with the aid the equations of compatibility, we eliminate the "redundant displacements" of the support joints, we obtain a set of N_{cc} equations with N_{cc} unknown displacements, and each equation will contain six unknowns. The difficulty is to solve this set of linear equations. In frameworks with a large

number of joints this set contains a large number of equations and solving them by determinants becomes extremely laborious.

Let us now consider the problem of residual stresses and strains in a framework when plastic strains occur in the rods under the action of external forces. Since from eqns. (2.18) R_{rk} vanish when the external forces P_n are removed, and since according to eqns. (2.19), the forces S_{ni} in the rods are linear homogeneous functions of the external forces (including the reactions at the supports), then after complete removal of the external forces the forces in the rods become zero, so that residual stresses in statically determinate frameworks do not occur.

In order to determine the residual strains we will make use of the concept of the total strain being the sum of the elastic and the plastic strains

$$\varepsilon_{ni} = \varepsilon_{ni}^{(p)} + \frac{S_{ni}}{E_{ni}F_{ni}}.$$

Since unloading takes place according to an elastic law, this expression has a residual strain if S_{ni} is taken to mean the residual forces in the rods:

$$\varepsilon_{ni}^{(o)} = \varepsilon_{ni}^{(p)} + \frac{S_{ni}^{(o)}}{E_{ni}F_{ni}}.$$

But these residual forces in the rods are zero after complete removal of the loads. Therefore

$$\varepsilon_{ni}^{(o)} = \varepsilon_{ni}^{(p)} = \varepsilon_{ni} - \frac{S_{ni}}{E_{ni}F_{ni}}, \tag{2.20}$$

i.e. the residual strains are equal to the difference between the total strains at the instant immediately before unloading commences (i.e. at the greatest values of the load) and the strains to which the truss would have been subjected at these (greatest) values of the applied load had it behaved completely elastically.

Substituting these values of $\varepsilon_{ni}^{(o)}$ in eqns. (2.15), we obtain a set of equations for the residual displacements

$$\begin{aligned}(u_i^{(o)} - u_n^{(o)})\, l_{ni} + (v_i^{(o)} - v_n^{(o)})\, m_{ni} + (w_i^{(o)} - w_n^{(o)})\, n_{ni} \\ = \varepsilon_{ni}^{(o)} b_{ni} \equiv b_{ni}\left(\varepsilon_{ni} - \frac{S_{ni}}{E_{ni}F_{ni}}\right) \equiv b_{ni}(\varepsilon_{ni} - \varepsilon_{ni}^{(e)}).\end{aligned} \tag{2.21}$$

We note that, according to (2.15), the left- and right-hand sides contain differences of the same type, the former corresponding to

the displacements at an instant immediately before unloading, and the latter to the displacements that the joints would have received for the same (maximum) loads, if the system had behaved perfectly elastically.

By generalizing eqns. (2.20) and (2.21), we can formulate the following unloading theorem for frameworks: in order to find the residual displacements, strains and stresses in any framework after complete removal of the load, subtract from the displacements, strains and stresses which occur in the system at this load the displacements, strains and stresses which would have occurred in the framework at this load if it had been completely elastic.

If we define $\Delta \boldsymbol{u}_n, \Delta \varepsilon_{ni}, \Delta \varrho_{ni}$ as the differences between the full values of the displacements, strains and stresses and their residual values, then

$$\left.\begin{aligned} \Delta \boldsymbol{u}_n &\equiv \boldsymbol{u}_n - \boldsymbol{u}_n^{(o)} = \boldsymbol{u}_n^{(e)}, \\ \Delta \varepsilon_{ni} &\equiv \varepsilon_{ni} - \varepsilon_{ni}^{(o)} = \varepsilon_{ni}^{(e)} \equiv \frac{S_{ni}}{E_{ni} F_{ni}}, \\ \Delta \sigma_{ni} &\equiv \sigma_{ni} - \sigma_{ni}^{(o)} = E_{ni} \varepsilon_{ni}^{(e)}. \end{aligned}\right\} \tag{2.22}$$

The first two equations can be derived from (2.21) together with (2.15), and from (2.20); in the third equation, for statically determinate trusses, $\sigma_{ni}^{(o)} = 0$.

This theorem presupposes that nowhere in the system do plastic strains of opposite sign occur—secondary plastic strains—after removal of the load.

(b) *Statically Indeterminate Frameworks*

In statically indeterminante frameworks $L = N_c - N_{cc} > 0$, i.e. there are a certain number of "redundancies"—forces in the rods or supports reactions. If, for example, in the truss of Fig. 68 the right-hand support is fixed, which decreases the number of degrees of freedom by one, there appears one "redundancy"—the horizontal reaction of the right-hand support.

In order to derive the equations for the forces, stresses, strains and displacements we make use of the general principles of theoretical mechanics.

Considering the nth joint (internal or support), we give it a virtual displacement $\Delta \boldsymbol{\delta}_n$, i.e. a displacement compatible with the confinements imposed on the system. The work done by the external

forces in these displacements will be $P_n \Delta\delta_n$ at each joint. For the support joint this work will be non-zero if, apart from the support reaction, an external force is applied to it which does not coincide in direction with the reaction. The support reaction in the case of a simple support connected to a fixed supporting surface does no work (it is unable to move in the direction of the reaction), but in the case of a compound support the reactions are in the nature of internal forces and do not feature in the balance of work done by the external forces. For compound supports it is necessary to take into account the work done by the external forces applied to the movable supporting body in the virtual displacements which this body can make. If on each kth movable body of the compound support, an external force $\boldsymbol{P}_k$ and a moment $\boldsymbol{M}_k$ are applied to a fixed point on the movable support surface (Fig. 67), we can find the work done by these forces in the virtual displacements, $\Delta \boldsymbol{d}_k$ and $\Delta \boldsymbol{\omega}_k$, of the movable supporting body. We then obtain the following expression for the total work done in the virtual displacements by the external forces applied to the framework:

$$\Delta A = \sum_n \boldsymbol{P}_n \Delta \boldsymbol{\delta}_n + \sum_k (\boldsymbol{P}_k \Delta \boldsymbol{d}_k + \boldsymbol{M}_k \Delta \boldsymbol{\omega}_k).$$

The force S_{ni} in the rod ni, which arises during the deformation, does the work

$$S_{ni} v_{ni} (\Delta\delta_i - \Delta\delta_n) = S_{ni} \Delta\varepsilon_{ni} b_{ni}.$$

According to Lagrange's principle, for a mechanical system in equilibrium the work done by the internal forces in the virtual displacements is equal to the work done by the external forces, i.e.

$$\sum_n \sum_i S_{ni} (\Delta\delta_i - \Delta\delta_n) \, v_{ni} = \sum_i \boldsymbol{P}_n \Delta \boldsymbol{\delta}_n + \sum_k (\boldsymbol{P}_k \Delta \boldsymbol{d}_k + \boldsymbol{M}_k \Delta \boldsymbol{\omega}_k). \tag{2.23}$$

The summation in the left-hand side is taken over all the rods in the system, so that here, $n \neq i$; the first summation in the right-hand side is taken over all the joints, including the support joints to which external forces are applied; the second summation is taken over all the movable absolutely rigid supporting bodies. If we consider only the non-support joints, then since $n \neq i$, we have from (2.23) for the nth (non-support) joint, that

$$-\Delta \boldsymbol{\delta}_n \sum_i S_{ni} v_{ni} = \boldsymbol{P}_n \Delta \boldsymbol{\delta}_n$$

or since $\Delta\boldsymbol{\delta}_n$ is arbitrary

$$\sum_i S_{ni}\boldsymbol{\nu}_{ni} + \boldsymbol{P}_n = 0. \tag{2.23'}$$

The summation is taken over all joints which are connected by rods to the nth joint.

Considering the qth support joint of the first type (with two degrees of freedom, Fig. 63) we have, from 2.23, that

$$-\Delta\boldsymbol{\delta}_q \sum_i S_{qi}\boldsymbol{\nu}_{qi} = \boldsymbol{P}_q\Delta\boldsymbol{\delta}_q.$$

But one equation of compatibility applies to the virtual displacements of this sort of joint (see eqns. (2.13)), which can be written in the form $\boldsymbol{\delta}_q = 0$ or in the form

$$\boldsymbol{\delta}_q = 0\boldsymbol{\nu}_q + \delta'_q\boldsymbol{\nu}'_q + \delta''_q\boldsymbol{\nu}''_q,$$

i.e.

$$\Delta\boldsymbol{\delta}_q = \boldsymbol{\nu}'_q\Delta\delta'_q + \boldsymbol{\nu}''_q\Delta\delta''_q.$$

The equation for the qth support joint can therefore be written in the form

$$\left(\sum_i S_{qi}\boldsymbol{\nu}_{qi} + \boldsymbol{P}_q\right)(\boldsymbol{\nu}'_q\,\Delta\delta'_q + \boldsymbol{\nu}''_q\,\Delta\delta''_q) = 0,$$

from which, since $\Delta\delta'_q$ and $\Delta\delta''_q$ are arbitrary, we get that

$$\left.\begin{aligned}\sum_i S_{qi}(\boldsymbol{\nu}_{qi}\boldsymbol{\nu}'_q) + \boldsymbol{P}_q\boldsymbol{\nu}'_q = 0,\\ \sum_i S_{qi}(\boldsymbol{\nu}_{qi}\boldsymbol{\nu}''_q) + \boldsymbol{P}_q\boldsymbol{\nu}''_q = 0.\end{aligned}\right\} \tag{2.23''}$$

At the support joints where no external forces are applied we must put $\boldsymbol{P}_q = 0$.

For the rth support of the second type (with one degree of freedom, Fig. 64), we have from (2.23) that:

$$\Delta\boldsymbol{\delta}_r\left(\sum_i S_{ri}\boldsymbol{\nu}_{ri} + \boldsymbol{P}_r\right) = 0.$$

But there are two equations of compatibility imposed on the virtual displacements of this type of joint which can be written in the form

$$\Delta\boldsymbol{\delta}_r = 0\boldsymbol{\nu}_r + 0\boldsymbol{\nu}'_r + \Delta\delta''_r\boldsymbol{\nu}''_r \equiv \Delta\delta''_r\boldsymbol{\nu}_r \times \boldsymbol{\nu}'_r.$$

Consequently the equation for the rth support joint of the second type becomes

$$\sum_i S_{ri}\boldsymbol{\nu}_{ri}(\boldsymbol{\nu}_r \times \boldsymbol{\nu}'_r) + \boldsymbol{P}_r(\boldsymbol{\nu}_r \times \boldsymbol{\nu}'_r) = 0. \tag{2.23'''}$$

If at some support no external force is applied we must put $\boldsymbol{P}_r = 0$. For a support of the third type all the virtual displacements are zero.

Thus each support of the first type gives two equations of the form (2.23″) and a support of the second type gives one equation of the form (2.23‴), whereas a support of the third type gives no equations.

For the jth support on the kth support body in a compound support, if we define $\boldsymbol{\varrho}_j^{(k)}$ as the radius vector of this support relative to the origin O_k of a coordinate system fixed to this body (Fig. 67), we have for its displacements

$$\boldsymbol{\delta}_j^{(k)} = \boldsymbol{d}_k + \boldsymbol{\varrho}_j^{(k)} \times \boldsymbol{\omega}_k,$$

so that for the virtual displacement $\Delta\boldsymbol{\delta}_j^{(k)}$, we have:

$$\Delta\boldsymbol{\delta}_j^{(k)} = \Delta\boldsymbol{d}_k + \boldsymbol{\varrho}_j^{(k)} \times \Delta\boldsymbol{\omega}_k.$$

From (2.23) we find that for the kth support body:

$$-\sum_i \sum_j S_{ij}^{(k)} \Delta\boldsymbol{\delta}_j^{(k)} \boldsymbol{v}_{ij}^{(k)} = \boldsymbol{P}_k \Delta\boldsymbol{d}_k + \boldsymbol{M}_j \Delta\boldsymbol{\omega}_k.$$

Since in the support body itself there are no rods connecting different supports, the summation with respect to j is taken over all supports lying on the kth support body, and the summation with respect to i is taken over all the joints of the other support bodies which are connected to each joint of the kth support by the rod b_{ij}. In other words, the summation is taken over all rods bearing on the kth support body. Considering the expression derived above for $\Delta\boldsymbol{\delta}_j^{(k)}$ in terms of $\Delta\boldsymbol{d}_k$ and $\Delta\boldsymbol{\omega}_k$, we can write this equation in the form

$$\left(\sum_i \sum_j S_{ij}^{(k)} \boldsymbol{v}_{ij}^{(k)} + \boldsymbol{P}_k\right) \Delta\boldsymbol{d}_k + \sum_i \sum_j S_{ij}^{(k)} \boldsymbol{v}_{ij}^{(k)} (\boldsymbol{\varrho}_j^{(k)} \times \Delta\boldsymbol{\omega}_k) + \boldsymbol{M}_k \Delta\boldsymbol{\omega}_k = 0$$

or, since $\boldsymbol{v}_{ij}^{(k)} (\boldsymbol{\varrho}_j^{(k)} \times \Delta\boldsymbol{\omega}_k) = (\boldsymbol{v}_{ij}^{(k)} \times \boldsymbol{\varrho}_j^{(k)}) \Delta\boldsymbol{\omega}_k$, we have that

$$\left(\sum_i \sum_j S_{ij}^{(k)} \boldsymbol{v}_{ij}^{(k)} + \boldsymbol{P}_k\right) \Delta\boldsymbol{d}_k + \left[\sum_i \sum_j S_{ij}^{(k)} (\boldsymbol{v}_{ij}^{(k)} \times \boldsymbol{\varrho}_j^{(k)}) + \boldsymbol{M}_k\right] \Delta\boldsymbol{\omega}_k = 0.$$

Since $\Delta\boldsymbol{d}_k$ and $\Delta\boldsymbol{\omega}_k$ are arbitrary, we obtain the two vector equations

$$\left.\begin{aligned} \sum_i \sum_j S_{ij}^{(k)} \boldsymbol{v}_{ij}^{(k)} + \boldsymbol{P}_k = 0, \\ \sum_i \sum_j S_{ij}^{(k)} (\boldsymbol{v}_{ij}^{(k)} \times \boldsymbol{\varrho}_j^{(k)}) + \boldsymbol{M}_k = 0, \end{aligned}\right\} \qquad (2.23'''')$$

which are equivalent to six scalar equations. If there are no external forces applied to some support body, we must put $\boldsymbol{P}_k = 0$ and $\boldsymbol{M}_k = 0$ in the eqns. (2.23''') for this body.

Thus we have three eqns. (2.23') for each non-support joint, two eqns. (2.23'') for each support joint of the first type, one eqn. (2.23''') for each support joint of the second type and six eqns. (2.23''') for each support body.

If we express all the forces S_{ni} in terms of the displacements of the internal joints $\boldsymbol{\delta}_n$, of the support joints $\boldsymbol{\delta}_s$ and of the support bodies $\boldsymbol{d}_k$, $\boldsymbol{\omega}_k$, we obtain a set of N_{cc} equations with N_{cc} unknowns.

Bearing in mind that for each rod there is a known relation between the stresses and strains in the form $\sigma_{ni} = E_{ni}\varepsilon_{ni}[1 - \omega_{ni}(\varepsilon_{ni})]$ we can write down that

$$S_{ni} = B_{ni}\varepsilon_{ni}\,[1 - \omega_{ni}(\varepsilon_{ni})], \tag{2.24}$$

where $B_{ni} = E_{ni}F_{ni}$ is the stiffness of the rod ni in tension. These expressions for S_{ni} can be substituted in eqns. (2.23')–(2.23''') which will now contain the strains of the rods as unknowns. We can then substitute for the strains their expressions (2.15) in terms of displacements which gives us a set of linear equations in the displacements of the joints (internal and support).

Retaining, for simplicity, the terms ε_{ni} instead of the right-hand sides of (2.15), and putting all terms containing $\omega_{ni}(\varepsilon_{ni})$ as $\boldsymbol{P}_n^{(\Phi)}$, we can replace eqns. (2.23') to (2·23''') by the equation

$$\sum_i (\boldsymbol{\nu}\boldsymbol{B})_{ni}\varepsilon_{ni} + \boldsymbol{P}_n - \boldsymbol{P}_n^{(\Phi)} = 0 \quad (n = 1, 2, \ldots, N_y), \tag{2.25'}$$

where N_y is the number of internal joints

$$\left.\begin{aligned} \sum_i (\boldsymbol{\nu}\boldsymbol{B})_{qi}\boldsymbol{\nu}'_q\varepsilon_{qi} + (\boldsymbol{P}_q - \boldsymbol{P}_q^{(\Phi)})\boldsymbol{\nu}'_q = 0, \\ \sum_i (\boldsymbol{\nu}\boldsymbol{B})_{qi}\boldsymbol{\nu}''_q\varepsilon_{qi} + (\boldsymbol{P}_q - \boldsymbol{P}_q^{(\Phi)})\boldsymbol{\nu}''_q = 0 \\ (q = 1, 2, \ldots, N_0^{(1)}), \end{aligned}\right\} \tag{2.25''}$$

where $N_0^{(1)}$ is the number of supports of the first type,

$$\sum_i (\boldsymbol{\nu}\boldsymbol{B})_{ri}(\boldsymbol{\nu}_r \times \boldsymbol{\nu}'_r)\,\varepsilon_{ri} + (\boldsymbol{P}_r - \boldsymbol{P}_r^{(\Phi)})(\boldsymbol{\nu}_r \times \boldsymbol{\nu}'_r) = 0$$
$$(r = 1, 2, \ldots, N_0^{(2)}), \tag{2.25'''}$$

where $N_0^{(2)}$ is the number of supports of the second type

$$\left.\begin{aligned} \sum_i \sum_j (\boldsymbol{\nu}\boldsymbol{B})_{ij}^{(k)}\varepsilon_{ij}^{(k)} + \boldsymbol{P}_k - \boldsymbol{P}_k^{(\Phi)} = 0, \\ \sum_i \sum_j (\boldsymbol{\nu}\boldsymbol{B})_{ij}^{(k)} \times \boldsymbol{\varrho}_j^{(k)}\varepsilon_{ij}^{(k)} + \boldsymbol{M}_k - \boldsymbol{M}_k^{(\Phi)} = 0 \\ (k = 1, 2, \ldots, k), \end{aligned}\right\} \tag{2.25''''}$$

where k is the number of movable support bodies. In these equations

$$\left.\begin{aligned} \boldsymbol{P}_n^{(\Phi)} &= \sum_i{}' (\boldsymbol{\nu B})_{ni}\varepsilon_{ni}{}'\omega_{ni}(\varepsilon_{ni}), \\ \boldsymbol{M}_k^{(\Phi)} &= \sum_i{}' \sum_j{}' (\boldsymbol{\nu B})_{ij}^{(k)} \times \boldsymbol{Q}_j^{(k)}\varepsilon_{ij}^{(k)}{}'\omega_{ij}\,(\varepsilon_{ij}^{(k)}) \end{aligned}\right\} \tag{2.26}$$

are the fictitious loads applied to the framework. In equations (2.25''), (2.25''') and (2.25'''') it is assumed that ε_{ij} are expressed by formulae (2.15) in terms of displacements, that the displacements of the support joint are expressed by formulae (2.13) in terms of the displacements $\boldsymbol{\delta}_n'$, $\boldsymbol{\delta}_n''$, and that the displacements of the support bodies are expressed by formulae (2.14) in terms of the displacements $\boldsymbol{d}_k$, $\boldsymbol{\omega}_k$. Eliminating terms containing $\omega_{ni}(\varepsilon_{ni})$ and writing the equations in the form (2.25') to (2.25''') is convenient for the application of the method of elastic solutions which was explained in § 4 of this chapter.

As a first approximation we solve the set of eqns. (2.25')–(2.25'''') for $\boldsymbol{P}_k^{(\Phi)} = 0$, $\boldsymbol{M}_k^{(\Phi)} = 0$. If we then find that $\varepsilon_{ni}' < \varepsilon_s^{(ni)}$ then this means that no plastic strains occur and the first approximation is the exact solution to the problem. If, however, some of the $\varepsilon_{ni}' > \varepsilon_s^{(ni)}$ then we must as a second approximation find from the known relation $\sigma_{ni} = \Phi_1^{(ni)}(\varepsilon_{ni})$ the values of $\omega_{ni} = \omega_{ni}(\varepsilon_{ni}')$ given by the formula

$$\omega = \frac{E\varepsilon - \Phi_1(\varepsilon)}{E\varepsilon}$$

(see formula (2.4)) and then find the value of the fictitious loads $\boldsymbol{P}_n^{(\Phi)}$ and $\boldsymbol{M}_k^{\Phi}$ as a first approximation from formulae (2.26). We then substitute these values of the fictitious loads in equations (2.25')–(2.25'''') and solve them, thus finding a second approximation to the values of the displacements and strains.

By repeating these operations we make successive approximations until the difference between the values of successive approximations is within the limits of the required accuracy.

7. The Resistance of a Material to Shear

In tests on a cylindrical specimen in tension or compression the only stress acting on the cross-section is a normal stress which can be found from the magnitude of the applied force; longitudinal

fibres experience only extensions which can be measured by an extensometer. This has enabled us to establish quantitative relations between normal stress and strain, both for increasing and decreasing loads, which describe the behaviour of the material under tension and compression. The next step is to devise an experiment which will enable us to describe the behaviour of the material in shear and to establish the relation between the shearing stress and the shear. For this purpose it is normal to make a torsion test on a thin-walled cylinder.

If we apply to the ends of a straight circular cylinder forces which reduce to a moment, the vector of which is directed along the axis of the cylinder and which is called a torque, then at some distance from the ends of the cylinder (of the order of its diameter) the state

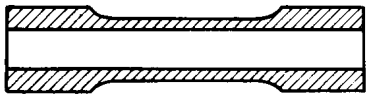

FIG. 70.

of stress in the material becomes uniform. In actual fact, as we shall see in the following paragraph the stress depends on the radius, i.e. it varies over the thickness of the cylinder, but when this thickness h is small compared with the mean radius a ($h/a \ll 1$), this variation can be ignored.

The sort of specimen used in shear tests is shown in Fig. 70. The thickened ends of the specimen are placed in the jaws of the testing machine and steel plugs are inserted into the cylinder at the ends to prevent crushing. One of the jaws remains still and the other rotates about an axis which coincides with the axis of the specimen. A lever or dynamometer arrangement is used to measure the torque. The strain is measured by an extensometer which gives the displacement in a circumferential direction of one point relative to another lying on the same generator.

As in the case of tension, we make use of the assumption that plane sections remain plane; that material points which before deformation were situated in planes perpendicular to the axis of the cylinder remain in this plane (or in a parallel plane) after deformation. The validity of this assumption can be confirmed by

observing a set of parallel circles drawn on the external (and sometimes also on the internal) surface of the specimen: these circles remain circles; since the thickness of the walls is small we are quite justified in assuming that particles on the internal points of the walls behave in exactly the same way.

In order to find the internal forces we make an imaginary section perpendicular to the axis of the cylinder, discard one part and investigate the equilibrium of the other. Since the external forces on this remaining half reduce to a torque, the internal forces on the section must also reduce to a moment of the same magnitude with a vector directed along the axis of the cylinder. Such a moment could be set up by stresses the vectors of which lie in the plane of

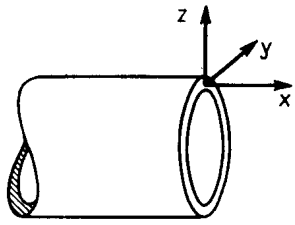

FIG. 71.

the section and which are directed along the tangents to circles with a common centre on the axis of the cylinder, i.e. by shearing stresses. From the loading conditions it is clear that there is no reason to assume that there occurs on the cross-section a self-balancing system of normal stresses or a self-balancing system of shearing stresses directed along the radius. The latter is particularly a valid assumption since the lateral surface of the specimen (external and internal) is free from loading: in particular, there are no components of load along the generators of the cylinder, and therefore, from the law of complementary shear stresses, there are no radial components of the shearing stresses at the edges of the cross-section. With thin walls it is quite obvious that there are none throughout the whole cross-section.

If at every point on the mean circumference of the cross-section we choose a local system of coordinates and direct the axis Ox, along the axis of the cylinder, the axis Oy along the tangent to the mean circumference of the section and the axis Oz along the radius

(Fig. 71), the stress acting on the section is $\sigma_{yx} = \sigma_{xy}$ and $\sigma_{xx} = \sigma_{zx} = 0$. Also, $\sigma_{yz} = \sigma_{zz} = 0$, which corresponds to the assumption that particles which before deformation lay on one radius remain on this radius after deformation, and the angles between radial fibres are not distorted, which satisfies the conditions required for the experiment. The stress σ_{yy} is also zero.

In future we shall define the sole shearing stress acting on the section, $\sigma_{yx} = \sigma_{xy}$ as τ.

In order to evaluate τ it is sufficient to write down the equilibrium condition for the remaining part of the cylinder (after we have discarded the other part). The cross-sectional area of the cylinder

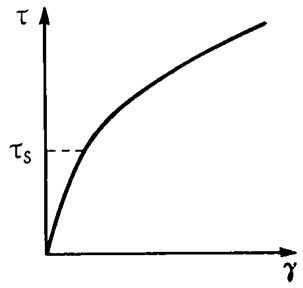

FIG. 72.

is $2\pi ah$, so that the moment of the internal forces about the axis Ox is $2\pi ah a\tau$. Equating this to the given external torque, we get that

$$\tau \equiv \sigma_{yx} = \frac{M}{2\pi a^2 h}. \tag{2.27}$$

If we observe an orthogonal set of generators and circumferences drawn on the surface of the specimen we notice a distortion of the right-angles after deformation. These distortions constitute the shear strain $2\varepsilon_{xy} = \gamma$ and can be measured by an extensometer.

If we measure M and γ during the course of the experiment we can construct the curve of the $\tau \sim \gamma$ relation. Its general shape is shown in Fig. 72. As a whole the nature of this relation is the same as the $\sigma \sim \varepsilon$ relation in the case of tension: there is a straight portion which corresponds to the elastic behaviour of the material, a curved portion which corresponds to the plastic region, and on

removal of the load we obtain a straight line parallel to the elastic portion. All our deductions therefore concerning the elasto-plastic properties of a material which were the result of tensile tests could have been made from the results of torsion experiments. As regards the numerical values, the yield points of material in shear are less than the yield points in tension. For example, for annealed steel containing 0·37 per cent carbon, $\sigma_S = 2460$ kg/cm^2 and $\tau_S = 1580$ kg/cm^2, for armco iron $\sigma_S = 1070$ kg/cm^2, $\tau_S = 910$ kg/cm^2. For many materials we can put

$$\sigma_S = \tau_S \sqrt{3}.$$

The ratio of the stress τ to the shear strain γ in the linear region of the $\tau \sim \gamma$ relation is called the modulus of rigidity and is denoted by G. For steel $G = 8 \times 10^5$ kg/cm^2, for cold rolled copper $G = 4 \times 10^5$ kg/cm^2, for aluminium $G = 2{\cdot}7 \times 10^5$ kg/cm^2.

8. Torsion of a Circular Rod

In the case of torsion of a rod of solid circular section or in the form of a thick-walled cylinder the assumption of a uniform stress distributed along a radius, which was valid in the previous paragraph, no longer applies. In order to establish the distribution of stress for a given external torque we make use of the assumption that plane sections remain plane and that radial fibres remain radial after deformation. Then every cross-section rotates as a whole about the axis of the rod, so that no shearing stresses occur between co-axial cylinders of which we can imagine the rod to be comprised. We can say then that at every point of the cross-section the shearing stress acts in a direction perpendicular to the radius and that τ is the function of r only (as a consequence of radial symmetry).

As before we imagine the rod to be cut into two parts, discard one part and consider the equilibrium of the other. In this way we find that the relation between the stress τ and the applied torque is given by

$$M = \int_0^a \tau 2\pi r^2 dr. \tag{2.28}$$

Since $\tau = \tau(r)$ this relation refers to an infinite number of unknown values of τ.

If we denote the angle of twist per unit length of rod (i.e. the angle of relative rotation of cross-sections unit distance apart)

by θ, the movement of any point is in a direction perpendicular to the radius and is

$$u_\vartheta = \vartheta r x,$$

where x is the distance from a section taken as fixed; the difference between the displacements of two points A and B (Fig. 73), which before deformation lay on a straight line parallel to the axis at a distance dx apart, is $\Delta u_\vartheta = \vartheta r\, dx$. We have therefore for the shear strain (see Fig. 73) that:

$$\gamma = \frac{\Delta u_\vartheta}{dx} = \vartheta r. \tag{2.29}$$

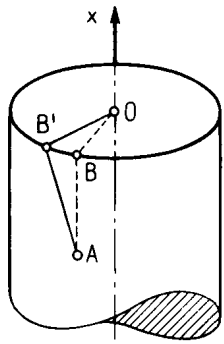

FIG. 73.

From shear experiments (torsion of thin-walled circular cylinders) we have the relation

$$\tau = \Psi(\gamma)$$

or

$$\tau = G\gamma[1 - \omega'(\gamma)] = G\vartheta r[1 - \omega'(\gamma)].$$

Since from (2.29) $dr = 1/\vartheta\, d\gamma$, we have from (2.28) that

$$M = \frac{2\pi}{\vartheta^3} \int_0^{\vartheta a} \Psi(\gamma)\gamma^2\, d\gamma \equiv \chi(\vartheta).$$

If we now express ϑ in terms of M, then from the relation $\gamma = \vartheta r$ we obtain an expression for the shear strain γ in terms of the torque M, and from the relation $\tau = \Psi(\gamma)$ we can express τ in terms of M. Conversely therefore, from torsion experiments on a circular specimen of solid section we can obtain the $\tau \sim \gamma$ relation.

If we make use of the expression for τ in terms of ω', we find from (2.28) that

$$M = G\vartheta J_p - \frac{2\pi G}{\vartheta^3} \int_{\gamma S}^{\vartheta a} \omega'(\gamma)\gamma^3 \, d\gamma, \tag{2.30}$$

where $J_p = \pi a^4/2$ is the polar moment of inertia of the cross-section of the rod and $\gamma_S = \tau_S/G$ is the limit of elastic shear strain.

For loading within the elastic limit, we have that $\omega'(\gamma) = 0$ and $M = G\vartheta J_p$. This gives the angle of twist ϑ

$$\vartheta = \frac{M}{GJ_p}, \tag{2.31}$$

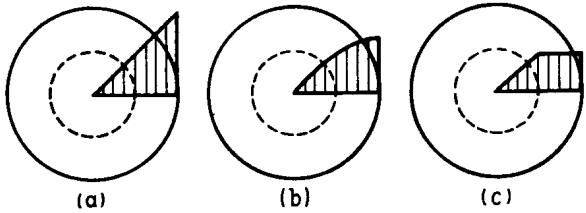

FIG. 74.

so that from (2.29) we have for the shear strain γ:

$$\gamma = \frac{Mr}{GJ_p}, \tag{2.32}$$

and thus

$$\tau = \frac{Mr}{J_p}. \tag{2.33}$$

The quantity GJ_p is called the torsional stiffness of a circular rod. We see that for torsion of a rod of circular section within the elastic limit the shearing stress increases from the centre to the periphery according to a linear law and reaches its greatest value at the surface of the rod. The diagram of the distribution of shearing stresses along a radius is shown in Fig. 74a. As the torque increases plastic strains occur, first of all at the surface of the rod, with an elastic core still remaining. As the torque increases further the radius of the elastic core (i.e. the radius of the cylindrical surface separating the regions of elastic and plastic strains) decreases, tending in the limit to zero. The part of the diagram of shearing stresses

from $r = \varrho$ (from the boundary between the regions of elastic and elasto-plastic strains) to $r = a$ will be curved (Fig. 74b). The magnitude of ϱ can be found from the relation $\varrho = \gamma_S/\vartheta$ if the magnitude of ϑ is known.

If the material of the rod has the property of linear strain hardening, so that the $\tau \sim \gamma$ curve is in the form of an open polygon, then

$$\omega'(\gamma) = \lambda'\left(1 - \frac{\gamma_S}{|\gamma|}\right),$$

where $\lambda' = (G - G')/G$ and G' is the strain hardening modulus in shear. We then have from the relation (2.30) that:

$$\begin{aligned} M &= GJ_p\vartheta - \frac{2\pi G\lambda'}{\vartheta^3}\left(\frac{\vartheta^4 a^4}{4} - \frac{\gamma_S}{3}a^3\vartheta^3 + \frac{1}{12}\gamma_S^4\right) \\ &= GJ_p\vartheta - \frac{G\lambda'}{\vartheta^3}\left(J_p\vartheta^4 - \gamma_S S_p\vartheta^3 + \frac{1}{6}\pi\gamma_S^4\right), \end{aligned} \tag{2.34}$$

where $S_p = \frac{2}{3}\pi a^3$ is the first moment of area of the cross-section.

In cases when the material of the rod displays only slight strain hardening, so that we can put $\lambda' = 0$, the problem is one of finding the carrying capacity of the rod in torsion, i.e. of evaluating the greatest torque which can be resisted by the rod. The shearing stress diagram for $G' = 0$ is of the form shown in Fig. 74c. The angle of twist for a fixed value of torque is prevented from increasing infinitely by the elastic core. From (2.34) for $\lambda' = 0$, we get that

$$M = GS_p\gamma_S - \frac{\pi G}{6\vartheta^3}\vartheta_S^3$$

or since $\vartheta = \gamma_S/\varrho$,

$$M = GS_p\gamma_S - \frac{1}{6}\pi G\varrho^3 = S_p\tau_S - \frac{1}{6}\pi G\varrho^3.$$

The carrying capacity of the rod will just be exhausted at a value of torque at which the radius of the elastic core becomes zero. At this value of the torque the angle of twist will continue to increase with no further increase in torque. From the last expression, when $\varrho = 0$ we obtain the formula for the limiting torque

$$M_{\text{lim}} = S_p\tau_S = \frac{2}{3}\pi a^3\tau_S.$$

It should be noted that the torque reaches its limiting value only after infinite increase in the angle of twist. In actual fact $\vartheta = \gamma_s/\varrho \to \infty$ as $\varrho \to 0$. Therefore the loss of carrying capacity really indicates, not that the torque has reached the above limiting value which is calculable, but simply that the angle of twist has increased very rapidly for very little increase in the torque—very rapidly, at any rate, compared with its increase during the elastic stage.

Let us consider now the problem of determining the residual stresses which remain in the rod after the removal of a torque which has caused plastic deformation of the rod. As M decreases, i.e. as ϑ decreases, the unloading process commences simultaneously at all points in the rod. Then since the τ–γ curve during unloading is

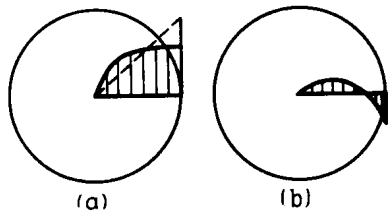

FIG. 75.

a straight line parallel to the elastic portion, a decrease in the torque by ΔM causes a decrease in stress at every point equal to the stress that would have resulted in the perfectly elastic rod due to the application of a torque ΔM. To find the residual stresses after complete removal of the torque we must therefore subtract from the stresses acting at each point of the section of the rod at the greatest value of torque, which can be found as shown above, the stresses which would have been set up in the rod for the same value of torque if the material had been perfectly elastic (this state of stress is called a fictitious elastic state of stress). If the diagram of shearing stresses at the greatest value of torque is of the form shown in Fig. 75a, the corresponding diagram at the same torque in the case of an ideally elastic rod would be that given by the dotted line. The diagram of the distribution of residual stresses therefore is as shown in Fig. 75b.

This method is a further illustration of the above mentioned theorem of unloading.

9. Combined Stress State in a Beam

As was pointed out in § 4 of this chapter rods and beams are usually assumed to be bodies the lateral dimensions of which are considerably less than the longitudinal dimensions. At every point of some line in a longitudinal direction we can make a section the area of which will be less than the area of any other section made through the same point. This section is known as a cross-section. The centroids of the cross-sections form a line which is called the axis of the rod or beam.

Many problems in practice can be reduced to the problem of beams. With a certain degree of approximation we can consider such things as the tooth on a gear wheel, a bridge, a ship's hull, a high building, etc., as examples of beams.

Let us consider a beam with a straight axis which we shall take as the axis Ox. We shall take the origin of coordinates at the centroid of the left-hand end of the beam and the y and z-axes as along the principal axes of inertia of the cross-section. Under the action of external forces (including the reactions of the supports)—distributed and concentrated—the beam is in equilibrium. In order to find the internal forces within the beam we make use of the method of sections. At some distance x from the left-hand end of the beam we make an imaginary section perpendicular to the axis Ox and discard the right-hand part of the beam. The internal forces (stresses) at this section reduce to the force

$$\boldsymbol{Q} = Q_x\boldsymbol{i} + Q_y\boldsymbol{j} + Q_z\boldsymbol{k},$$

applied at the centre of gravity of the section and to a moment

$$\boldsymbol{M} = M_x\boldsymbol{i} + M_y\boldsymbol{j} + M_z'\boldsymbol{k}.$$

One of the components of the force $Q_x = P$ is called the longitudinal (tensile or compressive) force—which is the resultant of the normal stresses over the section. The components Q_y and Q_z are called shear forces and are related to the shearing stresses on the section. The component M_x of the moment is the torque; it is also related to the shearing stresses on the section. The components M_y and M_z', which are called bending moments, arise due to the non-uniform distribution of normal stresses over the section. The force $\boldsymbol{Q}$ and the moment $\boldsymbol{M}$, to which the internal forces at the cross-section reduce, can be found from the external forces acting on the beam; for the remaining left-hand part of the beam is in equilibrium

under the action of the external forces applied to it and of the stresses at the section x. Consequently the internal forces on the section x are statically equivalent to the external forces acting on the discarded right-hand part of the beam. The distributed mass forces and the external surface forces reduce to the distributed force $\boldsymbol{q}(x) = q_x\boldsymbol{i} + q_y\boldsymbol{j} + q_z\boldsymbol{k}$ and to a distributed moment $\boldsymbol{m}(x) = m_x\boldsymbol{i} + m_y\boldsymbol{i} + m_z'\boldsymbol{k}$ per unit length of the beam, so that on an element of the beam of length dx (Fig. 76) there acts a force $\boldsymbol{q}(x)\,dx$ and a moment $\boldsymbol{m}(x)\,dx$. If the length of the beam is l then the equilibrium condition for the left-hand part of the beam is of the form

$$\boldsymbol{Q} = \int_x^l \boldsymbol{q}(\xi)\,d\xi + \Sigma \boldsymbol{R}_r,$$

$$\boldsymbol{M} = \int_x^l \boldsymbol{m}(\xi)d\xi + \int_x^l (\xi - x)\boldsymbol{i} \times \boldsymbol{q}(\xi)d\xi + \Sigma \mathrm{mom}_x \boldsymbol{R}_r + \Sigma \boldsymbol{M}_r. \quad (2.35)$$

where $\boldsymbol{R}_r$ is the concentrated force lying to the right of the section x, $\mathrm{mom}_x\boldsymbol{R}_r$ is the moment of this force about the centre of gravity of the section x and $\boldsymbol{M}_r$ is the concentrate moment applying to the right of the section x.

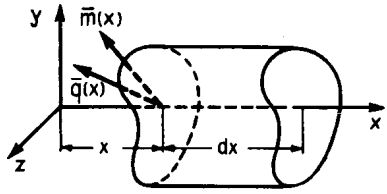

FIG. 76.

Equations (2.35), which relate the resultant internal forces on the section to the external forces, are in effect formulae for reducing the system of forces (acting on the discarded right-hand part of the beam) to one acting at a point (the centre of gravity of the section x). It is customary to represent the distribution of bending moments and shear forces along the axis of the beam, calculated on the basis of expressions (2.35) for given external forces, in the form of bending moment and shear force diagrams. From these diagrams we can see immediately at which sections the bending moments and shear forces reach their maximum values. These are

the "critical" sections from the point of view of the normal bending and shearing stresses.

We shall adopt the convention that Q_x, Q_y, Q_z, q_x, q_y and q_z will be considered positive if they act in the positive direction of the axes x, y, z when the external normal to the remaining left-hand part of the beam is directed along the x-axis. The moments M_x, $M_y, M_z', m_x, m_y, m_z'$ will be considered positive if they give a rotation in a clockwise direction when viewed from the side of the positive direction of the corresponding axis. Since

$$\boldsymbol{i} \times \boldsymbol{q} = \begin{vmatrix} \boldsymbol{i} & \boldsymbol{j} & \boldsymbol{k} \\ 1 & 0 & 0 \\ q_x & q_y & q_z \end{vmatrix} = -q_z \boldsymbol{j} + q_y \boldsymbol{k},$$

then from the second relation of (2.35) we have that:

$$\boldsymbol{M} = \int_x^l \boldsymbol{m}(\xi)\, d\xi - \boldsymbol{j} \int_x^l (\xi - x) q_z(\xi)\, d\xi + \boldsymbol{k} \int_x^l (\xi - x) q_y(\xi) d\xi + \Sigma \operatorname{mom}_x \boldsymbol{R}_r.$$

We see that for positive $q_y, q_z, R_y^{(r)}, R_z^{(r)}$ the corresponding part of the moment M_y is positive and that of the moment M_z' is negative. We shall therefore in future write $M_z' = -M_z$:

$$\boldsymbol{M} = M_x \boldsymbol{i} + M_y \boldsymbol{j} - M_z \boldsymbol{k}$$

and similarly

$$\boldsymbol{m} = m_x \boldsymbol{i} + m_y \boldsymbol{j} - m_z \boldsymbol{k}.$$

Differentiating the expressions for $\boldsymbol{Q}$ and $\boldsymbol{M}$ with respect to x, we get that:

$$\frac{d\boldsymbol{Q}}{dx} = -\boldsymbol{q}(x),$$

$$\frac{d\boldsymbol{M}}{dx} = -\boldsymbol{m}(x) + \boldsymbol{j} \int_x^l q_z(\xi)\, d\xi - \boldsymbol{k} \int_x^l q_y(\xi)\, d\xi = -\boldsymbol{m}(x) + \boldsymbol{j} Q_z - \boldsymbol{k} Q_y.$$

The relations

$$\left.\begin{aligned} \frac{d\boldsymbol{Q}}{dx} &= -\boldsymbol{q}(x), \\ \frac{d\boldsymbol{M}}{dx} &= -\boldsymbol{m}(x) + \boldsymbol{j} Q_z - \boldsymbol{k} Q_y \end{aligned}\right\} \tag{2.36}$$

are called the differential equations of Jouravsky (from the name of D. I. Jouravsky who derived them about 100 years ago). In terms of projections on the axes these relations become

$$\left.\begin{aligned} &\frac{dQ_x}{dx} = -q_x, \quad \frac{dQ_y}{dx} = -q_y, \quad \frac{dQ_z}{dx} = -q_z; \\ &\frac{dM_x}{dx} = -m_x, \quad \frac{dM_y}{dx} = -m_y + Q_z, \quad \frac{dM_z}{dx} = -m_z + Q_y. \end{aligned}\right\} \tag{2.37}$$

If we consider $\boldsymbol{Q}$ and $\boldsymbol{M}$ as the result of reducing the external forces acting on the right-hand part of the beam to the centre of gravity of the section x, then the relations (2.36) and (2.37) are identities. If however we consider $\boldsymbol{Q}$ and $\boldsymbol{M}$ as the resultant internal forces acting on the section x, then these expressions relate the internal forces to the external forces.

It should be noted that in evaluating the bending moment and shear force at some section in terms of external forces we assume that the beam is an absolutely rigid body. This is admissible since if we take into account the change in position of the force after deformation we introduce corrections which are small quantities of the second order, since the strains are small. Cases of very flexible beams in which this is not so will not be considered here.

Examples. **1.** The beam (bar) shown in Fig. 77 has a fixed hinged left-hand support (of the type shown in Fig. 64) and a movable hinged right-hand support (of the type shown in Fig. 63). This sort of beam is statically determinate in the sense that the equations of statics† are sufficient to determine the support reactions. The reactions of the supports in Fig. 77 are the two forces $\boldsymbol{A}$ and $\boldsymbol{B}$ acting vertically upwards. In order to evaluate them it is sufficient to take moments of all the forces (including the support reactions) about the hinges B and A:

$$\bar{A} = \frac{\Sigma \operatorname{mom}_B P_i + \Sigma M_i}{l}, \quad \bar{B} = -\frac{\Sigma \operatorname{mom}_A P_i + \Sigma M_i}{l},$$

where P_i is the vertical projection of the force acting on the beam, M_i is the concentrated moment. If the concentrated force has a horizontal component, then the fixed support A gives a horizontal reaction equal to the sum of the horizontal components of the forces $\boldsymbol{P}_i$.

† It is only in this sense that we talk of beams being statically determinate. The problem of finding the stresses in a beam is always statically indeterminate. In the same way in a statically determine truss (No. 5) the equations of statics determine the forces in the members, but not the stresses.

In this particular case

$$\bar{A} = \frac{Pb}{l}, \quad \bar{B} = \frac{Pa}{l} = \frac{P(l-b)}{l} = P - \bar{A}.$$

If at some point we imagine the beam to be cut, and discard the left-hand part, we get that:

$$Q = \bar{A} = \frac{Pb}{l},$$

if $x < a$, and for $x > a$

$$Q = -\bar{B} = -\frac{P(l-b)}{l}.$$

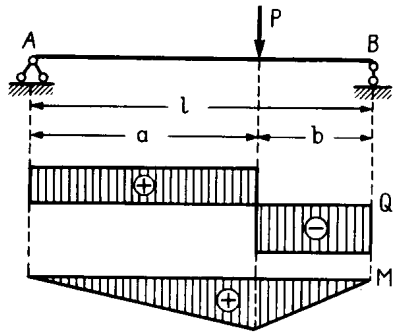

FIG. 77.

Similarly, on the first part

$$M(x) = \bar{A}x = \frac{Pb}{l}x,$$

and on the second part

$$M(x) = \bar{A}x - P(x-a).$$

The bending moment and shear force diagrams are shown in Fig. 77. We note the discontinuity in the shear force diagram, in which the magnitude of the step in the diagram is equal to the magnitude of the applied force, and in the bending moment diagram we notice a sharp change in slope under the point of application of the concentrated force. This is in agreement with Jouravsky's theorem (2.37). The values of Q at the points A and B (at the supports) are of course equal to the support reactions (at the point B, of opposite sign). The values of M at these points are zero since the hinged supports cannot resist moments.

2. For the beam shown in Fig. 78 the shear force and bending moment diagrams can be obtained by superimposing diagrams of the type shown in Fig. 77. They can of course be obtained as in the previous example by making an imaginary section in each of the three portions of the beam. We suggest that the reader solves the problem by this method as an exercise.

3. For a beam with a uniformly distributed load q (Fig. 79) we have that:

$$\bar{A} = \bar{B} = \frac{ql}{2},$$

$$Q(x) = \bar{A} - qx = \frac{ql}{2} - qx,$$

$$M(x) = \bar{A}x - q\frac{x^2}{2} = \frac{1}{2}qx(l - x).$$

The bending moment diagram is a parabola with a maximum at $x = l/2$. According to Jouravsky's theorem $Q = 0$ at $x = l/2$. The maximum value of M (at $x = l/2$) is $\frac{1}{8}ql^2$.

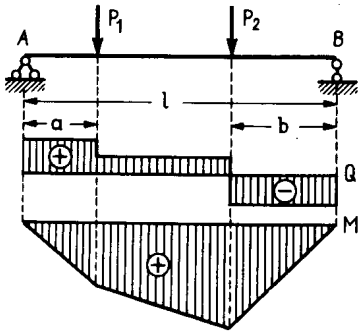

FIG. 78.

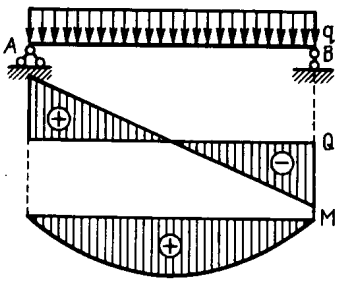

FIG. 79.

4. A cantilever with built-in left-hand end (Fig. 80) is also statically determinate since the support reaction at the point A is given only by two quantities: the vertical force A and the support moment M_A. We note that in this case it is unnecessary to work out the support reactions first. They can be determined during the process of constructing the shear force and bending moment diagrams if we imagine the cantilever to be cut at the point x, discard not the right-hand, but the left-hand side, and alter the resulting signs of Q and M. As a result we get that:

$$Q(x) = q(l - x),$$

$$M(x) = -\tfrac{1}{2}q(l - x)^2.$$

The bending moment diagram is a parabola with a maximum value at $x = l$. The values of $\bar{A}$ and M_A can be found from these expressions for $x = 0$:

$$\bar{A} = ql, \quad M_A = -\tfrac{1}{2}ql^2.$$

5. The beam shown in Fig. 81 can be imagined to be made up of two beams: of the cantilever BC at the "built-in" end of which we find the "support"

moment $M_B = -Pa$, and of the beam AB loaded by an "external" moment $-M_B$ and a concentrated force P at the support B. The shear force and bending moment diagrams for the whole beam are shown in Fig. 81, where

$$\bar{A} = -\frac{Pa}{l}, \quad \bar{B} = P\frac{l+a}{l}.$$

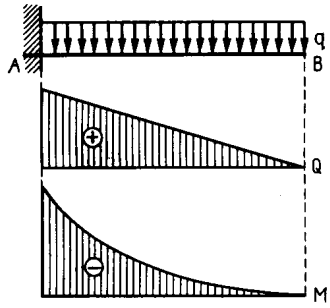

FIG. 80.

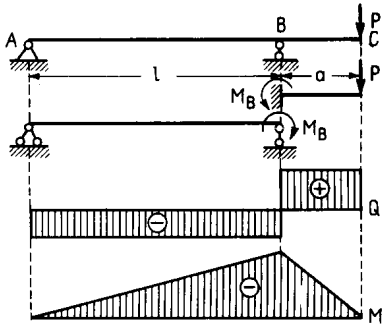

FIG. 81.

10. STRESSES AND STRAINS IN A BEAM

Let us now relate the external forces directly with the stresses acting on the section x. If $\boldsymbol{S}_x = \sigma_{xx}\boldsymbol{i} + \sigma_{xy}\boldsymbol{j} + \sigma_{xz}\boldsymbol{k}$ is the stress vector at some point (y, z) on the cross-section (Fig. 82), then

$$\boldsymbol{Q} = \iint_F \boldsymbol{S}_x \, dF,$$

$$\boldsymbol{M} = \iint_F \boldsymbol{r} \times \boldsymbol{S}_x \, dF,$$

where

$$\boldsymbol{r} = 0 \,.\, \boldsymbol{i} + y\boldsymbol{j} + z\boldsymbol{k}.$$

Considering the expressions for $\boldsymbol{Q}$ and $\boldsymbol{M}$ in terms of external forces given by (2.35), which in this case must be considered as the result of reducing the external forces acting on the part of the beam to the right of the section considered, to the centre of gravity of this section, we find in terms of projections on the axes that

$$\left.\begin{aligned} &Q_x = \iint_F \sigma_{xx}\, dF, \quad Q_y = \iint_F \sigma_{xy}\, dF, \quad Q_z = \iint_F \sigma_{xz}\, dF; \\ &M_x = \iint_F (y\sigma_{xz} - z\sigma_{xy})\, dF, \quad M_y = \iint_F \sigma_{xx} z\, dF, \quad M_z = \iint_F \sigma_{xx} y\, dF. \end{aligned}\right\} \tag{2.38}$$

Bearing in mind that the problem of torsion can be considered separately, we can assume that the external forces are such that $M_x = 0$. Equations (2.38) are not sufficient to determine the stresses σ_{xx}, σ_{xy}, σ_{xz} which are functions of the coordinates of the point. As usual we require to find certain relations of a geometrical nature which, together with the equations for the relation between stresses and strains, will enable us to find the stresses.

In order to determine the normal stresses σ_{xx} it is sufficient to make use of the assumption that plane sections remain plane. The shearing stresses σ_{xy}, σ_{xz} will be small compared with σ_{xx} if the length of the beam is considerably greater than the lateral dimensions. In order to estimate the magnitudes of the stresses we shall consider their mean values.

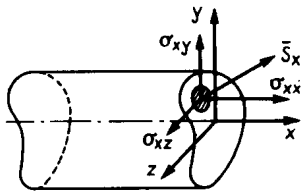

FIG. 82.

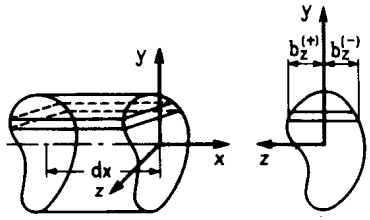

FIG. 83.

Let us consider a small strip in the beam of thickness dy and at a distance y from the plane (xz) (Fig. 83) and of width $b_z(y) = b_z^{(+)} + b_z^{(-)}$, which for a beam of constant cross-section is independent of x. The equation of the boundary of the cross-section can be written in the form $b_z = b_z(y)$. We define the mean stresses in the following way:

$$\bar{\sigma}_{xx}^{(z)} = \frac{1}{b_z^{(+)} + b_z^{(-)}} \int_{-b_z^{(-)}}^{b_z^{(+)}} \sigma_{xx}\, dz,$$

$$\bar{\sigma}_{xy}^{(z)} = \frac{1}{b_z^{(+)} + b_z^{(-)}} \int_{-b_z^{(-)}}^{b_z^{(+)}} \sigma_{xy}\, dz,$$

$$\bar{\sigma}_{xz}^{(z)} = \frac{1}{b_z^{(+)} + b_z^{(-)}} \int_{b_z^{(-)}}^{b_z^{(+)}} \sigma_{xz}\, dz.$$

Let us imagine this strip to be cut out of an element of the rod of length dx and let us consider the equilibrium equations for the resulting small plate. On the left- and right-hand edges of the strip (Fig. 84) uniformly distributed mean normal stresses $\bar{\sigma}_{xx}^{(z)}$ and $\bar{\sigma}_{xx}^{(z)'}$ act in the direction of the x-axis, where

$$\bar{\sigma}_{xx}^{(z)'} = \bar{\sigma}_{xx}^{(z)} + \frac{\partial \bar{\sigma}_{xx}^{(z)}}{\partial x} dx,$$

and on the upper and lower faces shearing stresses $\sigma_{yx}^{(z)'} = \bar{\sigma}_{xy}^{(z)}$ and $\bar{\sigma}_{xy}^{(z)'} = \sigma_{xy}^{(z)'}$ act in the direction of x, where $\sigma_{xy}^{(z)'} = \bar{\sigma}_{xy}^{(z)'} + \frac{\partial \bar{\sigma}_{xy}^{(z)}}{\partial y} dy$, so that the equilibrium equation in terms of projections on the x-axis is of the form

$$b_z \frac{\partial \bar{\sigma}_{xx}^{(z)}}{\partial x} + \frac{\partial}{\partial y}(b_z \bar{\sigma}_{xy}^{(z)}) = 0.$$

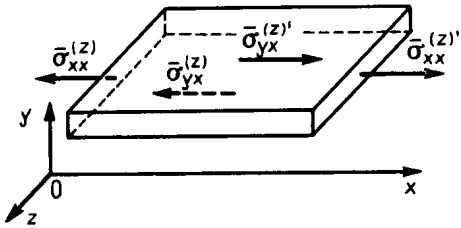

FIG. 84.

Integrating with respect to y from y to y', we get that:

$$b_z \bar{\sigma}_{xy}^{(z)} = \int_{y'}^{y} b_z \frac{\partial \bar{\sigma}_{xx}^{(z)}}{\partial x} dy.$$

Since the left-hand side is of the order of the magnitude of $b_1 \sigma_{xy}$ and the right-hand side of the order of $b_1^2 \sigma_{xx}/l$, then

$$\frac{\sigma_{xy}}{\sigma_{xx}} \sim \frac{b_1}{l},$$

where b_1 is the characteristic lateral dimension of the beam in the z-direction and l is the length of the rod. Similarly

$$\frac{\sigma_{xz}}{\sigma_{xx}} \sim \frac{b_2}{l},$$

where b_2 is the characteristic lateral dimension of the rod in the y direction. Therefore, if the lateral dimensions of the rod are small compared with its length ($b_1/l \ll 1$ and $b_2/l \ll 1$), the shearing stresses on the cross-section are very much less than the normal stresses.

The equilibrium equation of this strip (Fig. 84) in terms of projections on the y-axis is of the form

$$b_z \frac{\partial \bar{\sigma}_{xy}^{(x)}}{\partial x} + \frac{\partial}{\partial y}(b_z \sigma_{yy}) = 0,$$

which gives us an estimate of the magnitude of $\sigma_{yy}/\sigma_{yx} \sim b_1/l$ and similarly of $\sigma_{zz}/\sigma_{zx} \sim b_2/l$, so that the stresses σ_{yy} and σ_{zz} are quantities of a higher order of smallness compared with σ_{xx} when $b_1/l \ll 1$, $b_2/l \ll 1$, since

$$\sigma_{yy}, \quad \sigma_{zz} \sim \sigma_{xx} \frac{b^2}{l^2}.$$

In long beams therefore the main stress is the normal stress σ_{xx}.

In order to evaluate the normal stresses σ_{xx} we make use of the assumption that plane sections remain plane and assume that a plane cross-section perpendicular to the axis of the beam before deformation remains plane and normal to the deflected axis of the beam in the deformed state. This assumption is confirmed by experiment. If an orthogonal set of longitudinal and transverse lines are drawn on the lateral surface of a rubber beam, the transverse lines are not distorted after bending and remain orthogonal to the distorted longitudinal lines of the set. We note that the assumption that plane sections remain plane is incompatible with the occurrence of shearing stresses σ_{xy}, σ_{xz} associated with shear. It does however correspond approximately to the actual conditions, since these stresses are small compared with the normal stresses. The assumption of plane sections is absolutely accurate in the case of pure bending, when the beam is subjected to opposite couples which bend it in one of the principal planes.

If $\boldsymbol{w}_0 = u_0(x)\,\boldsymbol{i} + v_0(x)\,\boldsymbol{j} + w_0(x)\,\boldsymbol{k}$ is the displacement vector of a point on the axis of the beam, then the curvatures of the projections of the deformed axis of the beam in the planes (xz) and (xy) are respectively

$$\varkappa_y = \frac{d^2 w_0}{dx^2} = \frac{1}{\varrho_y}, \quad \varkappa_z = \frac{d^2 v_0}{dx^2} = \frac{1}{\varrho_z},$$

and the relative extension along the axis of the beam is

$$e = \frac{du_0}{dx}.$$

The quantities e, $\varkappa_y$, $\varkappa_z$ are the characteristic strains of the beam in the absence of a torque. We consider the curvature positive if the centre of curvature lies on the side of the axis of the beam in which the corresponding axis Oz or Oy is directed. From Fig. 85, which shows an element of the beam in its projection on the (xy)

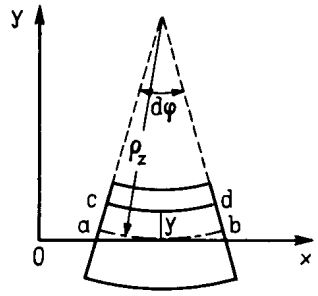

FIG. 85.

plane, we see that the relative extension due to bending in this plane is

$$\varepsilon' = \frac{cd - ab}{ab} = \frac{(\varrho_z - y)\,d\varphi - \varrho_z\,d\varphi}{\varrho_z\,d\varphi} = -\frac{y}{\varrho_z} = -\varkappa_z y.$$

Similarly for bending in the (xz) plane we have that $\varepsilon'' = -\varkappa_y z$. Thus the relative extension of a longitudinal fibre is

$$\varepsilon_{xx} = e - \varkappa_z y - \varkappa_y z. \tag{2.39}$$

Since σ_{xy}, σ_{yy}, σ_{xz}, σ_{yz}, σ_{zz} are small compared with σ_{xx}, we can put them equal to zero and consider that each longitudinal fibre of the beam is under conditions of uniaxial stress. Therefore we can make use of the stress–strain curve of a specimen for the relation between the normal stress σ_{xx} and the strain ε_{xx}:

$$\sigma_{xx} = \Phi_1(\varepsilon_{xx}) = E\varepsilon_{xx}[1 - \omega(\varepsilon_{xx})]. \tag{2.40}$$

Substituting here for ε_{xx} its expression (2.39), and then substituting the value obtained for σ_{xx} in the first, fifth and sixth equations of (2.38), we find that:

$$P \equiv Q_x = \iint_F E\varepsilon_{xx}[1 - \omega(\varepsilon_{xx})]\, dF = F \iint_F (e - \varkappa_z y - \varkappa_y z)\, dF - P_\omega,$$

$$M_y = E \iint_F (e - \varkappa_z y - \varkappa_y z)\, z\, dF - M_{y\omega},$$

$$M_z = E \iint_F (e - \varkappa_z y - \varkappa_y z)\, y dF - M_{z\omega},$$

where

$$\left.\begin{aligned} P_\omega &= E \iint_F \varepsilon_{xx}\omega(\varepsilon_{xx})\, dF, \\ M_{y\omega} &= E \iint_F \varepsilon_{xx}\omega(\varepsilon_{xx})\, z\, dF, \\ M_{z\omega} &= E \iint_F \varepsilon_{xx}\omega(\varepsilon_{xx})\, y\, dF. \end{aligned}\right\} \tag{2.41}$$

Since e, $\varkappa_y$, $\varkappa_z$ are functions of x, but not of y or z, if we take them outside the integral signs and consider that the axes y, z are the principal central axes of inertia of the section, so that

$$\iint_F y\, dF = \iint_F z\, dF = \iint_F yz\, dF = 0,$$

we get that:

$$\left.\begin{aligned} e &= \frac{P}{EF} + \frac{P_\omega}{EF}, \\ \varkappa_y &= -\frac{M_y}{EJ_y} - \frac{M_{y\omega}}{EJ_y}, \\ \varkappa_z &= -\frac{M_z}{EJ_z} - \frac{M_{z\omega}}{EJ_z}, \end{aligned}\right\} \tag{2.42}$$

where $J_y = \iint_F z^2\, dF$ and $J_z = \iint_F y^2\, dF$ are the moments of inertia of the cross-section of the beam about the axes Oy and Oz. Therefore

$$\varepsilon_{xx} = \frac{P}{EF} + \frac{M_y z}{EJ_y} + \frac{M_z y}{FJ_z} + \varepsilon_{xx}^{(\omega)},$$

where

$$\varepsilon_{xx}^{(\omega)} = \frac{P_\omega}{EF} + \frac{M_{y\omega} z}{EJ_y} + \frac{M_{z\omega} y}{EJ_z}.$$

The quantities EJ_y and EJ_z are called the flexural rigidities of the beam in the planes (xz) and (xy).

For the stress $\sigma_{xx} = E\varepsilon_{xx}[1 - \omega(\varepsilon_{xx})]$ we get that:

$$\sigma_{xx} = \frac{P}{F} + \frac{M_z}{J_z} y + \frac{M_y}{J_y} z + \sigma_{xx}^{(\omega)}, \tag{2.43}$$

where

$$\sigma_{xx}^{(\omega)} = E\varepsilon_{xx}^{(\omega)} - E\varepsilon_{xx}\omega(\varepsilon_{xx}).$$

If the material of the beam for the given external forces does not exceed the elastic limit, then $\omega = 0$ and $P_\omega = M_{y\omega} = M_{z\omega} = \varepsilon_{xx}^{(\omega)} = \sigma_{xx}^{(\omega)} = 0$. Then formulae (2.42) and (2.43) determine completely the strains and normal stresses since $Q_x = P$, M_y, M_z are expressed in terms of the given external forces by equations

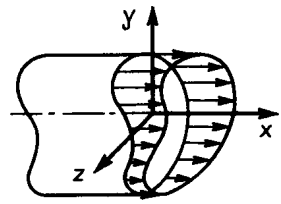

FIG. 86.

(2.35). It can be seen from formula (2.43), in which we must put $\sigma_{xx}^{(\omega)} = 0$, that the normal stresses are distributed linearly over the cross-section. The graph of normal stresses on the section, in which stress is measured in the direction of the x-axis (Fig. 86), is a plane inclined to the (yz) plane.

If plastic strains occur P_ω, $M_{y\omega}$, $M_{z\omega}$ are non-zero and contain the unknown quantity ε_{xx}. In this case it is convenient to put ε_{xx} and σ_{xx} in the form

$$\varepsilon_{xx} = \varepsilon + \varepsilon_\omega,$$

$$\sigma_{xx} = \sigma + \sigma_\omega,$$

where

$$\left.\begin{aligned} \varepsilon &= \frac{P}{EF} + \frac{M_z}{EJ_z} y + \frac{M_y}{EJ_y} z, \\ \sigma &= \frac{1}{F}\left(P + \frac{M_z}{i_z^2} y + \frac{M_y}{i_y^2} z\right) \end{aligned}\right\} \tag{2.44}$$

are the elastic portion of the strain and the fictitious elastic normal stress (where $i_y = \sqrt{(J_y/F)}$, $i_z = \sqrt{(J_z/F)}$ are the radii of gyration of the cross-section about the axes Oy and Oz), and

$$\left.\begin{aligned} \varepsilon_\omega &= \varepsilon_{xx}^{(\omega)} = \frac{P_\omega}{EF} + \frac{M_{z\omega}}{MJ_z}y + \frac{M_{y\omega}}{EJ_y}z, \\ \sigma_\omega &= E\varepsilon_\omega - \omega E(\varepsilon + \varepsilon_\omega) = (1 - \omega)\, E\varepsilon_\omega - \omega\sigma \end{aligned}\right\} \quad (2.45)$$

are the plastic portion of the strain and the additional normal stress. In the region of elastic strain $\varepsilon_\omega = 0$, $\sigma_\omega = 0$, since $\omega = 0$.

Applying the method of elastic solutions for the calculation beyond the elastic limit we make the zero approximation $\omega = 0$, so that $\varepsilon_{xx}^{(0)} = \varepsilon$ and $\sigma_{xx}^{(0)} = \sigma$ are given in terms of the external forces by formulae (2.44).

To obtain a first approximation we find $\omega^{(0)} = \omega(y, z)$, since we know from the stress–strain curve the form of the function $\omega(\varepsilon_{xx})$, and $\varepsilon_{xx}^{(0)} = \varepsilon$ has been found as a zero approximation as a function of y and z. Then, from formulae (2.41) we find that:

$$P_\omega^{(1)} = E\iint_F \varepsilon_{xx}^{(0)}\omega^{(0)}\, dF,$$

$$M_{y\omega}^{(1)} = E\iint_F \varepsilon_{xx}^{(0)}\omega^{(0)}z\, dF,$$

$$M_{z\omega}^{(1)} = E\iint_F \varepsilon_{xx}^{(0)}\omega^{(0)}y\, dF,$$

after which we find from formulae (2.45) that:

$$\varepsilon_\omega^{(1)} = \frac{P_\omega^{(1)}}{EF} + \frac{M_{z\omega}^{(1)}}{EJ_z}y + \frac{M_{y\omega}^{(1)}}{EJ_y}z,$$

$$\sigma_\omega^{(1)} = E[1 - \omega^0(\varepsilon)]\,\varepsilon_\omega^{(1)} - \omega^0\sigma.$$

Thus, as a first approximation, we have that:

$$\varepsilon_{xx}^{(1)} = \varepsilon + \varepsilon_\omega^{(1)}, \quad \sigma_{xx}^{(1)} = \sigma + \sigma_\omega^{(1)}.$$

Similarly we can go on to make further approximations. Usually the third approximation differs only slightly from the second, so that a second approximation is in most cases sufficient.

Examples. **1.** Let us suppose that the beam shown in Fig. 77 is of rectangular section 6 cm × 10 cm (the long side vertical), and that $l = 2a = 100$ cm, $P = 8000$ kg. The material of the beam is steel ($\sigma_S = 3400$ kg/cm^2). Let us find the maximum normal stress.

We find first of all the elastic solution. From the second formula of (2.44) we see that the greatest normal stress will occur on the section where M_z is a maximum and at the maximum value of y, i.e. for $y = h/2 = 5$ cm. The maximum value of M_z, at mid-span of the beam, is $M_{max} = Pl/4 = 200{,}000$ kg cm. For a rectangular section $J_z = bh^3/12$ where b is the width of the beam. In our case $J_z = 2000$ cm^4. Therefore, from formula (2.44)

$$\sigma_{max} = \frac{200000 \times 5}{2000} = 500 \text{ kg/cm}^2.$$

Since $\sigma_{max} < \sigma_S$ the elastic solution is the solution to the problem.

2. Design a beam of I-section, loaded as shown in Fig. 80, if $q = 1{\cdot}5 \times 10^3$ ton/m, $l = 3$ m, for which the greatest normal stress must not exceed the allowable stress $[\sigma] = 1400$ kg/cm^2.

Since $P = 0$, $M_y = 0$, we have from (2.44) that

$$\sigma_{max} = \frac{M_{max} h}{2J_z} \leqq [\sigma].$$

The quantity

$$W = \frac{J_z}{y_{max}}$$

is called the section modulus of the section. We require then that

$$W \geqq \frac{M_{max}}{[\sigma]}.$$

Since in our case

$$M_{max} = \frac{ql^2}{2} = 675 \times 10^3 \text{ kg cm},$$

then $W \geqq 482$ cm^3.

We then select from tables of rolled sections a beam which has a section modulus satisfying this condition.

11. Eccentric Loading. Core Points

Let us suppose that a beam is compressed by two forces parallel to the axis of the beam applied at points with coordinates $(0, \eta, \zeta)$ and (l, η, ζ) on the ends of the beam (Fig. 87). This is known as eccentric loading. The effect of the eccentrically applied force P would be the same as the effect of a force P acting along the axis of the beam together with bending moments

$$M_y = -P\zeta, \quad M_z = -P\eta$$

(according to the rule for signs of moments about the axes y and z which was established earlier).

If the material of the beam does not exceed the elastic limit, the normal stress given by formula (2.44) is

$$\sigma = -\frac{P}{F}\left(1 + \frac{\eta y}{i_z^2} + \frac{\zeta z}{i_y^2}\right), \tag{2.46}$$

where i_y, i_z are the radii of gyration of the section of the beam about the axes y and z. Here (y, z) are the coordinates of the point in the section at which the normal stress is evaluated.

Formula (2.46) shows that, depending on the magnitudes and signs of the point of application of the force (η, ζ) and the coordinates of the point at which the stress is calculated, the normal stress

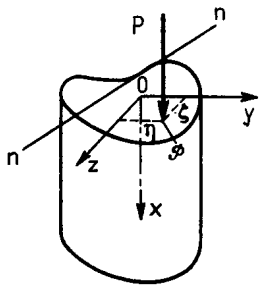

FIG. 87.

can be positive (tensile) or negative (compressive). Some materials (stone, brickwork, concrete, etc.) are considerably weaker in tension than in compression. It is important to know, therefore, in what region to apply the compressive force so that the stresses over the section of the beam are of the same sign (in this case, compressive).

The diagram of the normal stress σ is a plane intersecting the (yz) plane in some line n–n called the neutral axis (Fig. 87), since everywhere along this line the normal stress σ is zero. The equation of the neutral axis can be found from (2.46) by putting $\sigma = 0$:

$$\frac{\eta y}{i_z^2} + \frac{\zeta z}{i_y^2} = -1. \tag{2.47}$$

If the neutral axis intersects the cross-section, then on the parts of the cross-section lying on opposite sides of the neutral axis the stresses will be of opposite signs. If however the neutral axis lies

outside the section, the normal stresses are of the same sign everywhere in the cross-section. We require to find the limiting position of the neutral axis—the position when it becomes a tangent to the boundary of the section.

If we move this tangent around the boundary of the section in such a way that it nowhere intersects the section (i.e. if we move it along the curve of the envelope of the section), the point of application of the force (η, ζ) corresponding to each position of the neutral axis, which is sometimes called the pole, describes some closed curve, the area inside which is the core of the section.

We note that if the boundary of the section forms a salient angle at some point the tangent will rotate about this point through some finite angle. If in the equation of the neutral axis (2.47) we put y and z equal to the coordinates of this point, we see that as the neutral axis rotates about this point the pole moves along a straight line.

In order to construct the boundary of the core of the section it is convenient to write the equation of the neutral axis in the form

$$\frac{y}{a} + \frac{z}{b} = 1,$$

where, as can be seen from (2.47),

$$a = -\frac{i_z^2}{\eta}, \quad b = -\frac{i_y^2}{\zeta}.$$

For every given limiting position of the neutral axis a and b are known, and thus the corresponding positions of the pole can be found:

$$\eta = -\frac{i_z^2}{a}, \quad \zeta = -\frac{i_y^2}{b}. \tag{2.48}$$

It should be noted that the shape and dimensions of the core of the section are completely defined by the geometry of the section and in no way depend on the magnitude of the applied force, providing the deformation is elastic.

Examples. 1. For an I-section there are four limiting positions of the neutral axis: *1—1*, *2—2*, *3—3*, *4—4* (Fig. 88a), and to move from one to the other necessitates a rotation of $\pi/2$. Therefore the boundary of the core of the section is a quadrangle (a rhombus), and to construct it, it is sufficient to find the positions of its apices.

As an example, a certain beam 20 cm × 10 cm (Fig. 88a) has $i_y = 8{\cdot}15$ cm, $i_z = 2{\cdot}12$ cm.

In the position *1—1*, we have that $a_1 \to \infty$, $b_1 = 10$ cm.
From formula (2.48), $\eta_1 = 0$, $\zeta_1 = -8 \cdot 15^2/10 \approx -6 \cdot 65$ cm.
From symmetry, $\eta_3 = 0$, $\zeta_3 = +6 \cdot 65$ cm.
In the position *2—2*, we have that $a_2 = 5$ cm, $b_2 \to \infty$, so that

$$\eta_2 = -2 \cdot 12^2/5 \approx -0 \cdot 9 \text{ cm}, \quad \zeta_2 = 0;$$

$$\eta_4 = 0 \cdot 9 \text{ cm}, \quad \zeta_4 = 0.$$

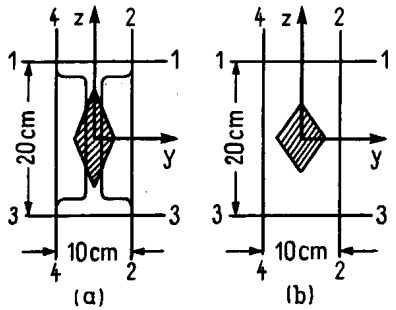

FIG. 88.

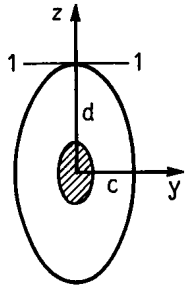

FIG. 89.

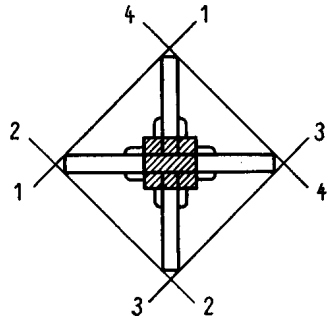

FIG. 90.

As a comparison we give the dimensions of the core of a rectangle of the same cross-sectional dimensions (Fig. 88b): $\eta_1 = \eta_3 = 0$; $\zeta_1 = -\zeta_3 = -3 \cdot 3$ cm, $\eta_2 = -\eta_4 = -1 \cdot 7$ cm, $\zeta_2 = \zeta_4 = 0$.

2. For an ellipse with semi-axes c and d we have that (Fig. 89):

$$J_y = \frac{\pi c d^3}{4}, \quad J_z = \frac{\pi c^3 d}{4}, \quad F = \pi c d, \quad i_z^2 = \frac{c^2}{4}, \quad i_y^2 = \frac{d^2}{4}.$$

As we move the tangent around the boundary of the ellipse the pole describes a smooth curve—an ellipse similar to the ellipse of the section. If we find, for example, the position of the pole corresponding to the position of the tangent

$1-1$ ($a_1 \to \infty$, $b_1 = d$) we see that $\eta_1 = 0$, $\zeta_1 = -c/4$, so that the semi-axes of the core ellipse are four times smaller than the semi-axes of the ellipse of the section.

3. For a column with a section the shape of a cross (Fig. 90) the core is a square, since the envelope curve is a square. This type of column is used, for example, in the construction of high buildings.

12. The Carrying Capacity of a Beam

If a material strain hardens only slightly beyond the elastic limit, the $\sigma - \varepsilon$ curve is often represented in the idealized form without any strain hardening (Fig. 91a). We might wish to know the maximum load which can be resisted by a beam, since when the

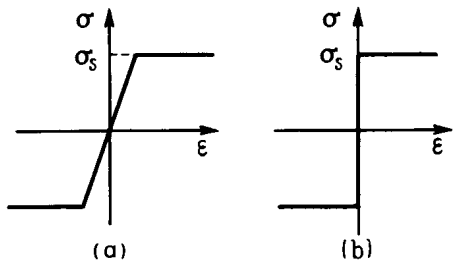

Fig. 91.

material at every section is in a plastic state, the beam is no longer able to offer further resistance to the load and the material "flows" at a constant value of the load. This state of affairs exists at strains exceeding ε_S and is not influenced by the magnitudes of the strains. To determine the carrying capacity, therefore, we can ignore the elastic strains and use a $\sigma - \varepsilon$ curve even more idealized (Fig. 91 b). In the absence of torque the limiting condition in the beam is reached when $\sigma_{xx} = \pm \sigma_T$ where $\sigma_T = \sigma_S$, the yield point. This corresponds to a certain combination of values of P, M_y, M_z.

We must distinguish between the following two cases:

(a) If the normal stresses over the whole cross-section are of the same sign, then, by definition (see formulae (2.38)),

$$P_{\text{lim}} = \iint_F \sigma_{xx}\, dF = \pm\sigma_T F,$$

$$M_y^{\text{lim}} = \iint_F \sigma_{xx} z\, dF = \pm\sigma_T \iint_F z\, dF = 0,$$

$$M_z^{\text{lim}} = \pm\sigma_T \iint_F y\, dF = 0,$$

since the axes Oy and Oz are the principal central axes of inertia of the cross-section.

(b) If the normal stresses on the section are of opposite signs the section must be divided into two parts by a line which is obtained by equating the expression

$$\varepsilon_{xx} = e - \varkappa_y z - \varkappa_z y$$

to zero:

$$\frac{y}{e:\varkappa_z} + \frac{z}{e:\varkappa_y} = 1 \quad \text{or} \quad \frac{y}{p_1} + \frac{z}{p_2} = 1. \tag{2.49}$$

This is the equation of a straight line which is specified by the values of the two parameters

$$p_1 = \frac{e}{\varkappa_z}, \quad p_2 = \frac{e}{\varkappa_y}.$$

In finding P, M_y, M_z from formulae (2.38), the integration must be taken separately over the part of the area F_1 where $\sigma_{xx} = \sigma_T$ and over the part of the area F_2 where $\sigma_{xx} = -\sigma_T$. If (y_{c1}, z_{c1}) and (y_{c2}, z_{c2}) are the centres of gravity of the areas F_1 and F_2, the limiting values of P, M_y, M_z are

$$\left.\begin{aligned} P &= \sigma_T(F_1 - F_2), \\ M_y &= \sigma_T(F_1 z_{c1} - F_2 z_{c2}), \\ M_z &= \sigma_T(F_1 y_{c1} - F_2 y_{c2}). \end{aligned}\right\} \tag{2.50}$$

The values of $F_1, F_2, y_{c1}, y_{c2}, z_{c1}, z_{c2}$ are given by the values of the parameters p_1 and p_2, i.e. by the position of the neutral axis (2.49).

Therefore (2.50) are parametric equations determining the carrying capacity of the beam:

$$\left.\begin{aligned} P &= \Psi_1(p_1, p_2), \\ M_y &= \Psi_2(p_1, p_2), \\ M_z &= \Psi_3(p_1, p_2). \end{aligned}\right\} \tag{2.51}$$

The relations (2.51), which are equivalent to one relation between P, M_y, M_z, represent a surface in the space (PM_yM_z). The values of P, M_y, M_z at every point on this surface correspond to the limiting condition of the beam.

The functions Ψ_1, Ψ_2, Ψ_3 of the parameters p_1, p_2 are related to the geometry of the cross-section of the beam. If we are required, therefore, to specify the shape and dimensions of a section for given values of P, M_y, M_z, so that the beam is in its limiting state,

the shape of the section must be specified to the accuracy of one parameter, the value of which is determined by the relations (2.51).

We note that the carrying capacity not only of a beam, but of any other member, is determined always only by one relation between the loads applied to the member.

Example. For a beam of rectangular section (Fig. 92) under the action of a longitudinal force P and a bending moment $M_y = M(M_z = 0)$, we have that

$$\varkappa_z = 0, \quad p_1 = \infty, \quad p_2 = \frac{e}{\varkappa_y} \neq 0.$$

The equation of the neutral axis is $z = p_2$. From (2.50) we have that

$$P = \sigma_T(F_1 - F_2),$$

$$M = \sigma_T(F_1 z_{c1} - F_2 z_{c2}),$$

and for the rectangle (Fig. 92),

$$z_{c1} = \frac{1}{2}\left(\frac{h}{2} + p_2\right)$$

and $z_{c1} - z_{c2} = h/2$ so that $z_{c2} = -\frac{1}{2}(h/2 - p_2)$. If, in addition, we make use of the identities (for any shape)

$$F_1 + F_2 = F, \quad F_1 z_{c1} + F_2 z_{c2} = 0,$$

then P and M will be expressed in terms of the one parameter p_2.

$$\left.\begin{aligned} P &= \sigma_T F\left(1 - \frac{4z_{c1}}{h}\right) = -\sigma_T F\frac{2p_2}{h}, \\ M &= 2\sigma_T F z_{c1}\left(1 - \frac{2z_{c1}}{h}\right) = \frac{1}{4}\sigma_T Fh\left(1 - \frac{2p_2}{h}\right)\left(1 + \frac{2p_2}{h}\right) \end{aligned}\right\} \quad (2.51')$$

In the absence of a bending moment the limiting value of the force P is $P_T = \sigma_T F$. If there is no force P we have that $F_1 = F_2 = F/2$, and for the limiting value of the bending moment M we find that $M_T = \frac{1}{4}\sigma_T Fh$. Making use of these values we can rewrite eqns. (2.51′) in the form

$$\frac{|P|}{P_T} = 1 - \frac{4z_{c1}}{h} = -\frac{2p_2}{h},$$

$$\frac{|M|}{M_T} = \frac{8z_{c1}}{h}\left(1 - \frac{2z_{c1}}{h}\right) = 1 - \frac{4p_2^2}{h^2}.$$

In order to eliminate p_2 we square the first of these and then add to the second:

$$\frac{|M|}{M_T} + \frac{P^2}{P_T^2} = 1. \quad (2.52)$$

Thus the carrying capacity of a beam of rectangular section is defined by a pair of parabolas (2.52) in the plane (PM) (Fig. 93). The values of P and M corresponding to a point within the parabolas are below the limiting condition of the beam.

We can find the parameter p_2 from the relations (2.51′):

$$p_2 = \frac{Ph}{2\sigma_T F} = \sqrt{\left(\frac{h^2}{4} - \frac{Mh}{\sigma_T F}\right)},$$

i.e. we can find the ratio of the relative axial extension e to the curvature $\varkappa_y$. But it is not possible to find the value of both of the quantities $e, \varkappa_y$. In problems of carrying capacity (for materials with no strain hardening) the values of the strains are always indeterminate and only their ratios can be found.

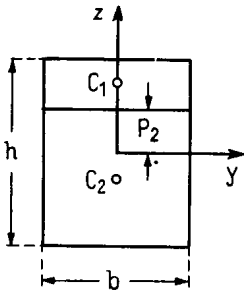

FIG. 92.

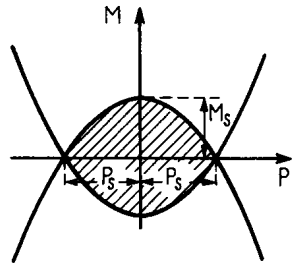

FIG. 93.

13. THE DEFLECTION OF A BEAM

For given external forces acting on a beam we can determine the normal stress σ_{xx} and the characteristic strains $e, \varkappa_y, \varkappa_z$. For example, in an elastic state the strains $e, \varkappa_y$ and $\varkappa_z$ are given immediately by formulae (2.42), in which we must put

$$P_\omega = M_{y\omega} = M_{z\omega} = 0,$$

$$e = \frac{P}{EF}, \quad \varkappa_y = -\frac{M_y}{EJ_y}, \quad \varkappa_z = -\frac{M_z}{EJ_z},$$

where P, M_y, M_z can be found in terms of the external forces from formulae (2.35). The question then arises as to the shape which the axis of the beam takes up after deformation.

In order to find the displacements of points on the axis of the beam we have the differential equations

$$\frac{du_0}{dx} = e, \quad \frac{d^2w_0}{dx^2} = \varkappa_y, \quad \frac{d^2v_0}{dx^2} = \varkappa_z,$$

in which the right-hand sides are known functions of x. Integrating these equations we find that:

$$u_0 = \int_0^x e\,dx + a_1,$$

$$v_0 = \int_0^x dx \int_0^x \varkappa_z\,dx + c_1 x + c_2,$$

$$w_0 = \int_0^x dx \int_0^x \varkappa_y\,dx + b_1 x + b_2,$$

or, if the origin of coordinates is attached to the left-hand end section, so that $a_1 = 0$:

$$\left.\begin{aligned} u_0 &= \int_0^x e\,dx, \\ v_0 &= \int_0^x \varkappa_z(\xi)(x-\xi)\,d\xi + c_1 x + c_2, \\ w_0 &= \int_0^x \varkappa_y(\xi)(x-\xi)\,d\xi + b_1 x + b_2. \end{aligned}\right\} \tag{2.53}$$

In order to find the constants c_1, c_2, b_1, b_2 we make use of the support conditions of the ends of the beam. For example, at a built-in end of a beam we have the conditions

$$v_0 = 0, \quad v_0' = 0; \quad w_0 = 0, \quad w_0' = 0,$$

and at a hinged end support

$$v_0 = 0, \quad v_0'' = 0; \quad w_0 = 0, \quad w_0'' = 0.$$

A solution to (2.53) exists both for elastic and for elasto-plastic strains. When there are no plastic strains, e, $\varkappa_y$, $\varkappa_z$ can be expressed in terms of P, M_y and M_z from formulae (2.42), so that from (2.53) we find that:

$$\left.\begin{aligned} u_0 &= \int_0^x \frac{P}{F}\,dx, \\ v_0 &= -\int_0^x \frac{M_z}{EJ_z}(x-\xi)\,d\xi + c_1 x + c_2, \\ w_0 &= -\int_0^x \frac{M_y}{EJ_y}(x-\xi)\,d\xi + b_1 x + b_2, \end{aligned}\right\} \tag{2.54}$$

where for beams of variable cross-section F, J_y, J_z are functions of x.

In statically determinate problems all the support reactions can be found from the equations of statics, so that all the external forces (including the support reactions) in the right-hand sides of eqns. (2.35) are known.

Then in the above expressions for u_0, v_0, w_0 we must put

$$M_y = -\int_x^l q_z(\xi)(\xi - x)\,d\xi + \int_x^l m_y(\xi)\,d\xi + M_{Ry},$$

$$M_z = -\int_x^l q_y(\xi)(\xi - x)\,d\xi + \int_x^l m_z(\xi)\,d\xi + M_{Rz}$$

(see the expression for M in § 9 and the rule given there for the signs of M_y and M_z).

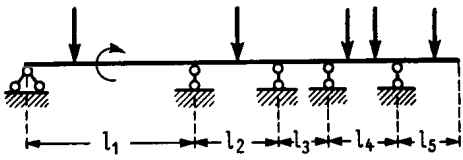

FIG. 94.

In statically indeterminate problems we cannot find all the support reactions; they must be found from considerations of the deflected form of the beam. In this case further conditions are imposed on the displacement of points on the axis of the beam and these additional conditions always give as many additional equations as there are additional unknown support reactions.

For example in a multi-span beam in plane bending (Fig. 94) we have only two equations of statics for finding five support reactions. The reactions of the three intermediate supports can be replaced by the forces X_1, X_2, X_3, which can for the time being be considered as known quantities. These forces will appear in the expressions for the displacements given by formulae (2.53), or in the case of an elastic problem, by (2.54). In order to find the redundancies X_1, X_2, X_3, we make use of the conditions that for $x = l_1$, $x = l_1 + l_2$, $x = l_1 + l_2 + l_3$ the deflections are zero.

In the case of a beam with two ends built in (Fig. 95), we can take as the redundancies the support moments M_1 and M_2, which can

then be found from the conditions that $v' = 0$ at $x = 0$ and $v' = 0$ at $x = l$.

There are several methods which enable us to simplify the problem of finding the deflected shape of a beam and the redundancies (in statically indeterminate problems): the Clebsch method, graphical methods, the equation of three moments, etc. (see for example the book by M. M. Filonenko-Borodich, *Strength of Materials*); these methods have been developed for the elastic problem. They do not, however, alter the general approach to the problem given here, and they are intended to decrease the number of mathematical operations and to create definite algorithms.

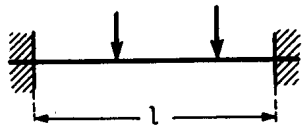

FIG. 95.

In an elastic problem it is sometimes convenient to write the differential equations for the shape of the deflected axis of the beam in another form.

From the Touravsky differential relations (2.37), in the absence of distributed moments m_y and m_z, we have that:

$$\frac{dM_y}{dx} = Q_z, \quad \frac{dM_z}{dx} = Q_y,$$

$$\frac{dQ_z}{dx} = -q_z, \quad \frac{dQ_y}{dx} = -q_y,$$

so that

$$\frac{d^2M_y}{dx^2} = -q_z, \quad \frac{d^2M_z}{dx^2} = -q_y.$$

therefore, differentiating twice the relations $EJ_y\varkappa_y = -M_y$, $EJ_z\varkappa_z = -M_z$ with respect to x, we get that:

$$\frac{d^2}{dx^2}\left(EJ_y\frac{d^2w_0}{dx^2}\right) = q_z, \quad \frac{d^2}{dx^2}\left(EJ_z\frac{d^2v_0}{dx^2}\right) = q_y.$$

In the case of a beam of constant cross-section J_y and J_z are constants. We then have the differential equations of the fourth order

$$\left.\begin{aligned} EJ_y \frac{d^4 w_0}{dx^4} &= q_z(x), \\ EJ_z \frac{d^4 v_0}{dx^4} &= q_y(x). \end{aligned}\right\} \tag{2.55}$$

The boundary conditions at the ends of the beam impose conditions on the displacements themselves and their first three derivatives, and we are thus able to find all the constants which result from integrating the equations (2.55). Taking into account the fact that in bending, for example, in the plane (xz) $EJ_y \varkappa_y = -M_y$, i.e. $EJ_y w_0'' = -M_y$, and that on differentiating this relation taking into account the Zhuravski differential relations, $EJ_y w_0''' = -Q_z$, we will have the further conditions for different cases of end support:

(a) at a built-in end

$$w_0 = 0, \quad w_0' = 0;$$

(b) at a hinged end support

$$w_0 = 0, \quad w_0'' = -\frac{M_0}{EJ_y},$$

where M_0 is the external moment at the support; if at a support there is no external moment applied, then $w_0'' = 0$ at this support;

(c) at a free end of a beam (at the end of cantilever)

$$w_0'' = -\frac{M_0}{EJ_y}, \quad w_0''' = -\frac{Q_0}{EJ_y},$$

where M_0 and Q_0 are the moment and force applied to this end of the beam.

14. A Beam on an Elastic Foundation

In many cases the beam is connected to an elastic body which deforms together with the beam. For example, the foundation of a building and the building itself deform together with the ground on which it stands. We can consider such things as dams, railway-tracks, etc., as examples of beams on elastic foundations.

The deflection of a beam lying on an elastic foundation (Fig. 96) is opposed by the foundation, and it is apparent that the greater the deflection of the beam the greater the reaction of the foundation.

The exact solution to this problem is extremely complex and comes within the scope of the theory of elasticity. As a simplification we often make use of Winkler's hypothesis according to which the reaction of the base is proportional to the deflection at a given point on the axis of the beam. This hypothesis amounts in effect to the assumption that the elastic support is made up of a number of springs perpendicular to the edge of the support and working independently of one another. According to this hypothesis the reaction of the elastic support per unit length of the axis of the beam is

$$q_{z0} = -kw_0. \tag{2.56}$$

The quantity k is called the modulus of the base and is considered to be constant for any type of soil and independent of the magnitude of the deflection w_0. In actual fact k is not constant.

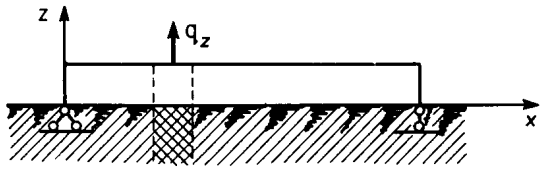

FIG. 96.

In the equation for the deflected axis of the beam of the type (2.55) we must add to the right-hand side the quantity q_z, which gives an equation of equilibrium for a beam on an elastic foundation in the form

$$EJ_y \frac{d^4w_0}{dx^4} + kw_0 = q_z(x). \tag{2.57}$$

If we put

$$\alpha = \sqrt[4]{\left(\frac{k}{4EJ_y}\right)},$$

then this equation becomes

$$w_0^{IV} + 4\alpha^4 w_0 = \frac{q_z(x)}{EJ_y} \equiv f(x),$$

where $f(x)$ is a known function. The general solution to this equation without the right-hand side is

$$w_0 = e^{\alpha x}(A \cos \alpha x + B \sin \alpha x) + e^{-\alpha x}(C \cos \alpha x + D \sin \alpha x).$$

Adding to this the particular solution to the equation with the right-hand side (we can find this, for example, from the method of variation of parameters), we obtain the general solution to the complete equation:

$$w_0 = w_0^p + e^{\alpha x}(A \cos \alpha x + B \sin \alpha x) + e^{-\alpha x}(C \cos \alpha x + D \sin \alpha x), \tag{2.58}$$

where $w_0^{(p)}$ depends on the external forces applied to the beam.

For the case shown in Fig. 96 we have the following boundary conditions:

$$w_0 = 0, \quad w_0'' = 0 \quad \text{at} \quad x = 0,$$
$$w_0 = 0, \quad w_0'' = 0 \quad \text{at} \quad x = l,$$

and from these we can find the constants A, B, C, D.

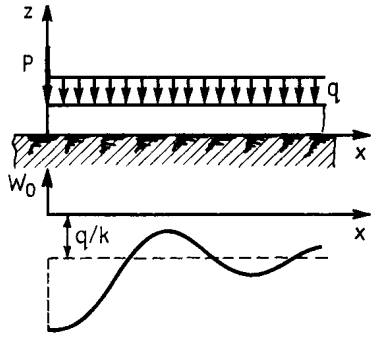

FIG. 97.

If the beam has no rigid supports and lies entirely on an elastic foundation, then at each end we have the conditions

$$w_0'' = 0, \quad w_0''' = 0,$$

and it is assumed that the beam remains in contact with the foundation (i.e. that the elastic base gives a reaction in both directions).

As an example let us consider a semi-infinite beam on an elastic foundation under the action of a uniform load $q_z = -q = \text{const.}$ and a concentrated force P applied at the end (Fig. 97). The particular solution in this case is of the form

$$w_0^p = -\frac{q}{k} = \text{const.}$$

The deflection as $x \to \infty$ must be constant since the influence of the left-hand end must vanish. Therefore the arbitrary constants $A = B = 0$, and the deflection is of the form

$$w_0 = -\frac{q}{k} + (C \cos \alpha x + D \sin \alpha x)\, e^{-\alpha x}.$$

In order to find C and D we have the conditions

$$M_y = 0, \quad Q_z = P \quad \text{at} \quad x = 0$$

or

$$w_0'' = 0, \quad w_0''' = -\frac{P}{EJ_y} \quad \text{at} \quad x = 0.$$

From this we find that:

$$D = 0, \quad C = -\frac{P}{2EJ_y\alpha^3},$$

and the deflection will therefore be

$$w_0 = -\frac{1}{k}\left[q + P\sqrt[4]{\left(\frac{4k}{EJ_y}\right)} \cos \alpha x \,.\, e^{-\alpha x}\right]. \tag{2.59}$$

Thus we see that the maximum deflection occurs under the force P and (at $x = 0$) is equal to

$$w_0^{\max} = -\frac{1}{k}\left[q + P\sqrt[4]{\left(\frac{4k}{EI_y}\right)}\right],$$

and the maximum stress will be at the section x_1, close to $x = 0$, at which the shear force vanishes, i.e. for

$$\tan \alpha x_1 = 1, \quad x_1 = \frac{\pi}{4\alpha}.$$

The bending moment at this section is a maximum and is equal to

$$M_y^{\max} = -EJ_y w_0''|_{x=x_1} = -2P\left(\frac{EJ_y}{k}\right)^{3/4} e^{-\frac{\pi}{4}}.$$

From (2.59) the deflection w_0 is a cosine curve with decreasing amplitude, and for a sufficiently large force P it can assume positive values, which from (2.56) gives a negative base reaction. For beams lying freely on an elastic base this is impossible and the solution is valid, therefore, only if the maximum deflection at the point $x_2 = 3\pi/4\alpha$ is not positive. From this condition we find that:

$$P \leqq q\sqrt[4]{\left(\frac{EJ_y}{k}\right)} e^{\frac{3\pi}{4}}.$$

If this condition is satisfied the beam will remain in contact with the foundation.

15. Longitudinal–Transverse Bending. The Stability of a Beam in Compression

In considering a beam under combined loading we evaluated the bending moments from the transverse and longitudinal forces without taking into account the deflection of the axis of the beam, since this deformation was considered to be small. But even in the case when the force is applied exactly along the axis of the beam the force creates a bending moment if the axis of the beam deflects. If this force is large or if the length of the beam is so great that a small deformation corresponds to large deflections, the moment from the longitudinal force can be considerable and as a result the deflection can increase without any increase in the applied longitudinal force. Therefore in slender rods, the length of which is considerably greater than the lateral dimensions, the application of a compressive force along the axis can lead to a loss of stability: at some value of the force a state of equilibrium becomes possible for which the axis of the rod is curved. In order to investigate the possibility of this type of equilibrium we must take into account the moments which are set up due to the deflection of the axis of the rod.

This means therefore that the problem of the stability (not only of a beam but of any other member) cannot be investigated if the equilibrium equations are written for the initial and not for the deformed state. The relation between the curvatures and moments

$$\varkappa_y = -\frac{M_y}{EJ_y}, \quad \varkappa_z = -\frac{M_z}{EJ_z}$$

remain, but we must modify the expressions for the bending moments in terms of the external forces. We will confine our attention for the present to the case when the material of the beam is in an elastic state.

Differentiating the first of the above relations, we have that:

$$\frac{d^2}{dx^2}(EJ_y\varkappa_y) = -\frac{d^2M_y}{dx^2} = -\frac{dQ_z}{dx} = q_z.$$

Let us suppose that apart from the transverse load q_z, acting perpendicular to the axis of the beam in the direction of z, the beam

is also subjected to a longitudinal force P. If the axis of the beam deflects (Fig. 98) then the forces P and P' acting along the deflected axis at the ends of an element of length dx (which can be assumed equal to an element of arc ds) give a projection on the z-axis of $-P\sin\varphi + P'\sin\varphi'$. For small deflections $\sin\varphi \approx \tan\varphi \approx dw_0/dx$, so that

$$-P\sin\varphi + P'\sin\varphi' = -P\frac{dw_0}{dx} + P\frac{dw_0}{dx} + d\left(P\frac{dw_0}{dx}\right)$$

$$= \frac{d}{dx}\left(P\frac{dw_0}{dx}\right)dx.$$

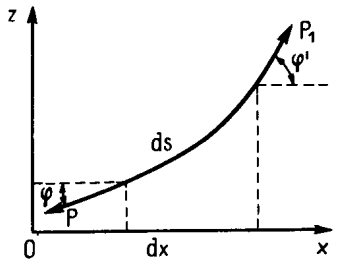

FIG. 98.

Per unit length of the beam, therefore, there is an additional force $d/dx(P\,dw_0/dx)$ acting in the direction of z. This force must be added to the load q_z in the equation between $\varkappa_y$ and q_z:

$$\frac{d^2}{dx^2}(EJ_y\varkappa_y) - \frac{d}{dx}\left(P\frac{dw_0}{dx}\right) = q_z(x). \qquad (2.60)$$

The curvature $\varkappa_y$ can be replaced by its approximate expression d^2w_0/dx^2. With the aid of eqn. (2.60) we can investigate the stability of beams of variable section with a longitudinal force distributed along the axis.

For simplicity we shall consider a beam of constant cross-section under the action of a compressive force P applied at the ends, so that $EJ_y = \text{const.}$ and $P = -P' = \text{const.}$ (the minus sign is introduced because loss of stability only occurs for compressive forces). Putting

$$\alpha^2 = \frac{P}{EJ_y},$$

we can rewrite eqn. (2.60) in the form

$$\frac{d^2\varkappa_y}{dx^2} + \alpha^2\varkappa_y = \frac{q_z}{EJ_y}. \tag{2.61}$$

This equation is of the same type as the equation for the oscillations of a pendulum. The general solution without the right-hand side is:

$$\varkappa_y = A\cos\alpha x + B\sin\alpha x.$$

The particular solution to the equation with the right-hand side can be found for example by the method of variation of parameters. The general solution will then be of the form

$$\varkappa_y = A\cos\alpha x + B\sin\alpha x + \frac{1}{\alpha EJ_y}\int_0^x \sin\alpha(x-\xi)\,.\,q_z(\xi)\,d\xi.$$

In order to find the constants A and B we make use of the boundary conditions.

If the beam is simply supported at its ends, then $M_y = 0$ at $x = 0$ and $x = l$, i.e. $\varkappa_y = 0$ at $x = 0$ and at $x = l$. Therefore $A = 0$. Making use of the condition at the end $x = l$, we have that:

$$B = -\frac{1}{\alpha EJ_y \sin\alpha l}\int_0^l \sin\alpha(l-\xi)\,.\,q_z(\xi)\,d\xi.$$

Thus

$$\varkappa_y = -\frac{\sin\alpha x}{\alpha EJ_y \sin\alpha l}\int_0^l \sin\alpha(l-\xi)\,.\,q_z(\xi)\,d\xi + \frac{1}{\alpha EJ_y}\int_0^x \sin\alpha(x-\xi)\,.\,q_z(\xi)\,d\xi \tag{2.62}$$

Each value of the force P (i.e. of the parameter α) corresponds to a definite value of the curvature $\varkappa_y$. But if P is such that

$$k \equiv \alpha l \equiv l\sqrt{\frac{P}{EJ_y}}$$

is a multiple of π, then the denominator in the first term vanishes and $\varkappa_y$ tends to infinity. Thus there is a series of values of P

$$P = \frac{k^2 EJ_y}{l^2} \quad \text{for} \quad k = \pi,\ 2\pi,\ 3\pi, \ldots$$

such that the curvature tends to infinity. The smallest of these values

$$P_{cr} = \frac{\pi^2 EJ_y}{l^2} \tag{2.63}$$

gives the critical force. We note that for critical values of the compressive force $\varkappa_y \to \infty$ independently of the value of the transverse load q_z. If $q_z = 0$ then from (2.62) we have indeterminate values for $\varkappa_y$ for $k = \pi, 2\pi, \ldots$, which is characteristic of problems on stability.

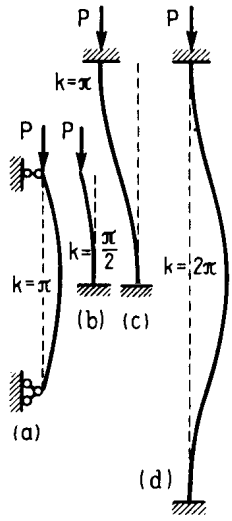

FIG. 99.

The fact that the curvature is indeterminate indicates that at the critical value of the force applied along the axis of the beam, apart from the case when the beam remains straight, which is possible but unstable, there exist other forms of equilibrium with a curved axis.

If in eqn. (2.60), instead of the approximate expression for the curvature, we make use of the exact expression $\varkappa_y = w_o''/(1 + w_o'^2)^{3/2}$, we obtain the same value for the critical load (2.63), but at the critical load the curvature will not be infinitely large.

The solution shows that from the moment the force reaches its critical value the curvature starts to increase very rapidly. The

shape of the deflected axis of the beam for large deflections after the force has reached its critical value was investigated by Leonard Euler. It was he who first derived the expression (2.63) for the critical compressive force at which loss of stability occurs. The critical force P_{cr} is therefore also called the Euler force P_E.

In formula (2.63) J_y occurs in the numerator. Since the whole argument could be repeated for bending in the (xy) plane, in evaluating the critical force we must put the smaller of the two principal moments of inertia of the cross-section in formula (2.63): after loss of stability (in the absence of transverse forces) bending occurs in the plane of the smallest stiffness of the beam.

From the relation (2.62) we see that for $q_z = 0$ the curvature of the beam varies according to a sinusoidal law. This means that after loss of stability the beam assumes the shape of some part of a sine curve. In the case of a beam with hinged end supports the smallest value of the critical load is obtained for $k \equiv \alpha l = \pi$. The expression for the curvature $\varkappa_y = B \sin \pi x/l$ shows that the deflected axis of a beam then represents a half sine wave (Fig. 99a). Knowing this we can find the values of the critical force for other types of support.

For instance, at mid-span the direction of the tangent to the deflected axis of the beam coincides with the initial direction of the straight axis. This means that each half of the beam is under the same conditions as a beam of length $l/2$ with one end built in and the other end free (Fig. 99b). Since loss of stability occurs at the same value of the critical force, then, if we now put l as the length of this half of the rod (i.e. of the rod with one end built in) we must replace l by $2l$ in the expression (2.63):

$$P_{cr} = \frac{\pi^2 EJ}{4l^2}. \tag{2.63'}$$

If now we continue this quarter sine wave upwards by a quarter wave (Fig. 99c), then this shape of the axis corresponds to a beam rigidly built in at both ends where one end can move perpendicular to the axis and along the axis, but cannot rotate; the value of the critical load will be as before—formula (2.63).

If we continue the half wave (Fig. 99a) in both directions by a quarter wave (Fig. 99d) then this will correspond to a beam built-in at both ends, where each end can move only along the axis of the beam. In formula (2.63), instead of l we must put $l/2$:

$$P_{cr} = \frac{4\pi^2 EJ}{l^2}. \tag{2.63''}$$

Figure 99 shows the various cases for different values of $k = \alpha l$.

Formula (2.63) was derived on the assumption that the material of the beam is entirely in the elastic range. If the length of the beam is insufficiently long compared with the lateral dimensions, the critical value of the force cannot be reached whilst the beam is still in an elastic state. In formula (2.63), dividing the right and left-hand sides by the cross-sectional area, we obtain the value for the critical normal stress

$$\sigma_{cr} = \frac{k^2 E J_y}{l^2 F} = \frac{k^2 E i_y^2}{l^2} = \frac{k^2 E}{\lambda_y^2},$$

where i_y is the radius of gyration of the cross-section about the axis Oy and $\lambda = l/i_y$ is the slenderness ratio of the beam in the plane (xz). From the condition that $\sigma_{cr} \leqq \sigma_S$, we have that: $\lambda_y \geqq k \sqrt{(E/\sigma_S)}$. For steel $\sqrt{(E/\sigma_S)} \approx 30$. Thus, for a beam simply supported at its ends ($k = \pi$) formula (2.63) applies if $\lambda_y > 100$. This would be very slender beam.

16. The Stability of a Rod beyond the Elastic Limit

If a system is in equilibrium under the action of some set of external forces, and if its restraints allow the system to be displaced in such a way that the work done by the internal forces in the displacements is less than that done by the external forces, then this state of equilibrium will be unstable; otherwise it will be stable. Single rods which are subjected to forces exceeding the minimum critical values found in § 15 will therefore be unstable. If however the rod is a member of some system and the force applied to the rod depends on the stiffness of the whole system and on its properties with respect to the rod under consideration, then the fact that the force in the rod has reached, or is even greater than, the above critical value does not necessarily mean that the equilibrium is unstable. This property applies to systems not in the elastic, but in the elasto-plastic range; it can be used to advantage in designing a structure of minimum weight.

Let us suppose that a rod with hinged ends is part of a system (for example, a truss) and that it loses stability at a compressive force P, after which it receives an additional infinitely small axial compression ε and a curvature $\varkappa = \varkappa_y$. To the accuracy of second order terms the decrease in length of the rod is

$$\Delta = \int_0^l \varepsilon dx \geqq 0,$$

where l is the length of the rod. As a result of the decrease in length Δ the unchanged external forces now re-distribute themselves throughout the structure, so that the force coming onto the rod considered now becomes $P + \delta P$ where δP depends on Δ and on the stiffness of the structure. Since ε, $\varkappa$ and Δ are small the relation between δP and Δ will, in general, be linear:

$$\delta P = -r\Delta, \tag{2.64}$$

where r is a stiffness coefficient of the structure. If $r > 0$, then for $\varepsilon > 0$ the buckling of the rod is accompanied by a decrease in the compressive force, and the structure is said to be self-unloading;

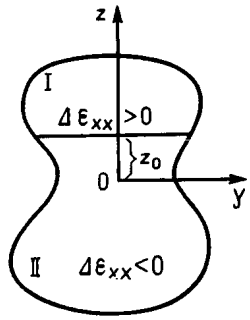

FIG. 100.

if $r < 0$ it is self-loading. The value of the coefficient r can always be found if the structure and external forces are given. We therefore consider r as a known quantity.

Let us consider a rod the cross-section of which has two axes of symmetry (Fig. 100). We will take stresses and extensions as positive for compression, and the curvature will be considered positive if the centre of curvature lies within $z > 0$. Then the additional extension of a longitudinal fibre at a distance z from the plane of symmetry (xy), assuming that plane sections remain plane, will be $\delta\varepsilon_{xx} = \varepsilon + \varkappa z$. It changes sign at $z = z_0$, where

$$z_0 = -\frac{\varepsilon}{\varkappa}, \tag{2.65}$$

so that $\delta\varepsilon_{xx} > 0$ for $z > z_0$ (self-loading) and $\delta\varepsilon_{xx} < 0$ for $z < z_0$ (self-unloading). For $\delta\varepsilon_{xx}$ we can put

$$\delta\varepsilon_{xx} = \varkappa(z - z_0), \quad (\varkappa z_0 = -\varepsilon). \tag{2.66}$$

If the compressive stress $\sigma = P/F$ exceeds the elastic limit before buckling occurs, then the expressions for the additional stresses $\delta\sigma_{xx}$ will be different for loading and unloading:

$$\left.\begin{aligned} \delta\sigma_{xx} &= E'\varkappa(z - z_0) \quad \text{for} \quad z \geqq z_0, \\ \delta\sigma_{xx} &= E\varkappa(z - z_0) \quad \text{for} \quad z \leqq z_0. \end{aligned}\right\} \tag{2.67}$$

Here $E' = d\sigma/d\varepsilon$ is the tangent modulus, i.e. the slope of the $\sigma \sim \varepsilon$ curve at $\sigma = P/F$. The additional force ΔP and the bending moment ΔM can be expressed in terms of the stress $\delta\sigma_{xx}$ by the formulae

$$\Delta P = \int_{-h/2}^{h/2} \delta\sigma_{xx} b\, dz, \quad \Delta M = \int_{-h/2}^{h/2} \delta\sigma_{xx} bz\, dz,$$

where $b = b(z)$ is the width of the section at a height z and h is the height of the section in the z-direction. Substituting the values of $\delta\sigma_{xx}$ given by (2.67) and integrating, we get that:

$$\left.\begin{aligned} \Delta P &= A(z_0) \,.\, \varkappa, \\ \Delta M &= D(z_0) \,.\, \varkappa, \end{aligned}\right\} \tag{2.68}$$

$$A(z_0) = \begin{cases} -z_0 EF = \dfrac{\varepsilon}{\varkappa} EF, & z_0 \geqq \dfrac{h}{2}; \\ (E - E')(S_2 - z_0 F_2) - z_0 E'F, & \dfrac{h}{2} \geqq z_0 \geqq -\dfrac{h}{2}; \\ -z_0 E'F = \dfrac{\varepsilon}{\varkappa} E'F, & z_0 \leqq -\dfrac{h}{2}; \end{cases} \tag{2.69}$$

$$D(z_0) = \begin{cases} EJ & z_0 \geqq \dfrac{h}{2}; \\ (E - E')(J_2 - z_0 S_2) + E'J, & \dfrac{h}{2} \geqq z_0 \geqq -\dfrac{h}{2}; \\ E'J, & z_0 \leqq -\dfrac{h}{2}. \end{cases} \tag{2.70}$$

Here F, J are the area and moment of inertia of the section about the axis Oy, and F_2, S_2, J_2 are the area, first moment and moment of inertia of the area of the section where the stress is reduced:

$$F_2 = \int_{-h/2}^{z_0} b dz, \quad S_2 = \int_{-h/2}^{z_0} bz\, dz, \quad J_2 = \int_{-h/2}^{z_0} bz^2\, dz, \tag{2.71}$$

i.e. they are known functions of z_0.

From the equilibrium equation for an element of the rod $d(\Delta P)/dx = 0$ it follows that ΔP is independent of x (it is constant); this means that instability occurs when $\Delta P \leqq \delta P$. When $\Delta P = \delta P$ we have that

$$A(z_0)\,\varkappa = r\int_0^l z_0\varkappa\,dx \equiv \delta P = \text{const.} \tag{2.72}$$

From the condition that the moment ΔM is equal to the moment of the external force $-(P + \delta P)\,w \approx -Pw$, we get that:

$$D(z_0)\frac{d^2w}{dx^2} + Pw = 0. \tag{2.73}$$

The two equations which must be satisfied by two unknown functions $z_0(x)$ and $\varkappa(x)$, being homogeneous in w, will have the solution $w = 0$ for any given value of $z_0(x)$ for the homogeneous boundary conditions

$$w = 0 \quad \text{at} \quad x = 0 \quad \text{and} \quad x = l \tag{2.74}$$

But at certain values of P there will exist non-trivial solutions. The smallest of these values of P gives the critical force at which the system, including the rod considered, becomes unstable.

For a perfectly elastic rod ($E' = E$) formulae (2.69) and (2.70) give the same values of A and D for any z_0: $A = -z_0EF$, $D = EJ$. Then from (2.72) we find that

$$-EF\varkappa z_0 = r\varkappa z_0 l,$$

and for $\varkappa \neq 0$ and $r \neq 0$ we therefore have that $z_0 = 0$, i.e. $\varepsilon = 0$ and $\delta P = 0$. Thus in any structure (for any r) slight buckling in the elastic range is not accompanied by a decrease in length ($\Delta = 0$), i.e. the rod behaves as if it were not confined by the structure. The Euler force P_E, given by (2.63), is the critical force independently of the value of r. In the elasto-plastic range this is not so.

Let us consider the reverse problem: in what structures (at what values of r) will loss of stability occur beyond the elastic limit ($E' < E$) for $z_0 \leqq -h/2$ (for any x)? In this case the whole cross-section should be in the state of plasticity; therefore $A = -z_0E'F$, $D = E'J$, and from (2.72) we have that:

$$-E'F\varkappa z_0 = r\varkappa z_0 l.$$

For $\varkappa \neq 0$, $z_0 \neq 0$; thus we get that

$$r = -r', \quad \text{where} \quad r' = E'F/l, \tag{2.75}$$

and instability occurs ($\Delta P \leqq \delta P$) for $r \leqq -r'$, i.e. $|r| \geqq r'$, since z_0 is negative ($\varkappa > 0$). The structure must therefore be self-loading. Putting $w = C \sin \pi x/l$ which satisfies (2.74), we find that the critical force, from (2.73), is

$$P_t = \frac{\pi^2 E' J}{l^2} = \frac{E'}{E} P_E, \tag{2.76}$$

which is called the tangent modular force.

For a single rod (for $r = 0$) we have from (2.72) that $A(z_0) = 0$, and since $z_0 \neq 0$, then in (2.69) and therefore in (2.70) $h/2 > z_0 > -h/2$, i.e. z_0 can be found from the equation

$$A(z_0) \equiv (E - E')[S_2(z_0) - z_0 F_2(z_0)] - z_0 E' F = 0. \tag{2.77}$$

Consequently, $z_0 = -c = \text{const.} < 0$. From (2.70) we have that:

$$D = (E - E')(J_2 + cS_2) + E'J = \text{const.} > 0. \tag{2.78}$$

This case was investigated by von Karman. The quantity

$$K = E' + (E - E')\frac{J_2 + cS_2}{J}, \quad (D = KJ) \tag{2.79}$$

is called Karman's modulus. From (2.73), putting $w = C \sin \pi x/l$, we find the Karman critical force

$$P_K = \frac{\pi^2 KJ}{l^2} = P_E \frac{K}{E}. \tag{2.80}$$

Since $K > E'$, this force is greater than the tangent modular force (2.76); since $K < E$ it is smaller than the Euler's critical force.

In the general case when $0 \geqq z_0 \geqq -h/2$ (when $\Delta > 0$) the changes in the stiffnesses (2.69) and (2.70) are related by the expression

$$\frac{dD}{dA} = \frac{(E - E')\, S_2}{(E - E')\, F_2 + E'F} < 0, \quad \text{since} \quad S_2 < 0.$$

From (2.68) we conclude that the more load the structure puts on the rod after loss of stability, the less is its stiffness D, and from (2.73) therefore, the smaller is the critical load.

Let us consider the case of a very rigid structure, when r, and therefore $\delta P = \Delta P$ as well, are extremely small. Then the case $z_0 = -c + \zeta$ will differ only slightly from the Karman case $-c$. From the expressions

$$A(z_0) = A(-c) + \delta A = \frac{\delta P}{\varkappa}, \quad D(z_0) = D(-c) + \frac{dD}{dA}\delta A,$$

where $\delta A = (dA/dz_0)_{z_0=-c} \cdot \zeta$, taking into account that $A(-c) = 0$, $D(-c) = KJ$, we get that

$$\left.\begin{aligned} D &= KJ + \left[\frac{(E - E')\,S_2}{(E - E')\,F_2 + E'F}\right]_{z_0=-c} \cdot \frac{\delta P}{\varkappa}, \\ z_0 + c = \zeta &= -\left[\frac{1}{(E - E')\,F_2 + E'F}\right]_{z_0=-c} \cdot \frac{\delta P}{\varkappa}. \end{aligned}\right\} \quad (2.81)$$

From (2.72) we now obtain to the accuracy of r^2

$$\delta P = -rc \int_0^l \varkappa\, dx. \quad (2.82)$$

The equation of stability (2.73), on the basis of (2.81), now becomes

$$KJ\frac{d^2w}{dx^2} + Pw = -\left[\frac{(E - E')\,S_2}{(E - E')\,F_2 + E'F}\right]_{z_0=-c} \cdot \delta P, \quad (2.83)$$

and the right-hand side must be considered extremely small compared with Pw for almost all values of x. The critical value of P will differ from the Karman force by a small quantity of the order of r, so that

$$\frac{P}{KJ} = \left(\frac{\pi + \alpha}{l}\right)^2, \quad P = P_K\left(1 + \frac{2\alpha}{\pi}\right), \quad (2.84)$$

where α is a small quantity of the order of r. The solution of eqn. (2.83)

$$w = C_1 \cos\frac{\pi + \alpha}{l}x + C_2 \sin\frac{\pi + \alpha}{l}x - \frac{(E - E')\,S_2}{(E - E')\,F_2 + E'F} \cdot \frac{\delta P}{P_K}$$

after substituting in (2.82) and satisfying the conditions (2.74), gives the following value for α (to the accuracy of r^2):

$$\alpha = -\left[\frac{4\pi rc(E - E')\,S_2}{lP_K\{(E - E')\,F_2 + E'F\}}\right]_{z_0=-c} \quad (2.85)$$

From this and from (2.84) we conclude that since $S_2 < 0$, in self-loading structures ($r < 0$) there must be $\alpha < 0$, i.e. the critical force is less than the Karman force, and in self-unloading structures ($r > 0$) it is greater.

From (2.84) and (2.85) we find that for a rectangular section

$$P = P_K + \frac{2rh^2}{l} \cdot \frac{\sqrt{E}}{\sqrt{E} + \sqrt{E'}}.$$

An example of a self-unloading structure is a freely supported beam of length L with its mid-point resting freely on the rod under consideration. If a load Q is applied at the centre, the deflection of the beam is $f = (Q - P)\,L^3/48(EI)_b$, where P is the force transmitted to the rod, and from this $\Delta f = \Delta = -L^3/48(EI)_b$. δP and the stiffness coefficient for the structure is therefore

$$r = + \frac{48(EJ)_b}{L^3}.$$

An example of a self-loading structure is a truss made up of two identical rods inclined at a small angle to the horizontal, in which the force is transmitted through an internal hinge to the vertical rod under consideration, which lies along the bisector of the angle.

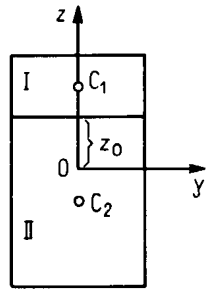

FIG. 101.

Example. For a beam of rectangular section (Fig. 101) with sides b and h in the directions of the axes Oy and Oz, we have that

$$J_y = J = \frac{bh^3}{12}, \quad F_2 = b\left(\frac{h}{2} + z_0\right), \quad S_2 = \frac{b}{2}\left(z_0^2 - \frac{h^2}{4}\right),$$

$$J_2 = \frac{b}{3}\left(z_0^3 + \frac{h^3}{8}\right),$$

so that from (2.79) we find that Karman's modulus is

$$K = 4EE'/(\sqrt{E} + \sqrt{E'})^2.$$

In the absence of any strain hardening ($E' = 0$), we have that $K = 0$ and the Karman critical force is zero. A single rod, therefore, of non-strain hardening material cannot resist a load greater than $F\sigma_T$, where σ_T is the yield point. Here, however, this force cannot be exceeded, not because of loss of stability, but because of loss of carrying capacity.

CHAPTER III

ELASTICITY AND PLASTICITY IN A STATE OF COMPOUND STRESS

1. Three-Dimensional Elasticity of Materials

The mechanical properties of materials examined in Chapter II were obtained by considering the tension or compression of a cylindrical specimen when one of the principal stresses (the axial stress) was non-zero and the other two principal stresses were zero everywhere within the test portion of the specimen. This state of stress is called uniaxial. In most machine and structural elements, however, there exists a state of compound stress, when all three principal stresses, or two of them, are non-zero.

In such cases a knowledge of the stress–strain curve of the material of the structure is insufficient in designing a structure with respect to its strength and deformability, for finding the stresses and corresponding strains which occur in it, and for determining the loads at which plastic deformation or failure of the structure occurs.

It is important, therefore, to establish experimentally the general relations between stresses and strains which occur in the material under conditions of compound stress.

In Chapter I we derived a mathematical apparatus which enabled us to describe the state of stress and strain within a body in the most general case. In particular, it was established that the relative change in any small volume is the sum of the relative extensions of three mutually perpendicular elements

$$\theta = 3\varepsilon = \varepsilon_{xx} + \varepsilon_{yy} + \varepsilon_{zz}, \tag{3.1}$$

and that the mean normal stress is equal to the arithmetic mean value of the three normal stresses acting on three mutually perpendicular areas

$$\sigma = \tfrac{1}{3}(\sigma_{xx} + \sigma_{yy} + \sigma_{zz}). \tag{3.2}$$

The directions of the axes of x, y, z within a small element of volume can be chosen completely arbitrarily (they are of course orthogonal), i.e. the numerical values of ε and σ do not depend on the choice of axes (they are invariant with respect to rotation of the coordinate axes).

The majority of homogeneous and quasi-isotropic (in the meaning given in Chapter I) solid bodies satisfy the following law of three-dimensional elasticity: the relative change in volume θ of a material during an isothermal (i.e. constant temperature) deformation process is a definite function only of the mean stress σ, and the deformation process is reversible. This is true also for adiabatic processes.

The relation between σ and θ can be established from comparatively simple experiments on the hydrostatic compression of specimens. A great number of such experiments have been carried out by Bridgman. By testing various materials in very strong cylinders under the action of very high liquid pressures of the order of 20–30 atm and more, Bridgman discovered that all the chemical elements and a very large majority of materials behave elastically: their volume decreases with increase in pressure and increases to its original value after release of the pressure. The relation between pressure and relative change in volume is therefore of the form

$$-\theta = \frac{p}{K}\left(1 - \frac{p}{K_1}\right),$$

where K is the bulk modulus, which for metals is of the order of 10^6 kg/cm^2, and K_1 is of the order of 10^5 kg/cm^2. It can be seen that the latter term is significant only for large pressures, and for pressures of the order of twice the yield point in tension the magnitude of the second term is only 1–2 per cent of the magnitude of the first. With the mean normal stresses usually met with in practice we can discard this second term and assume, to a high degree of accuracy, that the relation is linear. Since $p = -\sigma$, the relation between σ and $\theta = 3\varepsilon$ can, consequently, be written in the form

$$\sigma = 3K\varepsilon \equiv K\theta. \tag{3.3}$$

This law is valid not only for uniform all-round pressures, when the shape of the body remains similar to its original shape and does not experience any shear strain, but also for any stresses and strains,

The experiments of N. N. Davidenkov, and other experiments including those recently carried out in the materials laboratory o Moscow State University, have shown that the influence of plastic shear strains on the relation between σ and θ can be ignored.

The volumetric law of elasticity (3.3), which can be re-written in the form

$$\varepsilon = \frac{\sigma}{3K},$$

is sometimes replaced in calculations beyond the elastic limit by the condition of incompressibility

$$\varepsilon \equiv \tfrac{1}{3}(\varepsilon_{xx} + \varepsilon_{yy} + \varepsilon_{zz}) = 0, \tag{3.4}$$

since normally $K \gg \sigma$; this can be done in cases when the volumetric strain $\varepsilon = \sigma/3K$ is considerably smaller than the basic strains which occur in the body.

2. General Properties of Elasto-plastic Strains in Solid Bodies

It was established in Chapter I that the most general state of compound shear at some point in a body is given by the strain deviator which we define as $\varepsilon'_{mn}(m, n = x, y, z)$, and the components of which are expressed in terms of the strains ε_{mn} *by* the formulae

$$\varepsilon'_{mm} = \varepsilon_{mm} - \varepsilon; \quad \varepsilon'_{mn} = \varepsilon_{mn} \qquad (m \neq n). \tag{3.5}$$

The resultant shear strain γ_v is the shear strain of an octahedral fibre and coincides, to the accuracy of a numerical factor, with the strain intensity ε_i, i.e. $\gamma_v = \sqrt{(2)}\varepsilon_i$.

It was also established in Chapter I that the most general state of compound stress having zero mean stress (zero hydrostatic pressure) at any point in the body is given by the stress deviator, which we define as $\sigma'_{mn}(m, n = x, y, z)$ and the components of which can be expressed in terms of the stresses σ_{mn} by the formulae

$$\sigma'_{mn} = \sigma_{mm} - \sigma; \quad \sigma'_{mn} = \sigma_{mn} \qquad (m \neq n). \tag{3.6}$$

The resultant shear stress τ_v is the octahedral stress, which is related to the intensity of stress σ_i by the expression $\tau_v = (\sqrt{2}/3)\,\sigma_i$. It can easily be shown that the sums of the squares of the quantities ε'_{mn} and σ'_{mn} are proportional respectively to the square of the intensity of strain and the square of the intensity of stress:

$$\sum_{m,n} \varepsilon'^2_{mn} = \frac{3}{2}\varepsilon_i^2, \quad \sum_{m,n} \sigma'^2_{mn} = \frac{2}{3}\sigma_i^2,$$

where the summation is taken over all values of $m, n = x, y, z$; due to symmetry ($\varepsilon'_{mn} = \varepsilon'_{nm}$, $\sigma'_{mn} = \sigma'_{nm}$) each of these sums will contain six addends.

Since the components ε'_{mn} and σ'_{mn} are linearly dependent: $\sum_{m=1}^{3} \varepsilon'_{mm} = 0$, $\sum_{m=1}^{3} \sigma'_{mm} = 0$, then for the six quantities ε'_{mn} and σ'_{mn} we can, by linear transformation, substitute the five quantities Θ_k and S_k ($k = 1, 2, \ldots, 5$), which are linearly independent amongst themselves, so that

$$\sum_{m,n=x,y,z} \varepsilon'^2_{mn} \equiv \sum_{k=1}^{5} \Theta_k^2, \qquad \sum_{m,n=x,y,z} \sigma'^2_{mn} \equiv \sum_{k=1}^{5} S_k^2.$$

An example of such a transformation is

$$\left.\begin{aligned} \Theta_1 &= \varepsilon'_{11}\sqrt{\left(\frac{3}{2}\right)}, \quad \Theta_2 = (\varepsilon'_{22} - \varepsilon'_{33})\frac{\sqrt{2}}{2}, \quad \Theta_3 = \varepsilon'_{12}\sqrt{2}, \\ &\qquad \Theta_4 = \varepsilon'_{23}\sqrt{2}, \quad \Theta_5 = \varepsilon'_{31}\sqrt{2}, \\ S_1 &= \sigma'_{11}\sqrt{\left(\frac{3}{2}\right)}, \quad S_2 = (\sigma'_{22} - \sigma'_{33})\frac{\sqrt{2}}{2}, \quad S_3 = \sigma'_{12}\sqrt{2}, \\ &\qquad S_4 = \sigma'_{23}\sqrt{2}, \quad S_5 = \sigma'_{31}\sqrt{2}, \end{aligned}\right\} \tag{3.7}$$

and, denoting the sum of the squares of the components Θ_k and S_k respectively by Θ^2 and S^2, we get that

$$\left.\begin{aligned} \Theta^2 &= \sum_{k=1}^{5} \Theta_k^2, \quad |\Theta| = \sqrt{\left(\frac{3}{2}\right)}\varepsilon_i, \\ S^2 &= \sum_{k=1}^{5} S_k^2, \quad |S| = \sqrt{\left(\frac{2}{3}\right)}\sigma_i. \end{aligned}\right\} \tag{3.8}$$

The quantities Θ with components Θ_k ($k = 1, 2, \ldots, 5$), and $\boldsymbol{S}$ with components S_k ($k = 1, 2, \ldots, 5$) can now be considered as five dimensional orthogonal Cartesian vectors. Since all components Θ_k appear in the expression for the resultants hear strain ε_i in the same form, the space of the vector Θ (and similarly of $\boldsymbol{S}$) is homogeneous. On this basis we are able to investigate the general properties of the relation between $\boldsymbol{S}$ and Θ for materials which before deformation are homogeneous and isotropic.

For simplicity we shall consider the particular case of a state of plane stress when the vectors Θ and $\boldsymbol{S}$ are two-dimensional. In order to develop the laws of elasticity and plasticity of materials, i.e. in order to establish the relation between Θ and $\boldsymbol{S}$, we must rely on the results of experiments which enable us to measure at any

instant the stresses σ_{mn} and the strains ε_{mn} at every point in the body. For this purpose it is essential that the state of stress and strain in the specimen is uniform, i.e. the same at all points. In this case it is easy to find the stresses and strains in the body from the values of the external forces and of the displacements of the outer surfaces. In practice, however, a uniform state is achieved only in very few cases. We saw above that a body of any shape under a uniform external pressure over its whole surface is subjected to a uniform

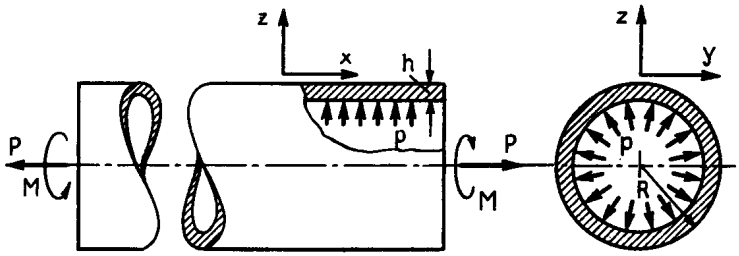

FIG. 102.

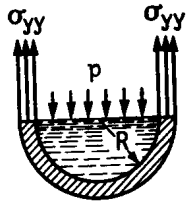

FIG. 103.

compressive strain, and in this way it is simple to investigate the behaviour of bodies under conditions of compression in three dimensions. We shall consider now the state of uniform compound butstress and the state of strain in a body.

The most common types of experiment in this field are those which investigate thin-walled cylindrical specimens under the simultaneous action of a torque, a tensile force uniformly distributed over the ends and a uniform internal pressure.

Let us take the axis Ox as along the axis of the cylinder, the axis Oy along the tangent to the circumference of the cross-section of the cylinder and the axis Oz along the radius (Fig. 102).

If we make an imaginary section, perpendicular to the axis of the cylinder, then on this section there will be normal stresses σ_{xx} from the tensile force P and shear stresses $\sigma_{xy} = \sigma_{yx}$ from the torque M. The magnitude of the normal stresses is found by dividing the tensile force by the cross-sectional area of the tube:

$$\sigma_{xx} = \frac{P}{F} = \frac{P}{2\pi Rh}.$$

As was shown in § 7 of Chapter II, if the thickness h of the cylinder is small compared with the radius R, the distribution of shear stresses can be considered uniform:

$$\sigma_{xy} = \frac{M}{RF} = \frac{M}{2\pi R^2 h}$$

(see formula (2.27)).

Let us now make a cut along the axis of the cylinder, discard one part and retain the other together with the liquid which it contains (Fig. 103). On the section of a thin-walled cylinder there will act a uniformly distributed stress σ_{yy}, which is independent both of the tensile force P and of the torque M, and on the part of the section filled with liquid, as well as over the whole internal volume of the cylinder, there will act a uniformly distributed pressure p.

If we consider the equilibrium of a section of the cylinder of unit length, the equilibrium equation will be

$$\sigma_{yy} \cdot 2h \cdot 1 = p \cdot 2R \cdot 1,$$

so that

$$\sigma_{yy} = \frac{pR}{h}.$$

In addition, the internal pressure gives rise to normal stresses σ_{zz}, which are equal to p on the internal surface of the cylinder and are zero on the external surface. These stresses are small compared with the others for $R \gg h$ (this can be seen immediately from the expression for σ_{yy}), and we shall put $\sigma_{zz} = 0$. Thus the state of stress at every point of the cylinder is defined by the components

$$\left.\begin{aligned} &\sigma_{xx} = \frac{P}{F}, \quad \sigma_{yy} = \frac{pR}{h}, \quad \sigma_{zz} = 0, \\ &\sigma_{yz} = \sigma_{zx} = 0, \quad \sigma_{xy} = \frac{M}{RF}; \quad \sigma = \frac{1}{3}(\sigma_{xx} + \sigma_{yy}) \\ &\qquad\qquad (F = 2\pi Rh). \end{aligned}\right\} \tag{3.9}$$

The axis Oz is a principal axis, since $\sigma_3 = \sigma_{zz} = 0$, so that we have a state of plane two-dimensional stress. It should be noted that each of the components σ_{xx}, σ_{yy}, σ_{xy} of this state of plane stress depends only on one of the external loads, P, p or M, so that by varying the latter we can attain any relation between σ_{xx}, σ_{yy}, σ_{xy}.

In order to find by experiment the strains ε_{xx}, ε_{yy}, ε_{xy} we must measure the change in the gange length l of the cylinder along the axis Ox (i.e. Δl, and then $\varepsilon_{xx} = \Delta l/l$) and the change in the radius of the cylinder ΔR. The relative change in the circumference of the cylinder will give the strain

$$\varepsilon_{yy} = \frac{\Delta(2\pi R)}{2\pi R} = \frac{\Delta R}{R}.$$

We shall define φ as the angle of rotation about the axis of x of the right-hand end of the gange length l relative to the left-hand end. Since a plane cross-section of the cylinder before deformation remains plane for any φ, the shear strain $2\varepsilon_{xy}$ is the angle of rotation of a straight generator of the cylinder due to the rotation φ; this angle (or more precisely, its tangent) is equal to the ratio of the circumferential movement $R\varphi$ to the length l, i.e.

$$2\varepsilon_{xy} = \frac{R\varphi}{l}.$$

Thus

$$\varepsilon_{xx} = \frac{\Delta l}{l}, \quad \varepsilon_{yy} = \frac{\Delta R}{R}, \quad \varepsilon_{xy} = \frac{R\varphi}{2l}. \tag{3.10}$$

The strain in the thickness of the wall of the cylinder, ε_{zz}, can be found either from experiment or by calculation on the basis of formula (3.3):

$$\varepsilon_{zz} = -\varepsilon_{xx} - \varepsilon_{yy} + \frac{\sigma}{3K}. \tag{3.10'}$$

The last term in the right-hand side of this expression is usually neglected.

Experiments on cylinders of various materials subjected simultaneously to the action of a force P, a pressure p and a torque M, are very complicated and require special equipment, particularly in cases when it is necessary to let these quantities vary with time according to a predetermined law. For this reason more straightforward experiments are usually carried out and they are of two different types: those with the combined action of P and p ($M = 0$)

and those with the combined action of P and $M (p = 0)$. A description of the equipment is given in Chapter VII.

3. P–p Experiments

Experiments on the deformation of cylindrical specimens under the action of a tensile force and an internal pressure can be carried out on normal loading machines by using specimens with closed ends and by using liquid or gas with special connecting pipes from a reservior with a regulating device to create the required internal pressure p. Loading of the specimen is carried out most easily by letting the force P and the pressure p vary with time according to a predetermined programme and measuring the extension Δl over the length l and the change ΔR in the radius.

The components of the stress vector $\boldsymbol{S}$ given by (3.9), (3.6) and (3.7), and of the strain vector $\boldsymbol{\Theta}$, given by (3.10), (3.5) and (3.7) are expressed in terms of P, p, Δl, ΔR by the formulae

$$\left.\begin{aligned} S_1 &= \sqrt{\left(\frac{2}{3}\right)}\left(\sigma_{xx} - \frac{1}{2}\sigma_{yy}\right) = \sqrt{\left(\frac{2}{3}\right)}\left(\frac{P}{F} - \frac{pR}{2h}\right), \\ S_2 &= \frac{\sqrt{2}}{2}\sigma_{yy} = \frac{pR}{h\sqrt{2}}, \\ \Theta_1 &= \sqrt{\left(\frac{3}{2}\right)}\varepsilon_{xx} = \sqrt{\left(\frac{3}{2}\right)}\frac{\Delta l}{l}, \\ \Theta_2 &= \sqrt{2}\left(\varepsilon_{yy} + \frac{1}{2}\varepsilon_{xx}\right) = \sqrt{2}\left(\frac{\Delta R}{R} + \frac{\Delta l}{2l}\right), \end{aligned}\right\} \tag{3.11}$$

the remaining components S_k and Θ_k being zero. For simplicity we have taken $K = \infty$, $\varepsilon = 0$.

Let $\boldsymbol{i}_1, \boldsymbol{i}_2$ be the unit vectors of the rectangular coordinate axes along which the components of the stress vector $\boldsymbol{S}(S_1, S_2)$ are measured from the origin, i.e. $\boldsymbol{S} = S_1\boldsymbol{i}_1 + S_2\boldsymbol{i}_2$, and let us suppose that in this plane $\boldsymbol{\Theta} = \Theta_1\boldsymbol{i}_1 + \Theta_2\boldsymbol{i}_2$ is the strain vector which is drawn from the end of the vector $\boldsymbol{S}$. The moduli of these vectors, as has already been pointed out (see formulae (3.8)); are, to the accuracy of a numerical factor, the resultant shearing stress (the intensity of stress) and the resultant shear strain (the intensity of strain):

$$\left.\begin{aligned} |\boldsymbol{S}| &= \sqrt{\left(\frac{2}{3}\right)}\sigma_i = \sqrt{\left(\frac{2}{3}\right)}\sqrt{(\sigma_{xx}^2 - \sigma_{xx}\sigma_{yy} + \sigma_{yy}^2)}, \\ |\boldsymbol{\Theta}| &= \sqrt{\left(\frac{3}{2}\right)}\varepsilon_i = \sqrt{2}\sqrt{(\varepsilon_{xx}^2 + \varepsilon_{xx}\varepsilon_{yy} + \varepsilon_{yy}^2)}. \end{aligned}\right\} \tag{3.12}$$

In carrying out the experiment with a cylindrical specimen we specify the force $P(t)$ and the pressure $p(t)$ as definite functions of time; in so doing we specify the components $S_1(t)$ and $S_2(t)$, i.e. the vector $\boldsymbol{S} = \boldsymbol{S}(t)$. The position of its end varies with time and describes a definite curve which is called the loading trajectory (Fig. 104). By measuring Δl and ΔR we can draw at every point on this trajectory the strain vector $\boldsymbol{\Theta}$. Also, since during the experiment we know the differential of the arc of the loading trajectory,

$$ds = \sqrt{\left[\left(\frac{dS_1}{dt}\right)^2 + \left(\frac{dS_2}{dt}\right)^2\right]} dt = \sqrt{(dS_1^2 + dS_2^2)},$$

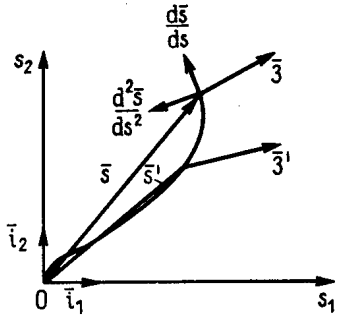

FIG. 104.

instead of the time t it is convenient to take as an independent variable the length of the arc

$$s = \int_0^t ds = \int_0^t \sqrt{\left[\left(\frac{dS_1}{dt}\right)^2 + \left(\frac{dS_2}{dt}\right)^2\right]} dt, \tag{3.13}$$

in which $\dot{s} = ds/dt$ is the rate of loading. The unit vector of the rate of loading is directed along the tangent to the trajectory and is

$$\frac{d\boldsymbol{S}}{ds} = \boldsymbol{T}.$$

The basic geometrical characteristic of the loading trajectory is its curvature $\varkappa = 1/\varrho$, where

$$\frac{1}{\varrho^2} = \left(\frac{d^2\boldsymbol{S}}{ds^2}\right)^2 = \left(\frac{\dot{S}_1\ddot{S}_2 - \ddot{S}_1\dot{S}_2}{\dot{s}^3}\right)^2, \tag{3.14}$$

where ϱ is the radius of curvature and the dots above S indicate differentiation with respect to the time t. We note that although the length of arc s and the curvature $1/\varrho$ involve the operations of differentiation and integration with respect to time t, the latter need not necessarily appear in these expressions, and we can eliminate it if we take, for example, the internal pressure p, i.e. the coordinate S_2, as the independent variable. Then

$$\left.\begin{aligned} s &= \int \sqrt{\left[1 + \left(\frac{dS_1}{dS_2}\right)^2\right]}\, dS_2, \\ \frac{1}{\varrho^2} &= \left(\frac{d^2S_1}{dS_2^2}\right)^2 : \left[1 + \left(\frac{dS_1}{dS_2}\right)^2\right]^3. \end{aligned}\right\} \tag{3.14'}$$

The unit vector normal to the loading trajectory, on the line of which is situated the centre of curvature, is $\boldsymbol{N} = \varrho\, d^2\boldsymbol{S}/ds^2$; together with the vector $\boldsymbol{T} = d\boldsymbol{S}/ds$ it forms a pair of orthogonal coordinate vectors, whose orientation at some point on the curve depends only on the intrinsic geometrical properties of the trajectory.

The problem of establishing the laws of elasticity and plasticity for any particular metal, from the point of view of experiments on cylindrical specimens, amounts to finding for all possible loading trajectories the strain vector $\mathfrak{Z}$ at any point, i.e. to finding the relation which we shall write in the form

$$\mathfrak{Z} = \mathfrak{Z}[\boldsymbol{S}].$$

In Chapter II we have already considered the most simple loading tests, which are the particular case of the P–p experiments when $p = 0$ and $S_1 = \sqrt{(2/3)}\,\sigma_{xx}$, $S_2 = (\sqrt{2/2})\,\sigma_{yy} = 0$, $|\boldsymbol{S}| = |S_1| = (\sqrt{2/3})\,\sigma_i = \sqrt{(2/3)}\,|\sigma_{xx}|$, $d\boldsymbol{S}/ds = \boldsymbol{T} = \boldsymbol{i}_1$; consequently, the experiments are carried out with loading trajectories coincident with the S_1-axis in Fig. 104. They show that for the majority of metals, for $|\sigma_{xx}| \leqq \sigma_s$ (σ_s is the yield point), the longitudinal strain is related to the stress by the expression $\varepsilon_{xx} = \sigma_{xx}/E$ and is reversible, and that the strain ε_{yy} is proportional to ε_{xx}: $\varepsilon_{yy} = -\nu\varepsilon_{xx}$. Since in evaluating the components of the strain vector (3.11) we made the approximation that $\varepsilon = 0$, in substituting in (3.11) the results of experiments on simple tension we must put $\nu = \frac{1}{2}$, and thus $\mathfrak{Z}_1 = \sqrt{(3/2)}\,\varepsilon_{xx}$, $\mathfrak{Z}_2 = \sqrt{2}(\varepsilon_{yy} + \frac{1}{2}\varepsilon_{xx}) \approx 0$. Experiments on simple tension show, therefore, that the vector $\mathfrak{Z}$ is directed along the

vector S and within the elastic range ($|S| < \sqrt{(2/3)}\,\sigma_s$) it is proportional to S:

$$\Im = \frac{3}{2E} S.$$

It was also shown that beyond the elastic limit

$$\Im = \frac{|\Im|}{|S|} S,$$

and $\sigma_{xx} = \Phi(\varepsilon_{xx})$, i.e. $|S| = (3/2)\,\Phi[\sqrt{(2/3)}|\Im|]$, $\sigma_i = \Phi(\varepsilon_i)$, where Φ is the function represented by the stress–strain curve.

By analogy with the case of simple tension we shall define simple loading in P–p experiments as a process in which the applied forces and the stresses caused by them give a loading trajectory which is a straight line starting at the origin of coordinates in the plane S_1S_2; otherwise the loading is known as combined loading. We see from formulae (3.11) that in P–p experiments simple loading corresponds to a change in the tensile force and internal pressure which is proportional only to one parameter (for example, time).

A great many P–p experiments with different homogeneous quasi-isotropic metals have shown that for all simple loading trajectories the strain vector $\Im$ is directed along the trajectory, i.e.

$$\frac{\Im}{|\Im|} = \frac{S}{|S|} \quad \text{or} \quad \Im = \frac{3\varepsilon_i}{2\sigma_i} S, \tag{3.15}$$

and the moduli of $\Im$ and S or ε_i and σ_i are inter-connected by the same relation as in simple tension. The function Φ, therefore, for a given material is universal for all cases of simple loading:

$$\sigma_i = \Phi(\varepsilon_i), \tag{3.16}$$

and consequently plastic strains start to occur at a constant value of $\sigma_i = \sigma_s$.

When some particular combination of stresses (or strains) reaches a value at which plastic strains appear, the condition of plasticity of the material is brought about. The condition of plasticity $\sigma_i = \sigma_s$ in the plane of the vector S (S_1S_2) is represented by the circle $|S| = \sqrt{(2/3)}\,\sigma_s$. Consequently, as soon as the loading trajectory crosses this circle, plastic strains occur in the cylinder.

Within the circle of plasticity $\sigma_i = \sigma_s$, (3.16) is replaced by the expression $\sigma_i = E\varepsilon_i$, so that (3.15) becomes $\Im = (3/2E)\,S$. This

relation applies irrespective of whether the loading is simple or combined, i.e. whether the loading trajectory is straight or curved, providing it does not go beyond the limits of the circle $\sigma_i = \sigma_s$. The vector equation $\mathfrak{Z} = (3/2E)\,S$ in this case, according to (3.11) in which the factor $\frac{1}{2}$ in front of σ_{yy} and ε_{xx} must be replaced by ν, is equivalent to two scalar equations which establish a linear relation between the stress and strain components. These equations are an example of the generalized Hooke's law in the case of compound stress.

It can easily be shown from formulae (3.11) that in an interval of time dt the work dW per unit volume of the material of the cylinder

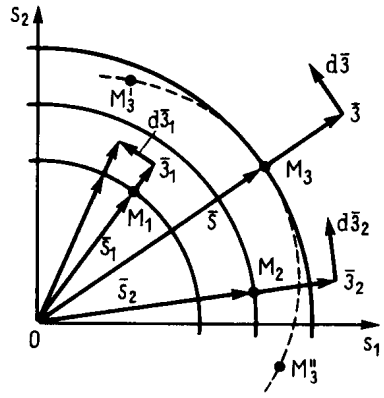

FIG. 105.

done by the internal stresses σ_{xx}, σ_{yy} in the strains $d\varepsilon_{xx}$, $d\varepsilon_{yy}$ is equal to the scalar product $S\,d\mathfrak{Z}$:

$$dW = \sigma_{xx}\,d\varepsilon_{xx} + \sigma_{yy}\,d\varepsilon_{yy} = S\,d\mathfrak{Z}.$$

A process in which a change in the state of the body requires a positive expenditure of energy by the external forces, i.e. one in which $dW > 0$ will, apparently, be a loading process. Otherwise ($dW < 0$) unloading is taking place. Therefore, transfer from loading to unloading occurs at $S\,d\mathfrak{Z} = 0$, i.e. when the vector of increase in $\mathfrak{Z}$ becomes orthogonal to the stress vector S.

Figure 105 shows the circle $|S| = \text{const.} < \sqrt{(2/3)}\,\sigma_S$, the circle of plasticity $|S| = \sqrt{(2/3)}\,\sigma_S$ and the circle $|S| = \text{const.} > \sqrt{(2/3)}\sigma_S$ which can be obtained by three experiments on the same tube: in the first experiment an initially isotropic tube is loaded in such a way as to produce the ray OM_1, and then the circular trajectory

with radius OM_1. Since the deformation will be elastic the strain vector $\mathfrak{Z}$ is directed along the radius and its modulus remains constant. Therefore $S\,d\mathfrak{Z} = 0$. Repeating the experiment with the same tube and taking it up to the circle of plasticity at the point M_2 and then loading it in accordance with this circle, we again find that $S\,d\mathfrak{Z} = 0$, since this circle is the limiting circle on which Hooke's law still applies. After complete removal of the load we still have, therefore, an undeformed isotropic tube. Repeating the experiment once more, we take the tube into the plastic range along the ray OM_3 and then load along the circle of constant radius OM_3. At the point M_3 the vector $\mathfrak{Z}$ is, of course, directed along the radius. Experiment shows that, with the exception of a small region in the neighbourhood of the point M_3, this will be a loading process ($S\,d\mathfrak{Z} > 0$). From considerations of continuity (since the radius OM_3 need exceed the radius OM_2 by only an extremely small amount), and also from the results of a number of experiments, it follows that a small region in the neighbourhood of the point M_3 on the circle of radius OM_3 will be an element of the limiting curve, i.e. $S\,d\mathfrak{Z} = 0$. Some authors, however, consider that the region of the point M_3 on the circle corresponds to a loading process ($S\,d\mathfrak{Z} > 0$) and that an element of the limiting curve is inclined to the tangent at the point M_3, i.e. they consider that the boundary between loading and unloading forms an angle at the point M_3.

The limiting curve which is the dividing line between loading and unloading processes is shown in Fig. 105 as the dotted line $M_3'M_3M_3''$ lying inside the circle of radius OM_3 and tangential to it at the point M_3.

In P–p experiments the axes Ox and Oy are principal axes and the stress σ_{xx}, σ_{yy} are principal stresses ($\sigma_{xy} = 0$), and the principal axes, therefore, do not rotate relative to physical points in the material. It is apparent, however, that it is possible to obtain curved loading trajectories in these experiments; this is the case for combined loading.

Thus, in order that the loading should be simple it is not sufficient for the principal axes to be fixed; as can be seen from expressions (3.11), it is also essential that the ratio of the principal stresses remains constant during variation of the external forces. If only one of these conditions is not satisfied the loading will be combined and will be represented by a curve in the plane of the vector S.

4. *P–M* Experiments and the Basic Principles of Plasticity

In the experiments we apply a tensile force P and a torque M (the pressure $p = O$) to a thin walled cylinder. The axes Ox, Oy in this case are not principal axes of stress and the principal axes do not remain unaltered under combined loading. *P–M* experiments are carried out on special machines (see Chapter VII); the operator fixes the values of the relative extension Δl of the cylinder and the angle of twist φ over the working portion l, and the force P and moment M induced in the specimen are measured by a dynamometer. The advantage of *P–M* experiments with given strains is that the strains Δl and φ can be varied independently over very wide ranges. This is not so in *P–p* experiments, nor is it so for *P–M* experiments if the loading is carried out on the basis of forces, especially if the material of the cylinder strain hardens only slightly. From the conditions of plasticity and the fact that strain hardening is only slight it follows that the modulus of the vector $\boldsymbol{S}$ can only slightly exceed the constant value $\sqrt{(2/3)}\,\sigma_s$, and we are unable, therefore, to obtain a trajectory in the plane of the vector $\boldsymbol{S}$ which differs noticeably from a circle. It would be more appropriate, therefore, to call these experiments not *P–M* experiments, but Δl–φ experiments.

From (3.9), (3.10), (3.5), (3.6) and (3.7), the components of the vectors $\boldsymbol{\Theta}$ and $\boldsymbol{S}$ can be expressed in terms of Δl, φ, P, M by the formulae

$$\left.\begin{aligned}
&\Theta_1 = \sqrt{\left(\frac{3}{2}\right)}\varepsilon_{xx} = \sqrt{\left(\frac{3}{2}\right)}\frac{\Delta l}{l},\\
&\Theta_3 = \sqrt{2}\,\varepsilon_{xy} = \frac{R\varphi}{l\sqrt{2}}, \quad |\boldsymbol{\Theta}| = \sqrt{(\Theta_1^2 + \Theta_3^2)} = \sqrt{\left(\frac{3}{2}\right)}\varepsilon_i,\\
&S_1 = \sqrt{\left(\frac{2}{3}\right)}\sigma_{xx} = \sqrt{\left(\frac{2}{3}\right)}\frac{P}{F},\\
&S_3 = \sqrt{2}\,\sigma_{xy} = \sqrt{2}\,\frac{M}{RF}, \quad |\boldsymbol{S}| = \sqrt{(S_1^2 + S_3^2)} = \sqrt{\left(\frac{2}{3}\right)}\sigma_i.
\end{aligned}\right\} \tag{3.17}$$

The remaining components of $\boldsymbol{\Theta}$ and $\boldsymbol{S}$ are zero.

During the experiment Δl and φ are varied in a definite manner with time and the strain vector $\boldsymbol{\Theta} = \Theta_1 \boldsymbol{i}_1 + \Theta_3 \boldsymbol{i}_3$ describes a strain trajectory in the plane of $\boldsymbol{\Theta}$; an element of arc $d\boldsymbol{\vartheta}$ of this

trajectory, its curvature $\varkappa$ and the unit vectors of the tangent T and normal N are expressed by the formulae

$$\left.\begin{aligned} d\vartheta &= \sqrt{(d\Theta_1^2 + d\Theta_3^2)}, \quad \vartheta = \int_0^t \sqrt{(d\Theta_1^2 + d\Theta_3^2)}, \\ \varkappa^2 &= \left(\frac{d^2\Theta}{d\vartheta^2}\right)^2, \quad T = \frac{d\Theta}{d\vartheta}, \quad N = \frac{1}{\varkappa}\frac{d^2\Theta}{d\vartheta^2}. \end{aligned}\right\} \tag{3.18}$$

We note that the length of arc ϑ and the curvature $\varkappa$ are the only intrinsic independent characteristics of the strain trajectory, and if the curvature $\varkappa(\vartheta)$ is given, all the derivatives of the vector Θ with

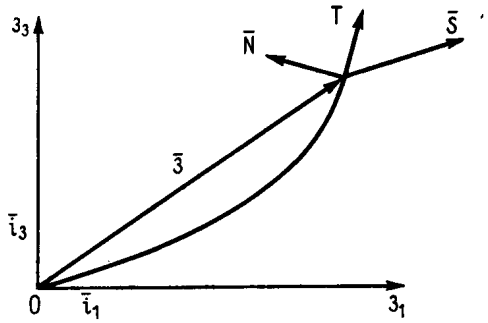

FIG. 106.

respect to ϑ can be expressed in terms of T, N and $\varkappa$ by Frenet's formulae

$$\frac{dT}{d\vartheta} = \frac{1}{\varkappa}N, \quad \frac{dN}{d\vartheta} = -\frac{1}{\varkappa}T. \tag{3.19}$$

Figure 106 shows the strain trajectory $\Theta(t)$, the vectors T and N, and the stress vector S, which is measured during the experiment, is shown at the end of the vector Θ. The work done by the internal forces $dW = S\,d\Theta$ in this case is the work done by the force S as the strain varies along the arc ϑ; consequently the loading condition $S\,d\Theta > 0$ means that the vector S forms an acute angle with T; the unloading condition $S\,d\Theta < 0$ means that S forms an obtuse angle with T, and the limiting state, when $S\,d\Theta = 0$ means that S and T are orthogonal.

Simple loading, as in P–p experiments, corresponds here to a strain trajectory which is any straight line drawn from the origin

of coordinates. Thus simple loading is defined as a process in which the ratio between all the applied external forces (in P–p experiments, the ratio P/p) remains constant with time, or alternatively, one in which the ratio between all the given displacements on the boundary of the body (in P–M experiments the ratio $\varphi/\Delta l$) remains constant with time. As we shall see later, these two definitions amount in effect to the same thing.

A trajectory $\Im_1(t)$ which is obtained by rotating $\Im(t)$ as a solid body about the origin of coordinates is called a rotational transform of the given trajectory $\Im(t)$. If α is the angle of rotation the transformation is given by

$$\left.\begin{aligned} \Im_1' &= \Im_1 \cos\alpha + \Im_3 \sin\alpha, \\ \Im_3' &= -\Im_1 \sin\alpha + \Im_3 \cos\alpha. \end{aligned}\right\} \tag{3.20}$$

A trajectory $\Im_1(t)$ which is the mirror image of $\Im(t)$ in any ray passing through the origin of coordinates is called an image of the given trajectory $\Im(t)$. In the plane of $\Im$ this transformation is given by

$$\left.\begin{aligned} \Im_1' &= \Im_1 \cos\alpha + \Im_3 \sin\alpha, \\ \Im_3' &= \Im_1 \sin\alpha - \Im_3 \cos\alpha. \end{aligned}\right\} \tag{3.21}$$

In (3.20) and (3.21) α is any constant angle (independent of t). We note that the determinant of (3.20) is $+1$ and the determinant of (3.21) is -1. It follows from their definitions that the length of arc ϑ of the strain trajectory and the curvature $\varkappa$ do not vary with either of the above transformations, i.e. they are invariant with respect to these transformations.

We shall go on now to consider the laws of elasticity and plasticity of initially isotropic materials which, within certain limits, have the property of linear elasticity and satisfy the condition of plasticity $\sigma_i = \sigma_s = \text{const.}$, and we shall derive the following more general laws of plasticity.†

The law of isotropy. The relation between the stress vector S and the strain vector $\Im$ is invariant with respect to the transformations of rotation and reflection. Consequently, when $\Im$ is transformed to $\Im_1$ according to formulae (3.20) or (3.21) the vector S is

† A. A. Ilyushin, Prikladnaya matematika i mekhanika, *Applied Mathematics and Mechanics*, 1954, No. 6.

transformed to the vector S_1 by the same formulae, and the unknown relation

$$S = L[\Theta] \tag{3.22}$$

retains its form: $S_1 = L[\Theta_1]$.

Corollary. (1) The relation $S = L[\Theta]$, i.e. the operation L with respect to the vector Θ, must be linear, since only in this case will the angle α not appear in the transformed relation (3.22). (2) The stress vector S can be represented in the natural axes of T and N by the expression

$$S = S_T T + S_N N, \tag{3.23}$$

where the coefficients S_T and S_N are invariant with respect to the transformations of reflection and rotation, i.e. they can be functions only of ϑ and $\varkappa$. (3) Since the vectors T and Θ are different the vector S can be represented in terms of the projections on these vectors:

$$S = S_1 \Theta + S_2 \frac{d\Theta}{d\vartheta}, \tag{3.24}$$

in which S_1 and S_2 can be functions only of ϑ and $\varkappa$. This means that (3.23) and (3.24) are, in effect, one and the same law and can be transformed one into the other. (4) Since the law of isotropy applies equally to P–p experiments, i.e. to the S space, (3.22) can be written in the form

$$\Theta = E_1 S + E_2 \frac{dS}{ds}, \tag{3.25}$$

where E_1 and E_2 are functions of s and ϱ.

The property of the law of plasticity (3.22), which enables us to represent it in the forms (3.23), (3.24) and also in other forms in the Θ space, in the form (3.25) and in other forms in the S space, and in similar forms in other spaces obtained from S and Θ by linear combinations, is known as isomorphism.

We note that a two-termed relation between S and Θ has resulted because we are considering P–p and P–M experiments. In general the Θ space will be five-dimensional and in its general form, therefore, (3.22) will be a five-termed expression for S in terms of the derivatives of the vector Θ.

For simple loading $N = 0$, $T = d\Theta/ds = \Theta/|\Theta|$, $dS/ds = S/|S|$, $|\Theta| = \vartheta$, $|S| = s$, and from the law of isotropy the law of plasticity (3.22) becomes $S/s = \Theta/\vartheta$, or

$$S = \frac{2\sigma_i}{3\varepsilon_i}\Theta, \tag{3.26}$$

where, since $\varkappa = 0$, the ratio of $|\boldsymbol{S}|$ to $|\boldsymbol{\Theta}|$ is a function only of ϑ or of s, or

$$\sigma_i = \Phi(\varepsilon_i), \tag{3.27}$$

where Φ is a universal function for all simple loadings of a given material. It can be seen from (3.26) that if the loading is simple in the $\boldsymbol{S}$ space, it also represents simple loading in the $\boldsymbol{\Theta}$ space.

The law of time lag. During the deformation process the angle between the stress vector $\boldsymbol{S}$ and the tangent vector to the strain trajectory $\boldsymbol{T} = d\boldsymbol{\Theta}/d\vartheta$ depends not on the whole previous geometry

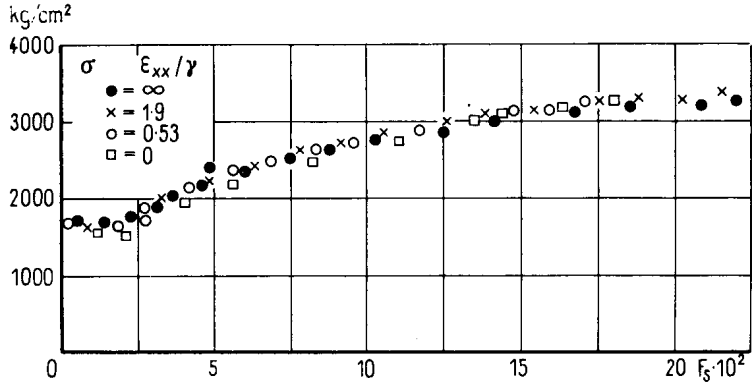

FIG. 107.

of the trajectory ϑ, but only on the preceding portion h, which is called the trace, and if over the length h of the trace the curvature $\varkappa < 1/h$, the stress vector coincides at the end of the trace with the tangent $\boldsymbol{T}$, i.e.

$$\boldsymbol{S} = |\boldsymbol{S}| \frac{d\boldsymbol{\Theta}}{d\vartheta} = \frac{2\sigma_i}{3v_i} \frac{d\boldsymbol{\Theta}}{dt} \quad \left(\varkappa < \frac{1}{h}\right), \tag{3.28}$$

where v_i is the intensity of the rates of deformation

$$v_i = \sqrt{\left(\frac{2}{3}\right)} \frac{d\vartheta}{dt} = \sqrt{\left(\frac{2}{3}\right)} \sqrt{\left[\left(\frac{d\Theta_1}{dt}\right)^2 + \left(\frac{d\Theta_3}{dt}\right)^2\right]}. \tag{3.29}$$

The law of time lag, therefore, defines only the direction of the stress vector $\boldsymbol{S}$ for trajectories of small curvature, but does not define the scalar relation between σ_i and ϑ, $\varkappa$, $d\vartheta/dt$.

Expressions (3.26) and (3.27), which are known as the laws of the theory of small elasto-plastic strains for simple loading, have been verified by numerous P–p and P–M experiments with various initially homogeneous and isotropic metals. As an example, Fig. 107 shows the results of P–M experiments carried out by Schmidt with an annealed steel containing 0·08 per cent C and 0·05 per cent Mn. The dots represent values of σ_i and ε_i for $k = \varepsilon_{xx}/\gamma = \infty$, the crosses for $k = 1{\cdot}9$, the circles for $k = 0{\cdot}53$ and the squares for $k = 0$. It can be seen that all the points lie very close to one common curve which represents graphically the relation $\sigma_i = \Phi(\varepsilon_i)$ for this steel.

During the experiments the specimens were partially and totally unloaded, and loadings were carried out with a constant initial value of k. The unloading was always elastic and the modulus of elasticity on the $\sigma_i = \Phi(\varepsilon_i)$ diagram during unloading was practically constant and equal to $3G$.

Recently some fairly accurate P–M experiments were carried out† in order to check the law of isotropy and the law of time lag by measuring the trace h, and in order to investigate certain properties of the coefficients S_T, S_N, S_1, S_2. Strain trajectories were obtained which differ considerably from the case of simple loading.

In these experiments thin cylindrical specimens of annealed red copper were used (their mean diameter was 20 mm, wall thicknesses 1 mm and 2 mm). The strain trajectories in the plane $(\vartheta_1\vartheta_3)$ were obtained on a machine of the kinematic type (see Chapter VII); they were found to be polygonal or curved, and in each group the trajectories represented mutual images in rays of different inclinations and rotations through various angles. Figure 108 shows the results of tests on two specimens loaded along trajectories which were the image of each other in the bisector of the angle between the coordinate axes. In the first test the specimen was first subjected to a tensile force (0–1); then, starting at the point 1, a torque was applied during which the tensile force necessary to maintain a constant extension decreased until at the point C it became zero, after which pure torsion continued until the point 2. At the point 2 a tensile force was again applied at a constant angle of twist and this was accompanied by a decrease in the torque until the point F,

† V.S. Lenskii, Izv. Akad. Nauk SSSR: Otdel Tekh. Nauk No. 11, 1958.

where the latter became zero. Commencing at the point 3 the specimen was then subjected to torsion at a constant extension. The second test started with torsion. The points S and S' correspond to the limiting elastic strains ($\Theta_{1s} = \varepsilon_s = \sigma_s/E$, $\Theta_{3s} = \gamma_s/\sqrt{3} = \tau_s/G\sqrt{3}$). The lengths of the intervals 01 and 01′, 12 and 12′, 23 and 23′ to the scale of the э plane are the same. By measuring the tensile force and torque during the experiment stress vectors were obtained at a number of points on the trajectory.

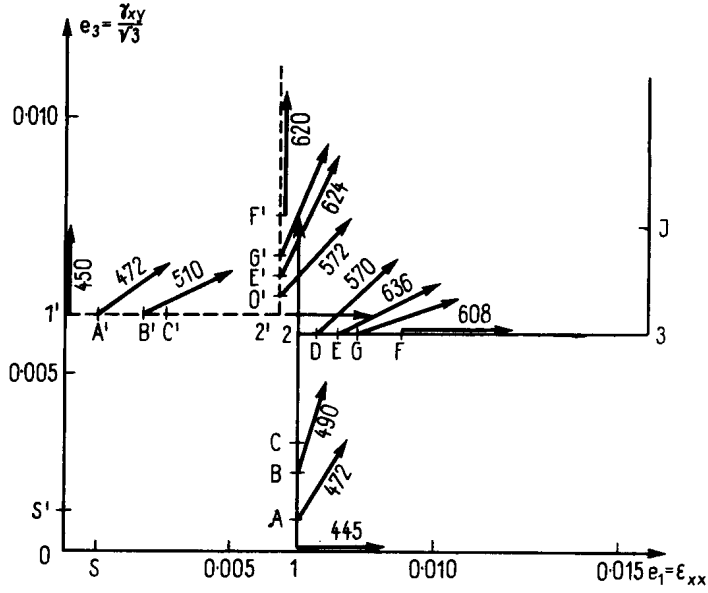

FIG. 108.

It can be seen that the stress vectors at corresponding points on the trajectories (A and A', B and B', C and C', 2 and 2′, D and D' etc.) have the same modulus and are identically inclined to the corresponding trajectories, which confirms the law of isotropy. Similar results were obtained for other types of trajectory. The coincidence of the directions of the stress vectors with the directions of the corresponding strain trajectories starting from the points C, C', D, D', 1 confirms the law of time lag. The magnitudes of the intervals $1C$, $1'C'$, $2F$, $2'F'$, $3J$ are approximately the same and equal to 3–$4\varepsilon_s$.

In order to check the corollaries of the law of time lag (in the case of a trajectory of small curvature the direction of the stress vector coincides with the direction of the tangent at the corresponding point on the strain trajectory) a number of experiments were carried out in which the strain trajectory was a semicircle of radius $R \approx 3h \approx 10\varepsilon_s$. The results of one experiment are shown in Fig. 109. It can be seen that almost everywhere the stress vectors lie in the direction of the tangents to the trajectory or are inclined only

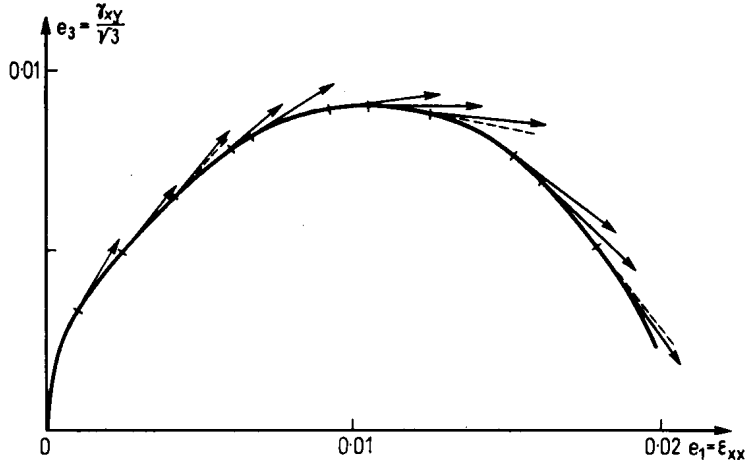

FIG. 109.

very slightly to these directions. Thus for trajectories, the radius of curvature of which is not less than $10\varepsilon_s$, in the case of copper, the law of plasticity in the form (3.28) is applicable.

5. THE GENERALIZATION OF HOOKE'S LAW AND THE LAWS OF SMALL ELASTO-PLASTIC STRAINS

In § 4 we established the following basic law of the relation between the stress vector S and the strain vector $\mathfrak{Z}$ for elastic strains in initially isotropic bodies and for simple loading beyond the elastic limit:

$$S = \frac{2\sigma_i}{3\varepsilon_i}\mathfrak{Z}.$$

Since the vectors S and Θ can be expressed in terms of the components of the stress deviator σ'_{mn} (3.6) and the strain deviator ε'_{mn} (3.5) by the linear relations (3.7), it follows that the components of σ'_{mn} and ε'_{mn} are interrelated by the same expressions as S and Θ, that is

$$\sigma'_{mn} = \frac{2\sigma_i}{3\varepsilon_i}\varepsilon'_{mn} \quad (m, n = x, y, z).$$

Considering again the total stresses σ_{mn} and strains ε_{mn}, we get that

$$\left.\begin{aligned} \sigma_{mn} - \sigma &= \frac{2\sigma_i}{3\varepsilon_i}(\varepsilon_{mn} - \varepsilon), \\ \sigma_{mn} &= \frac{2\sigma_i}{3\varepsilon_i}\varepsilon_{mn} \quad (m \neq 0) \\ (m, n &= x, y, z), \end{aligned}\right\} \tag{3.30}$$

and, if we consider that in (3.30)

$$\sigma = \tfrac{1}{3}(\sigma_{xx} + \sigma_{yy} + \sigma_{zz}),$$
$$\varepsilon = \tfrac{1}{3}(\varepsilon_{xx} + \varepsilon_{yy} + \varepsilon_{zz}),$$

identically, then the sum of the first three expressions of (3.30) gives the identity $0 \equiv 0$. If we also consider that in (3.30)

$$\sigma_i = \frac{1}{\sqrt{2}}\sqrt{[(\sigma_{xx} - \sigma_{yy})^2 + (\sigma_{yy} - \sigma_{zz})^2 + (\sigma_{zz} - \sigma_{xx})^2 + 6(\sigma_{yz}^2 + \sigma_{zx}^2 + \sigma_{xy}^2)]},$$

$$\varepsilon_i = \frac{\sqrt{2}}{3}[(\varepsilon_{xx} - \varepsilon_{yy})^2 + (\varepsilon_{yy} - \varepsilon_{zz})^2 + (\varepsilon_{zz} - \varepsilon_{xx})^2 + 6(\varepsilon_{yz}^2 + \varepsilon_{zx}^2 + \varepsilon_{xy}^2)],$$

identically, then (3.30) gives a further identity: $\sigma_i = \sigma_i$ (in order to show this it is sufficient to write down the expression under the root in the equation for σ_i in terms of the left-hand sides of (3.30)). Consequently (3.30) contains only four independent relations.

However, the law of volumetric elasticity (3.3) and the invariant law (3.27) give a further two relations

$$\sigma = 3K\varepsilon, \tag{3.31}$$
$$\sigma_i = \Phi(\varepsilon_i). \tag{3.32}$$

If σ and σ_i in the expressions (3.30) are replaced by their values given by (3.31) and (3.32), then (3.30) can be considered as six independent one-to-one relations between the six components of stress and the six components of strain. Their uniqueness follows from the uniqueness of the function $\sigma_i = \Phi(\varepsilon_i)$.

The relation $\sigma_i = \Phi(\varepsilon_i)$ can easily be found if the relation between octahedral stresses and strains $\tau_v = G(\gamma_v)$ is known from the results of experiments on thin walled cylinders in torsion. For, from formulae (1.18) and (1.32), §§ 5 and 6 of Chapter I, we have that

$$\sigma_i = \frac{3}{\sqrt{2}}\tau_v, \quad \varepsilon_i = \frac{\gamma_v^s}{\sqrt{2}},$$

and therefore

$$\sigma_i = \frac{3}{\sqrt{2}} G(\varepsilon_i \sqrt{2}) = \Phi(\varepsilon_i),$$

i.e. the function $\Phi(\varepsilon_i)$ can be found from $G(\gamma_v)$ by altering the scale of the abscissae and ordinates. In particular, within the elastic range $G(\gamma_v) = G\gamma_v$, and therefore

$$\sigma_i = 3G\varepsilon_i. \tag{3.33}$$

If we substitute the values of σ from (3.31) and of σ_i from (3.33) in the expressions (3.30), we obtain the generalized Hooke's law for elastic strains:

$$\left.\begin{aligned} \sigma_{mm} &= \left(K - \frac{2}{3}G\right)\theta + 2G\varepsilon_{mm}, \\ \sigma_{mn} &= 2G\varepsilon_{mn} \qquad (m \neq n), \end{aligned}\right\} \tag{3.34}$$

in which $K - 2/3G \equiv \lambda$ and $G \equiv \mu$ are known as the Lamé parameters. If we solve (3.30) for strains, we obtain Hooke's law in its general form—a form widely used in the strength of materials:

$$\left.\begin{aligned} \varepsilon_{xx} &= \frac{1}{E}[\sigma_{xx} - \nu(\sigma_{yy} + \sigma_{zz})], \quad \varepsilon_{yz} = \frac{1}{2G}\sigma_{yz}, \\ \varepsilon_{yy} &= \frac{1}{E}[\sigma_{yy} - \nu(\sigma_{zz} + \sigma_{xx})], \quad \varepsilon_{zx} = \frac{1}{2G}\sigma_{zx}, \\ \varepsilon_{zz} &= \frac{1}{E}[\sigma_{zz} - \nu(\sigma_{xx} + \sigma_{yy})], \quad \varepsilon_{xy} = \frac{1}{2G}\sigma_{xy}, \end{aligned}\right\} \tag{3.35}$$

in which E and ν can be taken as quantities related to K and G by the expressions

$$G = \frac{E}{2(1+\nu)}, \quad K = \frac{E}{3(1-2\nu)}. \tag{3.36}$$

It is quite obvious that E is Young's modulus, and ν is Poisson's ratio. In the case of a cylindrical specimen under the action of a tensile force along its axis Ox ($\sigma_{yy} = \sigma_{zz} = \sigma_{yz} = \sigma_{zx} = \sigma_{xy} = 0$)

we find from (3.35) that $E = \sigma_{xx}/\varepsilon_{xx}$, $\nu = -\varepsilon_{yy}/\varepsilon_{xx}$, which is in accordance with the definitions of E and ν given in § 1, Chapter II. The constant G is called the modulus of rigidity, and for metals is approximately $\frac{3}{8}E$.

The laws of elasto-plastic strains for the case of simple loading are given by (3.30), (3.31) and (3.32), or simply by (3.30), if for σ_i we put $\Phi(\varepsilon_i)$ and for σ, $3K\varepsilon$.

The graph of the relation $\sigma_i = \Phi(\varepsilon_i)$ is of the same form as that for $\sigma_1 = \Phi_1(\varepsilon_1)$ for a cylindrical specimen in simple tension, although there is a slight difference between the two. As in the case

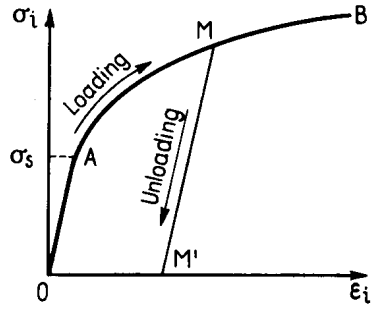

FIG. 110.

of simple tension, there is a linear part OA (Fig. 110), which corresponds to elastic strains and a curved part AB, which corresponds to elasto-plastic strains. The point A corresponds to the value of $\sigma_i = \sigma_s$—the yield point in tension.

A monotonic variation of the parameter λ_t,† which defines the variation of the external loads during the experiment, corresponds to a monotonic increase in the intensity of strain ε_i (and the intensity of stress σ_i).

A process in which an increase in the parameter λ_t corresponds to an increase in the intensity of strain, i.e. $d\varepsilon_i/d\lambda_t > 0$, is called a process of active deformation, in contrast to a process of passive deformation for which $d\varepsilon_i/d\lambda_t < 0$, which corresponds to a decrease in the external forces, i.e. to unloading. In a process of passive deformation commencing at some point M on the $\sigma_i \sim \varepsilon_i$

† λ_t is any monotonically increasing function of time.

diagram the relation $\sigma_i = \Phi(\varepsilon_i)$ will be represented by the straight line MM' parallel to the elastic part OA.

The laws (3.30)–(3.32) were derived from the results of experiments of initially isotropic (on the average) materials and do not apply for initially anisotropic materials. In a process of plastic deformation, however, the material becomes anisotropic, which is illustrated, for example, by Bauschinger's effect (see § 1, Chapter II). The question then arises, do the laws of the theory of small elasto–plastic strains apply if this anisotropy occurs? The answer is that the relations on which the laws were based were derived from experiments in which this anisotropy did occur. They do therefore take into account the anisotropy which exists during plastic deformation of a specimen in simple tension.

Certain materials possess the property of structural instability: during plastic deformation changes of phase are observed. For such materials the laws (3.30)–(3.32) require certain modifications which, however, we shall not consider here.

We may ask: is it necessary each time, for each new material, to carry out experiments on specimens in a state of compound stress under conditions of simple loading, in order to determine the relation $\sigma_i = \Phi(\varepsilon_i)$? Is it not possible to make use of the results of more straightforward experiments, for example, experiments on a cylindrical specimen in tension or a thin-walled cylinder in pure torsion?

The answer is that we can.

If, for instance, we make a torsion test on a cylinder, then

$$\sigma_{xx} = \sigma_{yy} = \sigma_{zz} = \sigma_{yz} = \sigma_{zx} = 0; \quad \sigma_{xy} \equiv \tau = \frac{M}{RF};$$

$$\varepsilon_{xx} = \varepsilon_{yy} = \varepsilon_{zz} = \varepsilon_{yz} = \varepsilon_{zx} = 0, \quad 2\varepsilon_{xy} \equiv \gamma = \frac{\varphi R}{l}$$

(the axes are chosen as in Fig. 102). Thus, from (1.18) and (1.32) $\sigma = \tau\sqrt{3}$, $\varepsilon_i = (\gamma/\sqrt{3})$. This test enables us to find the relation $\tau = G_1(\gamma)$. Consequently we can find the required relation $\sigma_i = \Phi(\varepsilon_i)$ by altering the scales:

$$\sigma_i = \sqrt{3}\, G_1(\varepsilon_i \sqrt{3}) = \Phi(\varepsilon_i).$$

It can be seen that the $\sigma_i \sim \varepsilon_i$ curve can be derived from the $\tau \sim \gamma$ curve by increasing the ordinates by $\sqrt{3}$ times and decreasing the abscissae in the same ratio.

We can, however, make use of an even simpler experiment. If we carry out a tensile test on a specimen (the axis of which we shall take as the axis of x), we find the relation

$$\sigma_1 = \Phi_1(\varepsilon), \quad \varepsilon_1 = \psi(\sigma_1) \equiv \Phi_1^{-1}(\sigma_1),$$

in which

$$\sigma_{xx} = \sigma_1, \quad \sigma_{yy} = \sigma_{zz} = \sigma_{yz} = \sigma_{zx} = \sigma_{xy} = 0;$$

$$\varepsilon_{xx} = \varepsilon_1, \quad \varepsilon_{yy} = \varepsilon_{zz} = -\nu\varepsilon_1, \quad \varepsilon_{yz} = \varepsilon_{zx} = \varepsilon_{xy} = 0,$$

so that

$$\sigma_i = \sigma_1, \quad \sigma = \frac{1}{3}\sigma_1;$$

$$\varepsilon_i = \frac{2(1+\nu)}{3}\varepsilon_1, \quad \varepsilon = \frac{1}{3}(1-2\nu)\varepsilon_1.$$

Poisson's ratio ν is constant in the elastic range and is variable during the plastic range. In order to find the relation between ν and the magnitude of the strain ε_1, we make use of the law of elastic change in volume $\sigma = 3K\varepsilon$, or

$$\sigma_1 = 3K(1-2\nu)\varepsilon_1.$$

Taking into account that $\sigma_1 = \Phi_1(\varepsilon_1)$, we obtain the theoretical value for Poisson's ratio

$$\nu = \frac{1}{2} - \frac{\Phi_1(\varepsilon_1)}{6K\varepsilon_1}. \tag{3.37}$$

Taking into consideration that $\sigma_1 = \sigma_i$ and taking the value of ν given by (3.37), we can now write down the three relations

$$\left.\begin{aligned} &\varepsilon_1 = \psi(\sigma_i), \\ &\sigma_i = 3K(1-2\nu)\varepsilon_1 = 3K(1-2\nu)\psi(\sigma_i), \\ &\varepsilon_i = \tfrac{2}{3}(1+\nu)\varepsilon_1 = \tfrac{2}{3}(1+\nu)\psi(\sigma_i). \end{aligned}\right\} \tag{3.38}$$

Eliminating ν from the last two expressions, we find that

$$\varepsilon_i = \psi(\sigma_i) - \frac{\sigma_i}{9K}, \quad \sigma_i = \Phi_1\left(\varepsilon_i + \frac{\sigma_i}{9K}\right). \tag{3.39}$$

Thus the required function $\sigma_i = \Phi(\varepsilon_i)$ has been found in a form solved for $\varepsilon_i = \Phi^{-1}(\sigma_i)$, i.e. we have found the inverse function

$$\varepsilon_i = \Phi_1^{-1}(\sigma_i) - \frac{\sigma_i}{9K}.$$

It is more convenient for purposes of calculation to write the relation $\sigma_i = \Phi(\varepsilon_i)$ in the form

$$\sigma_i = 3G\varepsilon_i[1 - \omega(\varepsilon_i)],$$

in which

$$\omega(\varepsilon_i) = 0 \quad \text{for} \quad \varepsilon_i \leqq \varepsilon_S. \tag{3.40}$$

6. The Conditions of Plasticity

Let us return now to the condition which determines the point of transition of a body into a plastic condition in a state of compound stress. As has already been pointed out, the material of a cylinder enters the plastic range when $\sigma_i = \sigma_s$, where σ_s is the yield point in tension. The expression

$$\sigma_i = \sigma_S = \text{const.} \tag{3.41}$$

is known as the Hencky–Mises condition of plasticity. According to this a material in a state of compound stress behaves elastically if the intensity of stress does not exceed the elastic limit in simple tension. This condition can be written in the expanded form:

$$\frac{1}{\sqrt{2}}\sqrt{[(\sigma_1 - \sigma_2)^2 + (\sigma_2 - \sigma_3)^2 + (\sigma_3 - \sigma_1)^2]} = \sigma_S \tag{3.41'}$$

or

$$\left[\frac{3}{2}\sum_{m,n=x,y,z}(\sigma_{mn} - \delta_{mn}\sigma)^2\right]^{1/2} = \sigma_S, \tag{3.41''}$$

where δ_{mn} is the Kronecker delta, or, finally, in the form

$$\sqrt{2}\sqrt{(\tau_{12}^2 + \tau_{23}^2 + \tau_{31}^2)} = \sigma_S. \tag{3.41'''}$$

In the case of a state of plane stress it is convenient to represent this condition graphically. If, for example, $\sigma_3 = 0$, the condition of plasticity (3.41′) becomes

$$(\sigma_1 - \sigma_2)^2 + \sigma_2^2 + \sigma_1^2 = 2\sigma_S^2$$

or

$$\sigma_1^2 + \sigma_2^2 - \sigma_1\sigma_2 = \sigma_S^2. \tag{3.42}$$

Expression (3.42) is the equation of an ellipse in the plane of the principal stresses ($\sigma_1\sigma_2$), sometimes called the Hencky–Mises ellipse (Fig. 111). The principal axes of this ellipse are inclined at an angle of 45° to the principal axes of plane stress, and the points of intersection of this ellipse with the axes σ_1 and σ_2 are at a distance of σ_s—the yield point in tension—from the origin of coordinates.

The Hencky–Mises condition of plasticity states that if a point in the $(\sigma_1\sigma_2)$ plane, which represents some state of plane stress, lies within the ellipse, then the material is in an elastic state.

It should be noted that the condition of plasticity (3.41) applies both for simple, and for combined loading. This is due to the fact that the relations between stresses and strains in the elastic range are of the same form, independently of whether the loading is combined or simple. At the elastic limit, in the case of combined loading, the principal axes of stress change their orientation and the ratio of the principal deviator stresses becomes variable, but

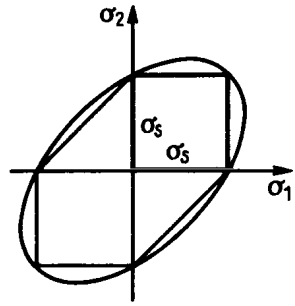

FIG. 111.

the principal axes of strain also change their orientation, following the principal axes of stress. The ratio of the principal deviator strains also varies but remains equal to the ratio of the principal deviator stresses, so that the stress and strain vectors remain colinear in the elastic range in the case of combined loading. Experiments recently carried out by Merino and Kotalik (U.S.A.) and also at the Central Scientific Research Institute of Industrial Structures (TsNIIPS) on biaxial compression and tension of plates has shown that in a process of combined loading the $\sigma_i \sim \varepsilon_i$ curves coincide with the $\sigma_i \sim \varepsilon_i$ curve for simple loading in the elastic range, and differ only slightly from this curve in the plastic range. It should, however, be noted that the loading in these experiments differed only slightly from simple loading.

In the theory of plasticity there is another condition of plasticity suggested first by Coulomb and again in the last century by St. Venant. According to this condition the material enters a plastic

state when the greatest shearing stress reaches some constant magnitude

$$\tau_{max} = \tau_S. \tag{3.43}$$

The maximum shear stress will be one of the principal shearing stresses $\tau_{12} = (\sigma_1 - \sigma_2)/2$, $\tau_{23} = (\sigma_2 - \sigma_3)/2$ or $\tau_{31} = (\sigma_3 - \sigma_1)/2$. In a state of plane stress when $\sigma_3 = 0$, τ_{max} is $(\sigma_1 - \sigma_2)/2$, $\sigma_1/2$ or $\sigma_2/2$. If σ_1, and σ_2 are of the same sign the maximum will be $\sigma_1/2$ or $\sigma_2/2$. This corresponds to uniaxial tension or compression in one or other direction. Therefore, in the first or third quadrants in the $(\sigma_1\sigma_2)$ plane condition (3.43) is represented by the straight lines $\sigma_1 = \pm\sigma_S$, $\sigma_2 = \pm\sigma_S$. In the second and fourth quadrants the maximum shearing stress will be $(\sigma_1 - \sigma_2)/2$, and here condition (3.43) is represented by straight lines parallel to the bisector of the angle between the σ_1 and σ_2 axes.

Thus, in a state of plane stress condition (3.43) can be represented by a hexagon, inscribed in the Hencky–Mises ellipse (Fig. 111), and the constant τ_S in (3.43) is

$$\tau_S = \tfrac{1}{2}\sigma_S, \tag{3.44}$$

where σ_S is the yield point in uniaxial tension.

The condition of plasticity (3.43) must apply also for pure shear. Therefore τ_S must be the yield point in shear (which is the condition suggested by Coulomb). According to (3.44), therefore, the yield point in shear must be equal to half the yield point in uniaxial tension. Experiment shows that normally $\tau_S = (0{\cdot}57 \sim 0{\cdot}60)\,\sigma_S$, which agrees more with the Hencky–Mises condition (3.41), since it follows from the latter that

$$\tau_S = \frac{\sigma_S}{\sqrt{3}}. \tag{3.45}$$

In general, as can be seen from Fig. 111, the Hencky–Mises and Coulomb–St. Venant conditions of plasticity differ only slightly. An estimate of the difference between the two can easily be made. In § 5 of Chapter I it was shown that the expression

$$\tau_v = 0{\cdot}933\,\frac{2\sqrt{2}}{3}\,|\tau_{max}|,$$

i.e.

$$\sigma_i = 0{\cdot}933 \times 2\,|\tau_{max}|,$$

is accurate to within 6·7 per cent. The expression $\sigma_s = 2\tau_s$ is also accurate to within this amount. The conditions of plasticity (3.41)

and (3.43) are sometimes called criteria of strength, and we talk of the Coulomb–St. Venant and Hencky–Mises theories of strength which refer to cases when plastic strains do not occur. If however we are interested in the conditions under which failure occurs, we will not be able to find them from expressions (3.41) and (3.43).

The question of finding the combination of stresses for which failure of the material occurs is considerably more complex than in the case of uniaxial tension. It should also be pointed out that although the diagrams of $\sigma_1 \sim \varepsilon_1$, for simple tension, and $\sigma_i \sim \varepsilon_i$ for compound stress practically coincide, the existence on the $\sigma_1 \sim \varepsilon_1$ diagram of a definite point corresponding to the instant of failure must not be assumed to indicate the existence of a similar point on the $\sigma_i \sim \varepsilon_i$ diagram. Indeed, failure can occur for a combination of stresses corresponding to any point on the $\sigma_i \sim \varepsilon_i$ curve. For example, let us suppose that a body is subjected to a uniform all-round tension, so that $\sigma_1 = \sigma_2 = \sigma_3 = \sigma$, and, consequently, $\sigma_i = 0$. At some value of σ failure occurs, but σ_i will still be zero. In this case, therefore, the point of failure coincides with the origin on the $\sigma_i \sim \varepsilon_i$ curve. For simple tension the point of failure on the $\sigma_i \sim \varepsilon_i$ curve will be the point corresponding to the value of $\sigma_i = \sigma_B$. Some years ago G. V. Uzhik, whilst carrying out some experiments on notched specimens, found that steel had a resistance to failure which corresponded to conditions of non-uniform all-round tension. Failure occurred at a maximum normal stress of the order of 30,000 kg/cm^2, which considerably exceeds the yield point and U.T.S. He found that on the $\sigma_i \sim \varepsilon_i$ diagram the instant of failure corresponded to a point very close to a value of $\sigma_i = \sigma_S$ (for steel).

The question of the criteria of failure has still to be answered, but so far a number of "points of failure" have been found, i.e. combinations of stresses at which the material fails.

If we examine the surface of failure of specimens which have been tested to destruction by various methods, we see in some specimens that the surface of failure is uneven and lustreless and that small randomly orientated crystal grains are visible, whereas in others the surface of failure is smoother with evidence of the sliding of grains over one another in definite directions and evidence of plastic deformation prior to failure. In the first case we talk of a brittle failure and the causes of failure are attributed to the normal stresses reaching certain critical values. In the second case we talk of a ductile failure of the shear type and its causes are attributed to

the shear stresses reaching certain limiting values. Thus both normal and shear stresses can cause failure, and any material can fail after the occurrence of considerable plastic strains.

In conclusion let us consider two further questions.

The laws of plasticity (3.30), (3.31), (3.32) were established on the basis of experiments in which the conditions of uniform stress and simple loading applied. But many structural elements are subjected to conditions of non-uniform stress. Is it possible then, for the conditions of simple loading to apply at all points in such a body? The answer to this question is provided by the theorem of simple loading,† which shows that the loading at every point in a body will be simple if all the external forces applied to the body increase with time in proportion to one and the same general function of time or to a parameter.

Finally, it is important to know the distribution of stress and strain in a body subjected to a non-uniform stress, when a monotonic increase of all the loads is replaced by a decrease, when unloading takes place. It is essential to know also the residual stresses and strains which remain in the body after removal of all external loads. During unloading stresses of opposite sign might occur, and these stresses could be so great that so-called secondary plastic strains occur. If we exclude these cases, then in order to calculate the stresses and strains during unloading, the unloading theorem † gives a simple and universal method, which was illustrated in the sections on frameworks and torsion of a circular rod. We calculate the difference between the greatest values attained by the external forces up to the instant the unloading commenced, and the values of these forces at the instant under consideration during the unloading process. We then calculate the stresses and strains which would have occurred if the body had behaved ideally elastically at loads equal to these differences. If we now subtract the elastic stresses and strains, calculated for the differences in the forces, from the stresses and strains calculated according to the laws of the theory of plasticity for values of the loads immediately prior to the start of the unloading, then this will give the values of the residual stresses and strains at the instant considered during the unloading process. In particular, the residual stresses and strains after complete removal of the external forces can be found as the difference between the

† See A. A. Iliushin, *Plasticity*, Gostekhizdat, 1948, sections 14, 15.

stresses and strains immediately before unloading, and the stresses and strains which would have occurred at the same (greatest) values of the forces, if the body had behaved ideally elastically.

7. Deformation of a Pipe under Internal and External Pressure (Lamé's Problem)

The problem of the stresses and strains in a thick-walled cylinder under the action of uniformly distributed internal and external pressures arose first of all in connection with the design of artillery

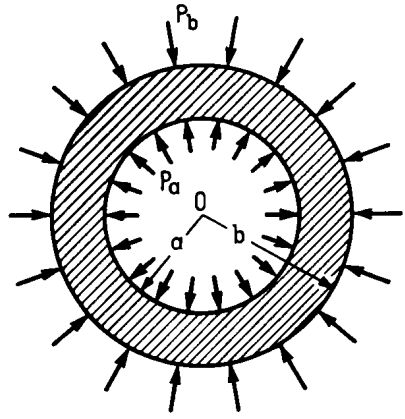

Fig. 112.

gun barrels. Problems of the same type are encountered also in other fields of engineering (high pressure pipework, compressor, cylinders, the extrusion of tubes, etc.).

Let us suppose that an infinitely long circular pipe (or a pipe supported at its ends on absolutely rigid plates) of internal radius a and external radius b is under the action of a uniformly distributed internal pressure p_a and an external pressure p_b (Fig. 112). It follows from symmetry that every point in the pipe will be displaced in a radial direction. We shall denote this displacement by u. Since points in the pipe cannot move in the direction of the axis of the pipe, which we shall take as the direction of the z-axis, and since the external load is uniformly distributed, the strains at all sections of the pipe perpendicular to the z-axis are the same. This

deformed state, which is independent of z and in which displacements occur in planes perpendicular to the z-axis, is known as a state of plane deformation.

We shall introduce a system of cylindrical coordinates r, ϑ, z. Figure 113 shows an element of the pipe $ABCD$ of unit length in the z-direction, formed by two radial sections and two cylindrical surfaces of radius r and $r + dr$. From the symmetry of the loading and of the shape of the pipe it follows that the magnitude of the radial displacement u depends only on r, and is independent of ϑ and z. Therefore, the points A and B are both displaced by an amount

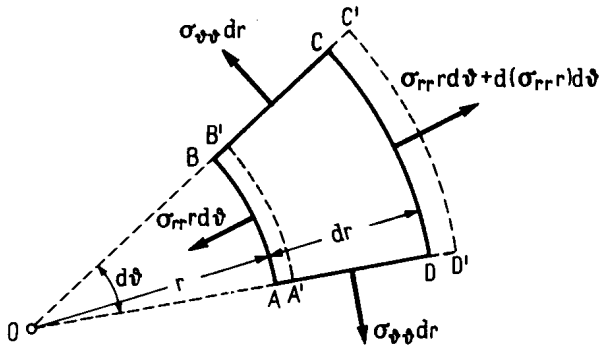

FIG. 113.

$u(r)$ after deformation, and the points C and D are both displaced by an amount $u + du/dr \,.\, dr$. Thus the relative extension ε_{rr} of a radial fibre is du/dr.

The length of the fibre AB before deformation is $r\,d\vartheta$ and after deformation $A'B' = (r + u)\,d\vartheta$. Therefore, the relative extension of a fibre in a circumferential direction is $\varepsilon_{\vartheta\vartheta} = u/r$.

No change takes place in the right-angle between BA and AD. Therefore, $\varepsilon_{r\vartheta} = 0$. Longitudinal fibres (parallel to the z-axis) do not extend, and they remain perpendicular to fibres in the $(r\vartheta)$ plane, so that

$$\varepsilon_{zz} = \varepsilon_{rz} = \varepsilon_{z\vartheta} = 0.$$

Let us consider first of all the case when no plastic strains occur in the pipe under the action of the pressures p_a and p_b. The generalized Hooke's law has already been given in Cartesian coordinates. But since we are considering the state of stress and strain at a

point, this law is of the same form in any curvilinear orthogonal system of coordinates. From the last three equations of (3.35) it follows that

$$\sigma_{r\vartheta} = \sigma_{\vartheta z} = \sigma_{zr} = 0,$$

i.e. at every point in the pipe, radial, circumferential and longitudinal directions are principal directions of stress and strain. The first three equations of (3.35) can be written in the form

$$\left.\begin{aligned} \frac{du}{dr} &= \frac{1}{E}[\sigma_{rr} - \nu(\sigma_{\vartheta\vartheta} + \sigma_{zz})], \\ \frac{u}{r} &= \frac{1}{E}[\sigma_{\vartheta\vartheta} - \nu(\sigma_{zz} + \sigma_{rr})], \\ 0 &= \frac{1}{E}[\sigma_{zz} - \nu(\sigma_{rr} + \sigma_{\vartheta\vartheta})]. \end{aligned}\right\} \tag{3.46}$$

It can be seen from these equations that $\sigma_{zz} \neq 0$ although $\varepsilon_{zz} = 0$. The stress σ_{zz} arises due to the fact that particles cannot be displaced in the direction of the axis of the pipe. Its value can be found if we know σ_{rr} and $\sigma_{\vartheta\vartheta}$:

$$\sigma_{zz} = \nu(\sigma_{rr} + \sigma_{\vartheta\vartheta}). \tag{3.47}$$

Considering the projection of all forces acting on the element $ABCD$ (see Fig. 113) in a direction perpendicular to the bisector of the angle BOA, we see that the stresses on the faces BC and AD are the same—which follows from considerations of symmetry. Projecting all the forces in the direction of the bisector of the angle BOA, we get that

$$\frac{d}{dr}(r\sigma_{rr})\, dr\, d\vartheta - 2\sigma_{\vartheta\vartheta}\, dr \sin\frac{d\vartheta}{2} = 0.$$

Since the angle $d\vartheta$ is small, we can put $\sin d\vartheta/2 = d\vartheta/2$. Then, dividing by $dr\, d\vartheta$, we obtain the differential equation of equilibrium

$$r\frac{d\sigma_{rr}}{dr} + \sigma_{rr} - \sigma_{\vartheta\vartheta} = 0. \tag{3.48}$$

The stresses σ_{rr} and $\sigma_{\vartheta\vartheta}$ are connected by a further relation. From the second equation of (3.46) we can find du/dr, which must be equal to the value of du/dr found from the first equation of (3.46). Therefore,

$$\sigma_{rr} - \nu(\sigma_{\vartheta\vartheta} + \sigma_{zz}) = r\frac{d}{dr}[\sigma_{\vartheta\vartheta} - \nu(\sigma_{rr} + \sigma_{zz})] + [\sigma_{\vartheta\vartheta} - \nu(\sigma_{rr} + \sigma_{zz})]$$

or,

$$r\frac{d}{dr}[\sigma_{\vartheta\vartheta} - \nu(\sigma_{rr} + \sigma_{zz})] + (1 + \nu)(\sigma_{\vartheta\vartheta} - \sigma_{rr}) = 0.$$

If we consider also expression (3.47) and divide by $(1 + \nu)$, we get that

$$r\frac{d}{dr}[(1 - \nu)\sigma_{\vartheta\vartheta} - \nu\sigma_{rr}] + \sigma_{\vartheta\vartheta} - \sigma_{rr} = 0. \tag{3.49}$$

Equations of the same type, which result, not from the equilibrium conditions, but from the relations between the strains, are called the equations of compatibility. Adding eqns. (3.48) and (3.49) we get that:

$$(1 - \nu)\, r\frac{d}{dr}(\sigma_{rr} + \sigma_{\vartheta\vartheta}) = 0.$$

Since $\nu \neq 1$ and $r \neq 0$, it follows that

$$\sigma_{rr} + \sigma_{\vartheta\vartheta} = \text{const.} = 2A.$$

As a result eqn. (3.48) reduces to the form

$$r\frac{d\sigma_{rr}}{dr} + 2\sigma_{rr} = 2A$$

or

$$\frac{d}{dr}(r^2\sigma_{rr}) = 2Ar.$$

Integrating, we find that:

$$\sigma_{rr} = A + \frac{B}{r^2}. \tag{3.50}$$

In order to find the constants A and B we make use of the boundary conditions corresponding to the particular problem:

$$\sigma_{rr} = -p_a \quad \text{for} \quad r = a,$$
$$\sigma_{rr} = -p_b \quad \text{for} \quad r = b.$$

These conditions reduce to two equations in A and B, from which we find that:

$$A = \frac{a^2p_a - b^2p_b}{b^2 - a^2}, \quad B = \frac{a^2b^2}{b^2 - a^2}(p_b - p_a).$$

Consequently,

$$\left.\begin{aligned}\sigma_{rr} &= \frac{a^2p_a - b^2p_b}{b^2 - a^2} + \frac{a^2(p_b - p_a)}{b^2 - a^2}\,\frac{b^2}{r^2},\\ \sigma_{\vartheta\vartheta} &= \frac{a^2p_a - b^2p_b}{b^2 - a^2} - \frac{a^2(p_b - p_a)}{b^2 - a^2}\,\frac{b^2}{r^2},\\ \sigma_{zz} &= 2\nu\,\frac{a^2p_a - b^2p_b}{b^2 - a^2}.\end{aligned}\right\} \tag{3.51}$$

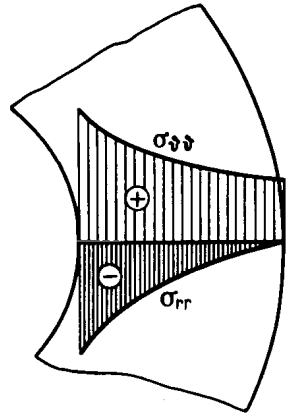

FIG. 114.

The expression for $\sigma_{\vartheta\vartheta}$ is obtained from the relation $\sigma_{rr} + \sigma_{\vartheta\vartheta} = 2A$, and the expression for σ_{zz} is found from (3.47). In the particular case when there is no external pressure ($p_b = 0$), we have that:

$$\left.\begin{aligned}\sigma_{rr} &= \frac{a^2p_a}{b^2 - a^2}\left(1 - \frac{b^2}{r^2}\right),\\ \sigma_{\vartheta\vartheta} &= \frac{a^2p_a}{b^2 - a^2}\left(1 + \frac{b^2}{r^2}\right),\\ \sigma_{zz} &= \frac{2\nu a^2p_a}{b^2 - a^2}.\end{aligned}\right\} \tag{3.52}$$

We see that $\sigma_{rr} < 0$ over the whole thickness of the wall of the pipe, i.e. this stress is compressive, and that $\sigma_{\vartheta\vartheta} > 0$, i.e. tensile. Graphs of the distribution of σ_{rr} and $\sigma_{\vartheta\vartheta}$ along a radius are shown for this case in Fig. 114.

Let us suppose now that the thickness of the wall of the pipe $\delta = b - a$ is small compared with the internal radius a. Then

$$b^2 - a^2 \equiv (b - a)(b + a) \approx 2a\delta, \quad r^2 + a^2 \approx 2a^2,$$

and from formulae (3.52) we get that

$$\sigma_{\vartheta\vartheta} = \frac{ap_a}{\delta}. \tag{3.53}$$

This is the well known Mariott formula for thin-walled cylindrical containers. The value of σ_{rr} varies from $-p_a$ at $r = a$ to zero a $r = b$. Consequently for $\delta \ll a$, $\sigma_{\vartheta\vartheta} \gg |\sigma_{rr}|$. In thin-walled containers, therefore, the stresses in the direction of the thickness of the wall will be negligibly small compared with the stresses in the surface of the wall, and these can be considered to be constant over its thickness.

Let us find now the points in the pipe at which plastic strains first occur under the action only of an internal pressure ($p_b = 0$). Since the axes of r, ϑ, z are principal axes of stress ($\sigma_{r\vartheta} = \sigma_{\vartheta z} = \sigma_{zr} = 0$),

$$\sigma_i = \frac{1}{\sqrt{2}} \sqrt{[(\sigma_{rr} - \sigma_{\vartheta\vartheta})^2 + (\sigma_{\vartheta\vartheta} - \sigma_{zz})^2 + (\sigma_{zz} - \sigma_{rr})^2]}$$

$$= \frac{a^2 p_a}{b^2 - a^2} \sqrt{\left[3\frac{b^4}{r^4} + (1 - 2\nu)^2\right]}.$$

It can be seen that σ_i reaches a maximum at $r = a$. Therefore, plastic stresses occur first of all on the internal surface of the pipe, and according to the condition of plasticity (3.41), this takes place when the pressure reaches a value

$$p_a' = \frac{(b^2 - a^2)\,\sigma_S}{\sqrt{[3b^4 + (1 - 2\nu)^2\, a^4]}}.$$

If the external diameter of the pipe is infinitely large, we have from formulae (3.52) that as $b \to \infty$

$$\sigma_{rr} = -\frac{a^2 p_a}{r^2},$$

$$\sigma_{\vartheta\vartheta} = \frac{a^2 p_a}{r^2}, \quad \sigma_{zz} = 0,$$

so that

$$\sigma_i = \frac{a^2 p_a}{r^2}\sqrt{3} \quad \text{and} \quad p_a' = \frac{\sigma_S}{\sqrt{3}},$$

i.e. the plastic state is reached on the surface of a cylindrical hole in an elastic space at the same pressure, independently of the radius of the hole. For example, for a steel pipe of internal diameter 76 mm ($a = 3{\cdot}8$ cm) and an external diameter 200 mm ($b = 10$ cm) for $\sigma_s = 6000$ kg/cm^2, $\nu = 0{\cdot}3$, we find that $p_a' = 3000$ kg/cm^2. If the external diameter of the pipe is increased to infinity, $p_a' \approx 3500$ kg/cm^2. Thus, even a considerable increase in the thickness of the wall of the pipe has only a slight effect on the limiting pressure at which plastic strains occur. This prompted artillery experts not to increase the thickness of the barrels of their guns, but to improve the properties of the steels they used, and to strengthen their barrels by shrinking on tubes, thus inducing an initial stress which

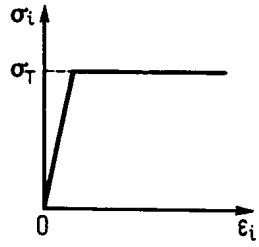

FIG. 115.

would give a more uniform stress distribution over the thickness of the wall, and cause the outer layers of the barrel to make a greater contribution to the resistance of the internal pressures.

With further increase in the internal pressure the boundary between the regions of elastic and elasto–plastic strains will move outwards towards the external surface of the pipe. Finally, at some value of $p_a = p$ the whole pipe enters an elasto–plastic state. Let us examine this state of affairs on the assumption that nowhere within the pipe does strain hardening occur. In other words, let us assume that the relation $\sigma_i = \Phi(\varepsilon_i)$ is of the form shown in Fig. 115. We know that Poisson's ratio beyond the elastic limit varies with increase in strain and tends to a value 0·5. For the sake of simplicity of calculation we shall assume that from the very beginning of plastic deformation $\nu = 0{\cdot}5$, i.e. that the material in the plastic state is incompressible, so that

$$\varepsilon \equiv \tfrac{1}{3}\theta \equiv \tfrac{1}{3}(\varepsilon_{rr} + \varepsilon_{\vartheta\vartheta} + \varepsilon_{zz}) = 0.$$

From the third equation of (3.30)

$$\sigma_{zz} - \sigma = \frac{2\sigma_i}{3\varepsilon_i}(\varepsilon_{zz} - \varepsilon)$$

for $\varepsilon = 0$ (from the condition of incompressibility) and $\varepsilon_{zz} = 0$, we get that,

$$\sigma_{zz} = \sigma = \frac{\sigma_{rr} + \sigma_{\vartheta\vartheta}}{2}. \tag{3.54}$$

Since we are considering the case when the whole of the material of the pipe is in a plastic state and there is no strain hardening, then at all points in the pipe $\sigma_i = \sigma_T$. Taking into account the relation (3.54) between σ_{rr}, $\sigma_{\vartheta\vartheta}$, σ_{zz}, we can rewrite this in the form

$$\frac{1}{\sqrt{2}}\sqrt{\left[(\sigma_{rr} - \sigma_{\vartheta\vartheta})^2 + \left(\sigma_{\vartheta\vartheta} - \frac{\sigma_{rr} + \sigma_{\vartheta\vartheta}}{2}\right)^2 + \left(\frac{\sigma_{rr} + \sigma_{\vartheta\vartheta}}{2} - \sigma_{rr}\right)^2\right]} = \sigma_T,$$

whence

$$\sigma_{rr} - \sigma_{\vartheta\vartheta} = \pm \frac{2\sigma_T}{\sqrt{3}}. \tag{3.55}$$

Since $\sigma_{rr} = 0$ on the external surface of the pipe, and since $\sigma_{\vartheta\vartheta}$ is tensile, i.e. positive, only the negative sign should be retained in the right-hand side of this expression.

The equilibrium eqn. (3.48) becomes therefore

$$r\frac{d\sigma_{rr}}{dr} = \frac{2\sigma_T}{\sqrt{3}}.$$

Integrating this equation, we find that

$$\sigma_{rr} = \frac{2\sigma_T}{\sqrt{3}} \ln r + C. \tag{3.56}$$

We note that there is only the one arbitrary constant C in this expression, whereas in the general solution of (3.48) in the case of elastic deformation, there were two arbitrary constants. This is to be expected, since in an elastic problem internal and external pressures could be given, whereas in the present example we know that the external pressure is zero, and we have to find only the internal pressure p at which plastic deformation occurs.

From the condition that $\sigma_{rr} = 0$ for $r = b$ we have, from (3.56), that

$$C = -\frac{2\sigma_T}{\sqrt{3}} \ln b,$$

and thus,

$$\sigma_{rr} = \frac{2\sigma_T}{\sqrt{3}} \ln \frac{r}{b}.$$

Also, making use of eqns. (3.54) and (3.55), we find that

$$\left.\begin{aligned} \sigma_{rr} &= \frac{2\sigma_T}{\sqrt{3}} \ln \frac{r}{b}, \\ \sigma_{\theta\theta} &= \frac{2\sigma_T}{\sqrt{3}} \left(1 + \ln \frac{r}{b}\right), \\ \sigma_{zz} &= \frac{2\sigma_T}{\sqrt{3}} \left(\frac{1}{2} + \ln \frac{r}{b}\right). \end{aligned}\right\} \tag{3.57}$$

The internal pressure at which the whole pipe enters the plastic region is given by the expression $\sigma_{rr} = -p$ for $r = a$, and consequently

$$p = \frac{2\sigma_T}{\sqrt{3}} \ln \frac{b}{a}. \tag{3.58}$$

We note one particular property of (3.58). In deriving it we did not need to make use of any relation between the strains, and it is valid, therefore, both for small and for large strains. From the condition that the volume remains constant at any instant of time t, we have that:

$$b^2(t) - a^2(t) = b_0^2 - a_0^2,$$

and therefore the ratio b/a decreases with time, and consequently, so also does p. The equilibrium, therefore, is unstable: a small strain at constant pressure destroys the equilibrium. Thus, as soon as the whole pipe enters the plastic region, in the absence of any strain-hardening, the material of the pipe will flow at a constant value of the internal pressure and then fail.

In exactly the same way, we can examine the case when the pipe enters the plastic region (without strain-hardening) under the action of an external pressure p'. Without going through the necessary computations, we note that the only difference between the two cases is that in eqn. (3.55) the plus sign should be retained, and in (3.56), in which a minus sign will occur before the first term, the constant C' will be given from the condition that $\sigma_{rr} = 0$ for $r = a$.

As a result we get that:

$$\left.\begin{aligned} \sigma_{rr} &= -\frac{2\sigma_T}{\sqrt{3}} \ln \frac{r}{a}, \\ \sigma_{\vartheta\vartheta} &= -\frac{2\sigma_T}{\sqrt{3}}\left(1 + \ln \frac{r}{a}\right), \\ \sigma_{zz} &= -\frac{2\sigma_T}{\sqrt{3}}\left(\frac{1}{2} + \ln \frac{r}{a}\right), \end{aligned}\right\} \tag{3.59}$$

and for p' we get the same value as for p:

$$p' = \frac{2\sigma_T}{\sqrt{3}} \ln \frac{b}{a}. \tag{3.60}$$

Thus, the external pressure at which the pipe starts to flow will be the same as the corresponding internal pressure. The difference is

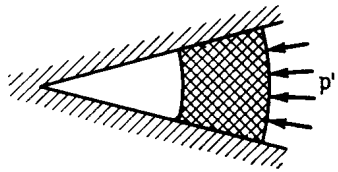

FIG. 116.

that, since during compression by an external pressure the ratio b/a increases, the equilibrium will be stable.

We have so far been considering only circular pipes. But there is nothing in the theory (both for elastic and for plastic deformation) that would be affected by assuming only axial symmetry, if we consider the case, not of a pipe, but a sector of a pipe lying with its meridian faces on absolutely rigid smooth planes in a radial direction (Fig. 116), along which it is free to slide without losing contact with these planes. Then, under the action of the external pressure given by formula (3.60), this sector will flow into the wedge. This type of problem is encountered, for example, in calculations for the pressure working of metals.

8. PLASTIC DEFORMATION OF A HOLLOW SPHERE

The elastic analysis of a hollow sphere with internal radius a and external radius b under the action of an internal pressure p_a and external pressure p_b is carried out in the same way as the analysis

of thick walled cylinders. If u is the radial displacement and r, ϑ, φ are the spherical coordinates, then

$$\left.\begin{aligned} &\varepsilon_{rr} = \frac{du}{dr}, \quad \varepsilon_{\vartheta\vartheta} = \varepsilon_{\varphi\varphi} = \frac{u}{r}, \quad \varepsilon_{r\vartheta} = \varepsilon_{\vartheta\varphi} = \varepsilon_{\varphi r} = 0, \\ &\sigma_{rr} = \frac{a^3 p_a - b^3 p_b}{b^3 - a^3} + \frac{a^3(p_b - p_a)}{b^3 - a^3}\,\frac{b^3}{r^3}, \\ &\sigma_{\vartheta\vartheta} = \sigma_{\varphi\varphi} = \frac{a^3 p_a - b^3 p_b}{b^3 - a^3} - \frac{a^3(p_b - p_a)}{b^3 - a^3}\,\frac{b^3}{2r^3}. \end{aligned}\right\} \quad (3.61)$$

Under the action of an internal pressure alone, plastic deformation occurs first of all on the internal surface of the sphere, and as the pressure increases, the boundary of the plastic region moves towards the outer surface.

Let us consider the limiting case, when the whole sphere under the action of a pressure p is in a plastic state. We shall confine our attention once more solely to the case when no strain hardening occurs (see Fig. 115), and when the material is incompressible. The equilibrium equation is of the form

$$r\frac{d\sigma_{rr}}{dr} + 2(\sigma_{rr} - \sigma_{\vartheta\vartheta}) = 0.$$

Since $\sigma_{\vartheta\vartheta} = \sigma_{\varphi\varphi}$,

$$\sigma_i = \pm(\sigma_{rr} - \sigma_{\vartheta\vartheta}).$$

Consequently, the condition of plasticity is of the form $\sigma_{rr} - \sigma_{\vartheta\vartheta} = \pm\sigma_T$. Since $\sigma_{rr} = 0$ and $\sigma_{\vartheta\vartheta} > 0$ for $r = b$, only the minus sign need be retained: $\sigma_{rr} - \sigma_{\vartheta\vartheta} = -\sigma_T$. From the differential equation of equilibrium we then have that:

$$\sigma_{rr} = 2\sigma_T \ln r + C.$$

After finding C from the condition that $\sigma_{rr} = 0$ for $r = b$, we get that

$$\sigma_{rr} = 2\sigma_T \ln\frac{r}{b},$$

$$\sigma_{\vartheta\vartheta} = \sigma_{\varphi\varphi} = 2\sigma_T\left(\frac{1}{2} + \ln\frac{r}{b}\right).$$

The pressure at which the whole of the hollow sphere enters the plastic state is thus

$$p = 2\sigma_T \ln\frac{b}{a}. \quad (3.62)$$

From the condition of incompressibility it follows that the ratio b/a decreases with increase in strain, so that the equilibrium will not be stable and the sphere will rapidly fail at a constant pressure p.

It is interesting to note that, for the same thickness and radius, a hollow sphere is approximately twice as strong as a cylinder. Instead of a sphere, we could have considered any part of a sphere formed by the surface of a cone (and not necessarily a circular cone) with its apex at the centre of the sphere. Formula (3.62) then gives the pressure necessary to induce plastic deformation and force the material into a conical die.

9. Thin-walled Containers

In the analysis of thin-walled containers (balloons, gas-holders, cisterns, etc.), we make use of the result obtained in the examination of thick-walled cylinders, that the stresses acting on areas parallel to the surface of the walls are negligibly small compared with the stresses acting on normal sections of the wall, and that the latter stresses can be considered to be uniformly distributed over the thickness h of the wall.

Let us consider a thin-walled container in the form of a surface of revolution (Fig. 117), on which there acts a pressure which varies along the meridian and which is uniformly distributed along each parallel. Let us consider an element formed by two meridian sections ab and cd and two sections bc and ad, normal to the meridian, at an angle $d\theta_2$ to each other.

We shall denote the principal radii of curvature at the point a as $R_1 = 0'a$ and $R_2 = 0''a$. On the faces ad and bc there will act a force $\sigma_2 h\, ds_1$, and on the faces ab and cd, a force $\sigma_1 h\, ds_2$, directed along the meridian and along the parallel respectively.

Resolving the resultant force due to the pressure, $p\, ds_1\, ds_2$, acting on the element $abcd$, and the forces $\sigma_1 h\, ds_2$ and $\sigma_2 h\, ds_1$ along the normal to the element at the point a, we get that:

$$p\, ds_1\, ds_2 = 2\sigma_2 h\, ds_1 \sin\frac{d\theta_2}{2} + 2\sigma_1 h\, ds_2 \sin\frac{d\theta_1}{2}.$$

Since $\sin\frac{d\theta_1}{2} \approx \frac{d\theta_1}{2}$ and $\sin\frac{d\theta_2}{2} \approx \frac{d\theta_2}{2}$, and since $ds_1 = R_1\, d\theta_1$, $ds_2 = R_2\, d\theta_2$, we have that

$$p\, ds_1\, ds_2 = \sigma_2 h\, ds_1 \frac{ds_2}{R_2} + \sigma_1 h\, ds_2 \frac{ds_1}{R_1},$$

from which

$$\frac{\sigma_1}{R_1} + \frac{\sigma_2}{R_2} = \frac{p}{h}. \tag{3.63}$$

This expression was derived by Laplace and is known as the Laplace equation. Mariott's formula (3.53) can be derived from this by letting the radius of curvature R_2 tend to infinity.

A second relation for finding the stresses can be found by considering the equilibrium of the part of the container, together with the liquid or gas, below a section formed by the surface of a cone, the generators of which are normal to the meridians (for example by the section *ad* produced; see Fig. 117b)

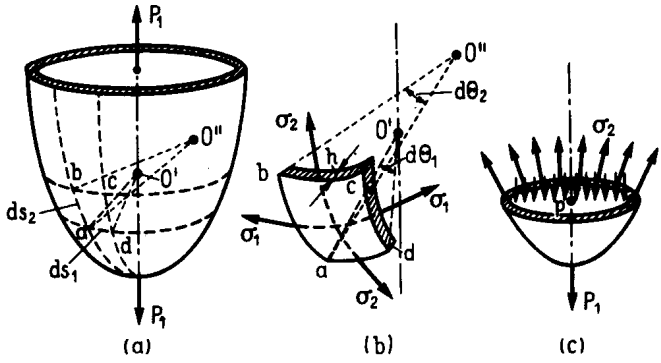

FIG. 117.

The equilibrium equation is of the form

$$\sigma_2 h\, 2\pi r \sin\theta_2 = p\pi r^2 + P_1,$$

where P_1 is the weight of the fluid filling the lower part of the container, or a tensile force acting along the axis of the container. Denoting the right-hand side by P, i.e. the sum of all the forces acting below the section, we get that:

$$\sigma_2 h = \frac{P}{2\pi r \sin\theta_2}. \tag{3.64}$$

Equations (3.63) and (3.64) give the values of σ_1 and σ_2.

It can be seen that thin-walled metal containers are extremely strong and are able to withstand very high pressures. For this reason they are widely used in engineering practice.

10. Shearing Stress Distribution in a Beam

Due to the shearing force $\boldsymbol{Q} = j\boldsymbol{Q}_y + k\boldsymbol{Q}_z$ there occur on cross-sections of a beam shearing stresses σ_{xy}, σ_{xz}, which, as has already been proved, are small compared with σ_{xx} if the lateral dimension of the beam is small compared with its length.

The stress vector $\boldsymbol{S}_x$ on the cross-section can be represented in the form

$$\boldsymbol{S}_x = \sigma_{xx}\boldsymbol{i} + \boldsymbol{\tau},$$

where $\boldsymbol{\tau}$ is the vector of the shearing stress

$$\boldsymbol{\tau} = \sigma_{xy}\boldsymbol{j} + \sigma_{xz}\boldsymbol{k}.$$

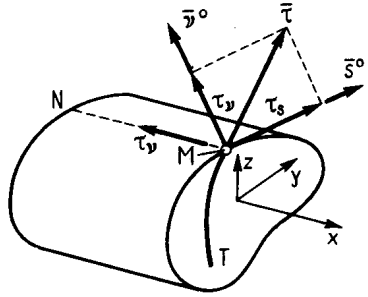

Fig. 118.

The vectors $\boldsymbol{\tau}$ depend uniquely on and vary continuously with the coordinates of points on the cross-section y, z, and therefore form a vector field. A line drawn in the plane of the cross-section, at every point on which the vector $\boldsymbol{\tau}$ is directed along a tangent, is called a shearing stress trajectory.

Let us suppose that some shearing stress trajectory T intersects the boundary of the cross-section at the point M (Fig. 118). Let $\boldsymbol{\nu}^0$, $\boldsymbol{s}^0$ be the unit vectors of the normal and tangent at the point M on the boundary. In terms of its projections on $\boldsymbol{\nu}^0$, $\boldsymbol{s}^0$,

$$\boldsymbol{\tau} = \tau_\nu\boldsymbol{\nu}^0 + \tau_s\boldsymbol{s}^0.$$

Since the component τ_ν acts in the plane of the cross-section, by the law of complementary shearing stresses, the same stress must act in the surface of the beam along the generator NM. But we assume that there is no shearing stress acting on the lateral surface of the beam, i.e. that this surface is free from load. Therefore $\tau_\nu = 0$

and, consequently, the vector of the shearing stress on the edge of the cross-section is directed along the tangent. Thus the boundary of the cross-section is a shearing stress trajectory.

A family of shearing stress trajectories on the cross-section forms a system of closed non-intersecting lines which include the line of the boundary of the cross-section.

The determination of the shearing stresses in a beam really belongs to the theory of elasticity and plasticity. However, a number of simple results can be obtained by the methods of the strength of materials.

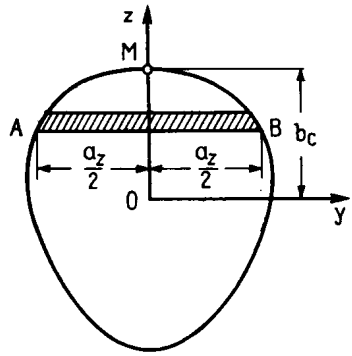

FIG. 119.

Let us consider a beam of constant cross-section which has an axis of symmetry z, and which is under the action of a moment M_y, and a shearing force $Q_z = dM_y/dx$ in the plane (xz) (Fig. 119).

The distance in the z-direction from the centre of gravity to the top of the cross-section will be denoted by b_c, and the width of the section at a distance z from the centre of gravity by a_z, so that the equation for the boundary can be written in the form $a_z = f(z)$. The mean shearing stress $\bar{\sigma}_{xz}$ on the line AB will be:

$$\bar{\sigma}_{xz} = \frac{1}{a_z} \int_0^{a_z} \sigma_{xz}\, dy,$$

and from symmetry the mean value of $\bar{\sigma}_{xy}$ over AB will be zero. The normal stress σ_{xx} on the line AB will, from (2.44), be constant and equal to

$$\sigma_{xx} = \bar{\sigma}_{xx} = \frac{P}{F} + \frac{M_y z}{J_y}. \tag{3.65}$$

We have already seen in § 10 of Chapter II that the following relation exists between $\bar{\sigma}_{xz}$ and $\bar{\sigma}_{xx}$:

$$\bar{\sigma}_{xz} = \frac{1}{a_z} \int_z^{b_c} a_z \frac{\partial \bar{\sigma}_{xx}}{\partial x} dz.$$

But $\frac{\partial \sigma_{xx}}{\partial x} = \frac{z}{J_y} \frac{dM_y}{dx} = \frac{z}{J_y} Q_z$; therefore, the mean shearing stress at a level z is given by the Jouravsky formula

$$\bar{\sigma}_{xz} = \frac{Q_z S_{zy}}{a_z J_y}, \tag{3.66}$$

where S_{zy} is the first moment about the y-axis of the part of the section above the line AB:

$$S_{zy} = \int_z^{bc} a_z z \, dz.$$

For example, for a rectangular section for which $a_z = a = \text{const.}$, $b_c = h/2$, we have that

$$S_{zy} = \frac{a}{2}\left(\frac{h^2}{2} - z^2\right), \quad J_y = \frac{ah^3}{12}$$

and therefore

$$\bar{\sigma}_{xz} = \frac{3}{2} \frac{Qz}{ah}\left(1 - \frac{4z^2}{h^2}\right).$$

The greatest value of $\bar{\sigma}_{xz}$ occurs when $z = 0$ and is one and a half times the mean shearing stress over the whole section:

$$\bar{\sigma}_{xz}^{\max} = \frac{3}{2} \frac{Qz}{F}.$$

Since there is no normal stress σ_{zz} and no shearing stress σ_{zy} in the plane of a longitudinal section (yx) of the beam, the stress σ_{xz}, the mean value of which we have just found, is the only force holding the lower part ($z < 0$) and the top part ($z > 0$) together. It ($\bar{\sigma}_{xz}$) is, therefore, of considerable importance in the design of the components of such structures as compound girders, etc.

For sections in which the dimension a_z varies smoothly with z and is small compared with the dimension b_c (i.e. with the height of the section), the true stress σ_{xz} will differ only slightly from the mean stress $\bar{\sigma}_{xz}$. For thin-walled sections of the type shown in

Fig. 120, therefore, the mean values will everywhere be close to the true values, with the exception of the internal angles.

For thin-walled sections the walls of which are inclined to the plane of bending (xz), formula (3.66) might give values which are very much different from the true values, which is obvious if we take into account the fact that the boundary of the cross-section must be a trajectory of the shearing stress τ.

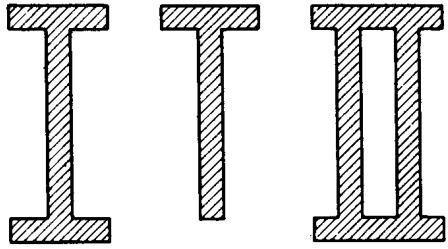

FIG. 120.

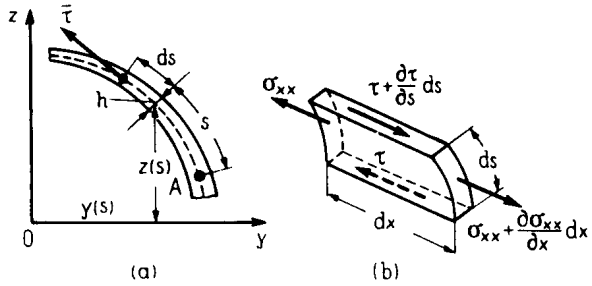

FIG. 121.

Let us consider a beam with an arbitrary thin-walled cross-section, for which, as before, the z-axis is an axis of symmetry. Figure 121a shows a part of the section in the right-hand quadrant, the dotted line indicates the centre line of the section, and h denotes the thickness at the point z.

The equation of the centre-line of the cross-section is $z = f(y)$ and we can assume, therefore, that we know also the parametric equations of the centre line

$$y = y(s), \quad z = z(s),$$

where s is the length of arc measured from any fixed point A in an anti-clockwise direction. From Fig. 121 b, which shows an infinitely small element of the section formed by the planes $x = \text{const.}$, $x + dx = \text{const.}$ and $s = \text{const.}$, $s + ds = \text{const.}$, so that the plane $s = \text{const.}$ is normal to the line s, it can be seen that the stress τ on the section $x = \text{const.}$ is directed along the arc s, and at the section $s = \text{const.}$, from the law of complementary shearing stresses, it is directed along the x-axis. Considering the equilibrium of the element, we have that:

$$\frac{\partial}{\partial s}(\tau h) + h\frac{\partial \sigma_{xx}}{\partial x} = 0$$

or, taking into account expression (3.65) for σ_{xx} when $P = \text{const.}$,

$$\frac{\partial}{\partial s}(\tau h) = -\frac{hz}{J_y}\frac{dM_y}{dx} = -\frac{hzQ_z}{J_y}.$$

Thus, integrating from $s = 0$ to s and denoting values at $s = 0$ by τ_0, h_0, we get that

$$\tau(s) = \frac{h_0}{h}\tau_0 - \frac{Q_z}{hJ_y}\int_0^s hz\, ds. \tag{3.67}$$

The integral

$$S_{yz} = \int_0^s hz\, ds$$

in this expression represents the static moment of the part of the section included between $s = 0$ and $s = s$, and therefore, for the shearing stress τ we have the expression

$$\tau(s) = \tau_0\frac{h_0}{h} - \frac{Q_z S_{yz}}{J_y h}. \tag{3.68}$$

which is known as Bredt's formula.

If the boundary of the cross-section is singly connected (open) or doubly-connected (closed), the origin for measuring the arc $s = 0$ can be taken as the lowest point of the intersection of the centre line with the z-axis. Due to symmetry the shearing stress at this point $\tau_0 = 0$, and therefore formula (3.68) defines fully the stress τ at any point. In particular, for a section of constant wall thickness $h = \text{const.}$,

$$\tau = -\frac{Q_z}{J_y}\int_0^s z\, ds. \tag{3.69}$$

This formula, together with (3.65), enables us to determine the elastic stresses in thin-walled structures such as plate and box girders, ships' hulls, etc.

If the material is loaded beyond the elastic range it is necessary first of all to find, by the methods already described, the distribution of the normal stress σ_{xx} over the cross-section and along the length of the component, and then the shearing stress can be found from the formula

$$\tau = -\frac{1}{h}\int_0^s h\frac{\partial \sigma_{xx}}{\partial x}\,ds.$$

CHAPTER IV

PLASTIC FLOW

1. The Strength and Plasticity of a Heated Metal

In many cases of plastic deformation of metals the loading process is not simple and the strains induced are not small. This applies particularly to the case of pressure working of metals, for example pressing, rolling and stamping operations, etc. The aim of these processes is to form billets or sheets of metal, finished or half-finished articles by means of plastic deformation. This means that after deformation the finished product differs in shape and dimensions from the body from which it was formed. This can be brought about by hot-working pressure processes, when, in order to improve the plasticity and decrease its resistance, the metal is deformed at a high temperature, or alternatively, by cold-working processes.

The process of the plastic deformation of a body is known as plastic flow. In pressure working processes, therefore, plastic flow of the metal takes place. The strain trajectories considered in Chapter III represent cases of uniform plastic flow.

At a temperature T_r, which is about 40 per cent of the absolute melting temperature T_m, and after further increase in temperature, recrystallization takes place in the metal at a definite rate. The crystal lattice distorted by the deformation is reformed, the micro-defects in the metal disappear and its density increases. This takes place as a result of the excess strain energy of the distorted structure and the fact that the elevated temperature greatly assists diffusion of the atoms. Plasticity is noticeably increased as a result of this recrystallization, i.e. other things being equal, the metal has a greater ability to deform without failure, but its strength (yield point, UTS) decreases.

If a previously deformed metal is heated above the recrystallization temperature, the change in dimensions of a grain, within certain limits, takes place as follows: at a constant temperature its size is less the greater the degree of deformation; at a constant

deformation its size is greater the higher the temperature. An important property of metals with deformation below and above the recrystallization temperature is that in the first case strain hardening takes place and in the second case it does not.

A process of plastic deformation of a metal at room temperature is usually considered a cold-working process, and at higher temperatures, at which the strength of the metal (its yield point, resistance to failure) decreases noticeably, the process is known as a hot-working process.

Some authors give a more precise definition and define a cold-working process of plastic flow as one which takes place at a temperature below T_r and a hot-working process as one which takes place at $T > T_r$.†

The melting points and recrystallization temperatures for certain metals are listed in Table 5.

TABLE 5. MELTING POINTS T_m AND RECRYSTALLIZATION TEMPERATURES T_r IN °C

Metal	Pb	Zn	Al, Mg	Au	Fe	Ni	W
T_r	0	0	150	200	450	620	1210
T_m	327	419	660	1060	1530	1450	3200

Thus, strictly speaking, the flow process for lead at room temperature is a "hot" process, whereas that of nickel at 600°C can be considered a "cold" process. With hot-working processes the yield point of the metal and the UTS are practically the same.

In hot-working pressure operations the metal is heated to within the appropriate temperature range determined beforehand by direct experiments. These experiments consist of subjecting specimens to tension at various temperatures and in this way finding the relation between the elasticity modulus E, the yield point σ_S, the UTS σ_B and the percentage elongation at failure δ, and the temperature of the specimen. Typical curves for X18 H25 C2 steel are given in Fig. 122; they illustrate the following points: E, σ_S, σ_B, δ

† Since the recrystallization process takes place at finite speed, this generalization, which assumes that in hot-working processes flow is accompanied by recrystallization, is not accurate; it is necessary to consider intermediate processes when recrystallization lags behind the flow process.

vary only slightly up to a temperature of the order of 400°C, after which they vary considerably. The yield point σ_S and the UTS σ_B practically coincide at a temperature of 800°C. The percentage elongation at failure (the plasticity) decreases first of all with increase in temperature and then increases to a first maximum at 500°C. It then falls off rapidly, then increases once more and reaches an absolute maximum at 700°C, after which the plasticity decreases as a result of the metal being "burnt", i.e. the boundaries between neighbouring grains oxidize and break down before the metal melts.

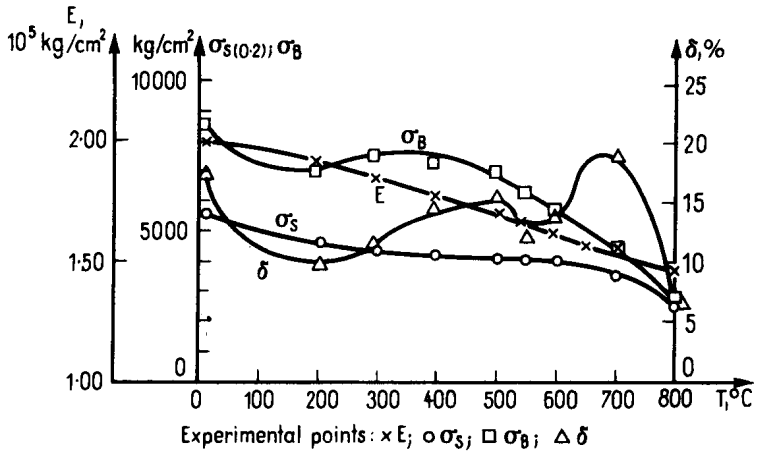

FIG. 122.

Since the relation $\sigma_S = \sigma_S(T)$ is known from experiment, the condition of plasticity in a state of compound stress for a metal at elevated temperatures is also known:

$$\sigma_i = \sigma_S(T). \tag{4.1}$$

In hot-working processes the working ("forging") temperature range is, of course, selected between the recrystallization temperature and the temperature at which the metal would be "burnt", (which is below the melting point) in the region of maximum plasticity.

Instead of using tensile tests for finding the working temperature range, other types of experiment are often used in practice, which represent more closely the actual conditions obtained during a hot-working process. For example, experiments on the compression of

a short specimen, torsion experiments, etc., are used, and the plasticity is determined by the deformation at which cracks first appear on the surface of the specimen.

The values of the maximum plastic strains for a particular metal obtained from different types of experiment (tension, compression, torsion tests) are, of course, different, and experiments have been carried out with very high all-round pressures in which the tension, compression and torsion are accompanied by very large plastic strains without failure. However, the temperature of maximum plasticity apparently depends only slightly on the nature of the state of stress, otherwise the working temperature range as found by the above-mentioned methods would not conform at all to the accepted practice of hot working of metals.

Thus, in determining the temperature range for hot-working pressure processes, and also, therefore, in the theory of plastic flow, we make use of the following hypothesis: within a particular range of pressures p the characteristic temperatures for a metal—the recrystallization temperature T_r, the melting point T_m, the temperature of maximum plasticity T_S (these are sometimes called homologous temperatures)—are independent of the nature of the state of stress. The magnitude of the pressure in a state of compound stress is the mean normal stress with a negative sign

$$p = -\sigma = -\tfrac{1}{3}(\sigma_1 + \sigma_2 + \sigma_3).$$

It is apparent that this hypothesis is valid only within a certain pressure range, since all the homologous temperatures, strictly speaking, depend on the pressure. For example, the absolute temperature of the melting point varies with pressure according to the differential equation (Clapeyron's equation)

$$\frac{dT_m}{dp} = \frac{T_m}{Q}\left(\frac{1}{\varrho_e} - \frac{1}{\varrho_s}\right),$$

where Q is the latent heat of liquefaction, ϱ_e and ϱ_s are the densities of the material in liquid and solid phases respectively for melting at given values of p and T_m. For the majority of materials melting is accompanied by a decrease in density, and the melting point, therefore, rises with increase in pressure.

Temperature is one of the parameters which define the most suitable régime for the hot working of a metal by pressure. In addition it is also necessary to take into account the way in which

the properties of the metal depend on the rate of deformation (for this purpose the dynamic characteristics of the metal are determined at various temperatures) and on the type of stressed state, since failure occurs at different values of intensity of stress for different types of stressed state. As regards the latter, the order of the various operations is of particular importance. Figure 123 shows the successive changes in a component for a bicycle frame from a piece of metal in the form of a flat rectangular plate to the final product (a seat attachment).

FIG. 123.

2. FINITE STRAINS AND THE TENSOR OF RATE OF DEFORMATION

Plastic flow of a material can be accompanied by considerable displacements of neighbouring particles, commensurable with the distances between them.

In Chapter I we introduced the concept of a small deformation as a set of three linear strains and three shear strains, expressed linearly in terms of the first derivatives of the displacements. It is easy to see that these quantities cannot be a characteristic of a finite (large) strain. For, suppose that in the neighbourhood of some point, which we shall take as the origin of coordinates O, there occurs a uniform strain in the (xy) plane, so that the displacements of points in this region are linear functions of the initial coordinates x_0, y_0:

$$x = x_0 + u = x_0 + A_1 x_0 + B_1 y_0,$$
$$y = y_0 + v = y_0 + A_2 x_0 + B_2 y_0,$$

where A_1, B_1, A_2, B_2 are certain functions of time which vanish at $t = 0$.

Considering the deformation of an element which at $t = 0$ is a square $OMPN$ of side 1 (Fig. 124), we see that the coordinates of the points M and N for $t > 0$ will be $M'(1 + A_1, A_2)$ and $N'(B_1, 1 + B_2)$, and therefore the relative extensions of fibres OM and ON will be

$$\varepsilon_x = \sqrt{[(1 + A_1)^2 + A_2^2]} - 1, \quad \varepsilon_y = \sqrt{[(1 + B_2)^2 + B_1^2]} - 1,$$

and the cosine of the angle ϑ between them will be

$$\cos\theta = \frac{(1 + A_1)\,B_1 + A_2(1 + B_2)}{(1 + \varepsilon_x)(1 + \varepsilon_y)}.$$

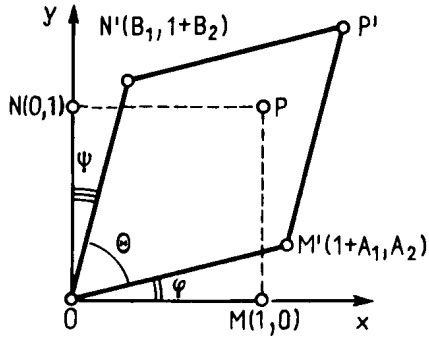

FIG. 124.

The quantities $\varepsilon_{xx}, \varepsilon_{yy}, \varepsilon_{xy}$ introduced in Chapter 1 (the components of a small strain) have the values

$$\varepsilon_{xx} = \frac{\partial u}{dx_0} = A_1,$$

$$\varepsilon_{yy} = \frac{\partial v}{dy_0} = B_2,$$

$$2\varepsilon_{xy} = \frac{\partial v}{\partial x_0} + \frac{\partial u}{\partial y_0} = B_1 + A_2,$$

and they cannot be expressed in terms of ε_x, ε_y and $\cos\theta$ because the three quantities A_1, B_2, $A_2 + B_1$ cannot.

The quantities ε_x, ε_y, $\cos\theta$, or any other functions of the first derivatives of the displacements which can be expressed in terms of ε_x, ε_y, $\cos\theta$, can be called strains. Examples of such functions are the so-called components of the tensor of finite strains, which,

in the case of plane deformation, can be expressed as follows in terms of the displacements u and v:

$$\left.\begin{aligned} \bar{\varepsilon}_{xx} &= \frac{\partial u}{\partial x_0} + \frac{1}{2}\left[\left(\frac{\partial u}{dx_0}\right)^2 + \left(\frac{\partial v}{\partial x_0}\right)^2\right], \\ \bar{\varepsilon}_{yy} &= \frac{\partial v}{\partial y_0} + \frac{1}{2}\left[\left(\frac{\partial u}{\partial y_0}\right)^2 + \left(\frac{\partial v}{\partial y_0}\right)^2\right], \\ 2\bar{\varepsilon}_{xy} &= \frac{\partial v}{\partial x_0} + \frac{\partial u}{\partial y_0} + \frac{\partial u}{\partial x_0}\frac{\partial u}{\partial y_0} + \frac{\partial v}{\partial x_0}\frac{dv}{\partial y_0}. \end{aligned}\right\} \tag{4.2}$$

These do, in fact, depend only on ε_x, ε_y, $\cos\theta$, as can be seen from the expressions for x and y in terms of x_0 and y_0:

$$\begin{aligned} 2\bar{\varepsilon}_{xx} &\equiv (1 + \varepsilon_x)^2 - 1, \\ 2\bar{\varepsilon}_{yy} &= (1 + \varepsilon_y)^2 - 1, \\ 2\bar{\varepsilon}_{xy} &= (1 + \varepsilon_x)(1 + \varepsilon_y)\cos\theta. \end{aligned}$$

Any three independent functions of the quantities (4.2) can also be called finite strains, since they allow the extensions of fibres and the changes in the angles between them to be found.

The advantage, therefore, of the quantities ε_x, ε_y, $\cos\theta$ and (4.2) is that they depend only on the internal deformation and are independent of the translational movement of an element as a whole, whereas the quantities ε_{ij} for finite strains do contain the translational movement, for example the angle φ or ψ (Fig. 124). It is obvious that internal stresses can depend only on internal strains and that they are independent of the translational movement. Therefore for finite strains there is no point in trying to find a relation between the stresses and the quantities ε_{ij}.

On the other hand, if we already know the principal axes of strain, then, taking these axes as the x and y-axes, and bearing in mind the fact that on the principal axes $B_1 = A_2 = 0$, $\varphi = \psi = 0$, we get that:

$$\begin{aligned} \varepsilon_{xx} &= A_1 = \varepsilon_x = \varepsilon_1, \\ \varepsilon_{yy} &= B_2 = \varepsilon_y = \varepsilon_2, \\ \varepsilon_{xy} &= 0 = \cos\theta; \end{aligned}$$

i.e. the expressions for ε_{ij} now characterize the principal strains, and any functions of them will be strains.

The so-called logarithmic principal strains

$$\left.\begin{aligned} \ddot{\varepsilon}_1 &= \ln(1 + \varepsilon_1), \\ \ddot{\varepsilon}_2 &= \ln(1 + \varepsilon_2), \\ \ddot{\varepsilon}_3 &= \ln(1 + \varepsilon_3), \end{aligned}\right\} \tag{4.3}$$

are now widely used, and these, without any apparent reason, are sometimes called actual strains.

Another approach to the problem of finding the strains, which is widespread in hydrodynamics, is based on the concept of a tensor of rates of strain. Let us suppose that the point O in Fig. 124 is now not a permanent physical point in the body (a particle) but a fixed point in space through which pass various physical points (particles) and at which, at an instant of time t, there is a particular physical point, and let us suppose that $OMPN$ is a definite constant element of volume in space in which, at an instant of time t, is located some particular physical element. u_x, u_y, u_z will denote the components of the velocity of this physical point, and x, y will be the coordinates of the point O. Then the velocity of the point M will be $u_x(x + \xi, y)$, $u_y(x + \xi, y)$; similarly the velocity of the point N will be $u_x(x, y + \eta)$, $u_y(x, y + \eta)$, where $\xi = OM$, $\eta = ON$; after a time dt there will take place the following infinitely small strains:

a relative extension of OM equal to $(\partial u_x/dx)\, dt$,

a relative extension of ON equal to $(\partial u_y/\partial y)\, dt$,

the cosine of the angle θ—a shear strain—equal to $(\partial u_y/\partial x + \partial u_x/dy)\, dt$. Dividing these expressions by dt we obtain the rates of strain of physical elements at any point in space:

$$v_{xx} = \frac{\partial u_x}{\partial x}, \quad v_{yy} = \frac{\partial u_y}{\partial y}, \quad 2v_{xy} = \frac{\partial u_y}{\partial x} + \frac{\partial u_x}{\partial y}.$$

If the flow is not in a plane, but takes place in three dimensions, we obtain expressions for the components of the rates of strain, which are of the same form as the expressions for small strains:

$$v_{mn} = \frac{1}{2}\left(\frac{\partial u_n}{dx_m} + \frac{\partial u_m}{\partial x_n}\right) \tag{4.4}$$

$$(m, n = 1, 2, 3)$$

(in this expression $x_1 = x$, $x_2 = y$, $x_3 = z$).

The set of quantities v_{mn} is known as the tensor of the rate of strain. The essential difference is that instead of the displacements u, v, w of a definite physical point, the tensor contains the velocities u_x, u_y, u_z of physical particles passing through a fixed point in space.

In the case of small strains the coordinates x_0, y_0, z_0 differ only slightly from x, y, z and, in view of continuity, we can assume that the velocities appearing in (4.4) are the derivatives with respect to time of the displacements appearing in the expressions for ε_{mn}, and therefore

$$v_{mn} = \frac{\partial \varepsilon_{mn}}{\partial t}. \tag{4.5}$$

We can establish the relation between the displacements of physical points and the velocities u_x, u_y, u_z at fixed points in space. Let us suppose that when $t = 0$ some physical point has coordinates x_0, y_0, z_0, and that for $t > 0$ its coordinates are x, y, z. Its velocities at an instant t when its coordinates are x, y, z, i.e. at the point (x, y, z) in space, will be dx/dt, dy/dt, dz/dt, and they must have the values u_x, u_y, u_z; thus we have the three ordinary differential equations

$$\left.\begin{aligned} \frac{dx}{dt} &= u_x(x, y, z, t), \\ \frac{dy}{dt} &= u_y(x, y, z, t), \\ \frac{dz}{dt} &= u_z(x, y, z, t) \end{aligned}\right\} \tag{4.6}$$

and the three initial conditions

$$\left.\begin{aligned} x &= x_0 \\ y &= y_0 \\ z &= z_0 \end{aligned}\right\} \quad \text{for} \quad t = 0. \tag{4.7}$$

If the velocities u_x, u_y, u_z are known, then by integrating (4.6) with the conditions (4.7), we get that:

$$\left.\begin{aligned} x - x_0 &= f_1(x_0, y_0, z_0, t), \\ y - y_0 &= f_2(x_0, y_0, z_0, t), \\ z - z_0 &= f_3(x_0, y_0, z_0, t), \end{aligned}\right\} \tag{4.8}$$

in which the quantities $x - x_0$, $y - y_0$, $z - z_0$ in the left-hand sides of these expressions are the displacements of the point considered (i.e. u, v, w which appear in the expressions for ε_{mn}). Since the displacements are known, we can also find the strains from one of the above formulae, for example (4.2).

In the same way that the resultant shearing strain is determined by the intensity of strain, the resultant rate of strain is determined by the intensity of the rate of strain, which is

$$v_i = \frac{\sqrt{2}}{3} \times$$

$$\times \sqrt{[(v_{xx} - v_{yy})^2 + (v_{yy} - v_{zz})^2 + (v_{zz} - v_{xx})^2 + 6(v_{yz}^2 + v_{zx}^2 + v_{xy}^2)]}. \tag{4.9}$$

It should be noted that even in the case of small strains when formulae (4.5) apply, the intensity of rate of strain is not equal to the derivative with respect to time of the intensity of strain. The expression $v_i = \partial\varepsilon_i/\partial t$ for small strains applies only in the case of simple loading.

3. The Relation between Stresses and Strains in the Theory of Plastic Flow

Since in metal working operations, when large plastic strains occur, the density of the material varies only slightly, the relation between the density ϱ (or the relative change in volume θ) and the pressure p (where $p = -\sigma$) can be replaced by the condition of incompressibility. Since $v_{xx} + v_{yy} + v_{zz}$ is the relative change in unit volume of the material in unit time, the condition of incompressibility is of the form

$$\frac{\partial u_x}{\partial x} + \frac{\partial u_y}{\partial y} + \frac{\partial u_z}{\partial z} = 0. \tag{4.10}$$

From the point of view of vectorial representation (Chapter III, § 4), the strain trajectories of unit volumes of the body in plastic flow processes are often trajectories of small curvature, and the stress vector, therefore, will be directed along the tangent to the strain trajectory, i.e. formula (3.28), $\boldsymbol{S} = (2\sigma_i/3\sigma_i)\,\partial\boldsymbol{\Im}/\partial t$, will apply; but $\partial\boldsymbol{\Im}/\partial t$ is the rate of strain given by the components of the rate of strain deviator, which, from (4.10) coincides with the tensor (4.4).

The stress vector $\boldsymbol{S}$ is characterized by the stress deviator σ'_{mn}, and in the same way that the tensor of rate of strain in the theory of flow was considered in a fixed geometrical space through which the material flows, the stress tensor σ_{mn} is also considered in this space. Thus σ_{mn} are not the stresses on specific physical surfaces of the body; these physical surfaces rapidly change their positions

with time; for example, initially orthogonal surfaces could after a time t, be inclined at angles differing considerably from 90°.

The stress vector S and the components of the stress tensor σ_{mn} are the stresses on geometrical surfaces which are fixed in space and always orthogonal, i.e. on physical areas which at an instant t coincide with these geometrical surfaces.

The above relations between the vectors S and $\mathfrak{D}$ in the theory of flow in terms of the components of stress σ_{mn} and of the rate of strain v_{mn} can be written in the form

$$\sigma_{mn} - \delta_{mn}\sigma = \frac{2\sigma_i}{3v_i} v_{mn} \quad (m, n = 1, 2, 3)$$

$$(\delta_{mm} = 1, \quad \delta_{mn} = 0 \quad \text{for} \quad m \neq n). \tag{4.11}$$

Here σ_i is either a known function of the temperature T (4.1) or, as follows from experiment, a known function of the temperature T, the intensity of the rate of strain v_i and the degree of deformation λ_i:

$$\sigma_i = \Phi(T, v_i, \lambda_i). \tag{4.12}$$

The degree of deformation λ_i is a quantity, the total derivative of which with respect to time is v_i:

$$\frac{d\lambda_i}{dt} \equiv \frac{\partial \lambda_i}{dt} + u_x \frac{\partial \lambda_i}{\partial x} + u_y \frac{\partial \lambda_i}{\partial y} + u_z \frac{\partial \lambda_i}{\partial z} = v_i,$$

so that

$$\lambda_i = \int_0^t v_i \, dt. \tag{4.13}$$

The problem of plastic flow in three dimensions comes within the province of the mathematical theory of plasticity, and in principle can be formulated as follows: the relations (4.11) express the six components of the stress tensor σ_{mn} in terms of the six components of the tensor of rate of strain v_{mn} and the mean stress σ, i.e. from (4.4), in terms of the three components of the velocities u_x, u_y, u_z and σ. If we substitute (4.11) in the three equations of motion of an infinitely small element, we obtain three equations in the above four unknown functions u_x, u_y, u_z, σ; adding to these the condition of incompressibility, we obtain the complete set of four differential equations. In addition, the loadings must be given on the surface of the body, i.e. the boundary conditions will be

expressed in terms of these four functions. The solution of this set of equations is the solution to the problem of plastic flow.

The strength of materials covers only the more simple cases of plastic flow which do not require laborious mathematical computations, and the differential equations of motion are often simplified by making use of additional kinematic and dynamic hypotheses, which enable an approximate solution to be found in sufficiently simple form.

4. Surface Friction

In metal working operations friction forces between the surface of the working parts of the machines and the metal being deformed are often considerable. For finite plastic strains of the metal the relative movement between these surfaces can be very large.

The shear stress at a common point on the surfaces of two bodies moving with relative velocity v and normal pressure p at a particular instant of time is called the friction τ between these two bodies. Due to the existence of this stress corresponding strains take place in the layers of every body in contact with another; in addition heat is generated. The temperatures of the surfaces at the point of contact can be the same providing there is no extraneous layer (oil, oxidation, etc.), but in general they will be different. Let $\lambda_{i1}, \lambda_{i2}, v_{i1}, v_{i2}, T_1, T_2$ be the degrees of deformation on the surfaces, the intensities of rate of strain and the temperatures of the first and second bodies respectively. We can estimate the upper limit of the value of the frictional stress in the following way: let us suppose that on at least one of the bodies, say for example in the first body, plastic strains occur in the surface layer, and let us take $\tau_s(p, \lambda_i, v_i, T)$ as the yield point in shear of the first body for the existing values of λ_i, v_i, T. Then obviously

$$|\tau| \leqq \tau_s(p, \lambda_i, v_i, T),$$

since the shear stress at a point in the thin surface layer of this body (or in a layer parallel and close to the surface) is less than on the slipping surface at this point (the surface of maximum shearing stresses, Fig. 125). The equals sign will apply if the surface of contact for this body is a slip surface.

Thus the greatest possible value of the frictional stress is given by the expression

$$|\tau| = \tau_s(p, \lambda_i, v_i, T). \tag{4.14}$$

The function τ_S can be found from experiment, as has already been mentioned, and in particular can be expressed in terms of σ_S by the formula $\tau_S = \sigma_S/\sqrt{3}$. It was shown by Prandtl that for an ideally plastic material moving between rigid rough plates the flow boundary is a slip plane (or more precisely, an envelope of slip planes), and on this plane the shearing stress reaches the value τ_S. It is essential, however, for the normal pressure p on the surface to be greater than a certain value p_S.

The maximum frictional stress (4.14) is not affected by the degree of roughness of the surfaces; the reason for this is that slipping at

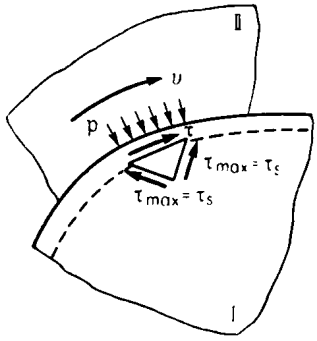

FIG. 125.

the limiting value of the frictional stress can take place either on the surface of contact or on a parallel surface within a thin layer of the body close to the surface of contact, the thickness of which in the case of a very rough surface will be greater than the undulations in the surface.

One of the basic mechanisms of dry surface friction on metal bodies is in fact the plastic deformation of a thin layer. As a result of the roughness of these surfaces, the compression acting on them and the relative slip even at low pressures, the surface is continually being worn away and further unevenness caused, i.e. the plastic deformation is accompanied by the tearing off of the "projections" in the surface to form new "hollows". In this process, of course, much depends on the crystal structure of the material, as this governs the formation of new "projections" and "hollows". At small pressures p the "hollows" will be only partly

filled, the number of "projections", which resist the pressure, will not be great and these "bearing" projections will be separated from each other, i.e. they will act independently. As a result of the pressure and sliding action plastic strains will occur in these projections and their carrying capacity under a pressure p will be directly proportional to the effective cross-sectional area F_p of all the "projections" per unit area of surface. Since the effective area in shear F_τ, which determines the carrying capacity of these projections for a shearing stress τ, is directly proportional to F_p, the frictional stress will be directly proportional to the pressure p (Coulomb's law):

$$|\tau| = \mu p. \tag{4.15}$$

The friction coefficient μ can be found in the following way: if σ_S is the mean yield point of the grains of the projections in compression, then $p = \sigma_S F_p$; denoting the shearing stress on F_p as τ_p, we have also that $\tau = \tau_p F_p$; thus we find that for small pressures

$$\mu = \frac{\tau_p}{\sigma_S}$$

and, since $\tau_p < \tau_S \approx \sigma_s/2$,

$$\mu \leqq 0{\cdot}5.$$

The discussion on which the derivation of formula (4.15) and the inequality $\mu \leqq 0{\cdot}5$ is based is only qualitative and is not to be taken as an accurate explanation; there are many other factors which could have been taken into account. But in practice formula (4.15) is widely used and is, in fact, the basis of the analysis of plastic flow in the presence of external friction.

Coulomb's law (4.15) can normally be applied not only to the case of dry friction, but also when there is oil present on the surfaces, and it also applies both for small and large pressures, up to values of τ given by formula (4.14). However, the frictional stress can have the values (4.14), (4.15) only at the points of contact of the surfaces where there is relative sliding. Moreover there might be points or lines of division of flow on the contact surface where the relative velocity is zero. Near these points and lines, therefore, there exist small areas with zero slip, which are called zones of total adhesion. In these zones there exists "static friction" and the stress $\tau < \mu p$, and at the points and lines of division of flow, due to symmetry, $\tau = 0$. Since the areas of the zones of adhesion are small, they are

often replaced by points or lines of division of flow, and are looked upon simply as changes in sign of the stress τ.

Formulae (4.14) and (4.15) are in effect the approximate law of surface friction widely used in the analysis of pressure working of metals. It can be represented mathematically as follows:

$$\left.\begin{aligned} \tau &= \mu p \operatorname{sign} v \quad \text{for} \quad p \leqq p_S \equiv \frac{\tau_S}{\mu}, \\ \tau &= \tau_S \operatorname{sign} v \quad \text{for} \quad p \geqq p_S, \end{aligned}\right\} \tag{4.16}$$

where sign $v = \pm 1$ is a symbol denoting that the friction stress acting on a given surface acts in the same direction as the movement of the surface of the other body relative to the given body. Since $\mu \leqq 0{\cdot}5$, p_S assumes the lower value:

$$p_S \geqq 2\tau_S \approx \sigma_S.$$

There is a great amount of literature dealing with the physical nature of surface friction, but further research is still needed. The friction coefficient μ depends on: (1) the state of the surface of the instrument causing the deformation; the higher the geometrical accuracy of this surface, the smaller is the coefficient of friction; (2) the lubrication of the surface, which reduces the coefficient of friction; in cold working processes various types of lubrication are used, for example fat oils, emulsions, etc; in hot working processes special pastes with graphite, glass, etc., are used; (3) the temperature of the surface; usually the friction coefficient μ increases as the surface temperature increases.

An experimental determination of the frictional stress τ and the friction coefficient μ, which occur during the plastic deformation of a piece of metal using a smooth instrument, is a complicated task, and is usually solved by indirected methods. In principle it is possible to make an accurate investigation of surface friction for soft materials at normal temperature if the instrument is made of optically active material, by finding the stresses on the friction surface by an optical method of stress analysis. It is possible to do this with metals by using special admixtures which come out on the surface of contact. In practice, however, indirect methods are normally used.

A very simple direct method would be as follows: a specimen C is compressed between the plates A and B of a press at constant speed v_1, and at the same time is displaced along the plate at a

given speed v_2 (Fig. 126). The ratio of the tangential force Q to the normal force P is the mean coefficient of friction on the contact surfaces $\mu = Q/P$. This is sometimes accepted as the true coefficient of friction which, however, depends upon a number of assumptions. In the first place, it is assumed that the coefficient of friction is independent of the pressure p, which is non-uniformly distributed over the surface of contact. Secondly, it is assumed that the conditions of lubrication are the same over the whole surface, whereas the pressure is variable and the conditions under which a

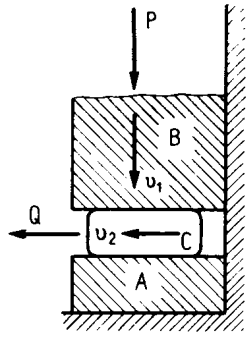

FIG. 126.

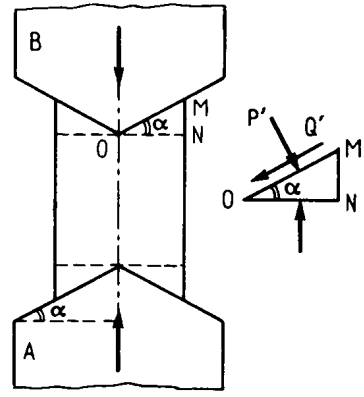

FIG. 127.

film of lubricant acts are therefore different at different points on the surface. Thirdly, even if $v_2 \gg v_1$, the sliding velocity at different points on the surface of contact differs both in magnitude and in direction, etc.

Another common method of finding μ is based on the compression of a cylindrical specimen between conical plates (Fig. 127). If a specimen of this sort is compressed between parallel plates, due to the friction at the ends, it will assume a barrel-like shape. If the angle α is chosen such that the specimen after compression retains its cylindrical shape, it is assumed that the coefficient of friction is equal to the tangent of this angle, i.e. $\mu = \tan \alpha$. Here again, we see that the first two of the above assumptions still apply, and in addition, the fact that the specimen retains its cylindrical shape is taken as evidence that it is in a state of simple axial compression. In this case, since the sum of the components in a radial direction

of the contact forces P' and $Q' = \mu P'$ acting on a sectorial element vanishes, we find that $P' \sin\alpha = Q' \cos\alpha$, i.e. $\mu = \tan\alpha$.

A number of other methods are based on the solution of simple problems on pressure working operations and will be dealt with later.

Table 6 gives values for the coefficient of friction of steel, copper and aluminium; it is assumed that the surface of the instrument is smooth and that the material is elastic.

TABLE 6. COEFFICIENTS OF FRICTION

Lubrication	T [°C]	μ		
		Steel	Copper	Aluminium
None	900–1200	0·3–0·5	–	–
	20	0·25–0·35	0·36	–
Machine oil	20	0·15–0·25	0·12	0·07
Oleic acid	20	–	0·06	0·04
Heavy oil and filings	900–1200	0·25–0·4	–	–

Table 7 shows the effect of high temperatures on the values of μ for steels.

TABLE 7. THE EFFECT OF TEMPERATURE ON μ

Material \ Temperature	700	800	900	1000	1100	1200
Steel 0·2% C	–	0·4	0·37	0·25	–	–
Steel 0·43% C	0·4	0·34	0·36	0·33	0·37	0·25
Steel Y7A	–	0·28	0·27	0·26	0·26	–
Steel Y12A	–	0·24	0·23	0·26	0·24	–

5. THE COMPRESSION OF A STRIP BETWEEN RIGID PLATES

As a simple example, let us consider the problem of compressing an infinitely long strip between two rigid plates A and B with parallel surfaces (Fig. 128). This problem was solved by Prandtl. The deformation will be plane: $u_x = u_x(x, y)$, $u_y = u_y(x, y)$,

$u_z = 0$. Consequently, from (4.4) $v_{zz} = v_{yz} = v_{zx} = 0$, and therefore, from (4.11), we have that:

$$\sigma_{xz} = \sigma_{yz} = 0,$$
$$\sigma_{zz} = \sigma = \tfrac{1}{3}(\sigma_{xx} + \sigma_{yy} + \sigma_{zz}),$$

so that $\sigma_{zz} = \sigma = \frac{1}{2}(\sigma_{xx} + \sigma_{yy})$, where σ_{xx}, σ_{yy} and σ_{xy} are functions only of x and y.

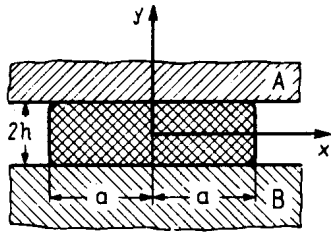

FIG. 128.

If $2h$ is the thickness of the strip, and $2a$ its width, then since the velocity of the plates is known, we have the kinematic boundary conditions

$$v = \pm \frac{dh}{dt} \quad \text{for} \quad y = \pm h(t). \tag{4.17}$$

Confining our attention to the case when $a/h \gg 1$ and when the plates are sufficiently rough, we shall assume that the regions on the surfaces of contact on which the law of dry friction (4.15) applies, and the regions of static friction (which due to symmetry are situated in the neighbourhood of the line $x = 0$, $y = \pm h$) are small compared to the regions on which the law of sliding $\tau = \tau_S \operatorname{sign} v$ applies. This leads to the boundary conditions for the stresses

$$\sigma_{xy} = \pm \tau_S \quad \text{for} \quad y = \mp h(t). \tag{4.18}$$

The condition of equilibrium of an element within the body (1.41) (§ 12, Chapter I), in the absence of mass forces, reduces to the two differential equations:

$$\left.\begin{aligned} \frac{\partial \sigma_{xx}}{\partial x} + \frac{\partial \sigma_{xy}}{\partial y} = 0, \\ \frac{\partial \sigma_{yx}}{\partial x} + \frac{\partial \sigma_{yy}}{\partial y} = 0. \end{aligned}\right\} \tag{4.19}$$

If the process takes place slowly so that the change in temperature and the influence of the rate of strain, as well as the effect of strain hardening on the mechanical properties of the material, can be ignored, we can put $\sigma_i = \sigma_S$, or, since $\sigma_S = \tau_S\sqrt{3}$ (§ 7, Chapter II) and since in this case $\sigma_i = (1/2)\sqrt{[(\sigma_{xx} - \sigma_{yy})^2 + 4\sigma_{xy}^2]}$, we obtain third relation between the stresses:

$$(\sigma_{xx} - \sigma_{yy})^2 + 4\sigma_{xy}^2 = 4\tau_S^2. \tag{4.20}$$

In this particular problem we shall assume that $\sigma_{xy} = f_1(y)$. Then, from the second equation of (4.19), we see that $\sigma_{yy} = f_2(x)$, and from (4.20), that $\sigma_{xx} = \sigma_{xx}(x, y)$ can then be represented as the sum

$$\sigma_{xx} = f_3(x) + f_4(y),$$

i.e. $\partial^2\sigma_{xx}/\partial x\,\partial y = 0$. Therefore, by differentiating the first equation of (4.19) with respect to y, we find that $\partial^2\sigma_{xy}/\partial y^2 = 0$, so that $\sigma_{xy} = cy + d$; here we must put $d = 0$, since from symmetry σ_{xy} must be zero at $y = 0$. Making use now of the boundary condition (4.18), we get that:

$$\sigma_{xy} = -\frac{\tau_S}{h}y.$$

We now see from the first equation of (4.19) that

$$f_3(x) = \frac{\tau_S}{h}x,$$

and consequently

$$\sigma_{xx} = \frac{\tau_S}{h}x + f_4(y)$$

$$\sigma_{yy} = f_2(x).$$

By substituting these values of σ_{xx}, σ_{yy} and σ_{xy} in eqn. (4.20), we arrive at the expression

$$\frac{\tau_S}{h}x + f_4(y) - f_2(x) = \pm 2\tau_S\sqrt{\left(1 - \frac{y^2}{h^2}\right)},$$

which is possible only if

$$\frac{\tau_S}{h}x - f_2(x) = b,$$

$$f_4(y) \mp 2\tau_S\sqrt{\left(1 - \frac{y^2}{h^2}\right)} = -b.$$

Consequently,

$$\sigma_{xx} = \frac{\tau_S}{h} x \pm 2\tau_S \sqrt{\left(1 - \frac{y^2}{h^2}\right)} - b, \quad \sigma_{yy} = \frac{\tau_S}{h} x - b.$$

Since at the edge of the strip $\sigma_{xx} = 0$ and $a/h \gg 1$ and $2\,[1 - (y^2/h^2)]$ is of the order of unity, then $b \approx \tau_S a/h$.

Retaining only the plus sign in the expression for σ_{xx}, we get finally that:

$$\left.\begin{aligned} &\sigma_{xx} = \tau_S \left[\frac{x}{h} + 2\sqrt{\left(1 - \frac{y^2}{h^2}\right)} - \frac{a}{h}\right]; \\ &\sigma_{yy} = \frac{\tau_S}{h}(x - a); \quad \sigma_{zz} = \tau_S \left[\frac{x}{h} + \sqrt{\left(1 - \frac{y^2}{h^2}\right)} - \frac{a}{h}\right]; \\ &\sigma_{xy} = -\frac{\tau_S}{h} y; \quad \sigma_{yz} = \sigma_{zx} = 0. \end{aligned}\right\} \tag{4.21}$$

The normal pressure $p = -\sigma_{yy}$ exerted by the plate on the strip increases linearly, and also rapidly, since $a/h \gg 1$, from the edges towards the centre of the strip. This confirms the assumption that the regions of dry friction are small. The resultant force P_1 per unit length of plate in the z-direction, which must be applied in order to compress the strip, is

$$P_1 = 2\int_0^a \sigma_{yy}\, dx = \frac{\tau_S a}{2h}.$$

Since $a/h \gg 1$ and $|y| \leqq h$, we see from expressions (4.21) that for areas at a sufficient distance from the line of division of flow $(x/h > 1)$ and from the edges of the strip $((a - x)/h > 1)$† the variation of the stresses σ_{xx} and σ_{yy} and, consequently, of the mean normal stress σ with variation of y, can be ignored, and that the deviator parts of the stresses σ_{xy} and $\sigma_{xx} - \sigma_{yy}$ are considerably less than the stresses σ_{xx} and σ_{yy} and the mean normal stress σ. On the basis of the first two of the relations (4.11) we conclude that on these same areas there is only slight variation in the magnitudes of the velocities v_{xx}, v_{yy} with variation in y.

Thus, generalizing these results and considering the plastic flow

† The remaining parts of the strip are small since $a/h \gg 1$.

of thin layers of arbitrary shape between rigid surfaces, we can assume as a simplification that:

1. the stress σ_3 normal to the surface of a layer does not vary over its thickness, and is equal to the pressure of the instrument on the layer: $\sigma_3 = -p$;

2. the stresses σ_1 and σ_2 on normal sections of the layer do not vary over its thickness and are equal in magnitude: $\sigma_1 \approx \sigma_2 = -q$;

3. the shearing stresses σ_{12} on the layer are small compared with σ_1 and σ_2 and, since they can be of the order of τ_S, they can be considered to be zero;

4. the lateral rates of flow of the plastic mass do not vary over the thickness of the layer.

From the first three assumptions, and from the condition that $\sigma_i = \sigma_S$, it follows that

$$p \approx q + \sigma_S. \tag{4.22}$$

6. Extrusion of Plates and Strips

Suppose that a strip of metal (Fig. 129) is extruded from between the rigid fixed walls of a die in a direction from right to left along the axis Ox. The origin of coordinates O will be taken as the inter-

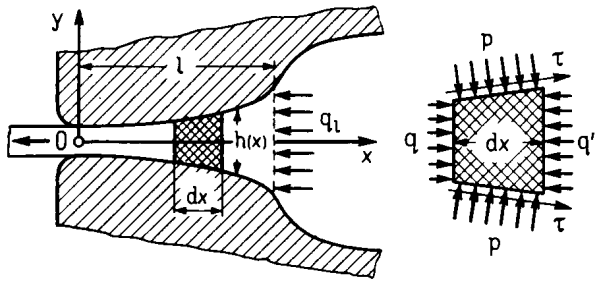

Fig. 129.

section of the outlet of the die with the axis Ox. The thickness $h(x)$ of the strip is equal to the gap between the walls and is a known function of x; we shall assume that it is small compared with the length l of the die, and that the tangent of the angle of inclination of the die dh/dx is small compared with unity.

The forces acting on an element dx of the strip are shown in Fig. 129. It is assumed that the width in the direction of the axis

Oz is considerably greater than 1, so that we can consider an element of unit width formed by sections at $z = z_0$ and $z = z_0 + 1$.

On the left-hand side of the element dx there will act a force $+qh$ along the axis Ox, and on the right-hand side a force $-(q + dq)(h + dh) = -qh - d(qh)$. On the lateral surface of the element dx there will act forces $p\,dx$ due to the pressure and frictional forces $\tau\,dx$. The former give a component $+p\,dh$ in the direction of Ox and the latter, due to the fact that the slope of the walls of the die is small, give a component $+2\tau\,dx$.

From the equilibrium condition for the element dx it follows that

$$-d(qh) + p\,dh + 2\tau\,dx = 0$$

or

$$\frac{dq}{dx} - \frac{p - q}{h}\frac{dh}{dx} - \frac{2\tau}{h} = 0. \tag{4.23}$$

At the exit from the die ($x = 0$) the strip is free-flowing, i.e. $q = 0$. At the section $x = l$ a pressure q_l must be applied to produce the strip, which is the quantity we wish to find.

If the friction coefficient μ between the strip and the walls of the die is less than 0·5 there will be a region of Coulomb friction adjoining the section $x = 0$. For, from the condition (4.22) we have that everywhere

$$p - q = \sigma_S \tag{4.24}$$

and therefore $p = \sigma_S$ at $x = 0$ and $\tau = \mu p < \tau_S \approx \sigma_S/2$. We shall put l_0 as the length of the region of Coulomb friction. Then for $0 \leqq x \leqq l_0$ we have that:

$$\tau = \mu p = \mu(q + \sigma_S), \quad 0 < x \leqq l_0. \tag{4.25}$$

Substituting (4.24) and (4.25) in (4.23), we get that:

$$\frac{dq}{dx} - \frac{2\mu q}{h} = \frac{\sigma_S}{h}\frac{dh}{dx} + \frac{2\mu\sigma_S}{h} \equiv \frac{\sigma_S}{h}\left(\frac{dh}{dx} + 2\mu\right). \tag{4.26}$$

The integral of this equation without the right-hand side will be

$$q = Cq(x), \quad q(x) = e^{2\mu\int_0^x \frac{dx}{h}}.$$

By the method of the variation of the parameter C we find the following general integral:

$$q = q(x)\left[D + \sigma_S \int \frac{1}{h}\left(\frac{dh}{dx} - 2\mu\right)\frac{1}{\varphi(x)}\,dx\right].$$

From the condition that $q = 0$ at $x = 0$ we find that for $0 \leqq x \leqq l_0$

$$q = \delta_S \varphi(x) \int_0^x \frac{1}{h}\left(\frac{dh}{dx} - 2\mu\right)\frac{1}{\varphi(x)}\,dx, \quad 0 \leqq x \leqq l_0. \quad (4.27)$$

At $x = l_0$ the Coulomb friction gives way to Prandtl friction, i.e. at $l = l_0$

$$\mu p \equiv \mu(q + \sigma_S) = \tau_S = \frac{\sigma_S}{2}$$

or $\mu q = (0{\cdot}5 - \mu)\,\sigma_S$. Thus l_0 can be found from the equation

$$\varphi(x) \int_0^{l_0} \frac{1}{h}\left(\frac{dh}{dx} - 2\mu\right)\frac{1}{\varphi(x)}\,dx = \frac{0{\cdot}5 - \mu}{\mu}. \quad (4.28)$$

Also, in the region $l_0 \leqq x \leqq l$ we find from (4.23) for $\tau = \tau_S = \sigma_S/2$, $p - q = \sigma_S$ that

$$q = C_1 + \sigma_S \int \frac{1}{h}\left(\frac{dh}{dx} + 1\right)dx = C_1 + \sigma_S\left(\ln h + \int \frac{dx}{h}\right),$$

where the constant C_1 can be found from the condition that the regions l_0 and $l - l_0$ are adjacent: $q = (0{\cdot}5 - \mu)/\mu$ at $x = l_0$. Thus we have finally that

$$q = \sigma_S\left[\frac{0{\cdot}5 - \mu}{\mu} + \ln\frac{h}{h_0} + \int_{l_0}^{x} \frac{dx}{h}\right], \quad l_0 \leqq x \leqq l, \quad (4.29)$$

where h_0 is the thickness at the section $x = l_0$, i.e. $h_0 = h(l_0)$. From this, by putting $x = l$, we can find the pressure q_l necessary to force the strip through the die:

$$q_l = \sigma_S\left[\frac{0{\cdot}5 - \mu}{\mu} + \ln\frac{h_l}{h_0} + \int_{l_0}^{l} \frac{dx}{h}\right], \quad (4.30)$$

where $h_l = h(l)$.

The distribution of the pressure p along the length of the die can be found from (4.27), (4.29) and (4.24); thus the die can be designed according to the methods of Chapter II; the power (force) required can be found by multiplying the pressure given by (4.30) by the total area in the yz plane at the section $x = l$.

The question of determining the rate of flow and the length of strip produced can be solved very simply by applying the condition of incompressibility. Suppose that v_l is the velocity of the material from right to left at the section $x = l$. From the condition that the volume per second passing any section is constant we find the velocity distribution

$$v = v_l \frac{h_l}{h}. \tag{4.31}$$

The length of the strip can be found from the condition that its volume is equal to the volume of material supplied at the section $x = l$.

This method can be applied to problems on the extrusion of thin-walled cylinders closed at one end (for example cartridge cases), and also to problems on the extrusion of long thin-walled tubes from short thick-walled tubes. If R is the mean radius of the tube produced, the area of the opening at $x = l$ will be $2\pi Rh$, and the force required to force the metal through the die will therefore be

$$Q = 2\pi Rh_l q_l, \tag{4.32}$$

where q_l is given by formula (4.30).

As an example, let us consider the extrusion of a thin-walled tube from a short section of a thicker tube of the same internal radius R. Let us suppose that h_1 is the thickness of the short tube, h_2 the thickness of the thin tube, and that the die is conical between these two thicknesses (Fig. 130):

$$h(x) = h_2 + \frac{h_1 - h_2}{l} x.$$

In order to simplify the calculations which follow from formula (4.27) and (4.30), we shall assume that there is no region of Coulomb friction and that $l_0 = 0$. In this case the specific pressure q_l can be found from formula (4.30), in which we must put $\mu = 0{\cdot}5$:

$$q_l = \left(1 + \frac{l}{h_1 - h_2}\right) \sigma_S \ln \frac{h_1}{h_2}. \tag{4.33}$$

The force on the section $x = l$ will be

$$Q = 2\pi Rh_1 \left(1 + \frac{l}{h_1 - h_2}\right) \sigma_S \ln \frac{h_1}{h_2}.$$

Let us suppose that a tube of radius $R = 10$ mm and thickness $h_2 = 2$ mm is to be produced from a section of a thick tube of titanium of internal radius $R = 10$ mm and external radius $R' = 15$ mm, i.e. the thickness $h_1 = 5$ mm. The angle of the die can be taken as 0·25 rad, so that $l = (h_1 - h_2) \cot 0{\cdot}25 = 11{\cdot}7$ mm.

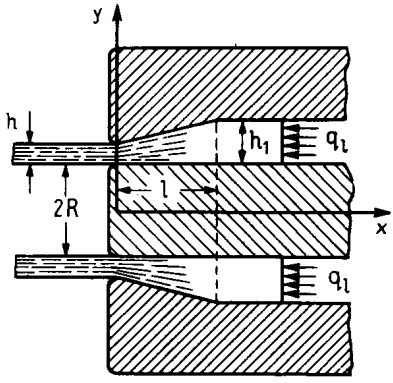

FIG. 130.

The force required will be

$$Q = 2\pi\, 10 \times 5(1 + \cot 0{\cdot}25) \ln \frac{5}{2} \sigma_S = 1420\sigma_S.$$

If the extrusion takes place at room temperature, for titanium $\sigma_S = 15{\cdot}4$ kg/mm^2 and $Q = 22$ (metric) tons. If it takes place at a temperature of 600°C, then $\sigma_S = 3{\cdot}9$ kg/mm^2 and $Q = 5{\cdot}5$ tons. The pressures will be respectively: in the first case $q_l = 69{\cdot}3$ kg/mm^2 and in the second, $q_l = 17{\cdot}5$ kg/mm^2. The maximum pressure on the wall of the die will be $p_l = q_l + \sigma_S$ and in the first case, therefore, $p_l = 84{\cdot}7$ kg/mm^2, i.e. 8470 atm, and in the second $p_l = 21{\cdot}4$ kg/mm^2, i.e. 2140 atm. The die must of course be designed on the basis of these pressures; it can be considered as a cylindrical thick-walled tube and analysed by making use of the formulae of § 7, Chapter III (Lamé's problem).

7. Flow over Rigid Plane Surfaces

A number of technological processes (stamping, pressing, etc.) can be considered as problems of the plastic flow of a metal over the rigid surfaces of the working parts of the machines (presses).

Let us examine the flow of a material between two rigid plane parallel plates, the distance h between which decreases with time. In solving this problem we shall make use of the results obtained in § 5, when we were considering the case of the compression of a strip of metal. We shall work with a system of rectangular co-ordinates Oxy on the working surface of the upper plate and consider an element of material of dimensions dx and dy in plan and of height h. The forces (per unit area) acting on the edges of the element are shown in Fig. 131. Since from the fourth conclusion

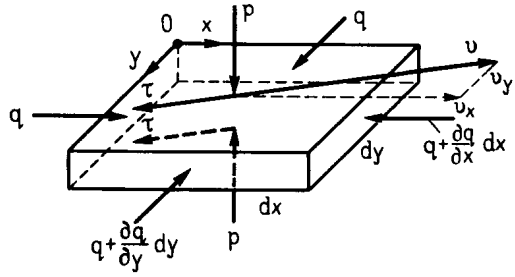

FIG. 131.

of § 5 the rate of flow can be considered to be constant over the thickness of the layer, and since the friction force acts in an opposite direction to the flow, the values of τ are the same in magnitude and direction on the upper and lower edges of the element. Putting v_x and v_y as the components of the velocity v, and resolving the forces acting on an element of material along the axes Ox and Oy, we have the following equilibrium conditions:

$$\frac{\partial q}{\partial x} dx h\, dy + 2\tau\, dx\, dy \frac{v_x}{v} = 0,$$

$$\frac{\partial q}{\partial y} dy h\, dx + 2\tau\, dx\, dy \frac{v_y}{v} = 0,$$

from which, after dividing by $h\, dx\, dy$, we get that:

$$\left.\begin{aligned} \frac{\partial q}{\partial x} &= -\frac{2\tau}{h}\frac{v_x}{v}, \\ \frac{\partial q}{\partial y} &= -\frac{2\tau}{h}\frac{v_y}{v}. \end{aligned}\right\} \tag{4.34}$$

Squaring and adding, we find that:

$$\left(\frac{\partial q}{\partial x}\right)^2 + \left(\frac{\partial q}{\partial y}\right)^2 = \frac{4\tau^2}{h^2}, \tag{4.35}$$

where τ is a function of the pressure p of the plate on the material. According to (4.22) $q = p - \sigma_S$. Thus from (4.35) we get that:

$$\left(\frac{\partial p}{\partial x}\right)^2 + \left(\frac{\partial p}{\partial y}\right)^2 = \frac{4\tau^2(p)}{h^2}. \tag{4.36}$$

This is the basic differential equation which, together with the boundary conditions on the edges of the material and the friction conditions on the surfaces, gives the pressure p, and consequently, the required force (the capacity of the press). From (4.22) $p \geqq \sigma_S$.

It is convenient to introduce the concept of a generalized pressure P on the basis of the expression

$$P = \int_{\sigma_S}^{p} \frac{dp}{2\tau(p)}; \tag{4.37}$$

then, instead of eqn. (4.36), we will have

$$\left(\frac{\partial P}{\partial x}\right)^2 + \left(\frac{\partial P}{\partial y}\right)^2 = \frac{1}{h^2}, \quad \text{i.e.} \quad (\text{grad } P)^2 = \frac{1}{h^2}, \tag{4.38}$$

where grad $P = \partial P/\partial x\, \boldsymbol{i} + \partial P/\partial y\, \boldsymbol{j}$, and instead of eqns. (4.34) we can write:

$$h \text{ grad } P = -\boldsymbol{V}^0, \tag{4.39}$$

where $\boldsymbol{V}^0$ is the unit vector of the velocity of flow.

Let us consider now the boundary conditions. If the boundary (the edges) of the material is free, then $q = 0$ there, and from (4.22) $p = \sigma_S$ and from (4.37) $P = 0$. Thus on a free edge

$$P = 0. \tag{4.40a}$$

If the material encounters a fixed obstacle, the velocity of flow at that point becomes tangential. Consequently, from (4.39) on a fixed boundary

$$\frac{\partial P}{\partial \nu} = 0, \tag{4.40b}$$

where ν is the normal to the boundary. If on one of the plates there is a groove or opening, and if the material flows into it, $q = \sigma_S$, i.e. here, from (4.22), $p = 2\sigma_S$. Thus the boundary condition in the case of a groove is of the form

$$P = \int_{\sigma_S}^{2\sigma_S} \frac{dp}{2\tau(p)} = \text{const}. \tag{4.40c}$$

If, finally, the groove has a finite (in general, variable) depth, then the material which has reached the bottom of the groove will prevent any further inflow of material. In this case, evidently,

$$P = P(s), \tag{4.40d}$$

where s is the length of arc along the boundary obstructing flow.

Let us now consider the following problem. Suppose that dry sand is sprinkled onto a horizontal plate of finite dimensions until it starts to overflow the edges, or flow over a vertical framing if one is set up around the edges of the plate. The surface of the heap of sand so formed will have rectilinear generators the inclination of which to the horizontal will be given by the coefficient of internal friction f of the sand: the tangent to the angle of inclination of a generator is equal to the coefficient of internal friction. Therefore, the equation of the surface of the heap of sand is of the form

$$(\text{grad } z)^2 = f^2, \tag{4.41}$$

where z is the distance along the vertical from the surface of the plate, which contains the axes Ox and Oy.

By comparing eqns. (4.38) and (4.41) we can establish the sand heap analogy† for the problem of flow over rigid surfaces, according to which the distribution of the generalized pressure P is of the same form as the surface of a sand heap, so that

$$P = \frac{z}{fh}.$$

To complete the analogy let us compare the boundary conditions. Condition (4.40a) corresponds to the free edge of the plate along which $z = 0$. Condition (4.40b) corresponds to a vertical framing sufficiently high to prevent overflow, so that $\partial z/\partial v = 0$. Condition (4.40c) corresponds to a frame of constant finite height along which $z = \text{const.}$, and over which the sand does flow, so that $\partial z/\partial v \neq 0$. Condition (4.40d) corresponds to a frame of variable height around the edge of the plate.

Let us transform eqn. (4.38) into curvilinear coordinates r and ψ, which are given by the expressions

$$\left.\begin{aligned} x &= \pm[r-\varphi(\psi)]\sqrt{[1-\varphi'^2(\psi)]}, \\ y &= \psi + [r-\varphi(\psi)]\varphi'(\psi), \end{aligned}\right\} \tag{4.42}$$

† A. A. Ilyushin, *Prikladnaya Matematika i Mekhanika* (Applied Mathematics and Mechanics) No. 6, 1955.

where φ is an arbitrary function of ψ. The coordinates r, ψ are orthogonal, so that in the first quadratic form

$$dx^2 + dy^2 = dr^2 + [1 - \varphi'^2 + (r - \varphi)\varphi'']^2 \frac{d\psi^2}{1 - \varphi'^2}$$

there is no term containing $dr\,d\psi$. When $\psi = \text{const.}$, the elimination of r from the expressions for x and y in terms of r and ψ leads to the equation of a straight line. Thus the lines $\psi = \text{const.}$ are straight lines. Equation (4.38) becomes

$$\left(\frac{\partial P}{\partial r}\right)^2 + \frac{1 - \varphi'^2}{[1 - \varphi'^2 + (r - \varphi)\varphi'']^2}\left(\frac{dP}{\partial \psi}\right)^2 = \frac{1}{h^2}.$$

But φ is an arbitrary function of ψ. This equation can therefore be satisfied for any value of ψ only if P does not depend on ψ. Consequently we have the following equation for P:

$$\frac{dP}{dr} = \pm \frac{1}{h},$$

the general solution of which is

$$\pm hP = r + C. \tag{4.43}$$

The expression (4.43) means that the lines $r = \text{const.}$ are lines of equal P and the lines $\psi = \text{const.}$ are flow lines, which are straight. By analogy with the sand heap we see that the flow lines coincide with the projections of the rectilinear generators—the lines of greatest slope, and the lines of equal P, with the horizontals in the surface of the heap. The lines or points of division of flow coincide with the projections of the edges (ridges) or the apexes of the sand heap.

The constant C in (4.43) can be found from the condition that $P = P_B$ on the edge of the plate where P_B is given by one the eqns. (4.40). As a result we have that

$$P = P_B \pm \frac{r_B - r}{h}, \tag{4.44}$$

where r_B is the distance from the origin of r to the point on the boundary. Thus, in order to find the generalized pressure it is in effect necessary to know the distribution of the flow lines (which can be determined by analogy with the sand heap) and the boundary conditions. Since the flow lines are straight, it is sufficient to find only their angles of intersection with the boundary. Since P

corresponds to the surface of the sand heap, the angle between the direction of a flow line and the direction of the arc of the boundary can be found from the expression

$$\cos(r, s) = \frac{dP_B/ds}{dP/dr}$$

or, on account of (4.43),

$$\cos(r, s) = \pm h \frac{dP_B}{ds}. \tag{4.45}$$

In the case of a free edge or a groove $dP_B/ds = 0$, and therefore the flow lines are normal to the boundary, which, of course, is obvious from the sand heap analogy. In formula (4.44) $r_B - r$ is in modulus the distance from the boundary to the point considered, measured along the line of flow. Thus, if we denote this distance by ξ, then

$$P = P_B + \frac{\xi}{h}. \tag{4.46}$$

In the region of dry (Coulomb) friction we have that $\tau(p) = \mu p$, and consequently, by definition (4.37)

$$p = \sigma_S e^{2\mu P} \quad \text{for} \quad p < p_S = \frac{\sigma_S}{2\mu}.$$

This region is contiguous with the boundary. Making use of (4.46), we have in the region of Coulomb friction that

$$p_K = p_B e^{2\mu\xi/h} \quad \text{for} \quad 0 \leqq \xi \leqq \xi_S = \frac{h}{2\mu} \ln \frac{\sigma_S}{2\mu p_B}, \tag{4.47}$$

where $p_B = \sigma_S e^{2\mu p_B}$ is the pressure p at the edge. The value of ξ_S for which solution (4.47) applies can be found from the condition that $p_K = p_S \equiv \sigma_S/2\mu$ for $\xi = \xi_S$. In the region where $\xi > \xi_S$ there is Prandtl friction: $\tau(p) = \tau_S = \sigma_S/2$. In this case the integral in (4.37) must be considered as an indefinite quantity

$$P = \frac{p}{\sigma_S} + A,$$

and the constant of integration A must be found in conjunction with (4.47). From the latter we have that

$$P_S = \frac{1}{2\mu} \ln \frac{P_S}{\sigma_S} = \frac{1}{2\mu} \ln \frac{1}{2\mu},$$

and therefore

$$\frac{1}{2\mu} + A = \frac{1}{2\mu} \ln \frac{1}{2\mu},$$

$$A = \frac{1}{2\mu}\left(\ln \frac{1}{2\mu} - 1\right) = -\frac{1}{2\mu}(1 + \ln 2\mu).$$

Thus, for $\xi > \xi_S$

$$p = \sigma_S\left[P + \frac{1}{2\mu}(1 + \ln 2\mu)\right],$$

where, according to (4.46), P is given by:

$$P = P_S + \frac{\xi - \xi_S}{h} = \frac{1}{2\mu} \ln \frac{1}{2\mu} + \frac{\xi - \xi_S}{h} = \frac{\xi - \xi_S}{h} - \frac{1}{2\mu} \ln 2\mu.$$

Consequently, in the region of Prandtl friction we have that:

$$p_p = \sigma_S\left(\frac{\xi - \xi_S}{h} + \frac{1}{2\mu}\right) \quad \text{for} \quad \xi > \xi_S. \tag{4.48}$$

Since we are not taking into account the region of static friction, formulae (4.47) and (4.48) define completely the pressure distribution.

8. Examples

1. A circular plate. If the boundary is a free edge or a circular groove the flow lines in both cases will be radial, and the lines of equal pressure will be concentric circles. The line of division of flow will in fact be a point—the centre of the plate.

In the case of a free edge $q_B = 0$ and $p_B = \sigma_S$. The boundary of dry friction is a circle of radius r_S, and from (4.47)

$$a - r_S = \frac{2}{2\mu} \ln \frac{1}{2\mu}, \quad r_S = a - \frac{h}{2\mu} \ln 2\mu.$$

It can be seen that for $\mu = 0{\cdot}5$, $r_S = a$, i.e. there will be no region of dry friction. For $r > r_S$

$$p_K = \sigma_S e^{2\mu(a-r)/h},$$

and for $r \leqq r_S$

$$p_p = \sigma_S\left(\frac{r_S - r}{h} + \frac{1}{2\mu}\right) = \sigma_S\left[\frac{1}{2\mu}(1 + \ln 2\mu) + \frac{a - r}{h}\right].$$

The pressure distribution along a diameter is of the form shown in Fig. 132.

The resultant force is given simply by

$$Q = \int_a^{r_s} p_K 2\pi r\, dr + \int_{r_s}^0 p_p 2\pi r\, dr.$$

Let us suppose now that at the edge $q_B = q_l$, $p_B = q_l + \sigma_S$, and that q_l is sufficiently large for there to be no region of dry friction. We then see from (4.37) that $P_B = q_l/\sigma_S$, and, therefore,

$$p = q_l + \sigma_S + \sigma_S \frac{a - r}{h}, \tag{4.49}$$

i.e. the pressure is distributed linearly along a radius.

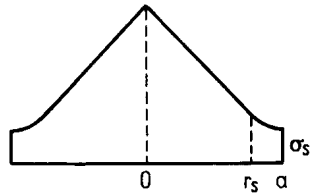

FIG. 132.

2. The extrusion of a cartridge case. By making use of this last solution and the example in § 6, we can determine approximately the force required to extrude a cartridge case from a cylindrical piece of metal (Fig. 133). A mandrel B with a conical end is inserted into the opening of the die A. The material is forced through the die by the piston C.†

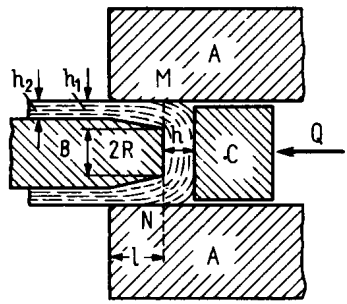

FIG. 133.

On the section MN there will be a pressure q_l given by formula (4.33). This must be substituted in formula (4.49) in order to find the pressure on the piston

$$p = \left(1 + \frac{l}{h_1 - h_2}\right)\sigma_S \ln \frac{h_1}{h_2} + \sigma_S + \sigma_S \frac{R + h_1 - r}{h}. \tag{4.50}$$

† This is the so-called direct method of extrusion; in back extrusion the piston C is fixed and the mandrel B moves to the right.

Here h is the thickness of the base of the cartridge. The greatest pressure is required at the end of the operation when h becomes a minimum. The total force required is

$$Q = \int_0^R p\, 2\pi r\, dr = \sigma_S \pi R^2 \left[1 + \frac{2}{3}\frac{R}{h} + \left(1 + \frac{l}{h_1 - h_2}\right) \ln \frac{h_1}{h_2}\right].$$

In the case of steel EI 123 we have that $\sigma_S = 19{\cdot}3$ kg/mm^2 at 20°C and $\sigma_S = 11{\cdot}4$ kg/mm^2 at 800°C. If $h_1 = 5$ mm, $h_2 = 2$ mm, $l = 12$ mm, $R = 15$ mm, $h = 8$ mm, for cold working we get that $Q = 75$ tons; for extrusion at 800°C, $Q = 44{\cdot}3$ tons.

3. A strip of metal. This problem was considered in § 5. With the axes arranged as shown in Fig. 128 the flow lines are the straight lines $z = \text{const}$. The sand heap would be the shape of a pitched roof, and the distribution of the generalized pressure is linear with respect to x. The boundary of the region of dry friction x is given by the expression

$$a - x_S = \frac{h}{2\mu} \ln \frac{1}{2\mu},$$

where $2a$ is the width of the strip. According to (4.47) and (4.48) the pressure distribution will be:

$$p_K = \sigma_S e^{2\mu(a-x)/h} \quad \text{for} \quad x_S \leqq x \leqq a,$$

$$p_p = \sigma_S \left(\frac{x_S - x}{h} + \frac{1}{2\mu}\right) \quad \text{for} \quad x \leqq x_S.$$

The pressure distribution curve with respect to x is shown in Fig. 134a. Fig. 134b shows the pressure distribution on the surface of a lead strip with $a/h = 8$ determined experimentally at the Central Scientific Research Institute of Technology and Engineering (TSNIITMash).

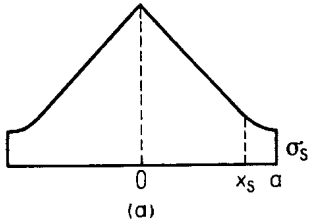

(a)

FIG. 134a.

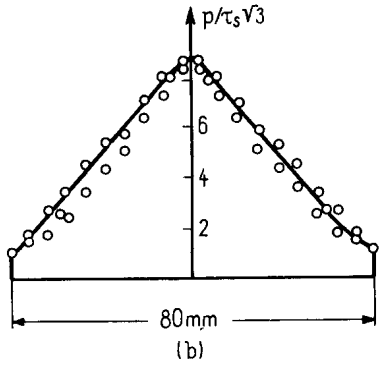

(b)

FIG. 134b.

4. A ribbed plate. This is an important structural element as it possesses considerable strength for only a small weight. Only very plastic materials can be used for pressed ribbed plates, and the theoretical analysis given below always

requires to be checked by experiment, since cracks are very likely to occur in the proximity of the ribs.

One of the plates of the press used in these operations contains parallel grooves of width δ at a distance $2a$ apart, into which the metal can flow freely (Fig. 135a). Considering a strip of width $2a$ between the grooves, we have, on the boundary coincident with the edges of the grooves, the condition that $q = \sigma_S$, $p = 2\sigma_S$. The sand heap is of the form shown in Fig. 135b. The line of division of flow, which is the projection of the ridge of the heap on the (xy) plane, lies in the centre of each strip.

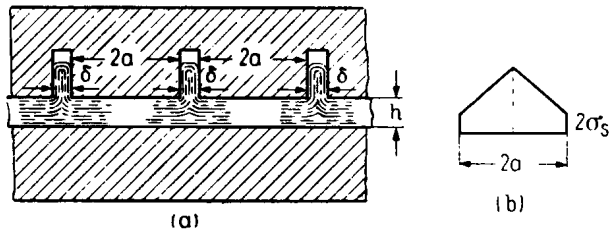

FIG. 135.

Since from (4.47) $p_K \geqq p_B$, and since in this case $p_B = 2\sigma_S$ there can exist regions of dry friction only for conditions of very good lubrication. Let us suppose that there are no such regions. Then (from 4.37) $p_B = 1$ and

$$p = \sigma_S\left(2 + \frac{a - x}{h}\right).$$

Per unit length of the strip of width $2a$ we have that

$$Q_1 \quad 2\int_0^a p\,dx = 2\sigma_S\left(2a + \frac{a^2}{2h}\right) = 4a\sigma_S\left(1 + \frac{a}{4h}\right).$$

If $2a = 10$ cm, $h = 1$ cm, $\sigma_S = 500$ kg/cm^2, we get that $Q_1 = 22{\cdot}5$ tons/cm. If we wish to form a plate 1 m $\times$ 1 m the force required would be $Q = 22{\cdot}500$ tons.

5. A plate with a square network of stiffening ribs. Here again $p = 2\sigma_S$ on the edge of a groove, and if there is no region of dry friction we have, as in the previous case, that

$$p = \sigma_S\left(2 + \frac{a - x}{h}\right) = \sigma_S\left(2 + \frac{\xi}{h}\right),$$

which applies in each of the four triangles into which the square is divided by the projections of the edges of the sand heap, which, in this case is the shape of a pyramid with apex O in the centre (Fig. 136). The diagram of distribution of the pressure p is of the same shape, where

$$OH = p_{\xi = a} = \sigma_S\left(2 + \frac{a}{h}\right).$$

The total force acting on one square panel is given by the volume of the pyramid in Fig. 136:

$$Q_1 = 8a^2\sigma_s\left(1 + \frac{a}{6h}\right). \tag{4.51}$$

With the data of the previous example $Q_1 = 183$ tons. On a square plate 1 m × 1 m there are 100 such panels. Thus the total force required is $Q = 18{,}300$ tons.

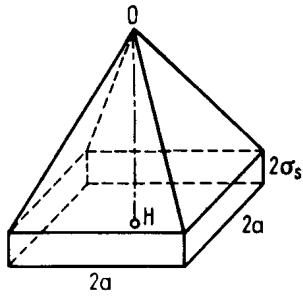

FIG. 136.

Let us suppose that we wish to form a plate with stiffening ribs of uniform height. We note that the central parts of the ribs in each bay will fill most rapidly. As soon as the material reaches the bottom of the groove any further inflow will be resisted, so that formula (4.51) applies only to the case of very deep grooves. The most restricted flow will occur in the grooves where they intersect, when the grooves have already been filled over their entire length. In finding the compressive force required we can make use of the sand heap analogy if we imagine the plate on to which the sand is poured to contain holes at the corners of the squares. If we consider these holes as points, the surface of the sand heap is the shape formed by the intersection of cones. The shape of the sand heap for one panel is shown in Fig. 137.

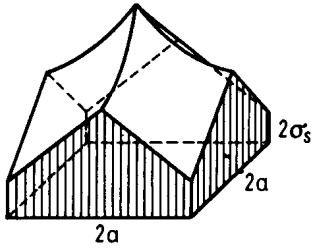

FIG. 137.

It can be shown that the force required is almost twice as large as that found above.

CHAPTER V

CREEP OF MATERIALS

1. Dependence of the Properties of Materials on Time

As was pointed out in Chapter II, the stresses and strains which arise in a body under load depend not only on the magnitude of the load, but also on the way in which the load varies with time. This is associated with the fact that the physical state of a body which is reached after a comparatively rapid application of load is not the equilibrium state for microvolumes, and that the regrouping of molecules and atoms from their initial to their final positions, corresponding to the equilibrium arrangement for given external conditions, requires a comparatively long interval of time, since a number of the necessary transition processes take place only slowly. The way in which the mechanical properties of materials depend on time can, therefore, be illustrated most clearly by the two extreme cases: (1) very rapid deformation, when there can be a time lag even in the most rapid transition processes, and (2) the case when the load is applied for a very long time, after which the effect of all the various microscopic and sub-microscopic mechanisms becomes evident. The behaviour of materials under impulse loading such as impact, explosion, etc., will be considered in the next chapter. In the present chapter we shall be mainly concerned with phenomena which take place in materials under load during a reasonably long interval of time.

(a) The visco-elastic behaviour of materials. The proportionality between stresses and strains which is illustrated, for example, by tensile tests on a cylindrical specimen is not exact and has definite deviations, these deviations being such that on removal of the external load the specimen is restored to its initial state, but the stress–strain curves for loading and unloading are, in general, different. For the majority of metals at normal temperatures and at the rates of deformation of the normal testing machines these

deviations from proportionality are not great and can often be ignored. They are, however, particularly noticeable in materials of organic origin, and they should not be confused with non-linear elasticity. Many high polymers, for example, rubber, possess the property of non-linear elasticity, which is illustrated by non-linearity of the relation between stresses and strains both for increase and for decrease in load. The loading curve, however, is almost coincident with the unloading curve, so that during the loading–unloading cycle no dissipation of energy occurs. In contrast to this, the non-linearity we shall be considering here is associated with the irrecoverable loss of energy in deforming the material. It is, of course, inherent also in the above non-linearly elastic materials. Quantitative relations between stresses and strains, which take into account this type of non-linearity, are often of the form that might be expected if, in addition to the basic properties of elasticity (linear or non-linear), which apply to the majority of solid bodies for small strains, the material possessed the properties of a viscous liquid. This aspect of the properties of materials is known as visco-elastic behaviour. We sometimes speak also of elastic recovery or time lag of the elastic properties.

The physical micromechanism of this phenomenon has not been investigated sufficiently in a quantitative respect. There exist results, mainly of a qualitative nature, which suggest that the visco-elastic behaviour of a material is associated with defects in the crystal lattice, with diffusion of atoms and with the flow of intergranular layers. Without going into this aspect of the problem, we will show that the visco-elastic behaviour of a material can be described in a simplified way with the aid of the following mechanical model (Focht's model).

Let us suppose that an ideally elastic spring is connected in parallel through a rigid system with a piston which moves in a cylinder containing a viscous liquid (Fig. 138). If the stiffness of the spring is equal to the Young's modulus E of the material we are investigating, the force which must be applied to the ends of the spring in order that it experiences a relative extension ε is $E\varepsilon$. The force exerted by the liquid in resisting the motion of the cylinder is directly proportional to the velocity of the piston; we shall denote the coefficient of proportionality by η. If we consider the resistance of the spring–dash-pot system as a stress σ, and the relative change in the distance between points A and B as a strain, the $\sigma \sim \varepsilon$

relation can be written in the form

$$\sigma = E\varepsilon + \eta\dot{\varepsilon}, \tag{5.1}$$

where $\dot{\varepsilon} = d\varepsilon/dt$ is the rate of strain.

The behaviour under load of the solid body so depicted can be investigated if σ is given as a function of time (if the variation of the loads applied to the body is given) by integrating the normal

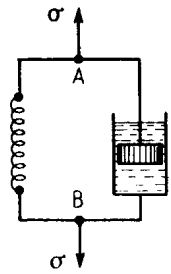

FIG. 138.

differential equation (5.1) for ε, or if $\varepsilon(t)$ is given (for given kinematic boundary conditions), by finding the magnitude of $\sigma(t)$ from (5.1). As an example, let us consider the case when a longitudinal force, which thereafter remains constant, is applied to a cylindrical rod at an instant $t = 0$. If we neglect the change in cross-section of the rod during deformation, we see that the rod is subjected to a constant tensile (or compressive) stress σ_0 starting from the instant $t = 0$. By integrating eqn. (5.1) and taking into account that $\varepsilon = 0$ at $t = 0$, we get that

$$\varepsilon = \frac{\sigma_0}{E}(1 - e^{-t/T}), \tag{5.2}$$

where by definition $T = \eta/E$. If the material is non-viscous ($\eta = 0$ and therefore $T = 0$) a strain $\varepsilon_0 = \sigma_0/E$ instantly occurs, which corresponds to elastic behaviour of the material. If the material is viscous ε_0 is reached only when $t \to \infty$. The curve of $\varepsilon = \varepsilon(t)$ is asymptotic to the line $\varepsilon = \varepsilon_0$ (Fig. 139).

If now at an instant $t = t_1$, the load is suddenly removed ($\sigma = 0$ for $t > t_1$) then, as can easily be seen by integrating (5.1) with $\sigma = 0$ and with the condition that ε has a value given by (5.2) for $t = t_1$, we get that for $t > t_1$,

$$\varepsilon = \frac{\sigma_0}{E}(1 - e^{-t_1/T})e^{\frac{t_1 - t}{T}},$$

so that $\varepsilon \to 0$ as $t \to \infty$. The curve of $\varepsilon = \varepsilon(t)$ for $t < t_1$ and for $t > t_1$ is shown in Fig. 139.

The constant T is usually called the period of recovery. It is the interval of time (starting from t_1) required for the strain to decrease e times.

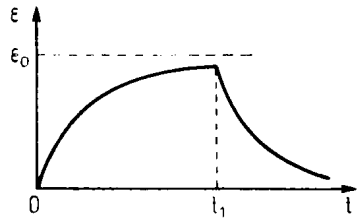

FIG. 139.

Without mentioning at present any other defects of Focht's model, we might note that it gives no explanation of relaxation of stress.

(b) Relaxation. If a solid body is rapidly deformed by some means, and if then its bounding surfaces are rigidly fixed so that the state of strain remains constant with time, the state of stress will alter and the magnitude of the stresses will decrease. For example, the force required to hold a rod at a given extension would decrease with time, at first rapidly, and then more slowly, tending to some limiting value. This continuous decrease in stress is known as relaxation. For the majority of metals relaxation is only slight at normal or low temperatures and becomes evident only at elevated temperatures. But in some metals (for example, lead, the recrystallization temperature of which is approximately room temperature) and also in materials of organic origin (plastics, rubber, etc.), this effect is noticeable even at normal temperature.

A model which represents in a simple manner the phenomenon of relaxation (Maxwell's model) is shown in Fig. 140 and comprises a spring and dash-pot joined together in series. The rate of relative extension ε_1 of the spring is related to the rate of change of load (stress) σ by the expression $\dot{\varepsilon}_1 = \dot{\sigma}/E$ and the rate of extension ε_2 of the dash-pot by the expression $\dot{\varepsilon}_2 = \sigma/\eta$. Thus for a material corresponding to this model, we have the following relation between stress and strain

$$E\frac{d\varepsilon}{dt} = \frac{d\sigma}{dt} + \frac{\sigma}{T}, \tag{5.3}$$

where the constant $T = \eta/E$ is called the period (time) of relaxation.

Let us consider a rod, the mechanical properties of which are described by (5.3), loaded in such a way that the strain is $\varepsilon_0 = \sigma_0/E$,

FIG. 140.

and let us imagine the rod to be fixed at an extension corresponding to this strain. If we integrate (5.3) as a differential equation in σ with the initial condition that $\sigma = \sigma_0$ at $t = 0$, we get that $\sigma = \sigma_0 e^{-t/T}$. Thus the stress tends to zero as $t \to \infty$. The period of relaxation is the time required for the instantaneous value of the applied stress to decrease e times.

The graph showing the change of stress with time at constant strain is called the relaxation curve. A number of curves for red copper at temperatures of 165 and 235°C, derived experimentally by Davis, are shown in Fig. 141. The initial portions of these

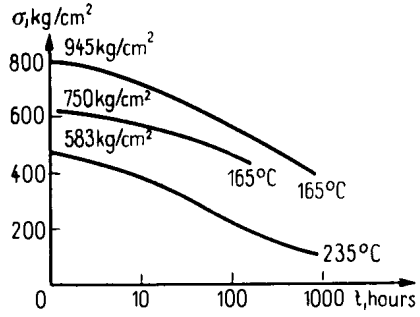

FIG. 141.

curves lie so close to the σ-axis that they are regarded as cutting it, and the initial stress is therefore indicated on each curve. The

behaviour of the relaxation curves in the initial time interval can be seen from the curves in Fig. 142 for cellulose acetate butyrate, derived recently by Watson, Kennedy and Armstrong.

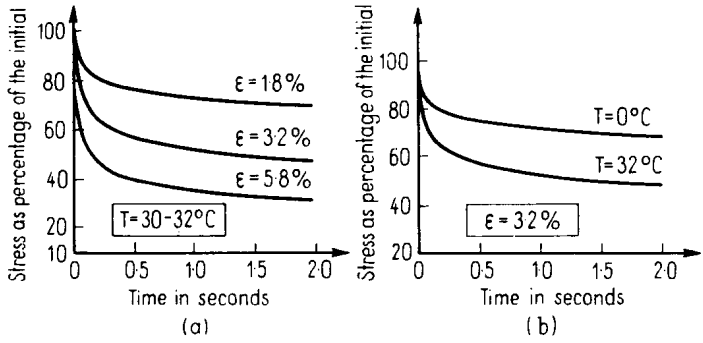

FIG. 142.

In analysing these curves we should note that: (a) the rate of relaxation (the slope of the tangent to the relaxation curve at a particular point) at corresponding instants of time during the experiment is greater, the greater is the initial stress (i.e. the greater the fixed strain), (b) that the rate of relaxation decreases with time and (c) that the stress during the relaxation tends to a finite value and not to zero, as is suggested by Maxwell's model.

Like Focht's model, Maxwell's model also does not conform satisfactorily with experiments on real bodies. These models do, however, represent qualitatively certain aspects of the behaviour of materials. In order, therefore, to portray the actual behaviour of materials these models are generalized: a number of Focht's models are combined in series and in parallel with a number of Maxwell's models.

A mathematical generalization of (5.1) and (5.3) is the expression

$$P_n\{\sigma\} = Q_{n+1}\{\varepsilon\}, \tag{5.4}$$

where P_n and Q_{n+1} are linear differential operators with respect to t of orders n and $n + 1$. The coefficients in these operators, in the same way as the coefficients E and η in the expressions (5.1) and (5.3), depend on temperature. Sometimes relaxation processes can be described by integral relations of the form

$$\sigma(t) = E\varepsilon(t) - \int_{-\infty}^{t} R(t - \tau)\,\varepsilon(\tau)\,d\tau. \tag{5.5}$$

Here the first term in the right-hand side is the instantaneous value of the stress, i.e. the value which the stress would have reached if the strain $\varepsilon(t)$ had been reached instantaneously. The second term takes into account the whole past history of the process. The form of $R(t)$, which plays the part of a "memory function", depends on the properties of the material and on the temperature.

(c) Creep. The irreversible change with time in the deformed state of a body at a constant load is known as creep. This phenomenon is observed in all materials, but for the majority of metals at room temperature and at low temperatures changes in strain take place so slowly that they can be ignored. The creep of plastics, rubber and other materials of organic origin and also soils is, however, noticeable at room temperature. In structural metals creep becomes noticeable at temperatures of 300–400°C, and at a temperature of about 800 C normal steels become practically useless due to their rapid creep. It is for this reason that heat-resistant alloys are made.

In order to derive quantitative characteristics of creep, cylindrical specimens are usually tested in tension at a constant value of the load and at constant temperature. In some cases, when the change in cross-sectional area of the specimen due to creep becomes noticeable, special apparatus is used in order to maintain the tensile stress at a constant value. The diagram of relative extension of the specimen against time at a constant load is called the creep

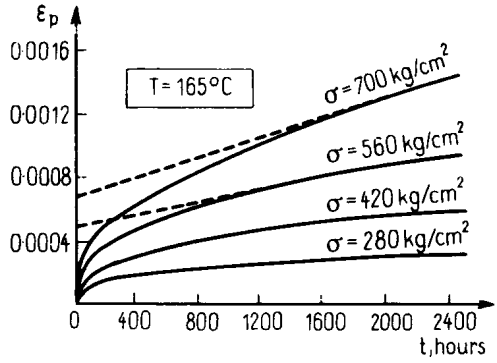

FIG. 143.

curve. Figure 143 shows a number of creep curves for red copper obtained by Davis. In these curves the values of the plastic part of the deformation are set out along the ordinate axis, and the origin

for each curve has been displaced by the magnitude of the strain (elastic or elasto-plastic) which occurs at the initial instant of application of the load. It can be seen that as the stress increases (its value is indicated on each curve) the rate of creep $\dot{\varepsilon}_p = d\varepsilon_p/dt$ increases, and that the creep curves for different stresses have approximately the same shape.

With increase in time the rate of creep for a given stress decreases monotonically, tending to some finite limiting value. At low stresses the rate of creep is so small and the creep strain so slight that it can be ignored. In this connection we talk of a limiting creep stress, which is the maximum stress for which creep strains can still be ignored.

For example, for the components of machines the maximum permissible creep strains are those not exceeding 1 per cent after the life of the machine. The limiting creep stress depends on the temperature. The question as to whether there exists an actual limiting creep stress, as the greatest stress at which creep strains are totally absent, remains unsolved. The fact remains that in certain materials creep takes place even at very low stresses.

We note that each of the curves of Fig. 143 has two characteristic parts: (1) a region of initial (unsteady) creep, in which the rate of creep varies rapidly, and (2) a region in which the rate of creep remains practically constant—a region of steady creep. If the experiments are continued for longer periods a third region is usually revealed, in which the rate of creep increases rapidly, and which is followed by failure. In designing for long-term creep the above curves are often replaced by the straight lines of steady creep (the dotted lines in Fig. 143). In this case the initial values of strain must be replaced by a step in the curve at the initial instant of time. This method of approach gives more accurate results in the design for creep.

On the other hand, in some cases (for example, for certain alloys at very high temperatures) it is essential to establish the nature of the creep during the initial period, since the increase in strain during this period can sometimes be excessive and failure can occur. The detailed curves of short-term creep in compression for a monocrystal of germanium at temperatures of 450–550°C derived by Patel are shown in Fig. 144.

A creep process depends to a very large extent on the temperature. Figure 145 shows creep curves derived by Davis for red copper at

a temperature of 235°C. Comparing these with Fig. 143, we see that for the same stress the rate of creep increases with increase in temperature. Figure 146 shows the relations between the minimum

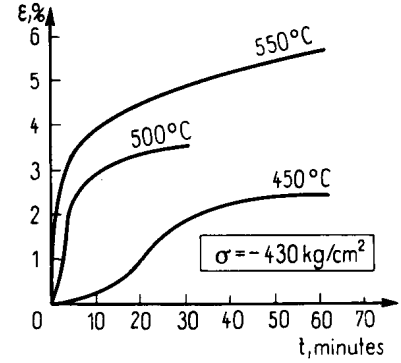

FIG. 144.

rate of creep (in the regions of steady creep) and the stress at different temperatures (derived by Davis).

With continuously varying temperatures we might expect to find, not only smooth, but also steep and irregular variations in the rate of creep due to recrystallization processes.

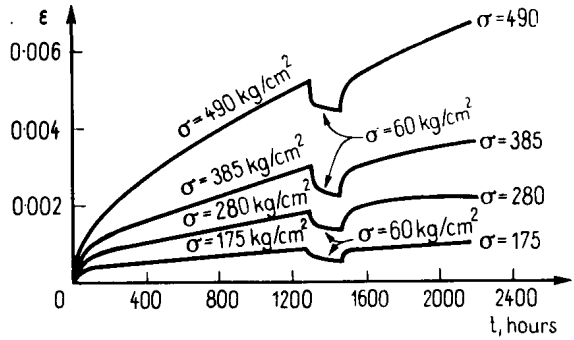

FIG. 145.

If at some instant during the experiment the load applied to the specimen is removed, then immediately after the sudden decrease in strain (which follows an elastic law) there takes place a process of gradual decrease in strain, with decreasing rate of strain, until some limiting value is reached. This process is known as reverse creep. The irregularities in the creep curves in Fig. 145 at $t = 1300$ hr

were caused by rapid temporary decreases in load. The regions indicated by arrows represent the process of reverse creep.

In their creep (and relaxation) properties many plastics and high polymers possess special characteristics which distinguish them from metals. In the first place creep strains in most plastics can

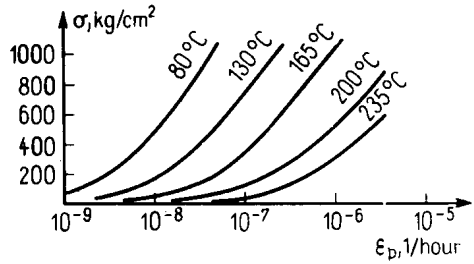

FIG. 146.

assume very high values, and the rate of creep, especially during the initial stages, can be very high. Secondly, reverse creep on removal of all loads acting on the body leads, as a rule, after a considerable time interval, to a complete (or almost complete) recovery of the initial shape and dimensions of the body (see Fig. 48, Chapter II), which is not the case with metals. This reversibility of strains applies not only to those built up during the process of creep, but also to the residual strains which arise as a result of the brief application of large loads. These characteristics must be taken into account most carefully if plastic components are to be used in a structural capacity. In some cases these characteristics are a disadvantage and require special measures to be taken to guard against failure. This is the case, for example, in machine tool construction where, as a rule, it is essential that the various components retain their shape and dimensions even after continued application of heavy loads. In other cases, however, these characteristics can be employed to advantage to improve the working properties of a product. This applies, for example, to components which repeatedly have to resist the same impact load: the flexibility of plastic components would enable them to absorb some of the impact and thus preserve the structure from damage; in addition, the residual strains, which occur on impact would disappear after a certain time and the component would continue to function normally.

The physical nature of the micro-processes which bring about the

phenomenon of creep is basically the same as the process of relaxation. Certain aspects of the phenomenon of creep can be explained by diffusion processes, the movement of dislocations (as is the case for plastic strains in general) and by the flow of intergranular substances, etc. However, an explanation which is satisfactory in a quantitative respect has yet to be found, and the so-called physical theories of creep are based on completely arbitrary assumptions, which are in no way supported by experiment.

A simplified explanation of the macroscopic nature of the phenomenon of creep can be obtained from Maxwell's model (Fig. 140). In addition, however, to the inability of such a simplified model to give a quantitative description of creep, this model is also unable to give a qualitative explanation. It does not explain, for instance, the phenomenon of reverse creep. Combined models do, however, give results in closer agreement with experiment.

(d) Delayed failure. This is the name given to the phenomenon of failure of a material which occurs, not immediately the load is applied, but after a certain interval of time; it is preceded by a creep process. In metals this phenomenon is normally observed only at elevated temperatures. The interval of time from the application of the load until failure depends on the magnitude of the greatest principal tensile stress: the greater this stress, the smaller is the period of delayed failure. The form of this relation for an alloy composed of Cu 92·51 per cent, Al 6·86 per cent, Zr 0·6 per cent at a temperature of 300°C is shown in Fig. 147. The type of failure depends on the period of delay: with a small period of delay, failure is preceded by considerable plastic deformation; with a long period of delay the failure is brittle and plastic strains are almost totally absent. The relation between the total extension of the specimen and time before failure has basically the same form as the relation between stress and period of delayed failure (Fig. 147).

The physical nature of delayed failure is apparently associated with the accelerated migration of defects in the atomic lattice with increase in temperature, which assists the formation of "weak points" on the surface and speeds up the development of failure cracks by the flow of voids in the lattice to the apexes of the cracks, and leads to a concentration of stress.

It is only recently that investigations have been commenced into

the occurrence of delayed failure. It is, however, important to take this phenomenon into account in the design of various heat engines and other plant.

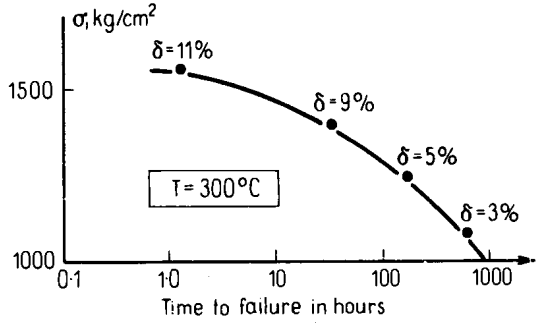

FIG. 147.

(e) Ageing of materials. In a number of materials a continuous change in mechanical properties takes place with time under constant external conditions and in the absence of any external load. It is usual to call these changes "ageing". The occurrence of ageing is an indication of internal instability within the material. In metals ageing is associated with structural instability brought about in some way by heat treatment or the conditions under which the metal solidified. In order to stabilize the properties of a metal, ageing is sometimes artificially accelerated by maintaining the metal at a slightly elevated temperature. Ageing of concrete, in this case associated with prolonged chemical reactions, is very noticeable. These processes, moreover, are exothermic, so that in large volumes of concrete there exists a changing field of temperature stresses which sometimes reach dangerous levels.

In plastics, rubber and other materials of organic origin ageing in the form of deep oxidizing processes leads to such extreme changes in properties that after some time these materials become unsuitable for structural purposes.

Of the above-mentioned effects of time on the mechanical properties of materials, creep and delayed failure are by far the most important from the point of view of the design of components of machinery, equipment and structures that are under conditions of static loading. In order to allow for delayed failure it is normal, in the absence of any systematized data, to make use of empirical formulae and rules derived from specially designed experiments.

Relaxation, in the strict sense of the word, is seldom encountered in practice, and as a rule it is of secondary importance compared with creep. In the majority of cases the components of machines and structures are subjected to definite loads, and the dynamic forces applied to these components are usually such that creep and flow at a particular rate predominate.

For example, the behaviour at high temperatures of turbine blades, engine casings, rotors, cantilever beams and shells and other similar structural elements is determined by given external forces (gas pressure, centrifugal forces, etc.), and in designing these components we need to know the creep curves for the material. Even in structures which have flange connections the resultant contact forces, due to the elasticity of the component elements of the joint, depend to a very large extent on the amount of creep, although relaxation does play some part.

In deriving the relation between stress and strain for metals at high temperature, we can therefore ignore elastic strain in the majority of cases and base our method of analysis mainly on a consideration of the creep of the material.

In the theory of creep, however, there are other phenomena associated with the dependence of the properties of a material on time which must be taken into account.

2. Mechanical Theories of Creep

So many different experiments in the field of one-dimensional creep have been carried out, and their results analysed in so many different ways, that various so-called theories of one-dimensional creep have now been developed. Although we can classify the results of a given series of experiments on creep at constant stress, and by a choice of functions and parameters place them under the headings of different theories, there are certain general conditions which are accepted as basic criteria of the correctness of any one theory: (1) the expressions derived in experiments at constant stress (load) must describe the behaviour of the specimen also at a stress (load) which varies during the experiment; (2) from the results of the creep experiments it should be possible to forecast the behaviour of the material at different constant rates of deformation; (3) from the expressions describing the results of the creep experiments it should be possible to derive relations between stress and time at a

constant extension for any given temperature, which are in agreement with the results of relaxation experiments. It follows, of course, that the relation between the various parameters in each theory should be such that they describe the results of creep experiments at different constant temperatures (experiments during which the temperature varies are not as a rule carried out).

(a) The equation of a family of creep curves can be written in the form

$$f_T(\sigma, \varepsilon, t) = 0, \tag{5.6}$$

where the suffix T indicates that temperature occurs in this expression in the form of parameters (coefficients). Relations of this type are called theories of ageing, since time occurs explicitly in the relation between stress and strain. If the creep curves for a given temperature, but for different constant stresses, are similar, as was noted above, expressions (5.6) can be written in the form

$$\varepsilon = \frac{\sigma}{E_T} + S_T(\sigma)\,\tau_T(t),$$

where the first term represents elastic strain. For example, experiments on certain plastics have shown that a family of creep curves can be conveniently represented by the equation

$$\varepsilon^{(p)} = \varepsilon_0 \left[1 + \left(\frac{t}{t_0}\right)^n\right] \operatorname{sh} \frac{\sigma}{\sigma_0},$$

where the parameters ε_0, t_0, n, σ_0, the characteristic properties of the material, depend on the temperature.

Expression (5.6) can be represented in the form of a surface in the space of the variables σ, ε, t (Fig. 148). If such a surface is con-

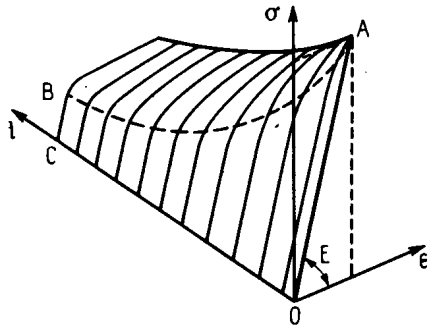

FIG. 148.

structed from the results of creep experiments performed at constant temperature, then according to the above remarks, the curves obtained by the intersections of this surface with the planes $\varepsilon =$ const. and projected on to the (σt) plane should coincide with the relaxation curves for the same temperature, and the projections on to the $(\sigma\varepsilon)$ plane of curves derived by the intersections with planes passing through the σ-axis should coincide with the $\sigma \sim \varepsilon$ curves for different constant rates of deformation. It should be pointed out that only for very few materials (plastics) are surfaces obtained which satisfy these requirements.

The discrepancy between this theory and experimental results is particularly noticeable in the case of variable load. If, for example, at some instant t, the stress is suddenly increased from σ_1 to $\sigma_2 > \sigma_1$, which is then maintained at a constant value, then according to (5.6) this should correspond to an instantaneous transfer to the creep curve obtained from an experiment at a constant stress σ_2 (from the curve OA in Fig. 149 to the curve DE). However,

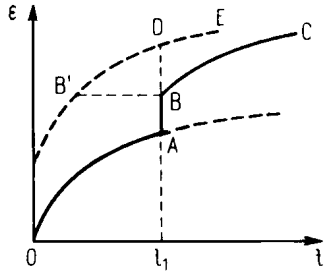

FIG. 149.

experiment shows that transfer takes place to BC, part of the σ_2 creep curve displaced parallel to the axis Ot starting from a point B' corresponding to the instantaneous value of the strain after the increase in load. Similarly, after a temporary decrease in load and subsequent increase to its previous value, we would expect, according to this theory, to arrive back on the same curve, which in actual fact does not take place (see Fig. 145).

It must of course be realized that expression (5.6), as all equations in the theory of creep, cannot be applied to every problem, and that its use in the calculations for processes the duration of which is considerably less than the period of relaxation is invalid. Equation (5.6) does, however, have the advantage of simplicity in the mathematical computations which result from it.

(b) The results of experiments on one-dimensional creep agree more closely with the actual behaviour of specimens under various conditions if they are presented in the form of the so-called theory of strain-hardening:

$$F_T(\sigma, \varepsilon, \dot{\varepsilon}) = 0, \tag{5.7}$$

where ε can be taken either as the total strain or its plastic part ($\varepsilon_p = \varepsilon - \sigma/E$). For example, we often use the expressions

$$\dot{\varepsilon}_p \varepsilon_p^k = A e^{\sigma/\sigma_0} \tag{5.7'}$$

and

$$\dot{\varepsilon}_p \varepsilon_p^k = A\sigma^n. \tag{5.7''}$$

By an appropriate choice of constants k, A, σ_0, n we can give a satisfactory description of the creep curves over a limited range of stresses, and at the same time describe relaxation and the various creep processes at variable stress. If the range over which the equations coincide with experimental results is to be widened, which is important if calculations are to be based on them, equations (5.7') or (5.7'') must be expressed in a more complicated form. This leads, however, to considerable mathematical difficulties. It is important, all the same, to establish for every material a universal expression (even if in a rather complex form) which satisfies the above mentioned requirements over sufficiently wide ranges of stress and temperatures, excluding, perhaps, special regions such as recrystallization intervals.

(c) It will be appreciated that considerable simplification is introduced by the concept of an initial "strain step", which means that the actual creep curve is replaced by a straight line diagram obtained by producing the region of steady creep back to the ε-axis. This gives sufficiently accurate results not only in cases of prolonged creep, when the main part of the strain is built up in the region of steady creep, but also in cases of short-term creep, providing, of course, that steady creep has taken place. In order to derive the corresponding expressions, we must determine from creep experiments at constant loads (stresses) the relation between the magnitude of the step in the plastic strain $\varepsilon_{p\Delta}$ and the stress:

$$\varepsilon_{p\Delta} \equiv \varepsilon_\Delta - \frac{\sigma}{E} = \varphi(\sigma),$$

and the relation between the rate of strain in the region of steady creep and the stress, $\dot{\varepsilon} = \psi(\sigma)$, where in the latter expression we can take ε to be either the total strain, or its plastic part. If these relations are known, the strain at any instant during the range of steady creep can be found from the expression

$$\varepsilon = \frac{\sigma}{E} + q(\sigma) + t\psi(\sigma).$$

On the basis of experimental data it is usual to approximate to the function $\varphi(\sigma)$ by using either the function $\varepsilon_{p\Delta} = Ne^{n\sigma}$ or the function $\varepsilon_{p\Delta} = N\sigma^n$. Similarly the function $\psi(\sigma)$ is normally expressed in the form $\dot{\varepsilon}_p = Ae^{k\sigma}$ or in the form $\dot{\varepsilon}_p = A\sigma^k$ for $\sigma \geqq \sigma_n$, where σ_n is the limiting creep stress. Often the instantaneous step in the plastic strain is small compared with the strain which builds up during the process of prolonged creep. In such cases we can use the even more simplified expression:

$$\dot{\varepsilon} = \psi(\sigma).$$

Let us consider now a process of unsteady creep which takes place under a load which increases monotonically (but sufficiently slowly). From the results of experiments on copper carried out by A. M. Zhukov, U.N. Rabotnov and F.S. Churikov at the same tem-

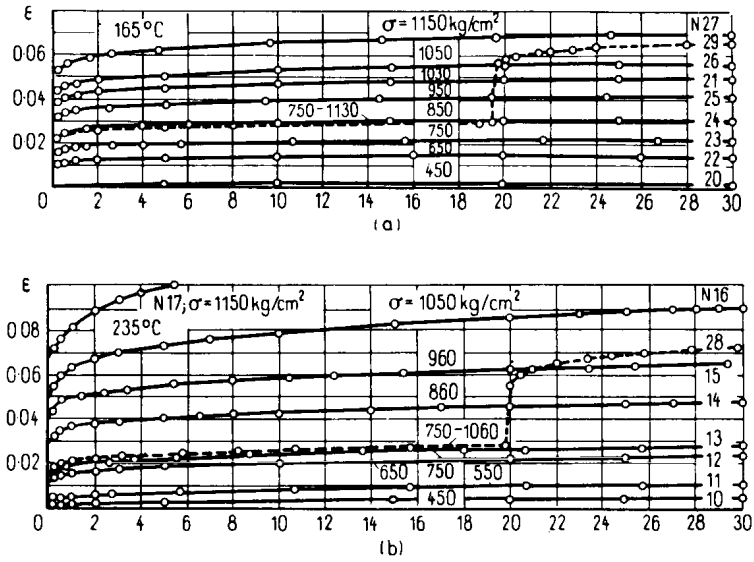

FIG. 150.

peratures as the experiments of Davis, it can be seen (Fig. 150) that a sudden increase in load causes a creep process over a certain range of stresses, starting from the instant the load is increased, which is identical to the process that would have resulted if the increased load had been applied to the undeformed specimen. Although this does not, apparently, apply to cases when the total strain at an instant immediately preceding the sudden increase in load exceeds the initial step in strain for a stress equal to the total stress after the step in the load, with the present simplification of the shape of the creep curves, we can assume that the rate of strain at every instant of time is made up of the rate of change of strain of the initial step and the rate of steady creep:

$$\dot{\varepsilon} = \frac{d}{dt}\left\{\frac{\sigma(t)}{E} + \varphi[\sigma(t)]\right\} + \psi(\sigma) \tag{5.8}$$

or

$$\dot{\varepsilon} = \Phi_T(\sigma)\,\dot{\sigma} + \psi_T(\sigma), \tag{5.8'}$$

where by definition

$$\Phi_T(\sigma) = \frac{1}{E_T} + \varphi'_T(\sigma).$$

The suffix T, as before, indicates that either the form of the functions, or the values of the constants occurring in them, depend on temperature.

3. Creep in a State of Compound Stress

Experimental investigations of the creep of materials under conditions of compound stress are at present still in their initial stages. Mathematical expressions have therefore been derived by analogy with the theory of plasticity, the relations between the invariant characteristics of stress and strain and time being expressed in the same form as that obtained from tensile (or compressive) tests. In other words, whatever form the strain trajectory has, the vectorial properties of the material at any given moment are described in the same way as in Chapter III (in the two-dimensional case):

$$\boldsymbol{S} = A\boldsymbol{\Im} + B\frac{d\boldsymbol{\Im}}{d\lambda_i} \tag{5.9}$$

or alternatively,

$$\frac{d\boldsymbol{\Im}}{dt} = A_1\frac{d\boldsymbol{S}}{dt} + B_1\boldsymbol{S}, \tag{5.9'}$$

where A and B (A_1 and B_1 respectively) depend not only on the arc length ϑ of the strain trajectory and its curvature $\varkappa$, but also on the derivatives of these quantities with respect to time, on the temperature T and in some cases on the time t directly. These expressions involving $\dot{\vartheta}$, $\dot{\varkappa}$ and t take into account to some extent the previous deformation.

For short-term creep processes the first term in expression (5.9) or (5.9′) is the most significant, so that in these cases we can put $B = 0$. Conversely, in processes of prolonged creep the second term in (5.9) or (5.9′) plays the major part, so that we can put $A = 0$ or $A_1 = 0$.

We shall understand by a process of steady creep in a state of compound stress one in which the strains vary with time, but in which the intensity of rate of strain v_i remains constant. Due to the unique relation between v_i and σ_i the intensity of stress also remains constant, although the magnitude of each of the stress components, in general, varies with time. For simplicity we shall not consider these changes in stress, and the components of the stress tensor in the case of steady creep will be considered constant. This will represent the state of stress to which conditions in the body tend asymptotically during creep.

Each of the strain components ε_{ij} in a state of compound stress can be considered to be composed of two parts: a strain ε'_{ij} equal to the value of the initial step and a strain ε''_{ij} which increases with time. If the external loading remains constant $\partial\varepsilon'_{ij}/\partial t = 0$, so that $\dot{\varepsilon}_{ij} = \dot{\varepsilon}''_{ij}$. The relations between the rates of strain and the stresses for strain trajectories of small curvature can be written in the normal form of the theory of flow:

$$\left.\begin{aligned} \dot{\varepsilon}_{ii} &= f(\sigma_i)(\sigma_{ii} - \sigma), \\ \dot{\varepsilon}_{ij} &= f(\sigma_i)\,\sigma_{ij} \quad (i \neq j), \end{aligned}\right\} \tag{5.10}$$

where σ_i is the intensity of stress, σ is the mean normal stress, and for the rates of strain we take the condition of incompressibility $\sum_{i=1}^{3} \dot{\varepsilon}_{ii} = 0$. The intensity of rate of strain

$$v_i = \frac{\sqrt{2}}{3} \times$$

$$\times \sqrt{[(\dot{\varepsilon}_{xx} - \dot{\varepsilon}_{yy})^2 + (\dot{\varepsilon}_{yy} - \dot{\varepsilon}_{zz})^2 + (\dot{\varepsilon}_{zz} - \dot{\varepsilon}_{xx})^2 + 6(\dot{\varepsilon}^2_{xy} + \dot{\varepsilon}^2_{yz} + \dot{\varepsilon}^2_{zx})]}$$

according to the remarks made at the beginning of this section, must

be related to the intensity of stress in the same way as the rate of steady one-dimensional creep is related to the tensile (or compressive) stress:

$$v_i = \psi(\sigma_i).$$

Since for uniaxial compression or tension $\sigma_i = \sigma_{xx}$, and from the condition of incompressibility $v_i = \dot{\varepsilon}_{xx} = \dot{\varepsilon}''_{xx}$, we get the following equation for v_i by expressing $\dot{\varepsilon}_{ij}$ given by (5.10) in terms σ_{ij}:

$$v_i = \tfrac{2}{3}\sigma_i f(\sigma_i).$$

Thus $f(\sigma_i)$ can be expressed in terms of the function $\psi(\sigma_i)$, which is known from creep experiments:

$$f(\sigma_i) = \frac{3}{2\sigma_i}\psi(\sigma_i),$$

and expression (5.10) becomes

$$\left.\begin{aligned} \dot{\varepsilon}_{ii} &= \frac{3}{2\sigma_i}\psi(\sigma_i)(\sigma_{ii} - \sigma), \\ \dot{\varepsilon}_{ij} &= \frac{3}{2\sigma_i}\psi(\sigma_i)\,\sigma_{ij} \quad (i \neq j). \end{aligned}\right\} \tag{5.11}$$

In problems with statical boundary conditions the state of stress can be found in a body from these relations. By integrating with respect to t in (5.11) and noting that at $t = 0$ ε_{ij} have the values of the initial step, we get for the case of steady creep that

$$\left.\begin{aligned} \varepsilon_{ii} &= \varepsilon'_{ii} + \frac{3t}{2\sigma_i}\psi(\sigma_i)(\sigma_{ii} - \sigma), \\ \varepsilon_{ij} &= \varepsilon'_{ij} + \frac{3t}{2\sigma_i}\psi(\sigma_i)\,\sigma_{ij} \quad (i \neq j). \end{aligned}\right\} \tag{5.11'}$$

In order to find ε'_{ij} we make use of the equations of the theory of small elasto-plastic strains

$$\begin{aligned} \varepsilon'_{ii} &= F(\sigma_i)(\sigma_{ii} - \sigma), \\ \varepsilon'_{ij} &= F(\sigma_i)\,\sigma_{ij} \quad (i \neq j) \end{aligned}$$

together with the fact that for simple tension the magnitude of the initial step is $\varepsilon_\Delta = \varphi(\sigma)$. Then, by making use of the condition of incompressibility, we get, in the same way as before, that

$$F(\sigma_i) = \frac{3}{2\sigma_i}\varphi(\sigma_i).$$

With this expression for the function $F(\sigma_i)$, the above equations of the theory of small elasto-plastic strains could be used to determine independently the state of stress in the body after the initial step. It would be found, however, that this state of stress does not in general coincide with that given by expressions (5.11). The reason for this is that the hypothesis of an initial step does not take into account the phenomenon of relaxation of stress, which is significant at the initial instant. In evaluating strains from the formulae

$$\left.\begin{aligned} \varepsilon_{ii} &= \frac{3}{2\sigma_i}[q(\sigma_i) + t\psi(\sigma_i)](\sigma_{ii} - \sigma), \\ \varepsilon_{ij} &= \frac{3}{2\sigma_i}[q(\sigma_i) + t\psi(\sigma_i)]\,\sigma_{ij} \quad (i \neq j) \end{aligned}\right\} \tag{5.12}$$

we must use values of the stresses given by eqns. (5.11).

In processes of prolonged creep, when it is known that the strains in the initial step are small compared with the strains which occur over the whole process, the first terms in the square brackets in expressions (5.12) should be discarded.

In the case of unsteady creep, when the state of stress in the body varies with time due to variations in the external loading, providing the deformation is simple at every point and the material is incompressible, we can replace (5.10) by the more general expressions:

$$\begin{aligned} \dot{\varepsilon}_{ii} &= f(\sigma_i, \dot{\sigma}_i)(\sigma_{ii} - \sigma), \\ \dot{\varepsilon}_{ij} &= f(\sigma_i, \dot{\sigma}_i)\,\sigma_{ij} \quad (i \neq j). \end{aligned}$$

Considering now, as in the case of steady creep, the one-dimensional problem, and making use of expression (5.8) or (5.8′), which is known from experiment, we get that:

$$\frac{2\sigma_i}{3} f(\sigma_i, \dot{\sigma}_i) = \frac{d}{dt}\left\{\frac{\sigma_i(t)}{E} + q\,[\sigma_i(t)]\right\} + \psi[\sigma_i(t)]$$

or

$$\frac{2\sigma_i}{3} f(\sigma_i, \dot{\sigma}_i) = \Phi(\sigma_i)\,\dot{\sigma}_i + \psi(\sigma_i),$$

so that

$$\begin{aligned} \dot{\varepsilon}_{ii}(t) &= \frac{3}{2\sigma_i(t)}\{\Phi[\sigma_i(t)]\,\dot{\sigma}_i(t) + \psi[\sigma_i(t)]\}\,[\sigma_{ii}(t) - \sigma(t)], \\ \dot{\varepsilon}_{ij}(t) &= \frac{3}{2\sigma_i(t)}\{\Phi[\sigma_i(t)]\,\dot{\sigma}_i(t) + \psi[\sigma_i(t)]\}\,\sigma_{ij}(t) \quad (i \neq j). \end{aligned}$$

By integrating, we arrived at the formulae

$$\left.\begin{aligned}\varepsilon_{ii} &= \frac{3}{2\sigma_i^0}\varphi(\sigma_i^0)(\sigma_{ii}^0 - \sigma^0) + \frac{3}{2}\int_0^t \frac{1}{\sigma_i}[\Phi(\sigma_i)\,\dot{\sigma}_i + \psi(\sigma_i)](\sigma_{ii} - \sigma)\,dt,\\ \varepsilon_{ij} &= \frac{3}{2\sigma_i^0}\varphi(\sigma_i^0)\,\sigma_{ij}^0 + \frac{3}{2}\int_0^t \frac{1}{\sigma_i}[\Phi(\sigma_i)\,\dot{\sigma}_i + \psi(\sigma_i)]\,\sigma_{ij}\,dt \quad (i \neq j).\end{aligned}\right\} \tag{5.13}$$

where suffixes "0" refer to the initial state of stress at the moment of application of the external loads.

In expressions (5.12) and (5.13) the form of all the functions and the values of the constants depend, of course, on the temperature. This dependence on temperature very much influences the method of solution of these problems, if there is a stationary non-uniform temperature distribution, or if the temperature in the body varies with time. In the first case we can make use of expressions (5.12) or (5.13), but in the second case they must be replaced by more general expressions derived by experiments on the one-dimensional creep of the material in question at variable temperature.

Experiment shows that the creep characteristics of certain materials are different for compression and for tension. It is possible that this phenomenon is associated with a slight initial anisotropy of the material (due, for example, to pressing operations), which is

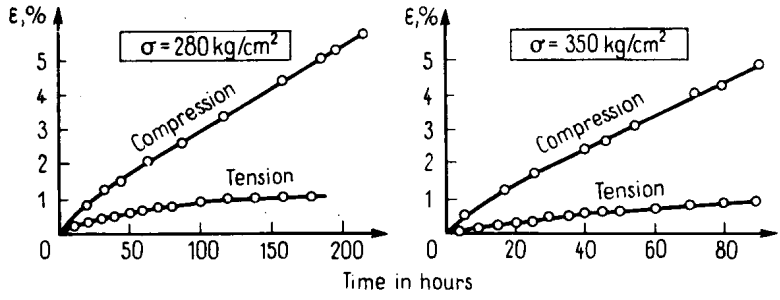

FIG. 151.

not revealed in the elasto-plastic behaviour of the material at normal temperatures in the relatively brief static tests, but which sometimes has a considerable influence on the creep process. In a number of cases these differences are so large that they must be taken into account in any calculations. Figure 151, for example, shows creep

curves in tension and compression for the heat-resistant alloy S-816 (43·2 per cent cobalt, 19·9 per cent nickel, 19·8 per cent chromium) at a temperature of 810°C (from experiments carried out by Erkovich and Guarneri, U.S.A.).

In cases when the principal stresses are all of the same sign no difficulty is involved in taking this difference into account: we simply alter the form of the functions φ (or Φ) and ψ in expressions (5.12) and (5.13). It is more difficult, however, when the principal stresses have different signs.

Let us suppose that $\dot{\varepsilon} = \psi(\sigma)$ is the law of steady one-dimensional creep in tension. In compression this rate of steady creep corresponds to some other absolute value of stress $\eta\sigma$, where η, in general, depends on σ; the law of creep in compression, therefore, is of the form $\dot{\varepsilon} = \psi(\eta\sigma)$. If we make the further assumption that the creep curves for tension and compression are similar, then by analogy with the expression for the step in strain in tension $\varepsilon' = \varphi(\sigma)$, we can write down an expression for the step in compression $\varepsilon' = \varphi(\eta\sigma)$.

Let us suppose that σ_1, for example, is a principal tensile stress and that σ_2 and σ_3 are principal compressive stresses. By applying the condition of incompresssibility, we can write down the relation between the rates of principal strain and the principal stresses in the form

$$\left.\begin{aligned} \dot{\varepsilon}_1 &= f(\Sigma_i)(\sigma_1 - \Sigma), \\ \dot{\varepsilon}_2 &= f(\Sigma_i)(\eta\sigma_2 - \Sigma), \\ \dot{\varepsilon}_3 &= f(\Sigma_i)(\eta\sigma_3 - \Sigma), \end{aligned}\right\} \tag{5.14}$$

where Σ_i and Σ differ from σ_i and σ in that σ_2 and σ_3 occur together with the factor η, which can be considered as a function of anisotropy. For the intensity of rate of strain we have, therefore, that

$$v_i = \tfrac{2}{3} f(\Sigma_i)\, \Sigma_i .$$

In the case of simple tension we have that $v_i = \dot{\varepsilon}_i$, $\Sigma_i = \sigma_i = \sigma_1$. But $\dot{\varepsilon}_1 = \psi(\sigma_1)$. Therefore,

$$f(\Sigma_i) = \frac{3}{2\Sigma_i}\psi(\Sigma_i). \tag{5.15}$$

In the case of simple compression $\Sigma_i = \eta\sigma_2$, $\Sigma = \frac{1}{3}\eta\sigma_2$, and from the second expression of (5.14) and from (5.15) we find that $\dot{\varepsilon}_2 = \psi(\eta\sigma_2)$. In this case, therefore, we can replace the initial

expressions (5.11) by the expressions

$$\left.\begin{aligned} \dot{\varepsilon}_1 &= \frac{3}{2\Sigma_i}\psi_p(\Sigma_i)(\sigma_1 - \Sigma), \\ \dot{\varepsilon}_2 &= \frac{3}{2\Sigma_i}\psi_p(\Sigma_i)(\eta\sigma_2 - \Sigma), \\ \dot{\varepsilon}_3 &= \frac{3}{2\Sigma_i}\psi_p(\Sigma_i)(\eta_1\sigma_3 - \Sigma). \end{aligned}\right\} \tag{5.16}$$

Then we can find by integration expressions to replace (5.12) or (5.13).

4. A Tube under Pressure (Plane Strain)

Let us investigate steady creep in a circular cylinder of internal radius a and external radius b subjected to an internal pressure p_1 and and external pressure p_2 and heated to a uniform temperature which does not vary with time. The ends of the cylinder will be considered fixed to smooth plates in such a way that the axial strain $\varepsilon_{zz} = 0$. The elastic strains for this type of problem were found in § 7, Chapter III. The condition of incompressibility, as before, will refer to the total (and not just the plastic) strains. It is apparent that the radial (σ_{rr}) and the circumferential ($\sigma_{\theta\theta}$) stresses are principal stresses, and that ε_{rr} and $\varepsilon_{\theta\theta}$ are principal strains.

As displacements occur only in a radial direction, and as the material of the tube is incompressible and the problem is axially symmetrical, we have from the condition of incompressibility that the rate of radial displacement is $\dot{u} = C/r$, where C is a constant as yet to be found. Thus

$$\dot{\varepsilon}_{rr} \equiv \frac{d\dot{u}}{dr} = -\frac{C}{r^2}, \quad \dot{\varepsilon}_{\theta\theta} \equiv \frac{\dot{u}}{r} = \frac{C}{r^2}, \quad v_i = \frac{2}{\sqrt{3}}\frac{C}{r^2}.$$

From (5.11), and taking into account that $\dot{\varepsilon}_{zz} = 0$, we find that:

$$\sigma_{zz} = \sigma = \tfrac{1}{2}(\sigma_{rr} + \sigma_{\theta\theta})$$

and therefore

$$\dot{\varepsilon}_{rr} = -\dot{\varepsilon}_{\theta\theta} = \frac{3}{4\sigma_i}\psi(\sigma_i)(\sigma_{rr} - \sigma_{\theta\theta}),$$

where

$$\sigma_i = \pm\frac{\sqrt{3}}{2}(\sigma_{rr} - \sigma_{\theta\theta}).$$

But there is compression in a radial direction ($\varepsilon_{rr} < 0$, $\sigma_i > 0$ and $\psi(\sigma_i) > 0$); thus $\sigma_{rr} < \sigma_{\theta\theta}$ and therefore

$$\sigma_i = -\frac{\sqrt{3}}{2}(\sigma_{rr} - \sigma_{\theta\theta}). \tag{5.17}$$

Consequently

$$\dot{\varepsilon}_{rr} = -\dot{\varepsilon}_{\theta\theta} = -\frac{\sqrt{3}}{2}\psi(\sigma_i),$$

i.e. $\psi(\sigma_i) = 2C/r^2\sqrt{3}$, whence

$$\sigma_i = \psi^{-1}\left(\frac{2C}{r^2\sqrt{3}}\right). \tag{5.18}$$

From the equilibrium condition (§ 7, Chapter III)

$$r\frac{d\sigma_{rr}}{dr} + \sigma_{rr} - \sigma_{\theta\theta} = 0$$

together with (5.17) and (5.18), we get that

$$\frac{d\sigma_{rr}}{dr} = \frac{2}{r\sqrt{3}}\psi^{-1}\left(\frac{2C}{r^2\sqrt{3}}\right).$$

Since $\sigma_{rr} = -p_1$ for $r = a$, we find by integrating this equation that

$$\sigma_{rr} + p_1 = \frac{2}{\sqrt{3}}\int_a^r \frac{1}{r}\psi^{-1}\left(\frac{2C}{r^2\sqrt{3}}\right)dr. \tag{5.19}$$

In order to find the constant C we make use of the condition that $\sigma_{rr} = -p_2$ at $r = b$:

$$p_1 - p_2 = \frac{2}{\sqrt{3}}\int_a^b \frac{1}{r}\psi^{-1}\left(\frac{2C}{r^2\sqrt{3}}\right)dr. \tag{5.20}$$

Having found C, we can find the distribution of radial stress from (5.19) and then find $\sigma_{\theta\theta}$ from the equilibrium equation:

$$\sigma_{\theta\theta} = \sigma_{rr} + r\frac{d\sigma_{rr}}{dr}.$$

At the same time the rate of radial displacement and the rate of strain become fully determinate. If we now integrate the expressions

$$\dot{\varepsilon}_{rr} = -\frac{C}{r^2}, \quad \dot{\varepsilon}_{\theta\theta} = \frac{C}{r^2},$$

noting that initially ε_{rr} and $\varepsilon_{\theta\theta}$ are equal to the values of the initial step:

$$\varepsilon_{rr} = -\frac{Ct}{r^2} + \varepsilon'_{rr}; \quad \varepsilon_{\theta\theta} = \frac{Ct}{r^2} + \varepsilon'_{\theta\theta}. \tag{5.21}$$

By analogy we find that:

$$\varepsilon'_{rr} = -\varepsilon'_{\theta\theta} = -\frac{\sqrt{3}}{2}\varphi(\sigma_i)$$

or, taking into account (5.18),

$$\varepsilon'_{rr} = -\varepsilon'_{\theta\theta} = -\frac{\sqrt{3}}{2}\varphi\left[\psi^{-1}\left(\frac{2C}{r^2\sqrt{3}}\right)\right], \tag{5.22}$$

where the constant C has the value found above.

Let us assume, for example, that the laws of one-dimensional creep (the law of the initial strain step and the law of steady creep) are given by the power functions:

$$\varepsilon' = \varphi(\sigma) \equiv A\sigma^m, \quad \dot{\varepsilon} = \psi(\sigma) \equiv B\sigma^n.$$

Then, we have from (5.20) that:

$$C = \frac{B\sqrt{3}}{2}\left[\frac{(p_1 - p_2)\sqrt{3}}{n(a^{-2/n} - b^{-2/n})}\right]^n.$$

Considering now (5.21) and (5.22), we find that at a time $t > 0$

$$\varepsilon_{rr} = -\varepsilon_{\theta\theta} = -\frac{Ct}{r^2} - \frac{A\sqrt{3}}{2}\left(\frac{2C}{B\sqrt{3}}\frac{1}{r^2}\right)^{m/n}.$$

It can be seen that these strains, whilst they satisfy the condition of incompressibility, do not satisfy the condition of compatibility, which can be seen from a comparison of solutions after the strain step. The condition of compatibility will be satisfied also if the material is such that $m = n$.

5. The Method of Similarity in the Determination of Steady Creep

Equations (5.11) for steady creep coincide with equations (4.11) in the theory of plastic flow in the case of small strains, since in this case

$$v_{mn} = \dot{\varepsilon}_{mn}, \quad \sigma_i = \sigma_v = \Psi^{-1}(v_i)$$

and in essence, therefore, these are one and the same theory applied to different ranges of rates of strain: to low rates of strain in the

case of creep and to medium and high rates of strain in the case of flow.

Equations (5.11), (4.11) also coincide in form with equations (3.30) in the theory of small elasto-plastic strains if we replace the strain hardening function $\Phi(\varepsilon_i)$ in the latter by the function $\Psi^{-1}(v_i)$, the strains ε_{mm} by the rates of strain $\dot{\varepsilon}_{mm}$ and the intensity ε_i by v_i, i.e. if we replace the vector of the displacement of a point by the vector of its velocity. From this coincidence in form of eqns. (5.11) and (3.30) we can derive the law of similarity of the displacements of bodies, which we considered in Chapter III under the action of specific loads, and the rates of steady creep of corresponding bodies under the action of corresponding loads, which we are considering in this chapter.

We can write down in two columns the corresponding equations of the theory of steady creep (5.11) and the theory of small elasto-plastic strains with the condition of incompressibility.

Theory of creep	Theory of elasto-plastic strains
$\sigma_{mm} - \sigma = \dfrac{2\sigma_i}{3v_i}\dot{\varepsilon}_{mm},$	$\sigma_{mm} - \sigma = \dfrac{2\sigma_i}{3\varepsilon_i}\varepsilon_{mm},$
$\sigma_{mn} = \dfrac{2\sigma_i}{3v_i}\dot{\varepsilon}_{mn},$	$\sigma_{mn} = \dfrac{2\sigma_i}{3\varepsilon_i}\varepsilon_{mn},$
$\dot{\varepsilon}_{11} + \dot{\varepsilon}_{22} + \dot{\varepsilon}_{33} = 0,$	$\varepsilon_{11} + \varepsilon_{22} + \varepsilon_{33} = 0,$
$v_i = \dfrac{\sqrt{2}}{3} \times \sqrt{[(\dot{\varepsilon}_{11} - \dot{\varepsilon}_{22})^2 + \cdots + 6(\dot{\varepsilon}_{31}^2 + \dot{\varepsilon}_{12}^2 + \dot{\varepsilon}_{23}^2)]},$	$\varepsilon_i = \dfrac{\sqrt{2}}{3} \times \sqrt{[(\varepsilon_{11} - \varepsilon_{22})^2 + \cdots + 6(\varepsilon_{23}^2 + \varepsilon_{31}^2 + \varepsilon_{12}^2)]},$
$\sigma_i = \Psi^{-1}(v_i) = \sigma_0 F\left(\dfrac{v_i}{v_0}\right),$	$\sigma_i = \Phi(\varepsilon_i) = \sigma_S F_1\left(\dfrac{\varepsilon_i}{\varepsilon_S}\right),$

where σ_0, v_0, σ_S, ε_S are the characteristic constant quantities.

Let us suppose that we wish to solve a creep problem on the basis of the formulae in the left-hand column for a body (A) which has a characteristic dimension l (a length, diameter, etc.), which is at a constant temperature T and is subjected to a given loading system P. We can form a geometrically similar body (A') in the following way: (1) the linear dimensions of the body (A') are made N times less than the dimensions of (A); (2) the material of body (A') is chosen so that the curves $\Psi^{-1}(v_i)$ and $\Phi(\varepsilon_i)$ are similar, i.e. so that $F(z) = F_1(z)$, where z is any number; (3) the loads on (A') are simi-

lar and at corresponding points proportional to the loads on (A), that is, concentrated forces P and P' (kg), forces distributed along a line Q and Q' (kg/cm), forces distributed over an area q and q' (kg/cm^2) and body forces K and K' (kg/cm^3) must satisfy respectively the formulae

$$\frac{N^2P'}{\sigma_S} = \frac{P}{\sigma_0}, \quad \frac{NQ'}{\sigma_S} = \frac{Q}{\sigma_0}, \quad \frac{q'}{\sigma_S} = \frac{q}{\sigma_0}, \quad \frac{K'}{N\sigma_S} = \frac{K}{\sigma_0}.$$

Since the equilibrium equations for bodies (A) and (A') will be the same, the solutions for the relative stresses σ_{mn}/σ_0, σ'_{mn}/σ_S, for the rates of strain and for the strains $\dot{\varepsilon}_{mn}/v_0$, $\varepsilon_{mn}/\varepsilon_S$ will also be the same

$$\frac{\sigma_i}{\sigma_0} = \frac{\sigma'_i}{\sigma_S}, \quad \frac{\sigma_{mn}}{\sigma_0} = \frac{\sigma'_{mn}}{\sigma_S}, \quad \frac{\dot{\varepsilon}_{mn}}{v_0} = \frac{\varepsilon'_{mn}}{\varepsilon_S}, \quad \frac{\dot{\varepsilon}_i}{v_0} = \frac{\varepsilon'_i}{\varepsilon_S},$$

and the velocity vector v at any point in body (A) will be expressed in terms of the displacement vector $\mathfrak{B}$ at a corresponding point in body (A') according to the formula

$$v = \frac{Nv_0}{\varepsilon_S}\mathfrak{B}. \tag{5.23}$$

Thus we have a simple experimental method of similarity for finding the rates of creep v of any complicated component based on an experimental determination of the displacement vector $\mathfrak{B}$ of an appropriate geometrically similar model.

Also, it follows from this similarity that the solutions found in Chapters II and III for various problems concerning the displacements in bodies in which elasto-plastic strains occur can be looked upon as the solutions to creep problems, if we make use of formula (5.23), and if the curves of $\sigma_i = \Phi(\varepsilon_i)$ and $\sigma_i = \Psi^{-1}(v_i)$ are similar.

Example. Let us consider a beam of rectangular section in the (xz) plane (Ox is the central axis of the beam, l is its length, b its breadth and h its depth). In Chapter II a formula (2.39) was derived, based on the assumption that plane sections remain plane, for the relative extension of a fibre parallel to the Ox axis:

$$\varepsilon_{xx} = e - \varkappa_z y - \varkappa_y z,$$

where $\varkappa_z$, $\varkappa_y$ are the curvatures. In this particular case $\varkappa_z = 0$, and the extension of the fibre can therefore be expressed in terms of the relative extension e of the axis and the curvature $\varkappa_y = \varkappa$:

$$\varepsilon_{xx} = e - \varkappa z.$$

Differentiating this expression with respect to time ($d\varepsilon_{xx}/dt = \dot{\varepsilon}_{xx}, \ldots$), we get that

$$\dot{\varepsilon}_{xx} = \dot{e} - \dot{\varkappa} z.$$

For a beam the intensity of stress σ_i is equal to the axial stress σ_{xx}, and the intensity of rate of strain is equal to $\dot{\varepsilon}_{xx}$. For convenience we shall put $\varepsilon_{xx} = \varepsilon$, $\sigma_{xx} = \sigma$.

For simplicity we shall assume that the creep law for the material of the beam can be expressed by the power function (where n is odd):

$$\sigma = \sigma_0 \left(\frac{\dot{\varepsilon}}{v_0}\right)^{1/n}, \quad \text{where} \quad \dot{\varepsilon} = \dot{e} - \dot{\varkappa} z.$$

Formulae (2.38) for the longitudinal force $Q_x \equiv P$ and the bending moment $M_z \equiv M$ give:

$$P = \int_{-h/2}^{h/2} b\sigma \, dz = b\sigma_0 \int_{-h/2}^{h/2} \left(\frac{\dot{e}}{v_0} - \frac{\dot{\varkappa}}{v_0}\right)^{1/n} dz$$

$$= \frac{nb\sigma_0}{n+1} \left[\left(\frac{2\dot{e} + \dot{\varkappa}h}{2v_0}\right)^{\frac{n+1}{n}} - \left(\frac{2\dot{e} - \dot{\varkappa}h}{2v_0} z\right)^{\frac{n+1}{n}} \right] \frac{v_0}{\dot{\varkappa}};$$

$$M = \int_{-h/2}^{h/2} b\sigma z \, dz = b\sigma_0 \int_{h/2}^{h/2} \left(\frac{\dot{e}}{v_0} - \frac{\dot{\varkappa}}{v_0} z\right)^{1/n} z \, dz$$

$$= \frac{v_0^2 nb\sigma_0}{\dot{\varkappa}^2(n+1)} \left\{ \frac{n}{2n+1} \left[\left(\frac{2\dot{e} + \dot{\varkappa}h}{2v_0}\right)^{\frac{2n+1}{n}} - \left(\frac{2\dot{e} - \varkappa h}{2v_0}\right)^{\frac{2n+1}{n}} \right] \right.$$

$$\left. - \frac{\varkappa h}{2v_0} \left[\left(\frac{2\dot{e} + \dot{\varkappa}h}{2v_0}\right)^{\frac{n+1}{n}} - \left(\frac{2\dot{e} - \dot{\varkappa}h}{2v_0}\right)^{\frac{n+1}{n}} \right] \right\}.$$

It can be seen that the rates of extension of the upper ($z = +h/2$) and lower ($z = -h/2$) layers of the beam

$$\dot{e}_1 = \dot{e} - \frac{\dot{\varkappa}h}{2}, \quad \dot{e}_2 = \dot{e} + \frac{\dot{\varkappa}h}{2},$$

can be found in terms of the given tensile force P and bending moment M by the rather involved algebraic equations:

$$\left.\begin{aligned} &\left(\frac{\dot{e}_2}{v_0}\right)^{\frac{n+1}{n}} - \left(\frac{\dot{e}_1}{v_0}\right)^{\frac{n+1}{n}} = \frac{\dot{e}_2 - \dot{e}_1}{v_0} p, \quad \text{where} \quad p = \frac{(n+1)P}{nbh\sigma_0}, \\ &\frac{2n}{2n+1} \left[\left(\frac{\dot{e}_2}{v_0}\right)^{\frac{2n+1}{n}} - \left(\frac{\dot{e}_1}{v_0}\right)^{\frac{2n+1}{n}} \right] - \frac{\dot{e}_2 - \dot{e}_1}{v_0} \left[\left(\frac{\dot{e}_2}{v_0}\right)^{\frac{n+1}{n}} + \left(\frac{\dot{e}_1}{v_0}\right)^{\frac{n+1}{n}} \right] \\ &\qquad = \left(\frac{\dot{e}_2 - \dot{e}_1}{v_0}\right)^2 m, \quad \text{where} \quad m = \frac{(n+1)M}{nbh^2\sigma_0}. \end{aligned}\right\} \tag{5.24}$$

In the particular case of simple tension ($M = 0$) we have that $\dot{\varkappa} = 0$, and therefore $\dot{e}_1 = \dot{e}_2 = \dot{e}$, where $\dot{e}$ can be found from the first formula (by expanding in a series for $\dot{\varkappa}$, dividing by $\dot{\varkappa}$ and then putting $\dot{\varkappa} = 0$; or more simply, directly form the expression for P):

$$\dot{e} = v_0 \left(\frac{P}{bh\sigma_0} \right)^n .$$

In the case of pure bending ($P = 0$) we have that $\dot{e} = 0$ and therefore $-\dot{e}_1 = \dot{e}_2 = \dot{\varkappa} h/2$; from the second formula we get that

$$\dot{\varkappa} = -\frac{2}{h} \left(2m \frac{2n+1}{n+1} \right)^n .$$

In the general case ($P \neq 0$, $M \neq 0$) the above equations can be solved numerically or approximately.

P and M might be given as functions of x. For example, in the case of a turbine blade, we have centrifugal forces which create a tensile force $P(x)$ which is variable along the length of the blade, together with a gas pressure which creates a bending moment $M(x)$. In a similar case of a beam of variable width $b(x)$ and depth $h(x)$ the quantities p and m will be known functions of x and, therefore, solving equations (5.24) for $\varkappa$ and $\dot{e}$ and finding that

$$\dot{e} = f_1(x), \quad \dot{\varkappa} = f_2(x),$$

we get for the longitudinal displacement $u(x)$ ($e = \partial u/\partial x$) and the deflection $w(x)$ ($\varkappa = \partial^2 w/\partial x^2$) that

$$u = t \int f_1(x)\, dx, \quad w = t \iint f_2(x)\, dx\, dx .$$

Turbine blades usually have a very complicated shape, and due to the centrifugal forces and the pressure of the gas, bending, torsional and tensile stresses occur in them. To evaluate them, even on the basis of the theory of flow considered here, is extremely involved, and it will readily be appreciated therefore how useful is the method of similarity.

CHAPTER VI

DYNAMIC RESISTANCE OF MATERIALS

1. Dynamic Forces of Resistance

Experiment shows that the resistance of materials to rapidly changing strains differs from their resistance to strains which take place very slowly, i.e. to "static strains". The following fundamental phenomena have been discovered.

1. The dynamic moduli of metals and other solid bodies having a crystal structure differ only slightly from their static values, i.e. in solid bodies strained within the elastic range the effect of the rate of strain is insignificant. In organic bodies with a high molecular structure (rubber, plastics, high polymers) and in solidified liquids (glass, asphalt) the effect of the rate of strain is noticeable even within the elastic range.

2. With increased rate of strain the elastic limit (yield point) increases, this effect being particularly noticeable in materials having a pronounced yield point (iron, low-carbon steel).

3. The ultimate tensile stress and, in general, the stress at failure, depend on the rate of strain and increase with increase in the latter. In general the magnitude of the residual strain is less with failure after a high rate of strain than with failure under similar conditions after a low rate of strain. We see from points 2 and 3 that the whole shape of the plastic portion of the $\sigma \sim \varepsilon$ curve is altered.

4. With an instantaneously applied stress which exceeds the static yield point, yield occurs not immediately, but after a certain interval of time which depends on the magnitude of the stress and the properties of the material ("delayed yield").

5. With an instantaneously applied stress which exceeds the static ultimate tensile stress failure occurs after a certain interval of time ("delayed failure").

The effect of the rate of strain on the resistance of the material is understood in general, although the mechanism of this effect has

not yet been investigated in detail. Elastic deformation in normal solid bodies is not accompanied by any significant irreversible changes in the crystal structure of the material: the distance between elementary particles changes and a corresponding change takes place in the forces of interaction, but the relative positions of particles remains basically unaltered. The effect of rate of strain is therefore not very significant. In high molecular compounds, for example in high polymers such as rubber, with their molecules in the form of long chains, transfer from a random disposition of molecules with maximum entropy to a more ordered disposition with a decreased value of entropy requires a fairly long interval of time. With a very high rate of strain the interaction between the atoms in each chain and the interaction along the lines of the local connections between molecules are the important factors, whereas the component of strain due to change in entropy, in view of the considerable time required for relaxation to take place, becomes less significant.

Plastic strains are accompanied by irreversible changes in the structure of the material. This is due either to the displacement of irregularities in the structure (dislocations) or to the displacement of particles caused by thermal diffusion, or some other process which requires a definite interval of time and which is associated with considerable relative movement of particles and the rearrangement of the relative positions of particles over a considerable volume, which requires a definite interval of time. It will be seen that with a high rate of strain these processes will lag behind the deformation, which therefore takes place for the most part due to the elastic change in distance between particles, whereas at a slow rate of strain deformation takes place due mainly to the above-mentioned irreversible processes.

The remarks of § 1 of the previous chapter concerning the properties of materials in relation to time still hold good in the case of very high rates of deformation. Of all the many attempts to give a detailed explanation of the influence of rate of strain, we shall give only the theory put forward recently concerning the phenomenon of delayed yield in mild steel. Plastic deformation, according to this theory, is associated with the movement of free, unconnected dislocations (disruptions of the crystal structure). For such a dislocation to start to move, a stress equal to the yield point must be applied. But in carbon steels each dislocation is surrounded

by a cloud of carbon atoms which prevents movement of the dislocation. An additional external stress is therefore required in order to free the dislocation from the surrounding carbon. This explains why mild steels and iron have an upper and a lower yield point. The upper yield point is the stress which is necessary to start off the yield process (to free the dislocation, according to the present theory), and the lower yield point is the stress which is sufficient to maintain the yield process after it has commenced (to keep the dislocation in motion). With an instaneously applied stress which exceeds the upper yield point, the process of freeing the dislocation commences. If this stress is removed before the process is completed there will be no residual strains. If, however, this stress is maintained for some time plastic deformation of the material commences. A number of quantitative relations have been found, based on the atomic–molecular theory of interaction of particles. These relations conform satisfactorily over a certain range with the results of experimental investigations into delayed yield.

2. The Effect of Rate of Strain on the Yield Point

Experiments with mild steel wire carried out by J. Hopkinson (1872) and B. Hopkinson (1905) have shown that the yield point for impact loading is approximately double the static value. In these experiments the yield point was measured by the height through which the load P (Fig. 152) fell before striking the collar A attached to the lower end of the wire. The upper end of the wire was attached to a rigid support.

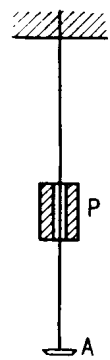

Fig. 152.

Davis (1949) determined the value of the yield point in impact by using a falling sphere. A hardened steel sphere was dropped on to a plate of the material under investigation and the minimum height of fall for which an imprint was left was noted. The stress corresponding to this height could then be calculated from the impact theory of the theory of elasticity. The stresses which occur in these cases can be very large. For example, a sphere of 0·6 cm diameter falling from a height of 0·1 cm causes a stress in a steel plate immediately under the centre of the sphere of 15,500 kg/cm^2; if the height of fall is increased to 100 cm the stress becomes 62,000 kg/cm^2. The static yield point was found by pressing the spheres into the plate. The results of experiments with two materials are given in the following table:

Yield point	Mild steel [kg/cm^2]	Armour plate [kg/cm^2]
Static	4500	13,170
Dynamic	9150	15,500

Warnock and Pope (1947) carried out impact tests on high-quality low-carbon steel (0·22 per cent C), in which the specimen with a head at the top was dropped together with a weight fixed to its lower end. After falling a certain height the head of the specimen struck a stop and the specimen was extended by the weight which continued to move. Figure 153 (in which the circles represent experimental results) shows the results of their experiments and the relation between the yield point and speed of fall.

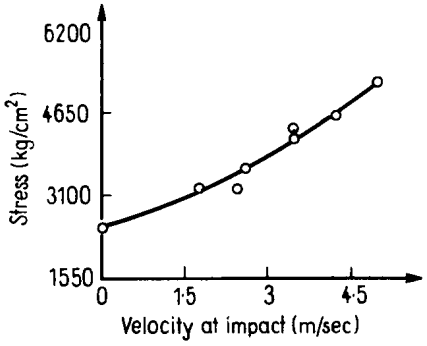

FIG. 153.

J. Taylor (1946) used the method of firing specimens at a rigid target to determine the required dynamic properties.

For paraffin wax the yield point has been determined by loss of transparency. Whereas its static yield point is 34 kg/cm^2, the dynamic yield point of paraffin has been found to vary from 42–53 kg/cm^2. Data for some other materials are given in the table below:

Yield point	Low-carbon steel	Medium-carbon steel	Duralumin
Static [kg/cm^2]	2800	3200	3000
Dynamic [kg/cm^2]	6500–7400	7500	4500

A comparison of the results of different experiments has led to the conclusion that, for a given material with different heat treatment and with different alloying admixtures, the increase in the yield point at a high rate of strain is greater, the lower the static yield point.

3. The Effect of Rate of Strain on the Ultimate Tensile Stress

Failure under dynamic loading occurs as a rule at stresses which exceed the corresponding static values. A very detailed investigation into failure under dynamic loading was carried out by Clark and Wood (1950). In their experiments a tensile force was applied to the specimen by means of a bracket on a fast moving flywheel, which was arranged to catch the head of the specimen after the flywheel had attained the required speed of rotation. Tests were made with various steels, aluminium alloys and copper, which had been subjected to various forms of heat treatment. It was found that the ultimate tensile stress of the steels increased, depending on the heat treatment, from 0–55 per cent. In certain cases it was observed that the UTS even decreased from the static value when the heat treatment had been such that it had made the steel brittle or structurally unstable.

For copper the increase in UTS ranged between 20 and 38 per cent, for the aluminium alloys, up to 33 per cent, and for magnesium alloys, up to 54 per cent.

The change in percentage elongation at failure with increased rate of strain was found to depend on the heat treatment. The

general tendency in the case of steels was that with increase in rate of strain the percentage elongation at failure at first increased slightly, and then decreased.

4. Delayed Yield and Delayed Failure

The results of experiments on delayed yield (by Johnson, Wood and Clark, 1953) for low-carbon steel (0·1 per cent) are given in Fig. 154, in which the dots represent the results of tests in which a tensile stress was suddenly applied, and the circles represent the results of tests in which compressive stresses were applied.

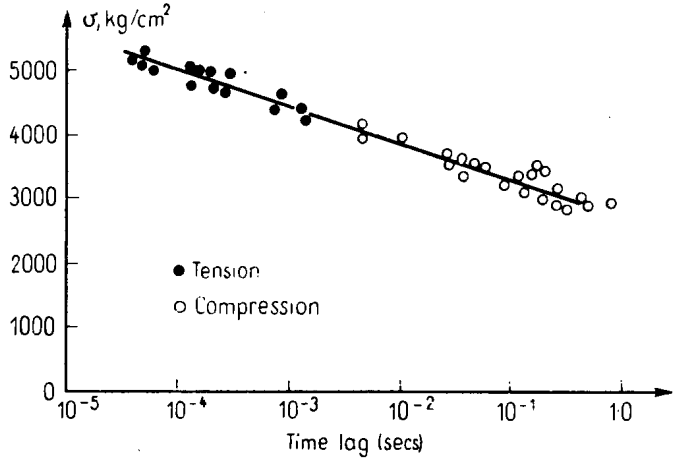

Fig. 154.

The abscissa of a point represents, on a logarithmic scale, the time in seconds which passes before yield in the specimen takes place at the constant stress given by the corresponding ordinate. The relation between the period of delayed yield t_1 and the applied stress σ over the stress range investigated can be expressed analytically by the equation

$$t_1 = t_0 e^{-\sigma/\sigma_0}, \tag{6.1}$$

where t_0 and σ_0 are constants.

The commencement of yield was found from a strain-time trace given by an electrical resistance strain gauge fixed to the surface of the specimen close to the end on which the impact occurs. The signal from the strain gauge is transmitted to a cathode ray oscillo-

graph which traces out the strain–time curve on its screen. A typical curve is shown in Fig. 155, from which it can be seen that during 0·298 msec the strain remained practically constant and then started to increase rapidly at the same value of stress. The lower part of Fig. 155 shows a sinusoidal curve produced by the oscillation of a standard electromagnetic oscillator, which serves as a time scale.

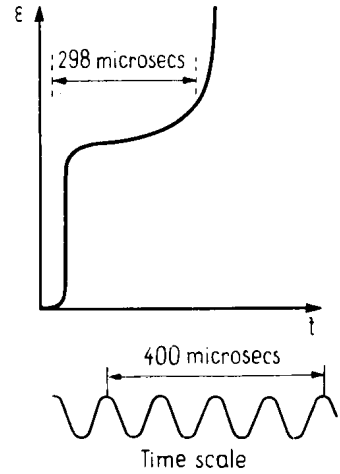

FIG. 155.

Delayed failure at constant stress is analogous in every respect to delayed yield. According to results obtained by Zhurkov and Narsullayev (1953) the time τ before failure occurs at a stress σ is given approximately by the formula

$$\tau = Ae^{-\chi\sigma}, \tag{6.2}$$

where A and χ are constants which depend on the material and the temperature.

In experiments in which the rate of strain is constant the quantity $1/\tau$ is proportional to the rate of strain $\dot{\varepsilon}$, so that formula (6.2), rewritten in the form $e^{\chi\sigma} = A/\tau$ is analogous to the formula

$$\sigma = \sigma_0 + B \ln \varkappa\dot{\varepsilon},$$

which was used in § 2, Chapter II, and which was derived by P. Ludwick (1908).

It would appear from expressions (6.1) and (6.2) that yield, and similarly failure, can occur at any stress however small after a sufficiently long time interval, i.e. that the static (in the full sense

of the word) yield point and UTS are zero. For solid bodies having a crystal structure, however, it has been established that failure and plastic deformation do not occur even after a very long time if the applied stress is less than the static ultimate tensile stress and the static yield point respectively, which are non-zero quantities. Equations (6.1) and (6.2) for such bodies can therefore be applied only over a limited range.

In the case of materials such as glass, asphalt, plastics and other similar materials which do not have a crystal structure, plastic deformation followed by failure may take place at some very low stress after a sufficiently long period of time. Such materials can be considered in this respect as supercooled, very viscous liquids. It is not known if equations (6.1) and (6.2) would still apply in this case, as they were obtained on the basis of limited intervals of time t_1 and τ.

5. Stress–Strain Curve for Dynamic Loading

The experiments described in §§ 2, 3, 4 were only concerned with two characteristic points on the stress–strain curve: the yield point (elastic limit) and the ultimate tensile stress. The derivation of the complete stress–strain diagram, however, for different rates of strain meets with serious experimental difficulties when the rate of strain becomes high. These difficulties are of two types. In the first place, on the application of impact loads the oscillations of the measuring apparatus become so noticeable that the errors introduced by these oscillations exceed the quantities being measured. It would appear that these difficulties could be overcome by the use of electrical resistance strain gauges—thin wires stuck to the specimen which change their electrical resistance with increase or decrease in length and have very little inertia. But here unfortunately difficulties of a second type occur. The point is, as we shall see later, that mechanical disturbances in any medium are propagated at finite velocity in the form of waves. At a low rate of strain these waves travel backwards and forwards along the specimen many times during the course of the experiment, so that the state of stress and strain in the aggregate is uniform. At a high rate of strain the state of stress and strain is not uniform over the length of the specimen. This means in the first place that the strain, for example, calculated as the ratio of the total extension to the length of the spe-

cimen, does not even on an average reflect the state of strain in the specimen, and the rate of strain calculated as the rate of change of the distance between the ends of the specimen divided by its length is not even on an average the true rate of strain, which, like the strain itself, varies along the length of the specimen and with time. Moreover, the longer the specimen the more apparent does this non-uniformity become. In the second place, the waves travelling backwards and forwards along the specimen are picked up by the electrical strain gauges and transmitted to the measuring apparatus in the form of fluctuating traces, the frequency of which is of the same order as or exceeds the natural frequency of oscillation of the electrical parts of the apparatus, which distorts the signals received from the gauges; the shorter is the specimen the greater these difficulties become. A typical stress–strain trace for impact loading at a rate of 9 m/sec is shown in Fig. 156 (derived by Taylor). It would be very difficult to give a satisfactory interpretation of this diagram with any great degree of accuracy.

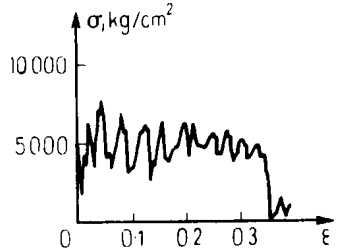

FIG. 156.

The difficulties involved in deriving stress–strain diagrams for high rates of strain brought about by the finite velocity of propagation of mechanical disturbances can be illustrated by the following numerical example. Suppose we wish to find the stress–strain diagram for a rate of strain $\dot{\varepsilon} = 1 \times 10^4$/sec, and that we propose to do so by compressing a cylindrical specimen with some form of solid body moving at high velocity. Assuming that we propose to use electrical strain gauges, we can make the length of the specimen 2 cm. In order to obtain a mean rate of strain of 1×10^4/sec, the striking hammer must have a velocity $v = l \,.\, \dot{\varepsilon} = 2\text{ cm} \times 10^4\text{ sec}^{-1} = 200$ m/sec, which can easily be attained. The mean yield strain $\varepsilon_S = 0{\cdot}002$ will be reached in the specimen when the hammer has travelled a distance $\Delta l = \varepsilon_S \,.\, l = 4 \times 10^{-3}$ cm $= 4 \times 10^{-5}$ m (the

opposite end of the specimen is assumed to be fixed). With a speed of 200 m/sec this requires a time of 2×10^{-7} sec. The elastic strains will be propagated most rapidly; for example, in steel and aluminium elastic waves are propagated at a velocity of the order of 5×10^5 cm/sec. After a time of 2×10^{-7} sec a wave front will therefore move through a distance of 5×10^5 cm/sec $\times$ 2×10^{-7} sec $= 10^{-1}$ cm, i.e. only 1/20th of the length of the specimen. At this instant all the deformation will be concentrated in this part of the specimen, whereas the method of measurement presupposes a more or less uniform deformation over the full length of the specimen. But even in this small part of the specimen, where the mean strain is 20 times greater than the yield point, the deformation will be far from uniformly distributed, since plastic strains are propagated much more slowly than elastic strains.

An investigation of the mechanical properties of materials at high rates of strain leads, therefore, to the necessity to investigate

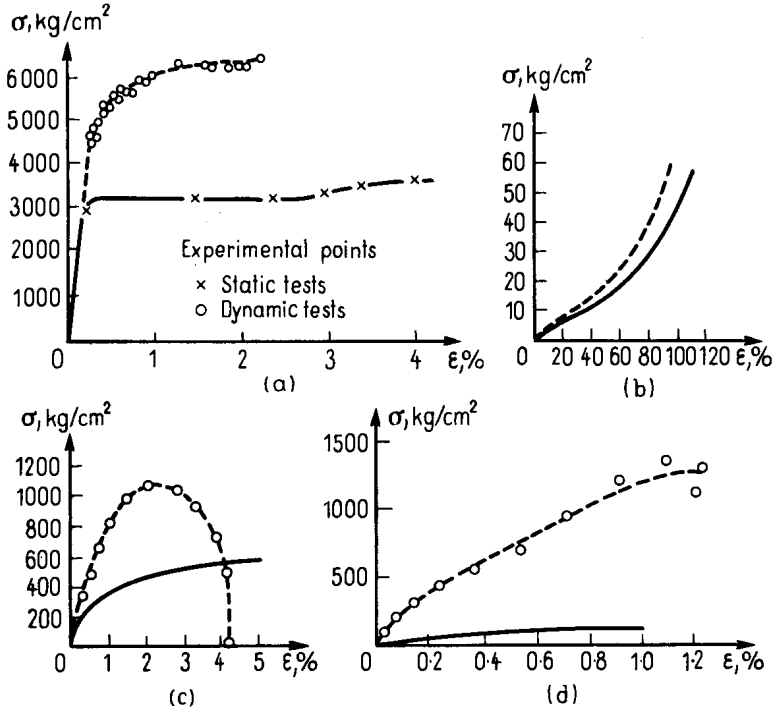

FIG. 157.

the process of wave propagation. We should note that the above experimental results produced by Hopkinson and Taylor were obtained by an analysis of the observations on the basis of the wave propagation theory.

Certain aspects of the theory of wave propagation will be dealt with later. For the moment we shall only give the results of attempts to derive the relation $\sigma = \Phi_1(\varepsilon)$ for dynamic loading which have so far been obtained by experiments based on the wave theory.

Figure 157 shows the static and dynamic curves for mild steel (Fig. 157a), for natural rubber (Fig. 157b), copper (Fig. 157c) and Plexiglas (Fig. 157d). The curves for steel and rubber were obtained in the materials laboratory of Moscow University by the methods of residual strain distribution and rate of impulse propagation respectively, and those for copper and Plexiglas were derived by G. Kolsky (England) by means of the so-called Davis measuring rod. The continuous lines represent the results of static experiments and the broken lines give the results of dynamic tests. All the dynamic curves were derived from impact tests and correspond to very high rates of strain. The results show that the rate of strain has a very large influence on the shape of the stress–strain curve.

Analytically the relation between stresses and strains for an arbitrary loading process can be written in the form (see formula (5.7) of the previous chapter)

$$\sigma = \Phi(\varepsilon, \dot{\varepsilon}), \tag{6.3}$$

and unloading, i.e. a process accompanied by a decrease in strain, can be assumed to take place according to an elastic law as for static deformation. Geometrically the relation (6.3) can be represented by a surface in the $(\sigma, \varepsilon, \dot{\varepsilon})$ space, and any loading process can be represented by a curve on this surface (Fig. 158). In particular, the creep curve can be found by projecting the intersection of this surface with the plane $\sigma = \text{const.}$ on to the $(\varepsilon\dot{\varepsilon})$ plane. By integrating the equation of this curve $f(\varepsilon, \dot{\varepsilon}) = 0$ we can obtain the equation for the creep curve

$$\varepsilon = \varepsilon(t) \quad \text{for} \quad \sigma = \text{const.}$$

A surface in the (σ, ε, t) space given by the following expression and shown in Fig. 159 can also be used to represent the behaviour of a specimen under load:

$$F(\sigma, \varepsilon, t) = 0. \tag{6.4}$$

This surface, which we shall call the stress–strain–time surface, consists of a part of the plane $OABC$ passing through the axis Ot and the normal OA, the slope of which in the $(\sigma\varepsilon)$ plane relative to the ε-axis is equal to the elasticity modulus E. The curve AB which

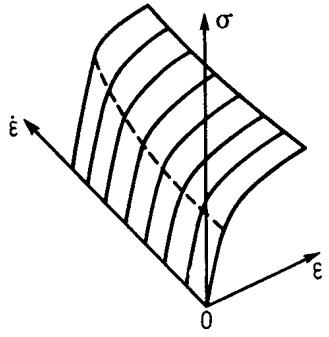

FIG. 158.

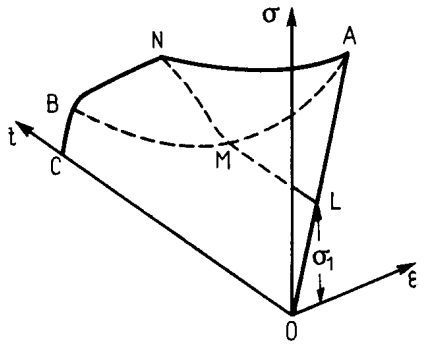

FIG. 159.

divides the plane part of the surface from the curved part tends asymptotically as $t \to \infty$ to the plane $\sigma = \bar{\sigma}_T$, where $\bar{\sigma}_T$ is the static yield point derived experimentally with an infinitely small rate of strain, or is asymptotic to the axis Ot if the static yield point of the material is zero. The same remarks apply to the line AN which indicates the position of failure. Points on this curve can, depending on the properties of the material determined by its composition and heat-treatment, have coordinates σ, ε which are smaller or greater in magnitude than the coordinates of the point A, which is the point of failure for an infinitely high rate of strain. A compression process can be represented by a surface symmetrical about

the axis Ot. The shape of this surface changes with change in temperature.

The curve of the intersection of this surface with a cylindrical surface, the generator of which is parallel to the σ-axis and the directrix of which is the curve $\varepsilon = \varepsilon(t)$ in the (ε, t) plane, describes a loading process which follows any required law of increase in strain with time. The $\sigma \sim \varepsilon$ relation is given by the projection of this curve on to the (σ, ε) plane. In particular the curve given by the intersection of this surface with a plane passing through the σ-axis corresponds to loading at a constant rate of strain. The $\sigma \sim \varepsilon$ curve for a given law of variation in stress with time can be defined in an analogous way.

Unloading (a decrease in strain) which commences at any instant of time can be represented by a curve passing through the corresponding point on the stress–strain surface in a plane parallel to the plane $OABC$.

The creep curve for a given stress σ_1 is given by the projection on to the (εt) plane of the curve LMN, which is the intersection of the plane $\sigma = \sigma_1$ with the stress–strain surface. The length LM corresponds to the period of delayed yield at constant stress. This interval, which projected onto the (σ, ε) plane constitutes a point, is normally not encountered on creep curves, since the period of delayed yield is very small compared with the times required for carrying out normal creep experiments.

If at some instant during the loading the stress σ_1 is decreased by a small amount $\Delta\sigma$, and if this decreased stress is then maintained, initially the strain which results after the sudden removal of the load will remain constant. This process can be represented in the (σ, ε, t) space by a straight line parallel to the axis Ot and lying below the stress–strain surface. But immediately this line intersects the stress–strain surface deformation once more starts to increase, and follows the curve of the intersection of this surface with the plane $\sigma = \sigma_1 - \Delta\sigma$.

Creep is observed at stresses which are less than the static yield point σ_T. This means that the static yield point $\bar{\sigma}_T$ found by an ideal experiment with an infinitely low rate of strain is less than the quasi-static yield point σ_T found from experiments with a low but finite rate of strain.

The relaxation curves $F(\sigma, \varepsilon_1, t) = 0$ are given by the intersection of the stress–strain surface with the plane $\varepsilon = \varepsilon_1$.

In order to construct the stress–strain surface for a material, it is necessary to conduct a series of experiments on creep at various stresses, or a series of experiments on relaxation at different strains or, finally, derive a series of $\sigma \sim \varepsilon$ curves for different constant rates of strain.

6. The Theory of Impact

A number of problems in engineering are concerned with the compression of cylindrical bodies by impact. Cylinders can be used in this way for measuring high pressures caused by explosions: the residual strain in the cylinder is a measure of the pressure. The elementary theory of impact is derived from energy considerations.

Suppose that a cylinder A on an absolutely rigid fixed block B is subjected to a longitudinal impact by an absolutely rigid body M of mass m moving prior to impact with a velocity V (Fig. 160).

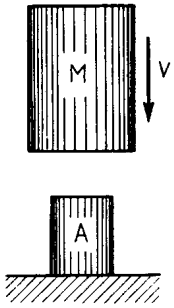

Fig. 160.

At the instant of maximum compression the velocity of the body M becomes zero, and its kinetic energy is converted into the strain energy of the cylinder. If F is the cross-sectional area of the cylinder and l its length, then by equating the kinetic energy of the mass m to the strain energy of the cylinder, we get that:

$$\frac{1}{2} mV^2 = \int_0^{\delta} Fl\sigma \, d\varepsilon, \tag{6.5}$$

where δ is the greatest relative decrease in length of the cylinder. The integration is carried out over the dynamic curve $\sigma = \Phi_1(\varepsilon)$. If the material is incompressible (which is approximately the case

for plastic deformation), the quantity Fl, which is equal to the volume of the cylinder A, remains constant, so that

$$\frac{1}{2}mV^2 = Fl\int_0^{\delta}\sigma\,d\varepsilon. \tag{6.6}$$

Here the integral represents the area ONP under the dynamic curve $\sigma = \Phi_1(\varepsilon)$ (Fig. 161). The compression of the cylinder (the maximum decrease in length) can be found from eqn. (6.6), and the greatest stress $\sigma_1 = \Phi_1(\delta)$ can then be found from the curve $\sigma = \Phi_1(\varepsilon)$.

After the compression period the length of the cylinder starts to increase slightly due to the elastic part of the deformation. After this period of partial recovery the body M separates from the cylinder at a velocity V', which can be found by equating its kinetic energy to the elastic strain energy of the cylinder given by the triangle NPQ (see Fig. 161):

$$\frac{1}{2}mV'^2 = \frac{1}{2}Fl(\delta - \varepsilon')\Phi_1(\delta), \tag{6.7}$$

where ε' is the residual strain.

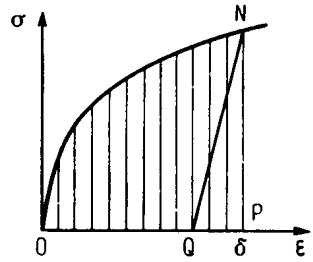

FIG. 161.

If the impact does not cause plastic deformation in the cylinder. then in (6.6)

$$\int_0^{\delta}\sigma d\varepsilon = E\int_0^{\delta}\varepsilon\,d\varepsilon = \frac{1}{2}E\delta^2,$$

and in equation (6.7) $\varepsilon' = 0$ and $\Phi_1(\delta) = E\delta$ so that

$$mV^2 = EFl\delta^2 \tag{6.8}$$

and $V' = V$. From (6.8) we can find the maximum elastic compres-

sive strain δ:

$$\delta = V\sqrt{\left(\frac{m}{EFl}\right)},$$

and the maximum stress due to impact is

$$\sigma_1 = E\delta = V\sqrt{\left(\frac{Em}{Fl}\right)}.$$

For materials which strain-harden only very slightly we can put $\sigma = \sigma_T$ in (6.6), where σ_T is the yield point, and the elastic strain in the case of large compression can be ignored. Then we get from (6.6) that

$$\delta = \frac{1}{2}\frac{mV^2}{Fl\sigma_T}.$$

For example, if the diameter of the cylinder is 2 cm, the material is mild steel having a dynamic yield point $\sigma_T = 5000$ kg/cm^2, and if this cylinder is struck by a hammer weighing 20 kg travelling at 10 m/sec, we find that the absolute compression $\Delta = \delta l$ is

$$\Delta \approx 0{\cdot}65 \text{ cm}.$$

In the case of a cylinder of length l and cross-sectional area F, moving along its axis with velocity V and then striking a rigid fixed stop, we have that $m = Fl\varrho$, where ϱ is its density, so that

$$\frac{1}{2}Fl\varrho V^2 = Fl\int_0^\delta \sigma\, d\varepsilon \quad \text{or} \quad \frac{1}{2}\varrho V^2 = \int \sigma\, d\varepsilon.$$

In particular, if the strains are elastic

$$\varrho V^2 = E\delta^2, \quad \delta = \frac{V}{a_0},$$

where $a_0 = \sqrt{(E/\varrho)}$. Thus, in order that no plastic strains occur on impact, it is necessary that

$$V < a_0\varepsilon_S, \tag{6.9}$$

where ε_S is the strain at the yield point (elastic limit).

This theory is sometimes used in experiments for finding the $\sigma \sim \varepsilon$ relation for dynamic loading. For example, in the above-mentioned experiments of Warnock and Pope measurements were taken of the maximum strain on impact ε_1, the rebound kinetic

energy T' of the striking body and the residual strain ε', and the stress σ_1 for the strain ε_1 was then found from an equation of the type (6.7).

In the elementary theory of impact it is assumed that the stresses and strains are uniformly distributed along the length of the cylinder, which is not always the case for two reasons: (1) due to friction on the ends, the specimen assumes a barrel shape after compression, and (2) at a high rate of strain the finite rate of propagation of disturbances becomes important.

7. Longitudinal Waves in Rods

In the theory of longitudinal waves in long thin rods the movement of particles in directions perpendicular to the axis of the rod is neglected. Let us take the x-axis as the axis of the rod, and denote the longitudinal displacement of a particle in the rod, which is a function of x and of the time t, as u. At any instant the stresses and strains on each cross-section of the rod are uniformly distributed.

In order to determine the propagation velocity of a disturbance we consider the wave front, i.e. the moving plane AB, perpendicular to the axis of the rod, which separates the part of the rod in which the disturbances caused by the application of forces to the left-hand end of the rod already exist, from the part of the rod which the disturbances have not yet reached (Fig. 162). This plane (in

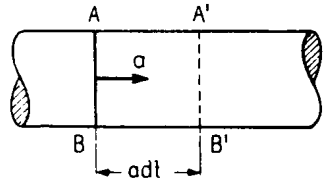

Fig. 162.

the general case of a three-dimensional problem, a surface) is called a wave front. Since the displacements are continuous functions of x and t (otherwise the condition of continuity of the material would not be satisfied), at an instant of time t, $u(x, t) = 0$ at the section x which corresponds to the position of the front AB. After a time dt this plane, which is moving with a velocity a, as yet unknown, will move through a distance $a\,dt$ to the position

$A'B'$ and in this new position of the wave front the equation

$$u(x + dx, t + dt) = 0$$

is still satisfied. Expanding this into a Taylor's series and retaining only terms of the first order, we get that

$$u(x, t) + \frac{\partial u}{\partial x} dx + \frac{\partial u}{\partial t} dt = 0.$$

Since $u(x, t) = 0$, and $dx = a\,dt$, $\partial u/\partial x = \varepsilon$ and $\partial u/dt = v$, we can find the relation between the strain ε and the velocity v of a particle (this velocity should not be confused with the velocity of propagation of the disturbance) on the wave front

$$v = -a\varepsilon. \tag{6.10}$$

This is the particular case of so-called kinematic conditions on the wave front. If the wave front (the plane AB) is the boundary between the parts of the rod in which the velocities of particles and the strains, and therefore the stress, differ by a finite quantity (are discontinuous at the plane AB), then condition (6.10) can be rewritten in the form

$$v_1 - v_2 = -a(\varepsilon_1 - \varepsilon_2), \tag{6.10'}$$

where $v_1, \varepsilon_1, v_2, \varepsilon_2$ are the velocities of particles and the strains to the left and right of the wave front. In this case we talk of a shock wave. With a continuous distribution of the disturbances, expression (6.10') can be applied at any cross-section in the disturbed region, if we consider any moving disturbance as the limiting case of a shock wave when the magnitude of the discontinuity in the velocities and strains tends to zero. In this case (6.10) can be written in the differential form:

$$dv = -a\,d\varepsilon. \tag{6.10''}$$

Let us consider now the so-called dynamic conditions on the wave front AB. After a time dt all the particles situated between AB and $A'B'$ (see Fig. 162) will be disturbed from their state of rest and brought into a state of motion with velocity v. This will be caused by a longitudinal stress σ acting on the section AB. If ϱ is the density of the material, F the cross-sectional area of the rod, the mass which during the time dt has been set in motion from a state of rest will be $Fa\varrho\,dt$, so that from the momentum theorem we have that

$$Fa\varrho\,dt\,v = -F\sigma\,dt,$$

from which we obtain the relation between the stress and the velocity of particles

$$a\varrho v = -\sigma. \tag{6.11}$$

For a shock wave condition (6.11) becomes

$$a\varrho(v_1 - v_2) = \sigma_2 - \sigma_1. \tag{6.11'}$$

With a continuous distribution of the disturbances, (6.11') for any point in the disturbed region can be written in the differential form

$$a\varrho\, dv = -d\sigma. \tag{6.11''}$$

Substituting in (6.11'') the value of dv given by (6.10''), we get that

$$a = \sqrt{\left(\frac{1}{\varrho}\frac{d\sigma}{d\varepsilon}\right)}. \tag{6.12}$$

Thus, any longitudinal disturbance characterized by a particle velocity v, by a strain ε and a stress σ will in fact be propagated at a finite speed which, according to (6.12), depends on the density ϱ of the material and on $d\sigma/d\varepsilon$, the slope relative to the ε-axis of the tangent at the corresponding point on the stress–strain curve. We see then that the propagation velocity of a disturbance depends, in general, on the magnitude of the deformation. In particular, for elastic disturbances $d\sigma/d\varepsilon = E$, the modulus of elasticity of the material, so that the propagation velocity of an elastic wave is

$$a_0 = \sqrt{\left(\frac{E}{\varrho}\right)} \tag{6.13}$$

and does not depend on the magnitude of the deformation within the elastic limit. For steel, for example, $E = 2{\cdot}1 \times 10^6$ kg/cm^2 and $\varrho = 7{\cdot}8/981$ gm . sec^2/cm^4, so that $a_0 \approx 5000$ m/sec. The propagation velocity of an elastic wave in an aluminium rod has approximately the same value.

The law of propagation of disturbances along a rod can conveniently be represented in graphical form in the (xt) plane. The propagation of each disturbance, characterized by the quantities v, ε, σ can, according to (6.12), be represented by a straight line, the slope of which relative to the axis Ot is a. If, for example, we apply a variable pressure to the end of the rod $x = 0$ which causes a strain on this end which varies according to the law $\varepsilon = f(t)$ (this law is represented graphically on the left side of Fig. 163), then the picture of the distribution of the disturbances in the (xt)

plane is as shown on the right side of Fig. 163. Until the moment τ, when the stress on the end of the rod reaches the yield point, elastic waves will be propagated from the end of the rod with the same velocity a_0. They can be represented by a series of parallel

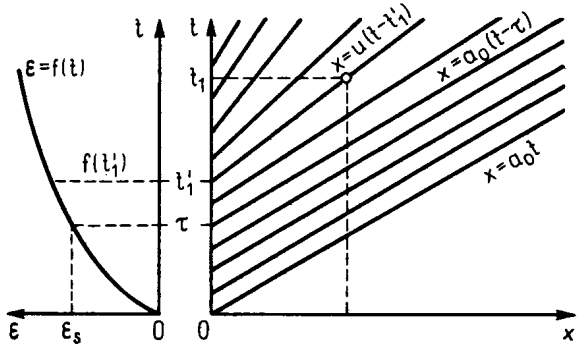

FIG. 163.

straight lines of slope a_0. At the instant τ plastic waves will start to be propagated with velocities which depend on the magnitude of the deformation. They can be represented by a cluster of divergent straight lines if the $\sigma \sim \varepsilon$ diagram is convex on the side of the σ-axis, so that $d\sigma/d\varepsilon$ decreases with increase in ε.

The law of the variation in strain at any cross-section x can easily be found from Fig. 163 by drawing the line $x = x_1$, and for any instant of time t_1, following along the line $x = a(t - t_1')$ to the axis Ot at the point t_1', which corresponds to the strain $\varepsilon_1 = f(t_1')$. Thus, the strain at the section x at an instant of time t is

$$\varepsilon = f\left(t - \frac{x}{a}\right). \tag{6.14}$$

Thus the problem of propagation of elasto-plastic waves with active strains reduces to solving the eqn. (6.14), in which $a = a(\varepsilon)$ is given by the $\sigma \sim \varepsilon$ diagram. In particular, in the case of elastic strains, we obtain the solution

$$\varepsilon = f\left(t - \frac{x}{a_0}\right), \quad v = -a_0 f\left(t - \frac{x}{a_0}\right), \tag{6.14'}$$

which shows that on every section x the strain (and therefore the stress and the particle velocity) varies according to the same law

as on the end of the rod, but with a time lag x/a_0 required for the elastic disturbance travelling at velocity a_0 to reach the section at time t.

In order to establish the strain distribution along the length of the rod at any instant of time $t_1 > 0$, we draw the straight line $t = t_1$ in the (xt) plane in Fig. 163 and then follow the line $x = a(t - t_1')$ to the axis Ot to find the strain $\varepsilon_1 = f(t_1')$ at any section x_1. In particular, we see that in the case of elastic strains the disturbances travel without distortion in their distribution along the length of the rod.

The longitudinal displacement u of the particles in an elastic rod can be described by a second order partial differential equation. In order to derive this equation we make use of eqn. (2.6) of Chapter II:

$$\frac{d^2u}{dx^2} = \frac{Q(x)}{EF},$$

where $Q(x) = F\varrho R_x(x)$, in which $R_x(x)$ is the mass force acting in the direction of the axis of the rod. In this case the mass force is the inertia force: $R_x(x) = \partial^2 u/\partial t^2$. Instead of the total derivative in eqn. (2.6) we must write partial derivatives, since $u = u(x, t)$. As a result we arrive at the equation

$$\frac{\partial^2 u}{\partial t^2} = a_0^2 \frac{\partial^2 u}{\partial x^2}, \tag{6.15}$$

called the wave equation.

It can easily be shown that its solution is

$$u(x, t) = f_1(x - a_0 t) + f_2(x + a_0 t), \tag{6.16}$$

where f_1 and f_2 are arbitrary twice-differentiable functions. We see that this solution is the general solution, as it contains two arbitrary functions. The first function $f_1(x - a_0 t)$ describes the propagation of disturbances in the positive direction of the axis Ox with velocity a_0, since it remains constant for $x - a_0 t = \text{const.}$, i.e. for $dx/dt = a_0$. Similarly the second function describes the propagation of disturbances in the negative direction of the axis Ox. The form of the functions f_1 and f_2 is determined by the initial and boundary conditions.

8. Transverse Waves

If the motion of the medium is such that the displacements of its particles takes place in a direction perpendicular to the direction of propagation, the waves are called transverse waves. In the case of waves of this kind we can repeat all the calculations of the previous section simply replacing $u(x, t)$ by $w(x, t)$, σ by τ and ε by γ. As a result, instead of (6.10) we have that $\xi = -b\gamma$, where $\xi = \partial w/\partial t$ is the particle velocity, b is the velocity of propagation of the transverse wave and γ is the shearing strain; instead of (6.11) we have

$$bp\xi = -\tau,$$

and instead of (6.12),

$$b = \sqrt{\left(\frac{1}{\varrho}\frac{d\tau}{d\gamma}\right)}.$$

In particular, the velocity of propagation of an elastic transverse wave is

$$b_0 = \sqrt{\left(\frac{G}{\varrho}\right)},$$

where G is the shear modulus.

Elastic transverse waves occur, for instance, in a circular rod when a torque is applied to its end. In this case we speak of torsion waves.

The solution of problems on the propagation of transverse waves is analogous to the solutions for longitudinal waves. In our future work, therefore, we shall only consider the latter.

9. Reflection of Longitudinal Elastic Waves

If a rod has a finite length l, then from the moment $t_1 = l/a_0$, when the front of an elastic wave reaches the end of the rod $x = l$, reflected waves start to be propagated from this end. We shall consider here only those cases when the incident wave, and also the incident and reflected wave together, cause stresses which do not exceed the elastic limit. Since within the elastic limit the problem is linear, the motion within the region where the effect of reflection is felt can be found by linear superposition (algebraic addition) of the incident and reflected waves (this refers to the displacements, strains, particle velocities and stresses).

In order to construct a reflected wave we imagine that the rod extends to the right to infinity. Then, as an incident wave passes the section $x = l$ there occur stresses, strains and particle velocities, the variation of which with time is given by (6.14′).

If the end of the rod $x = l$ is free, the stresses and strains at $x = l$ must be zero. For reflected waves to be generated in this case, it is therefore necessary for an external stress to be applied to the end $x = l$ equal in magnitude but opposite in sign to that which arises at the section $x = l$ due to the incident wave, i.e. from (6.14′) a pressure

$$p_1 = -Ef\left(t - \frac{l}{a_0}\right).$$

Since in § 7 we considered $f(t) = 0$ for $t < 0$ (the load is applied at the instant $t = 0$), it follows that $p_1 \neq 0$ for $t \geqq l/a_0$, which is obvious: wave reflection commences at an instant $t = l/a_0$. But exactly the same stress p_1 would have occurred at the section $x = l$ if the length of the rod had been $2l$ and a load $-f(t)$ had been acting on the right-hand end of the rod since the instant $t = 0$. The solution for this case can be found from (6.14′) by replacing f by $-f$, a_0 by $-a_0$ (since the wave is being propagated towards the left) and x by $x - 2l$ (since the origin of coordinates must be displaced to the right a distance $2l$), so that in the reflected wave

$$\varepsilon' = -f\left(t + \frac{x - 2l}{a_0}\right), \quad v' = -a_0 f\left(t + \frac{x - 2l}{a_0}\right).$$

The resultant strains and particle velocities in the region in which the effect of the reflection is felt are, therefore,

$$\begin{cases} \varepsilon = f\left(t - \dfrac{x}{a_0}\right) - f\left(t + \dfrac{x - 2l}{a_0}\right), \\ v = -a_0 f\left(t - \dfrac{x}{a_0}\right) - a_0 f\left(t + \dfrac{x - 2l}{a_0}\right). \end{cases}$$

In particular, during the whole time at $x = l$,

$$\begin{cases} \varepsilon = 0, \\ v = -2a_0 f\left(t - \dfrac{l}{a_0}\right), \end{cases}$$

i.e. the strains are zero (as must be the case for a free end) and the velocities of particles are twice those that would have occurred at $x = l$ in a semi-infinite rod.

The values of ε and v can be found graphically as follows (Fig. 164): for any instant $t > l/a_0$ draw the curve of the distribution of ε given by (6.14'), including the part for $x > l$ (this part of the curve is shown by the broken line in Fig. 164a); draw the curve derived from the former by reflection about the point $x = l$ with the latter as the centre of symmetry (the dotted line in Fig. 164a).

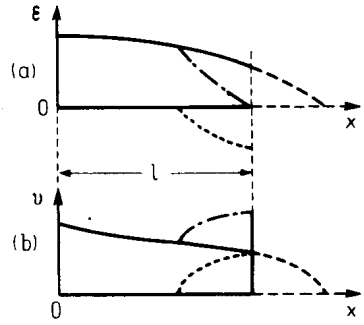

FIG. 164.

Add the curves in the region $x < l$ geometrically. The resulting curve is shown by the dash-dot line in Fig. 164a. The graph of v is derived in a similar way by reflecting the v diagram in the line $x = l$ as an axis of symmetry (Fig. 164b). The curve for the stresses σ is derived in the same way as the ε curve.

If the end of the rod $x = l$ is rigidly fixed, then in order to generate a reflected wave, external stresses must be applied at the section $x = l$ in such a way that the displacements and particle velocity at this section remain zero. In the same way as before, it can easily be shown that an external load $+f(t)$ must be applied to the end $x = 2l$ of the imaginary extended rod, the solution then being

$$\varepsilon' = f\left(t + \frac{x - 2l}{a_0}\right), \quad v' = a_0 f\left(t + \frac{x - 2l}{a_0}\right),$$

and the resultant strains and particle velocities in the region through which reflected waves are travelling are

$$\varepsilon = f\left(t - \frac{x}{a_0}\right) + f\left(t + \frac{x - 2l}{a_0}\right),$$

$$v = -a_0 f\left(t - \frac{x}{a_0}\right) + a_0 f\left(t + \frac{x - 2l}{a_0}\right).$$

In particular, at $x = l$

$$\varepsilon = 2f\left(t - \frac{l}{a_0}\right),$$

$$v = 0,$$

i.e. the particle velocities are zero (as the conditions require) and the strains (and therefore the stresses also) are twice those that would have arisen at the section $x = l$ of a semi-infinite rod. The distribution of ε and v is shown graphically in Fig. 165.

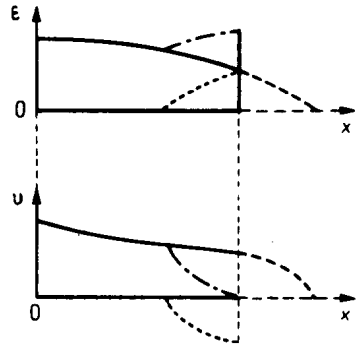

Fig. 165.

10. Impact of a Rod on a Stationary Obstacle

Suppose that a rod of length l and cross-sectional area F is moving along its axis with a velocity V when it strikes an absolutely rigid fixed plane obstacle (Fig. 166a).

Let us assume that the material of the rod strain-hardens linearly so that only two propagation velocities are possible for longitudinal waves: $a_0 = \sqrt{(E/\varrho)}$ for elastic strains, and $a_1 = \sqrt{(E_1/\varrho)}$ for plastic strains, where E_1 is the strain-hardening modulus. Particles adjacent to the leading end of the rod are brought to rest on impact. Their velocity changes by V, which gives rise to a compressive strain in accordance with (6.11). If the stress corresponding to this strain exceeds the elastic limit, two waves will be generated at the surface of contact and these will travel along the rod with velocities a_0 and a_1, both being shock waves (Fig. 166b). Indeed, all the elastic strains which occur simultaneously at the end of the rod will be propagated at the same velocity a_0 and will reach any given section of the rod simultaneously. The same applies to all the

plastic strains. Ahead (to the right) of the elastic wave front

$$\varepsilon_0 = 0, \quad v_0 = -V, \quad \sigma_0 = 0.$$

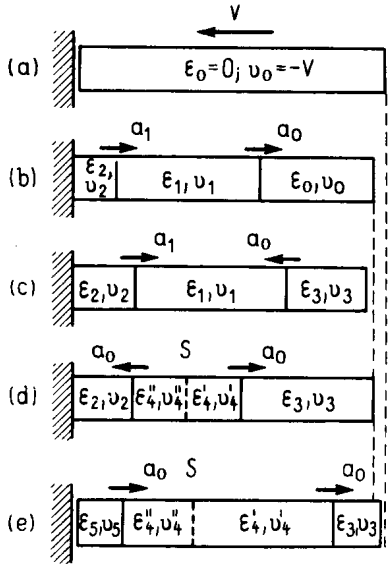

FIG. 166.

Behind (to the left of) this front $\varepsilon_1 = -\varepsilon_S$, $\sigma_1 = -E\varepsilon_S$, and v_1 can be found. From (6.11) we have that

$$a_0\varrho(v_1 + V) = E\varepsilon_S,$$

whence

$$v_1 = -V + a_0\varepsilon_S.$$

Behind the plastic wave front $v_2 = 0$, since the obstacle is fixed, and ε_2 and σ_2 can also be found. Since in the case of linear strain-hardening

$$\sigma = -E\varepsilon_S + E_1(\varepsilon + \varepsilon_S),$$

for compression beyond the elastic limit, we have from (6.11′) that:

$$-a_1\varrho v_1 = -E\varepsilon_S + E\varepsilon_S - E_1(\varepsilon_2 + \varepsilon_S),$$

from which, substituting the value found for v_1, we find that:

$$\varepsilon_2 = \frac{1}{a_1}(a_0\varepsilon_S - V) - \varepsilon_S,$$

$$\sigma_2 = (E - E_1)\,\varepsilon_S + E_1\varepsilon_2.$$

We see, therefore, that plastic strains will occur in the rod if

$$V > a_0\varepsilon_S, \tag{6.17}$$

which is in accordance with condition (6.9) derived from the elementary theory of impact.

After a time l/a_0 the elastic wave will reach the right-hand end of the rod, and after reflection will move to the left with velocity a_0 (Fig. 166c). Since the right-hand end of the rod is free, $\sigma_3 = 0$ and $\varepsilon_3 = 0$ behind (to the right of) the front of the reflected wave, and from an expression of the type (6.14) we find that the velocity v_3 is:

$$v_3 = 2a_0\varepsilon_S - V.$$

The process is as if from the moment reflection from the right-hand (free) end of the rod occurs, a tension wave of the same intensity (i.e. with the same numerical values of ε and σ) as the incident compression wave starts to travel along the rod.

When the reflected elastic wave and the incident plastic wave meet at the section S (Fig. 166d), it is as if two rods were in collision: the right-hand part moving with velocity v_3 and the left-hand part moving with velocity v_2. As a result of this "internal collision" shock waves will be propagated to right and left from the section S. Depending on the velocity of impact V, these waves could be elastic or plastic, but the wave travelling to the left will always have a velocity a_0, at least, providing $v_3 - v_2 > 0$, so that particles in the right-hand part of the rod, by exerting a pull on the particles of the left-hand part, will cause the load on the left-hand part to be reduced. Since this reduction in load takes place according to an elastic law, the velocity of propagation of such a shock wave, called an unloading wave (first discovered by K. A. Rakhmatulin), will be a_0. Considering the values of v_2 and v_3, we see that an elastic wave will travel to the left, providing that

$$V < 2a_0\varepsilon_S.$$

It can be shown that this will be the case also for any other velocity.

Let us suppose that the velocity of impact V is such that only an elastic wave travels to the right from the section S. The point P on the $\sigma \sim \varepsilon$ diagram (Fig. 167) will correspond to particles to the left of S which are in the process of being unloaded, and the point Q will correspond to particles to the right of S where no plastic strains have occurred. By the law of action and reaction

$\sigma_4' = \sigma_4''$, and from the condition of continuity of the material $v_4' = v_4''$. The strains ε_4' and ε_4'' are, however, different, since the points P and Q are on different parts of the $\sigma \sim \varepsilon$ curve (Fig. 167). The section S is therefore a stationary front of second order discontinuity in strain. In contrast to the fronts of shock waves, which are also fronts of second order discontinuity, moving with velocities a_0 and a_1, this front is stationary.

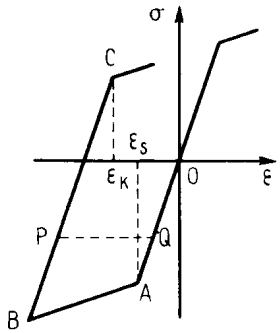

FIG. 167.

Taking into account that $\sigma_4' = \sigma_4''$, $v_4' = v_4''$ and the relation between stresses and strains $\sigma = E\varepsilon - (E - E_1)(\varepsilon_2 + \varepsilon_S)$ on the part BC of the $\sigma \sim \varepsilon$ curve (Fig. 167) and $\sigma = E\varepsilon$ on the part OA, we find from equations of the type (6.14) that on each of the fronts:

$$\varepsilon_4' = \frac{a_0 + a_1}{2a_0^2}(a_0\varepsilon_S - V),$$

$$v_4' = v_4'' = \frac{3a_0 - a_1}{2a_0}(a_0\varepsilon_S - V) + V,$$

$$\varepsilon_4'' = \frac{2a_0^2 + a_0a_1 - a_1^2}{2a_0^2a_1}(a_0\varepsilon_S - V).$$

From the conditions that $-\varepsilon_S < \varepsilon_4' < \varepsilon_S$ and $-\varepsilon_k > \varepsilon_4'' > \varepsilon_2$, where ε_k is the new elastic limit (Fig. 167), we find that the waves leaving the stationary front of second order discontinuity will both be elastic if

$$V < \left(1 + \frac{2a_0}{a_0 + a_1}\right)\varepsilon_S a_0. \tag{6.18}$$

It can easily be shown that in this case $v_4' = v_4'' > 0$. Therefore, when the wave moving to the left from the section S arrives at the

point of contact with the obstacle, the contact can be broken.† If this occurs the motion is as shown in Fig. 166e: an elastic wave is propagated to the right from the left-hand end of the rod with velocity a_0 and $\varepsilon_S = -\varepsilon^*$, i.e. ε_S is equal to the residual strain (since the end has been released from the pressure of the plate). From the relation $\sigma = E\varepsilon - (E - E_1)(\varepsilon_2 + \varepsilon_S)$ we find the residual strain ε^* for $\sigma = 0$, so that

$$\varepsilon_5 = -\varepsilon^* = \frac{a_0^2 - a_1^2}{a_0^2 a_1}(a_0\varepsilon_S - V),$$

and from an equation of the type (6.14) we then find that

$$v_5 = 2a_0\varepsilon_S - V.$$

The assumption that the two bodies are no longer in contact amounts to the requirement that $v_5 > 0$. The case described occurs, therefore, providing

$$V < 2a_0\varepsilon_S, \tag{6.19}$$

which is in accordance with condition (6.18). The rod would then be in contact with the obstacle for a time

$$T = \frac{2l}{a_0}. \tag{6.20}$$

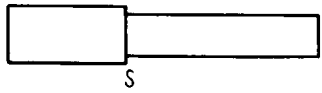

FIG. 168.

After contact ceases the rod will move to the right, and at the same time will vibrate. In the part to the right of the section S only elastic strains occurred, and in the part of the left of S there exist the same residual strains: as a result the rod has assumed the shape shown in Fig. 168. The length λ_p of the region where the residual strains exist can easily be found by examining the way in which the elastic and plastic waves are propagated from the moment they arise to the moment they meet at the section S:

$$\lambda_p = \frac{2a_1 l}{a_0 + a_1}. \tag{6.21}$$

† We note that the condition that $v_4'' > 0$, in general, is not sufficient for the contact to cease. Although particles in the part of the rod adjacent to the obstacle have a velocity to the right, the rod can be looked upon as a form of compressed spring; if slight movement to the right occurs it will expand and the contact can be maintained.

The magnitude of the residual strain is

$$\varepsilon^* = \frac{a_0^2 - a_1^2}{a_0^2 a_1}(V - a_0\varepsilon_S). \tag{6.22}$$

In an experiment on the longitudinal impact of a rod against a rigid obstacle we can measure the residual strain ε^*, the length λ_p of the zone over which it occurs and the time the bodies are in contact T. We can also measure the density ϱ of the material. We can then find from (6.20) $a_0 = \sqrt{(E/\varrho)}$, i.e. the dynamic modulus of elasticity, and from (6.21) and (6.22) we can find ε_S and $a_1 = \sqrt{(E_1/\varrho)}$, i.e. the dynamic elastic limit and the dynamic strain-hardening modulus. In this way we can derive experimentally the dynamic $\sigma \sim \varepsilon$ diagram, providing it is linear in its plastic range. It should, however, be pointed out that this is not so for the majority of materials.

If condition (6.19) is not observed, i.e. if

$$2a_0\varepsilon_S < V < \left(1 + \frac{2a_0}{a_0 + a_1}\right)a_0\varepsilon_S,$$

it can be shown that contact ceases after a time

$$T = \frac{4l}{a_0 + a_1},$$

and as before there remains one zone of constant residual strains.

If condition (6.18) also is not observed, i.e. if

$$V > \left(1 + \frac{2a_0}{a_0 + a_1}\right)a_0\varepsilon_S,$$

a plastic wave will travel to the right from S, a second stationary front of second order discontinuity S' will be formed to the right of S, and after impact there will be two zones of constant residual strains ε^* and $\varepsilon^{*\prime}$ in the rod. With further increase in the velocity of impact three, four, etc., zones of constant residual strain will be formed (Fig. 169).

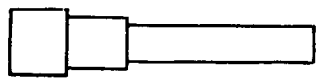

FIG. 169.

11. The Measuring Rod Theory

The phenomenon of propagation and reflection of longitudinal waves is applied in the theory of an apparatus used for deriving the pressure–time curve for explosion and impact—an apparatus known as Hopkinson's measuring rod.

Hopkinson's measuring rod consists of a long rod A made of steel with another rod B of the same diameter (Fig. 170) called a "chronograph" stuck to its end with grease. If a small explosion occurs on the left-hand end of the rod A, an elastic wave will travel along the rod, the shape of which (i.e. the distribution of the

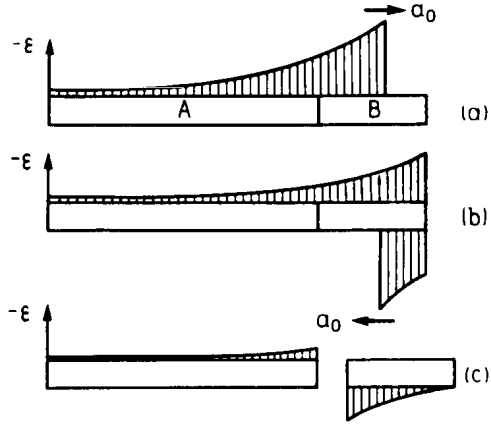

Fig. 170.

stresses or particle velocities) will reproduce to some scale the shape of the pressure–time curve on the left-hand end of the rod (Fig. 170a). This wave will pass undistorted through the junction of the rods A and B and will then be reflected from the right-hand end of rod B in the same way as if a wave of the same shape but of opposite sign (Fig. 170b) had started from this end of the rod. If as a result of the superposition of the reflected wave on the incident wave at the point of junction of the two rods a tensile stress is generated (Fig. 170c) the rod B will fall off, since the joint cannot withstand tensile stresses.

Repeating the test with "chronographs" of different length, and measuring each time the momentum of the "chronograph" and of the main rod, we obtain a pressure–time curve in the form of a step-curve (Fig. 171). The momentum of the "chronograph" is

numerically equal to the part of the area under the pressure–time curve extending from zero along the time axis to $\tau = 2l/a_0$, where l is the length of the "chronograph" and a_0 is the velocity of the elastic wave.

Instead of one "chronograph" several discs can be used, a measurement of the velocities of which gives immediately several small "steps" in the p—t curve. These discs can be stuck in a recess in the face opposite to that at which the explosion or impact occurs. A curve similar to Fig. 171 then gives the pressures reaching the back of the plate.

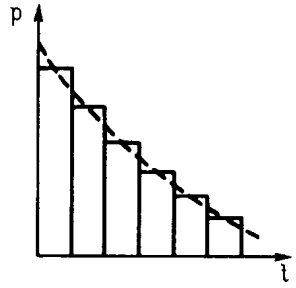

FIG. 171.

12. DERIVATION OF THE DYNAMIC $\sigma \sim \varepsilon$ DIAGRAM FROM THE DISTRIBUTION OF RESIDUAL STRAINS

The method given in § 10 of deriving the dynamic relation between stresses and strains is limited by the fact that the $\sigma \sim \varepsilon$ curve for the majority of materials is non-linear beyond the yield point. On impact with an obstacle an elastic shock wave will be generated but the front of the plastic wave will be indistinct, since each plastic wave travels with its own velocity $a = \sqrt{(1/\varrho)(d\sigma/d\varepsilon)}$. On impact with a rigid obstacle an infinite number of strains with

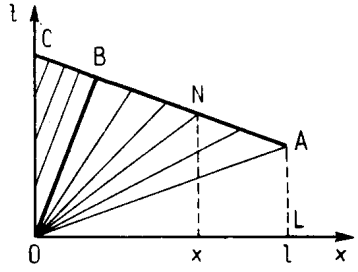

FIG. 172.

different velocities will be propagated simultaneously along the rod from the point of contact. In the (x, t) plane this can be represented by a cluster of straight lines radiating from the origin of coordinates and called Riemann waves (Fig. 172) if, as is the case for the majority of solid bodies, the $\sigma \sim \varepsilon$ diagram is convex on the side of the σ-axis.

On impact the straight line OA corresponds to the front of the elastic shock wave on which the strains increase discontinuously to ε_S, and the line OB corresponds to the propagation of the maximum strain caused by the impact. In the region OAL the

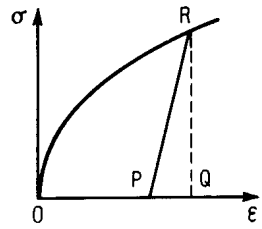

FIG. 173.

particles are in their initial (pre-impact) state: the stresses and strains are zero and the velocity of all the particles is V. In the region OAB the strains vary with x and with t. In the region above OB the strains are constant (equal to the maximum strain).

The front of the elastic shock wave OA will be reflected from the right-hand free end of the rod as an unloading wave moving with the velocity a_0 of an elastic wave. This can be represented in the (x, t) plane by the straight line AC. It will pass through the Riemann waves and at each section will leave behind a residual strain $\varepsilon^* = \varepsilon^*(x)$, which can be measured experimentally. If, in addition, we could also find the greatest strain reached at each section before the decrease in load caused by the reflected wave, we could draw the dynamic $\sigma \sim \varepsilon$ curve.

For, if we know $OP = \varepsilon^*$ and $OQ = \varepsilon_{\max}$ (Fig. 173), by drawing PR with slope E (the Young's modulus) and the perpendicular to the ε-axis from the point Q, we can determine the corresponding value of $\sigma = RQ$:

$$\sigma = E(\varepsilon_{\max} - \varepsilon^*) = \chi(x). \tag{6.23}$$

The relation $\sigma = \sigma(\varepsilon)$ can thus be found in parametric form

$$\left.\begin{aligned} \sigma &= \chi(x), \\ \varepsilon &= \varepsilon_{\max}(x). \end{aligned}\right\}$$

It is, however, extremely difficult in practice to measure the maximum strain at each section, but this difficulty can be overcome.

If at some section x the maximum strain caused by the impact is ε, and if the required relation between stress and strain is of the form $\sigma = \Phi(\varepsilon)$, the residual strain at this section is

$$\varepsilon^* = \varepsilon - \frac{1}{E}\Phi(\varepsilon), \tag{6.24}$$

whence

$$\frac{d\varepsilon^*}{dx} = \frac{d\varepsilon}{dx} - \frac{1}{E}\frac{d\Phi}{d\varepsilon}\frac{d\varepsilon}{dx}$$

or

$$\frac{d\varepsilon^*}{dx} = \frac{d\varepsilon}{dx}\left(1 - \frac{1}{a_0^2}\frac{1}{\varrho}\frac{d\Phi}{d\varepsilon}\right), \tag{6.25}$$

where we have made use of the relation $a^2 = E/\varrho$. But $(1/\varrho)(d\Phi/d\varepsilon) = a^2$. i.e. the square of the velocity of propagation of the strain ε.

From Fig. 172 it can easily be shown that the point where the strain ε, travelling at velocity a, meets the unloading wave AC is given by the expression $x = 2al/(a_0 + a)$, i.e. at this section the maximum strain was ε. Substituting $a = a_0 x/(2l - x)$ in expression (6.25), we get that

$$\frac{d\varepsilon^*}{dx} = \frac{d\varepsilon}{dx}\left[1 - \left(\frac{x}{2l - x}\right)^2\right] \quad \text{or} \quad \frac{d\varepsilon}{dx} = \frac{\dfrac{d\varepsilon^*}{dx}}{1 - \left(\dfrac{x}{2l - x}\right)^2}.$$

By integrating with respect to x we can find the maximum strain reached before unloading occurs at every section x:

$$\varepsilon(x) = \varepsilon_S - \int_x^l \frac{\dfrac{d\varepsilon^*}{dx}}{1 - \left(\dfrac{x}{2l - x}\right)^2} dx.$$

In the integration we have taken into account the fact that on the extreme right-hand section $x = l$ the maximum strain is ε_S. The above expression is in fact the required solution, since $\varepsilon^* = \varepsilon^*(x)$ can easily be found by experiment by measuring the cross-sectional

area after impact. In order to avoid the necessity of differentiating the experimental curve of $\varepsilon^* = \varepsilon^*(x)$, which leads to considerable errors, we carry out the integration by parts. As a result we get that

$$\varepsilon(x) = \varepsilon_S + \frac{\varepsilon^*(x)}{1 - \left(\frac{x}{2l - x}\right)^2} + \int_x^l \frac{x(2l - x)\,\varepsilon^*(x)}{4l(l - x)^2}\,dx, \quad (6.26)$$

after which, from (6.23), we find that:

$$\sigma(x) = \sigma_S + \frac{Ex^2\varepsilon^*(x)}{4l(l - x)} + \frac{E}{4l}\int_x^l \frac{x(2l - x)\,\varepsilon^*(x)}{(l - x)^2}\,dx. \quad (6.27)$$

The expressions (6.26) and (6.27) are the parametric equations of the required relation $\sigma = \Phi(\varepsilon)$.

R. I. Nadeevaya of Moscow University used this method to determine the $\sigma \sim \varepsilon$ relation for steel shown in Fig. 157a. The points in this diagram in the plastic range correspond to different rates of strain which are higher, the closer the point is to the elastic limit. The difference in slope between the static and dynamic diagrams is also greater close to the elastic limit. A dynamic curve, therefore, whilst not coinciding exactly with the curve corresponding to an infinite rate of strain is very close to this curve.

13. The Method of Impulses

The method given in the previous section of determining the $\sigma \sim \varepsilon$ relation cannot be used when the material has a $\sigma \sim \varepsilon$ curve which is convex on the side of the ε-axis, since in this case the greater the strain the greater is its propagation velocity. The stronger waves then overtake the weaker, which results in a pheno-

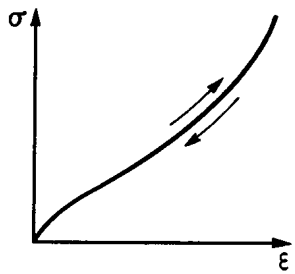

Fig. 174.

menon analogous to the breaking of waves at sea, which is difficult to subject to theoretical analysis. Furthermore, the method described is not applicable to non-linearly elastic bodies for which the stress–strain relation for active strains is non-linear, but where the curve for decreasing loads approximately coincides with that for increasing loads, so that after removal of the load no residual strains occur. A typical curve which has both these properties is that for rubber (Fig. 174).

To derive the dynamic $\sigma \sim \varepsilon$ curve for this type of material we proceed as follows.

We extend statically a long cylindrical specimen of the material to some point M on the $\sigma \sim \varepsilon$ curve and fix it in this position. By striking the end of the rod we create an impulse of not very large magnitude, the propagation velocity of which along the rod can easily be measured. It is found that this velocity corresponds not to the slope of the static $\sigma \sim \varepsilon$ curve at the point M, but to the slope of the dynamic $\sigma \sim \varepsilon$ curve at the corresponding point M'. By varying the static tension we can derive the curve of the relation between the velocity of propagation of strains $a = a(\varepsilon)$ and the strain due to the static tension. Since $a^2 = (1/\varrho)\, d\sigma/d\varepsilon$, we can find from this curve the dynamic $\sigma \sim \varepsilon$ relation:

$$\sigma = \varrho \int_0^{\varepsilon} a^2(\varepsilon)\, d\varepsilon.$$

This method was used by V. S. Lenskii and M. A. Tarasovaya at Moscow University to derive the dynamic relation for rubber shown in Fig. 157b.

14. Spalling and Resistance to Bursting

The importance of the study of waves is not restricted to providing a means of determining the dynamic properties of materials. It is very much more important in the study of the effects of dynamic loading and in providing the means of protecting equipment and structures from failure.

Seismology—one of the most important branches of knowledge—has as its basis the study of the theory of waves. A disturbance originating within a small volume of the earth's crust is propagated in all directions and decreases in intensity with increase in distance travelled. The propagation of these disturbances, their reflection

from and interaction with natural obstacles (mountain ranges, gorges, seas and oceans) is studied on the basis of wave theory.

Seismic methods were given considerable impetus by the need to carry out surveys for minerals. By producing an explosion at a certain depth and observing the waves arriving at a seismograph it is possible to detect underlying rock formations at great depths.

The effect of an explosion on a structure situated some distance away or underground is also transmitted by waves.

Due to an explosion or impact a phenomenon is observed on the surface of, for example, a steel plate, which is known as spalling:

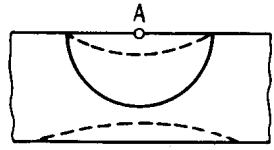

FIG. 175.

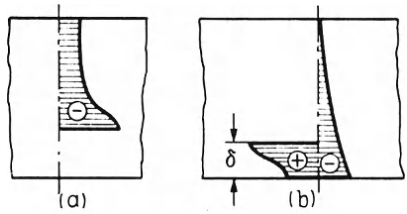

FIG. 176.

pieces of material the shape of a plano-convex lenses (the spalled surface is shown by the broken lines in Fig. 175) fly off from both faces of the plate. In order to study quantitatively this phenomenon Reinhart (1951) assumed as a simplification that the pressure caused by the explosion was uniformly distributed over the face of the plate. This one-dimensional theory of spalling is analogous to the measuring rod theory (§ 11) and is based on the assumption that the strains are elastic.

If the pressure is instantaneously built up and then rapidly diminishes, the compression wave (Fig. 176a), on reflection from the free surface as a tension wave of the same shape (Fig. 176b), is superimposed on the compression wave, and at some distance from the free surface gives rise to tensile stresses. If the material can withstand large compressive stresses but fails at very much smaller tensile stresses (which is the case for many materials), at

some distance δ from the rear (free) surface of the plate the tensile stress caused by the superposition of the incident and reflected waves can reach failing point σ_p and it is here that a spalling crack is formed. The relation between the pressure caused by the explosion and time was found in Reinhart's experiments by measuring the velocities of small discs stuck in recesses in the back of the plate, as was described in § 11. Knowing the law $p = p(t)$, and measuring the depth of spalling δ, we can determine the magnitude of the stress required to give the spalling type of failure. From formula (6.14), multiplying both sides by the elasticity modulus E, we have for the compressive stress in the plane of spalling

$$\sigma' = -p\left(t - \frac{H - \delta}{a_0}\right),$$

where H is the thickness of the plate; the tensile stress in this plane is $\sigma'' = p(0) = p_0$. Thus the failure stress is

$$\sigma_p = \sigma'' + \sigma' = p_0 - p\left(t - \frac{H - \delta}{a_0}\right).$$

Reinhart found the following values for the spalling failure stress: for duralumin (an alloy of the type D. 16), 9800 kg/cm^2, for copper, 30,000 kg/cm^2, for steel (Mk. 1020), 11,000–15,000 kg/cm^2, for steel (Mk. 4130), 30,800 kg/cm^2. These values are considerably greater than the ultimate tensile stresses, which is due partly to the effect of the rate of strain, but mainly to the conditions of failure under an almost uniform all-round tension. It is of interest that the results obtained for spalling failure for steel Mk. 1020 are very close to those for a bursting type of failure obtained by G. V. Uzhik, who carried out tensile tests on notched specimens. At the point of failure in the latter the conditions were close to the conditions of all-round tension.

The actual mechanism of spalling caused by impact or explosion is much more implicated than that given by the one-dimensional theory. For thick plates the explosion (and even more so, the impact) can often be considered to act at a point. The front of the compression wave is a hemisphere with centre at the point of the explosion A (see Fig. 175). As a result of the wave being reflected from the upper surface of the plate tensile stresses occur, which at a certain depth, being superimposed on the compression wave, create the conditions required for spalling of the face of the plate.

Reflection from the lower surface of the plate leads to spalling of the back of the plate.

If the pressure from the explosion is sufficiently large, further spalling may occur due to reflection from the free surface formed by the first spalling. This is known as multiple spalling and is a phenomenon not unheard of in practice.

15. Hollow Charges

It was discovered as far back as the eighteenth century that a charge with a conical depression or hollow was more effective than one with a plane surface. The effect of a hollow charge is concentrated around the axis of the cone and produces a high pressure, reaching 200,000–300,000 atm over a small area. Mining engineers made use of this phenomenon for breaking through large rock formations by forming in this way the cylindrical holes into which the blasting charge is then placed, and also for forming the radial chambers leading from main oil wells in an effort to increase the flow of oil, etc.

If the internal surface of the depression in a shaped charge is coated with a thin layer of metal this metal forms on explosion a concentrated jet of metal moving at great velocity (up to 5–10 km/sec) and possessing great penetrating power. This type of charge was used during the second world war in armour-piercing shells such as the American "bazooka" and the German "faustpatron". It should be noted that the high velocity of the concentrated jet does

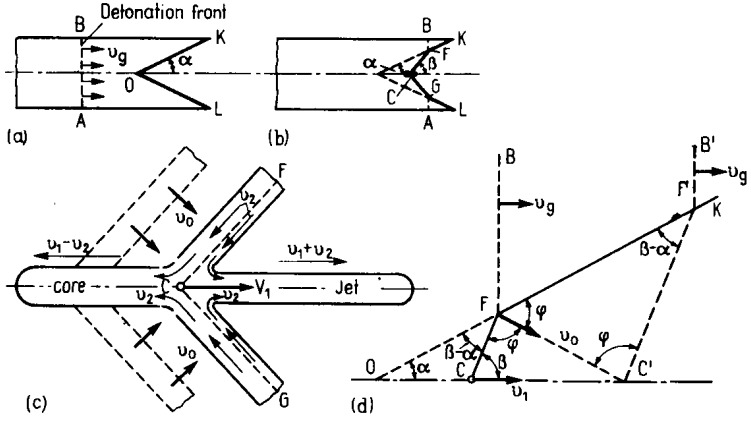

FIG. 177.

not require a high velocity of the armour-piercing shell.† A coated shaped charge in the form of a wedge in which the metal coating forms a thin plane jet of great velocity can be used for cutting plate metal, steel joists, cables, etc.

The mechanism of the formation of concentrated jets in a coated hollow charge and its action on an obstacle have been studied by a great number of scientists. We shall give here only the elementary theory suggested by Taylor, which refers to charges with either a wedge-shaped or a conical hollow.

Let us consider a longitudinal section of such a charge (Fig. 177a). The detonation front AB moving with velocity v_D passes over the coating. The instantaneous pressure on this front imparts a velocity v_0 on each particle of the coating, the direction and magnitude of which we shall find later. If we ignore the change in the intensity of pressure on the detonation front due to decrease in the explosive towards the base of the wedge (cone), and if we ignore also the increase in mass per unit length of the conical layer of the coating, then the velocity v_0 can be considered to be constant. Then the moving part of the layer will be in the shape of a wedge (cone) FCG (Fig. 177b) with angle $\beta > \alpha$. In the parts of the coating converging on the axis of the wedge (cone) a high pressure is set up and plastic flow takes place. The part of the metal on the internal surface of the layer is pushed out in the direction of motion of the detonation front (to the right) and forms a thin jet moving at high velocity (Fig. 177c). The part of the metal on the external surface of the layer is pushed in the opposite direction and forms a so-called "core" also moving to the right but at a lower velocity than the jet. An observer moving together with the apex of the deformed wedge C would see a picture of established flow.

A metal under high pressures can be considered as an almost ideal fluid, the velocity v of which is related to the pressure p at the place of formation of the jet by the well-known Bernoulli equation of the theory of hydrodynamics:

$$p + \tfrac{1}{2}\varrho v^2 = \text{const.},$$

in which the density ϱ can be considered to be constant. Thus the material in the jet and in the core move away from the apex C at

† The Japanese, for example, used armour-piercing shells which were simply attached to the armour of a tank.

the same velocity v_2. If the velocity of the apex C is v_1, the velocities of the jet and of the core are therefore

$$v_i = v_1 + v_2, \quad v_S = v_1 - v_2, \tag{6.28}$$

respectively, where $v_1 > v_2$, so that $v_S > 0$, but $v_S < v_i$ (Fig. 177c).

We shall now find the direction and magnitude of the velocity v_0 of particles of the coating material in the deformed state. Suppose that at an instant t the layer occupies a position CFK (Fig. 177d). After an interval of time Δt the point F, which starts to move at a velocity v_0, is situated at the point C'. During this time the detonation front moves a distance $v_0 \Delta t$ and intersects the layer in the point F', and the part FF' of the layer, without changing its length, moves to a position $F'C' \| FC$, so that $\angle CFC' = \angle FC'F'$. But $\Delta FF'C'$ is an isosceles triangle, and $\angle FC'F = \angle C'FF' = \varphi$. The velocity v_0 is therefore directed along the bisector of the angle CFK. Its magnitude, or, what is equivalent, the magnitude of the angle β is determined by the pressure on the detonation front, so that one of them, for example β, can from now on be considered to be the unknown quantity. Then, since $FC' = v_0 \Delta t$ and $FF' \cos\alpha = v_D \Delta t$, we find the relation between v_0 and v_D, taking into account that $\varphi = \frac{1}{2}(\pi - \beta + \alpha)$:

$$v_0 = \frac{\sin(\beta - \alpha)\cos\dfrac{\beta - \alpha}{2}}{\cos\alpha} v_D. \tag{6.29}$$

On the other hand, since $FC' = v_0 \Delta t$ and $CC' = v_1 \Delta t$, we find the relation between v_0 and v_1:

$$v_1 = \frac{\cos\dfrac{\beta - \alpha}{2}}{\sin\beta} v_0. \tag{6.30}$$

We see from Fig. 177 that the velocity of divergence of the material relative to the point C, assuming that the material is incompressible, is the same as the velocity of convergence of the material from the side of the point F. Therefore,

$$v_2 = \left(\frac{\cos\dfrac{\beta - \alpha}{2}}{\tan\beta} + \sin\frac{\beta - \alpha}{2} \right) v_0 = \frac{\cos\dfrac{\beta + \alpha}{2}}{\sin\beta} v_0. \tag{6.31}$$

From (6.28) to (6.31) we obtain the following expressions for the absolute velocities of the jet and the core:

$$\left.\begin{aligned} v_j &= v_D \frac{\sin(\beta - \alpha)}{\cos\alpha}\left(\operatorname{cosec}\beta + \cot\beta + \tan\frac{\beta - \alpha}{2}\right), \\ v_S &= v_D \frac{\sin(\beta - \alpha)}{\cos\alpha}\left(\operatorname{cosec}\beta - \cot\beta - \tan\frac{\beta - \alpha}{2}\right). \end{aligned}\right\} \tag{6.32}$$

We see that the velocity of the jet is greater, the smaller the angle at the apex of the cone (wedge) of the coating of metal, since the angle β then becomes smaller as well. In particular, as $\alpha \to 0$, we have that $v_j = 2v_D$ and $v_S = 0$.

We can determine now what part of the mass of coating material was used to form the jet. If in the case of a wedge m is the mass of the coating material per unit length in the direction CF (Fig. 177c), and m_j and m_S are the masses which go to make up the jet and core respectively, then the condition that the component of the momentum in a horizontal direction is constant before and after division of the mass into the jet and the core gives:

$$mv_2 \cos\beta = m_S v_2 - m_j v_2.$$

Since also $m_j + m_S = m$, we have that

$$m_j = \frac{m}{2}(1 - \cos\beta), \quad m_S = \frac{m}{2}(1 + \cos\beta). \tag{6.33}$$

As $\alpha \to 0$, β also tends to zero, and then $m_j \to 0$. Thus a decrease in the angle α gives an increased velocity and decreased mass of the jet.

The action of hollow charges on a metal plate may be explained as follows: the jet penetrates to a considerable depth in the plate and causes plastic flow of the material in directions perpendicular to the axis of the charge. For this reason the diameter of the hole formed exceeds that of the jet. The pressure of the jet on the plate can be calculated from Bernoulli's equation if the instantaneous loss of velocity Δv_j of the jet on striking the plate can be found:

$$p = \tfrac{1}{2}\varrho(\Delta v_j)^2.$$

For example, if on striking a steel plate the loss in velocity is of the order of 3000 m/sec, the pressure under the jet will be of the order of 400,000 atm.

The above theory of hollow charges can be refined by taking into account the decrease in the intensity of the detonation wave

and the increase in the mass of the material of the conical shell which is brought into motion as the detonation wave approaches the base of the cone. In this case the deformed surface would not be the cone *FCG* (Fig. 177b), but a surface of revolution with a curved generator. Different parts of the jet would have different velocities.

The laws governing the formation of these jets and their penetration into an obstacle can be investigated experimentally with the aid of Röntgen-impulse apparatus. It has been found that the theory conforms very satisfactorily with the results of such experiments.

16. Penetration of one Body by Another

Several different approaches have been made to the solution of the problem of penetration of a sharp body into an obstacle. Some of these theories are based on the assumption that the obstacle consists of a viscous liquid into which an absolutely rigid body penetrates at a very high velocity. Other theories consider the material of the obstacle as a solid medium possessing the properties of elasticity and plasticity. There are also a number of different approaches within the latter category. We can, for example, consider penetration either as a static problem on the basis of a conical or wedge-shaped body being pressed into an elasto-plastic medium and apply the dynamic, as opposed to the static, relation between stress and strain, taking into account in this way the dynamic nature of the problem. Approached on this basis, penetration is analogous to the problems which were dealt with in Chapter III. In the case of a shell penetrating a piece of armour at high velocity, it would sometimes be more accurate to approach the problem in a way which takes into account the finite velocity of propagation of the disturbances, i.e. on the basis of the wave theory.

In order to explain the application of the wave theory to the problem of penetration, let us consider the following plane problem. Suppose that an absolutely rigid wedge-shaped body with curved sides (Fig. 178a), of infinite length in a direction perpendicular to the drawing, is moving with a known velocity $V(t)$ in its plane of symmetry. For a small layer of the medium of thickness h at a sufficient depth H and perpendicular to the plane of symmetry of the penetrating body, the problem can be formulated as follows:

if we ignore the friction between the medium and the penetrating body, we can consider that any cross-section of the layer parallel to the plane of symmetry of the body remains plane, that it moves in a direction perpendicular to the plane of symmetry and remains parallel to its original position (the assumption of plane sections remaining plane). If we ignore also the friction between different layers of the medium, we arrive at a problem of propagation of plane longitudinal elasto-plastic waves in a rod contained in an absolutely rigid and smooth cylinder, the ends of the rods being given a velocity $v(t)$, which is related to time by the function $V(t)$

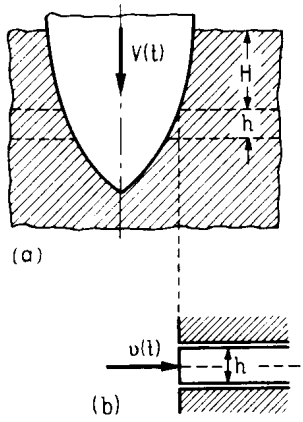

FIG. 178.

and the shape of the lateral surface of the penetrating body (Fig. 178b).

An interesting feature of this problem is that the deformation of the rod takes place solely on account of a change in volume with a corresponding change in density. At present our information concerning the equation of state for solid bodies is incomplete. On the basis of experimental data on the behaviour of bodies at high pressure F. A. Bakhshiyan (1950) has suggested the following relation between the pressure p and density ϱ:

$$p = \frac{A}{n}\left[\left(\frac{\varrho}{\varrho_0}\right)^n - 1\right], \tag{6.34}$$

where A is a constant with the dimensions kg/cm^2, n is a dimensionless quantity (an integer) and ϱ_0 is the density at zero pressure.

From the law of conservation of mass $\varrho\Omega = \varrho_0\Omega_0$, where Ω_0 and Ω are the volumes before and after compression, we have that

$$\frac{\varrho}{\varrho_0} = \frac{1}{1+\theta},$$

where $\theta = (\Omega - \Omega_0)/\Omega_0$ is the relative change in volume. In our case of confined longitudinal compression of a rod contained in a rigid layer we have that $\theta = \partial u/\partial x = \varepsilon$. Therefore, from (6.34) the relation between the longitudinal stress σ and the strain ε is of the form

$$\sigma = -\frac{A}{n}\left[\left(\frac{1}{1+\varepsilon}\right)^n - 1\right]. \tag{6.35}$$

From this, according to formula (6.12), we can find the propagation velocity of the longitudinal wave

$$a \equiv \sqrt{\left(\frac{1}{\varrho}\frac{d\sigma}{d\varepsilon}\right)} = \sqrt{\left[\frac{A}{\varrho_0}\left(\frac{1}{1+\varepsilon}\right)^n\right]}. \tag{6.36}$$

If we put $n = 6$, we get that

$$a = \frac{1}{(1+\varepsilon)^3}\sqrt{\left(\frac{A}{\varrho_0}\right)}. \tag{6.37}$$

The present problem differs from that given in § 7 (Fig. 163) in that on the end of the semi-infinite rod in this case we are given as a function of time not the strain, but the velocity of particles. But if we know the velocity of the particles at the end of the rod, we also know the strain. From (6.10″) $v = -\int_0^{\varepsilon} a(\varepsilon)\,d\varepsilon$, which applies everywhere within the moving region, we get that

$$v(t) = -\sqrt{\left(\frac{A}{\varrho_0}\right)}\int_0^{\varepsilon}\frac{d\varepsilon}{(1+\varepsilon)^3} = \frac{1}{2}\sqrt{\left(\frac{A}{\varrho_0}\right)}\left|\frac{1}{(1+\varepsilon)^2} - 1\right|,$$

from which

$$\varepsilon(t) = \left[1 + 2\sqrt{\left(\frac{\varrho_0}{A}\right)}v(t)\right]^{-1/2} - 1. \tag{6.38}$$

We see from formula (6.37) that as the strain ε increases the propagation velocity a of the wave decreases. In the (x, t) plane, therefore, the curves of propagation of different strains is represented by a non-concurrent cluster of divergent straight lines (Fig. 179). When a series of these curves has been drawn on the basis of eqn. (6.37) and (6.38), as we know from § 7 (Fig. 163), it is not difficult to find the strain at any section x at any instant of time t.

We can then determine from (6.35) the variation with time of the stress at any section.

In particular we can find the stress $\sigma_H = \sigma_H(t)$ on the end of the rod, i.e. the pressure exerted by the penetrating body on the medium at any depth. If we solve simultaneously the problem of propagation of waves at different layers in the medium and the problem of motion of a penetrating body of given mass against the reaction of the medium, we can also determine the law governing the motion

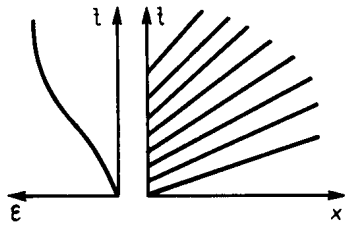

FIG. 179.

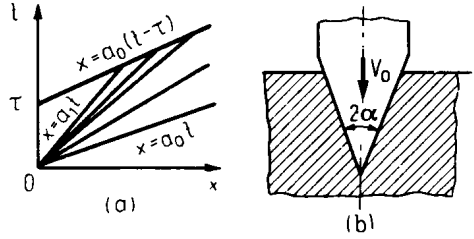

FIG. 180.

of the penetrating body. The difficulty is that a retardation of the body corresponds to a retardation at the ends of at least some of the layers, i.e. to a decrease in the load acting on them. This leads to a very complex mathematical problem on the propagation of unloading waves, since the waves in the region of decrease in load are propagated with the velocities of elastic waves and overtake the previously generated plastic waves. In the (x, t) plane the propagation curves of these waves will intersect those of the active elasto-plastic waves.

In the case of a plane wedge with angle 2α penetrating a medium at a constant velocity V_0, we have from (6.38) that

$$\varepsilon = \left[1 + 2v_0 \sqrt{\left(\frac{\varrho_0}{A}\right)}\right]^{-1/2} - 1 = \varepsilon_0 = \text{const.} \qquad (6.39)$$

where $v_0 = V_0 \tan \alpha$, i.e. the imaginary rod is under conditions of end impact at constant velocity. The non-concurrent cluster of wave propagation lines in the (x, t) plane becomes a concurrent cluster (see Fig. 172, § 12), the slope a_1 of the outer ray of which is given by (6.37) by putting $\varepsilon = \varepsilon_0$ from (6.39) (Fig. 180a).

If the pointed part of the body is followed by a plane parallel part (Fig. 180b), then immediately the point of change passes through the layer under consideration the pressure exerted by the wedge on the layer instantaneously vanishes. The resulting shock wave of decrease in load is propagated with the velocity of an elastic wave $a_0 = \sqrt{(A/\varrho_0)}$ (from formula 6.37 for $\varepsilon = 0$), and in the (x, t) plane we have the equation $x = a_0(t - \tau)$. This allows us to find, as in the problem of a rod striking an obstacle (§ 12), the

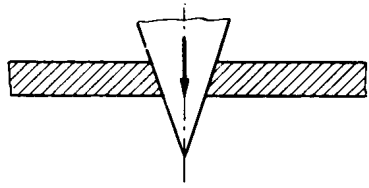

FIG. 181.

distribution of residual strains and, in particular, the size of the hole left by the penetrating body.

For a wedge penetrating a thin plate at high velocity the problem becomes completely analogous to the problem of impact of a rod on an obstacle, since the whole plate can be considered as one layer with free surfaces (Fig. 181).

The various theoretical approaches to the process of penetration are not always borne out by observed results, and for this reason empirical formulae are quite often used. The velocity V_0, for example, which is necessary for a normal modern artillery shell of weight q and calibre d to penetrate an armoured plate of thickness H is given by the formula

$$V_0 = kd\left[H\left(\frac{H}{d}\right)^n\right]^{1/2} V_0 = k\frac{d^{0.75}H^{0.7}}{q^{0.5}}, \qquad (6.40)$$

where k is a constant which depends on the mechanical properties of the plate. For penetration of thick plates, in which a small, neat hole is left, $n = 1$, for thin plates $n = 2$, and in the case of stamping

small solid cylinders of material from a thick plate we take $n = 2$. In the case of high velocity shells ($V > 1200$ m/sec) the depth of penetration on normal impact with a metal object is given by the formula

$$H = k(MV^2)^{1/3}, \tag{6.41}$$

where k is a coefficient which depends on the material of the object and is found experimentally.

17. Impact on Structures

As an approximation we can consider the mass of the structure to be concentrated at certain points. In particular the mass m_k of a structure with planes of symmetry (xz) and (yz) can be considered as made up of a mass at the supports and a mass at a point on the z-axis. We shall denote this mass as $m = km_k$ where $k < 1$. If the stiffness B of the structure is known, the displacement of the mass m caused by the static action of a force Q on the structure along the z-axis is given by the formula

$$w = Q/B. \tag{6.42}$$

Suppose now that a solid body of mass m_0 moving along the z-axis with velocity V_0 strikes the structure in the region of the concentration of the mass m and that the body remains in contact with the structure. At the time of impact $w = 0$, and therefore free impact of masses m_0 and m takes place without separation. By the law of conservation of momentum the velocity V of the two masses immediately after impact is $V = V_0 m/(m + m_0)$. The kinetic energy of the structure and of the striking body after impact are, therefore,

$$\frac{1}{2}(m + m_0)\, V^2 = \frac{1}{2} \cdot \frac{m^2}{m + m_0} \cdot V_0^2. \tag{6.43}$$

This energy is absorbed by the structure, and at maximum displacement w_m the kinetic energy (6.43) is entirely transformed into the potential energy of elastic deformation of the structure which is $\frac{1}{2} w_m Q_m = \frac{1}{2} \cdot B w_m^2$. Therefore, from (6.43),

$$w_m = mV_0/\sqrt{[B(m + m_0)]}. \tag{6.44}$$

Knowing w_m we can calculate the maximum forces, strains and stresses set up in the various elements of the structure by the impact. This semi-statical approach is, of course, approximate.

CHAPTER VII

VIBRATIONS OF ELASTIC BODIES AND FATIGUE OF MATERIALS

1. The Behaviour of Materials and Structures under Oscillating Loads

The periodic motion of the various components of engines, machines and mechanisms, irrespective of the nature of the external forces, sets up periodically varying inertia forces which act on these components as well as on the supports, foundations or structures connected to the machine. These inertia forces can be looked upon as external forces when finding the internal forces of interaction between particles of the body. The external forces acting on a component or on a structure can also vary periodically; the pressure inside an internal combustion engine acts in this way on the piston and on the sides and head of the cylinder, and so also does the resistance of the materials on the working parts of stamping machines and presses. Oscillations which set up periodically varying stresses can occur as a result of the interaction of an elastic body on the surrounding medium: the wing of an aeroplane, a turbine blade, a ship's propellor, all of which move relative to a liquid or gaseous surrounding medium, are, under certain conditions, set into an oscillatory motion due to changes in the angle of incidence to the resisting medium coupled to the restoring elastic forces of the oscillating body. Examples of this type of motion, which comes under the heading of self-induced vibration, are the oscillations of bridges, masts, cables, etc., in an air stream. Periodically varying stresses can also occur in periodically varying temperature and radiation fields.

The mechanical behaviour of bodies under oscillating loads, or, in general, repeated (though not necessarily periodic) loads, differs from their behaviour under constant loads. The design criteria for a body under the action of a repeated load are different from those for a constant load: a combination of stresses and strains which is

"safe" under a constant load is not necessarily so in the case of repeated application and removal of the load. We can go a little way toward understanding the reason for this if we bear in mind that a stress is in fact the mean of the internal forces, which are distributed non-uniformly and act in random directions between different microvolumes. In the experimental derivation of the strength criteria for constant, static loads this non-uniformity is taken account of in the actual behaviour of the material during the experiment. But the results of these experiments and the strength criteria derived from them cannot automatically be applied to cases of repeated loads. Indeed, even in the case of deformation within the elastic range, when each repetition of the load gives the same state of stress and strain, local plastic strains and microfailures can occur within small regions of the body, especially if there exist defects within or on the surface of the body (cracks, cuts, inclusions, etc.). The local state of stress and strain in these regions would then be quite different in the case of repeated loading. The accumulation of the changes that take place in these small regions can lead to the development of failure cracks, or in other words to fatigue of the material under periodic loading.

If the external load is a repeatedly varying temperature field, then for a sufficiently wide temperature range the various parts of the body will be subjected to various types of heat treatment, which are accompanied, in general, by irreversible structural changes which in some cases can lead to failure of the material. Failures such as these are sometimes referred to as thermal breakdown of the material.

Oscillating loads causing resonance can lead to a marked increase in the amplitude of the vibrations of the various parts of a structure, which is undesirable and dangerous, not only because excessive stresses can be set up, but also because large displacements, even when they correspond to relatively small stresses, can prevent the structure from functioning properly. In the first case (the case of failure) the problem is one concerned with the actual strength of the structure or machine, and in the second case (the case of excessive displacements) it is a problem of stability.

Loads which vary with time and conditions which give rise to vibration are frequently encountered in practice and for this reason the study of oscillations of solid bodies and the accompanying phenomena is of considerable importance.

We shall deal only with elastic vibrations. The theory of elasto-plastic vibrations has not as yet been fully developed, and so far the general method of analysis of oscillations for repeated elasto-plastic strains has not been found.

2. Longitudinal Standing Waves and Longitudinal Vibrations in Rods

We shall make use of the results of §§ 7–9 of Chapter VI to consider the following problem. Suppose that at an instant $t = 0$ a pressure

$$p \equiv -\sigma|_{x=0} = EA \sin 2\pi k t,$$

which varies according to a sinusoidal law, is applied to the left-hand end ($x = 0$) of a homogeneous rod of constant cross-section and length l, and let us assume that $k = a_0/(2l)$, i.e. the inverse of the time taken by an elastic wave to travel twice the length of the rod. Here E is the longitudinal modulus of elasticity, A is the amplitude factor (a constant) such that $|p| < \sigma_S$. This pressure causes a longitudinal strain at this end of the rod which also varies according to a sinusoidal law:

$$\varepsilon|_{x=0} = f(t) \equiv -A \sin 2\pi k t.$$

We require to find the distribution of stresses, strains and particle velocities at any section of the rod and at any instant of time $t > 0$.

From (6.14′), at a section $x > 0$ which the elastic wave has already reached, but which has not yet been affected by the reflection of the wave from the end $x = l$, we have that

$$\left.\begin{aligned} \varepsilon &= -A \sin 2\pi k \left(t - \frac{x}{a_0}\right), \\ v &= a_0 A \sin 2\pi k \left(t - \frac{x}{a_0}\right), \end{aligned}\right\} \tag{7.1}$$

the law of variation of σ being similar to that for ε.

If the right-hand end of the rod $x = l$ is free, superposition of the reflected wave gives (see § 9, Chapter VI):

$$\varepsilon = -A \sin 2\pi k \left(t - \frac{x}{a_0}\right) + A \sin 2\pi k \left(t + \frac{x - 2l}{a_0}\right),$$

$$v = a_0 A \sin 2\pi k \left(t - \frac{x}{a_0}\right) + a_0 A \sin 2\pi k \left(t + \frac{x - 2l}{a_0}\right),$$

or

$$\left.\begin{aligned} \varepsilon &= 2A\cos\frac{\pi a_0}{l}\left(t-\frac{l}{a_0}\right)\sin\frac{\pi}{l}(x-l), \\ v &= 2a_0 A\sin\frac{\pi a_0}{l}\left(t-\frac{l}{a_0}\right)\cos\frac{\pi}{l}(x-l). \end{aligned}\right\} \tag{7.2}$$

We see from this that the variation in the velocity v of particles at each section x reached by the reflected wave has a phase lead of $\pi/2$ over the strain ε and also, therefore, over the stress σ.

At the instant $t_1 = 2l/a_0$ the reflected wave reaches the left-hand section $x = 0$. We see from (7.2) that $\varepsilon = 0$ at $x = 0$ (and also at $x = l$) for any value of t. In order to find the solution for $t > t_1$, therefore, we must add (7.2) and (7.1) for $t_1 < t < 3l/a_0$ and double (7.2) for $3l/a_0 < t < 4l/a_0$ in the region affected by the second reflection. Thus each time the wave travels along the rod and back the amplitude of the strains, stresses and velocities of all points doubles.

If at the instant $t_1 = 2l/a_0$ the pressure on the left-hand end of the rod is released, and if this end, as well as the right-hand end, then becomes free, the subsequent motion of the rod is described by formulae (7.2), which give $\varepsilon = 0$ at $x = 0$ and $x = l$ for any t, which corresponds to the boundary conditions for a rod with free ends. The free motion described by formulae (7.2) forms a so-called standing wave, which is the result of superimposing two sinusoidal waves (the incident and reflected waves) which have the same amplitude and frequency but opposite directions of propagation.

The characteristics of this type of motion, as can be seen from (7.2), are as follows: (1) every point in the body performs harmonic motio; (2) the amplitude of the oscillation of any point depends on the position of the point (on x) but is independent of time; (3) the frequency of the oscillations is the same for all points and has the same phase; (4) the displacement is a continuous function of the coordinate x, so that the continuity condition for the rod is satisfied.

A standing wave of the same frequency could have been obtained if the right-hand side of the rod, instead of being free, had been built-in. A similar result would have been obtained if, instead of $a_0/2l$ we had taken k as $2(a_0/2l)$, $3(a_0/2l)$ and, in general, $n(a_0/2l)$ where n is an integer, i.e. if the frequency of the disturbing force

had been a multiple of the inverse of the time taken by the wave to travel twice the length of the rod.

Instead of applying to the end of the rod a force acting during the time $t_1 = 2l/a_0$ according to a sinusoidal law and considering the free motion from the time $t = t_1$, we could have taken the origin as the instant t_1 and considered the distribution of the disturbances as a known quantity at this instant (as initial conditions) given by formulae (7.2) for $t = t_1 = 2l/a_0$.

It can be seen that with this particular initial distribution of the disturbances the rod performs free longitudinal oscillations which can be distinguished by the above-mentioned properties. This type of free oscillation of an elastic body (or a system of material points), in which each point performs harmonic oscillations, in which all the points oscillate synchronously and in phase, and in which continuity conditions are observed, is usually called normal oscillation (or natural oscillation), and the frequency, the natural frequency. In other words, in the case of normal oscillation the picture of displacements in the body varies but remains similar. In the above example the amplitude factor A can be found from the amplitude of the applied pressure. It can lie within the limits $0 < |A| < \sigma_S/E$, where σ_S is the yield point.

We see then that in the case of longitudinal oscillation an infinite number of normal oscillations are possible, which correspond to an infinite number of natural frequencies, multiples of the inverse of the time taken for the elastic longitudinal wave to travel twice the length of the rod.†

If we apply to the end of the rod a longitudinal force which varies periodically with a frequency equal to one of the natural frequencies, then, as can be seen from the above example, resonance occurs: the amplitude of the oscillations increases. If there were no forces of internal and external resistance the amplitude would increase to infinity. In practice there always exists internal and external friction, and the amplitude increases only to a definite

† It is shown in theoretical mechanics that the number of normal oscillations and the corresponding number of natural frequencies is equal to the number of degrees of freedom in the system of material points. An elastic body can be considered as an infinite number of material points with elastic connections, the number of degrees of freedom of which is infinite. In any elastic body, therefore, there is an infinite number of normal oscillations and an infinite number of corresponding natural frequencies.

limit at which the energy generated by the external force becomes equal to the loss of energy in overcoming internal and external friction.

The mode of a normal oscillation (and of any other type of oscillation) is given by the distribution of the displacements at any instant, for example, by the distribution of the amplitudes. In the above example, as can be seen from (7.2), the longitudinal displacement u is

$$u = -2\frac{Al}{\pi}\cos\frac{\pi a_0}{l}\left(t - \frac{l}{a_0}\right)\cos\frac{\pi}{l}\left(x - l\right). \qquad (7.3)$$

Thus the distribution of displacements, particle velocities and strains along the length of a rod with free ends at any one instant of time is as shown in Fig. 182a. The distribution of stress will be similar to the strain distribution.

Points which for normal oscillation do not move are called nodes, and points the amplitudes of which are maxima are called antinodes. In the above example there is one node (at $x = l/2$) and two antinodes (at $x = 0$ and $x = l$). For normal oscillation at one of the higher natural frequencies there will be several nodes and several antinodes. The distribution of displacements, particle velocities and strains shown in Fig. 182b corresponds to the second natural frequency.

If initially a longitudinal disturbing force is applied to the rod according to an arbitrary law (and not according to (7.2)), the free oscillations will not be normal oscillations. In this case the force acting on the end of the rod does not vary according to a sinusoidal law during the time $2l/a_0$. But the function of time which represents the law of variation of this force can be expanded in a Fourier series in sines with periods which are multiples of $a_0/2l$. For each factor after the instant $t_1 = 2l/a_0$ we obtain a standing wave of the type (7.2). Thus an arbitrary free oscillation can be represented as the result of superimposing normal oscillations.

In order to determine the mode of the normal oscillations and the magnitudes of the natural frequencies, according to the definition of normal oscillation, we must try to find a solution to the equation of longitudinal motion (see eqn. (6.15), Chapter VI),

$$\frac{\partial^2 u}{\partial t^2} = a_0{}^2\frac{\partial^2 u}{\partial x^2}$$

in the form

$$u = X(x)\cos(pt + \varphi), \qquad (7.4)$$

where p is the so-called angular frequency related to the frequency of oscillation ν by the expression $p = 2\pi\nu$, φ is the initial phase angle given by the initial conditions,† and $X(x)$ is a function which characterizes the shape of the oscillation. The function $X(x)$ and the frequency of the natural oscillations are given by the boundary conditions.

In the previous example of a rod with free ends we have the following boundary conditions:

$$\left.\begin{aligned} \varepsilon \equiv \frac{\partial u}{\partial x} = 0 \text{ at } x = 0, \\ \varepsilon \equiv \frac{\partial u}{\partial x} = 0 \text{ at } x = l. \end{aligned}\right\} \tag{7.5}$$

Substituting expression (7.4) in the equation of motion and dividing by $\cos(pt + \varphi)$, we arrive at an ordinary differential equation in $X(x)$:

$$X'' + \frac{p^2}{a_0^2} X = 0,$$

the general solution of which is

$$X(x) = C_1 \sin\frac{p}{a_0} x + C_2 \cos\frac{p}{a_0} x. \tag{7.6}$$

From the first boundary condition in (7.5) we find that $C_1 = 0$, and the second then gives the equation

$$C_2 \sin\frac{p}{a_0} l = 0.$$

Since $C_2 \neq 0$ (otherwise $u = 0$, i.e. no oscillations would occur), we have the equation

$$\sin\frac{p}{a_0} l = 0, \tag{7.7}$$

called the frequency equation. It shows that normal oscillation is possible, not at any frequency p, but only at frequencies corresponding to the roots of eqn. (7.7). Taking into account that $p = 2\pi\nu$, we have from (7.7) the values of the natural frequencies

$$\nu_n = \frac{a_0}{2l} n, \tag{7.8}$$

† For example, in the previously considered example the initial instant was taken as $t_1 = 2l/a_0$, and the initial state was given by formulae (7.2), since $\varphi = 0$. We could have taken any instant $t_2 > t_1$ as the starting point, and the initial state that given by (7.2) for $t = t_2$. We could then have had that $\varphi \neq 0$.

the value of $n = 0$ corresponds to translational movement of the rod.

Thus, we obtain a value for the function $X(x)$ corresponding to the nth natural frequency

$$X_n(x) = C_2 \cos \frac{n\pi}{l} x,$$

which defines the mode of the nth normal oscillation, the amplitude factor C_2 remaining constant. From (7.4) the displacements for the nth normal oscillation are given by

$$u_n = C_2 \cos \frac{n\pi}{l} x \cos\left(\frac{n\pi a_0}{l} t + \varphi\right).$$

For $n = 1$ we obtain an expression for u which coincides basically with (7.3).

The positions of the nodes for the nth normal oscillation are given by the equation

$$X_n(x) = 0,$$

which in this case has the solution

$$\frac{n\pi x_i}{l} = \frac{\pi}{2}(2i + 1)$$

or

$$x_i = \frac{l}{2n}(2i + 1),$$

in which $0 \leqq x_i \leqq l$. We see that for $n = 1$ there is only the one root $x_0 = l/2$ which corresponds to $i = 0$. For $n = 2$ (the second normal oscillation) there are two roots: $x_0 = l/4$ and $x_1 = 3l/4$ (Fig. 182b).

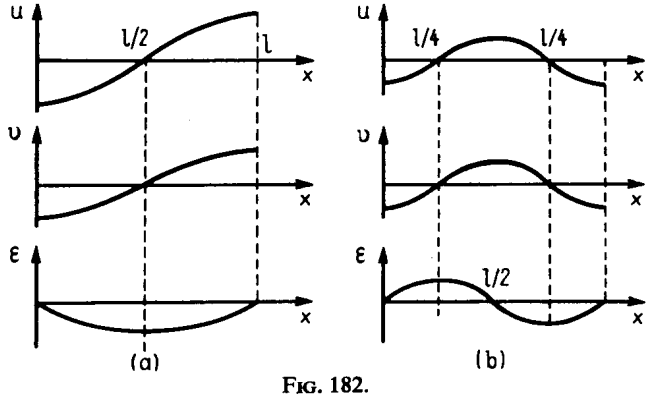

FIG. 182.

Indeterminancy of the amplitude factor C_2 is not peculiar to this particular problem: in all cases, since the initial conditions are not given, the shape of the normal oscillations is determined only to within a scale factor; if the initial conditions are known the motion is fully determinate.

In the case of a rod with fixed ends we have the boundary conditions

$$u = 0 \text{ at } x = 0,$$
$$u = 0 \text{ at } x = l.$$

Substituting expression (7.6), we find from the first that $C_2 = 0$. The second equation leads to a frequency equation which coincides with (7.7), so that the natural frequencies are given by formula (7.8), and the shape of the nth normal oscillation is given by the function

$$X_n(x) = C_1 \sin \frac{n\pi}{l} x,$$

and consequently the nodes occur at the points at which the anti-nodes occur in the case of a rod with free ends. In particular, for the first normal oscillation we have that:

$$u_1 = C_1 \sin \frac{\pi x}{l} \cos \left(\frac{\pi a_0}{l} t + q \right),$$

so that the nodes occur at the ends of the rod $x = 0$ and $x = l$ (Fig. 183). These points are also nodes for any higher form of oscillation, but there would then be in addition intermediate nodes.

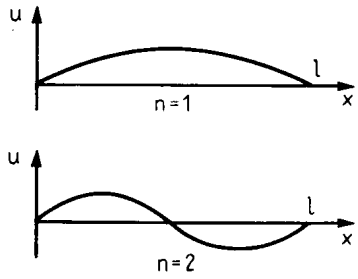

FIG. 183.

At high frequencies, when the lateral dimensions of the rod are not small compared with the length of the longitudinal wave, the theory given above is no longer in agreement with results derived

experimentally. This is in consequence of the fact that in the initial differential equations no account is taken of the inertia of particles moving in directions perpendicular to the axis of the rod. In order to take this inertia into account we must resort to the exact equations of the theory of elasticity.

In practice it is extremely important to determine the natural frequencies of structures: in order to avoid dangerously high stresses or deflections we must ensure that the frequency of the disturbing force does not coincide with one of the natural frequencies of oscillation (especially one of the lower frequencies), and in order to do so it is essential, of course, to determine these natural frequencies. In certain vibrating machines, on the other hand, resonance can be used to advantage, since the energy required is then a minimum.

Experiments on longitudinal elastic vibrations of rods can be used to determine the longitudinal modulus of elasticity of the material. Since $a_0 = \sqrt{(E/\varrho)}$, we have from (7.8) that

$$E = \frac{4l^2\nu_n^2\varrho}{n^2}.$$

If we measure the natural frequencies ν_n and the quantities l and ϱ we obtain a value of E for each of the natural frequencies. For the lower frequencies we usually obtain values close to the results of static experiments. But at high frequencies, especially for highly elastic materials (rubber, plastics, etc.), the results obtained differ considerably from the static values, illustrating the effect of rate of strain on the mechanical properties of the material. Values for the elasticity modulus E found from oscillation experiments are sometimes called adiabatic values, in contrast to the isothermal values which are those found from static experiments.

3. Torsional Vibrations in Rods

The analysis of torsional vibrations in rods is analogous in every respect to the theory of longitudinal vibrations. It is sufficient simply to replace a_0 by $b_0 = \sqrt{(G/\varrho)}$, the displacement u by the angle ϑ and the longitudinal stiffness EF by the torsional stiffness $C = GT$, where, for a circular section $T = J_p$, the polar moment of inertia.

A study of torsional oscillations is important for the design of

engine shafts, drilling rigs, etc. Although perhaps not an exact analysis, the same elementary theory of torsional oscillation can be applied to rods of non-circular section. Whole structures (masts, aircraft wings, helicopter blades, etc.) must be designed for torsional vibration. Experiments on the torsional vibration of rods can be used to find the value of the rigidity modulus G (the adiabatic value).

So as not simply to repeat the various steps of the last section, we shall consider the problem of the torsional oscillations of a rod with a stiffness which varies discontinuously along its length under the action of concentrated masses. The problem is in fact one of a shaft with flywheels attached (Fig. 184). At every section of the shaft a solution to the equation of motion

$$\frac{\partial^2 \vartheta}{\partial t^2} = b^2 \frac{\partial^2 \vartheta}{\partial x^2}, \tag{7.9}$$

where ϑ is the angle of rotation of a section, $b = \sqrt{(G/\varrho)}$ in the case of a shaft of circular section or $b = \sqrt{(GJ_p/m)}$ (where m is the moment of inertia of the rod per unit length about the axis of rotation), is required in a form analogous to (7.4):

$$\vartheta(x, t) = \theta(x) \cos(pt + q), \tag{7.10}$$

for $\theta(x)$ we obtain the ordinary differential equation

$$\theta'' + \frac{p^2}{b^2}\theta = 0, \tag{7.11}$$

the general solution of which is of the form

$$\theta = C_1 \sin \frac{p}{b} x + C_2 \cos \frac{p}{b} x. \tag{7.12}$$

The constants C_1 and C_2 can be expressed in terms of the amplitudes of the angle of rotation and torque, for example, at the left-hand end of the section. If we take into account that the torque is $M = GT\,\partial\vartheta/\partial x$, we get that:

$$C_{2i} = \theta_{0i}, \quad C_{1i} = \frac{M_{0i}}{(GT)_i} \frac{b}{p}, \tag{7.13}$$

where θ_{0i} and M_{0i} are the amplitudes of the angle of rotation and the torque at the left-hand end of the ith section, $(GT)_i$ is the torsional stiffness of the ith section of the shaft. In addition to the boundary conditions on the ends of the shaft, we must also take

into account the conditions at the junctions between the various sections of the shaft. If at the junction between the $(i-1)$th and the ith section there is a concentrated mass (a flywheel) with moment of inertia J_i about axis of the shaft, the necessary conditions are that:

$$\theta_{i-1} = \theta_i \text{ at } x = x_i, \tag{7.14}$$

$$M_{i-1} = M_i - J_i p^2 \theta_i \text{ at } x = x_i. \tag{7.15}$$

If at a junction there are no concentrated masses we must put $J_i = 0$ in (7.15). If within the nth section the moment of inertia m_n per unit length is small compared to the moment of inertia J_{n-1} of the concentrated mass situated at the left-hand end of the $(n+1)$th section, the nth section can be assumed to act simply as an elastic connection: a solution of the type (7.12) is unnecessary in this case, and the solutions for the $(n-1)$th and $(n+1)$th sections together give

$$\left.\begin{aligned} M_{n-1}^{(\text{right})} + J_n p^2 \theta_{n-1}^{(\text{right})} &= M_{n+1}^{(\text{left})} - J_{n+1} p^2 \theta_{n+1}^{(\text{left})}, \\ \theta_{n-1}^{(\text{right})} + M_n^{(\text{left})} \frac{b_n}{(GT)_n} &= \theta_{n+1}^{(\text{left})}, \end{aligned}\right\} \tag{7.16}$$

where $M_n^{(\text{left})} = M_{n-1}^{(\text{right})} + J_n p^2 \theta_{n-1}^{(\text{right})}$. Here the first equation expresses the fact that the torque is constant along the length l_n and the second takes into account the relative rotation of the ends of the nth section.

Let us suppose that this section is the section l_2 in the arrangement shown in Fig. 184; let us assume also that $l_3 = 0$, i.e. that the right-hand bearing is situated immediately next to the flywheel M_2. Since the left-hand end of the first section is simply supported, we have the condition that $M_0 = 0$ at $x = 0$. Therefore, in (7.12) written for the first section, $C_1 = 0$. From (7.15) we have that

$$M_2^{(\text{left})} = -C_2 \frac{p}{b} (GT)_1 \sin \frac{p}{b} l_1 + J_1 p^2 C_2 \cos \frac{p}{b} l_1,$$

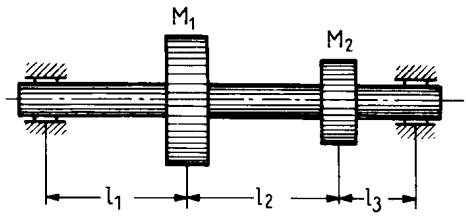

FIG. 184.

and from the second expression in (7.16) we find that

$$\theta_3^{(\text{left})} = C_2 \cos \frac{p}{b} l_1 + \frac{M_2^{(\text{left})} l_2}{(GT)_2},$$

and from the first expression in (7.16) we then get that

$$M_3^{(\text{left})} = -C_2 \frac{p}{b} (GT)_1 \sin \frac{p}{b} l_1 + J_1 p^2 C_2 \cos \frac{p}{b} l_1 + J_2 p^2 \left[C_2 \cos \frac{p}{b} l_1 + \frac{M_2^{(\text{left})} l_2}{(GT)_2} \right].$$

The condition $M^3_{(\text{left})} = 0$ leads, after division by C_2, to a transcendental frequency equation for the angular frequency p. The solutions to equations of this sort can often be found graphically.

4. Bending Oscillations in Rods

In engineering practice we often encounter cases of bending oscillations in rods and sometimes in whole structures.

The equation for free bending oscillations in a beam can be found from the differential equation for the deflection v (eqn. (2.55) in Chapter II)

$$EJ \frac{d^4 v}{dx^4} = q.$$

if we take the distributed load $q(x)$ as the inertia force per unit length of the rod, equal to $(-\varrho F \partial^2 v/\partial t^2)$, where F is the cross-sectional area and v is taken as a function of x and t. As a result we get that

$$\lambda^2 \frac{\partial^4 v}{\partial x^4} + \frac{\partial^2 v}{\partial t^2} = 0, \tag{7.17}$$

where we have introduced the definition

$$\lambda^2 = \frac{EJ}{\varrho F} = a_0^2 i^2. \tag{7.18}$$

Here a_0 is the velocity of propagation of longitudinal elastic waves in the rod, i is the radius of gyration of the cross-section.

From the definition of normal oscillation, we must try to find a solution to eqn. (7.17) in the form

$$v(x, t) = X(x) \cos(pt + \varphi).$$

After substitution in (7.17) we arrive at the ordinary differential equation in $X(x)$:

where
$$X^{(IV)} - k^4 X = 0, \tag{7.19}$$

$$k^4 = \frac{p^2}{\lambda^2} = \frac{4\pi^2 \varrho F \nu^2}{EJ}. \tag{7.20}$$

The general solution to this equation is:

$$X(x) = C_1' \sin kx + C_2' \cos kx + C_3' e^{kx} + C_4' e^{-kx}.$$

It is convenient to express this solution in terms of functions first suggested by A. N. Krylov:

$$S_1(x) = \tfrac{1}{2}(\cosh x + \cos x),$$
$$S_2(x) = \tfrac{1}{2}(\sinh x + \sin x),$$
$$S_3(x) = \tfrac{1}{2}(\cosh x - \cos x),$$
$$S_4(x) = \tfrac{1}{2}(\sinh x - \sin x),$$

These functions have a special property which is that the derivatives up to the fourth order inclusively satisfy the conditions:

$$S_4' = S_3; \quad S_4'' = S_3' = S_2; \quad S_4''' = S_3'' = S_2' = S_1;$$
$$S_4^{(IV)} = S_3''' = S_2'' = S_1' = S_4; \quad S_3^{(IV)} = S_2''' = S_1'' = S_4' = S_3; \cdots$$

Also
$$S_1(0) = 1; \quad S_2(0) = S_3(0) = S_4(0) = 0.$$

Special tables exist for these functions.† The general solution to eqn. (7.19) is

$$X(x) = C_1 S_1(kx) + C_2 S_2(kx) + C_3 S_3(kx) + C_4 S_4(kx). \tag{7.21}$$

In a beam of infinite length the shape of the oscillations is limited only by the form of (7.21), in the absence of any limitations on the constants C_1, C_2, C_3, C_4, k, and any frequency can be considered a natural frequency: the spectrum of natural frequencies is continuous and unlimited. The fixing conditions impose limitations on the constants. We shall consider now a number of particular cases.

(a) A simply supported rod. If the length of the rod is l, the boundary conditions which express the fact that deflections and

† See, for example, I. V. Ananyev, Spravochnik po raschetu sobstvennikh kolebanii uprugikh sistem (Reference book of natural frequencies of elastic systems, Moscow, 1946).

bending moments are zero at the ends of the rod are

$$X(0) = 0; \quad X''|_{x=0} = 0; \tag{7.22}$$

$$X(l) = 0; \quad X''|_{x=l} = 0. \tag{7.23}$$

Conditions (7.22) are satisfied only if $C_1 = C_3 = 0$. Conditions (7.23) then lead to a set of equations in C_2 and C_4:

$$S_2(kl)\, C_2 + S_4(kl)\, C_4 = 0,$$

$$S_4(kl)\, C_2 + S_2(kl)\, C_4 = 0.$$

The requirement that non-trivial solutions exist for this set of equations, which amounts to the requirement that oscillations do in fact occur, leads to the frequency equation

$$S_2^2(kl) - S_4^2(kl) = 0$$

or

$$\sin kl \,.\, \sinh kl = 0. \tag{7.24}$$

The zero solution $k_0 = 0$ (and also, therefore, $\nu_0 = 0$), as follows from (7.21), corresponds to the state of rest: $X(x) = 0$ for any values of x, and therefore $v(x, t) = 0$. The non-zero positive roots of eqn. (7.24) are

$$k_1 l = \pi; \quad k_2 l = 2\pi; \quad k_3 l = 3\pi; \quad \ldots; \quad k_n l = n\pi,$$

so that the natural frequencies are given by the formulae

$$\nu_1 = \frac{\pi\lambda}{2l^2}; \quad \nu_2 = \frac{4\pi\lambda}{2l^2}; \quad \nu_3 = \frac{9\pi\lambda}{2l^2}; \quad \ldots, \quad \nu_n = \frac{n^2\pi\lambda}{2l^2}.$$

For C_2 and C_4 we have, evidently, for each natural value of $k = k_n$, that $(C_2)_n = -(C_4)_n$ so that the nth natural shape of the oscillations is sinusoidal:

$$X_n(x) = A_n \sin k_n x = A_n \sin \frac{n\pi x}{l}.$$

The supports are nodes for any form of oscillation. The number of antinodes is equal to the order number of the natural oscillation.

(b) A rod with free ends. Since in this case the bending moments and shear forces at the ends of the rod are zero, the boundary conditions are

$$X''|_{x=0} = 0; \quad X'''|_{x=0} = 0; \quad X''|_{x=l} = 0; \quad X'''|_{x=l} = 0,$$

so that $C_3 = C_4 = 0$ and the frequency equation is:

$$S_3^2(kl) - S_2(kl)\, S_4(kl) = 0$$

or
$$\cos kl \cosh kl - 1 = 0. \tag{7.25}$$

The roots of this equation are†:

$$k_1 l = 0; \quad k_2 l = 4{\cdot}730; \quad k_3 l = 7{\cdot}853; \quad k_4 l = 10{\cdot}996; \quad \ldots,$$

and for $n > 3$ we can with sufficient accuracy put:

$$k_n l = \frac{2n - 1}{3}\pi.$$

The zero solution refers to the linear form of equilibrium. The remaining roots correspond to the natural frequencies

$$\nu_2 = \frac{\lambda}{2\pi}\left(\frac{4{\cdot}730}{l}\right)^2; \quad \nu_3 = \frac{\lambda}{2\pi}\left(\frac{7{\cdot}853}{l}\right)^2; \quad \nu_4 = \frac{\lambda}{2\pi}\left(\frac{10{\cdot}996}{l}\right)^2; \ldots,$$

and for C_1/C_2 we have that:

$$\left(\frac{C_1}{C_2}\right)_n = -\frac{S_4(k_n l)}{S_3(k_n l)} = -\frac{S_3(k_n l)}{S_2(k_n l)},$$

so that
$$A_n X_n(x) = S_4(k_n l)\, S_1(k_n x) - S_3(k_n l)\, S_2(k_n x).$$

The shapes of the deformed axes for natural frequencies ν_2, ν_3 and ν_4 are shown diagrammatically in Fig. 185.

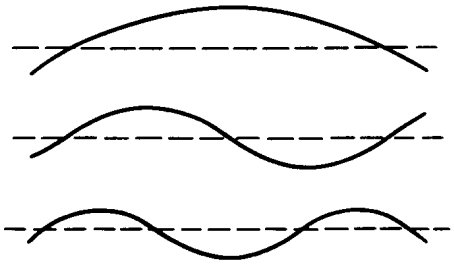

FIG. 185.

The ratios of the distances of the nodes from the left-hand end of the rod to the length of the rod are given in the table on the next page.

(c) A rod with one end built-in, the other free. The boundary conditions
$$X(0) = 0; \quad X'|_{x=0} = 0;$$
$$X''|_{x=l} = 0; \quad X'''|_{x=l} = 0$$

† See, for example, Rayleigh, Teoriya Zvuka, *Theory of Sound*, Moscow, 1955, Vol. I, p. 299. In future the roots of frequency equations and the positions of nodes will also be taken from this book.

lead to the equalities $C_1 = C_2 = 0$ and to the frequency equation

$$\cos kl \cosh kl + 1 = 0, \tag{7.26}$$

Order number of the natural oscillation	Positions of nodes			
	1st	2nd	3rd	4th
II	0·224	0·776	–	–
III	0·132	0·500	0·868	–
IV	0·094	0·356	0·644	0·906

the roots of which are

$$k_1 l = 1{\cdot}875; \quad k_2 l = 4{\cdot}694; \quad k_3 l = 7{\cdot}855; \quad k_4 l = 10{\cdot}996; \quad \ldots;$$

$$k_n l \approx \frac{2n-1}{2}\pi,$$

so that for the natural frequences we have:

$$\nu_1 = \frac{\lambda}{2\pi}\left(\frac{1{\cdot}875}{l}\right)^2; \quad \nu_2 = \frac{\lambda}{2\pi}\left(\frac{4{\cdot}694}{l}\right)^2;$$

$$\nu_3 = \frac{\lambda}{2\pi}\left(\frac{7{\cdot}855}{l}\right)^2; \quad \nu_4 = \frac{\lambda}{2\pi}\left(\frac{10{\cdot}996}{l}\right)^2; \quad \ldots$$

Also,

$$\left(\frac{C_3}{C_4}\right)_n = -\frac{S_2(k_n l)}{S_1(k_n l)} = -\frac{S_1(k_n l)}{S_4(k_n l)}$$

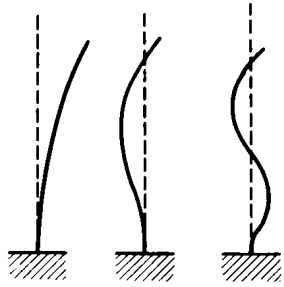

FIG. 186.

and the form of the natural oscillations is given by the function

$$A_n X_n(x) = S_2(k_n l)\, S_3(k_n x) - S_1(k_n l)\, S_4(k_n x).$$

The first three natural forms of oscillation are shown diagrammati-

cally in Fig. 186, and the relative distances of the nodes from the free end are given in the following table:

Order number of the natural oscillation	Positions of intermediate nodes		
	1st	2nd	3rd
I	–	–	–
II	0·226	–	–
III	0·132	0·499	–
IV	0·094	0·356	0·6439

In order to find the adiabatic values of the modulus of longitudinal elasticity from experiments on bending oscillations we have that:

$$E_n = \frac{4\pi^2 \varrho F l^4 \nu_n^2}{J(k_n l)^4}.$$

Experiments on bending and also on torsional oscillations are very widely used for determining the adiabatic moduli of elasticity, since they are easier to carry out than experiments on longitudinal oscillations.

It should be noted that at high frequencies and large curvatures the theory given above does not agree with the experimental results. This is explained to a large extent by the fact that the initial eqn. (7.17) does not contain terms which take into account the inertia of rotation of the cross-section and the effect of lateral forces. In literature specializing in the theory of oscillations of elastic systems the complete equations are given, but their solution is accompanied by considerable mathematical difficulties.

5. Fatigue

Under the application of loads which vary periodically with a sufficiently large amplitude a material will fail after a certain number of cycles. Sometimes this failure starts on the surface of the body, in which case it can be discovered by visual inspection; in other cases failure first occurs within the body and can be detected, for example, by a change in the natural frequency of oscillation, by means of ultrasonic flaw detection and other methods. Failure occurs at a combination of macro-stresses which, if of constant magnitude or if the number of cycles is not large, would not cause

failure. In cases of complete failure of this sort, plastic deformation is noticeable only in the immediate vicinity of the failure crack, in spite of the fact that the material under the static application of loads which cause the same state of stress would behave plastically. For example, in a cylindrical low-carbon steel specimen under the action of a static uniaxial tensile force very large residual strains (of the order of 30 per cent or more) occur after failure: under the action of alternating longitudinal stresses, the amplitude of which is less than the static UTS, failure occurs without noticeable residual deformation.

Failure of a material after a certain number of cycles of a periodically varying applied load is known as fatigue, and this type of failure is known as a fatigue failure. The ability of a material to withstand an infinitely large number or a sufficiently large finite number of cycles of a periodically repeated load is a measure of the endurance of the material.

An investigation of the possibility of fatigue failure is particularly important in the design of components of machines, aircraft, ships and of certain building structures which are subjected to periodic loading. The problem is most frequently encountered, however, in mechanical engineering design.

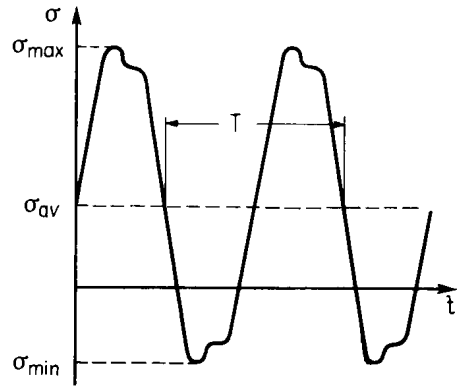

FIG. 187.

A periodic load which gives rise to some characteristic stress in the body (tensile or compressive stress in the case of axial tension, compression or bending in a beam, shearing stress on the circular cross-section of a specimen in torsion) can be characterized by the following quantities (Fig. 187): the maximum (σ_{max} or τ_{max}) and minimum

(σ_{min} or τ_{min}) stresses of the cycle, which can be of the same or opposite sign; the amplitude of the cycle $\sigma_A = \frac{1}{2}(\sigma_{max} - \sigma_{min})$, where σ_{max} and σ_{min} must include their signs; the mean stress of the cycle $\sigma_{av} = \frac{1}{2}(\sigma_{max} + \sigma_{min})$, which can be looked upon as the static load on which is superposed an alternating load; the coefficient of asymmetry of the cycle $r = \sigma_{max}/\sigma_{min}$; the period T or the frequency $\nu = 1/T$. In the case of a symmetrical alternating cycle $\sigma_{max} = -\sigma_{min}$, so that $\sigma_{av} = 0$. For an asymmetrical alternating cycle $\sigma_{av} > 0$ or $\sigma_{av} < 0$, and $0 > r > -1$. For a constant-sign cycle $\sigma_{av} > 0$ or $\sigma_{av} < 0$, and $1 > r > 0$. The value of $r = 1$ corresponds to a static load. In all cases σ_{max} and σ_{min} (or τ_{max} and τ_{min}) refer to the stresses at points in the specimen where they have their greatest absolute magnitude (for example, at points on the surface of a circular specimen in torsion, or at points farthest away from the neutral surface in the case of a beam in plane bending). In the case of a state of compound stress analogous characteristics are introduced for the principal stresses, for the maximum shearing stresses and for the intensity of stress. In general the orientation of the principal directions will vary periodically with time.

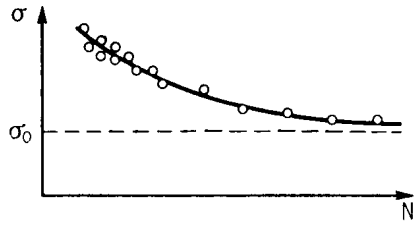

FIG. 188.

The resistance of a material to fatigue failure can be characterized in the following way. Let us suppose that a number of specimens of the same shape and dimensions, made from the same material, which is in the same state for all specimens (the same temperature, the same conditions of smelting, mechanical and heat treatment, etc.), are tested under a symmetrical alternating tensile–compressive load, and that the amplitude of the stresses remains constant for each specimen but varies from specimen to specimen. If for each specimen we plot in a plane a point the abscissa of which is equal to the number of cycles N before failure occurs, and the ordinate of which represents the maximum stress σ, then these points enable us to draw an experimental curve known as a Wöhler

curve (Fig. 188). For the majority of alloys with an iron base the Wöhler curve has an asymptote $\sigma = \sigma_0 \neq 0$. This means that in the case of a symmetrical cycle with the greatest stress not exceeding the magnitude of σ_0, the specimen has unlimited endurance, i.e. it is able to withstand any number of cycles without failure. For every stress exceeding σ_0 the specimen fails due to fatigue after a finite number of cycles given by the abscissa of the corresponding point on the Wöhler curve. The quantity σ_0 is known as the fatigue limit. The region between the Wöhler curve and the asymptote $\sigma = \sigma_0$ is called the region of limited endurance. For the majority of steels the fatigue limit for a symmetrical tension–compression cycle is from 30–50 per cent of the static UTS.

The Wöhler curve is often drawn in semi-logarithmetic coordinates $\sigma \sim \ln N$, in which case the curve is represented approximately by two straight lines, one inclined, the other horizontal (Fig. 189), and it is customary to use the curve in this form.

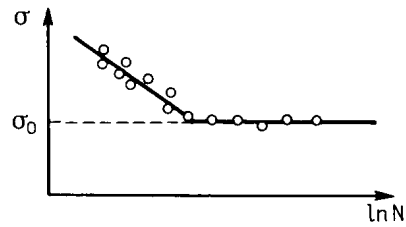

FIG. 189.

Non-ferrous metals, as a rule, do not have a fatigue limit: although the slope of their Wöhler curves becomes less as the amplitude of stress decreases there is no indication of a horizontal asymptote. In this case we talk of the nominal fatigue limit as the maximum stress (amplitude of stress) which the specimen can withstand without failure of the fatigue type after a given number of cycles (for example 5×10^7 cycles).

It is, of course, impossible in practice to carry out an experiment with an infinite number of cycles. In order to determine the fatigue limit, therefore, we consider as an experimental base a definite number of cycles which is chosen bearing in mind the actual length of use of the component, then the greatest stress which the specimen is able to withstand after this number of cycles is then found experimentally. For steel an experimental base is usually chosen within the range $10^6 \sim 10^7$ cycles, and for non-ferrous metals—up to

$5–10 \times 10^7$ cycles and more. It is then assumed that at stresses (stress amplitudes in the case of a symmetrical cycle) which do not exceed the fatigue limit found in this way the specimen will not fail after any number of cycles, although in actual fact, of course, failure might occur.

With an asymmetrical stress cycle the results of fatigue experiments can be represented in the form of a Haigh diagram (Fig. 190). If we set out the mean stress of the cycle as abscissa and the amplitude of the variable component of the stress as ordinate, the fatigue limit is given by a point on the curve MN. The point M represents the fatigue limit for a symmetrical cycle, and the point N the static UTS.

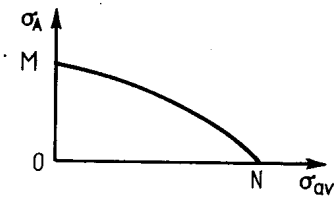

FIG. 190.

In many cases the stresses in a structure subjected to periodic loading exceed the fatigue limit. This applies, for instance, to components of aircraft engines, helicopter blades and to various items of military equipment, the useful life of which is limited for a number of other reasons. In such cases it is essential to know the limited endurance characteristics, which determine the strength reserve of the component or structure, and its resistance to fatigue failure after a definite period, i.e. after a certain number of cycles. Therefore, whereas in fatigue calculations it is important to know exactly only one point on the Wöhler curve—the fatigue limit, in estimating the limited endurance we are interested in the upper part of the Wöhler curve. The nature of the function which the component is intended to perform and its expected length of service, since this depends also on other considerations, usually give a reduced base for the fatigue experiments. For this reason it is important to reproduce as closely as possible in the experiments the true conditions under which the component is to function, and to establish the static characteristics which might show that the component will fail at stresses other than the nominal fatigue limit found from these experiments, and at a number of cycles which differs

from the experimental base. The latter is particularly important, since at stresses considerably in excess of the true fatigue limit and close to the static UTS wide scatter is observed in the experimental results. In recent years much attention has been devoted to the use of statistical methods in the analysis of the results of fatigue experiments.

6. Factors influencing Fatigue Characteristics

Fatigue characteristics derived experimentally are very sensitive to changes in the conditions under which the experiment is conducted. Apart from such factors as chemical composition, microstructure, temperature, heat treatment, which influence considerably the results of static experiments, these results depend very much on such factors as the accuracy to which the surface of the specimen is machined, the shape and dimensions of the specimen and the nature of the experiment, etc. For example, the yield point determined for a particular material from tensile tests on a cylindrical specimen and from bending tests, in both cases with the use of polished specimens, would be the same as the results of tests on specimens machined on a lathe. The fatigue limits found from tension–compression tests are sometimes very different from those found from bending tests, and in some cases they may differ by as much as 40–50 per cent (relative to the smaller quantity). Inconsistent results for the fatigue characteristics can also be obtained from experiments on two specimens, one of which is polished and the other very roughly turned out on the lathe, all other conditions being identical. The results are also influenced by such factors as whether or not the experiments are carried out with symmetrical alternating bending in one and the same physical plane in the cylindrical specimen, or by rotation about the curved axis of the deflected specimen, as is the case in a number of fatigue testing machines, when all the diametrical sections undergo the same sequence of stress. Reference books usually give fatigue data for three typical experiments: bending, uniaxial tension–compression and torsion (the corresponding fatigue limits being denoted by $\sigma_{-1b}, \sigma_{-1p}, \tau_{-1}$ where the "-1" corresponds to a coefficient of asymmetry $r = -1$, i.e. to a symmetrical cycle).

Let us examine the influence of some of these factors.

1. The shape and dimensions of the specimen and geometrical defects. In the case of a specimen with a cylindrical working portion,

the proximity of the enlarged ends of the normal specimen has a considerable effect on the results, since inaccuracies in its manufacture, which more often than not occur in these places, can give rise to stress concentrations which influence the fatigue characteristics. For this reason it is better to use specimens, the working portion of which narrows down very gently towards the centre where fatigue failure usually occurs.

Cuts, notches, scratches, dents, etc., on the surface of the specimen and various internal defects (voids, inclusions) reduce resistance to fatigue failure. The effect of sharp notches and cracks is particularly noticeable, as it is around such defects that stress concentrations occur. Stress concentrations also affect the nature of the failure and the general behaviour of the specimen in static experiments. But whereas in static experiments a defect such as a scratch, which causes a stress concentration only in a very small region at the bottom of the scratch, has no effect on the results, in fatigue experiments a scratch can alter the result by 100 per cent.

In order to find approximately the range of variation of fatigue characteristics it is normal to construct two Wöhler curves: one for well polished cylindrical specimens (or specimens with a working portion which narrows gradually towards the centre) and another for specimens with sharp notches in the surface. The Wöhler curves for specimens of other shapes and dimensions and with other defects will, apparently, lie somewhere between the two.

The absolute dimensions of the specimen also affect its fatigue characteristics, although not its static characteristics, for the latter, the so-called scale factor as such does not exist. An increase in the dimensions of a specimen leads to a decrease in the fatigue limit.

In order to derive reliable and consistent fatigue data, therefore, it is very important to standardize the shape and dimensions of the specimens used. Standard specimens have a working portion of 7–10 mm diameter. Unfortunately specimens used in fatigue experiments have not as yet been fully standardized.

If the aim of an experiment is to determine the fatigue characteristics of a component which has a complicated shape, reliable results can only be obtained by reproducing exactly the shape and dimensions of the component.

2. Accuracy of machining. As was mentioned above the accuracy with which the surface of the specimen is machined is of considerable importance. For this reason it is normal to use specimens with

a polished working portion. It is, however, important to bear in mind the whole machining process. If the specimen is machined by a blunt cutting instrument the surface layer will be strain-hardened, and this increases the fatigue strength and can lead to errors. During polishing, small fragments of the abrasive can penetrate the surface of the specimen and lead to a decrease in its fatigue strength.

The fatigue strength of machinery components can be increased by special mechanical processes (surface hardening, shot-blasting, etc.).

3. Deleterious media. If the application of a periodic load is accompanied by the action of some deleterious medium and by corrosion of the material, as is the case, for example, in the components of internal combustion engines, turbines, chemical engineering equipment, the fatigue characteristics, as a rule, decrease considerably. An estimate of the effect of such factors is usually made by reproducing or modelling the true conditions.

4. Loading. The effect of the type of stressed state was mentioned above. The ability to reproduce exactly a particular state of stress in a series of experiments is particularly important. This requires care and thought, both in designing the machines and apparatus necessary for the fatigue experiments, and in setting them up for the tests, in attaching the specimen and in controlling the loading equipment. Irregularity in the application of the load in the form of a temporary increase in amplitude of the cycle, or prolonged breaks in the experiments, can be reflected in the results.

5. Temperature. Experiments carried out at different temperatures give different results for the fatigue characteristics. At temperatures close to absolute zero there is a sharp increase in fatigue strength. Experiments at these very low temperatures are being carried out at present in many countries. In these experiments the specimen is usually surrounded by liquified gas (for example, liquid helium). For normalized steel with a 0·3 per cent carbon content, an increase in the fatigue limit (on a base of 10^7 cycles) to 7500 kg/cm^2 has been obtained at 196°C, compared with 4000 kg/cm^2 at room temperature, and for the aluminium alloy 75 S–T the corresponding values for the fatigue limit are 4200 kg/cm^2 and 2000 kg/cm^2. On the other hand, for specimens with sharp notches in their surfaces a number of experiments have shown decreases in the fatigue limit with decrease in temperature.

The effect of non-uniform temperature fields and of heat radiation which varies with time has as yet been only superficially in-

vestigated. There is no information available on the effect of radioactive radiation on fatigue strength.

6. Frequency of the vibrations. Within a sufficiently wide range the frequency ν (or period T) has no noticeable effect on the fatigue characteristics. Information exists, however, which suggests that in the higher audio frequencies some change takes place in the fatigue strength. Some change can also be expected at very low frequencies. Experiments at very low frequencies, which naturally are of very long duration, are being carried out at present in a number of research laboratories. They are of particular importance for the design of components which have a large period of oscillation and which are intended for prolonged use.

7. The Development of Fatigue Failures

A fatigue fracture in a specimen with a circular section which had been rotated about its deflected axis is shown in Fig. 191. The outer region of the fracture is a smooth shiny surface whereas the inner region has a mat granular surface. This type of fracture suggests the following explanation of the way in which the failure developed. Initially a number of fatigue cracks formed on the surface of the specimen where the normal stress is a maximum. These cracks then merged and spread towards the centre of the specimen.

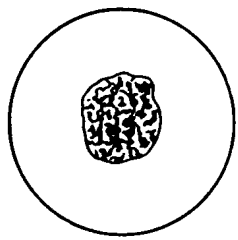

Fig. 191.

At the same time the surface of the crack in the compression zone was worn smooth. At some instant when the crack had spread to a sufficient depth the stress concentration created conditions for a brittle failure of the remaining part of the section, in this way completing the fatigue failure.

In the case of failure of a cylindrical specimen in tension–compression fatigue tests, the smooth parts of the fracture surface sometimes occur not on the outer part of the section but in the

centre, often in several places. This shows that failure first occurred inside the specimen and that the failure cracks spread from inside the section.

Analysis of fatigue fractures shows that various defects promote fatigue failures: cuts, scratches, voids, inclusions within the structure, etc., all of which cause local stress concentrations. This is in accordance with the fact that values for the fatigue limit found experimentally are smaller for specimens of large dimensions. For in large specimens, even if they are carefully prepared, there is always more likelihood of some defect liable to initiate failure. The unavoidable scatter in the results of fatigue experiments is a consequence of this fact.

The micro-mechanism of a fatigue failure has not as yet been thoroughly investigated, in spite of the fact that a great deal of experimental work on the subject of fatigue has been carried out in many countries. There is no reason to believe that this mechanism differs fundamentally from the mechanism of plastic deformation and failure under static or semi-static conditions, in spite of the fact that fatigue failure occurs at macro-stresses too small to cause static failure. When we speak of the effect of such things as quality of the surface, cuts, scratches and internal defects, when in effect we are replacing the actual problem, which is one dealing with the fatigue of a material, by one on the fatigue of a body prepared in some particular way from this material, we should bear in mind that a detailed analysis of the state of stress in the neighbourhood of these defects and in the specimen as a whole would give us the complete picture of the occurrence and development of fatigue failures under different conditions in terms of definite criteria, which would include the characteristics of the state of stress and strain.

Fatigue experiments with specimens which, as far as possible, are free from defects and in which a uniform state of compound stress is applied, are becoming increasingly important. For this purpose it is possible to use thin-walled cylindrical specimens and subject them to periodic tension and compression together with torsion and internal pressure. Unfortunately a complete and systematic investigation into fatigue under conditions of compound stress has as yet not been made, and the information that does exist only allows us to understand its general character. It appears that a very important part is played in the development of a fatigue failure under a state of compound stress by the stress intensity and the amplitude

of its variation. At present no information is available on the effect of the type of the state of stress, which undoubtedly, as in the case of static conditions, has a very great influence on the results. More thorough investigations are necessary in this field.

An analysis of fatigue failures under conditions of compound stress should be supplemented by investigations into the static characteristics of the structure of the material in relation to the different methods of manufacture. Such an investigation should give quantitative information on the likelihood and distribution of defects and differences in the physical and geometrical properties, which would give some guidance as to the possible magnitudes and distribution of the stresses which are likely to occur in the body together with some estimate of possible stress concentrations.

A static approach to the subject of fatigue failures has been developed in the U.S.S.R. by N. N. Afanasyev. This approach, however, has not been exploited as widely as it should have been. It consists, essentially, of a macroscopic analysis, and allows us to study the micromechanism of fatigue failure on the basis of the assumptions made concerning plastic deformation and failure under quasi-static conditions. For example, the idea that in the dislocational mechanism the velocity at which a dislocation moves depends on the temperature suggests that with decreases in temperature the fatigue limit should increase, which is in fact confirmed by experiment.

CHAPTER VIII

METHODS AND EQUIPMENT FOR MECHANICAL TESTING

1. Introduction

In this chapter we shall describe some experimental methods of investigating the elastic and plastic properties of materials under laboratory conditions. Special methods and equipment used for investigating specific properties of concrete, ceramics, rocks, soils, timber and plastics will not be dealt with. In certain respects, these special methods are not different in principle from the methods used in the mechanical testing of metals.

In an experimental determination of mechanical properties we always have at our disposal three items: (1) the material under investigation in the form of a specimen of some particular shape, (2) a loading apparatus, (3) measuring apparatus which records the loads applied to the specimen and the stresses and strains which result.

Of the many different testing machines and measuring equipment in existence today we shall describe only those which are appropriate to the laboratories of higher academic institutions and those laboratories specializing in the investigation of the elasto-plastic properties of materials. Particular examples will be given of equipment and apparatus used at Moscow University.

2. Preparation of the Specimen

In the preparation of an experiment it is important to exercise considerable care in the manufacture of the specimen and to have some knowledge of the general physical properties of the material and to be able to derive information on the mechanical (elasto-plastic) properties of the material during the course of the experiment.

First of all it is essential, of course, to know something about the material. The specimen or a number of specimens of the same material are, therefore, subjected to a chemical or spectroscopic analysis, which determines the chemical constituents. For this purpose shavings of the material can be used. If it is suspected that different castings of the material have different properties tests should be made on samples from different castings.

Since the chemical composition alone does not determine the structural state of the material, since this depends also on the heat-treatment and casting technique, the material should be subjected to microscopic analysis. Without a knowledge of the chemical composition and structural characteristics and, what is more important, if it is not certain that specimens are identical (in this respect), the experimental results obtained will not be reliable or consistent and will be difficult to reproduce.

The following points are important in the preparation of the specimens.

(1) Geometrical accuracy of the specimen is essential if the results are to be interpreted accurately and if it is required to be able to reproduce them in other experiments. It will be appreciated that if the diameter of the working portion of a specimen varies along its length the relative extension in the case of tension and relative angle of twist in the case of torsion will be greater in that part of the specimen where the diameter is smaller. Curvature of the axis of the specimen in compressive or tensile tests gives rise to bending stresses and strains which can lead to inaccurate results. Inaccuracies are also introduced if the section of an apparently circular section is elliptical or if the walls of cylindrical specimens vary in thickness, etc. The tolerance in these quantities should be determined in each case in accordance with the nature of the experiment and the dimensions of the specimen. The above remarks do not exclude, of course, specimens of shapes more complicated than cylindrical (notched specimens, specimens with a working portion which gradually decreases in area towards the centre, etc.). But in all cases geometrical accuracy in the working portion must be guaranteed and check measurements made on each specimen before the experiment commences.

(2) The quality of the surface of the specimen must be such that local non-uniformity in the state of stress caused by stress concentrations around sharp grooves, dents and scratches does

not noticeably distort the macroscopic observations of the behaviour of the specimen. In the majority of cases specimens are prepared by a cutting process (on a lathe, milling, drilling or planing machine), and less frequently they are made by casting or pressing. The quality of surface finish which can usually be attained on a lathe for example by an experienced operator is as a rule sufficient for static experiments on cylindrical specimens (solid or hollow) under conditions of combined or simple tension–compression, torsion and internal pressure. In fatigue experiments, however, when the quality of the surface is one of the most important factors, in experiments on notched specimens, when the effect of a local non-uniform state of stress is being investigated, and in certain dynamic experiments on impact, more precision is required in the surface finish and the specimens must be ground or polished.

(3) Homogeneity (macro-homogeneity) of the specimen must be ensured, both in its chemical composition, and in its microstructure. When specimens are prepared from castings each group of specimens must be taken from the part of the casting which has the most uniform structure, from parts close to the surface, since the central part of a casting usually has a coarser or less regular structure, providing, of course, that the experiment is not intended as a comparison of the elasto-plastic characteristics of different parts of the casting. If the specimens are prepared from rods or rolled sheet each group of specimens should as far as possible be cut from same rod (or sheet) or at least from the same series of rods. The material should be free from blisters, internal cracks and inclusions, which cause stress concentrations. This, of course, does not apply to experiments on materials for which porosity (sponge rubber, foam glass, certain ceramics) or non-homogeneity (concrete) are properties upon which the structural value of the material depends. But we must not, for example, judge the mechanical properties of cast rubber on the basis of the results of experiments with foam rubber.

(4) Since the structural state of the material very much depends on the degree of heat treatment, the latter must be known exactly for every specimen. A knowledge of the state "as supplied" is not sufficient. It is necessary in addition to take into account that during the cutting operation, especially if the cutting tool is rather blunt, non-homogeneity of the structure can be caused by the pressure on the surface, which is particularly noticeable in thin-walled

specimens. The same remarks apply to pressure forming and to casting. Each group of specimens should therefore be subjected to the appropriate heat treatment (annealing, quenching, tempering, etc.), with proper control by means of microscopic analysis. Care should be taken, however, to avoid the formation of oxidizing films. Annealing assists in reducing the initial anisotropy caused by rolling, wire-drawing, etc. It should be remembered that if quenching is used the structural characteristics of the material in specimens of large dimensions will not be the same towards the centre, since the depth to which the quenching is effective is not large—which could perhaps be a reason for the so-called "scale-factor" effect.

3. Geometry of the Specimen

In dealing with the geometry of specimens we must bear in mind two types of experiments: experiments for finding the elasto-plastic properties and strength characteristics, and experiments for finding the so-called structural strength. The latter refer both to experiments on parts of structures or on complete structures (frames, aircraft, wings, rocket structures, etc.), and also to experiments on individual components (rods, plates, shells). Some experiments are intended to check basic analytical assumptions (for example, the assumption that plane sections remain plane in the bending theory). We shall deal here with specimens used for determining the mechanical properties of materials.

Fig. 192.

(1) Specimens used in tensile tests have a cylindrical (Fig. 192) or prismatic (Fig. 193) working portion which ensures that over a certain length the state of stress and strain is uniform. If necessary an ordinary long rod of constant section can be used (a wire of some particular gauge, for example). But with large strains such a rod would start to yield or fail at the jaws of the testing machine and the control of the experiment would be lost. For this reason

specimens are made with thickened ends which fit into the jaws of the testing machine (Figs. 192 and 193). The change of section is gradual, so as to avoid undesirable stress concentrations. The length of the working portion is made several times larger than the greatest lateral dimension. This ensures that in the central part of the specimen the state of stress is uniform and uniaxial, which is not the case near the change in section (see St. Venant's principle, Chapter II).

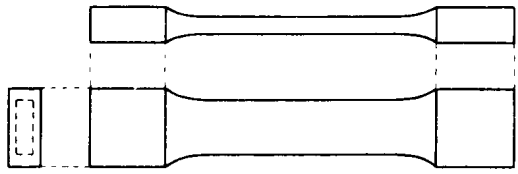

FIG. 193.

(2) It is difficult to make specimens for compression tests with thickened ends, since the long working portion that would be necessary would cause instability. A specimen in the form of a short cylinder with smooth ends (Fig. 194a) is also unsuitable

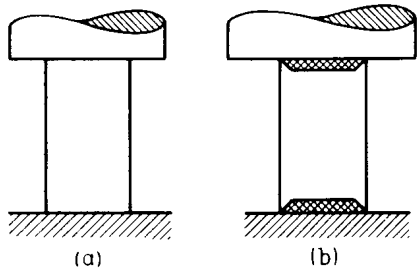

FIG. 194.

since even with good lubrication friction between the plates and the ends of the cylinder leads to non-uniform and non-uniaxial deformation (a barrel shape results). One method of avoiding this is shown in Fig. 194b. A sharp ridge is formed round the ends of the specimen and the space between the specimen and the plate is filled with a thick lubricant (for example, paraffin wax). The height of the specimen should not exceed two or three times the diameter, so as to avoid instability.

(3) Specimens for P–p, P–M and P–M–p experiments are thin-walled cylinders with external appearance similar to Fig. 192.

(4) Specimens for investigating the behaviour of materials (their strength) in a state of triaxial stress are made in the form of cylinders with a circumferential notch (Fig. 195). At the bottom of the notch a state of compound stress is set up which approximates to all-round tension. The analysis of the results of experiments with this type of specimen requires a knowledge of the theory of the state of stress under such conditions.

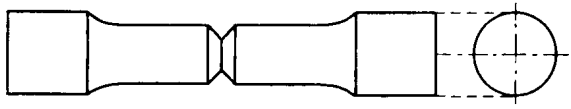

FIG. 195.

(5) Specimens for studying the propagation of waves and the behaviour of materials under high rates of strain are made in the form of long cylinders capable of withstanding a tensile, compressive or torsional impact on the end or a transverse impact at any point. The presence of a notch under these conditions cannot as yet be used to determine any basic characteristic, since our present knowledge of wave theory does not enable us to analyse wave propagation in the vicinity of notches and grooves.

(6) Specimens used for experiments on impact viscosity are of prismatic or cylindrical shape with a notch. Experiments on impact (usually lateral) are used to obtain data on the plasticity of a material in various states of heat treatment and at different temperatures.

(7) Specimens for fatigue experiments are cylindrical with a working portion which narrows gradually towards the centre. For fatigue experiments in a state of compound stress tubular specimens are used, as these ensure a uniform state of stress.

(8) Various other shapes are used for special experiments. For example, a plate in two-directional tension can be used for P–p experiments. For experiments on all-round compression practically any shape of specimen is possible.

4. STATIC TESTING MACHINES

Static testing machines can be divided into two classes: (1) machines of the kinematic type, in which the quantity actually measured is the relative movement of the grips of the machine; (2) machines of the force type, in which the force transmitted to the specimen

by the grips is measured. In the first the moving parts are operated (by motors or manually) through a system of gears and levers, and in the second, the load is usually applied either hydraulically or pneumatically. Some machines, known as universal testing machines or universal presses, enable tension, compression and bending tests to be carried out. Others, known as compound stress machines, are used for *P–p*, *P–M* or *P–M–p* experiments.

(1) The MAN universal testing machine (Fig. 196) is of the kinematic type. The cross-beam T_1 is moved in a vertical direction by

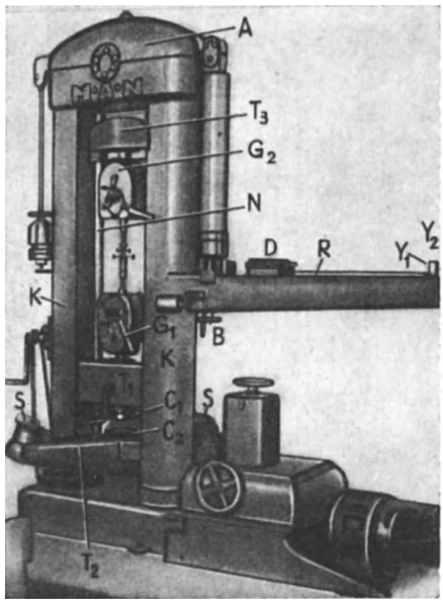

FIG. 196.

screws situated inside the columns *K* and slides along the guides *N*. At the centre of the cross-beam at the top there is a grip G_1 which holds the specimen in a tensile test and at the bottom a flat bearer C_1 for compression tests. Flat specimens are held in the grips by wedges which slide in guides which narrow towards the top and automatically grip the head of the specimen. Circular specimens bear on a bush held in a semi-cylindrical (self-centring) bearing which rests on the cylindrical surface of the grip.

An upper grip G_2 in the same way as the bottom, is located in a fixed cross-beam T_3 attached to the guides *N* which, by means of

a prism, bear on a lever inside the head A. Another fixed cross-beam T_2 contains a bearing plate C_2 (for compression tests) and two roller supports S. In bending tests the beam is placed on these supports. The distance between the supports can be varied. The load is then applied through C_1.

A weight D moves along the balance lever R, and its position can be controlled by the wheel B and recorded on a scale on the side of the lever. The weight D is moved one way or another along the

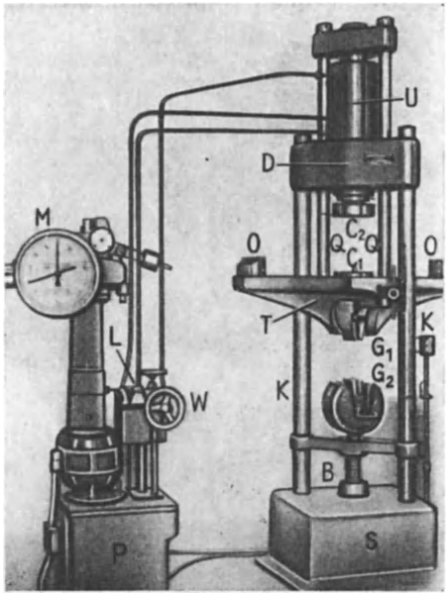

FIG. 197.

lever R until the pointer Y_1 is opposite Y_2. The vertical load (the tensile or compressive force) applied to the specimen is read off on the scale.

The rigidity of its frame, its smooth action and high accuracy and ease of measurement of the applied load make this machine very reliable and suitable for precise scientific experiments providing, of course, the strains are measured accurately.

The maximum load (the capacity of the machine) is 35 tons. The maximum cross-beam movement is 350 mm.

(2) The Mohr and Federhaff universal press (Fig. 197) is a machine of the force type. The cross-beam T, which has a bearing

plate C_1 and roller supports O on its upper surface and a grip G_1 underneath, slides along rigid guides K. It is rigidly connected to the piston in an oil cylinder U attached to the (fixed) beam B; this beam has a flat bearing plate C_2 underneath. At the base S of the machine there is a motor which, by means of the screw B, moves the lower grip G_2 up or down. The grips G_1 and G_2 are of the wedge type. When oil is pumped into the cylinder by the pump P the piston, together with the crossbeam T, is raised. If a specimen is placed between the plates C_1 and C_2 it is compressed; if it is placed in the grips G_1 and G_2 it is extended; if a beam is placed on the roller supports O and an inverted roller support attached to the plate C_2 the beam can be subjected to bending.

The force applied to the specimen is determined by the pressure of the oil in the cylinder U, which is measured on a pressure gauge M. The speed of movement of the cross-beam can be regulated by a valve (operated by the lever L and the wheel W) which controls the supply of oil to the cylinder; the speed can vary from 10 to 120 mm/min. Smaller speeds can be obtained, but this may cause overheating of the oil. A tensile force can be applied by a motor which moves the grip G_2 downwards, but the speed of movement of G_2 is quite high, which renders precise readings difficult to make.

The maximum travel of the cross-beam is 300 mm and the maximum load is 35 tons. The measuring range can be varied by means of a counterbalance weight. The pressure gauge has three scales: 0–7000 kg, 0–17,500 kg and 0–35000 kg, the smallest divisions being respectively 20, 50 and 100 kg. There is a special device which records automatically on a drum the P–Δl diagram.

(3) The Schopper universal 100-ton press in principle is the same as the Mohr and Federhaff press described above. The large travel of the machine (250 mm for the upper cross-beam and for the lower grip) and its large capacity make it suitable for experiments on large specimens. By means of special attachments it can be adapted to enable pressing and stamping tests, etc., to be made on smaller specimens.

Laboratory presses and testing machines of 500, 1000 tons capacity and more can be obtained.

(4) The Schopper compression–tension testing machine (Fig. 198) is of the kinematic type. It is one of the best of the latest models and is portable. Its speed can be regulated (from 5–30 mm/min by a motor, and as low as required by manual operation); it has cross-

beams and a lever system and a dynamometer with an indicating dial. The 10-ton machine has three scales: 0–2000 kg (in divisions of 5 kg), 0–5000 kg (in divisions

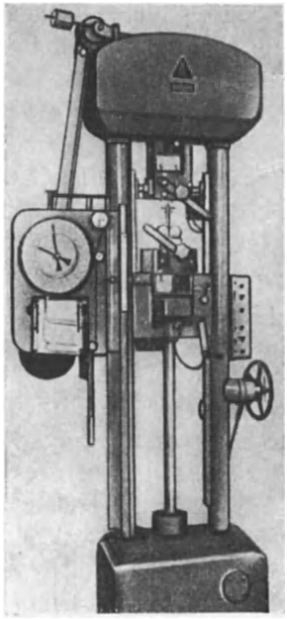

FIG. 198.

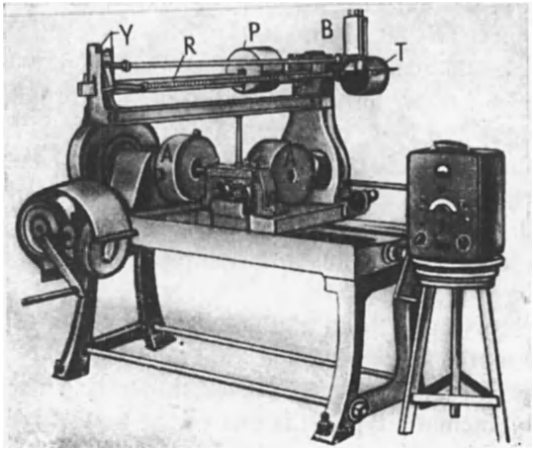

FIG. 199.

of 20 kg). The maximum travel of the cross-beam is 900 mm, 5-ton machines are also available.

(5) The Mohr and Federhaff torsion testing machine (Fig. 199) is of the kinematic type and is of 30,000 kg.cm capacity. The cylindrical specimen is held in the two grips *A*. The left-hand grip is rotated by hand through a reduction gear about a horizontal axis. The right-hand grip is connected to a lever system. A balance weight *P* slides along the lever *R* which has an inlaid scale (graduated in

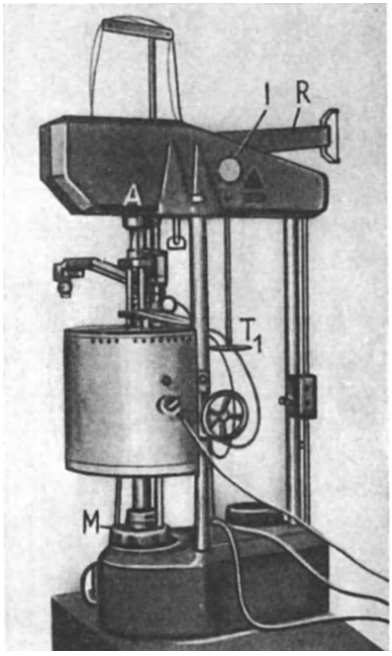

FIG. 200.

divisions of 100 kg.cm). The torque applied to the specimen is given by the position of the weight *P* for which the pointers *Y* coincide in position. The lever system can be standardized by the weight *T*. The M–φ diagram is automatically recorded on the drum *B*. The right-hand grip can be moved to right and left along the stand to suit the length of the specimen.

(6) The Schopper creep machine (Fig. 200) is an example of a machine of the force type with a lever system and can be used for creep tests on cylindrical specimens at temperatures up to 1000°C.

The specimen is held in the grips by bushes in the form of a half-ring (in a similar way to the MAN machine). The lower grip is connected to an adjusting screw; its position can be regulated before the start of the experiment by the hand-wheel M. The upper grip is connected to the head of the machine A, which is part of the lever system through which the load is applied. On a small lever there is a hanger T_1, on which a weight P_1 is placed for an initial loading of the specimen. At the end of a large lever is hung a weight

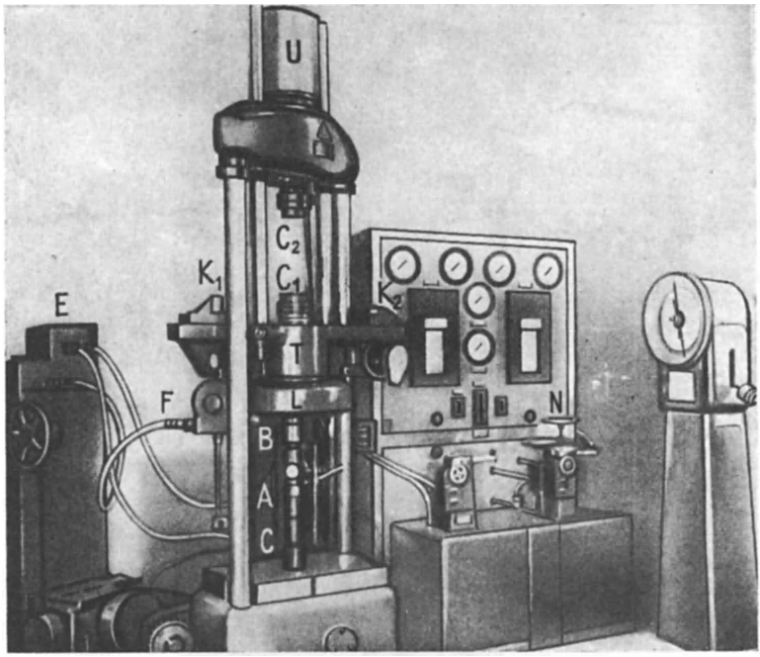

FIG. 201.

P_2 which sets up a tensile force in the specimen. The stress set up in a standard specimen is indicated on the weights. When the lever rotates as a result of elongation of the specimen it can be brought back to its original position by lowering the bottom grip. The zero (equilibrium) position of the lever is shown by the indicator I. The grips together with the specimen are situated in an electric oven the temperature of which is controlled by a thermostat. The capacity of the machine is 5000 kg.

(7) The Schopper compound stress machine (Fig. 201) is of the force type. It is designed for experiments with hollow cylindrical

specimens under combined tension, torsion and internal pressure, i.e. for *P–p*, *P–M* or *P–M–p* experiments. The specimen *A* is subjected to tension by movement of the cross-beam *T* actuated by the pressure of oil on a piston in the cylinder *U*. A change in pressure in the cylinder, and also in the whole hydraulic system when the pump is switched off, or a change in pressure due to change in volume of the cylinder, which could occur due to deformation of the specimen, is eliminated by a pneumatic compensator situated on the stand *N*. The torque is transmitted kinematically to the specimen from the motor *E* through the flexible pipe *F*. A worm gear in the box *L* rotates the grip *B* whilst the lower grip *C* remains fixed. The cross-beam *T* is prevented from rotating by supports in the form of guide columns which are in fact dynamometers (for example, hydraulic dynamometers). The internal pressure is generated by forcing oil into the hollow specimen which is filled with oil before commencement of the experiment. Measurement of the tensile force is carried out by a manometer connected to the cylinder *U* and graduated in force units. The internal pressure is also measured by a manometer. The maximum tensile force that can be applied is 30,000 kg, the maximum torque, 20,000 kg.cm and the greatest internal pressure, 300 kg/cm^2. The maximum travel of the cross-beam is 250 mm and the maximum angle of twist, 360°.

The machine is also provided with flat bearing plates C_1 and C_2 and supports K_1 and K_2 with rollers which allow the machine to be used as a universal press (for compression and bending experiments).

(8) A compound stress machine Mk. 04–1 of Soviet manufacture is shown in Fig. 202. It is the kinematic type of machine. It is designed for experiments on specimens subjected to combined tension, torsion and internal pressure, i.e. for Δl–φ experiments (the kinematic variant of *P–M* experiments) and also for *P–p* and *P–M–p* experiments (the mixed variants). A cylindrical specimen *A* is held in the grips *B* by bolts which hold the thickened walls of the specimen (Fig. 202) against locating plugs. The cross-beam *T* can be moved up and down by means of a worm gear (operated by a motor M_1 or by hand), and it is prevented from rotating by the guide columns *K*. The head of the machine is in the form of a portal frame *R* resting on an upper base plate *D* and can be rotated about a vertical axis (by a motor M_2 or by hand) and transmit the rotation to a spindle through the lugs *E* which support the end of a

lever F. The lower end of the spindle forms the upper grip B, and the upper end H in the shape of a portal frame rests on a sphere located in a hollow in an elastic dynamometer I which measures the tensile force. The latter bears on the upper base plate through a system

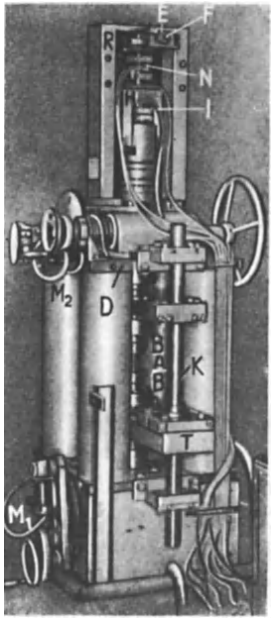

FIG. 202.

of ball-bearings L. The connecting rod between the lever F and the spindle frame acts as a dynamometer for measuring the torque N. In this way the tension and torsion apparatus are kept separate. Measurement of the applied force and moment is based on measurement of the strain of the dynamometers by means of a pneumatic device (see below).

The internal pressure is generated by pumping oil into the specimen from a pump situated on the control panel. It is measured by a manometer.

The maximum tensile force of the machine is 5000 kg, the maximum torque 2000 kg.cm and the maximum internal pressure 800 kg/cm^2. The maximum travel of the cross-beam is 200 mm.

(9) Hardness testing machines. Hardness is a measure of the strength and plastic characteristics of materials and is convenient

for comparison and quality control purposes. It is measured by the indentation of a hard body in the surface of the material.

The Brinell hardness H_B is measured by the indentation produced by a hardened steel ball under a specific load P (kg). It is normal to take $P = 30d^2$ for steels and $P = 10d^2$ for non-ferrous alloys, where d is the diameter of the ball in millimetres. The Brinell hardness is taken as the ratio of the force P to the area of spherical indentation produced:

$$H_B = \frac{P}{\frac{1}{2}\pi d[d - \sqrt{(d^2 - \delta^2)}]}, \tag{8.1}$$

where δ is the diameter of the indentation. H_B is approximately proportional to the UTS. In order to standardize these experiments a Brinell testing machine is used (Fig. 203).

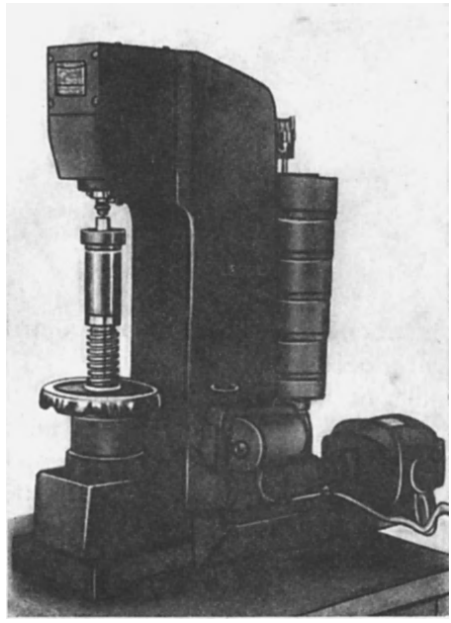

FIG. 203.

The Rockwell hardness is defined as the depth of the indentation produced by a hard steel 120° cone, or a ball of diameter 1·59 mm, under the action of a specific force. There are three scales of hardness (*A*, *B* and *C*) corresponding to three values of the applied

force 60, 100 and 150 kg respectively, the hardnesses being denoted by H_{RA}, H_{RB}, H_{RC}. A special Rockwell testing machine is used to determine these quantities (Fig. 204).

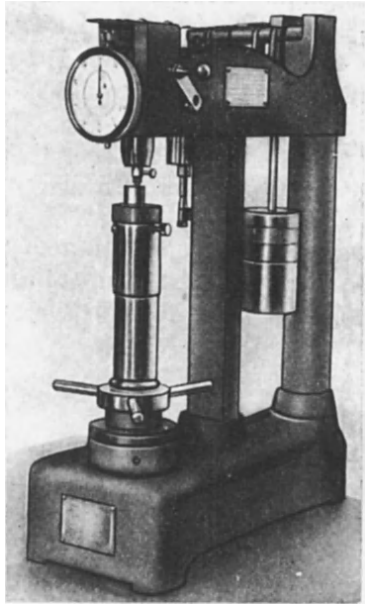

FIG. 204.

Hardness tests are a convenient means of control, for example, of heat treatment processes.

A method similar to the Brinell test is used for the dynamic testing of materials. In this a ball either falls freely or forms a striking surface of a pendulum. The analysis of the indentation formed enables estimates to be made of the effect of rate of strain on the plastic characteristics of a material. A Brinell impact test can be used for the same purpose as the static test: to compare and control the properties of materials. The equipment necessary in this case is simpler than the actual Brinell testing machine and can be used under any production or field conditions.

Apart from the machines described above there are numerous other types of equipment which can be used for testing materials. It should always be borne in mind that sometimes the simplest equipment gives the most reliable results. For example, for tensile tests we can use a calibrated wire (providing such is readily avail-

able) with the top held in a vice and a weight hanger attached to the bottom. In the case of a wire of diameter 2 mm made of steel C_T–5 (σ_S = 2800 kg/cm^2, σ_B = 5500 kg/cm^2) the force required to cause failure is of the order of 160 kg. This force can easily be applied by weights placed on the hanger. If the length of the wire is 3 m, the overall extension when the yield point is reached will be 3 mm. This extension (the movement of the bottom of the wire or the weight hanger) can be measured with a high degree of accuracy by means of dial gauges reading to 0·01 mm (see below). The advantage of this method is that the loads are applied directly to the specimen. The disadvantages have been pointed out in § 2. It is a particularly useful method for testing highly elastic materials (rubber, nylon, etc.).

(10) Structural testing is the investigation of stress, strains and conditions of failure in full size structures or in large scale models of these structures. The advantage of this type of testing is that it is possible to apply large forces accurately. Special floors are constructed for supporting the structures (of high strength reinforced concrete with cast-in channels and I-beams to take the holding down bolts). Special travelling gantries are used for applying vertical loads (in the structures laboratory of Moscow University there are two such gantries capable of applying loads up to 100 tons) and there are various methods of applying horizontal loads (for example, by hydraulic jacks).

5. Dynamic Testing Machines

In this section we shall give a brief description of machines and equipment used for vibration and fatigue tests and the equipment used for dynamic experiments with unrepeated loading.

(1) A mechanical vibrator is a machine used to set up periodic oscillations in a specimen or structure. It comprises a mass mounted eccentrically on a rotating shaft. If it is required to make the action of the vibrator directional two eccentric masses are used rotating synchronously in opposite directions. Vibrators of this sort can be used by themselves (for example in structural testing) or as part of vibration or fatigue machines. The effectiveness of the vibrator depends on the weight and the eccentricity and also on the speed of rotation. Hydraulic and pneumatic vibrators work on the principle of a variable pressure applied to a piston.

Electromagnetic vibrators comprise an electromagnet activated by an alternating electric current of given frequency. If the material under investigation is a ferromagnetic alloy the alternating magnetic field can be applied directly. Otherwise a shoe of transformer iron or the electromagnet itself, working together with an externally attached mass, is attached to the object under investigation. In some cases, when a specimen of non-magnetic material is massive, interaction with the electromagnet occurs on account of induced currents. Electromagnetic vibrators are sometimes used in conjunction with mechanical resonators.

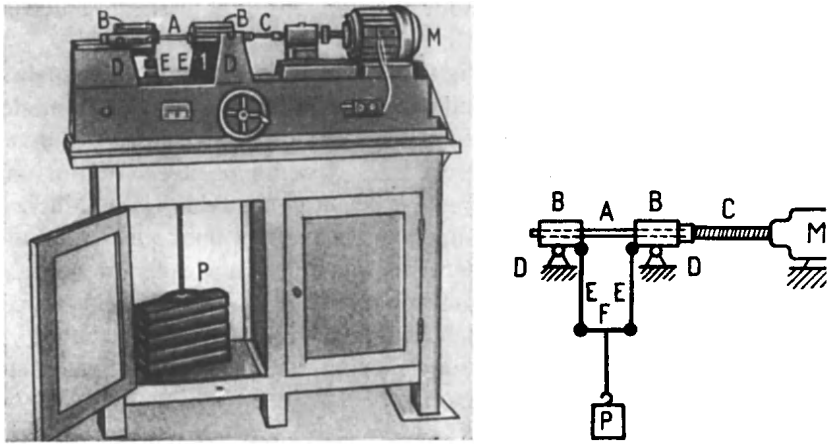

a b

FIG. 205.

(2) A rotary bending fatigue machine (Fig. 205a) is shown diagrammatically in Fig. 205b. A specimen *A* with circular section is held in the grips *B* and is rotated by the motor *M* through the flexible shaft *C*. The grips rotate on hinged supports *D*. A load *P* is applied to the grips through the beam *F* and the rods *E* and sets up a bending moment in the specimen (i.e. conditions of pure bending). On rotation the bending plane remains fixed in space and every meridian section passes through this plane in turn. The angular velocity of the motor is 2860 r.p.m.; this determines the frequency of the bending oscillations. The bending moment remains constant during the experiment and its magnitude is determined by the load *P*.

(3) A fatigue testing machine for bending in one plane is shown diagrammatically in Fig. 206. A flat specimen is held in grips *B* and *C* which rotate in hinged supports. As the flywheel *M* rotates the hinge *D* moves in a horizontal direction, causing the grips *C* and *B* to rotate (in opposite directions), thus subjecting the specimen to alternating bending moments applied at the ends (i.e. conditions of pure bending).

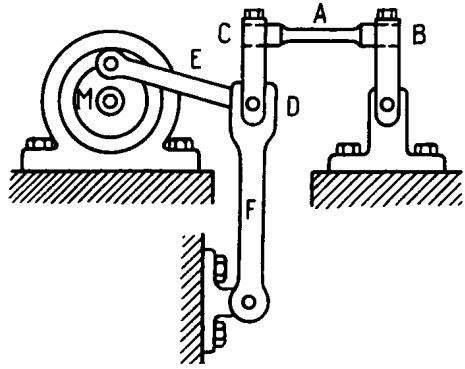

FIG. 206.

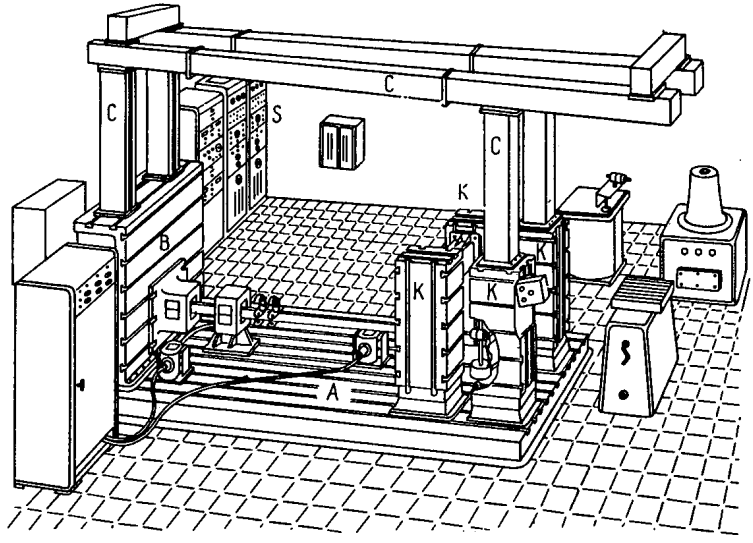

FIG. 207.

(4) A universal vibration and fatigue testing machine P–50 (Figs. 207 and 208) of Soviet manufacture uses electromagnets and a control system to set up and stabilize various types of vibration. The specimen is attached to the stand (Fig. 207) consisting of the base plate A, $4 \times 2{\cdot}5$ m, the wall B, the four columns K and the

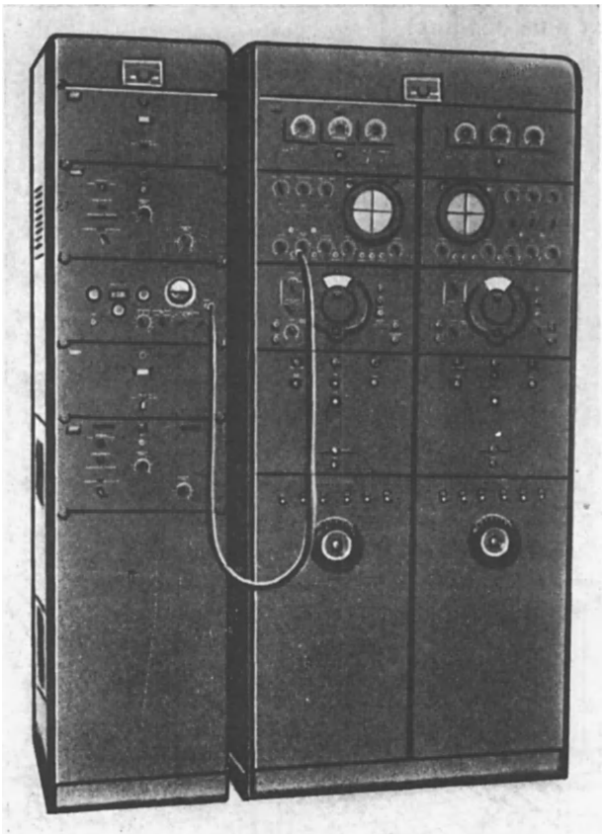

FIG. 208.

frame C of height 3·2 m. The electromagnets are energized by a direct current generator; the current passes through an invertor in the control panel (Fig. 208) and is transformed into an alternating current. The frequency is determined by the frequency of the supply generator, which sets up an alternating voltage across a thyratron valve contained in the invertor. When this voltage reaches a certain value ionization of the gas (mercury vapour, hydrogen)

filling the thyratron occurs, and an are discharge takes place, i.e. the current from the generator flows through the thyratron. The current ceases suddenly when the anode potential falls below the arcing potential; the invertor is wired so as to ensure that this happens. The maximum frequency at which the current passes through the thyratron is limited by the time necessary for de-ionization of the gas, which is comparatively large for mercury vapour (several hundred microseconds) and very small for hydrogen (a few microseconds). In spite of the high power of the supply to the magnets (4000 V in both cases), the force set up is insufficient to generate forced oscillations of the required magnitude. The apparatus usually works, therefore, at resonance frequencies, when the frequency of the load coincides with one of the natural frequencies of the specimen under the given conditions of fixing. In order to produce forced oscillations resonators are used (in the form, for example, of elastic rods with movable weights attached) which can be tuned to the required frequency and help to vibrate the structure.

The apparatus includes a number of "extras" which enable special types of experiments to be carried out: there is a platform for horizontal vibrations, a table for vertical vibrations, a machine for fatigue experiments in torsion, a device for pure bending tests, a device for fatigue experiments in tension–compression and also a device for vibration tests on plates and shells.

The control panel (Fig. 208) contains equipment for controlling and measuring the vibrations. An important feature of the control panel, amongst many others, is the stabilizer, which automatically ensures constancy of the amplitude of the displacements (or the velocities or accelerations) of a point in the structure, which is very important, for example, in fatigue experiments. As the arrangement is multi-channel and includes a stabilizer, it is able to generate so-called compound oscillations (for example, bending and torsional oscillations in a rod) with a given ratio of amplitudes in each component. This allows, in particular, fatigue experiments to be carried out for a state of compound stress.

(5) The pneumatic impact machine PSK–3† shown in Fig. 209 is a linear accelerator. The casing of the machine is in the form of a steel tube with stiffening ribs which absorb the reaction from the

† A. A. Iliushin, P. M. Ogibalov, *Izvestiya Akademii Nauk* (Bulletin of the Soviet Academy of Science, No. 3, 1957).

pneumatic gun and part of the force of impact on the target block. A pneumatic gun *A* is mounted on the rear flange of the casing (a simplified diagram is shown in Fig. 210) with a firing mechanism and a high pressure cylinder (up to 200 kg/cm^2) rigidly fixed to the barrel of the gun. The striker *C* is fired from the gun at a floating block *D* which transmits the force of impact to the casing through the oil damper *E*. The specimen *F* under investigation is attached to the front of the block. The travel of the striker is 2500 mm, the velocity of impact up to 300 m/sec, the energy of impact more than 35,000 kg.m, the diameter of the striker 98 mm and its weight from 10–30 kg.

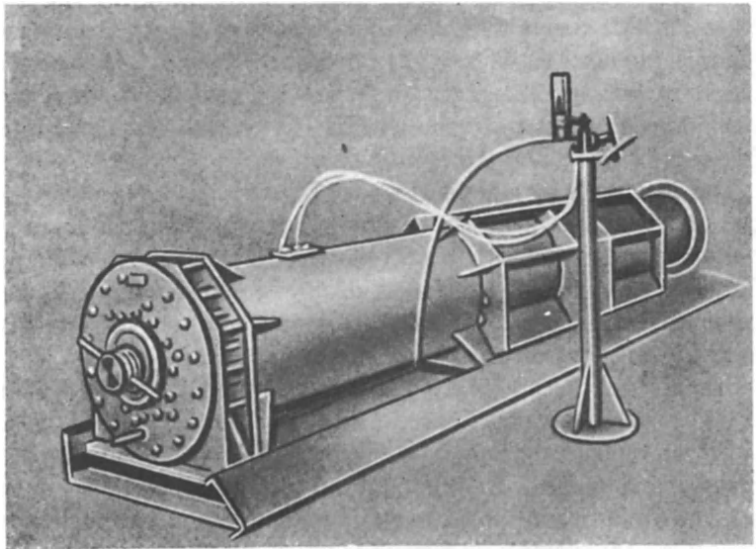

FIG. 209.

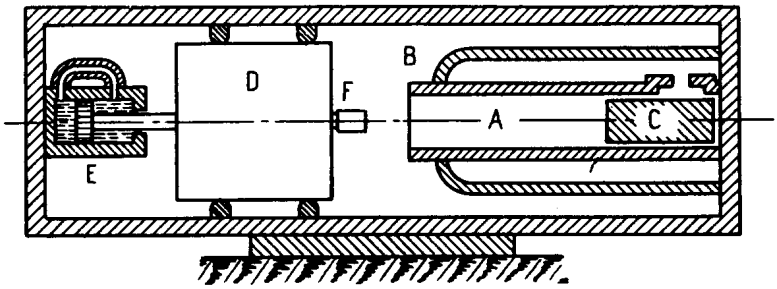

FIG. 210.

By virtue of the high velocity and the high energy of impact the machine can be used for testing the mechanical properties of materials under very high rates of strain and also for experiments on armour-piercing, on the deformation and failure of shells under high dynamic internal pressures, on impact stamping and pressing,

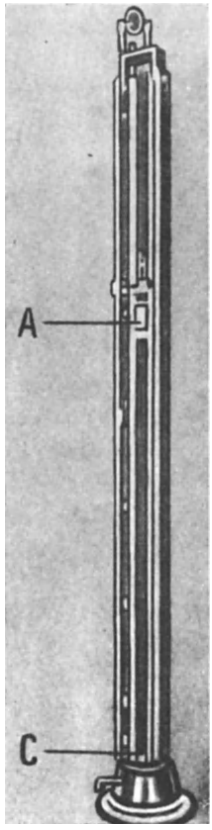

FIG. 211.

etc. If the striker is made hollow and filled with an appropriate material, and if the specimen F is replaced by a suitably designed damping system, the apparatus can be used to investigate the behaviour of bodies subjected to very high loads of short duration.

(6) An impact testing machine with a falling weight (Fig. 211) is the simplest type of linear impact machine. The velocity and energy of impact are given by the height of fall and the mass of the

weight *A*. The specimen *B* sits on the base plate *C*. In order to find the energy absorbed by the specimen, it is simply necessary to measure the height of rebound of the weight.

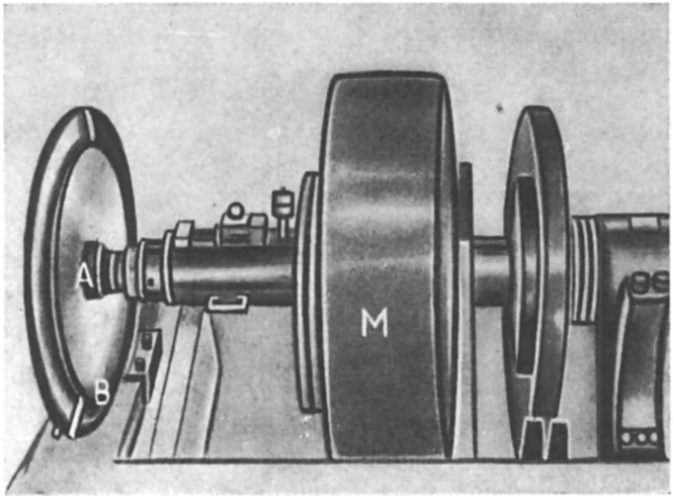

FIG. 212.

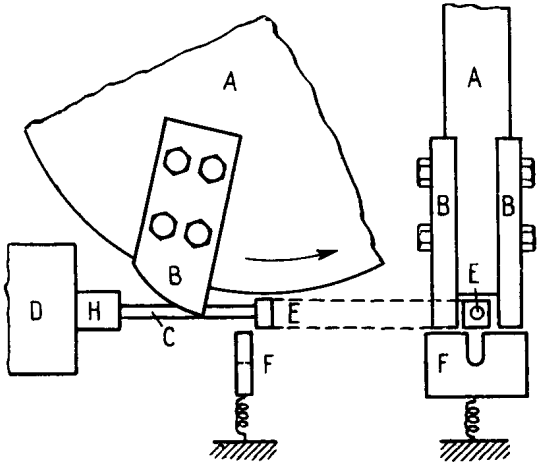

FIG. 213.

(7) A rotary impact machine, which was designed by the California Institute of Technology and which is used mainly for tensile tests, is shown in Fig. 212. The steel disc *A* of diameter approxi-

mately 1100 mm is mounted on the shaft of the d.c. motor *M* of 250 h.p. and is integral with the rotor of the motor. The total weight of this part is about 900 kg. At normal revolutions (750 r.p.m.) the linear velocity at the rim of the disc is 46 m/sec but can be increased to 80 m/sec. At one place (or two) on the disc steel plates *B* shaped as shown in Fig. 213 are bolted on so as to overhang the rim. The specimen *C* has one end screwed into a massive block *D* (weighing about 325 kg) which moves in guides in the direction of the axis of the specimen; the other end of the specimen has a head *E* of square section 25 × 25 mm. This head passes freely between the plates on the disc. When the disc has attained sufficient speed a slotted steel plate *F* mounted on a spiral spring is released and moves so that the working portion of the specimen enters the slot. The plates on the disc catch the slotted plate together with the head of the specimen. Due to the large mass of the rotating parts the angular velocity remains practically constant and the specimen is loaded to destruction at a practically constant linear velocity. An elastic dynamometer *H* is used to measure the tensile force, the change of which with time is recorded on a cathode-ray oscillograph. The extension of the specimen at any time can be found from the angular velocity of the disc.

(8) The pendulum impact machine MK 30 (Fig. 214) is one of the most common types of rotary machines. It is intended for experiments on impact resistance. Impact resistance is defined as the ratio of the energy expended in loading the specimen to destruction, to the area of the surface of failure under specified conditions of temperature and heat treatment. It is a very important characteristic of a material and is related to its plasticity and strength characteristics. The apparatus comprises a stand *A* with a rigid frame *B*, a pendulum *C* rotating about an axis *O*, a movable frame *D*, the position of which can be fixed by the ratchet *E*, a measuring device and a device for holding the specimen. The movable frame is first of all set at the required height and the pendulum is then attached to it by means of a special catch. The top of the pendulum, as it rotates, raises the scale *F* of the measuring device. A notched specimen is set up with its ends on the bearing plates *H*, which can be set at various distances apart. The catch is released, the pendulum falls and its striker *K* strikes the specimen in the plane of the notches; having broken the specimen the pendulum continues to rotate, rising to a height less than the original. In so doing

the top of the pendulum lifts the block L with a pointer attached and leaves it in its highest position. The energy absorbed in breaking the specimen is given by the difference between the initial and final height of the pendulum:

$$\mathfrak{Z} = Mgr(\cos\alpha_1 - \cos\alpha_2),$$

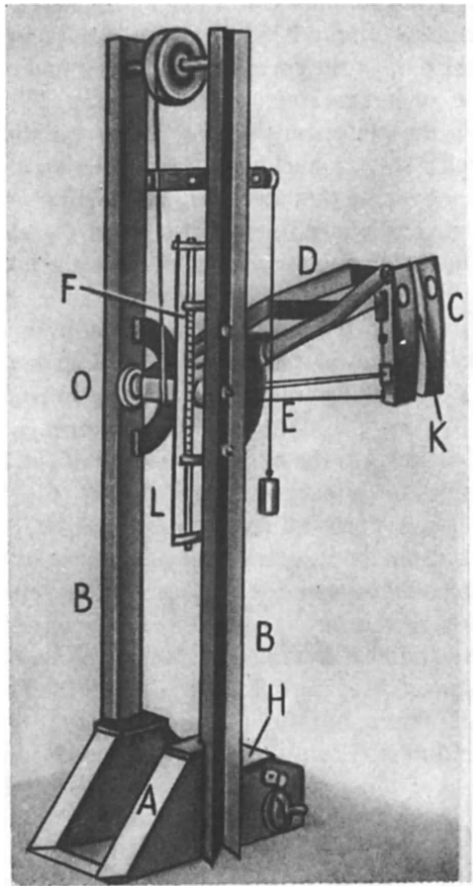

FIG. 214.

where M is the mass of the pendulum, g is the acceleration due to gravity, r is the radius to the centre of gravity of the pendulum, α_1 and α_2 are the angles of inclination to the vertical of the pendulum before and after impact. The scale F is graduated so that the

pointer L indicates directly the loss of energy in kg.m. The maximum energy of impact is 30 kg.m.

(9) There are many different pieces of apparatus for studying wave processes, and their design depends upon the particular type of problem to be investigated. We shall give two examples of this type of apparatus.

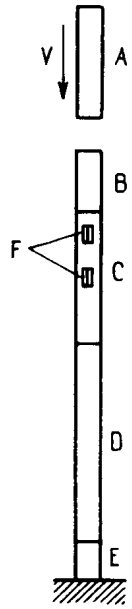

FIG. 215.

Figure 215 shows diagrammatically the apparatus used for measuring the period of delayed yield (see Chapter VI). The annealed steel rod C under investigation stands on a long rod D of hardened steel, which in turn rests on a rod E of a soft material (for example, copper) standing on a base. Above the rod under investigation there is another rod B of hardened steel which receives a longitudinal impact from the hardened rod A. All rods are of the same diameter and their ends ground together so that the compression wave travels undistorted through the joints, but tensile stresses are not transmitted. The rod A is arranged to travel at a velocity V at impact, so that the stress in the compression wave given by formula (6.11) exceeds the static ultimate stress. The sum

of the lengths of rods B, C and D is considerably greater than the length l_a of the rod A. Also, since the propagation velocities of the waves in all the rods are the same, a compression wave will arrive at the damping rod E with a constant stress $\sigma = \varrho a_0 V$ and wavelength $\lambda = 2l_a$, since the compression wave set up at the junction of rods A and B becomes, after reflection from the free end of rod A, a shock wave of total unloading. The rod B evens out the distribution of stress, and rod E reduces the effect on the rod under investigation of waves reflected from this end of rod D. Two electrical strain gauges F are attached to rod C (see below), and are connected to oscillographs which record the deformation process at these sections. Figure 155 (Chapter VI) shows the trace produced by the upper gauge.

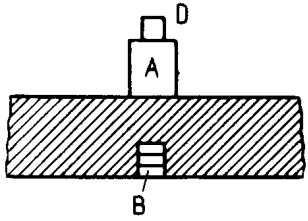

FIG. 216.

Figure 216 shows the apparatus used in an experiment on spalling on a plate due to an explosion. A charge A with a detonator D is placed on the upper surface of the plate. A cylindrical hole is bored in the bottom surface of the plate in which are placed washers B of different thicknesses. By measuring the velocities of these washers after the explosion, we can draw a curve of the variation of pressure with time (see the measuring rod theory in Chapter VI). By repeating the experiment on a plate without the hole and measuring the depth at which the spalling crack is formed we can determine the stresses which cause spalling of the material.

When carrying out investigations into impact and explosive effects we must take into account the interaction between the load and the specimen. For example, the theory given in Chapter VI shows that the stress in a longitudinal wave generated by the longitudinal impact of two rods depends not only on the properties of the material and the velocity of the moving rod, but also on the properties of the material of the rod which receives the impact. In

the same way the pressure on a plate caused by an explosion depends not only on the properties and dimensions of the charge and the method of detonation, but also on the material of the plate. The values found from one experiment for the pressure set up by the explosion must not, therefore, be assumed to be the same for another experiment with a different material. Although this remark may seem quite obvious experience has shown that it is a point that requires to be emphasized.

6. The Measurement of Small Displacements

In order to measure very small displacements we must use some device or other which magnifies these displacements so that they become visible. There are various mechanical, optical, optical–mechanical and electrical methods of realizing this.

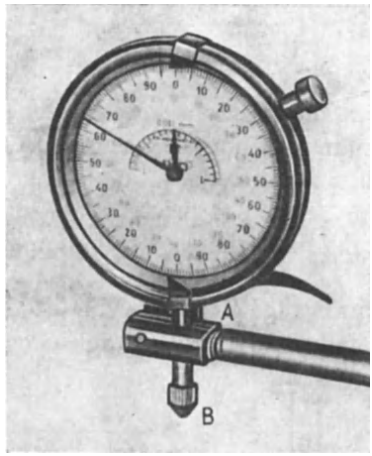

Fig. 217.

(1) The dial gauge (Fig. 217) is fixed to a rigid clamp by a cylindrical clip *A* and the spherical end of the plunger *B*, which is spring-mounted, is arranged to bear on the surface of the body the displacement of which it is required to measure. The movement of the plunger is converted by a gear-wheel into the angular movement of the large pointer. Gauges which measure to 0·01 mm are quite common, and it is also possible to obtain gauges which read to 0·001 mm (one micron). The small pointer (sometimes replaced

by a pointer connected directly to the rod *B*) gives the displacement in millimetres.

(2) The differential hydraulic gauge (shown diagrammatically in Fig. 218) converts a small movement of the piston *A*, which

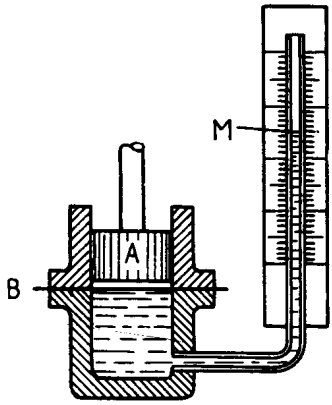

FIG. 218.

displaces the membrane *B*, into a large movement of the meniscus *M* of a slender column of liquid measured on a millimetre scale. The magnification is equal to the ratio of the cross-sectional area *S* of the piston *A* to the area of the tube *s*. A disadvantage of this apparatus is that the force that has to be applied to the piston is quite large.

(3) The pneumatic gauge shown in Fig. 219, on the other hand, requires only a small pressure to be applied by the body the dis-

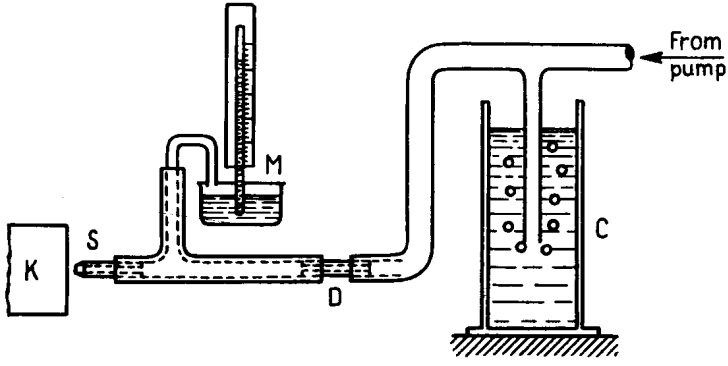

FIG. 219.

placement of which is measured. It works on the basis of the change in dynamic pressure in a tube when the distance between the nozzle S and the surface of the body K changes: when the clearance increases the air is able to discharge more easily and the dynamic pressure falls, which is indicated on the manometer M. The pressure applied to the system is stabilized (for example by a liquid stabilizer as shown in Fig. 219). The sensitivity of the instrument and the magnification produced can be regulated by altering the diameter of the throttle D. The smaller is the diameter of the throttle, the greater is the magnification. Strictly speaking the scale is non-linear (the curve of clearance against column height is S-shaped), but in the region of the point of inflection the curve is almost linear.

All the three gauges described so far are based on the mechanical conversion of displacements. We shall consider now two examples of purely optical methods of conversion.

(4) A microscope which includes in its optical system a plane glass with a graduated scale or grid, in the background of which can be seen points on the surface of the body under investigation, can be used for measuring small displacements. The microscope is attached to a rigid stand. Measurements over a comparatively small range can be made to the accuracy of 1 μ.

(5) An interferometer (shown diagrammatically in simplified form in Fig. 220) enables displacements to be measured to the accuracy of a tenth of the length of a light wave (to a hundredth or thousandth of a micron) over a wide range. Monochromatic light

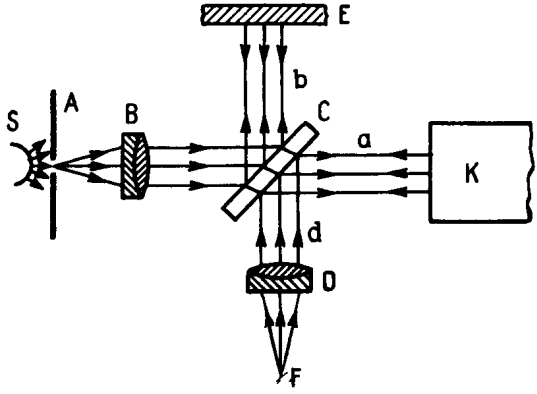

FIG. 220.

from a source S passes through a slot in the diaphragm A situated at the focal point of the objective lens B, and is transformed by the latter into a parallel ray. Part of this ray (the beam a) passes through a semi-transparent plate C inclined at 45° to the ray, and part is reflected by the plate (the ray b). The ray a, having been reflected from the optically flat surface of the specimen and from the plate C, unites with the ray b, which after reflection from a fixed mirror E passes through the plate C, to form the ray d. The eyepiece D focuses the ray into the eye of the observer. With the position of the body K fixed the observer will see an interference picture in the form of lines (strips). If K is displaced in the direction of ray a the interference lines will move. If a measuring device (a glass with a scale) is added to the system, any small displacement of the body K can easily be measured.

The combined method (optical–mechanical) method of measurement is illustrated by the following three examples.

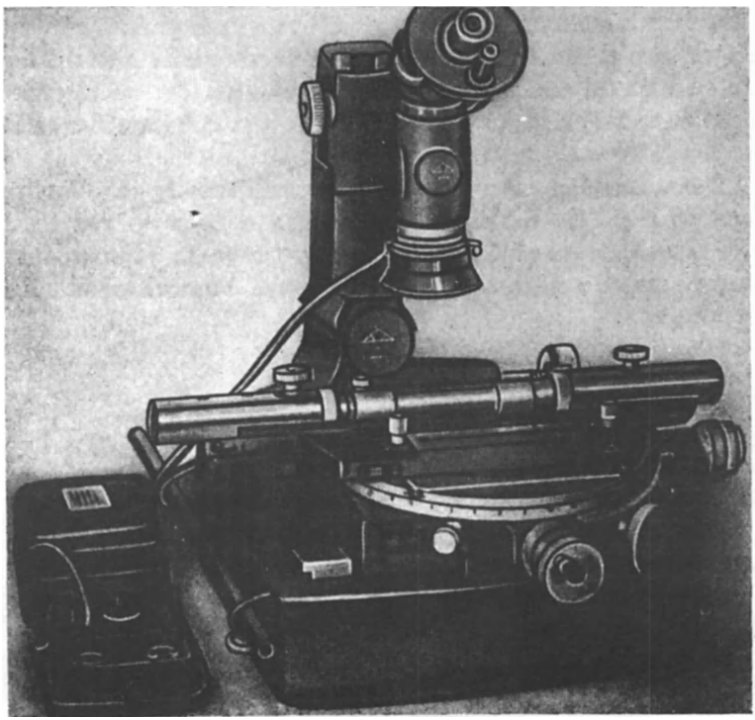

FIG. 221.

(6) A travelling microscope has in its field of vision two mutually perpendicular sighting axes (hair-lines). The position of the microscope is adjusted until the sighting axis coincides with a point on the object under observation: a reading is taken on the scale of a measuring device. As the body is displaced the intersection of the hair-lines is adjusted to coincide once more with the point on the body and the new reading on the scale is noted. The difference in the two readings gives the displacement of the point. The microscope shown in Fig. 221 is an example of this type of instrument and measures to an accuracy of 0·005 mm over a range of 75 mm. It is used for controlling dimensions of various components.

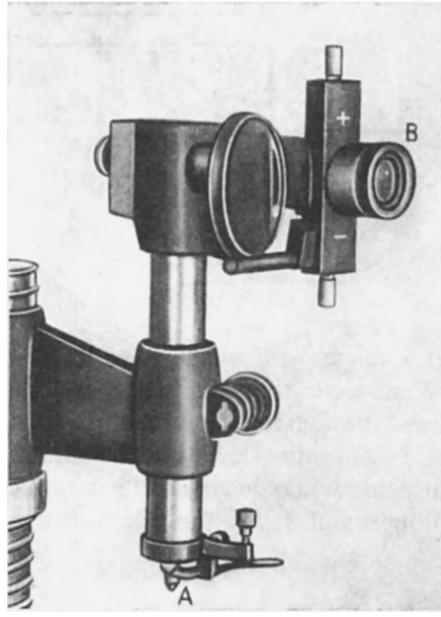

FIG. 222.

(7) The Zeiss optical gauge (Fig. 222) is attached to a rigid stand and is arranged so that the movable rod *A* bears on the surface of the object under investigation. As the object moves the displacement of the rod *A*, magnified mechanically, is shown on a micron scale viewed through the eyepiece *B*. The scale is illuminated through an opening in the instrument. The accuracy of measurement is better than 1 μ.

(8) The Martens mirror gauge (shown diagrammatically in Fig. 223) comprises a spring A with one end rigidly fixed; between this and the body K there is a prism with a mirror B. A linear scale (or, more accurately, a circular scale) L reflected in the mirror is

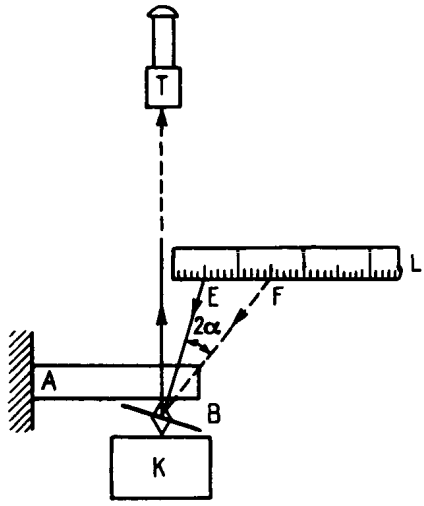

FIG. 223.

viewed through a telescope T which has a hair-line sighting axis. As the object K moves to the right or left the scale will appear to move when viewed through the telescope T. In this case magnification is obtained by an optical lever (instead of a mechanical lever). With a small displacement δ the angle of rotation of the prism (and the mirror) will be small. If h is the height of the prism, then

$$\delta = h\sin\alpha \approx h\tan\alpha.$$

The sighting axis will then coincide with the image, not of the point E, but of the point F, the angle between the rays BE and BF being 2α. If H is the distance from the mirror B to the scale L, then

$$EF = H\tan 2\alpha \approx 2H\tan\alpha;$$

therefore

$$EF = \delta\frac{2H}{h}. \tag{8.2}$$

The ratio $2H/h$ gives the magnification of the instrument. Usually the scale is displaced a distance such that $2H/h = 500$. A displace-

ment of 2μ then corresponds to an apparent movement of the scale of 1 mm, which can easily be observed.

We shall consider now some electrical devices for magnifying displacements.

(9) An electrical resistance deflectometer in the form of a rheostat is shown diagrammatically in Fig. 224. A contact C is arranged to slide along the high-resistance wire AB, the ends A and B of which are fixed in insulators. The circuit with power supply D

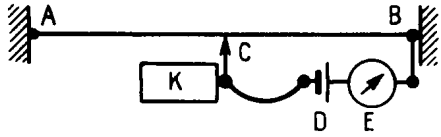

FIG. 224.

is closed through the section BC of the wire and includes an accurate voltmeter E (for example, a millivoltmeter) connected in series. If the contact C is connected to a body K under investigation, a displacement of the latter will alter the resistance of BC due to its change in length, and this change in resistance will alter the reading of E.

A more usual arrangement is when the contact C is fixed to the resistance wire and the part AC is discarded. Then as the body K moves to the left the wire BC will be extended and its change of resistance will be given by the reading of E.

The arrangement shown is, however, found to be unstable in operation and the apparatus used in practice is very much more complex. This will be dealt with in more detail in § 8.

(10) A capacitance gauge. If one plate of a plane condenser is connected to the body under investigation and if the other is fixed, then as the body moves in a direction perpendicular to the plate the capacitance varies. This can be observed, for example, as a change in frequency if the condenser is connected to an oscillatory circuit.

(11) An inductance gauge works on a principle similar to the capacitance gauge, but in this case the movement of the body causes two coils to approach or move away from each other or a core to move into or out of the coil, in this way altering the self-inductance of the coil. This can be also be measured by the change in frequency of an oscillatory circuit.

(12) A photoelectric gauge comprises a photoelectric cell situated in a closed box with slot. If a parallel beam of light is directed at the slot and if a shutter is attached to the body so that it partly covers the slot, then as the body moves more of the slot will be covered and the amount of light reaching the cell will decrease together with its electromotive force. This can be measured by the appropriate electrical apparatus. In this way the displacement of the body is transformed directly into an electromotive force.

If a mechanical quantity is converted into an electromotive force then with the aid of integration and differentiation circuits it is possible to find an approximate value of the integral of the measured quantity or its derivative with respect to time. An example of

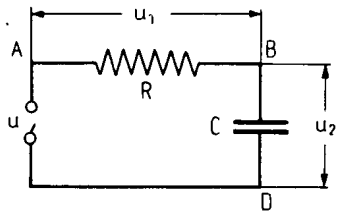

FIG. 225.

such a circuit is shown in Fig. 225. It contains a resistance R and a constant capacitance (the condenser) C. Let us suppose that the input voltage is $u(t)$, and that the current is $i(t)$. From Kirchhoff's law we have that:

$$iR + \frac{1}{C}\int i\,dt = u(t) \tag{8.3}$$

or

$$R\frac{di}{dt} + \frac{i}{C} = \frac{du}{dt}. \tag{8.4}$$

Let us suppose that u_1 and u_2 are the voltage drops across R and C (Fig. 225). If R and C are such that $u_1/R \ll 1/C\,du_2/dt$, the first term in (8.3) can be ignored, so that from (8.4) we have:

$$i = C\frac{du}{dt}.$$

Since $u_1 = iR$, we have that in an instrument connected to terminals at A and B, $u_1 = RC\,du/dt$, i.e. the voltage across it is proportional to the derivative with respect to time of the input voltage

u, which is proportional to the mechanical quantity we are measuring. If R and C are such that $u_1/R \gg 1/C\, du_2/dt$, the second term in (8.3) can be ignored, so that $i = u/R$. In an instrument connected to terminals B and D we then have that $u_2 = (1/C)\int i\, dt = (1/RC)\int u\, dt$, i.e. the voltage across it is proportional to the integral of the input voltage $u(t)$.

This system has been employed, for example, in the P–50 machine. The main measuring device in this machine is the vibration meter, in which a coil moves in a constant magnetic field. The induced e.m.f. is proportional to its velocity. The basic quantity measured, therefore, is the change with time of the velocity of the body under investigation. With the aid of an integration circuit we can find the change in its displacement with time, and with the aid of a differentiation circuit we can find the change in its acceleration with time. We see from this how it is possible to stabilize vibrations not only with respect to the amplitude of velocity, but also with respect to the amplitude of the displacements or accelerations.

It should be noted that the accuracy of the differentiation and integration operations depends on the quantity RC, the so-called time constant of the apparatus. In order to find the limits of the possible error it is necessary to analyse the integral of the complete eqn. (8.4).

7. Force Measuring Devices

The most simple and reliable method of measuring the forces applied to a specimen or structure is to "weigh" them, since the measurement of any force reduces in the end to a comparison with the force of gravity, since the practical unit of force is taken as the weight of 1 cm^3 of pure water. This method of measuring forces is used when weights are applied directly to the specimen and when a lever system of loading is employed (the MAN machine, the creep machine, etc.). In lever systems, however, the magnitude of the force applied to the specimen should not be calculated from the mechanical advantage principle, since to do so would introduce errors due to inaccuracy of the measurement of the distances between the points of support and also to the impossibility of assessing accurately various losses. Instead the force applied should be measured by calibrating the machine with the aid of some sort of dynamometer.

The vast majority of dynamometers contain an elastic element, the displacement of some point of which is proportional to the force applied, and can be measured by various means. An exception is, of course, the liquid (mercury, alcohol) manometer, in which the pressure is given directly by the weight of a cylindrical column of liquid per cm^2 of horizontal cross-sectional area. The movement of a point on the elastic element of a dynamometer is usually magnified (most often by a lever system) and is measured on a scale.

Every dynamometer, like any force measuring device, must be calibrated by comparing its readings with those of a standard dynamometer or by loading it with known weights. A force-measuring device can if necessary be calibrated by comparison with another device which has already been calibrated. If successive calibrations are made by this method, however, the accuracy of the last calibration is, of course, reduced. Dynamometers in the Soviet Union which are used for important scientific investigations, like any other measuring equipment, are subjected periodically to government inspections by a number of organizations acting on behalf of the Board of Weights and Measures: apparatus and machines are checked against standard equipment. After the inspection a certificate is issued which shows the range of the instrument, the divisions of its scale and possible errors in the readings.

Linearity of a dynamometer, i.e. the proportionality of displacement to applied load is a convenient, but not essential, property of the instrument. A much more important property is its ability to give identical readings for increase and decrease in load; an essential property is its ability to reproduce readings. For this reason the elastic element of a dynamometer is usually made of hardened steel, which within the elastic range has an extremely narrow hysteresis loop and retains its elastic properties for a very long time.

(1) The standard compressive force dynamometer (Fig. 226) comprises a closed irregular ring of variable section. If a compressive force is applied through the ball-bearings 1, the bearing plates of the dynamometer move towards each other and this movement is measured by the micron dial gauge 2. The certificate for the instrument gives the readings corresponding to different values of applied force over the whole range of measurements.

The instrument is designed for static measurements but is included in the P–50 vibration machine for measuring the ampli-

tude of the longitudinal force in the arrangement used for tension-compression fatigue experiments. One bearing plate is rigidly fixed on a stand and a luminous point (a small drop of luminous paint or a piece of glass illuminated by reflected light) is placed on the

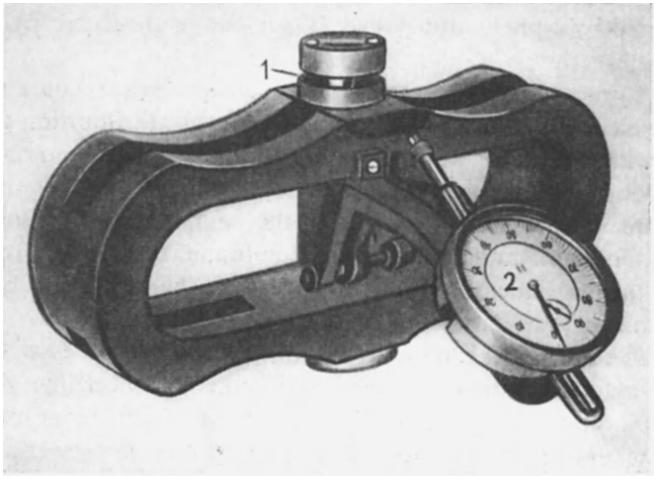

FIG. 226.

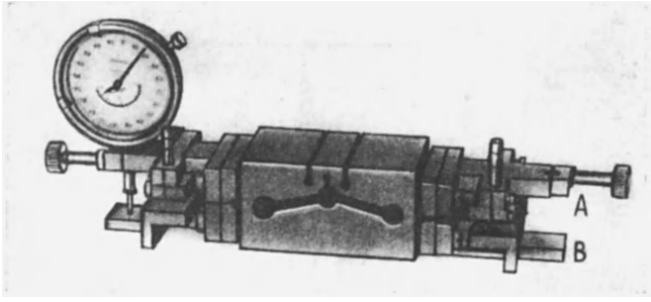

FIG. 227.

other, which is attached to the specimen; with vibration this point becomes a line the length of which is measured with a microscope and which represents to some scale the amplitude of the force.

(2) The tensile force dynamometer with a pneumatic contact shown in Fig. 227 is used in the 04–1 combined loading machine, In principle it differs from the dynamometer described above only in the method of measuring the displacement: instead of a dial

gauge a pneumatic gauge is used to measure the change in distance between the ends of the levers *A* and *B*.

(3) The torque dynamometer in the 04–1 machine is a circular cylindrical rod held rigidly at the ends by grips which almost meet in a meridian plane. A change in distance between the grips is measured by a pneumatic gauge. It can also be measured by a dial gauge.

(4) A manometer (a pressure-measuring device) contains an elastic element either in the form of a bent tube (a Bourdon gauge) filled with liquid or gas, or in the form of a membrane on one side of which is the liquid or gas, the pressure of which it is required to measure. As the pressure increases the bent tube in the Bourdon gauge tends to straighten, and the membrane is distended. In both cases the movement can be converted mechanically (or by any other means) and measured on a scale.

(5) The sylphon bellows shown in Fig. 228 comprises a hollow metal cylinder with corrugated sides like a concertina. As the pressure inside the sylphon bellows increases the cylinder extends. The movement of one end relative to the other can be measured in a number of ways. In the 04–1 machine, for example, these instruments are used as intermediate elements in the measuring

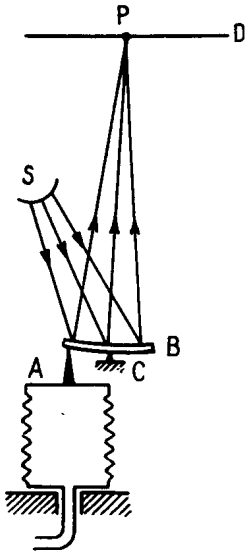

FIG. 228.

system, and the movement of the top of the cylinder, by means of the pin *A*, causes the spherical concave mirror *B* to rotate about the hinge *C*. A spot of light *D* which is focused from the light source *S* by the mirror *B* then moves over the semi-transparent screen *D* by an amount proportional to the angle of rotation of the mirror, i.e. proportional to the pressure in the cylinder.

(6) An electrical resistance strain gauge dynamometer is a circular cylindrical rod with electrical strain gauge wires arranged longitudinally on the outside and attached by means of some form of insulating layer. The extension of the dynamometer, which is proportional to the applied tensile force, is measured by an electrical apparatus which can be calibrated in forces. The change in the resistance of the gauges is measured by a Wheatstone bridge arrangement; as the gauge is extended the bridge becomes unbalanced by an amount which can be measured directly or by the compensation method (for further details see the description of electrical resistance strain gauges, § 9). If the gauge-wire is attached at 45° to a generator, the change in its resistance will be proportional to the relative angle of twist of the rod (since a direction at 45° to a generator is a principal direction of strain in torsion). In this form the dynamometer can be used to measure torque. Dynamometers of this type are used both for static and for dynamic experiments. In the latter case oscillographs can be used to record the changes in stress.

(7) A carbon resistance dynamometer comprises a column built up of carbon discs, the resistance of which changes if it is compressed. In order to measure this change the dynamometer is connected to a bridge circuit. The only difference from the previous example is that the resistance gauge is the actual dynamometer itself.

The instrument can be used for dynamic as well as static measurements.

(8) In a piezo-electric dynamometer use is made of the piezo-electric property of certain minerals (a crystal of quartz, barium, titanate, etc.), which is that under compression a difference in potential proportional to the compression is set up between the top and bottom faces of the crystal holder. This difference in potential can be measured in a number of ways.

It is useful for dynamic experiments, but is unsuitable for static

experiments, since the potential difference decreases rapidly as a result of discharge through the crystal itself.

In conclusion it might be pointed out that any elastic body can be used as a dynamometer: the important part is the system for measuring the displacements.

8. Mechanical, Optical and Optical-Mechanical Methods of Measuring Strains

A tensiometer (or extensometer) is a device for measuring strains (linear and shear strains). Extensometers are used to measure the relative movements of points in a body under investigation and the same principles are employed in their construction as were described in § 5, when we were dealing with instruments for measuring displacements.

A purely optical method of measuring strains, which is more reliable than any other method, is the use of two or more universal travelling microscopes each of which is mounted on a fixed base and follows the movement of a particular point on the specimen. The magnitude of the strain can easily be found from the difference in movement of two or more such points. In practice more convenient methods are used, a number of examples of which will now be described.

(1) A simplified diagram of the Chalmers interference extensometer, with the balancing device not included, is shown in Fig. 229.

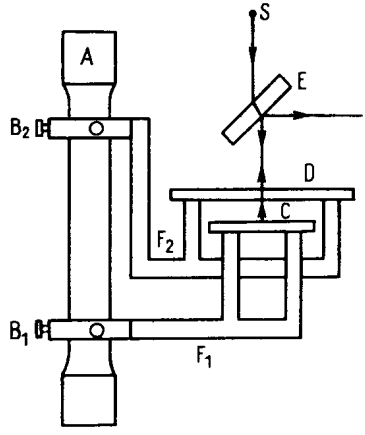

Fig. 229.

Two screw-clips B_1 and B_2 are fixed to the specimen A, and to these clips are attached the brackets F_1 and F_2 which support flat parallel glass plates C and D. Monochromatic light from the source S passes through the glass plate E inclined at 45° and arrives at the plate D. Part of the light is transmitted through this plate and part is reflected from its bottom surface. The light transmitted is then reflected from the top surface of plate C so that superimposed rays which have travelled different paths arrive back at the glass plate E. After reflection from the bottom surface of E the rays are viewed by an observer who sees an interference picture. This picture will change as the specimen extends, and this change, which can be measured, gives the relative movement of the sections of the specimen to which the screw-clips B_1 and B_2 are attached. A change in the interference picture with plates C and D exactly parallel will be observed as periodic fading and brightening of fixed interference bands, as the distance between C and D changes by one light wavelength. If, however, the plates form a small angle with each other, the interference bands will be displaced discontinuously but will remain parallel. In this case the measurements can be made in terms of intervals corresponding to a change in distance between C and D of one tenth (or less) of a wavelength. The accuracy of the measurements of strain possible with this instrument with a 30 mm gauge-length is to within 10^{-7}, i.e. 10^{-5} per cent of the relative extension. (The gauge-length of an extensometer is the distance between the points observed through the instrument).

If the glass plates C and D are placed in meridian planes, the same instrument can be used to measure the relative angle of twist of a specimen in torsion, i.e. a shear strain.

(2) A torque meter is used for measuring relative angles of twist, and comprises two clamps attached to two sections of the specimen at a specific distance apart (the gauge length), to which are fixed mirrors, the planes of which lie in meridian sections of the specimen. As the specimen twists the mirrors rotate through different angles and the difference between these angles, referred to the gauge length, is the relative angle of twist from which the shear strain is determined (see § 7, Chapter II). The angle of rotation of each mirror can be measured, for example, by the movement of a spot of reflected light over a circular scale. It is more usual, however, to use the method employed in the Martens mirror gauge (see

Fig. 223). A linear scale is set up in front of each mirror and the movement of the image of the scale is observed through a telescope with a hairline. If Δ is the apparent (observed) movement of the scale and H is the distance from the scale to the mirror, the angle of rotation of the mirror α (i.e. the angle of rotation of the section) is given by:

$$\tan 2\alpha = \frac{\Delta}{H},$$

and for small angles of rotation measured in radians we can put $\tan 2\alpha = 2\alpha$, so that $\alpha_1 - \alpha_2 = \frac{1}{2}(\Delta_1/H_1 - \Delta_2/H_2)$ is the difference in angles of rotation, and $\vartheta = (1/B)(\alpha_1 - \alpha_2)$, where B is the gauge-length (the distance between the two sections), ϑ is the relative angle of twist. The shear strain on the surface of a circular specimen is therefore

$$\gamma = a\vartheta = \frac{a}{2B}\left[\frac{\Delta_1}{H_1} - \frac{\Delta_2}{H_2}\right], \tag{8.5}$$

where a is the radius of the specimen.

The relative angle of rotation of two cross-sections in the plane of bending can be measured in the same way in tests of beams subjected to bending.

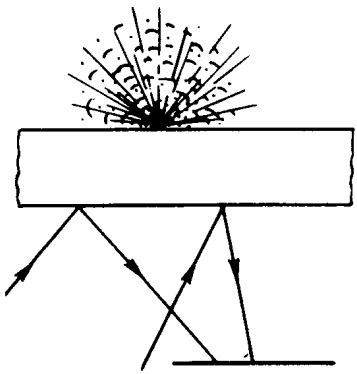

FIG. 230.

(3) The method of mirror surfaces makes use of polished surfaces on the actual specimen itself and is usually employed for investigating the behaviour of plates and slabs, especially under the action of dynamic loads. An explosion is produced on the upper surface of the plate (Fig. 230) and narrow beams of light are projected on to

a number of polished areas on the lower surfaces. Immediately the deformation waves reach the lower surface of the plate the polished areas are displaced and, in general, rotate. By photographing the path followed by a spot of light reflected from each polished area the shape of the lower surface of the plate at any instant of time can be calculated.

(4) The grid method: if a geometrically accurate grid is drawn on the surface of the specimen before the experiment, any deformation of the specimen will cause the grid to distort. By measuring the distorted grid (for instance, with the aid of a travelling microscope) the deformation of the specimen can be determined. The method is suitable for large strains.

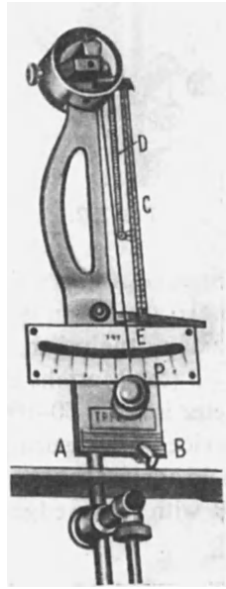

FIG. 231.

(5) The Huggenberger extensometer (Fig. 231) is of the mechanical type. The point *A*, which is part of the frame of the instrument, and the prism *B* are held by means of a spring clamp at two points on one generator of the specimen. The prism *B* which rotates with increase or decrease in length of the specimen is connected to a lever *C* which transmits the movement through the rod *D* to the pointer *E* which moves over a circular scale *P*. The magnification

produced by the specimen is about 1000–1200. It is used solely for static experiments.

(6) The Martens mirror extensometer (Fig. 232) is one of the most reliable strain measuring instruments of the lever-mirror

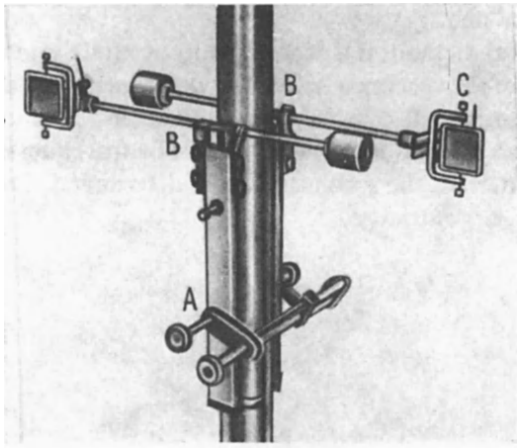

FIG. 232.

type. It comprises a knife edge *A* and a prism *B* held between the frame and the specimen. To the prism is attached a mirror which rotates about the same axis as the prism. Measurements are made in the way described in § 5 (the Martens mirror gauge). The gauge length of the extensometer is from 50–100 mm.

(7) An optical lever device for measuring lateral strain (Fig. 233) comprises two shoes *A* held against the specimen *L* by spring-loaded clamps *F*, two plates *B* with knife edges *C* and two cylindrical

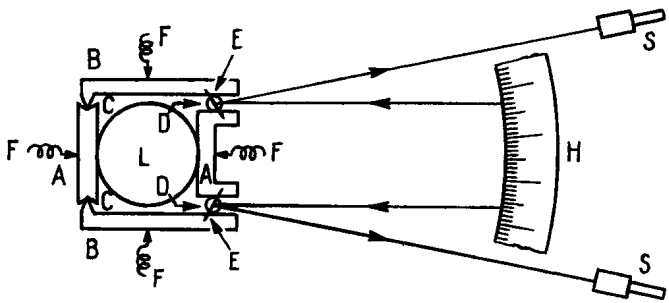

FIG. 233.

rollers D with axially mounted plane mirrors E; the plates B are held against the shoes A through the lugs C and the rollers D by means of clamps (which in the diagram are represented by the coils). As the diameter of the specimen changes the right-hand shoe A moves relative to the plates, and in so doing rotates the rollers D. The movement of the shoes, which is equal to the change in diameter of the specimen, is measured by the apparent displacement of a circular scale H reflected in the mirrors E and observed through the telescopes S in the same way as for the Martens lever-mirror extensometers. The accuracy of this device is the same as that of the Martens extensometer.

The Huggenberger extensometer can also be used to measure lateral strains in flat specimens.

(8) A vibrating wire extensometer is shown diagrammatically in Fig. 234. A knife edge A, which is integral with the frame of the

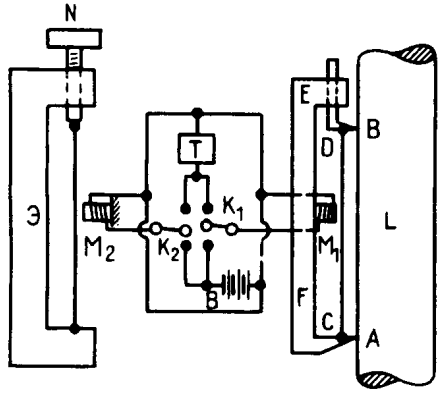

FIG. 234.

instrument, and a knife edge B, which can move along the axis of the instrument in the guides E, are attached firmly to the specimen L. A wire CD is stretched between A and B. A magnet M_1, which by means of the switch K_1 can be connected for a short interval of time to the battery B, sets up vibrations in the wire CD the frequency ν of which depends on the tension in the wire:

$$\nu = \frac{1}{2l}\sqrt{\left(\frac{S}{\varrho_1}\right)}, \tag{8.6}$$

where S is the tensile force in the wire, ϱ_1 is the mass per unit

length of the wire, l is the length of the wire CD. Since according to Hooke's law

$$S = \sigma \frac{\pi d^2}{4} = E\varepsilon \frac{\pi d^2}{4}, \tag{8.7}$$

where d is the diameter of the wire, E is the longitudinal modulus of elasticity, we find, by comparing (8.6) and (8.7), that the relative extension is

$$\varepsilon = \frac{16\varrho_1 l^2}{\pi d^2 E} \nu^2, \tag{8.8}$$

which is equal to the relative extension of the section AB of the specimen.

The frequency ν can be found by comparison with a standard apparatus Э, in which the tension in the string is produced by a micrometer screw N connected to a scale which shows the frequency of vibration of the standard wire. The comparison is carried out as follows. The magnets M_1 and M_2 are used in turn to set up vibrations in the wire of the instrument and in the standard wire. The switches K_1 and K_2 are then reversed so as to connect the magnets M_1 and M_2 to the telephone T (the electromagnets then function as electrodynamic microphones) and the pitch of the notes is compared. By turning the screw N so as to tighten the standard wire the notes can be matched and the frequency of the vibrations of the standard wire can be read off on the scale.

The instrument is accurate to within 0·1 per cent of the relative extension. It is used for static experiments.

The accuracy of the instrument can be increased if the standard instrument is replaced by a precise electromagnetic generator, and if the telephone is replaced by a cathode-ray oscillograph. The generator is connected to the Y–Y plates of the oscillograph and the electromagnet M_1, which now functions as a microphone, is connected to the X–X plates. By varying the frequency of the generator we can obtain a stationary curve (a Lissajous figure) on the oscillograph screen and the frequency ν can then be read off on the generator scale.

All of the extensometers described above (with the exception of the grid method) measure only one component of the deformation: either an extension or an angle of twist. We shall describe now a two-component extensometer used in the 04–1 combined loading

machine where the nature of the experiment requires the extension and angle of twist of the specimen to be measured simultaneously.

(9) The two-component extensometer "Mechanical ray" (Fig. 235) is attached by the base plate *P* to the cross-beam of the machine, and, in the same way as two travelling microscopes, follows

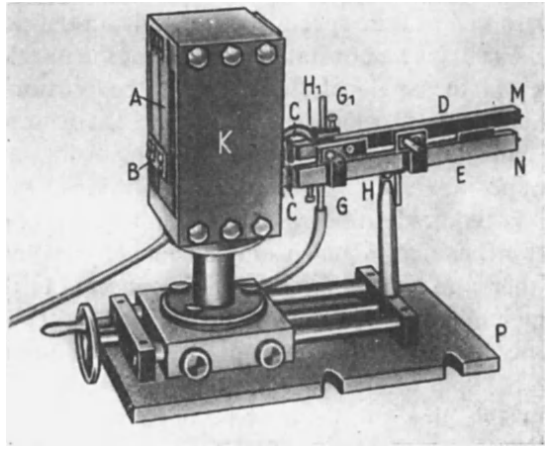

FIG. 235.

the movement of two points on the specimen lying on one generator before deformation. In this case, however, the rays of light are replaced by long metal rods, and the measuring device of the microscopes, by pneumatic gauges.

Two pairs of leaf springs *A*, connected at the bottom by two rods *B*, are attached at the top to the frame of the instrument *K* which can be wound along a horizontal axis. To each pair of springs are connected rods *D* and *E* 200 mm long through ball and socket joints *C*, and the conical pointed ends *M* and *N* of these rods make contact with the specimen. The rods are of rectangular section with polished faces; the side faces are parallel and the upper and lower faces are perpendicular to the axis of the specimen. Two nozzles *G* and *H* are screwed into the lower rod *E* so as to point towards the lower and side surfaces of the upper rod *D*. If the specimen moves as a rigid body and if movement is of the order of 3–5 mm, in view of the length of the rods *D* and *E*, the gaps between the nozzles *G* and *H* and the faces of the rod *D* alter only by very small amounts. Spirit manometers, therefore, connected to the nozzles would only

record relative movement of the rods. Also, in the case of simple tension the side of rod D will move along the nozzle H without altering the gap, and a manometer for measuring the angle of twist φ will give a constant reading, whereas the gap between the nozzle G and the lower face of the rod D will increase, and the column of spirit in the manometer will fall, indicating an extension of the portion MN of the specimen. Similarly, in the case of torsion the nozzle G will give a constant reading, but the nozzle H will give the change in the angle of twist φ over the portion MN of the specimen. The nozzle which can be seen in the figure beneath the nozzle G, and another nozzle which is not visible and which is situated opposite H, serve to compensate for air losses.

When it is required to derive a continuous trace of the readings this purely mechanical system is supplemented by a pneumatic device in which there are two sylphon bellows connected to the nozzles G and H which make contact with a concave mirror at two points on mutually perpendicular diameters of the mirror, so that in the case of tension the spot of light moves over the semi-transparent screen along a straight line, and in the case of torsion, along a line perpendicular to the former. In the case of combined tension and torsion the spot of light moves along a curve which in coordinates Δl and φ represents a strain trajectory (see Chapter III).†

The instrument is calibrated in each component on a special calibration instrument which measures the displacement of the moving part by an optical micron gauge (§ 5). Lateral strains can

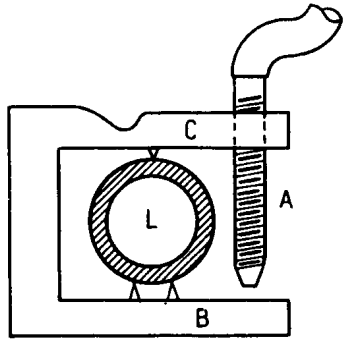

FIG. 236.

† Similar pneumatic–optical devices are used to derive traces of the $P - M$, $P - \Delta l$, $M - \varphi$ curves.

also be measured by the pneumatic method. The principle of this type of instrument will readily be seen from Fig. 236, where L is the specimen, A is the nozzle of the pneumatic gauge, B is a fixed leg and C a movable (sprung) leg.

9. Electrical Methods of Measuring Strains

Electrical methods of measuring strains, as was pointed out in § 5, are based on the conversion of mechanical displacements into electrical quantities.

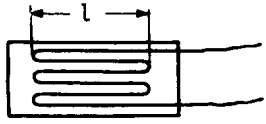

Fig. 237.

(1) An electrical resistance strain gauge is a wire arranged as shown in Fig. 237 in between two pieces of paper stuck together. If the gauge has n turns (rows) its electrical resistance R_1 is

$$R_1 = n\varrho\frac{l}{F},$$

where ϱ is the specific resistance of the material of the wire, F is its cross-sectional area and l is the length of one turn (the gauge-length). The gauge, by means of a special glue, is stuck to the specimen so that the gauge-length changes together with the length of the section of the surface of the specimen to which the gauge is attached. As the specimen deforms, therefore, R_1 will vary, and

$$\frac{R_1 + \Delta R_1}{R_1} = \frac{l + \Delta l}{l}\left(\frac{d}{d + \Delta d}\right)^2,$$

where d is the diameter of the wire, the change in specific resistance being ignored. Since $\Delta l/l = \varepsilon$, and $\Delta d/d = -\nu\varepsilon$, where ν is Poisson's ratio, we get, after discarding small quantities of order higher than the first, that

$$\frac{\Delta R_1}{R_1} = \varepsilon(1 + 2\nu)$$

or, in general,

$$\frac{\Delta R_1}{R_1} = S\varepsilon. \tag{8.9}$$

The quantity S is called the gauge factor, and usually lies between 1.8 and 2.3. The strains measured by these gauges do not normally exceed 1 per cent. If the initial resistance of the gauge is 200 Ω we have, therefore, that $\Delta R_1 < 4\,\Omega$. In order to facilitate the measurement of small changes in resistance, the resistance R_1 is included in one arm of a Wheatstone bridge (Fig. 238).† The diagonal of the

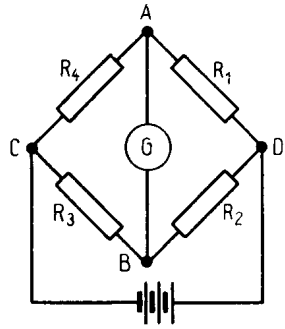

FIG. 238.

bridge contains a sensitive measuring instrument G (a galvanometer, microammeter, etc.). For the bridge to be in balance, as is well known, the relation

$$R_1R_3 = R_2R_4 \tag{8.10}$$

must be satisfied.

One of the resistances, for example, R_2, is variable. It is made in the form of an electrical resistance strain gauge and is stuck to a cantilever beam the deflection of which is measured by a micrometer screw. Suppose that initially, before the body under investigation is loaded, the bridge is balanced by means of the variable resistance R_2 so that the pointer on G stands at zero. As loading takes place the body deforms, the resistance R_1 alters, the bridge is thrown out of balance and the pointer on G moves away from the zero mark. The scale of the galvanometer can be graduated directly in values of the strain ε.

It is more usual, however, to use a compensation method: the cantilever beam is deflected by means of a micrometer screw so as to alter the resistance R_2 until the condition (8.10) is once more satisfied:

$$R_1'R_3 = R_2'R_4.$$

† In practice the circuit used is more complicated than that shown in Fig 238.

The deflection of the end of the cantilever can be measured by a dial gauge. It is these dial gauges that are normally calibrated in values of the strain ε.

A few gauges, selected at random from a particular batch, can be calibrated by sticking them to a beam the elastic strain of which under load is known.

The resistance of a gauge varies considerably with temperature. In order to compensate for likely variations in temperature the same type of gauge as R_1 is used for the resistance R_4. It is subjected to the same conditions as R_1 (for example it is stuck to an identical piece of material and placed adjacent to R_1); the same procedure is followed for the resistances R_2 and R_3. With change in temperature the resistances of R_1 and R_4 will then increase or decrease by k_1 times and R_2 and R_3 by k_2 times. As a result we have that

$$k_1 R_1 k_2 R_3 = k_2 R_2 k_1 R_4,$$

which is equivalent to (8.10), so that the bridge remains balanced.

The error in measurements taken with a gauge length of 10 mm is within 0·1 per cent of the highest of the quantities measured.

Electrical resistance strain gauges are very convenient to use. They can be stuck in any required position on the structure under investigation. They can be attached in large numbers and by means of a special switch they can be switched in turn to the measuring apparatus. This is important, for example, in the experimental stress analysis of aircraft, bridges, etc., when a large number of strain gauge points are required.

The almost complete absence of inertia in these gauges allows them to be used for dynamic experiments (both as a means of measuring the deformation of the structure, and as a converting element in a dynamometer). The readings of the gauges in this case are recorded with the aid of an oscillograph.

(2) The carbon (semi-conductor) extensometer is a modification of the electrical resistance strain gauge. It is shown diagrammatically in Fig. 239. The pointed ends of a fixed leg A and a movable (in the plane of the hinge E) leg B bear against the specimen. A column of carbon discs is compressed between A and B. A similar column D is compressed between B and the frame of the instrument. As the specimen extends the column D is compressed and the compression in column C is reduced. The resistances of the two columns vary in opposite senses. If they are wired so as to form

adjacent arms of a Wheatstone bridge the balance of the bridge will be destroyed and a current will flow through the diagonal. A trace on an oscillograph of the variations of this current provide information on the deformation. In the case of static measurements the zero method can be employed, i.e. the bridge can be re-balanced with the aid of its other arms.

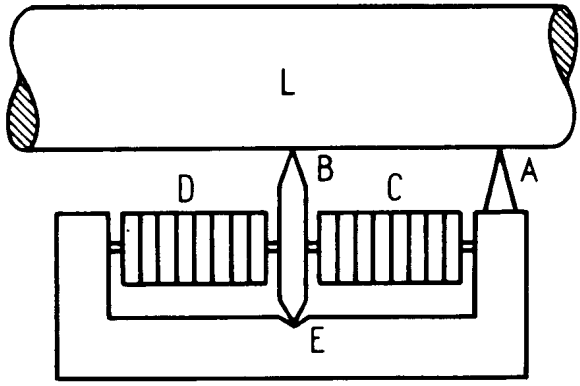

FIG. 239.

(3) A capacitance strain gauge consists of a condenser the capacitance of which varies as a result of the deformation. The use of capacitance strain gauges is accompanied by considerable technical difficulties and for this reason they are not nearly as widespread as resistance strain gauges. We shall illustrate the way in which they can be used by describing as an example Davis's measuring rod, which is an improved version of Hopkinson's measuring rod (see Chapter VI) and is used for investigating wave processes.

A flat plate parallel to the end of the rod *C* and charged to a high potential from the supply *I* forms one electrode of a plate

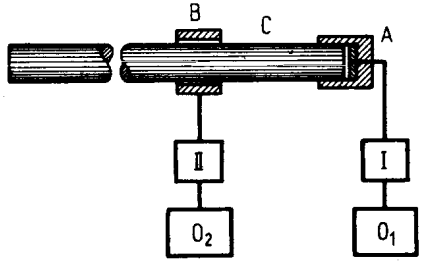

FIG. 240.

condenser microphone A (Fig. 240). The end of the rod C, which is earthed, forms the second. The lateral surface of the earthed rod C acts as one electrode of a cylindrical condenser microphone B which is charged from the supply II.

Let us suppose that a pressure is applied to the left-hand end of rod C which sets up an elastic wave, the stress σ in which is related to the particle velocity v by expression (6.11):

$$\sigma = -\varrho a_0 v,$$

where $a_0 = \sqrt{(E/\varrho)}$ is the propagation velocity of an elastic wave and ϱ is the density of the material of the rod. After the wave is reflected from the free end the particle velocity is doubled, so that if we measure the change with time of the longitudinal velocity $v_1(t)$ of the right-hand end, and, therefore, the change in the stress σ also, the change in pressure $p(t)$ on the left-hand end of the rod will be

$$p(t) = \tfrac{1}{2}\varrho a_0 v_1(t). \tag{8.11}$$

If the displacement $u_1(t)$ of the end is measured we can substitute in (8.11) its derivative: $v_1 = \partial u_1/\partial t$.

Let us suppose now that we measure the radial displacement of the lateral surface $w(t)$. Since the rod remains within the elastic range the lateral strain, which is w/a, where a is the radius of the rod cross-section, is related to the longitudinal strain by the expression

$$\frac{w}{a} = -\nu \frac{\sigma}{E}.$$

Thus, if we measure the radial displacement under the incident wave the pressure on the end of the rod is given by

$$p(t) = \frac{Ew}{a\nu}, \tag{8.12}$$

so that in this case there is no need to differentiate the expression for $w(t)$.

The microphone A is a sliding fit on the rod. Thus, when the compression wave reaches the right-hand end the microphone does not move and the rod moves rapidly into it. The sudden change in the gap between the electrodes of the plate condenser increases the potential difference, which for small displacements is proportional to the change in the gap. This change in potential is

recorded by the cathode-ray oscillograph O_1, which gives to some scale the curve of $u_1(t)$ from which, on the basis of (8.11), the curve of $p(t)$ can be derived.

A similar process in the cylindrical condenser microphone B gives a curve of $w(t)$, i.e. it gives to some scale the $p(t)$ curve according to (8.12).

(4) The Molchanov induction extensometer, a simplified diagram of which is shown in Fig. 241, consists of two legs A and B connected

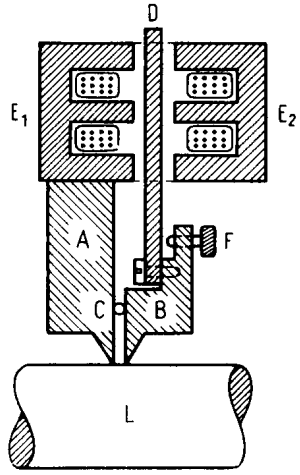

FIG. 241.

through a hinge C and resting on pointed ends on the specimen L. The leg A at its top carries two coils E_1 and E_2 shown in section (a conductor wound on a central glass core). Between the coils there is a mild steel armature D fixed rigidly to leg B. As the specimen extends the armature approaches the core of coil E_1 and moves away from coil E_2, so that the inductances of the coils vary in opposite senses. The screw F is used to zero the armature before taking a measurement.

The coils E_1 and E_2 are connected to neighbouring arms of an a.c. bridge (Fig. 242) which contains: (1) differential transformers T_1 and T_2, the magnetomotive forces of which act in opposite directions; (2) coils P_1 and P_2 which are the secondary windings of the transformers and (3) a galvanometer G in the diagonal. Before a measurement is taken the rheostats R_1 and R_2 are adjusted so that

the currents flowing through the rectifiers B_1 and B_2 from the secondary windings (coils P_1 and P_2), which flow in opposite directions, are balanced—the galvanometer G gives a zero reading.

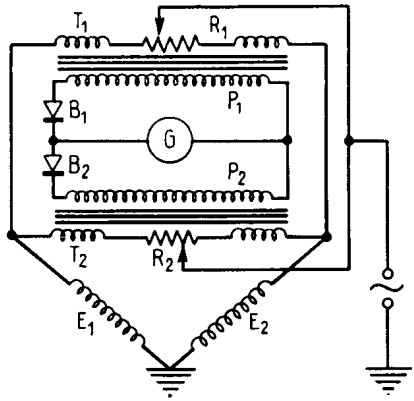

FIG. 242.

As the specimen deforms the inductances of coils E_1 and E_2 alter by the same amounts but in opposite senses; this alters the currents in coils P_1 and P_2 by similar amounts in opposite senses, so that the galvanometer records the sum of these values. The instrument is linear for small readings.

(5) Magneto-elastic extensometers are based on the fact that certain alloys with a nickel base, usually called permalloys, have a high magnetic permeability which is affected by deformation. If a coil is wound on one arm A of a frame as shown in Fig. 243 cut

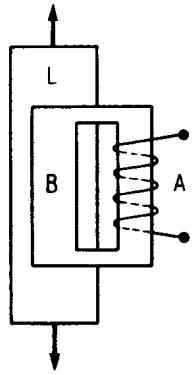

FIG. 243.

from a permalloy plate, and if the arm B is attached to the surface of the body under investigation L, then as the latter deforms the arm B also deforms and the magnetic permeability of the frame alters, which alters the inductance of the coil, which, as in the previous example, can be included in an a.c. bridge circuit. In practice these extensometers are found to be unstable with high sensitivity; this is associated with residual changes in the properties of permalloy after deformation.

(6) The photoelectric extensometer is based on the principle illustrated by Fig. 244. To the clamps H_1 and H_2, which are

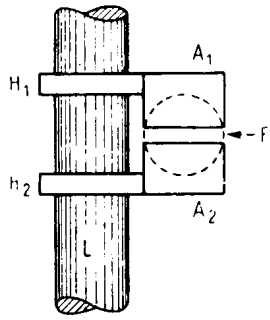

FIG. 244.

attached to the specimen L, are fixed plates A_1 and A_2. The width of the slit formed by these plates alters as the specimen deforms, which alters the amounts of light falling on the photo-electric cell F.

An important property of electrical extensometers is that they can be used for dynamic measurements and that a continuous trace of their readings can be recorded on an oscillograph. This, together with the fact that they enable readings to be taken easily in large numbers, justifies the use of complex electrical and electronic apparatus in stress analysis.

10. THE PHOTOELASTIC METHOD OF STRESS ANALYSIS

The photoelastic method of stress analysis has been developed from the discovery made in the nineteenth century by Brewster that certain amorphous optically isotropic materials (glass, celluloid, plastics, etc.), become optically anisotropic after deformation, or in other words, they assume the property of double refraction. At

every point in an optically anisotropic material we can draw an ellipsoid of refraction indices, the principal axes of which coincide with the principal axes of strain. The principal values of the refraction indices n_1, n_2, n_3 are related to the principal strains $\varepsilon_1, \varepsilon_2, \varepsilon_3$ by the expressions

$$\left.\begin{aligned} n_1 - n_0 &= a\varepsilon_1 + b(\varepsilon_2 + \varepsilon_3), \\ n_2 - n_0 &= a\varepsilon_2 + b(\varepsilon_3 + \varepsilon_1), \\ n_3 - n_0 &= a\varepsilon_3 + b(\varepsilon_1 + \varepsilon_2), \end{aligned}\right\}$$

where n_0 is the refraction index for the undeformed material, a and b are constants. We find from these expressions that:

$$\left.\begin{aligned} n_1 - n_2 &= k(\varepsilon_1 - \varepsilon_2), \\ n_2 - n_3 &= k(\varepsilon_2 - \varepsilon_3), \\ n_3 - n_1 &= k(\varepsilon_3 - \varepsilon_1), \end{aligned}\right\} \tag{8.13}$$

where by definition $k = a - b$. By making use of Hooke's law we find that:

$$n_i - n_j = C(\sigma_i - \sigma_j), \quad i, j = 1, 2, 3, \tag{8.14}$$

where C is a constant known as the photoelastic constant of the material, $\sigma_1, \sigma_2, \sigma_3$ are the principal stresses. The material is called optically active if $C \neq 0$ (or if $k \neq 0$).

If a plate of such material is deformed in its own plane (if a state of plane stress is set up so that $\sigma_3 = 0$) and if a normal ray of plane polarized light is passed through the plate, the resulting ray can be represented as the superposition of rays polarized in planes passing through the normal and the axes of principal strain. One of these rays, moreover, will lag behind the other, due to the difference in propagation velocities. Since the speed of light in a medium is $v = nv_0$, where n is the refraction index and v_0 is the speed of light in a vacuum, if we make use of the first of the expressions (8.14), namely,

$$n_1 - n_2 = C(\sigma_1 - \sigma_2), \tag{8.15}$$

we find that the retardation δ of the principal light vibrations is

$$\delta = h(n_1 - n_2)\, v_0 = hC'(\sigma_1 - \sigma_2) = 2hC'\tau_{\max}, \tag{8.16}$$

where h is the thickness of the plate and $\tau_{\max} = (\sigma_1 - \sigma_2)/2$ is the maximum shear stress in the plane of the plate.

In the case of a non-uniform state of stress different retardations depending on the magnitude of $\sigma_1-\sigma_2$ will be obtained for different points on the plate. Therefore, if we derive experimentally the field of retardations we can derive from this the diagram of principal stress differences.

Let us suppose that a ray of monochromatic light before reaching the specimen passes through a polarizer and becomes polarized, say, in the x–x plane. After the specimen the light passes through an analyser, i.e. through a polarizing plate the plane of polarization of which is perpendicular to the x–x plane; we shall define this as the y–y plane (Fig. 245). The planes of polarization of the rays

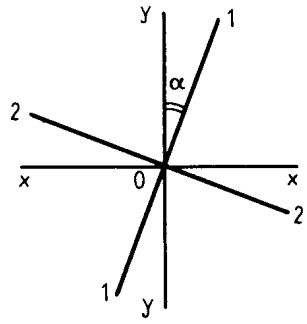

FIG 245.

after passing through the specimen coincide with the principal directions 1–1 and 2–2. After passing through the analyser both rays are once more polarized in one plane and since these rays were derived by the splitting (double refraction) of one ray, the light vibrations superimposed one on the other after the analyser will have one frequency, but they will have a phase difference which depends on the retardation δ.

It is known from the theory of optics that if the plane of polarization of an incident ray differs by an angle α from the plane of polarization of the ray after leaving the analyser, the intensity I_1 after the analyser is related to the intensity I_0 of the incident ray by the expression

$$I_1 = I_0 \cos^2\alpha.$$

After passing through the specimen, therefore, the intensity of the

light in rays polarized in planes 1–1 and 2–2 will be respectively (Fig. 246)

$$I_1 = I_0 \cos^2\left(\frac{\pi}{2} - \alpha\right) = I_0 \sin^2\alpha,$$

$$I_2 = I_0 \cos^2\alpha,$$

and after the analyser

$$I_1' = I_0 \sin^2\alpha \cos^2\alpha = \tfrac{1}{4} I_0 \sin^2 2\alpha,$$

$$I_2' = I_0 \cos^2\alpha \cos^2\left(\frac{\pi}{2} - \alpha\right) = \frac{1}{4} I_0 \sin^2 2\alpha,$$

so that $I_1' = I_2' = I'$. But these rays, which have the same intensity and the same frequency, will have a phase difference which depends on the magnitude of δ:

$$\varphi = hD(\sigma_1 - \sigma_2), \tag{8.17}$$

where D is a constant depending on the wavelength.

For the intensity after the analyser we have

$$I_m = I_0 \sin^2 2\alpha \sin^2\frac{\varphi}{2} = I_0 \sin^2 2\alpha \sin^2\frac{hD(\sigma_1 - \sigma_2)}{2}. \tag{8.18}$$

Formula (8.18) applies at every point on the specimen. But in the case of a non-uniform state of stress the orientation of the principal axes relative to some fixed direction changes from point to point. For instance, in general we can always find a number of points lying on one line, called an isoclinic, at which $\alpha = 0$ or $\alpha = \pi/2$, so that along this line $\sin 2\alpha = 0$, i.e. on a screen beyond the analyser a dark line will be seen. If the specimen or polarizer–analyser system is rotated through an angle $\Delta\alpha$ another dark line—an isoclinic—will be seen on the screen. In this way by rotating the polarizer–analyser system, we can obtain a field of isoclinics.

We recall that in order to determine a non-uniform state of plane stress at any point we must know three quantities as functions of the position of the point, which are: the principal stresses and the angle which defines the orientation of the principal axes (or, what amounts to the same thing, the quantities σ_{xx}, σ_{yy}, σ_{xy}). The field of isoclinics determines one of these quantities—the angle of orientation of the principal axes.

If we know the field of isoclinics we can find the field of isostatics, or the trajectories of principal normal and shearing stresses. The

tangent and normal at any point on an isostatic coincide in direction with the principal normal stresses. The isostatics can be found in the following way. Let us suppose that we have determined a field of isoclinics in increments of $\Delta\alpha = 5°$ (Fig. 246). Let us start

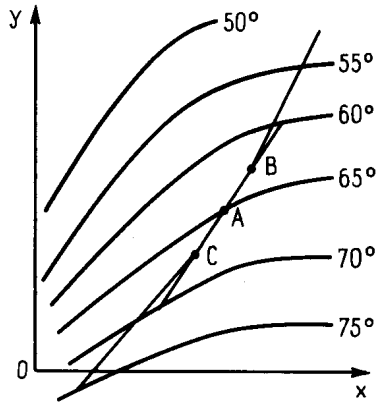

FIG. 246.

at some point A on the isostatic $\alpha = 65°$. We draw through this point a short line inclined at 65° to the Oy axis to intersect the neighbouring isostatics. From the centres B and C of the two parts of this line on either side of the initial isoclinic we draw lines at 60° and 70° respectively and so on. The required isostatic will be the smooth curve drawn through these lines. A second family of isostatics will be orthogonal to the first, and families of isostatics corresponding to the maximum shear stresses form angles of 45° to the families of isostatics for the normal stresses.

Let us consider now the last term in eqn. (8.18). It will be seen that it vanishes where

$$\frac{hD(\sigma_1 - \sigma_2)}{2} = n\pi, \quad n = 0, 1, 2, \ldots \tag{8.19}$$

On a screen beyond the analyser, therefore, there will be seen (in the case of monochromatic light) a set of dark lines, known as isochromatics, corresponding to different values of n and called respectively isochromatics of zero, first orders, etc. The stress difference corresponding to an isochromatic of any particular order can be found from a simple tensile test on the specimen. If natural (white) light is used, then since D depends on the wave-

length, coloured bands would be formed, since extinction for any given $\sigma_1-\sigma_2$ will occur only for a particular wavelength.

We see then that the field of isoclinics gives the stress difference $\sigma_1-\sigma_2$ as a function of the position of a particular point. Thus the fields of isoclinics and isostatics found by experiment give two relations between the three unknowns σ_1, σ_2 and α. The third relation necessary for the complete solution of a problem cannot, however, be found purely from optical observations. This is to be expected, since, as can be seen from (8.13) or (8.14), the optical effects result from the deviator parts of the stresses. This can also be seen from (8.18), since in the case of uniform tension or compression in two directions we have that $\sigma_1 = \sigma_2$ and, therefore, $I_m = 0$ everywhere for any angle of rotation α.

The third relation can be found either by numerical integration or by constructing experimentally so-called isopachics. Since in a state of plane stress $\sigma_3 = 0$, we have from Hooke's law that

$$\varepsilon_3 = -\frac{\nu}{E}(\sigma_1 + \sigma_2),$$

so that

$$\sigma_1 + \sigma_2 = -\frac{E}{\nu}\frac{\Delta h}{h}. \tag{8.20}$$

If we measure $\Delta h/h$ at various points and if we know the properties of the material, ν and E, we can draw lines of equal (and numerically determinate) values of $\sigma_1 + \sigma_2$. The line along which $\Delta h/h$ (and therefore $\sigma_1 + \sigma_2$ as well) is constant is called an isopachic. We can find the complete field of these lines if we cover the plate under investigation, which must be flat before the experiment, by an optically plane glass plate and if we observe the interference picture in the air gap between the undeformed glass plate and the specimen.

The photoelastic method of stress analysis would be of very little value if it enabled us to derive the stress distribution only in optically active materials. The importance of this method lies in the fact that it gives a model of the stress distribution in plates of optically inactive and in opaque materials in general, for example in metals. The point is, as the theory of elasticity shows, that in the case of a state of plane stress (or plane strain) the stress distribution under a loading which is given on the boundary of the body does not depend on the mechanical properties of the material. This is

true for simply connected regions or for multiply connected regions when the resultant of the system of forces acting on each boundary is zero. If a model is made from an optically active material and is made geometrically similar (in its plane) to the plate we wish to investigate, and if the scale factor (the ratio of a linear dimension on the model to the corresponding dimension on the plate) is k_s, the ratio of the forces on the model to the true forces is k_c, and the ratio of the thickness of the model to the thickness of the plate is k_h, then the ratio k_0 of the stress (normal or shearing stress) at some point in the model to the stress at the corresponding point in the plate is

$$k_\sigma = \frac{k_c}{k_s k_h},$$

i.e.

$$\sigma = \sigma_M \frac{k_s k_h}{k_c}, \tag{8.21}$$

where σ is the stress in the plate and σ_M the corresponding stress in the model.

The photoelastic method of stress analysis is used mainly when the deformation is kept within the elastic range. The method can however be extended to cover elasto-plastic deformation and today research is being carried out in this field. This development of photoelasticity is possible primarily because the relation (8.13) between the principal indices of refraction and the principal strains applies also over a certain range of plastic strains. In addition, there are indirect methods, one of which makes use of plates glued to the specimen. A thin plate of optically active material is stuck on the model which is in the form of a metal plate with one face polished. The elastic limit of the optically active material must be greater than that of the metal. The required picture is produced by the light which is reflected from the mirror surface of the specimen and passes twice through the layer of optically active material. The elastic strains in the optically active layer then correspond up to some limit to the plastic strains in the metal. This method is also in the development stage.

In the application of photoelasticity to a three-dimensional problem the method of stress freezing is used. This can be explained as follows. A model made of optically active material is heated uniformly to some "softening" temperature (of the order of $+100°C$) and a load is then applied. The model with the load still

applied is then cooled to room temperature, after which the load is removed. It is considered that the changes in the refraction index (optical anisotropy) caused by the deformation are "frozen in" and retained in the body after removal of the load. The model is then divided up into a number of thin slices and the optical picture in each is studied to determine the state of stress in the three-dimensional model under load. Whereas in the case of a state of plane stress the variations in the state of stress can be recorded with a cine-camera, i.e. the photoelastic method can be applied to dynamic problems (vibrations, waves), the method of stress freezing in the form described above can only be used in static experiments.

The method of inset plates, which is still in the development stage, is very useful for dynamic experiments. In this method a three-dimensional model made of optically inactive material is split up and a plane layer of optically active material, which has the same mechanical properties as the model, is inserted. As the model is deformed only the optically active layer will give an interference pattern, the variation of which can be observed directly.

11. Photographic Recording

In experiments on the static deformation of bodies it is sometimes convenient to use photographic recording in order to obtain a complete and accurate record of the observations made during the experiment. Quite often photography is used to record interference patterns and in the 04–1 machine, for instance, photographic methods are used in combined loading tests to give a continuous diagram of the recordings of the pneumatic–optical instruments. In dynamic experiments the photographic method is often the only one possible, since direct observation of short-lived events is, as a rule, impossible, so that we have the choice of estimating the nature of the events that occurred during the experiment either on the basis of the residual effects on the material or from the traces produced by the measuring instruments, which can often be carried out photographically. In order to obtain photographic records the most important items of equipment are, of course, a camera and lighting.

The lighting must be sufficiently bright to give a well defined picture with the exposures possible for any particular process, without producing a blurred effect. As a source of continuous

lighting incandescent lamps are used (often with a short-duration boost device which improves the spectral composition of the light). Other sources are arc lamps and vapour lamps; it is also possible to use daylight and, in particular, direct sunlight. Sometimes a powerful instantaneous source is sufficient: an electric spark, a magnesium flash, a metal wire fused by a large electric current, etc. Serious attention, however, must be paid in these cases to the synchronization of the flash and the required instant during the experiment. As regards the shutter of the camera, sometimes it can be left open if the illumination of the specimen is only weak prior to the flash; otherwise it is necessary to synchronize the shutter

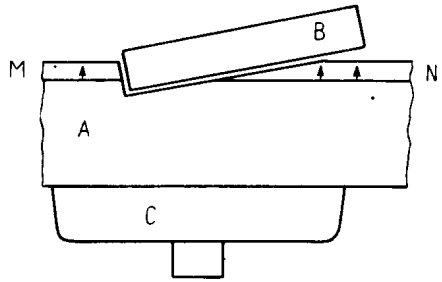

FIG. 247.

with the flash equipment, which is usually very easy to do: the shutter control is connected directly to the flash device. For example, operation of the shutter can be arranged to close a discharge circuit which ionizes the spark gap between the electrodes of a discharger. Sometimes it is required to produce several successive flashes in order to record the various stages in a deformation process. We shall describe three methods which can be used for this purpose: (1) successive switching on by means of a special synchronizing device of a number of momentary light sources (for example electric spark dischargers); (2) repeated switching on of the same light source, for example, by the periodic application of a high voltage to the terminals of a gas-filled discharge tube; (3) a stroboscope can be used to admit light as required from a continuous source. The duration of the flash in all cases can be controlled to one microsecond and less.

Sometimes the observed phenomena are self-illuminating and do not require additional illumination: the image on the screen of an oscillograph (sometimes with a considerable afterglow), a detona-

tion and explosion, the luminescence of gases in a shock wave. As an example Fig. 247 shows diagrammatically the apparatus used in an experiment to determine the propagation velocity of a shock wave in a metal.† A charge C exploded on the lower surface of the plate A sets up a shock wave MN which is propagated at a velocity of several kilometres per second. The wave itself, of course, is not visible in the metal. But in the top surface of the plate a pocket is formed with one surface at 10° to the surface of the plate and a flat plate B of transparent material (leucite) is placed with $\frac{1}{4}$ mm clearance in the pocket. The gap between the two plates contains air or argon. After the front of the shock wave MN reaches the bottom of the gap a shock wave is set up in the gas which is accompanied by luminescence of the air (and a more intense luminescence of argon). A small vertical displacement of the front of MN corresponds approximately to a horizontal displacement of the front of luminescence six times greater, which can be recorded photographically from above.

Sometimes, depending on the nature of the experiment, a standard camera is not suitable and a special design has to be used. We can differentiate between cameras with a fixed film (or plate), those with an intermittently moving film and those with a continuously moving film. Normal cameras with a fixed film can be used for individual photographs of static processes or processes of short duration. The exposure for a photograph of a fixed object with a given light intensity is limited solely by the sensitivity of the film. In photography of moving objects the maximum permissible exposure is determined by the required accuracy of the photograph. If Δ is the permissible image overlap of the photograph (i.e. the displacement of the image of a point over the film during the exposure time), V is the velocity of the object in a direction parallel to the plane of the film, H and h are the distances from the objective to the object and to the film respectively, we have for the exposure τ:

$$\tau \leqq \frac{H\Delta}{hV}. \tag{8.22}$$

In many cases the exposure given by a mechanical shutter (up to the order of one-thousandth of a second) is too long. In this case the

† Walsh and Christian, *Phys. Review*, **97**, 6, 1955.

exposure can be controlled by the duration of the flash. As a shutter with a very brief exposure a Kerr cell (Fig. 248) can be used. The Kerr cell is based on the fact that certain substances (nitrobenzol, chloroform, orthonitrotoluene, etc.), assume the property of double refraction. A Kerr cell comprises an air-tight container K with plane parallel transparent walls and with metal plates M and N connected to an electric power supply. If a Kerr cell together with crossed polarizer P and analyser A is placed between

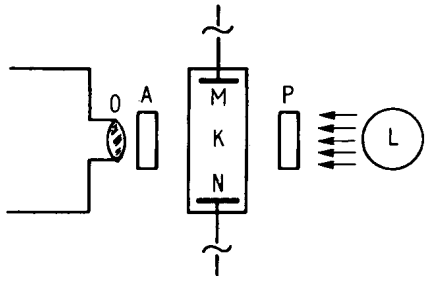

FIG. 248.

the object L and the objective O of a camera, and if the supply is not switched on, light which is plane-polarized by the polarizer will not pass through the analyser. If the supply is now connected so as to set up a potential difference between M and N, light which is plane-polarized in P, after passing through the Kerr cell, becomes elliptically polarized and will therefore pass through the analyser A and reach the objective of the camera. The small exposure which can be attained by means of the Kerr cell is 0·01 μsec. Its disadvantage, however, is the considerable loss of light (up to 70 per cent).

Cameras with fixed films can be designed so as to produce a series of photographs of a moving object or of the changes which take place in the object. A simplified diagram of this type of apparatus is shown in Fig. 249. The object L is illuminated by an intermittent light source. The image (unfocused) falls on a plane mirror K which rotates about a horizontal axis and which reflects the image (focused) on to the film P fixed to a circular rim. The speed of rotation of the mirror is chosen so that no two images coincide and the duration of the flash is made sufficiently short so that the image is not blurred. Instead of an intermittent light

source, a high frequency shutter device, such as the Kerr cell, can, of course, be used. Cameras of this sort are able to take photographs at the rate of several million per second.

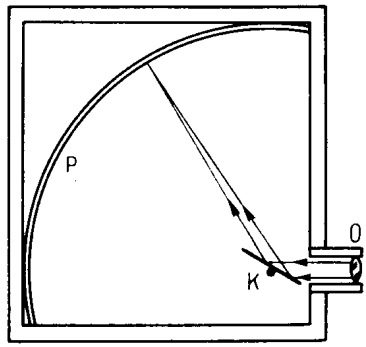

FIG. 249.

Cameras with a film which moves intermittently have the advantage that exposure occurs at the instant when the film is stationary, and if blurring of the image results it is due solely to the movement of the object. Their use is, however, somewhat limited by the tendency of the rapidly moving film to tear, not to mention the difficulties inherent in their construction. This type of camera is capable of taking only 250 photographs per second approximately, and for this reason it is not very often used.

Cameras with a continuously moving film are the most commonly used. They can be either the normal cine-camera or the high-velocity or ultra-high-velocity type. In order to obtain a series of images the motion of the film is synchronized with the opening and closing of the shutter or with the intermittent illumination of the object. In the case of a relatively slow-moving object, the image will be exact to within a tolerance Δ if the exposure τ satisfies the inequality:

$$\tau \leqq \frac{\Delta}{v}, \tag{8.23}$$

where v is the velocity of the film. If the object is moving, inequalities (8.23) and (8.22) must both be satisfied. In order that separate photographs do not overlap, the condition

$$v \leqq \frac{vH}{Lh}, \tag{8.24}$$

must be satisfied, where v is the frequency of the shutter (or of the intermittent illumination), v is the velocity of the film, H and h are the distances from the objective lens to the object and to the film respectively, and L is the height of the object.

Examples of cameras with continuously moving films are those in which the film is wound from one reel onto another (cine-cameras), cameras of the drum type, in which the film is attached to the rim of a continuously rotating drum, and cameras of the disc type in which the film is fixed to one surface of a rotating disc. The last two types of camera require some means of stopping automatically the opening of the shutter or of switching off the illumination after one revolution, so that the film is not exposed for a second time.

Cameras with a continuously moving film are used for outline or silhouette photography when a record of the motion of the body as a whole is required, as opposed to its motion at various points. For example, in order to find the propagation velocity of the front of a shock wave caused by an explosion, the camera is focused on the explosive and arranged so that the direction of motion of the film is perpendicular to the direction of motion of the wave front. With all illumination switched off the shutter is opened, the film is set in motion and the charge exploded. In the case of a wave front moving at constant velocity, the boundary between the illuminated and dark parts on the film will be a straight line, the slope of which determines the velocity of the front of the shock wave D:

$$D = \frac{vH}{h} \tan\alpha, \tag{8.25}$$

where v is the velocity of the film, H and h are the distances from the objective lens to the explosive and to the film respectively.

In the same way we can determine, for example, the change in velocity of a hammer after impact—by photographing the shadow of the leading edge of the hammer. A similar procedure is followed in dynamic experiments on the compression of cylindrical specimens under a falling weight. In these experiments, instead of photographic methods, the required record is sometimes obtained by producing a trace on a rotating drum.

Cine-cameras can also be used to give a record of the instrument readings in processes which take place at moderate rates.

INDEX

Ageing of materials 272, 274
Amorphous body 6
Analyser 426
Analysis of materials 368
Angle of twist 130
Anisotropy 6, 11, 19, 200
Annealing 87
Antinodes 344
Armstrong 266

Bauschinger effect 78, 200
Beam 138
  cantilever 140
  carrying capacity of 153
  continuous 158
  deflection of 156
  in bending 138, 149, 221
  I-section 151
  on elastic supports 160
  semi-infinite 162
  stability of 164
  stress and strains in 141
  thin-walled 222
  under combined loading 135
Bending, plane 158
  combined longitudinal and transverse 164
  moment 135
  pure 144, 290
Bernoulli equation 330
Bredt's formula 224
Brinell hardness 381

Carrying capacity 133, 153
Central Scientific Research Institute of Industrial Structures 203
Chalmers extensometer 408
Change of shape 40, 44, 52, 55
Change of volume 39, 44, 52, 55
Chronograph 321
CHURIKOV, F. S. 277
Cine-camera 435
Clapeyron's equation 229
Clark 295
Coefficient 119
  influence of friction 239
Complementary shearing stresses 30
Components
  of strain tensor 47
  of stress tensor 28
Concentration, stress 364, 369
Condition of incompressibility 235
Condition, yield 202, 228
  COULOMB, ST. VENANT 203, 204
  HENCKY–MISES 202, 204
Continuum, material 7, 27
Coordination number 10
Core points 149
Corrosion 93
Coulomb's law 239
Cracks 14
Creep 4, 7, 83, 261, 267, 273
  curve 267, 303
  in a state of compound stress 278
  of polymers 270
  reversible 270
  steady 268, 276, 279, 284, 286
  theory of 273
  unsteady 268, 277
Critical load 3

Damping of vibrations 85
DAVIDENKOV, N. N. 178
DAVIS 265, 267, 269, 278, 294
Degree
  of deformation 236
  of freedom 111, 116
Delayed yield 291

Deviator
  strain 52
  stress 40
Diagram
  constitution 86
  dynamic stress–strain 322
  Haigh 360
  stress–strain 73, 79, 129, 298, 299
Dislocation 102, 271, 292
Displacement 21, 53, 64
  measurement of 395
  relative 44
Double refraction 424
Dynamometer 403
Δl–φ experiments 189

Eccentric tension (compression) 149
Elastic body 2
Elastic constants 75, 198
Elastic core 132
Elastic limit 73, 169, 291
Elasticity 2, 75, 176
  non-linear 261
  volumetric 176
Electron cloud 11
Endurance 357
  limited 359
Equation of compatibility 210
Equlibrium, condition of 64
ERKOVICH 283
Extension
  mean 49
  relative 47
Extensometers 408
External influences 1, 30

Failure 2, 3, 7, 205
  Afanasyev's theory of 366
  brittle 205, 364
  dynamic 295
  fatigue 356, 364
  surface 205
Fatigue 4, 356
  limit 359
FOCHT 262, 266
Force
  body 25, 62
  centrifugal 64, 290
  concentrated 60
  dynamic 291
  Euler critical 168, 173
  external 1, 21, 58
    mass 58, 62, 64
    surface 58, 60
  internal 6, 53, 69
  longitudinal 135
  of gravity 64
  of interaction of particles 6, 20, 53, 66, 293
  transverse (shear) 135
Fracture, fatigue 364
Frameworks 109
Frequency
  angular, of vibrations 345
  effect of, on fatigue 364
  equation 345
  natural 343
Friction
  internal 4
  Prandtl 248
  surface 237
Front
  detonation 330
  wave 307

Geometry of specimens 368
GUARNIERI 283

Heat-resistant alloys 267
Heat-treatment of metals 13, 86
Hencky–Mises ellipse 202
Hinged supports 111
Hollow charge 329
Hooke's Law 75, 106, 425
  generalized 196, 208
HOPKINSON, B. 293, 301
HOPKINSON, J. 203, 301
Hypothesis of plane sections 72, 106, 127, 130, 142, 144
Hysteresis 85

Impact 293, 304
  of a rod on an obstacle 315, 337

Impact, (*cont.*)
on a structure 338
theory of 304
Impulse loading 325
Intensity
of rate of strain 235
of stress 41, 178
Inter-atomic forces 11
Interferometer 397
Isochromatic 428
Isoclinic 427
Isomorphism 192
Isostatic 427
Isotropy 6, 11, 19, 70, 75, 191, 200

Jouravsky equations 138, 159, 222

KENNEDY 266
KOLSKY 301
KOTALIK 203
Krylov's function 352

Lagrange's principle 122
Lagrange's variational equation 66
Lamé parameters 198
Lamé's problem 207, 250
Laplace formula 219
Lattice
crystalline 9, 20, 26
distortion of 21, 95, 102, 262, 271
parameter 9
Limit of proportionality 73
Linear accelerator 387
Load 183, 186
critical 3
dynamic 291
impulse 325
limiting 153
oscillating 339
repeated 4, 85
Loading
combined 186
simple 186, 191, 192, 206
shock 293, 304
Ludwick's formula 297
Lüders lines 101

Machines, testing 372
dynamic 383
fatigue 383
static 372
Macrostructure 12
Manometer 406
Mariott's formula 212, 219
Material (of solid bodies) 2, 79
brittle 4, 80
incompressible 75
non-homogeneous 19
of organic origin 95, 272, 291
optically active 425
structurally unstable 200
visco-elastic 261
MAXWELL 264, 266, 271
Maxwell's equation 83
Measurement
of displacements 395
of forces 403
of strains 408 f.
optical method of 408
Measuring rod 321
Mechanics
of a continuum (a continuous medium) 6
of a deformable body 1
structural 6
theoretical 121
MERINO 203
Metals 9, 70, 79, 86
Method
general, of finding stresses, strains and displacements 64
of elastic solutions 104, 109, 148
of impulses 325
of residual strains 322
of similarity 286
of stress "freezing" 430
photo-elastic, of stress analysis 424
Microstructure 12
Model, mechanical 262, 264
Modulus
dynamic 291
of longitudinal elasticity (Young's modulus) 75, 93, 97, 323, 348
adiabatic 348, 356
isothermal 348

Modulus (*cont*).
shear 130
strain-hardening 75
in shear 133
von Karman 173
Mohr and Federhaff testing machine 374
Monocrystal 11, 27

NARSULLAYEV 297
Neutron bombardment 95
Node 110
in a framework (vibration) 344
Non-linearly elastic body 326
Normalization 89

Orientation
of grains 15, 27
parameter 15
Oscillation
mode of 344
natural 343

Period
of recovery 264
of relaxation 265
Phase of metals 13, 87
Photo-elastic constant 425
Photographic methods 431
Plastic flow 226, 250
three-dimensional 233, 236
Plastic range 109
Plasticity 4, 176, 186, 189
ideal 100
laws of 189
Plastics 272, 274
P–M experiments 189, 194
Poisson's ratio 75
Polarizer 426
POPE 294, 306
P–p experiments 183
Prandtl's problem 242
Pressure
generalized 252
hydrostatic 39, 56
working 216, 226, 235
Principal axes 49, 425
of strain 49, 425
of stress 31
Principal plane of stress 32
Proof stress 74
Properties of materials 1, 7, 13, 69, 74, 79, 89, 429
effect of creep and recovery on 83
effect of heat-treatment on 86
effect of radiation on 95
effect of rate of strain on 81
effect of relaxation on 82
effect of repeated loading on 85
effect of temperature on 90
effect of time on 261
fatigue 361
structural 9

RABOTNIKOV, U. N. 277
Radioactivity, effect of 95
Rate of deformation 81, 235, 291, 293
high 299
Recovery 83, 264
Recrystallization 226, 269
Redundancy 121
REINHART 327
Relaxation 7, 82, 264, 281, 304
curve 265
Resonance 3, 348
Rockwell hardness 381
Rod
eccentrically loaded 149
in tension (compression) 55
measuring 321
of constant section 104
of variable section 104, 105
slender 164

Schopper machines 375
Shaft, analysis of 350
Shear 11, 126
elasto-plastic 178
maximum 49, 51
octahedral 52
Slip planes 11
Solid derformable body 7
Spalling 326
State of compound stress 176, 178, 202, 278
State of plastic stress in a hollow sphere 216
State of stress 26, 33
at a point 27, 37

Statically indeterminate frames 108, 121, 158
Stiffness
  flexural 147
  in tension–compression 106
  torsional 132
Strain 1, 2, 5, 9, 64, 83, 141, 232
  active 76
  elasto-plastic 69, 73, 76, 192, 194, 196
  finite 2, 230, 237
  hardening 75, 133
  in the neighbourhood of a point 43
  irreversible 77
  logarithmic principal 232
  non-linear elastic 77
  passive 77
  plane 54, 284
  plane shear 57
  plastic 1, 4, 73, 76, 105, 109, 132, 226, 292
    mechanism of 100
  principal 232
  principal axes of 49, 425
  rate 81
  residual 73, 76, 120, 301, 322
  reversible 77
  small 46
  temperature 58
  tensor 46
  total 120
  trajectory 189, 194, 235
    reflection of 191
    rotation of 191
Stress 5, 9, 22, 27, 58, 64, 141, 235
  at a point 28
  external 58
  frictional 237
  hydrostatic 39
  initial 58, 87
  normal 27, 35, 142, 150, 221
    mean 39
    principal 30
  principal 32, 33, 36
  residual 120
  shearing 27, 33, 126, 132, 220
    law of complementary 30
    octahedral 38
  temperature 58
Strip forming 61
Support
  compound 114
  fixed 112, 114
  hinged 111
  rigid 111
Sylphon 406

TAYLOR, J. 295, 299
Temperature, effect of
  on creep 268
  on fatigue 363
  on friction 242
  on mechanical properties 90, 274, 282
Tension
  hydrostatic 56
  simple uniaxial 55
Tensor
  of rate of strain 230, 233
  of relative displacement 46
  strain 47
    deviator of 52
    spherical 52
  stress 24, 40
    deviator of 40
    spherical 40
Theorem
  of Jouravsky 138
  of simple loading 206
  of unloading 121, 206
Theory
  of ageing 272
  of creep 267
  of elasticity 7
  of impact 304
  of plasticity 7
  of small elasto-plastic strains 192, 287
  of strain hardening 276
Thin-walled containers 218
Three-dimensional elasticity 176, 197
Time, effect of, on mechanical properties 261, 292
Torque 127, 135
  meter 409
Torsion
  of circular rod 130

Torsion (*cont.*)
of thin-walled cylinder 127
Trajectory
loading 184
shearing stress 220
Tubes
thin-walled 207, 218, 249
under pressure 207, 284

Ultimate tensile stress 74
Uniaxial stress 55
Uniform stress 180
UZHIK, G. V. 205, 328

Vector
displacement 21
of internal stresses 58
strain 184
stress 21
Vibrations 2, 85, 339
bending 351
free 343
longitudinal 341
torsional 348
Vibrator 383
Viscosity 7, 84, 261

WARNOCK 294, 306
WATSON 266
Wave equation 311
Waves
elastic 307
plastic 322
shock 308
standing 341
unloading 317
Waves on long rods 307
longitudinal 307
propagation of 299
reflected 312
Riemann 323
torsional 312
transverse 312
Wear 238
Winkler's hypothesis 161
Wöhler's curve 358, 362
WOOD 296
Work
done by internal forces 53
in a change of shape 55
in a change of volume 55

Yield, delayed 296
Yield point 73, 88, 130, 291, 292
local 76
lower 74, 292
upper 74, 292
well-defined 73

ZHUKOV, A. M. 277
ZHURKOV 297

MADE IN GREAT BRITAIN